RV SONNE
CRUISE REPORT SO173/1, 3 & 4

SUBDUCTION II:
THE CENTRAL AMERICAN CONTINENTAL MARGIN

SO173/1: 9.7.-6.8. 2003
BALBOA (PANAMA) - CALDERA (COSTA RICA)
SO173/3: 3.9.-16.9.2003
CALDERA (COSTA RICA) - CALDERA (COSTA RICA)
SO173/4: 17.9.-29.9.2003
CALDERA (COSTA RICA) - BALBOA (PANAMA)

Edited by
Ernst Flueh, Emanuel Soeding, Erwin Suess
with contributions of cruise participants

Investigations in the frame of SFB574
"Volatiles and Fluids in Subduction Zones:
Climate Feedback and Trigger Mechanisms for Natural Disasters"

Contribution Nr. **52** of SFB574

GEOMAR
Forschungszentrum
für marine Geowissenschaften
der Christian-Albrechts-
Universität
zu Kiel

KIEL 2004

GEOMAR REPORT 115

GEOMAR
Research Center
for Marine Geosciences
Christian Albrechts University
in Kiel

Redaktion dieses Reports:
Ernst Flueh, Emanuel Söding und Erwin Suess

Layout: Emanuel Söding

GEOMAR REPORT
ISSN 0936 - 5788

GEOMAR
Forschungszentrum
für marine Geowissenschaften
Wischhofstr. 1-3
D - 24148 Kiel
Tel. (0431) 600-2555, 600-2505

Editors of this issue:
Ernst Flueh, Emanuel Söding und Erwin Suess

Layout: Emanuel Söding

GEOMAR REPORT
ISSN 0936 - 5788

GEOMAR
Research Center
for Marine Geosciences
Wischhofstr. 1-3
D - 24148 Kiel
Tel. (49) 431 / 600-2555, 600-2505

Content

1 Summary

R/V SONNE cruise SO 173 is the latest in a series of research cruises to the Central American convergent margin. The cruise was initiated, planned, and carried out by members of the "Sonderforschungsbereich SFB 574", established in 2001 as a long-term "Cooperative Research Center" at the University of Kiel. Nearly all subprojects of the SFB 574 participated in various aspects of the cruise and contributed to cruise-related research.

The SFB 574 studies budgets, reactions, and recycling of fluids and volatiles in subduction zones to understand how they are regulating and mediating global processes such as the geochemical evolution of hydro- and atmosphere, long-term changes in Earth's climate, and the dynamics of sedimentary architecture of continental margins. The convergent Central American margin offshore Costa Rica and Nicaragua is a type example of an erosive subduction zone where these interconnected processes can be studied.

Volatiles are carried into the subduction zone with pelagic sediments, alteration products of the oceanic crust, and the trench fill derived from sediments transported downslope. They are recycled via fluid venting at the deformation front, mud diapirism at the margin, and magmatic devolatilization at the volcanic arc. Inside the subduction zone the incoming material is transformed, mobilized or fractionated into different volatile reservoirs and phases. These phases are either ejected into the exosphere through the upper plate, accreted to the leading edge of the continental plate, or they are transported into the lower mantle.

Several factors affect the mode of volatile recycling at subduction zones: the tectonic style of subduction as well as the geometry and composition of the margin wedge and the subducted plate determine the volatile budget, its transformation, and return pathways. There are intricate feedback loops between tectonic style, volatile behavior and metamorphic processes that the SFB 574 is attempting to unravel. To address these issues the 12 subprojects of the SFB 574 are grouped under three overarching themes as follows:

A: Material input and tectonic behavior during plate subduction.

Convergent margins are frequently characterized by accretionary superstructures built up by deformed pelagic and hemipelagic sediments. At erosive convergent margins, however, sediments carried on the incoming oceanic plate and slope material mobilized through mass wasting are completely consumed in the subduction zone. As significant amounts of carbon, sulphur, water, and halogenes are removed from the exosphere through subduction erosion, SFB 574 research is focused on the locus of this exchange process, the slope of the erosive Central American margin. Of particular interest are sediment diagenesis and alteration of oceanic crust, two major processes that are considerably modifying the input of carbon, sulphur, and water into the subduction zone. Compressive tectonic stresses at the front of the subduction zone lead to progressive expulsion of intergranular fluids from deforming unlithified sediments, and, combined with higher temperatures at depth, to mineral dehydration. The "excess" fluids are extruded on a small scale through localized vents and diapiric processes or on a broader scale through focussed flow along faults and fractures. Therefore one of the key questions for this theme is the magnitude and connection between the different dewatering mechanisms.

B: Transformation and partitioning of volatiles into different reservoirs.

During subduction volatiles can be partioned into several transient reservoirs such as mud diapirs and gas

hydrate layers, in which considerable amounts of methane, carbon dioxide and water are retained. Transient reservoirs strongly modulate the return flow of volatiles into the hydrosphere, by accumulating them over long periods of time and releasing them rapidly under certain conditions, such as hydrate dissociation or eruption of mud volcanoes. The dynamics and external control of these reservoirs - such as short-term climate change and slope stability - are among the least understood parameters in element recycling at subduction zones.

C: Devolatilization by magmas and metamorphic processes in the forearc.

The majority of the world's active subaerial volcanoes are concentrated along convergent plate margins, mostly around the rim of the Pacific Ocean. These volcanoes are not only characterized by their explosive activity causing major loss of life and property, but also known as a major source of climate-influencing volatiles in the Earth's atmosphere. Volcanic systems at subduction zones represent the most important factor in global material cycling and influence on the biosphere compared to other tectonic environments. A realistic estimate of the magmatic volatile input into the hydrosphere and atmosphere at subduction zones is only possible if the interactions and interdependencies between slab, mantle and crustal reservoirs, petrogenetic processes, and the characteristics of volatile release and entrainment during magma ascent can be reconstructed qualitatively and quantitatively over long time-scales. The main objectives of Theme C are to evaluate the mass balance of volatiles that are subducted into the mantle, incorporated into the crust, and released into the hydrosphere and atmosphere at subduction zones, as well as the transport dynamics of magmas and their volatiles.

The research carried out under Theme C of the SFB 574 is expected to improve our understanding of volatile flux in subduction zones and its effects on global material cycling and the Earth's climate. The results of these studies will also be important to assess the impact of toxic volcanic emissions on the environment and to contribute to volcanic hazard mitigation in Nicaragua and Costa Rica, countries that are frequently affected by major natural disasters.

All subprojects of the SFB 574 are tied closely together through common goals and overarching questions that can not be addressed by one group or one scientific discipline alone. Such questions are:

- Is there a detectable and quantifiable relationship between tectonic movements, tidal and other forces, on one hand, and dewatering rates and fluid venting, as well as volcanic activities, on the other?
- How do subduction velocity, plate composition, and variable temperature and pressure regimes affect the depth of maximum devolatilization and earthquakes?
- How much of the return flux to the ocean and the atmosphere occurs through vent sites, mud diapirism, and volcanoes? What is the recycling efficiency of these pathways?
- What are the processes controlling the formation and decomposition of gas hydrates and how is methane transport affected by mud diapirism? Do gas hydrates trigger large slumps, how often do such events occur and how much mass is moved by individual slumps?
- How do fluid and gas fluxes at subduction zones affect benthic communities, water column chemistry, and sea-air exchange of green house gases and what role does biologically mediated transformation of volatiles in the ocean play?
- What are the quantities of different volatile phases expelled from volcanoes into the atmosphere, from which sources do they originate, and which are the processes controlling their composition?

Leg SO 173/1 was dedicated to collecting a wide range of geophysical data in the working area such as standard MCS, high resolution deep tow seismic and sidescan sonar information to aid further planning and sampling.

Legs SO 173/3 and SO 173/4 were dedicated to geochemical, sedimentological, biological, and oceanographic measurements and sampling as well as video sled and lander-based seafloor observations and measurements.

2 Introduction

2.1 Objectives of Cruise SO 173/1

SO 173 continues a series of R/V SONNE cruises to the Pacific convergent continental margin off Costa Rica and Nicaragua. The series began in 1991 with cruise SO 76 in 1991, followed by SO 81 in 1993, SO 107 in 1996, SO 144 (6 legs) in 1999 and SO 163 (2 legs) in 2002. Moreover, this area has been investigated by several cruises of other institutions with different research vessels (R/V EWING, ROGER REVELLE, R/V METEOR). In addition, it has been probed by drilling with JOIDES RESOLUTION. Therefore the question arises: Why is this section of the margins of the Pacific plates so much in the focus of current geoscientific research?

The segment of the Central American continental margin off Costa Rica and Nicaragua provides - over a relatively short distance - a wide spectrum of considerably different subduction styles and scenarios. The main differences are age and source of the subducted oceanic crusts, subduction angle, depth of the melting zone and earthquake focal depths. Characteristic features are the seamount province parallel to the Cocos Ridge, which is subducted under Costa Rica, and the heavily fragmented plate segment cut by numerous normal faults, subducted off Nicaragua. As such, the segment off Costa Rica and Nicaragua is a natural laboratory to investigate causes, consequences, and relationships between these different parameters.

At convergent margins, gravitational downslope mass transport takes place in varying dimensions. Submarine slides occur as large megaslumps of several hundreds to thousands of km^3, but also as a sequence of individual slumps, generated by oversteepened submarine slopes. Major slides are often attributed to high sedimentation rates leading to overpressuring. Earthquakes are considered the likely immediate triggers for failure along the continental margins, yet compelling evidence for these causal factors is inconclusive. In the Costa Rica area, special downslope transport is associated with seamount subduction (Ranero and von Huene, 2000; von Huene et al., 2000).

All these dynamic processes are shaping and changing the seafloor. Cruise SO 173 set out to map in detail the surface of the continental margin off Costa Rica in a multiscale approach, applying a whole set of different mapping tools with different resolution. High resolution surveys will aim to identify local features such as tectonic structures, slides, and fluid venting-related manifestations on the seafloor. To assist interpretation, direct observations and detailed optical imaging of the seafloor by TV-sled are necessary. At the same time, the results of TV-guided investigations provide an important basis for sample site selection for most of the other subprojects of the SFB 574.

The scientific goals of the first leg of SO 173 centered around geophysical investigations using OBH and OBS systems as well as DTS sidescan sonar and multichannel seismic streamer. Planned surveys included seismic measurements ranging from conventional crustal scale wide-angle surveys to high resolution deep tow seismic investigation and deep tow sidescan sonar imaging. Geologic features identified on previous cruises, such as Mound 11 and 12, Mound Culebra and the BGR slide area were the primary targets of the cruise. In addition, a seismological network, deployed in October 2002 during the METEOR M 54 cruise, had to be recovered. During transits Simrad multibeam bathymetry and magnetic data were collected.

2.2 Objectives of Cruise SO 173/3 and SO 173/4

A summary of cruise targets and objectives for SO 173 legs 3 and 4 includes the following high priority goals, briefly described in the following overview:

- Mapping and sampling of most of the newly discovered mounds on the Nicaragua and Northern Costa Rica margin. These mounds were discovered by the Deep-towed Sidescan Sonar System (DTS) employed during SO 173-1.
- Continuation of geochemical studies on Mound Culebra, Mound 10, Mound 11 and Mound 12 in order to better constrain rates and activity of venting; recovery of near-surface gas hydrates.
- Mapping and sampling of faults near Mound Culebra to look at genetic relationships between tectonics and mud diapirism; of particular interest here is clarification of whether or not the faults are active fluid conduits along their entire surface tracks or only at points of intersection.
- Additional coring and video observations at the BGR and GEOMAR slides to better constrain the age and mechanisms of hydrate dissociation related shallow mass wasting in the area.
- Detailed water column and sediment sampling at the suspected freshwater seep site off Quepos slide including deployment of lander systems.
- Sampling of ash layers off Nicaragua to correlate them to land-based volcanic events and to develop an along-arc para-stratigraphy which ties in the history of volcanic eruptions on the Central American volcanic arc.
- Assessment of interannual variability of methane emissions from vent sites as well as bottom current control on methane plume distribution.
- Selected sampling of sediments and carbonates at sites of high methane turnover for biomarker investigations.
- Sediment physical property studies on canyon systems off Nicaragua, sampling of high reflectivity backscatter anomalies.
- Lander deployments on Mound Culebra (BCL and Long Ranger) to look for possible fluid flow anomalies (here occurrence of crystalline clasts indicates higher rates of sediment transport).
- Deployments of moorings/current meters near Mound Culebra and Jaco Scar in support of water column studies.
- Revisiting Rio Bongo scarp for sampling of carbonates in order to complete regional coverage of lower-slope vent sites primarily based on video sled (OFOS) observations to search for evidence of seepage in areas not surveyed in detail.

2.3 Geological Setting of the Study Area and Maps

The working area of cruise SO 173 was located at the Pacific continental margin off Costa Rica and Nicaragua. This area contains the boundary between the Caribbean and Cocos plates, marked by the Middle America Trench (Fig. 2.3.1). The Cocos Plate subducts beneath the Caribbean plate at a relatively shallow angle, dragging down crustal material as well as various kinds of sediments and fluids deposited there. The subduction, transformation, mobilization and recycling of this material results in large well-known prominent features like the back arc volcanoes that make up most of Costa Rica and Nicaragua, but also in many small and medium-sized seafloor features, like slides, mounds and margin escarpments which can be observed along the slope of the overriding plate. During SO 173 the latter features were of special interest for the investigations, as sources of subducted and recycled material .

At the Costa Rica margin the Cocos Plate can be divided into three different areas based on morphology: 1) Northwest of Fisher Seamount, the smooth Pacific basin seafloor, created at the East Pacific Rise facing the Nicoya Peninsula, is similar to the less rugged continental slope morphology; 2) Opposite, the ocean floor created at the Galapagos Rift System is covered with seamounts, the continental margin has some large embayments, the continental slope is indented and has a more rugged morphology; 3) The Cocos Ridge, formed as a hotspot trace by the Galapagos Hotspot, subducts beneath a narrow continental slope that rises steeply up to a shelf of the uplifted Osa Peninsula. The general areas visited on cruise SO 173/1, 3 and 4 are pictured in Figure 2.3.2, the location of stations is shown in detail on the following maps 2.3.3 to 2.3.22.

The area of normal faulting on the subducted plate off Nicaragua shows a system of half-grabens bordered by faults parallel to the trench, progressing downwards into the trench as the Cocos Plate subducts. These faults are likely to act as fluid venting systems, transporting material from the deeper crust to the surface. The small basins between these half-grabens are filled with pelagic and hemi-pelagic dark olive green clayey muds, which frequently contain ash layers, blown offshore from the Central American volcanoes. These ashes were among the most important targets of this cruise (see chapter 6.6).

On the continental plate the slope along the Middle America Trench (MAT) contains many relatively tiny seafloor features related to dewatering at the margin. Among them are several submarine slumps and slides, occurring in water depths between 450 and 3500m. Some slides are only a few hundered meters wide, some span up to several kilometers along the margin slope. Other dewatering features include mounds of various heights from a few meters up to several hundered meters. Cracks and faults within the sediment body of the overriding plate may as well show characteristics of dewatering like biological and chemical indicators for deep fluid outflow. In order to ascertain differences in dewatering signals and activity related to tectonic style of the subducting Cocos Plate, the features situated off the northern part with smooth topography of the downgoing plate were compared to those off the southern part with rough topography.

The following maps show details of the seafloor features investigated during SO 173/1, 3 and 4, starting in the north, continuing southwards. Most of the features have previously been targets during cruises SONNE 163 and METEOR 54, while others were surveyed for the first time. During leg 1 of this cruise they underwent a geophysical survey, followed by thorough investigation using video techniques during legs 3 and 4. Among these features are a series of mounds in the northern part of the working area (fig. 2.3.2 - 2.3.6), with the biggest, Mound Baula, being approx 130m high and the smallest, Mound Iguana, elevating only approximately 10-15m. More detailed descriptions of all mounds can be found in chapter 6.5. (Seafloor Observations).

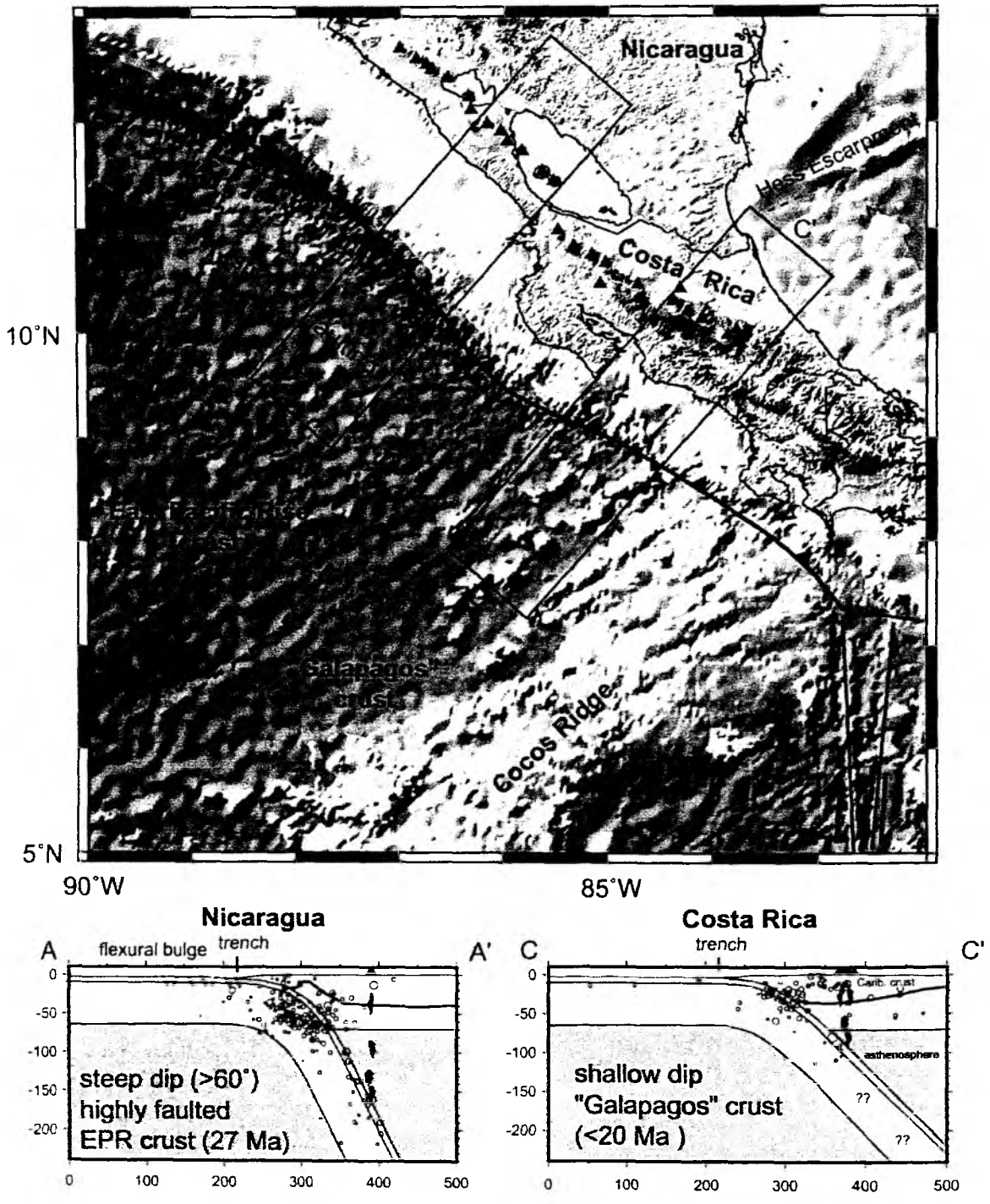

Fig. 2.3.1.: Geodynamic setting of the Nicaragua-Costa Rica convergent margin.

The other main prominent features present on the continental margin are scarps, carved into the slope by subducted seamounds. These features have previously been found to contain among the most active venting sites in this area. One of them, Jaco Scarp (Fig. 2.3.12), has been revisited during this cruise to add information about water currents to the existing dataset.

Many canyons and gullies are prominent in the bathymetry, they cut through the margin, transporting sediments from the shelf into the trench. They had not been explored for vent sites before, but have been giving attention recently, as they showed some backscatter anomalies. Fig 2.3.20 shows one example, station 25-GC was taken in another canyon location.

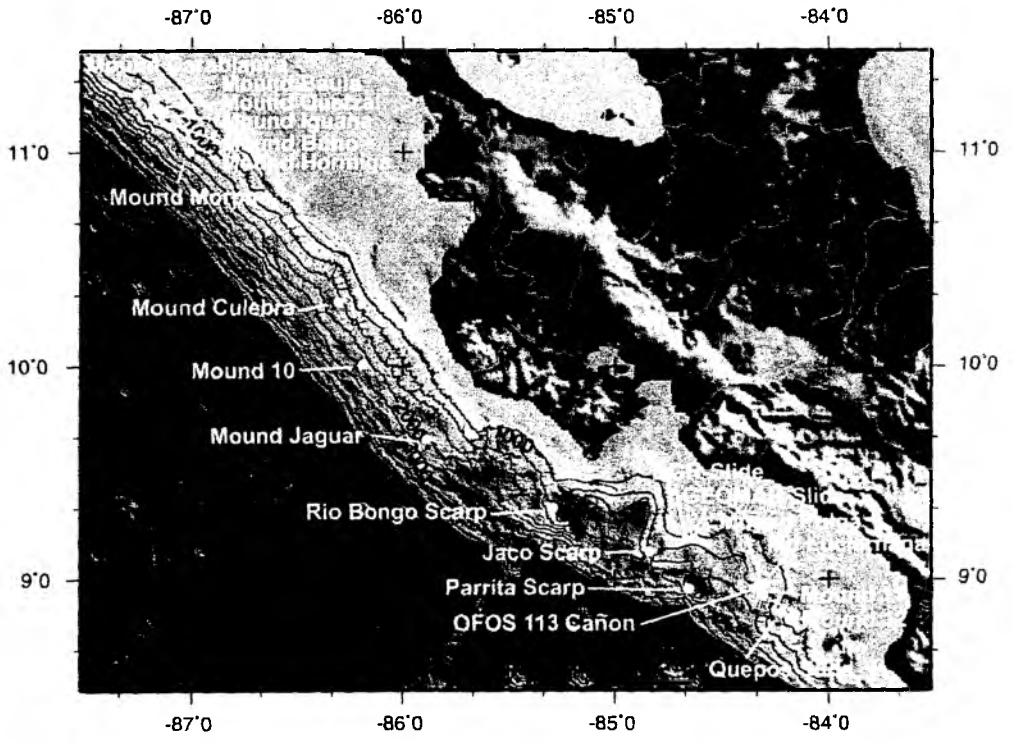

Fig. 2.3.2: *Special seafloor features such as mounds and scarps visited during SO 173/3 and 4; see maps on the following pages for details.*

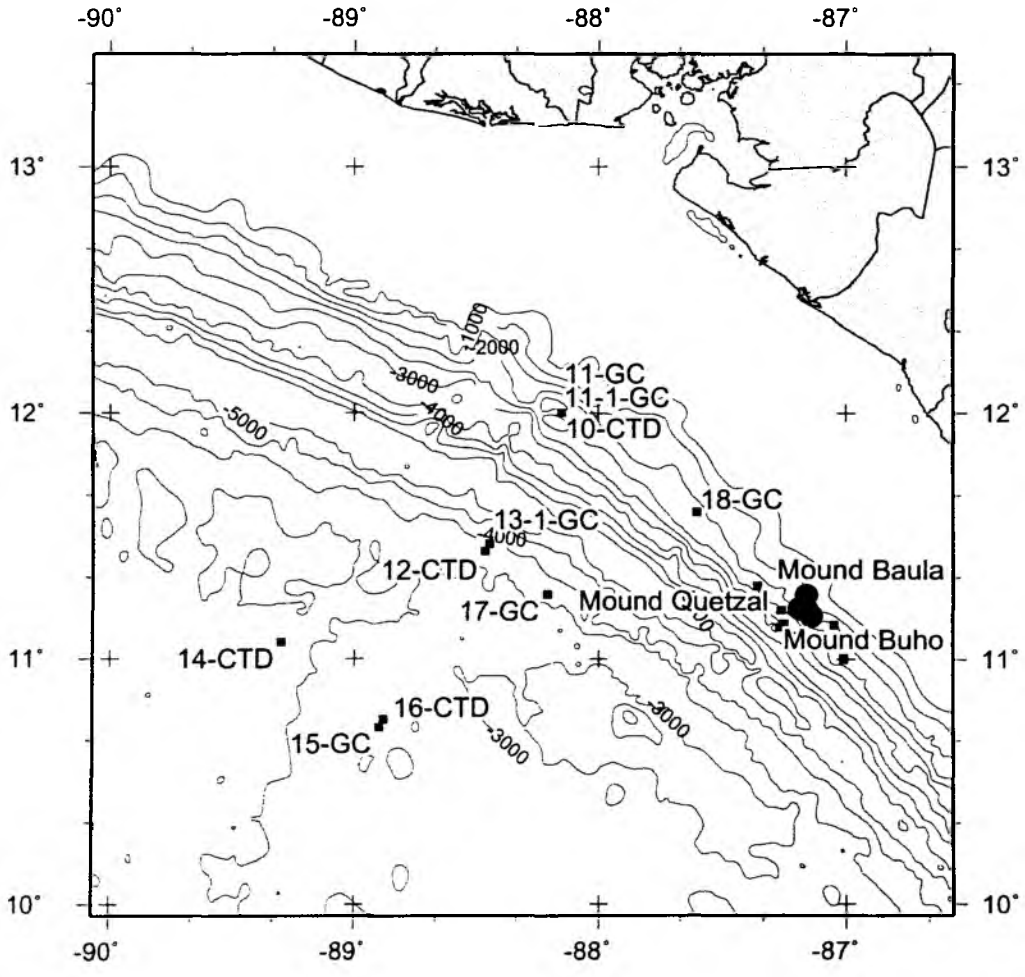

Fig. 2.3.3: Northern stations off Nicoya visited during cruise SO 173-3.

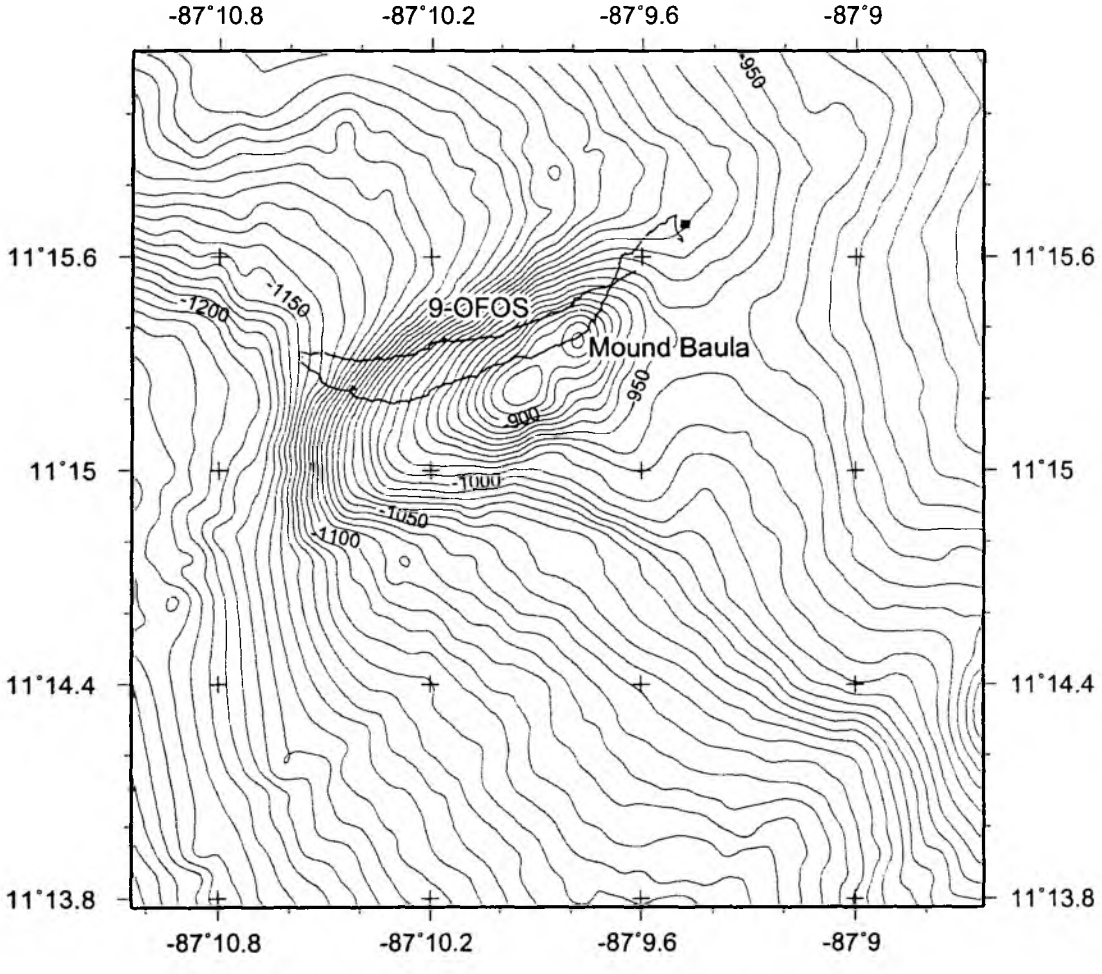

Fig. 2.3.4: OFOS station on Mound Baula visited during cruise SO 173-3.

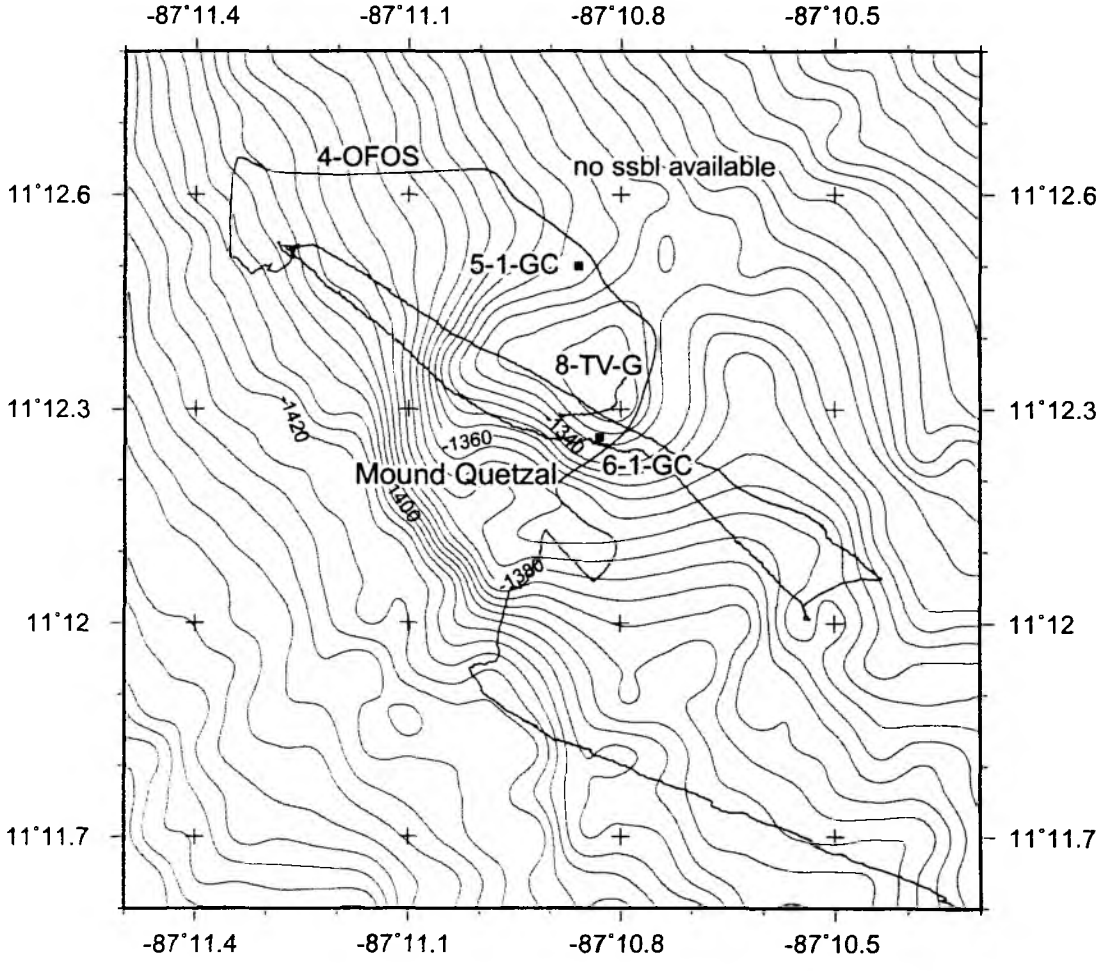

Fig. 2.3.5: Stations on Mound Quetzal visited during SO 173-3. Note that at portions of the track no ssbl was available, hence the shiptrack was plotted, which is slightly offset from the subbottom position.

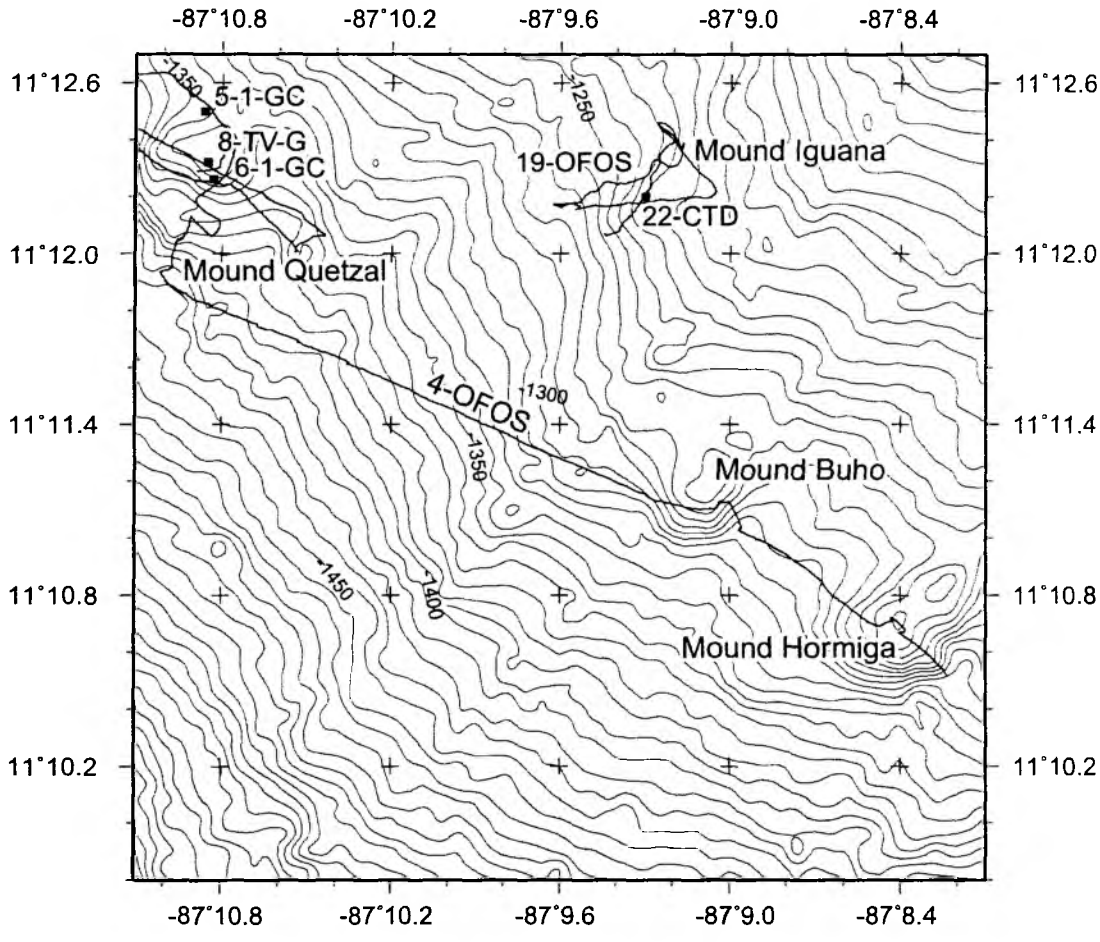

Fig. 2.3.6: *Stations near Mounds Quetzal, Iguana, Buho and Hormiga visited during SO 173-3.*

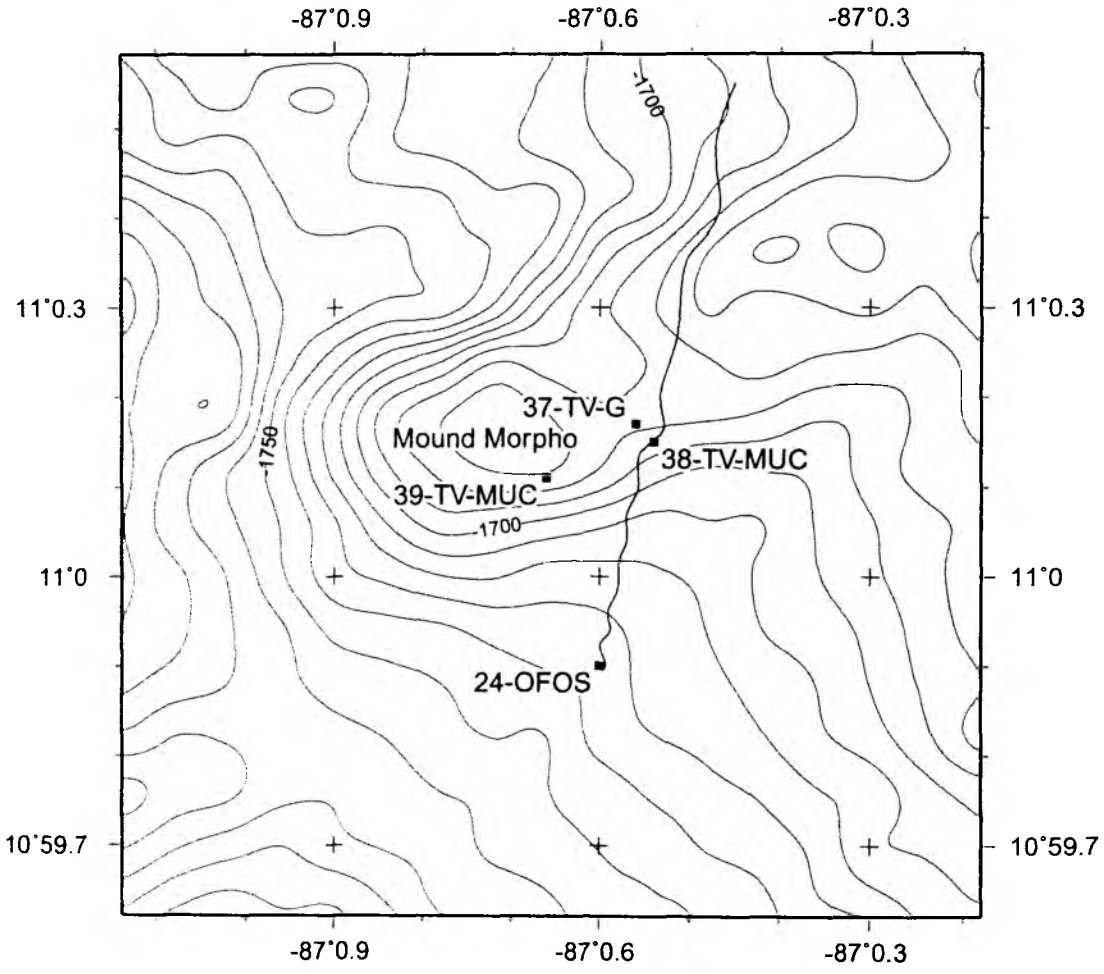

Fig. 2.3.7: Stations on Mound Morpho visited during SO 173-3.

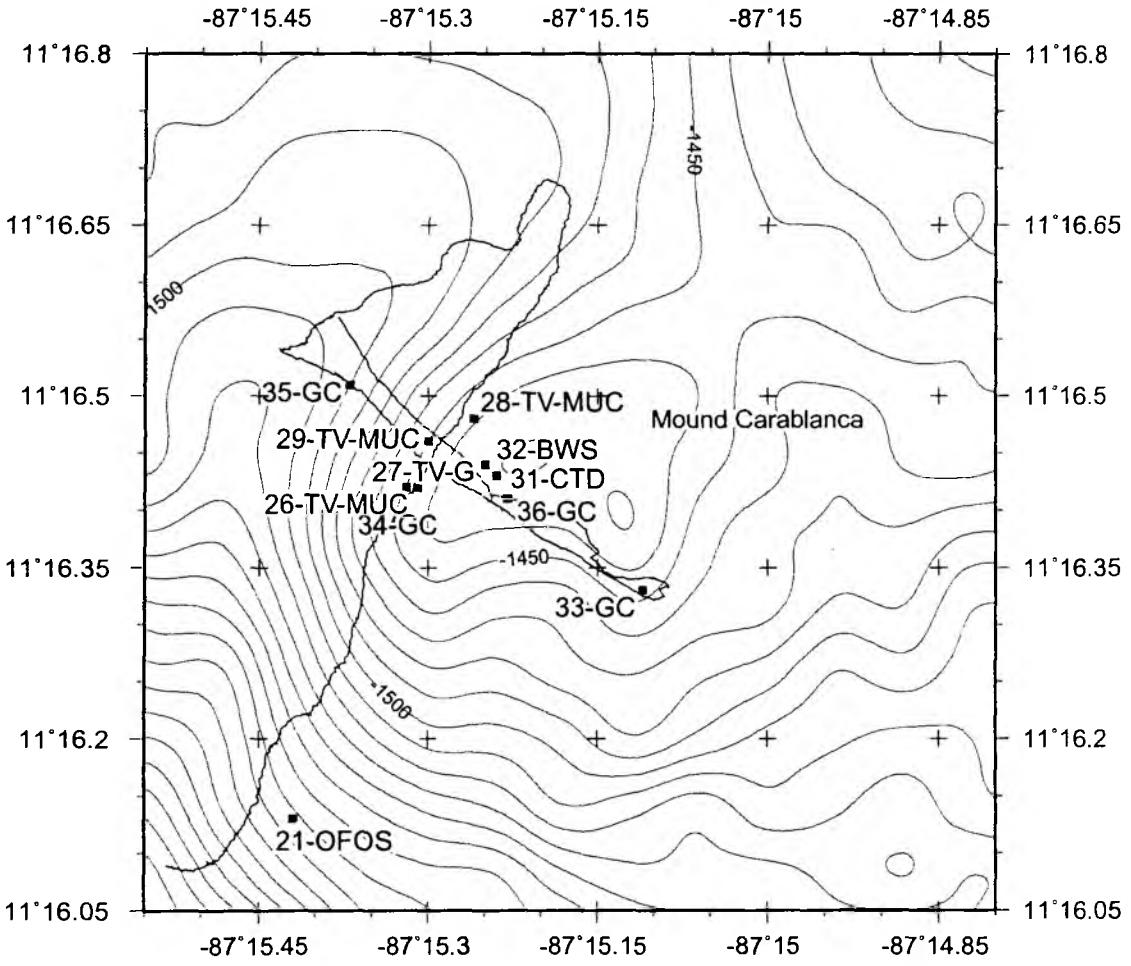

Fig. 2.3.8: Stations on Mound Carablanca visited during SO 173-3.

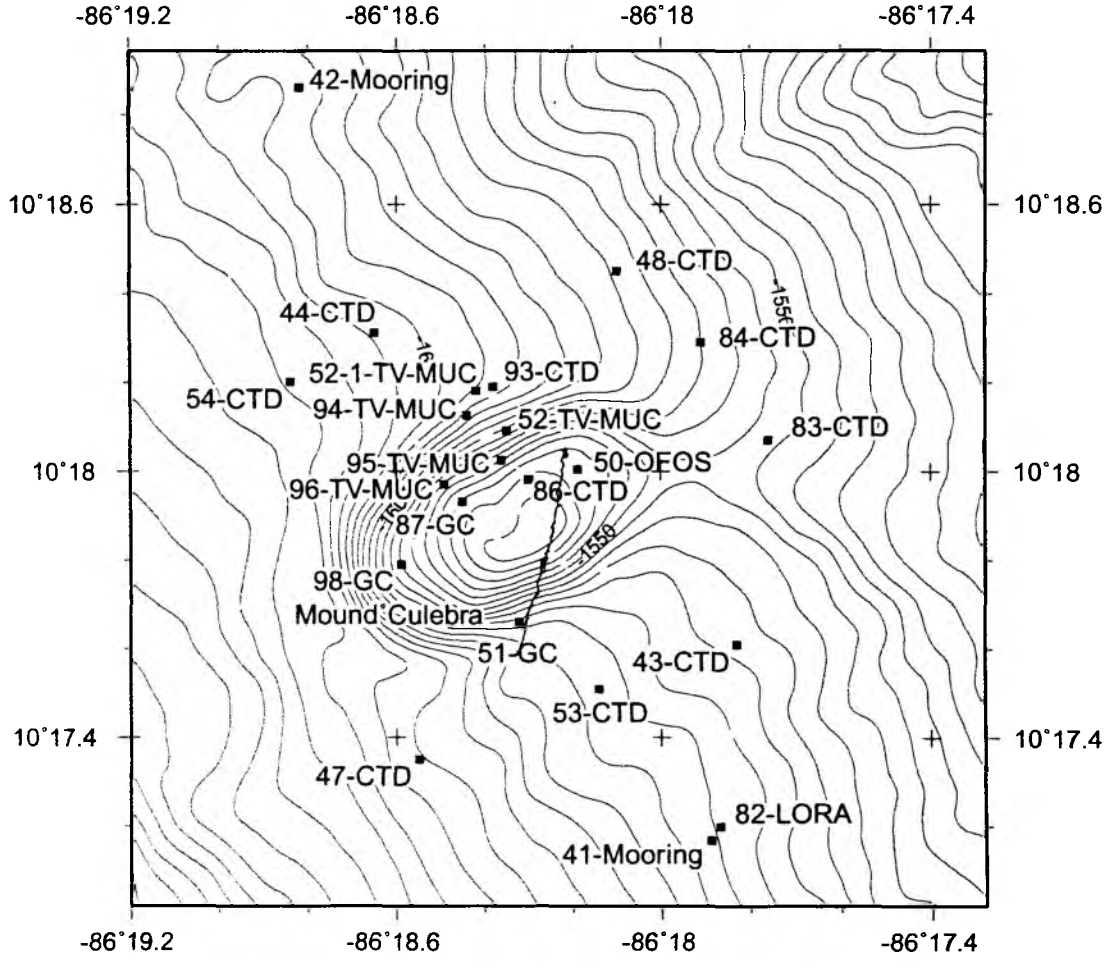

Fig. 2.3.9: Stations on Mound Culebra visited during SO 173-3 and 4. Gray squares mark stations from previous SFB cruises SONNE 163 and METEOR 54. See the respective reports for details.

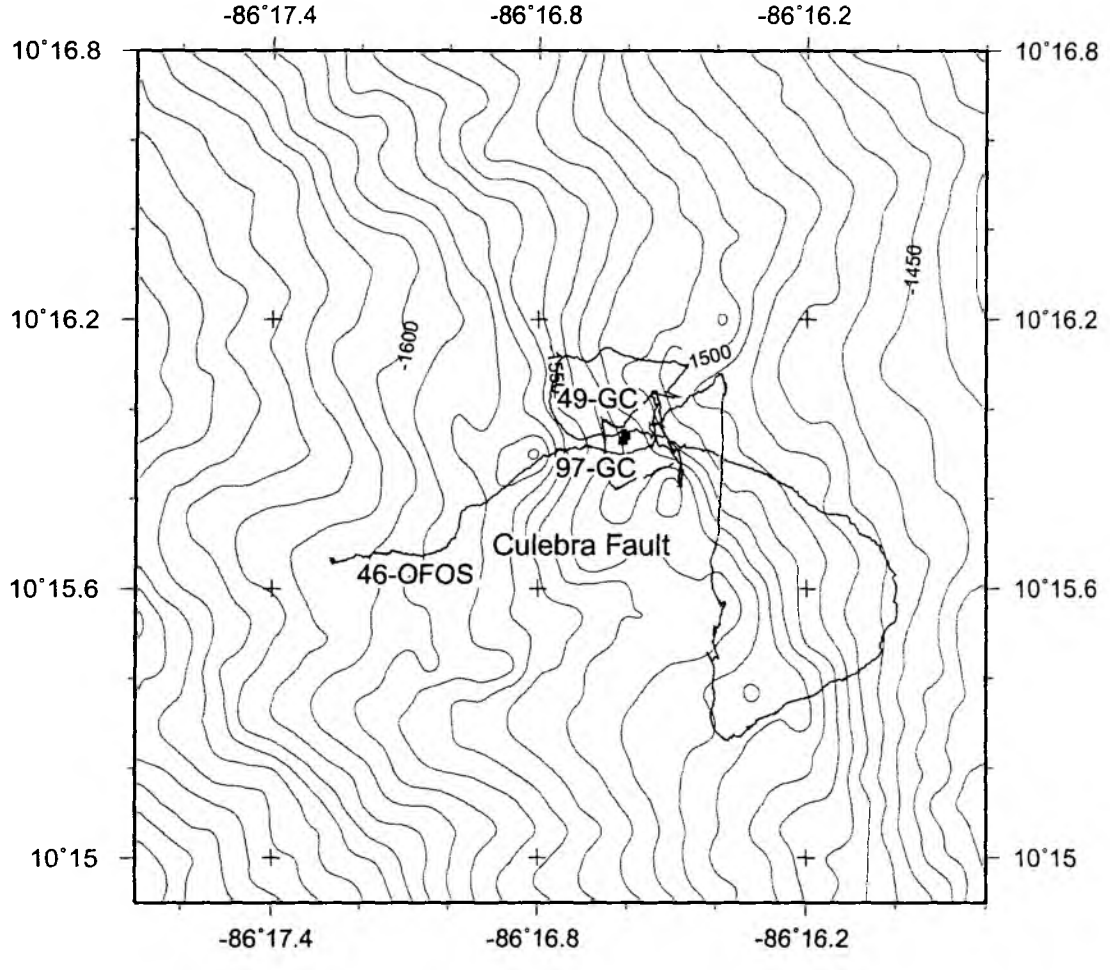

Fig. 2.3.10: *Stations near Mound Culebra Fault visited during SO 173-3 and 4.*

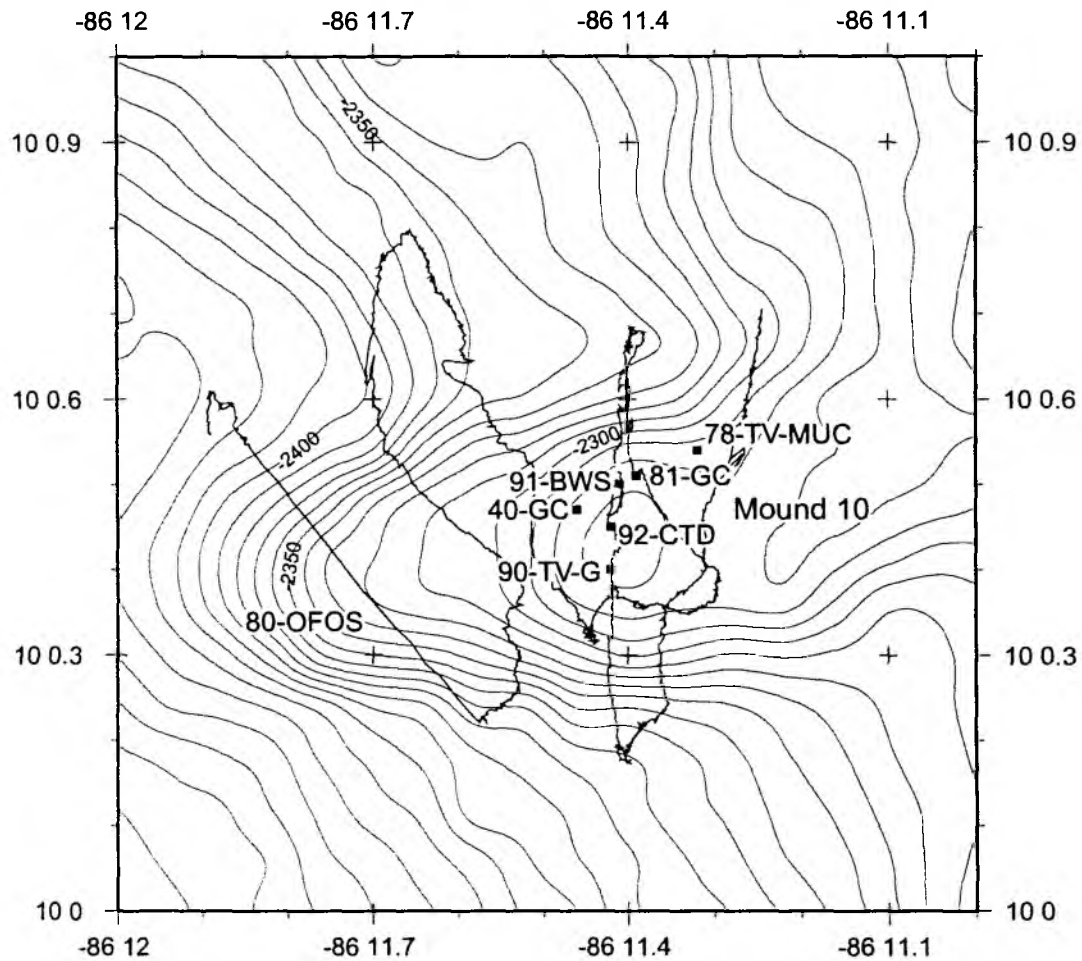

Fig. 2.3.11: Stations on Mound 10 visited during SO 173-3 and 4. Gray squares mark stations from previous SFB cruises SONNE 163 and METEOR 54. See the respective reports for details.

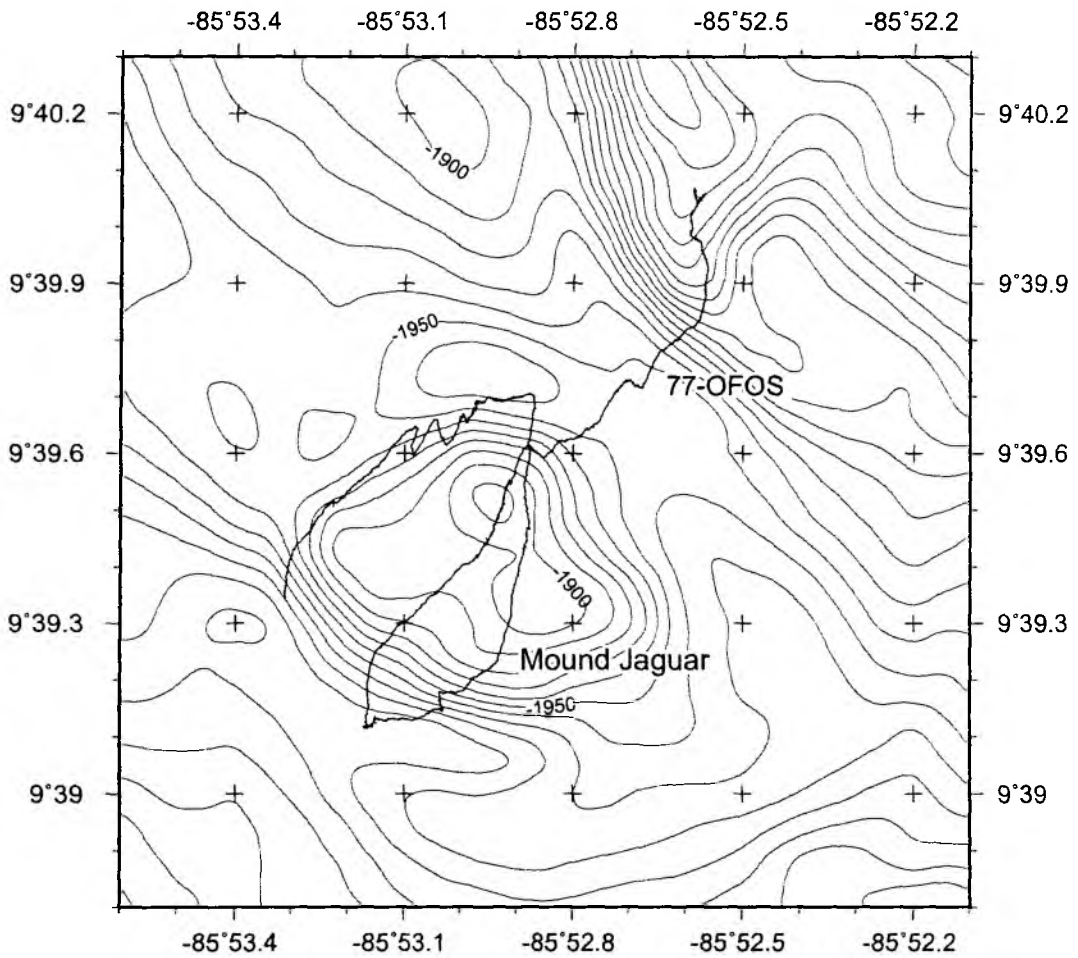

Fig. 2.3.12: *OFOS station on Mound Jaguar visited during SO 173-4.*

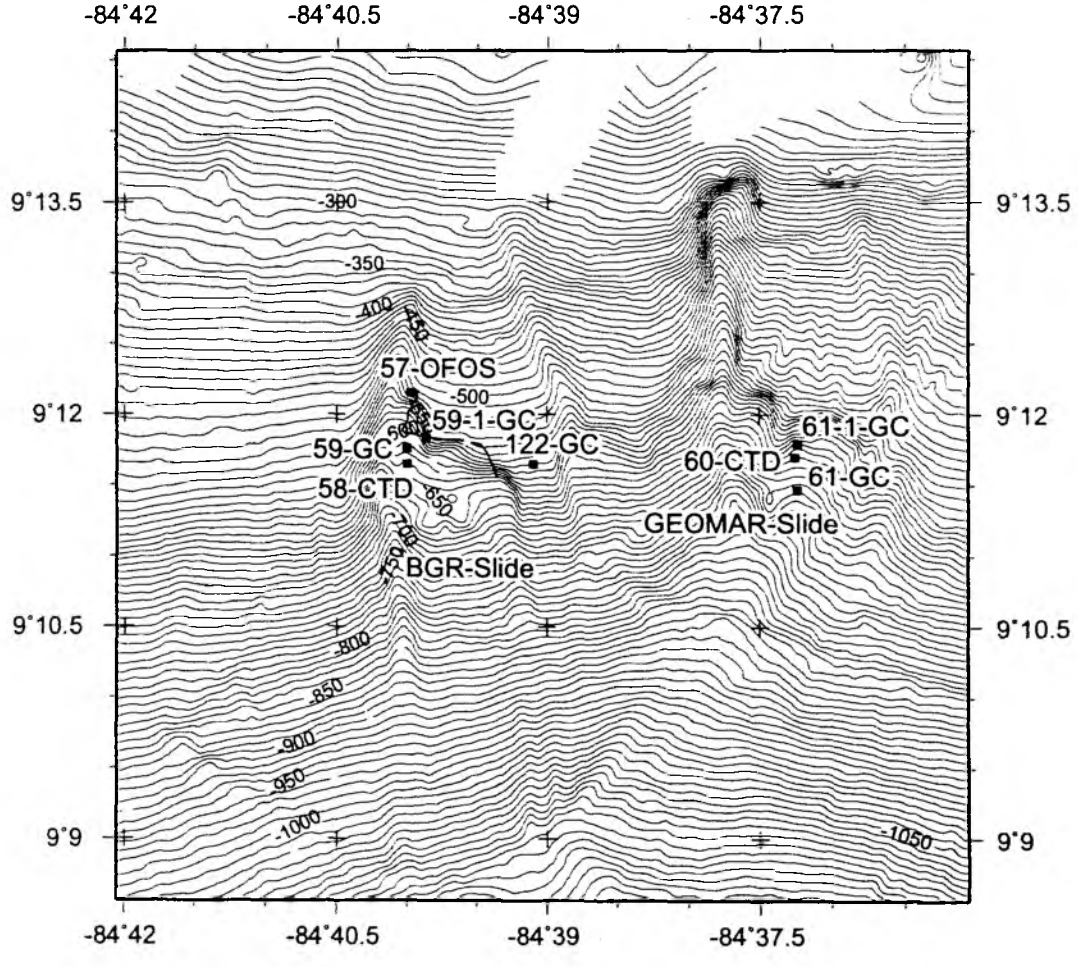

Fig. 2.3.13: *Stations near BGR and GEOMAR slides visited during SO 173-3 and 4. Gray squares mark stations from previous SFB cruises SONNE 163 and METEOR 54. See the respective reports for details.*

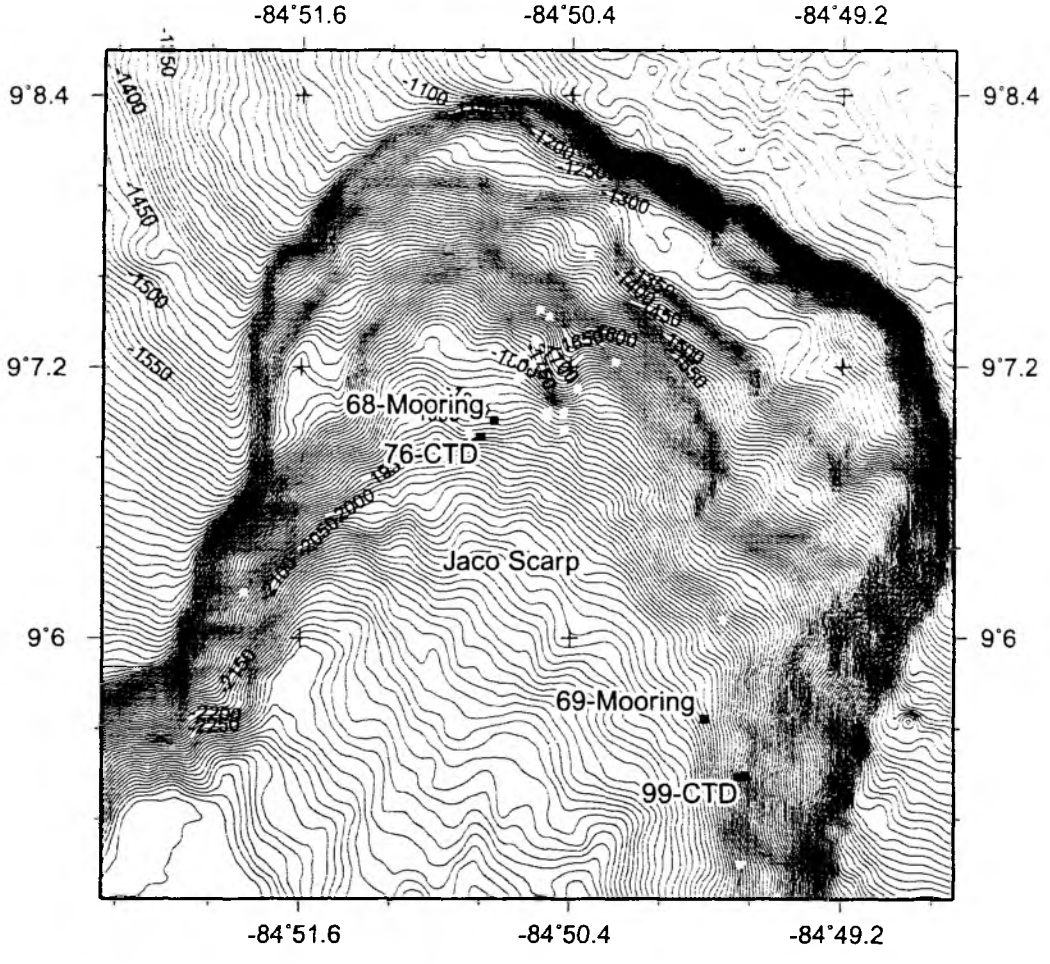

Fig. 2.3.14: *Stations at Jaco Scarp visited during SO 173-3 and 4. Gray squares mark stations from previous SFB cruises SONNE 163 and METEOR 54. See the respective reports for details.*

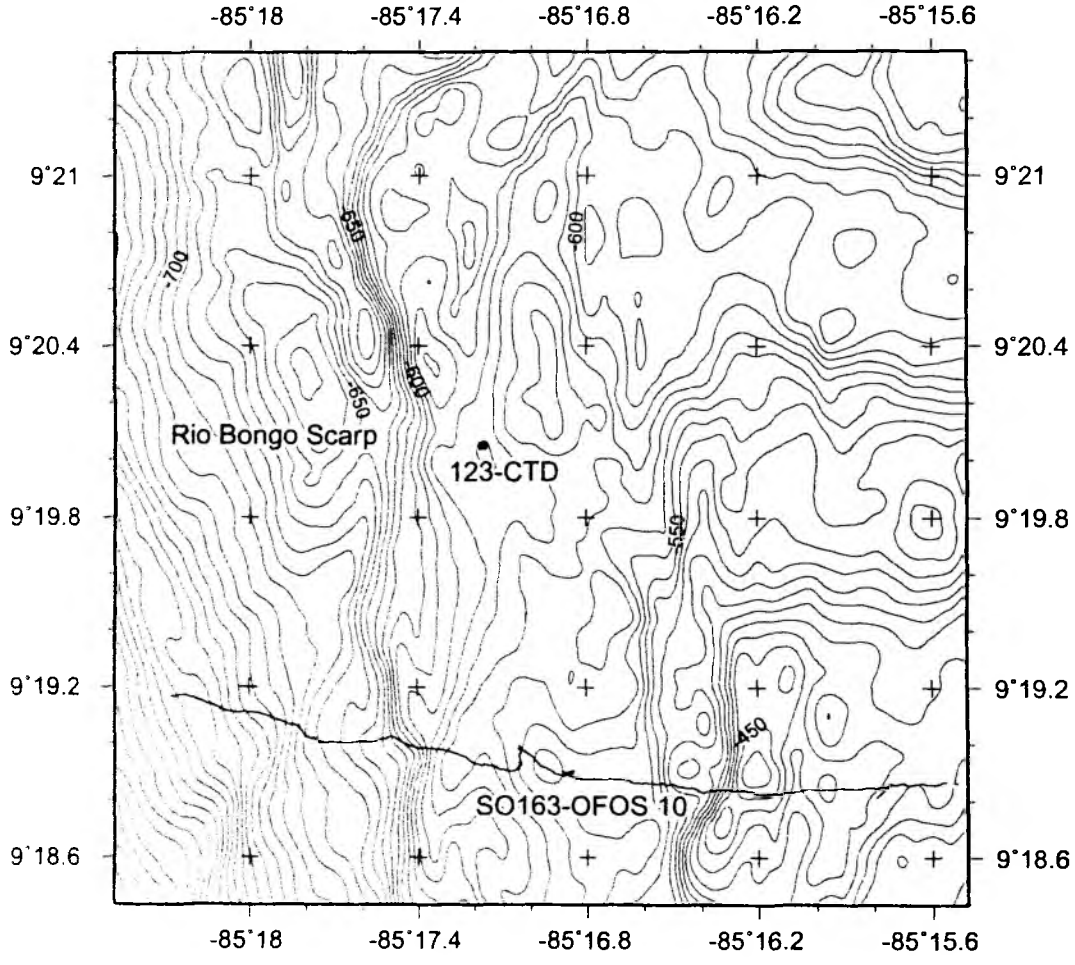

Fig. 2.3.15: Station at Rio Bongo Scarp visited during SO 173-4.

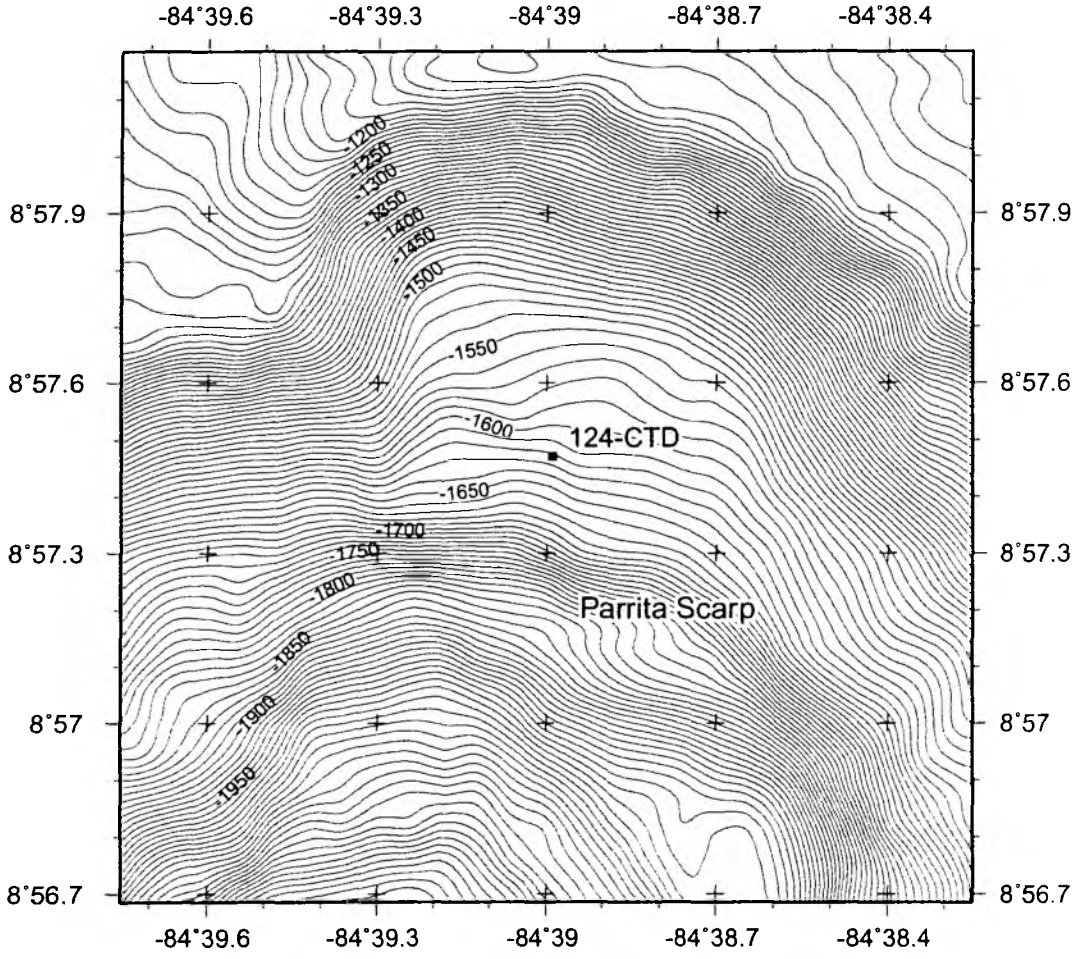

Fig. 2.3.16: *Station at Parrita Scarp visited during SO 173-4.*

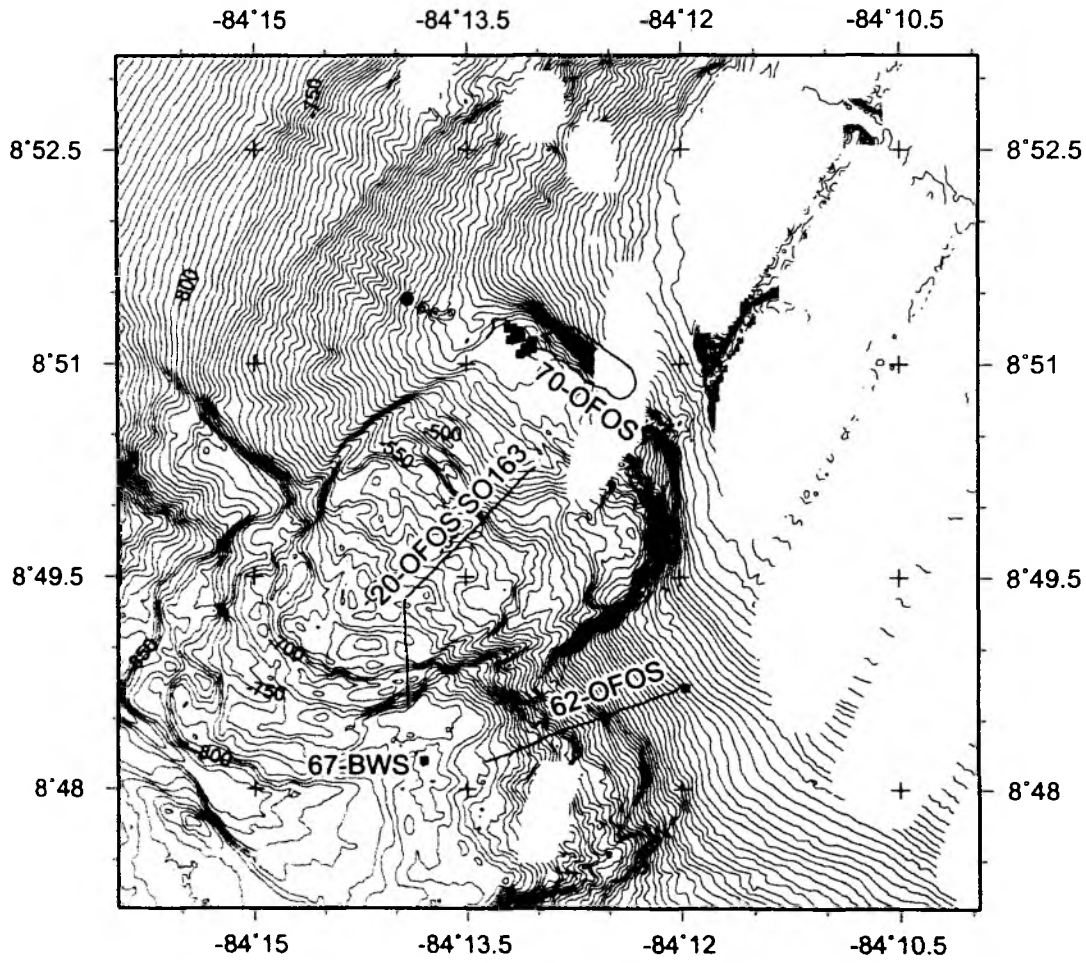

Fig. 2.3.17: Overview of stations at Quepos slide visited during SO 173-3 and 4.

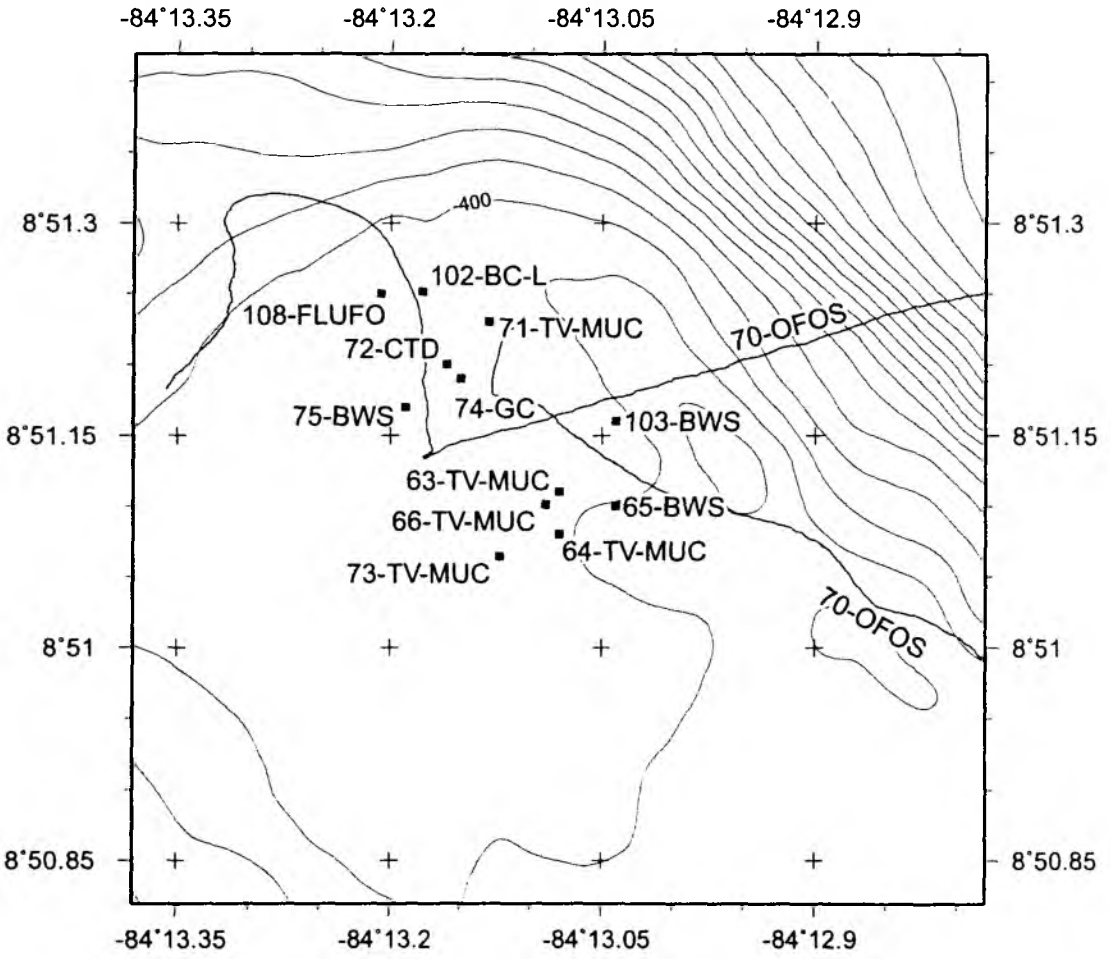

Fig. 2.3.18: *Stations at Quepos slides' northern hanging wall visited during SO 173-3 and 4. Gray squares mark stations from previous SFB cruises SONNE 163 and METEOR 54. See the respective reports for details.*

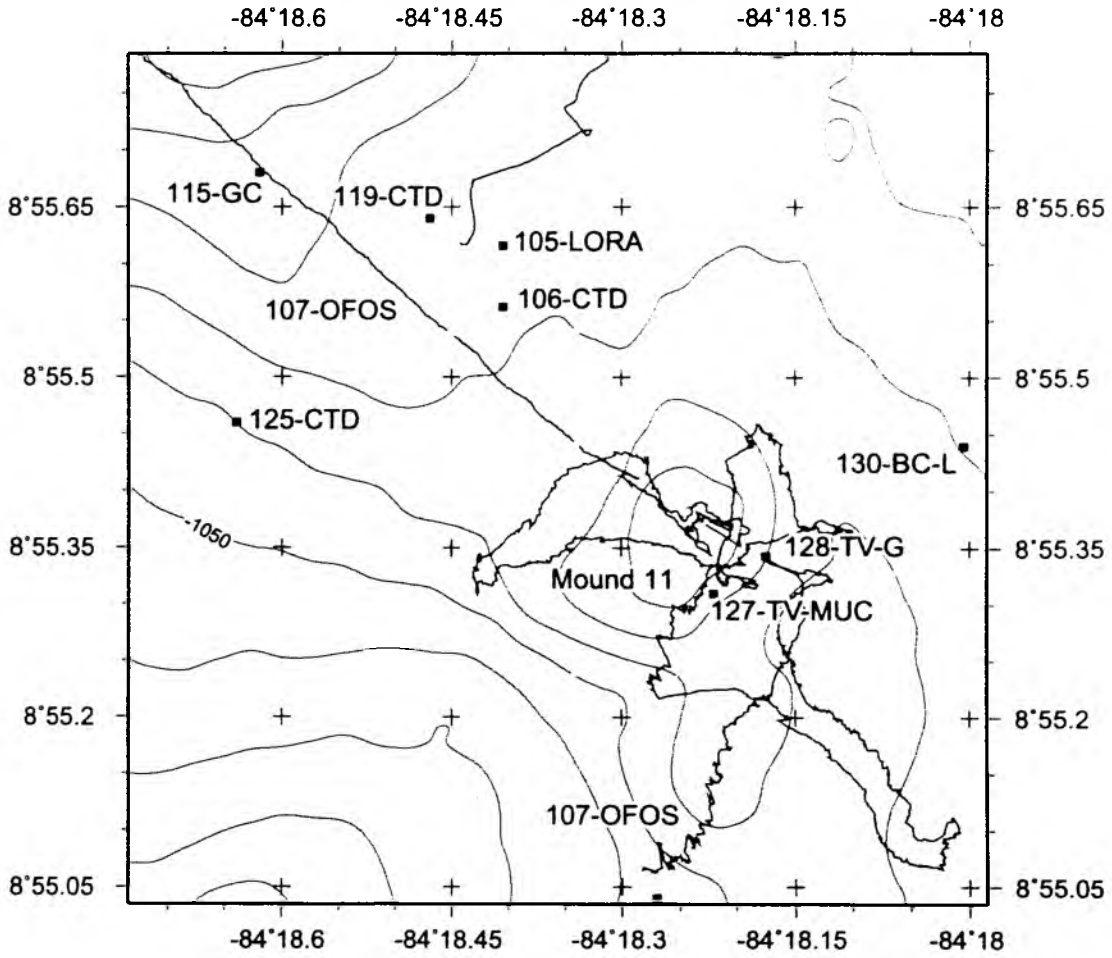

Fig. 2.3.19: Stations on Mound 11 visited during SO 173-4. Gray squares mark stations from previous SFB cruises SONNE 163 and METEOR 54. See the respective reports for details.

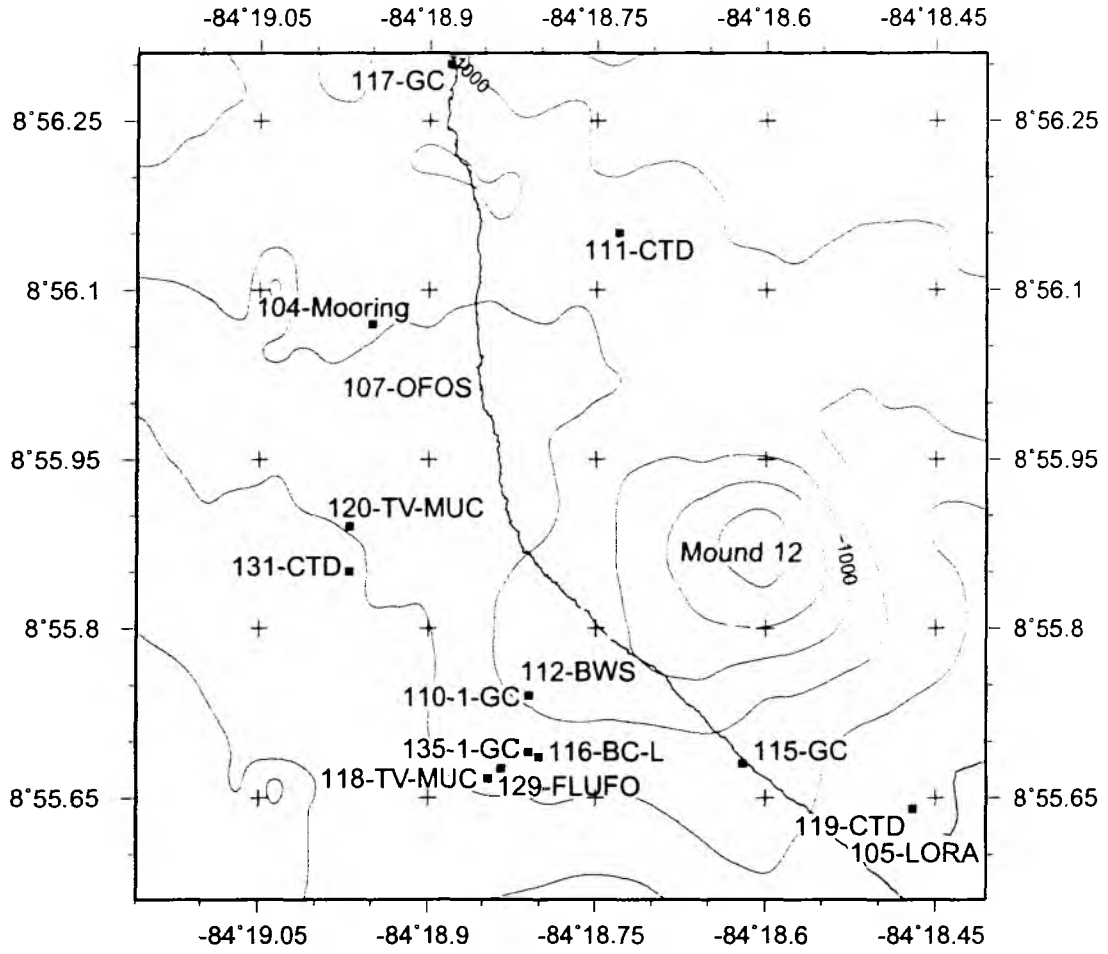

Fig. 2.3.20: *Stations on Mound 12 visited during SO 173-4. Gray squares mark stations from previous SFB cruises SONNE 163 and METEOR 54. See the respective reports for details.*

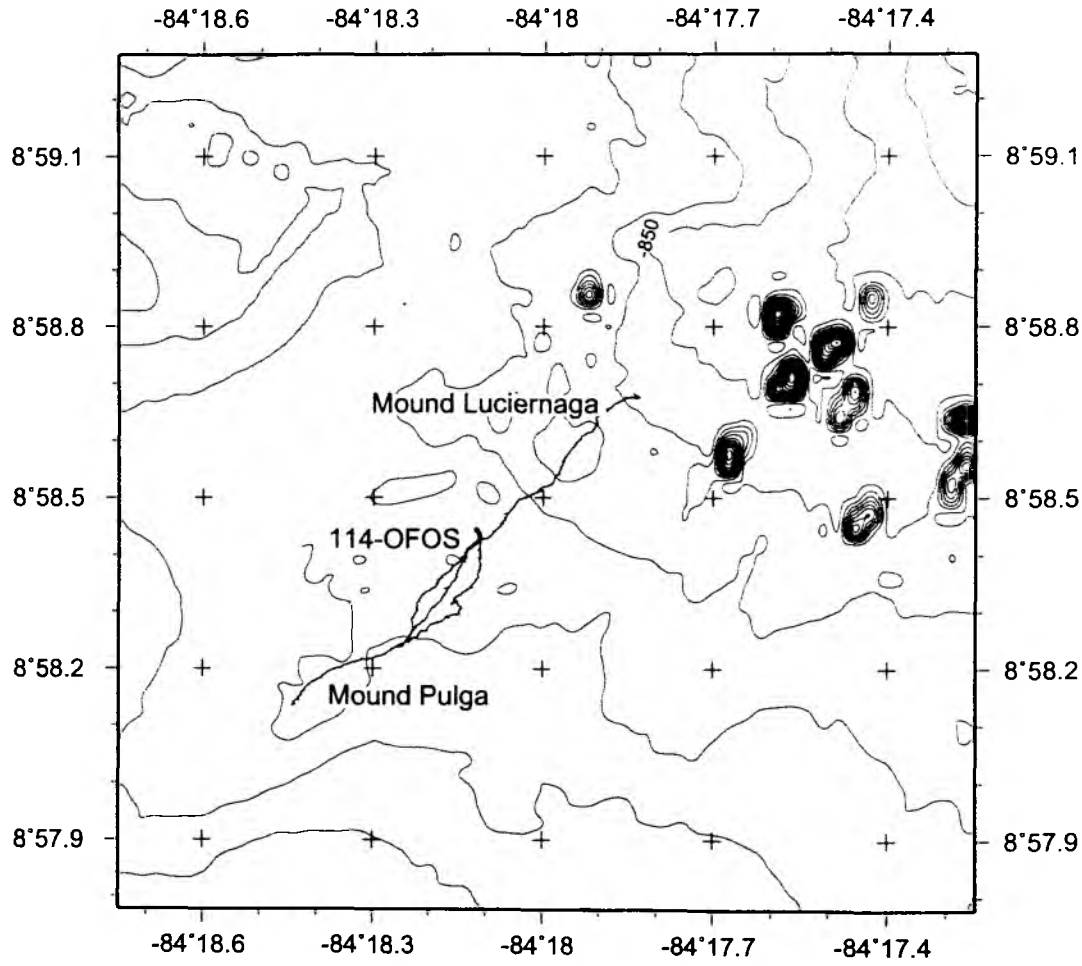

Fig. 2.3.21: OFOS track at Mound Luciernaga and Mound Pulga visited during SO 173-4. Small „mounds" in the eastern part of the map are artifacts.

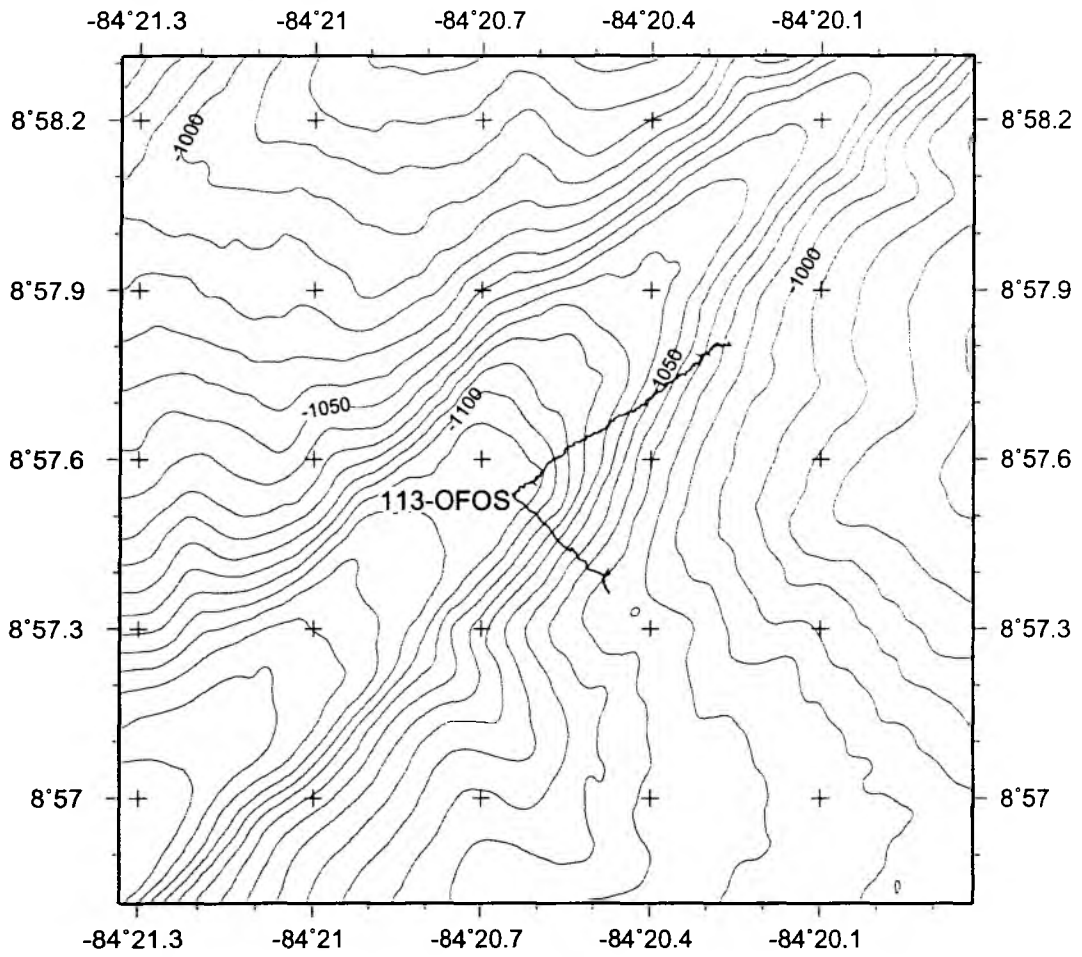

Fig. 2.3.22: OFOS track 0n canyon northwest of Mound 12 visited during SO 173-4.

3 Participants

3.1 Scientists

3.1.1 Scientists - SO 173-Leg 1

Prof. Dr. Ernst R. Flüh	GEOMAR, chief scientist
Juan José Alvarado	CIMAR-UCR
Ivonne Arroyo	SFB 574
Dr. Jörg Bialas	GEOMAR
Ileana Boschini	ICE
Dr. Monika Breitzke	GEOMAR
Dietmar Buerk	SFB574
Noemi Fekete	SFB574
Dr. Jürgen Gossler	SFB574
Dr. Dirk Kläschen	GEOMAR
Dr. Ingo Klaucke	GEOMAR
Lepolt Linkimer	LIS-RSN (UCR)
Dr. Mauricio Mora	ECG-UCR
Cord Papenberg	GEOMAR
Dr. Peter Sak	Bucknell University
Klaus-Peter Steffen	KUM
Natalia Zamora	ECG-UCR

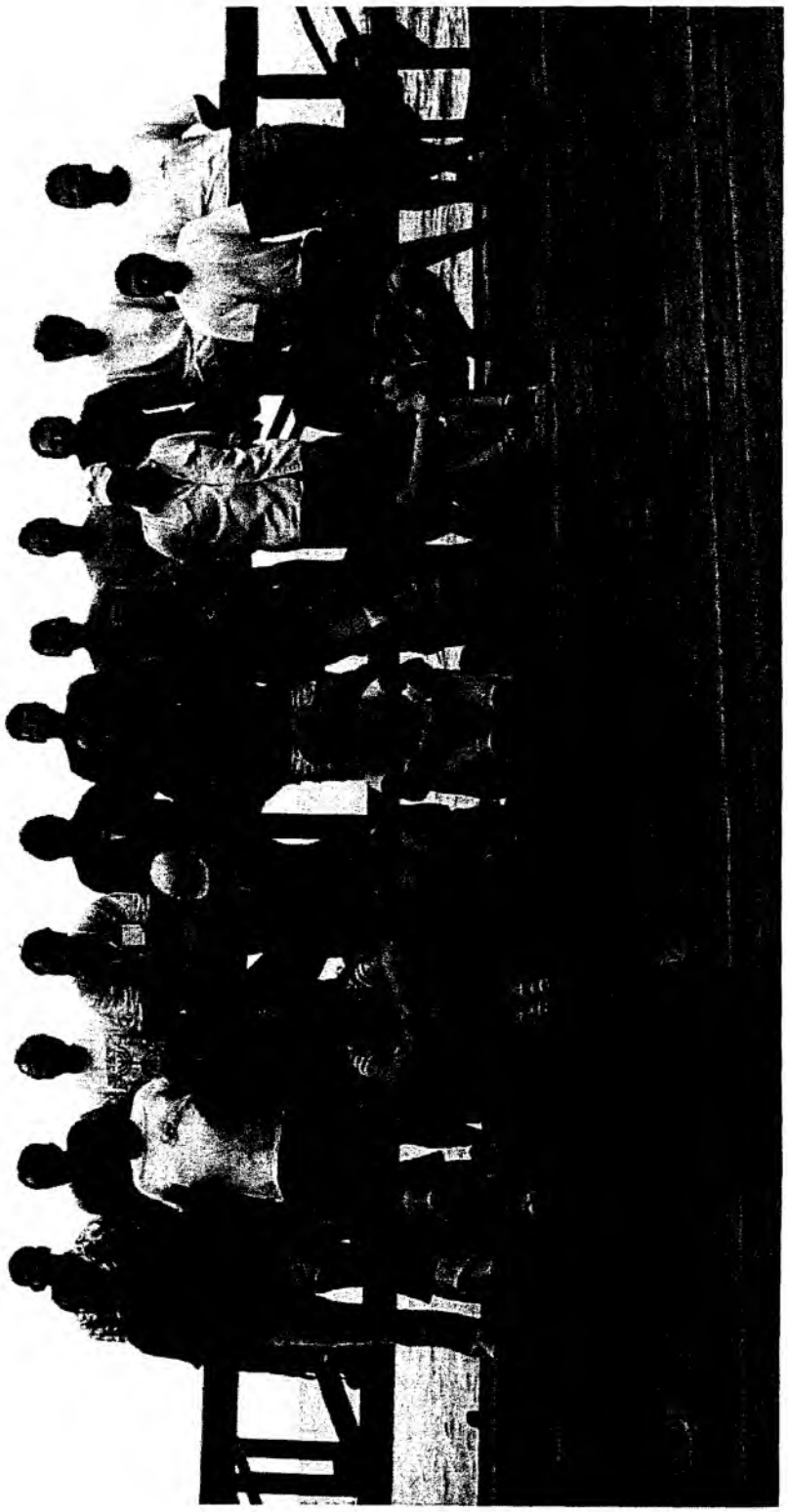

Fig. 3.1.2: Participants of Cruise SO 173/3.

3.1.3 Scientists SO173-Leg 4

Erwin Suess	SFB574, chief scientist
Ingrun Albrecht	SFB574
Emelina Corrales Cordero	ECG
Bettina Domeyer	SFB574
Silvia Echeverría Sáenz	ECG
Christian Hensen	SFB574
Volker Liebetrau	SFB574
Peter Linke	GEOMAR
Bert Manzke	SFB574
Susan Mau	SFB574
Tobias Mörz	SFB574
Kristin Nass	SFB574
Martin Pieper	KUM
Thomas Posch	IFGK
Michael Poser	OKTOPUS
Wolfgang Queisser	GEOMAR
Heiko Sahling	RCOM
Ulrike Schacht	SFB574
Jan Scholten	IFGK
Thorsten Schott	OKTOPUS
Mark Schmidt	IFGK
Emanuel Söding	SFB574
Karen Stange	SFB574
Klaus Wallmann	GEOMAR
Ulrike Westernströer	IFGK

Fig. 3.1.3: Participants of Cruise SO 173/4.

3.2 Crew

3.2.1 Crew SO 173-Leg 1

Martin Kull	Master
Carsten Simon	Chief Mate
Ha-Jo Lübbermann	1st Mate
Matthias Linnenbecker	Radio Officer
Dr. Holger Dietz	Surgeon
Volker Hartig	Chief Engineer
Norman Lindhorst	2nd Engineer
Matthias Häckel	2nd Engineer
Rainer Papendieck	Electrician
Rudi Angermann	Chief Electronic Engineer
Olliver Rottkemper	Electronic Engineer
Jörg Leppin	System Operator
Hartwig Allmer	System Operator
Rainer Rosemeyer	Fitter
Gerd Behrmann	Motorman
Heinrich Riedler	Motorman
Uwe Szych	Motorman
Hermann Rademacher	Motorman
Klaus Hermann	Chief Cook
Arnold Ernst	2nd Cook
Andreas Wege	Chief Steward
Anette Nickel	2nd Steward
Jan Hoppe	2nd Steward
Peter Mucke	Boatswain
Eugenius Dracopoulos	A. B.
Ringo Gollnest	A. B.
Günther Stängl	A. B.
Jürgen Kraft	A. B.
Götz von Berg	A. B.
Andreas Schrapel	A. B.

3.2.2 Crew SO 173-Leg3

Hartmut Andresen	Master
Carsten Simon	1st Mate
Matthias Linnenbecker	2nd Mate
Ronald Stern	2nd Mate
Konrad Raabe	Surgeon
Volker Hartig	Chief Engineer
Ralf Michael Kroesche	2nd Engineer
Klaus Dieter Klinder	2nd Engineer
Uwe Rieper	Electrician

Rudi Angermann	Chief Electronic Engineer
Michael Dorer	Electronic Engineer
Jörg Leppin	System Operator
Peter Holler	System Operator
Rainer Rosemeyer	Fitter
Holger Zeitz	Motorman
Uwe Szych	Motorman
Klaus Otto Hermann	Chief Cook
Volkhard Falk	2nd Cook
Michael Both	Chief Steward
Bernd Gerischewski	2nd Steward
Rainer Götze	2nd Steward
Winfried Jahns	Boatswain
Detlef Etzdorf	A. B.
Hans Jürgen Vor	A. B.
Andreas Schrapel	A. B.
Werner Hoedl	A. B.
Jürgen Kraft	A. B.
Christian Milhahn	Trainee
Manfred Walderstein	Trainee

3.2.3 Crew SO 173-Leg 4

Hartmut Andresen	Master
Carsten Simon	1st Mate
Matthias Linnenbecker	2nd Mate
Ronald Stern	2nd Mate
Konrad Raabe	Surgeon
Volker Hartig	Chief Engineer
Ralf Michael Kroesche	2nd Engineer
Klaus Dieter Klinder	2nd Engineer
Uwe Rieper	Electrician
Hilmar Hoffmann	Chief Electronic Engineer
Michael Dorer	Electronic Engineer
Martin Tormann	System Operator
Peter Holler	System Operator
Rainer Rosemeyer	Fitter
Holger Zeitz	Motorman
Uwe Szych	Motorman
Frank Sebastian	Motorman
Klaus Otto Hermann	Chief Cook
Volkhard Falk	2nd Cook
Michael Both	Chief Steward
Bernd Gerischewski	2nd Steward
Rainer Götze	2nd Steward

Winfried Jahns	Boatswain
Detlef Etzdorf	A. B.
Hans Jürgen Vor	A. B.
Andreas Schrapel	A. B.
Werner Hoedl	A. B.
Jürgen Kraft	A. B.
Christian Milhahn	Trainee

3.3 Addresses of Participating Institutions

GEOMAR: GEOMAR Forschungszentrum für marine Geowissenschaften
der Christian-Albrechts-Universität zu Kiel
Wischhofstr. 1-3
24148 Kiel, Germany
Tel.: +49 - 431 - 600 - 2972
Fax: +49 - 431 - 600 - 2922
Internet: www.ifm-geomar.de

SFB 574: Sonderforschungsbereich 574
Christian-Albrechts-Universität zu Kiel
c/o GEOMAR Forschungszentrum
Wischhofstr. 1-3
24148 Kiel, Germany
Tel.: +506 - 220 - 6394
Fax: +506 - 220 - 8212
Internet: www.sfb574.geomar.de

Bucknell University: Geology Department
Lewisburg, PA 17837, USA
Tel.: +1 (570) - 577 - 3029
Fax: +1 (570) - 577 - 3031

CIMAR: Centro de Investigaciones en Ciencias del Mar y Limnologia
Universidad de Costa Rica
Apartado 2060-1000 San Pedro
Costa Rica
Tel.: +506 - 207 - 3201
Fax: +506 - 207 - 3028

ECG: Escuela Centroamericana de Geologia
Universidad de Costa Rica
Apartado 214 - 2060 San José
Costa Rica
Tel.: +506 - 253 - 8407
Fax: +506 - 253 - 2586

ICE: Instituto Costarricense de Electricidad
C.S. Exploración Subterránea, Sabana Norte
Apartado 10032 San José, Costa Rica
Tel.: +506 - 220 - 6394
Fax: +506 - 220 - 8212

IFGK: Institut für Geowissenschaften
Christian-Albrechts-Universität zu Kiel
Ludewig-Meyn-Str. 10
24118 Kiel Germany

KUM: K.U.M. Umwelt- und Meerestechnik Kiel GmbH
Wischhofstraße 1-3, Geb. D5
24148 Kiel, Germany
Tel.: +49 - 431 - 7209 - 220
Fax: +49 - 431 - 7209 - 244
e-mail: KUM.Umweltmeerestechnik *a* t-online.de

LIS: Laboratorio de Ingenieria Sismica
Instituto de Investigaciones en Ingenieria
Universidad de Costa Rica
Apartado 36 - 2060 San José, Costa Rica
Tel: +506 - 207 - 4696
Fax: +506 - 224 - 2619

OKTOPUS: Gesellschaft für angewandte Wissenschaft, innovative
Technologien und Service in der Meeresforschung mbH
Kieler Straße 51
24594 Hohenweststedt

RCOM: DFG Forschungszentrum Ozeanränder (RCOM)
der Universität Bremen
Klagenfurter Str.
28359 Bremen

RSN: Red Sismológica Nacional
ICE – UCR
Apartado 214 - 2060 San José
Costa Rica
Tel.: +506 - 253 - 8407
Fax: +506 - 253 - 2586

TUB: Technische Universität Berlin
Fachgebiet Grundbau und Bodenchemie
Gustav-Meyer-Allee 25
13355 Berlin
GERMANY

On July 19 profiling was terminated and all OBH/S were safely recovered. Nine of them were redeployed later that day on a profile across Mound 11 and Mound 12. Several profiles were acquired with DTS in this area, unfortunately, the deep tow streamer was not working. A seismic line with the GI-Gun was acquired. While attempts to repair the deep tow streamer continued, the area of the BGR slide was surveyed with several sidescan lines and several reflection profiles using the surface streamer. Two more sidescan profiles using both the 75 and the 410 khz sidescan frequencies were acquired on mounds 11 and 12 before the nine OBH/S were recovered and R/V SONNE set course for a 190 nm transit to the outer rise of Nicoya peninsula.

During this transit the magnetometer was deployed again.

On July 23, 18 OBH/S were deployed along a 50-nm-long profile, in part coincident with a MCS line collected on an earlier cruise by R/V MAURICE EWING. At 22:00 the three Bolt airguns were deployed and shot across the array at 3.0 kn with a 60 sec trigger interval. Shooting was finished at 19:00 on July 24. Subsequently three short profiles were shot with the GI-Gun, in order to determine the orientation of the seismometers. All instruments had been recovered at 17:00 on July 25. After a few instruments had been tested for functionality at depth of 4300m, four OBH (53 to 56) were deployed on the outer rise to monitor the local seismicity. These instruments are to be recovered at the end of leg 2.

In the morning of July 26 the POSIDONIA antenna was recalibrated, and DTS profiles were run in the area of Mound Culebra. After two days of continuous work the deep tow streamer failed and profiling had to be interrupted for repair. This repair time was used to recover one tiltmeter station (OBT52), that had been deployed close to the profiling area. After 5 hours the system was deployed again, and at 24:00 on July 28 R/V SONNE set course for Caldera, where equipment and people had to be transfered. At 12:30 R/V SONNE docked at the pier in Caldera, terminating leg SO 173/1a.

Leg SO173-1b began when R/V SONNE left the port of Caldera on July 30 at 08:00 heading North to Nicaraguan waters. After 14 hours of transit R/V SONNE arrived in the working area at the continental slope off Nicaragua at about 11°10' N where the next couple of days were dedicated to sidescan and deep tow streamer observations across mound structures and slumps known from previous bathymetry mapping. The deep tow system was deployed on July 31 at 03:30 local time. It operated continuously until 13:00 on August 05 when profiling need to be terminated to be back in the port of Caldera in due time. On August 06 at 08:00 R/V SONNE docked in the port of Caldera, where cruise SO 173/1 ended.

4.2 Cruise Narrative of Legs 3 and 4

4.2.1. Introduction

During R/V SONNE expedition SO 173 leg 3 and 4 geochemical, hydrographic and sedimentological investigations were conducted along the Central American subduction zone. The cruise objectives were fluid transport in the forearc and the distribution of volcanic ash on the adjacent oceanic plate. Because of logistical constraints sediment coring was the main focus during leg 3 while lander deployments were concentrated on leg 4; on both legs. CTD casts, bottom water sampling, TV-guided multi-coring, current mooring deployments, and sea floor observations using the system OFOS were carried out on both legs. The scientific party on board of the vessel consisted of members of the respective subprojects of SFB 574 ("Volatiles and fluids in subduction zones") who were complemented by experts and guests from other institutes.

4.2.2 Leg 3

3 - 10 September 2003

On September 03-04, the containers and equipment were unloaded and loaded during the port call at Caldera (Costa Rica) under rainy skies and in humid air of 30° C. Thunderstorms and heavy rain showers in the late afternoons brought a welcome cooling and a break in the port activities as did the visit of the impressive 3-mast full sailing ship "Gloria Columbia" of the Columbian navy which docked alongside R/V SONNE. At 17:00 on September 04 we departed Caldera in a north-easterly direction towards the margin off Nicaragua. Here our investigations were concentrated on an area known as "New Mounds" as well as on an oceanic plate transect running parallel to the El Salvador – Nicaragua offshore line.

On the way north we retrieved a long-term mooring at "Mound Culebra" that should have recorded the current distribution over 2 months but had not. We reached the New Mounds area in the morning of September 06 and started work. Here, a large number of fluid venting targets had been documented by sidescan sonar surveys during the previous expedition SO 173 Leg 1. A total of 126 possible sites for detailed investigation of fluid and gas venting had been mapped by several surveys. They mostly consisted of mounds, canyons, slides and slumps. We eventually selected several mound structures and patches of different backscatter patterns with and without morphological expressions. All mounds investigated showed manifestations of active fluid flow based on OFOS, TV-grab and TV-multicorer deployments as well as methane anomalies in the water column.

The mounds were dominated by authigenic carbonates of considerable thickness and extent either in the form of crusts, concretions or odd-shaped chemoherms, followed by colonies of vent clams and pogonophorans. Bacterial mats were conspicuously absent.

The mounds located at water depths between 900-1300m seem to be more completely covered with impenetrable carbonate caps and contained fewer vent organisms than those situated on the lower slope, e.g. between 1400-1700m. The former appeared larger and more mature than the latter.

A list of results included preserved fluid structures in semi-cemented sediments and interlayered carbonate-sediment strata retrieved by TV-grabs (iron-sulfide-coated channels, "fritted carbonates", carbonate-lined burrows, enrichment of coarse particles, formation of pseudomorphose etc.). Gravity cores and TV-guided multicores contained overconsolidated mudclasts, which indicate extrusions of material from considerable depth. These samples are important in settling the question of whether muds erupt or extrude and if continuous or periodic material transport causes the build up of these mounds. The pore water investigations provided indications of diagenetic processes which proceed more intensely in

sediments affected by ascending fluids than in those surrounding vent sites.

The small-scale investigations in the New Mounds area alternated with large-scale sampling of volcanic ash distribution patterns. An array of gravity cores was set up which extended up to 100 nautical miles from the margin onto the oceanic plate.

As the research clearance for the EEZ of El Salvador had expired just days before, we were not able to extend the transect NW-ward as originally planned. Nevertheless the distribution pattern of ash layers was sampled over an area of more than 1000 km^2 which is reached by the volcanic chain of Central America. 59 ash layers in 6 cores were identified on the basis of density and magnetic susceptibility changes in the core logs. They served as samples for detailed shore-based analyses, and a preliminary correlation was established between the layers. Sampling of ash layers was complemented by the investigation of pore waters of the adjacent strata which provided information on alteration reactions of ashes with sediment and seawater. Some prominent eruptions known from land-based studies of Nicaragua, El Salvador and Guatemala were documented in the sediments. A comparison with previously sampled material gave reason to assume that the ashes covered the last 150.000 years. Along the coring profiles a hydrographic transect of the uppermost 1000 m recorded the distribution of methane and other parameters in the oxygen-minimum-zone. This provided criteria for the differentiation of methane from venting and methane generated "in-situ" in the water column.

11 – 17 September 03

At the beginning of the week starting on September 11, work in the area of "New Mounds" focused on two active structures: "Mound Carablanca" and "Mound Morpho". The previous designation of the mounds had been by geographic and other cruise-related terms which caused some confusion. Therefore we named all structures in the "New Mounds" area which were actually investigated after indigenous species of Central America. For example, the sidescan sonar backscatter pattern of Mound Carablanca (=white faced monkey) has a faint resemblance to the face of a monkey with eyes, nose (bright spots) and a surrounding mane (changing bright and dark circular bands). The backscatter pattern of Mound Morpho (=butterfly) suggests the high-contrast patchy pattern of a butterfly wing.

Several gravitycores, TV-guided multicores, bottom water samples, CTD- and TV-grab deployments were conducted at the outer margin of Mound Carablanca, which is characterized by circular structures, as well as at the center of the mound. All deployments were successful. Studies of sediment fabric revealed clay clasts, slick-in-sides, and other elements suggesting mud extrusions. At Mound Morpho TV-multicorer deployments on clam fields showed specimens of remarkable size; TV-grab-deployment brought on deck carbonate blocks with chemoherm structures and authigenic carbonate precipitates without embedded sediment.

September 12-14 work concentrated on Mounds # 10 and Culebra, located farther SE. These structures had been investigated on an earlier cruise (M 54). New work was done along a NW-SE striking fault which cuts through the center of Mound Culebra. After having arrived in the area we deployed 2 moorings to collect current data to better understand the dispersal and transport of methane released into the water column. This objective was supplemented by several CTD casts taken during the current meter deployment.

Cores were taken at the southern flank of Mound # 10 where previous evidence had suggested an inflow of fresh seawater. whereas at the southern flank of Mound Culebra large amounts of clay clasts and

altered crystalline clasts were extracted from sediments sampled by a gravity corer. Further we obtained evidence for substantial freshening of pore waters from a core at the NW-SE-fault. This suggests an ascent of deep fluids at a segment of the fault at a point where it is slightly offset. Data from this 9-m gravity core showed a continuous decrease in chloride to as low as 290 mMol. Also other dissolved components, namely calcium, point to deep-sourced fluids which ascend relatively slowly but apparently over a considerable area. The fluid chemistry will approximate the pure end-member composition.

For the last part of the week (September 15-16) R/V SONNE steamed to an area where several slides have originated from the upper continental slope at shallow depth (300-600 m). Based on previous work the following areas were investigated: BGR slide, GEOMAR slide, and Quepos slide. During the transit to the area at night a multibeam survey was completed as well as several hydrocasts. We aim at reaching a common understanding of what triggers these slides which have so far been treated as isolated occurrences. At the BGR and GEOMAR slides we cored into the slide plane immediately below the head wall where only thin hemipelagic sediments had accumulated since the slide event. The sediments showed considerable over-consolidation as well as high shear strength; density estimates by logging confirmed this interpretation. We also cored into an undisturbed slide block at the base of the head wall. Laminations, cross-bedding and slightly rotated clasts support this preliminary interpretation. The chaotic slide mass farther downslope was not investigated although the high methane content in the bottom water clearly suggests that the slide mass itself or the undisturbed sediment beneath may be the source of degassing.

At the Quepos slide TV-guided multicorer deployments and bottom water sampling showed a considerable fluid venting activity which had not been known previously. Extented bacterial mats were known from the base of the slide and the samples retrieved suggest a seep of ground water instead of deepsourced fluids. Such a phenomenon had previously been assumed because of "light" oxygen and relatively "heavy" carbon (non-biogenic) isotope values obtained from a carbonate crust. Now pore water analyses further support typical freshwater criteria for the venting fluid: low Cl- and Ca-values.

After completing work in the morning of 16 September we took course towards Caldera. On our way we deployed two current meter moorings at the axis of Jaco Scarp. At 16:00 R/V SONNE docked at the pier and between 18:00 and 20:00 an exchange of scientists and crew members took place. The following day several more crew members were exchanged and we departed Caldera at 20:00 on September 17.

4.2.3. Leg 4

18 – 29 September 2003

After exchanging several crew members, scientists and guests, welcoming the lander-team on board, and loading air freight, R/V SONNE departed Caldera in the evening of September 17 and took course to the nearby working area Quepos slide. Observations with TV-guided systems, measurements of methane in the near-bottom water column, and pore water analyses showed that at the foot of the slump massive fluid emissions are responsible for the wide-spread colonization by bacteria and the freshening of pore waters. As the start-up of the lander systems for a determination of fluid flow rates would still have required extra time, we relocated to the area of the mounds north of Caldera.

On the way, methane measurements at selected stations which had been visited previously (SO 144 cruise in 1999, SO 163 cruise in April 2003 and M 54 cruise in July and September 2002) showed that surprisingly all known anomalies were now significantly reduced. This strongly suggests that not only currents and circulation influence the methane distribution but that the source strength of the fluid

emissions seems to be subject to large-scale inter-annual fluctuations. During the course of the expedition this observation was confirmed, with Mounds #11 and #12 showing additional anomalous behavior. Here the maximum concentration of methane in the water column was also reduced compared to previous measurements but within a large area surrounding Mound #12 the near-bottom methane emissions were greatly increased, which had not been observed before.

Work at mounds Culebra and #10 turned out to be difficult, as during a TV-multicorer deployment at 2300 m the underwater power supply system was completely destroyed by implosion of the pressure housing. To ensure subsequent deployment of this important instrument, parts of the lander system were installed which, however, required a constant interchange of parts between the instruments and hence cost precious time. Furthermore, substandard material used to attach the weights at the benthic chamber lander (BC-L) caused premature launches. This problem could fortunately be solved during the later part of the cruise. In addition to these instrumental and material problems the targets for the lander deployment exhibited a complicated topography, contained carbonate structures, and were exceedingly small so that no successful deployment was possible during the scheduled time at these sites. However, several TV-multicores and gravity cores compensated for this failure.

Before R/V SONNE departed the northern working area on September 23 the Long Ranger was picked up. This lander contains an upward looking current meter (ADCP = Acoustic Doppler Current Profiler) which had registered data for several days at the summit of Mound Culebra. During the deployment time of the Long Ranger an array of CTD casts were sampled around Mound Culebra to monitor the methane distribution. Also before departing, another gravity core was taken at the NW-SE-trending fault which cuts through Mound Culebra. The pore waters again showed an apparent discharge of deep fluids based on decreasing Cl contents. Based on 2 cores at different distances to the fault zone we could define an area affected by ascending fluids.

On steaming towards Mounds #11 and #12, two current moorings were retrieved at Jaco Scarp, before intensive lander deployment was carried out. The Benthic Chamber Lander (BC-L) and the Fluid Flow Lander (FLUFO) were first deployed at the discharge area at Quepos Slide and later at Mounds #11 and #12. At all locations we succeeded in optimally positioning the equipment onto the most active fluid vents for a 24-hour-deployment. At Quepos Slide all systems worked well and preliminary results document high rates of fluid and methane flow, intense material turnover, complete oxygen depletion, exceedingly high methane contents near gas saturation levels, and a significant build-up of peculiarly shaped authigenic carbonate crusts. Also at Mound #12 both lander types recorded optimal data. This is extremely interesting in light of the increased colonization by bacterial mats in the area. Unfortunately, a technical failure of the BC-Lander on Mound #11 precluded registration of equally good data at this location. But here as well as at Mound #12, TV-multi-corer deployments yielded undisturbed sediment cores with clear negative Cl anomalies which suggests the presence of deep fluids as well as a high flow rates.

Between the lander deployments OFOS and multibeam surveys were conducted. OFOS was used to get the ground truth of backscatter anomalies as well as to investigate new hitherto unknown features of fluid flow. The multibeam survey mapped a possible slide (Quepos East) at the upper slope, east of the active Quepos Slide in detail. This structure is well-defined bathymetrically; it is about 5 nm long, 3 nm wide at the shallow end and 5 nm wide at its deeper end. The head wall lies at 230 m of water depth, has its steepest gradient between 350 and 280 m and ends at a water depth of 500 m. Quepos East shows no slump mass at the foot, instead 3 canyons traverse along the longitudinal axis with numerous feeder

channels. It is probably an old slump feature, similar to the Quepos slide but significantly bigger. Currently it is denuded by erosion and its canyons have taken over sediment transport from the shelf to the slope. No detailed OFOS-observation nor methane measurements were carried out because of time limitation; therefore it is still unclear whether or not Quepos East is still actively venting fluids.

Similar to Mound Culebra, a detailed program of methane and current measurements was carried out at Mound #12 . The Long Ranger was deployed as well as a conventional current meter mooring, and seven hydrographic stations complemented the array to obtain a simultaneous picture of methane and current distribution. Near the end of the cruise on September 27, a TV-grab deployment was planned in the area of the increased bacterial colonization at Mound #12, however, the plan was abandoned because of a damaged fibre optic cable. As its repair would have taken more time than was available, two gravity corer deployments were carried out. As it is almost tradition, the last one of them contained several layers of gas hydrate at between 200 - 300 cmbsf (= cm below sea floor) Obviously, at this bacterial site the increased flow of methane is reflected in gas hydrate formation as well as increased methane contents within the bottom water layer.

With the scientific program coming to an end in the evening of September 27, the following 36-hour transit from the working area to Balboa/Panama brought the vessel into port around midday on Monday September 29.

In summary, several highlights and considerable station work were accomplished. One of the results directly and significantly contributing to the SFB objectives was the discovery of the Quepos slide vent, which might be a ground water flow from as far as 80 km offshore and which may have triggered the slide. Furthermore, equally significant are the documentation of deep fluid flow along the Culebra Fault as well as the widespread inter-annual fluctuation of methane emissions. Gas hydrates from a biogenetic (?) and a thermogenetic (?) methane source side by side, at Mounds #12 and #11 respectively document the high spatial variability and differing source depths of dewatering. The identification of different types of clasts related to extrusion features in the mound sediments considerably enhances our understanding of fluid and mass transport from depth. Once again, the importance of our Lander systems in obtaining direct fluid and dissolved component flow rates cannot be emphasized enough. Although this approach is technically complex and demanding, it is unique worldwide and provides essential data directly that contribute directly to the overall SFB objectives. They determine the quantity of element recycling in an observational time frame which may be extrapolated to the subduction framework, and they validate modelling.

Such results can only be achieved through the excellent and continued cooperation between the vessel's crew and the scientific party and the cooperation among the SFB subprojects, as well as the dedication of all participants. Thanks to all of the persons involved.

5 Scientific Equipment

5.1 Shipboard Equipment

5.1.1 Navigation

A crucial prerequisite for all kinds of marine surveys is the precise knowledge of position information (latitude, longitude, altitude above/below a reference level). Since 1993 the global positioning system (GPS) has been commercially available and widely used for marine surveys. It operates 24 satellites in synchronous orbits, thus at least 3 satellites are visible anywhere at any moment (Seeber, 1996). The full precision of this originally military service yields positioning accuracies of a few meters. In the past this service was restricted to military forces and inaccessible to commercial users (Blondel and Murton, 1997). For about two years the full resolution has been generally available.

The resolution of GPS can be enhanced with the Differential GPS (D-GPS) scheme (Blondel and Murton, 1997, Knickmeyer, 1996). Using several reference stations, the determination of the ship's position can be corrected in real time and enhanced to a 1 m to 5 m accuracy. Since cruise SO 109 (1996) D-GPS service is available onboard R/V SONNE. The ship's ASHTEC system provides a validated accuracy better than 5 - 10 m in the area off Costa Rica.

D-GPS values as well as most other cruise parameters are continuously stored in the navigation database, and are distributed via the DVS ("data distribution system") on the ship's network.

Unfortunately, the precision of the position information does not correspond to the accuracy of the time base in the navigation database, as the navigation processing unit Atlas ANP 2000 does not copy the precise GPS-time values, but adds time stamps of its internal unsynchronized clock.

5.1.2 Simrad EM120

The EM120 system is a multibeam echosounder (with 191 beams) providing accurate bathymetric mapping to depths up to more than 11000 m. It is composed of two transducer arrays fixed on the hull of the ship, which send successive frequency-coded acoustic signals (11.25 to 12.6 kHz). The data acquisition is based on successive emission-reception cycles of this signal. The emission beam covers 150° across track direction, and 2° along track. The reception is obtained from 191 overlapping beams, with widths of 2° across track and 20° along track. The beam spacing can be defined as equidistant or equiangular, and the maximum seafloor coverage can be fixed or not. The echoes from the intersection area (2°*2°) between transmission and reception patterns produce a signal from which depth and reflectivity are extracted.

For depth measurements, 191 isolated depth values are obtained perpendicular to the track for each signal. Using the 2-way travel time and the beam angle known for each beam, and taking into account the ray bending due to refraction in the water column by sound speed variations, depth is estimated for each beam. A combination of phase (for the central beams) and amplitude (lateral beams) is used to provide a measurement accuracy practically independent of the beam pointing angle. The raw depth data then need to be processed to obtain depth-contour maps. In the first step, the data are merged with navigation files to compute their geographic position, and the depth values are plotted on a regular grid to obtain a digital terrain model (*DTM*). In the last stage, the grid is interpolated, and finally smoothed to obtain a better graphic representation.

Together with depth measurements, the acoustic signal is sampled each 3.2 ms and processed to obtain a cartographic representation, commonly named mosaic, where grey levels are representative of

backscatter amplitudes. These data thus provide information on the seafloor nature and texture; it can be simply said that a smooth and soft seabed will backscatter little energy whereas a rough and hard relief will return a stronger echo.

During the SO 173 cruise, the Simrad EM 120 Multibeam echosounder, available on R/V SONNE since June 2001, was used continuously. During deep tow profiling dense line offset was used to reduce the opening angles of the beams in order to receive higher resolution images while still covering the complete area. Bathymetric data were processed routinely onboard during the survey, using the NEPTUNE software from Simrad, which is available on board and the academic software MB-System from Lamont-Doherty Earth Observatory. At the beginning of the cruise, a water velocity profile was measured to a depth of 2000 m. The results were used throughout the cruise to produce maps. The data are shown in Figure 5.1.1

5.1.3 PARASOUND

The PARASOUND system works both as a low-frequency sediment echosounder and as a high-frequency narrow beam sounder to determine the water depth. It utilizes the parametric effect, which produces additional frequencies through nonlinear acoustic interaction of finite amplitude waves. If two sound waves of similar frequencies (here 18 kHz and e.g. 22 kHz) are emitted simultaneously, a signal of the difference frequency (e.g. 4 kHz) is generated for sufficiently high primary amplitudes. The new component travels within the emission cone of the original high frequency waves, which are limited to an angle of only 4° for the equipment used. Therefore, the footprint size of 7% of the water depth is much smaller than for conventional systems and both vertical and lateral resolution are significantly improved.

The PARASOUND system is permanently installed on the ship. The hull-mounted transducer array has 128 elements within an area of 1 m^2. It requires up to 70 kW of electric power due to the low degree of efficiency of the parametric effect. In 2 electronic cabinets, beam formation, signal generation and the

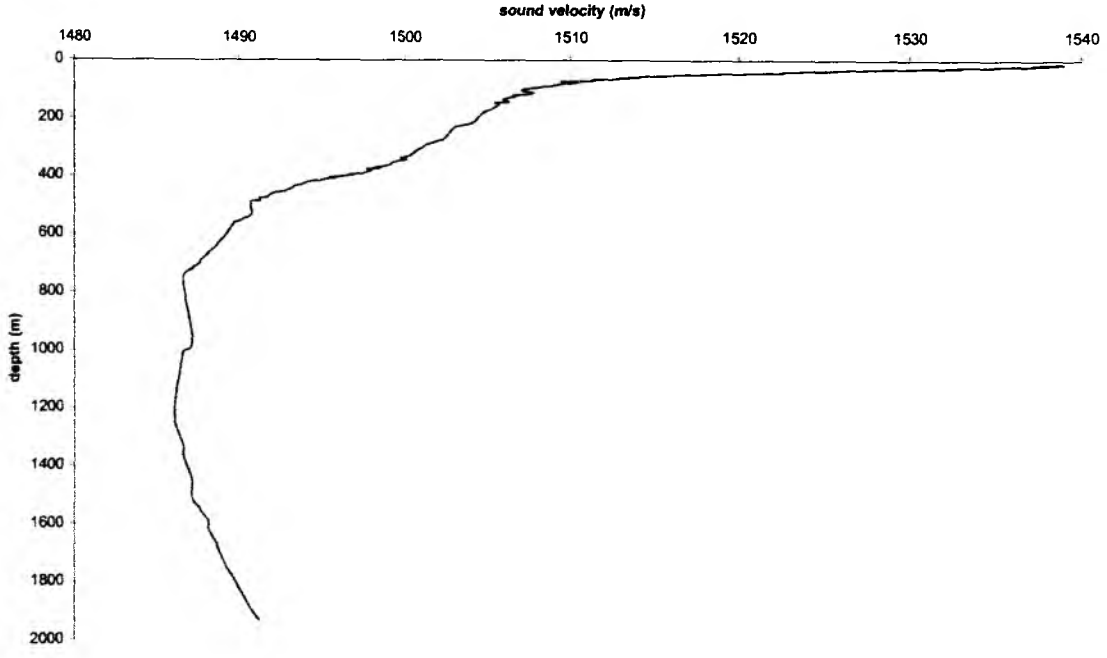

Fig. 5.1.1: Water velocity profile to a depth of 2000 m measured during cruise 173/1. These results were used throughout the cruise to generate bathymetric maps.

separation of the primary (18, 22 kHz) and secondary frequencies (4 kHz) is carried out. Using the third electronic cabinet located in the echosounder control room, the system is operated on a 24-hour watch schedule.

Since the two-way travel time in the deep sea is long compared to the length of the reception window of up to 266 ms, the PARASOUND System sends out a burst of pulses at 400 ms intervals, until the first echo returns. The coverage in this discontinuous mode is dependent on the water depth and also produces non-equidistant shot distances between bursts.

The main tasks of the operators are system and quality control and to adjust the start of the reception window. Because of the limited penetration of the echosounding signal into the sediment, only a short time window close to the sea floor is recorded.

In addition to the analog recording features with the b/w DESO 25 device, the PARASOUND System is equipped with the digital data acquisition system ParaDigMA, developed at the University of Bremen. The data are stored on removable hard disks using the standard, industry-compatible SEGY-format. The 486-processor-based PC allows for buffering, transfer and storage of the digital seismograms at very high repetition rates. Of the emitted series of pulses, usually only every second pulse can be digitized and stored, resulting in recording intervals of 800 ms for a given pulse sequence. The seismograms were sampled at a frequency of 40 kHz, with a typical registration length of 266 ms for a depth window of ~200 m. The source signal was a band limited, 2-6 kHz sinusoidal wavelet with a dominant frequency of 4 kHz and duration of 1 period (250 µs total length). The data were stored on DAT tapes using Windows NT backup software.

5.2 Computer Facilities for Bathymetry, Magnetics, and Seismic Data Processing

The experiments and investigations carried out during SO 173 required special computing facilities in addition to the existing shipboard systems. For programming of ocean bottom stations, processing and interpretation of seismic data and analysis of magnetics several workstations and a dedicated PC laptop were installed by the wide angle and seismology groups of GEOMAR.

In order to handle the large amount of data transfer GEOMAR installed a workstation cluster onboard comprising the following systems:

1	"moho"	SUN Sparc 20	2 CPU, 192 MB memory	no disks, DAT, CD	Sun Solaris 2.8
2	"devonia"	SUN Ultra 60	2 CPU 1 GB memory	150 GB disks, 1x DLT, 1x DAT	Sun Solaris 2.6
3	"hotblack"	SUN Ultra 1	1 CPU, 320 MB memory	4 GB disks, CD, DLT, DAT	Sun Solaris 2.8
4	"galicia"	SUN Sparc 10	2 CPU, 240 MB memory	no disks	Sun Solaris 2.9
5	"crimea"	AMD Duron 700 MHz	1 CPU, 128 MB memory	200 GB disks, 6x PCMCIA	Windows2000
6	"pinta"	AMD Duron 700 MHz	1 CPU, 128 MB memory	68 GB disks, 6x PCMCIA	Windows2000

For seismic modelling one Macintosh G4 Powerbook was installed:

7	Macintosh G4 Powerbook

In addition to these computers, several laptops were used. For plotting and printing two HP Postscript laser printers (paper size A3 and A4) as well as the shipboard color plotters were available.

The workstation cluster was placed in the Magnetiklabor where it was set up according to a "client-server" model, with "moho" being the server. All important file systems from the main server at GEOMAR were duplicated onto the "moho"-disks. Using NFS-, NIS-, and automounter services the computing environment was nearly identical to that at GEOMAR, so every user found his/her familiar user interface. The convenience of network-mounted file systems has to be paid for with a heavy network load, particularly during playback of OBH data (c.f. SO 123 cruise report, Flueh et al., 1997). This required a high-performance network, which was accomplished by a switched twisted-pair ethernet. A 12-port ethernet switching hub (3COM-SuperstackII 1000) with an uplink connection of 100 Mbps to the server "moho" and dedicated 10 Mbps ports for the client workstations maintained the necessary network performance. In order to keep the shipboard network undisturbed by the workstation cluster, but to allow for communication between them, the server "moho" was equipped with two network interfaces and served as a router. This provided the additional benefit of a simplified network configuration. Considerable

setup work was dedicated to "moho", while the other workstations used the same IP addresses and network configuration as used at GEOMAR.

A small secondary cluster ("hotblack" and "pinta") was installed in the Reinlabor for the seismology group to split up the heavy network load.

The raw and processed data was stored onto two 8-hard drive system (Raid "STOR3 Triple Stor") with a total capacity of 1080 Gbytes each connected to the "devonia" and "hotblack". An additional backup device was installed within the Raid system to restore lost data after a possible hard disk failure.

To preserve power supply in case of a ship's internal power breakdown, two UPSs (uninterruptible power supplies) secured both clusters. The Raid system, hard drives and "devonia" as well as "hotblack" were each secured by an UPS to maintain network operation and to avoid a complete system crash, which could lead to a loss of data.

This network setup showed a reliable and stable performance, and no breakdowns were observed.

5.3 Seismic Instrumentation

E. Flueh, J. Bialas, K. Steffen and watch standers

5.3.1 GEOMAR Ocean Bottom Hydrophone/Seismometer (OBH/S)

The Ocean Bottom Hydrophone

The first GEOMAR Ocean Bottom Hydrophone was built in 1991 and tested at sea in January 1992. A total of 17 OBH and 5 OBS instruments were available for SO 173/1. This type of instrument has proven to be highly reliable. In fact, more than 2000 successful deployments have been carried out since. 56 sites altogether were occupied during the SO 173/1 cruise.

The principal design of the instrument is shown in Figure 5.3.2, and a photograph showing the instrument upon deployment can be seen in Figure 5.3.1. The design is described in further detail by Flueh and Bialas (1996). The construction of the OBH is centered around a steel pipe, to which the system components are mounted. At the top of the pipe is a flotation buoy made of syntactic foam that is rated, as are all other components of the system, for a water depth of 6000 m. Attached to the buoy are a radio beacon, a strobe light, a flag and a floating line to aid in retrieval. The hydrophone for the acoustic release is also mounted here, and connected to a model RT661CE release transponder (MORS Technology). Communication with the instrument is possible through the ship's transducer system, allowing successful release and range commands even at 5 kn speed and distances of 7 to 9 km. Opposite the release transponder is an E-2PD hydrophone sensor from OAS Inc. is attached, and in its own pressure tube an MBS recorder from SEND GmbH with D-cells or rechargeable batteries. Finally, approximately 1 m below the steel pipe an anchor is suspended, constructed from pieces of railway tracks weighing about 40 kg each.

The Ocean Bottom Seismometer

The construction of the Ocean Bottom Seismometer (OBS) (Bialas and Flueh, 1999) is based on the GEOMAR OBH, with a few minor changes (Fig. 5.3.3). In contrast to the OBH, the OBS has three legs around a center post to which the anchor weight is attached (Fig. 5.3.4). When deployed, the OBS is positioned directly on the sea bottom to avoid collisions between the seismometer cable and the anchor. A larger floatation buoy is used to compensate for the heavier payload of instruments and the seismometer release lever. During this cruise two types of release for the seismometer were used. The larger housing of the gimbaled KUM seismometers required the use of a 2.5-m-long sledge system (Fig. 5.3.3). Two clock-controlled burn wires will first disconnect the seismometer from the buoyant body, and a flexible rope held under tension will force the sensor to slide off the boom. The second burn wire will later disconnect the flexible rope from the seismometer to ensure that no mechanical forces are transmitted from the carrier to the sensor. An internal clock will activate the gimbal mechanism of the seismometer at a pre-selected time after deployment. A second type of short-period seismometer does not provide a gimbal mechanism and therefore the housing is much smaller. Due to the reduced weight and size a simple stick serves as deploy lever. Again a burn wire is used to release the sensor. This type of burn wire works without a clock. A battery is stored water proof and depth resistant inside a copper tube, which at one end offers a corroding wire as a hook. Once the instrument has been deployed into the water, an electrical current will establish between copper tube and wire, resulting in corrosion of the wire. The size of the wire controls the amount of time (2 hours) needed to release the connected payload. Both seismometers are equipped with I/O 4.5 Hz sensors. All three channels are preamplified within the seismometer housing and recorded by the standard Methusalem recorder as used in the OBH units. Parallel to these three

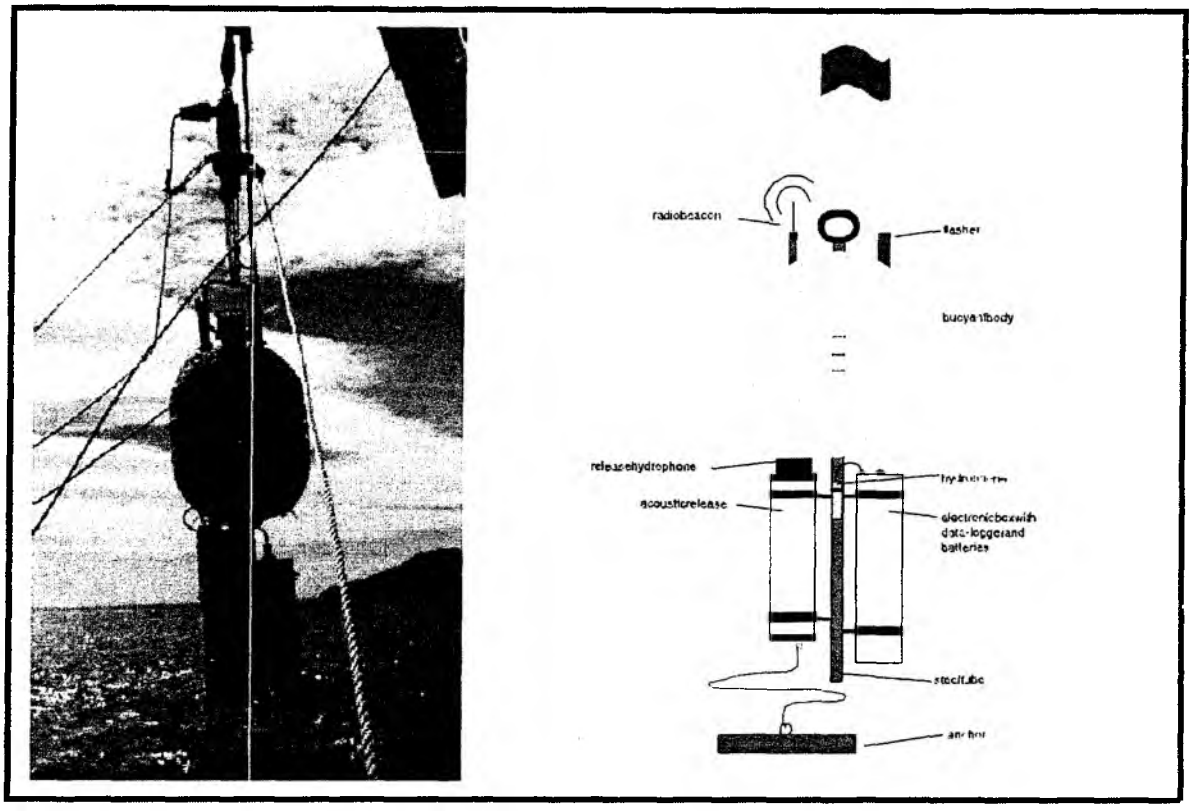

Figure 5.3.1. & 5.3.2.: *Ocean Bottom Hydrophone ready for deployment (left). Schematics of a completely equipped Ocean Bottom Hydrophone (right).*

channels the standard hydrophone is recorded on the fourth channel. For system compatibility the acoustic release, the pressure tubes, and the hydrophone are identical to those used for the OBH.

Marine Broadband Seismic Recorder (MBS)

The so-called Marine Broadband Seismic recorder (MBS; Bialas and Flueh, 1999), manufactured by SEND GmbH, was developed based upon experience with the DAT based recording unit Methusalem (Flueh and Bialas, 1996) over the last years. PCMCIA technology allows for static flash memory cards to be used as unpowered storage media. Thus mechanically driven recording media and read/write errors due to failure in tape handling operations can be avoided. In addition, a data compression algorithm is implemented to increase data capacity. A redesign of the electronic layout enables a power consumption (1.5 W) decreased by about 25% compared to the Methusalem system. Data output can be in 16- to 18-bit signed data, depending on the sampling rate. Based on digital decimation filtering, the system was developed to serve a variety of seismic recording requirements. Therefore, the bandwidth reaches from 0.1 Hz for seismological observations to the 50-Hz range for refraction seismic experiments and up to 10 kHz for high resolution seismic surveys. The basic system is adapted to the required frequency range by setting up the appropriate analog front module. Alternatively, 1, 2, 3 or 4 analogue input channels may be processed. The operational handling of the recording unit is similar to the Methusalem system or works by loading a file via command or automatically after power-on. The time base is kept on a temperature-compensated DTCXO with a 0.05 PPM accuracy. Setting and synchronization of the time as well as drift monitoring is carried out automatically by synchronization signals (DCF77 format) from a GPS-based coded time signal generator. Clock synchronization and drift are checked after recovery and compared with the original GPS units. After software preamplification, the signals are low-pass filtered using a

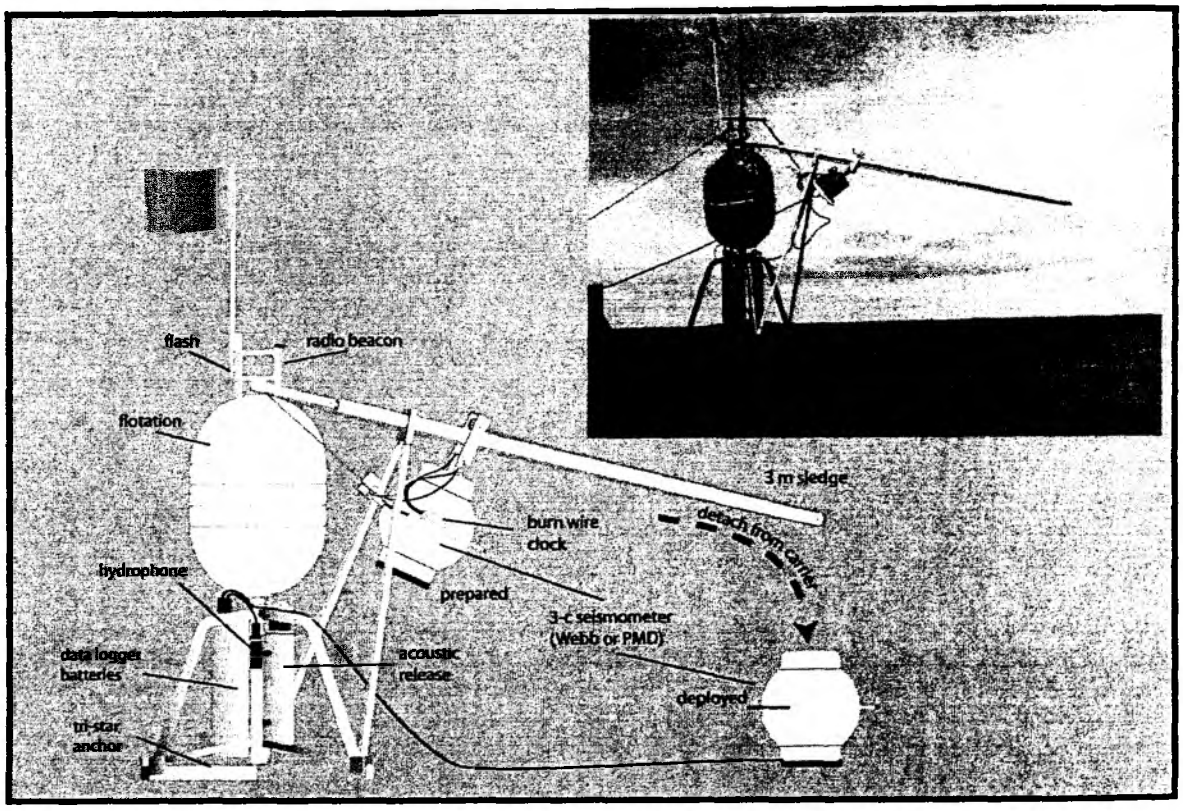

Fig. 5.3.3 and 5.3.4.: *GEOMAR Ocean Bottom Seismometer equipped with sledge for large seismometers (here broadband sensor) OBS equipped with gimbaled short-period KUM seismometer (inset).*

5-pole Bessel filter with a -3 dB corner frequency of 10 kHz. Then each channel is digitized using a sigma-delta A/D converter at a resolution of 22 bits producing 32-bit signed digital data. After delta modulation and Huffman coding the samples are saved on PCMCIA storage cards together with timing information. Up to 4 storage cards may be used, with up to 440 MB per card available. Data compression allows a data capacity of more than 2 GB. Recently, technical specifications of flash disks (disk drives of PCMCIA technology) have been modified to operate below 10°C, making 1-GB-drives available for data storage. The flash cards need to be copied to a PC workstation after recording. During this transcription the data are decompressed and data files from a maximum of 4 flash memory cards are combined into one data set and formatted according to the PASSCAL data scheme used by the Methusalem system. This enables full compatibility with the established processing system. While the Methusalem system provided 16-bit integer data, the 18-bit data resolution of the MBS can be fully utilized using a 32-bit data format.

The Marine Longtime Seismograph

Although power consumption was reduced with the MBS data logger, long-term deployments (up to one year), which are useful for seismological observations, could not be achieved. For this purpose the prototype of a new data logger, the Marine Longtime Seismograph (MLS) was developed by SEND GmbH under the direction of GEOMAR.

The MLS is also a four-channel data logger whose input channels have been optimized for 3-component seismometers and one hydrophone channel. The modular design of the analog front end allows the use of

different seismometers and hydrophones or pressure sensors. Currently, front ends for the Spahr Webb, the Guralp and the PMD seismometer as well as for a differential pressure gauge (DPG), and the OAS hydrophone have been developed. With these sensors we are able to record events between 50 Hz and 120 s. A greatly reduced power consumption of 250 mW during recording combined with a high -precision internal clock (0.05 PPM drift) allows data acquisition for one year. The data are stored on up to 12 PCMCIA type II flashcards. The instrument can be parameterized and programmed via a RS232 interface. After low-pass filtering the signals of the input channels are digitized using Sigma-Delta A/D converters. A final sharp digital low-pass filter is incorporated into the software by a Digital Signal Processor. The effective signal resolution depends on the sample rate and varies between 18.5 bit at 20 ms and 22 bits at 1 s. Playback of the data is done under the same scheme as previously described for the MBS. After playback and decompression the data is provided in PASSCAL format, at which point it may easily be transformed into standard seismological data formats. During cruise SO 173/1, 23 OBH and OBS stations were recovered from a 9 month deployment using the MLS device with the sensors described above (see Ch. 6.4.1).

The Marine Exploration Seismic Recorder (MES)

During cruise SO 173/1 the prototype of a new generation of recording devices was available for first test deployments. This data logger is based on the experiences with the MBS and MLS devices. It is supposed to replace the MBS system in the future. New features are a 24 bit A/D converter which provides a signal to noise ratio above 120 dB. As the development of PC cards did not allow the use of high capacity cards (2 GB and higher) in low-temperature surroundings like the ocean floor the new data logger uses an internal hard disk. From developments in laptop technology, drives are available that withstand a harsh working environment and need only a small amount of power. High data transfer through a firewire (5 GB < 10 min) ensures that the entire 20 GB disk drive can be copied within 40 min. Further features are similar to the MBS. Together with the data logger a new set of Linux-based programs allows to run the complete data transformation up to SEGY formatted trace segmentation without switching between different operating systems or computing platforms.

During laboratory tests the MES recording worked and data could be copied from the system. Unfortunately the unit could not be accessed after a first deployment and the data could not be saved from disk.

5.3.2 GEOMAR Mini-Streamer

In addition to the deep tow, a mini-streamer was onboard to record reflection seismic events. This streamer was manufactured by SIG (Service et Instruments de Geophysique, France). The system comprises several parts: four 50-m-long active sections with 20 hydrophones spaced at 2.50 m, two 2.50-m-long lead-in sections separating the depth transducer (Philips P30) in the tail and the depth transducer and preamplifier in the head from the active sections. The lead-in cable is 150 m long, and a 50-m-long deck cable can be laid out to connect the winch to the lab. The individual hydrophones are omnidirectional and have a flat frequency response from 10 to 1000 Hz. The sensitivity is –90db, re 1V/mbar, +-1 dB. The hydrophones are mounted in an oil-filled polyurethane pipe of 34 mm in diameter, with a nominal density of 1.12 gr/cm3. The lead-in cable can be trimmed to the required depth using air and seawater. A control unit provides power to the preamplifier, displays the depths of the head and tail depth transducers and provides the analog signals of the four channels. Different preamplifications can be chosen by a selector, either each channel by its own, two neighboring channels added, or all four channels added. We used the

amplification of each single channel. The depth readings are also available on RS232 interfaces for storage on a PC.

The signals recorded by the streamer were stored on a four-channel MBS recorder, identical to those used in the ocean bottom seismic recorders. The streamer winch was placed amidships about 8 m away from the aft of the vessel.

5.3.3 Seismic Sources

Two types of airguns were available during this cruise. One 2.4-l GI gun was used during deep tow operation and reflection seismic profiling while up to three 32-l Bolt airguns were operated simultaneously during wide angle experiments (see Figure 5.3.3. for towing configuration). Both gun types were fired through a LongShot airgun controller operating on external trigger signals.

External Trigger

During deep tow operation the shot trigger was provided by the INGGAS controller, described in chapter 5.5.4. For wide angle and surface streamer profiling the trigger signal was supplied from the ship's Ashtech GG24 GPS/Glonass receiver, which can provide a 1-ms-long 5 V-TTL pulse at intervals between 0.2 and 999 s. The impulse has to be stable to within the accuracy of the GPS time, which is 70 ns. Shot breaks, necessary for subsequent data processing and instrument location, were stored on a MBS recorder and displayed in real time for quality control. For this process, the same procedure as for the OBHs was used (see Chapter 5.3.1) and the trigger signal was converted into a 5 V-TTL pulse of 300 ms length by a circuit provided by the ship's technical support staff (WTD). The pulse was delivered to the Real Time Systems LongShot Seismic Source Controller and the MBS recording units. As the LongShot triggered on the falling flank, the ship's trigger signal was inverted. The source controller verifies that all guns are fired at the pre-selected aim point after the external trigger is detected. The ignition pulse is sent out to each gun according to the trigger delay time prior to this aim point. Exact positions for the shot times were calculated by post-processing using shot time and UTC time values stored with D-GPS coordinates in the ship's database. From earlier cruises it was known that the coordinates stored within the database were provided by the Atlas ANP 2000 system, which does not copy the exact GPS time values, but adds time stamps of its internal uncontrolled clock to the high precision coordinates of the D-GPS system. The accuracy of the time values mainly depends on the operator's ability to manually set the ANP clock to GPS time. This is clearly a somewhat biased method compared to the efforts of precise positioning.

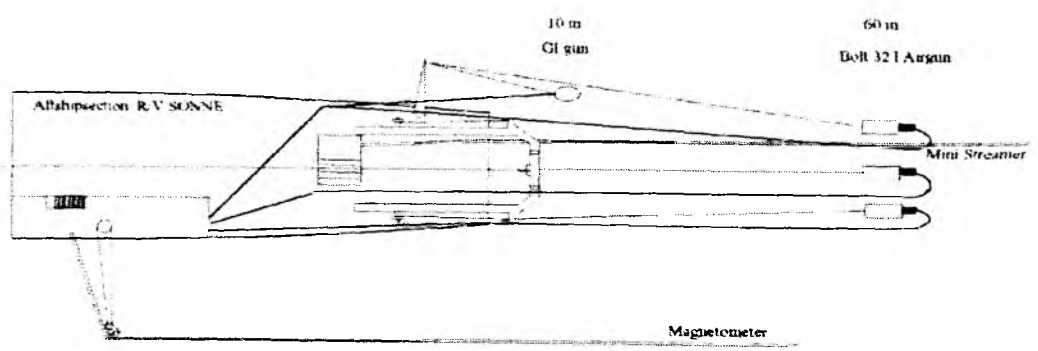

Fig. 5.3.5.: *Tow configuration at the stern of R/V SONNE. Extension of the starbord crane allows to tow all three 32-l guns at same distance. The mini streamer can not be towed together with the three guns.*

GI-GUN

For SO 173/1 a GI-Gun (Generator-Injector gun; manufactured by Sodera) for high-resolution survey, with a generator and injector volume of 1.7 l each was available (Fig. 5.3.6). Basically a GI-Gun consists of two airguns in one. The first gun, the generator, produces the primary pulse. Depending on the chamber

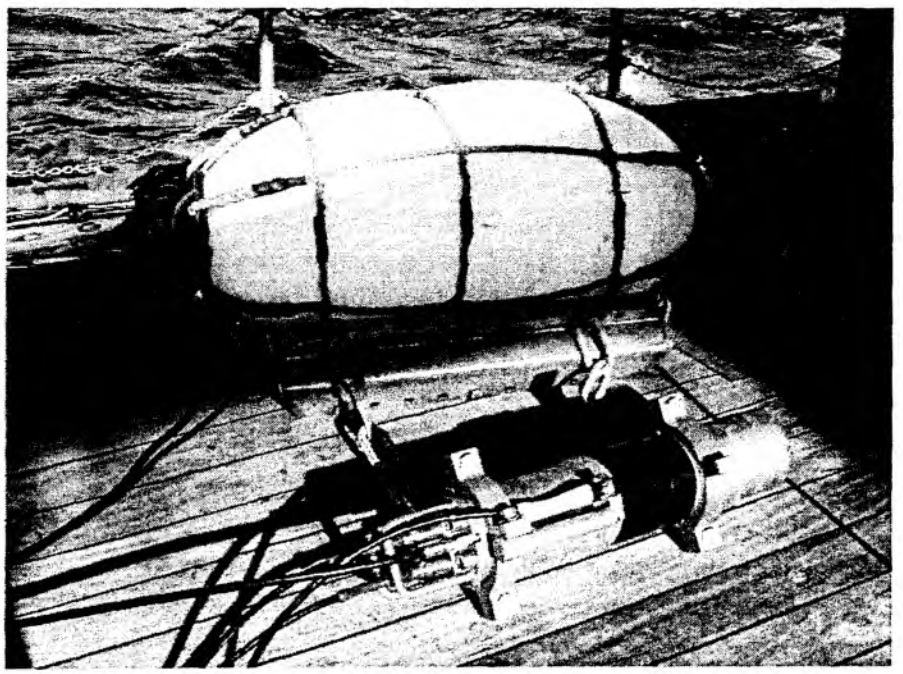

Fig. 5.3.6: *GI-gun model 210 with gun hanger and buoyancy.*

Fig. 5.3.7: *32 l Bolt gun during midship deployment.*

volume, which can be adjusted by volume reducers, the bubble can be significantly suppressed by triggering the second part of the gun, the injector, after a delay if the bubble collapses. Operation of this gun is very simple, especially as it is unnecessary to pressure it up prior to deployment.

The following GI-Gun configuration has been used:

Mode	Generator Volume (in^3)	Injector Volume (in^3)	Delay (ms)	Discharge Port
Harmonic	105	105	58	large

The GI-gun was operated through the LongShot seismic source controller where ports 7 and 8 were reconfigured for GI-gun mode. A special software layout, provided by RealTime through GEOMAR accounts, enabled the use of the Bolt guns (see Chapter 5.3.3) and the GI-gun without major reconfiguration of the control unit. The attached shot break hydrophone was used for automatic shot point adjustment. With the LongShot sensor display, the near field source wavelet was controlled and remained constant over the entire survey. A single gun hanger towed the GI-Gun approximately 10 m behind the ship's stern at a water depth of 1,5m. Towing depth remained stable due to a fender on top of the gun hanger. Following the recommendation of the Sodera handbook, the gun was operated at a pressure of 140 bar and with a shot interval of 7 s, and worked without problems.

32L BOLT-GUN

The seismic signals of the lower frequency band were generated by up to three Model 800 CT BOLT airguns (one on loan from UTIG); a photo of one of the guns is shown in Figure 5.3.7. Each gun has a volume of 32 l (2000 in^3), and generates a signal with a main frequency centered around 6 to 8 Hz, including higher harmonics. The pier winches at the port and starboard side towed one gun each, while the third gun was towed by the deep sea cable through the center of the A-frame. On the port side the towing wire was attached to a block on the A-frame, while on the starboard side the extension of the small crane was used. Trigger cables and air hoses were deployed manually. Each gun was suspended from two fenders with an additional float attached to the supply lines to prevent contact between the gun and the towing wire. A sketch of the towing configuration is shown in Figure 5.3.5. The guns were towed 60 m behind the vessel and operated at 140 bar at a depth of 7 to 8 m. Due to the extension of the starboard crane all three guns could be towed at the same distance behind the vessel.

Gun handling and compressor operation went smooth throughout the entire cruise.

Table 5.3.1: Table showing the delay times used with the LongShot source controller
- Aim point is the time at which the guns are aligned
- Trigger delay is the time at which the ignition pulse is prior to the aim point

	trigger delay	aim point	injector delay
Bolt gun	0	60	N/A.
GI-gun	20.2	60	58

5.4 Magnetometer

During cruise SO 173 a GeoMetrics G801/3 Marine Proton Magnetometer was used. This unit consists of a gasoline-filled sensor attached to a 250-m-long marine cable and a control unit. During the polarization cycle an electric current generates a strong magnetic field in the coil and forces the magnetic moments of the protons to be aligned for a short time parallel to the existing field. During the following measuring cycle, i.e. when the electric current is turned off, the field generated previously is removed and the protons start realigning themselves with the Earth's magnetic field. According to the moment preservation law, this happens by precession of the protons with a frequency directly proportional to the intensity of the geomagnetic field. It is this frequency, which is then measured as AC electric current created by magnetic induction in the coil, amplified, counted and transformed into magnetic field intensity values (measuring unit: 10^{-9} Tesla = 1 nT), which is recorded.

In order to minimize the influence of the ship's hull, the sensor of the Magnetometer is towed 180 m behind the ship. The distance between the ship and the sensor is sufficient to minimize the magnetic influence of the vessel resulting in a resolution of about 5 nT.

On board of R/V SONNE, the winch was placed on the port back deck and the sensor towed to the port side of the vessel. A boom led the cable about 7 m to the side of the ship in order to prevent it from colliding with the ship. Before data acquisition, the tow fish was dissemble and the membrane condition checked, after which the gasoline was filled in. After some minor problems at the beginning, the system worked well throughout the trip.

The measured values of the total intensity magnetic field were displayed on a console and written as digital output coded in BCD values. The system was set to deliver one data value every 3 seconds via digital multiport interface to a PC, where a special software was used to store the data together with UTC time in ASCII tables.

After data backup the files were transferred to a SUN workstation. GPS coordinates and time were taken from the ship's navigation system and assigned to each magnetic stamp on the basis of the recorded time. The magnetic and the navigation data were resampled to a 10-s interval. After optional median filtering they were displayed using GMT plot routines (Wessel and Smith, 1995).

5.5 Deep Tow Acoustic and Seismic Investigations

M. Breitzke, J. Bialas, D. Buerk, N. Fekete, E. Flueh, I. Klaucke, C. Papenberg, C. Ranero

5.5.1 General Scientific Background

The vertical and lateral resolution of marine subsurface structures in reflection seismic images strongly depends on the marine seismic source and streamer system used for signal generation and data acquisition. The vertical resolution is controlled by the dominant frequency and bandwidth of the reflected signals and can be improved by using high(er)-frequency sources like GI- or waterguns in deep water and boomers or sparkers in shallow water. Deconvolution tries to improve the vertical resolution by increasing the bandwidth. The lateral resolution is determined by the size of the Fresnel zone whose radius depends on the source and streamer depth and on the depth of the reflector, respectively, on the velocity above the reflector and on the dominant frequency. Migration decreases the in-line resolution and radius of the Fresnel zone to a minimum of a quarter wavelength but has no influence on the cross-line resolution. The cross-line resolution can only be improved by lowering the streamer and - in the ideal case - the source towards the sea floor.

Whereas reflection seismic studies provide an image of the subsurface structures sidescan sonar surveys are intended to map the acoustic properties of the seafloor. Generally, the principle of sidescan sonar mapping is that an acoustic beam is scattered at targets on the seafloor, and the amount of scattering that is directed back to the instrument is recorded. This amount of backscattering is related in decreasing order to the regional slope, the microtopography of the seafloor and the physical properties of the material on the seafloor. Knowing the regional slope, it is principally possible to relate the backscatter signal to lithology if the regional slope is known *a proiri*, and the backscatter return is correctly calibrated. The resolution of these backscatter images and the penetration depth of the acoustic beam, and thus the depth interval over which the backscatter image is averaged, depends on the frequency used by the sidescan sonar instrument. Well-known very low- and low-frequency and low-resolution instruments are the GLORIA or the TOBI system operating with acoustic beams of 6.5 and 30 kHz, respectively. In contrast to these low-resolution instruments, a high-resolution dual-frequency deep towed sidescan sonar instrument (DTS-1) with center frequencies of 75 and 410 kHz will be used during R/V SONNE cruise SO 173/1 in order to map the extent of diapiric mounds and the detailed distribution of carbonate crusts that are related to fluid escape structures. A more thorough and detailed summary of the theory and principles of sidescan sonar imagery and data processing is presented elsewhere (Blondell and Murton, 1998).

5.5.2 The Deep Tow Sidescan Sonar and Digital Multichannel Seismic Streamer System

5.5.2.1 Introduction

The hybrid multichannel digital deep tow seismic streamer used during this cruise has been developed within the INGGAS project (subproject 3) of the gas hydrate initiative of the GEOTECHNOLOGIEN program (BMBF) in order to collect marine seismic data with an improved lateral in- and cross-line resolution particularly in regions of special interest for gas hydrate research. In this context, hybrid system means that conventional marine seismic sources like air-, GI- or waterguns shot close to the surface are still used, whereas the streamer is lowered to the seafloor and - combined with a sidescan sonar system acquired within the OMEGA project of the gas hydrate initiative of the GEOTECHNOLOGIEN program - forms a deep towed device. A depressor of about 2 tons in weight completes the deep tow system and ensures that the sidescan sonar and streamer to keep in depth and as close to the towing ship as possible (Figure 5.5.1).

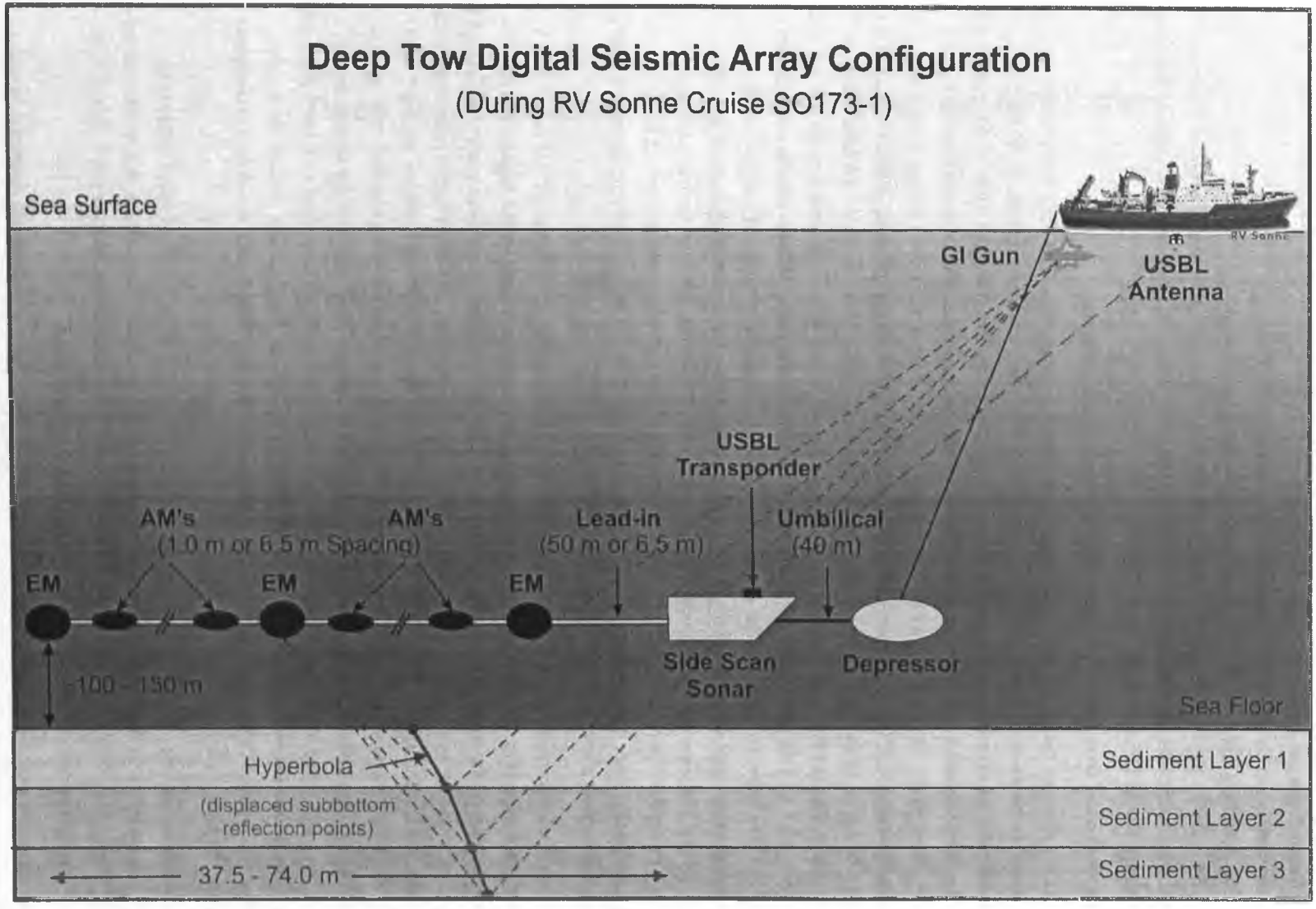

Fig. 5.5.1: *Deep tow digital seismic array and sidescan sonar configuration used during R/V SONNE cruise SO 173/1.*

In the following the main components of the deep towed sidescan sonar and multichannel seismic streamer system are described, i.e.

(1) the technical details of the sidescan sonar instrument DTS-1,
(2) the multichannel seismic streamer configuration,
(3) the ultra short baseline (USBL) positioning system POSIDONIA,
(4) the recording and control system of the complete deep tow device
(5) the software used to operate the deep towed sidescan sonar and multichannel seismic streamer.

Finally, the deployment and recovery procedures, the operational settings used during this cruise and first preliminary results (cf. sect. 6.2) are presented.

5.5.2.2 Technical Description of the DTS-1 Sidescan Sonar System

The DTS-1 sidescan sonar is a dual-frequency, chirp sidescan sonar (*EdgeTech Full-Spectrum*) working with center frequencies of 75 and 410 kHz. The 410-kHz sidescan sonar emits a pulse of 40 kHz in bandwidth and for a duration of 2.4 ms (providing a range resolution of 1.8 cm), and the 75-kHz sidescan sonar enables a choice between two pulses of 7.5 and 2 kHz in bandwidth with 14 and 50 ms pulse lengths, respectively. They provide a maximum across-track resolution of 10 cm. Towing speeds of 2.5 to 3.0 kn and a range of 750 m were used during this cruise, so that the maximum along-track resolution is on the order of 1.5 m. In addition to the sidescan sonar sensors, the DTS-1 contains a 2 - 16 kHz chirp subbottom profiler providing a choice of three different pulses, each with a pulse length of 20 ms: a 2 - 10-kHz pulse, a 2 – 12 kHz pulse and a 2 – 15 kHz pulse resulting in a nominal vertical resolution between 6 and 10 cm. The sidescan sonar and the subbottom profiler can be run with different trigger modes, internal, external, coupled and gated triggers. Coupled and gated trigger modes also allow to specify trigger delays. The sonar electronics provide four serial ports (RS232) to attach up to four additional sensors. One of these ports is used for a Honeywell attitude sensor providing information on heading, roll and pitch. Finally, there is the possibility of recording data directly in the underwater unit through a mass-storage option with a total storage capacity of 60 GByte.

The sonar electronics are housed in a titanium pressure vessel mounted on a towfish of 2.8 m x 0.8 m x 0.9 m in dimension (Fig. 5.5.2). The towfish houses a second titanium pressure vessel containing the underwater part of the telemetry system (*SEND DSC-Link*) and the Linux-based Bottom-PC (*SEND*) of the seismic streamer data acquisition system (cf. sect. 5.5.4). In addition, a releaser capable to work with the USBL positioning system POSIDONIA (*IXSEA-OCEANO*) with a separate receiver head (cf. sect. 5.5.3), and an emergency flash and radio beacon (*NOVATECH*) are included in the towfish. The towfish can also be equipped with a forward-looking sonar, but this sensor had been removed for this cruise in order to gain additional buoyancy at the nose of the fish. Additional syntactic foam had also been placed in the front of the towfish to further improve the fish's towing behaviour. For the same reason the towfish had been fitted with a deflector at the rear. This deflector has five positions from 0 to –5 and is designed to reduce the pitch of the towfish.

The towfish is connected to the sea cable via the depressor through a 40 m long umbilical cable (Fig. 5.5.1). The umbilical cable is tied to a buoyant rope that bears the actual towing forces. An additional rope has been taped to the buoyant rope and serves to pull in the instrument during recovery (cf. sect. 5.5.6).

5.5.2.3 Deep Tow Multichannel Seismic Streamer Configuration

The streamer is a modular digital seismic array (*HTI, High Tech, Inc.*) which can be operated in water depths of up to 6000 m. It consists of a 50-m-long lead-in cable towed behind the sidescan sonar fish and

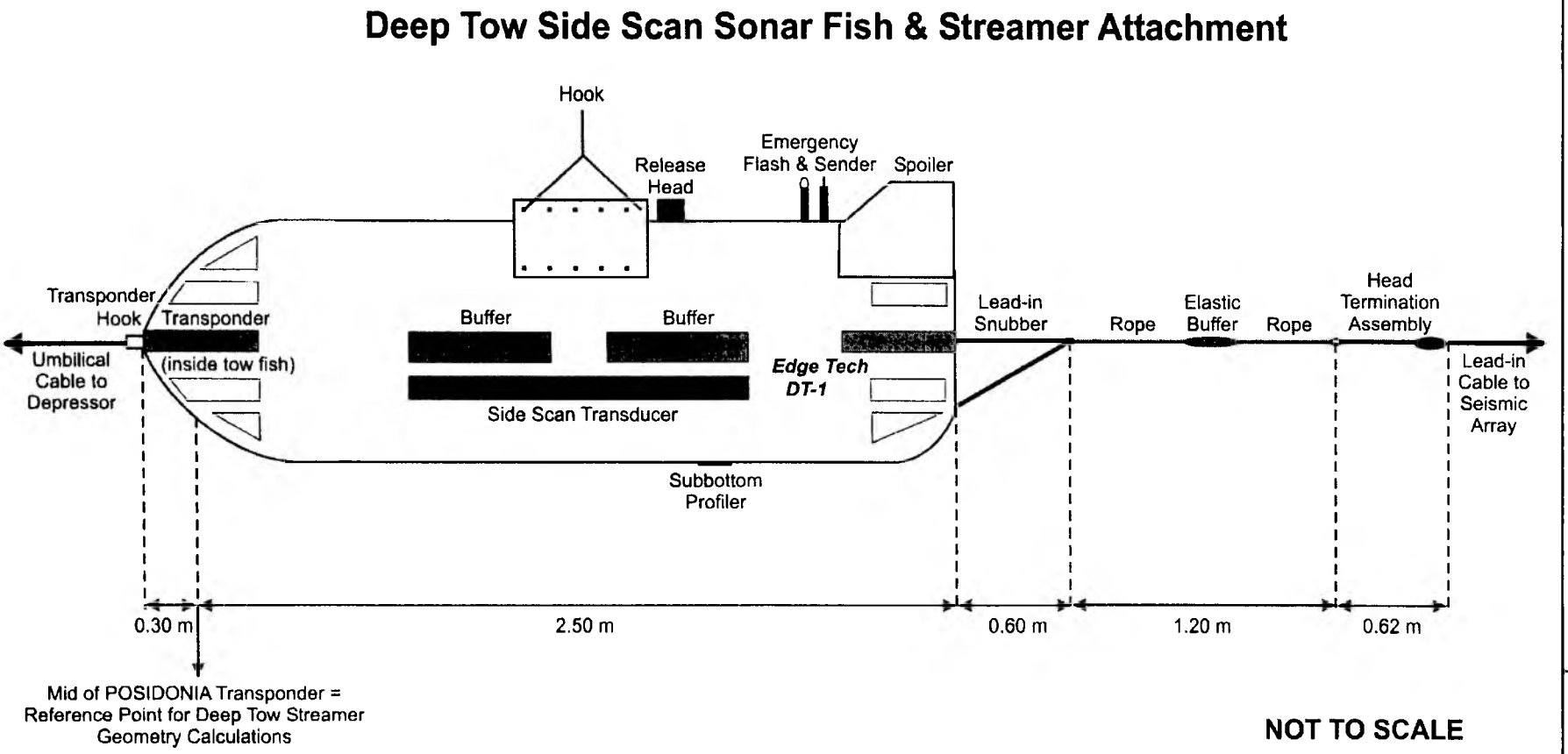

Fig. 5.5.2: Geometry and dimensions of the deep tow sidescan sonar fish and streamer attachment.

single modules for each channel (Figure 5.5.1). There are two different modules, i.e. acoustic and engineering modules. Each acoustic module (AM) houses a single hydrophone, low- and high-cut filter, pre-amplifier and 24-bit AD converter in a pressure vessel. Special engineering modules (EM) additionally include a compass, a pressure sensor and a motion sensor (*Crossbow*) which provide information on the depth of the module below the sea surface, on its geographical position (magnetic heading) and on its roll and pitch during the survey. Modules are interchangeable and can be connected arbitrarily by cables of 1 or 6.5 m in length. Up to 96 channels can be combined. Selectable sample intervals and pre-amplifier gains between 0.25 - 500 ms and 0 - 36 dB, respectively as well as two different high-pass filters with 4 Hz low-cut frequency allow to use different and sufficiently high-frequency seismic sources to guarantee both a very high vertical and lateral resolution.

A special lead-in snubber combined with an elastic rope buffer is used to fix the streamer to the sidescan sonar towfish. Figure 5.5.2 shows the lengths and dimensions of these different parts together with the dimension of the sidescan sonar fish. These lengths have to be taken into account if the geographical positions of the different streamer nodes are computed during a later post-processing step.

During R/V SONNE cruise SO 173/1 the configuration of the deep tow streamer changed from one survey area to the other due to contact and corrosion problems at the pins and within the plugs of the cables and short cuts within the streamer nodes. Hence, detailed listings of the streamer configuration, node numbers, node types and cable lengths used are given in section 6.2.2 for each survey area.

5.5.3 Ultra Short Base Line (USBL) Positioning System POSIDONIA

Underwater navigation, depth and position measurement of the sidescan sonar tow fish is carried out by the ultra-short base line (USBL) system POSIDONIA (*IXSEA-OCEANO*). It mainly consists of a deployable acoustic array (antenna) installed in the moon-pool, and a responder with a remote receiver head mounted on the sidescan sonar fish housing an additional pressure sensor (cf. sect. 5.5.2.2). Either the responder function is triggered via cable link through a coaxial or fibre optic deep sea cable transmitted via the telemetry system or transponder mode is used triggered by an acoustic signal through the acoustic array antenna (cf. sect. 5.5.4).

The USBL positioning principle of the POSIDONIA system is based on a bi-directional exchange of submarine acoustic signals between one or several acoustic transponders and the acoustic array consisting of one transmission transducer and two pairs of hydrophones (Fig. 5.5.3). The acoustic transponders are interrogated either by a trigger pulse transmitted via the deep sea cable telemetry (trigger 2) or by an acoustic signal and will send a 25 ms M-FSK (multi-frequency shift keying) reply. The 25 ms M-FSK signal is a succession of ten monochromatic pulses (each 2.5 ms long) of ten different frequencies ranging from 14.5 to 17.5 kHz. The order of frequencies during the pulse is determined by the M-FSK code. For best detection of the signal with POSIDONIA, codes 22 or 23 should be selected. The four reception hydrophones of the array receive this signal that is then transmitted to the processing unit, which measure the phases of the signals and the time between interrogation and reply in order to deduce the relative position of the transponder and calculate its geographical position. The minimum ping interval depends on the range of the transponder. It was kept constant at 10 s during this cruise, in order to reduce interferences with the side scan sonar. Together with the D-GPS, gyro compass and motion sensor (MRU) information provided by the ship the *POSIDONIA* system allows to determine the depth and position of the sidescan sonar fish with an absolute accuracy of 0.5 - 1% of the water depth if the sidescan sonar fish's position is within a cone of 60° or 120° opening angle, and with an accuracy of 2 -

POSIDONIA USBL-Positioning Principle

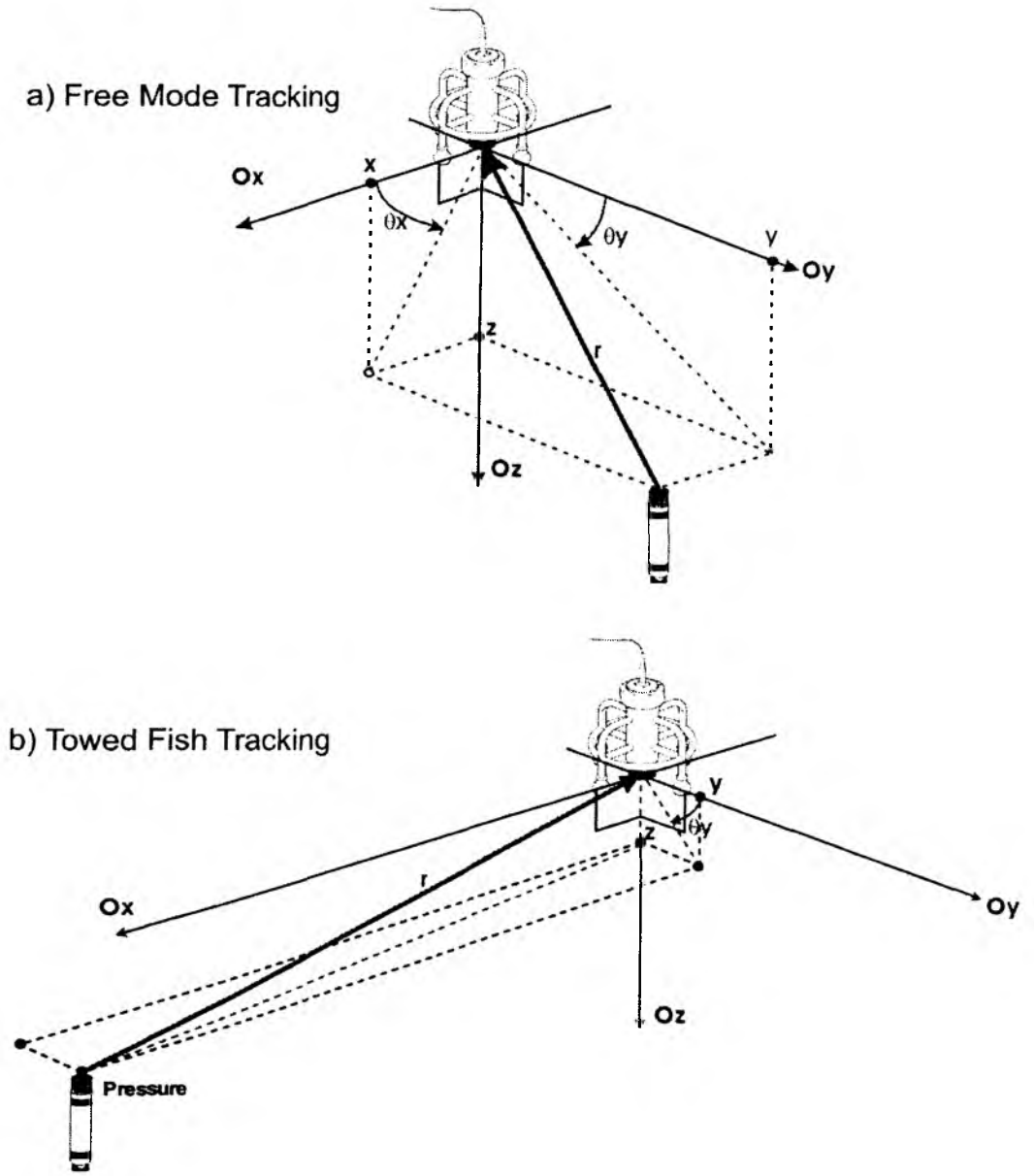

	Deployable Acoustic Array			
Conical Angle	60°	120°	140°	170°
Accuracy % of the slant range	0.5%	1%	2%	5%

Fig. 5.5.3: *Positioning arrangement and accuray of the ultra-short baseline (USBL) system POSIDONIA, (a) using the free tracking mode for conical angles to a maxium of 60°, and (b) using the towed fish tracking mode for conical angles larger than 60°.*

5% if the position is within a cone of 140° or 170° opening angle.

The *POSIDONIA* positioning system can be run in two different tracking modes, the free mode tracking (Fig. 5.5.3a) and the towed fish mode tracking (Fig. 5.5.3b). In the free mode all four hydrophones are used to calculate the position of the transponder. In the towed fish mode only the hydrophones aligned with the towed vehicle are used together with depth information provided by a built-in depth sensor. The free mode should be used when the transponder is located in a cone of 60° underneath the ship, but this mode will work fine up to an angle of 120 degrees. Beyond this angle the towed fish mode should be used.

As the *POSIDONIA* antenna is not fixed to the hull of the ship, the antenna has to be calibrated prior to using the *POSIDONIA* system, in order to determine the vertical, longitudinal and transverse offsets of the acoustic array axes relative to the corresponding ship axes (Fig. 5.5.4b), and taking the position of the *POSIDONIA* acoustic array relative to a common reference point (CRP) on the ship, usually the position of the D-GPS receiver, into account (Fig. 5.5.4a). For this calibration an acoustic transponder has to be moored on the seafloor in water depths ranging from 1000 - 2000 metres, but should be free from any acoustic shadows, i.e. ideally some metres above the ground. The ship will then sail a figure of eight above the mooring point in order to interrogate the transponder at any angle and from either side of the vessel (Fig. 5.5.5). The dimension of this figure of eight depends on the water depth and the designated maximum vertical observation angle that shall be included. It is designed to obtain a minimum of 1000 data points. As example Figure 5.5.5 displays the dimension of this figure of eight for a water depth of 1250 m, a maximum angle of the cone of 50° and a ship's velocity of 3 kn. After the ship having sailed this calibration curve the *POSIDONIA* software calculates correction factors of roll, pitch and yaw in order to correctly position the transponder.

The latest version of the software *ABYSS* also allows setting of filters in order to eliminate bad navigation points from the final data file. This filter function also allows smoothing of the underwater navigation, a feature particularly interesting for towed instruments.

Based on the geographical positions of the sidescan sonar tow fish (*POSIDONIA* transponder position) determined by the *POSIDONIA* system, the (magnetic) heading values measured by the engineering nodes (EM's) of the streamer and the D-GPS data provided by the ship's antenna the geographical positions of each streamer node as well as the seismic source can be determined at each shot trigger time by temporal and spatial interpolation of the D-GPS, *POSIDONIA* and engineering data sets.

Prior to the calibration run a water sound velocity profile was recorded down to 2000 m water depth, the limit of the ship´s sound probe which belongs to the *SIMRAD* multibeam system, and copied into the *POSIDONIA* data base. Unfortunately the serial interface cards used to read the ships sensor information did not operate continuously and hence several parts of the first calibration could not be recorded (Fig. 5.5.6). Nevertheless enough data points could be sampled to allow a first calibration which was then used for a second smaller figure eight. After application of both calibration results the moored calibration transponder could be located with a precision of +/- 7 m (better than 1% of the 1179 m water depth). During the first deep-tow sidescan sonar and seismic profiles the transponder of the tow fish was operated in responder mode, avoiding two transmissions through the water column. Again problems occurred with the serial ports and the DSP board connection of the processing unit, which finally resulted into a drop out of *POSIDONIA* positioning during the first profile. Remote investigations by the manufacturer pointed towards a malfunction of the processor and serial boards, which could only be replaced at the factory. In order to minimize the time consuming needs of calibration runs the acoustic

POSIDONIA USBL-Calibration Procedure

a) Posidonia Array Offsets relative to the Ship's Common Reference Point (CRP) - Constant Offsets

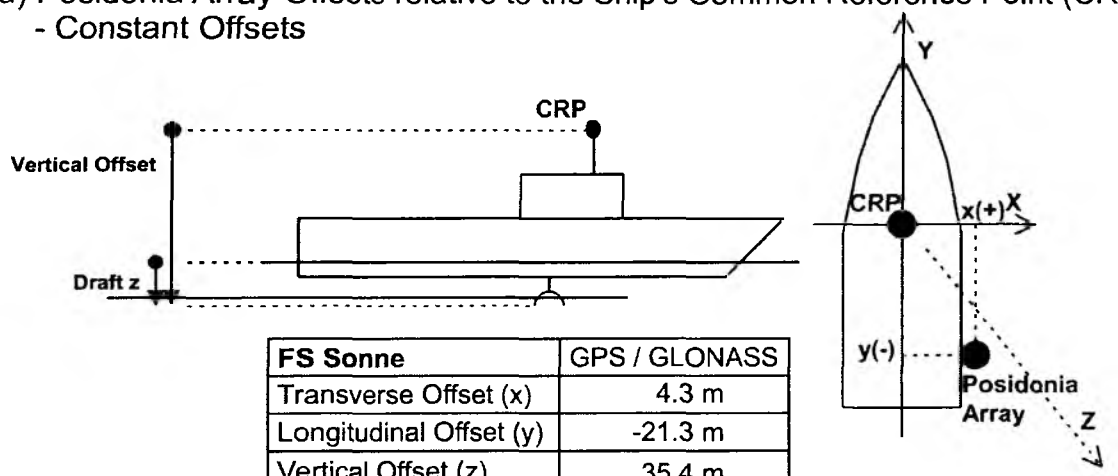

FS Sonne	GPS / GLONASS
Transverse Offset (x)	4.3 m
Longitudinal Offset (y)	-21.3 m
Vertical Offset (z)	35.4 m
Draft (z)	7.8 m

b) Posidonia Array Offsets relative to the Ship's Horizontal and Vertical Reference Unit (VHRU) - Calibration Offsets

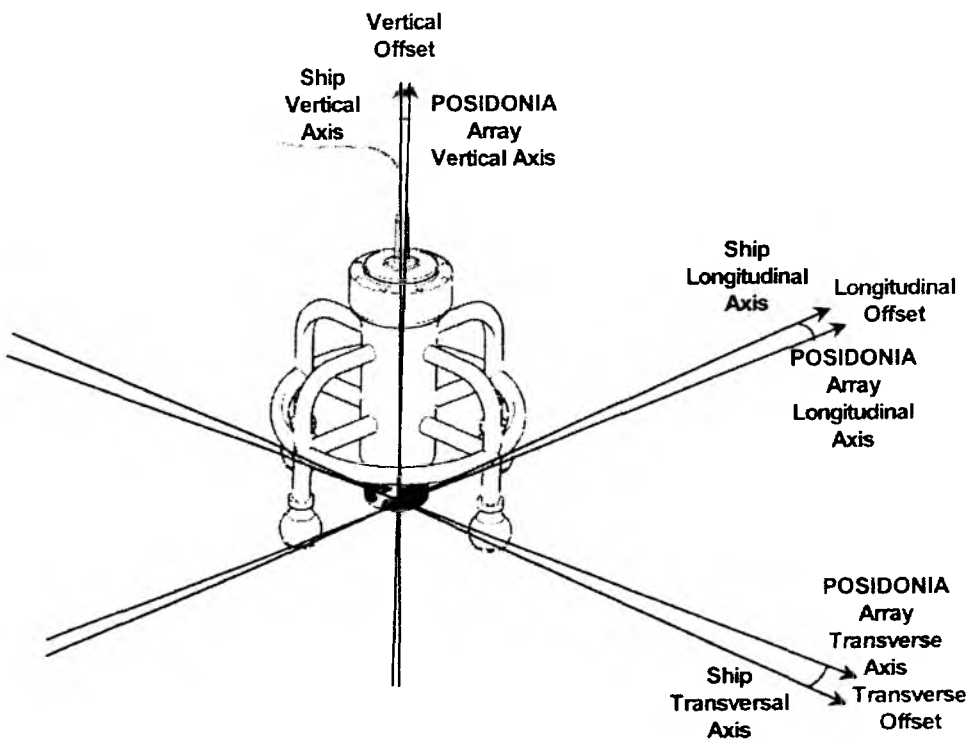

Fig. 5.5.4: *Calibration procedure of the ultra-short baseline (USBL) system POSIDONIA. a) POSIDONIA array offsets relative to a common reference point (CRP), usually the position of the (D)GPS antenna. (b) POSIDONIA array offsets relative to the ship's vertical, longitudinal and transversal axes.*

array was kept in deployed position while the ship was not allowed to sail faster than 8 kn through water. For a second operation the transponder was set into transponder mode, avoiding the serial link through the questionable boards. It was found that the originally installed transponder does not reply on acoustic interrogation and was therefore replaced by a spare unit. Additionally the transmission of pressure values was omitted as the manufacturer reported unsolved problems with this option. After these changes the *POSIDONIA* system operated over most of the remaining time. Nevertheless it was necessary to reboot both, the PC and PPU system at arbitrary intervals several times. It was noted as well that the displayed time and the time within the recorded positions was set one day, two days, etc. more behind UTC. As it could be assumed that the time stamp should be copied from the DGPS strings no attempts were made to change this during the cruise in order to keep the known offset constant for all recordings. During a second and third calibration a second figure eight was skipped as the accuracy of positioning was already better than 1% of the water depth after the first run (+/- 12 m at 1236 m, Figs. 5.5.7, 5.5.8).

5.5.4 Recording and Control System

The deep-tow recording and control system consists of a top and a bottom side part (Fig. 5.5.9). The top side part includes a Linux-based Top-PC (*SEND*), a DSC-Link (*SEND*) as top side part of the telemetry system, the surface Full Spectrum Interface Unit (*FS-IU*) of the sidescan sonar system (*EdgeTech*) and two 2 PC's running the *HydroStar Online* (*ELAC*) and the *Geometrics StrataVisor NX* (*GEOMETRICS*) software for the deep-tow sidescan sonar and multichannel seismic online data recording and quality control. In addition, there is the processing unit of the USBL positioning system *POSIDONIA* and a PC for the online recording and display of measured positions of the sidescan sonar tow fish. An optional obstacle avoidance sonar with it's display and control unit completes the laboratory set-up of the deep-tow recording and control system.

At the bottom side a Linux-based PC with 120 GB storage capacity and the underwater part of the telemetry system (*SEND*), which handles the data transfer between underwater and onboard systems and provide all necessary power supplies for the bottom electronics, are installed in a pressure-proofed housing mounted on the sidescan sonar fish. Additionally, the Full Spectrum Deep Water (*FS-DW*) part of the sidescan sonar system (*Edge Tech*) is installed in a second pressure vessel mounted on the sidescan sonar fish, too. An obstacle avoidance sonar is available as optional add on system as well but was not included during this cruise.

The deep-tow seismic streamer and side scan sonar system can completely be controlled from the top side by the Linux-based Top-PC and the dedicated HydroStar PC. Seismic and sidescan sonar data are stored both underwater on the Linux-based Bottom-PC and the FS-DW as well as onboard on the hard disc of the PC's running the *HydroStar Online* and the *Geometrics StrataVisor NX* software or on two connected *DLT 8000* devices with 40 (uncompressed) or 80 GByte (compressed) storage capacity connected to the Geometrics-PC. Commands which control the seismic recording parameters like sample interval, record length, delay, filter or pre-amplifier gain, and which initialize the data transfer between underwater and onboard systems, are sent from the top to the bottom side via low-speed downlink, whereas seismic and sidescan sonar data are transferred from the underwater to the top side via telemetry and high-speed uplink through a coaxial or fibre optic deep sea cable. During a final system check at GEOMAR prior to shipping a problem with the fibre optic modem was detected. In order to avoid expensive airfreight for late shipping of the complete data control system it was decided to restrict to the coaxial transmission onboard R/V SONNE. From earlier cruises it was known that the available

Posidonia USBL-Calibration Curve

PARAMETERS	
Ship's Speed (knots)	3
Cadence (sec)	7
Depth (m)	1250
Maximum angle (deg)	50

FIGURE	
Diameter of 1 loop (m)	1490
Total Distance (m)	9355
Duration (min.)	115
Number of Points	1386
Max. Slant Range (m)	1945
MinimuM Cadence (s)	4

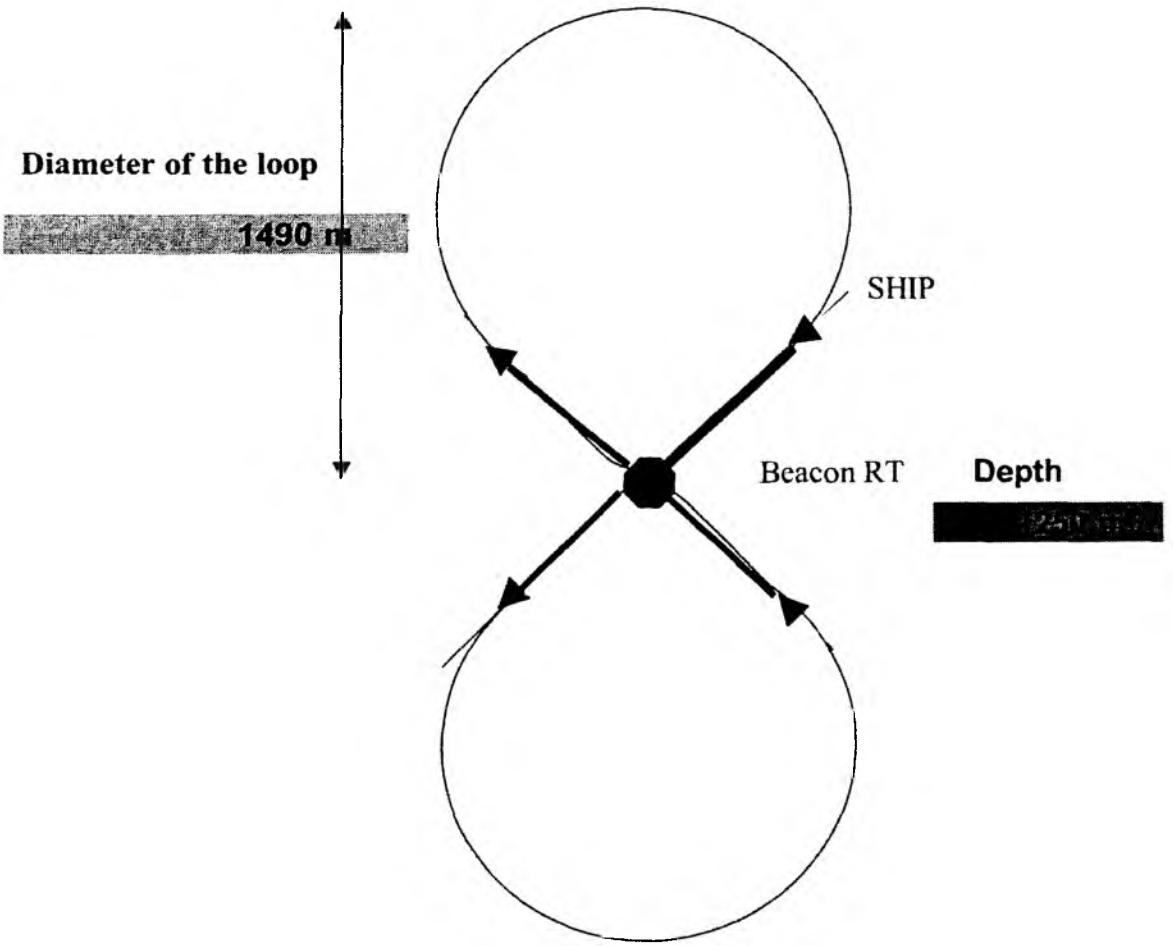

Fig. 5.5.5: Calibration curve based on figure-eight-configuration for the ultra-short baseline (USBL) system POSIDONIA computed for a water depth of 1250 m, a maximum conical angle of 50° and a ship's velocity of 3 kn.

bandwidth would be enough to transmit all required online data, if a record length of 3.072 s, a sample interval of 0.25 ms (resulting in 12288 samples per trace) and a 7-s shot interval were chosen during seismic and sidescan sonar profiling, and as long as the sidescan sonar would operate without the 410 kHz sensor. Only if recording parameters were changed, one or two shots would sometimes be lost at the moment the new parameter set was sent to the bottom side.

All bottom and top side components as well as the air gun shooting were synchronized by D-GPS time-based trigger signals generated by a Linux Top-PC via the LPT10 link. Additionally, all surface and underwater components controlling the deep tow device are linked via ethernet with the Linux Top-PC serving as gateway and form a small PC cluster within the computer network on board of the research vessel.

5.5.5 Software

5.5.5.1 DTS-1 Sidescan Sonar

The main operations of the DTS-1 sidescan sonar are essentially run using *HydroStar Online*, a multibeam bathymetry software developed by *ELAC NAUTIK GmbH* and recently adapted to the acquisition of *EdgeTech* sidescan sonar data. This software package allows onscreen presentation of the data, of the tow fish's attitude, and the tow fish's navigation when connected to the POSIDONIA USBL-positioning system. It also allows to set the main parameters of the sonar electronics, such as selected pulse, range, power output, gain, ping rate, and range of registered data. With *HydroStar Online* it is also possible to start and stop data storage either in XSE format on the *HydroStar Online* PC or in JSF format underwater on the *FS-DW*. Simultaneous storage in both XSE and JSF formats is also possible. Some additional settings such as trigger mode or data window size can only be changed by accessing the underwater electronics directly via the surface *FS-IU*. The *FS-IU* also runs *JStar*, a diagnostic software tool, that also allows running some basic data acquisition and data display functions.

HydroStar Online creates a new XSE file when a file size of 10 MB is reached, while a new JSF file is created every 20 MB. How fast this file size is reached depends on the amount of data generated, which in turn essentially depends on whether the high-frequency (410 kHz) sidescan sonar is used. The amount of data generated is also a function of the sidescan sonar and subbottom pulses and of the data window that is specified in the initialization file (sonar.ini) on the *FS-DW*. The data window specifies the range over which data are sampled. Proper selection of this parameter strongly depends on the selected range of the sidescan sonar system in order to avoid good data to be cut off, or to prevent storage space from being wated by too large amounts of useless data. It also proved practical to switch off data recording while the ship was turning. During the present cruise a new file was created every 3 minutes on average, resulting in a total of 5705 files and 56.2 GByte of data.

Further handling and processing of the sidescan sonar data can be done either by the *PRISM* software package (Southampton Oceanography Centre) or the *CARAIBES* software package (IFREMER). The figures in this report have been processed using *CARAIBES*, which was available onboard.

5.5.5.2 Deep Tow Multichannel Seismic Streamer

In order to start the digital multichannel seismic data acquisition both the Linux Bottom-and Top-PC have to be started and the operator has to log in as root into both PCs by opening two windows on the Top-PC screen and starting the scripts *tpcroot* and *bpcroot*. Subsequently, several drivers, which organize and control the down- and uplink and the data transfer from the bottom to the top side, have to be started on the Bottom and Top-PC by running the scripts *tpc start* and *bpc start*. Prior to starting the drivers on the

Bottom-PC, the *Geometrics Controller Interface* (GCI), which enables the transfer of the multiplexed digital data from the Linux Top-PC to the Geometrics-PC, and the *Geometrics StrataVisor NX* software have to be started and the trigger enabled. Finally, the *INGGAS-Controller* software (*SEND*), which allows to set the main recording parameters and displays the depth and heading values of the engineering nodes of the streamer graphically onscreen, has to be run on the Linux Top-PC. Actually, the main recording parameters for the digital multichannel seismic data acquisition, such as recording length, delay, sample interval, filter and pre-amplifier gain, have to be set twice, once in the *INGGAS-Controller* software (*SEND*) running on the Linux Top-PC and again in the *Geometrics StrataVisor NX* software running on the Geometrics-PC, because these parameters are not transferred directly from the Linux Top-PC to the Geometrics-PC via the *Geometrics Controller Interface* (GCI).

The *Geometrics Stratavisor NX* software allows to display the complete shot gathers, their amplitude spectra and a continuous single-fold profile of one selected trace onscreen, to print the continuous single-fold profile on an online printer and to store the acquired data on hard disc or the two connected *DLT 8000* devices in standard seismic SEG-D, SEG-Y or SEG-2 format, so that the data can easily be processed by conventional public domain or commercial software packages like *Seismic Unix, SEISMOS, FOCUS,* etc. Various bandpass-filter and gain options exist to optimize the display on the screen and on the online printer.

5.5.6 Deployment and Recovery

The operations for deployment and recovery of the deep tow multichannel seismic streamer and sidescan sonar are a bit demanding and require a relatively calm sea, to ensure that handling is safe for both crew and instrument. Five persons are ideal for safe operation. Ideally, the complete deep towed sidescan sonar and seismic streamer system is towed via the A-frame.

Deployment starts when the ship sails through the water with no more than 1 kn . First the seismic streamer including the knotted rope at the end is put overboard, node by node, letting it drift away. Then the sidescan sonar towfish is heaved into the water and released with a special hook that allows to detach the crane cable. The towfish then also drifts astern while the ship moves at minimal speed. Meanwhile, the buoyant rope is secured. Then the depressor is put in place below the A-frame, the buoyant towing rope fitted to the end termination of the sea cable and the umbilical cable connected to the sea cable. Any loose ends are tied securely and the depressor, with the towfish attached to it, heaved into the water. At this stage it is important that no strain is exerted on the cable connection.

During recovery, first the depressor is pulled and secured on deck. Then the towfish is pulled close to the stern of the ship with the additional rope taped to the umbilical cable. This way the towfish can be recovered using the support winches on the A-frame. Prior to lifting the towfish, safety lines are connected to the top holder used during deployment by long sticks. This technique has proved practical under good weather conditions, because during recovery, the sidescan sonar fish is only secured at one point for a short time and can then turn freely along its long axis.

5.5.7 Seismic Source and Operational Settings

The deep towed streamer and sidescan sonar system has been deployed six times during R/V SONNE cruise SO 173/1. The system was towed with an average ship velocity of 3 kn.

For seismic measurements a standard GI-Gun (Generator-Injector (GI) Gun; *Sodera*) with anormal chamber volume (2 x 1.7 l) was towed on the starboard side using the extension of the small tumable

crane at R/V SONNE's aft deck. The umbilical of the GI-gun was connected to the small piece of fixed rail set up to support the starboard 32 l BOLT gun, and towed about 3 - 10 m behind the ship's stern, depending on the survey area (cf. sect. 6.2). The towing wire was connected to a bow with the GI-Gun hanging on two chains 0.5 m beneath. An elongated buoy, which stabilized the gun at a horizontal position in a water depth of about 1.6 - 1.7 m, was connected to the bow by two rope loops. The injector was triggered with a delay of 58 ms with respect to the generator signal essentially eliminating the bubble signal. The shot interval was 7 s, resulting in an average shot point spacing of about 10.8 m.

For the sidescan sonar measurements the 75-kHz option was used as standard while the 410-kHz sonar was operated at Mounds 11 & 12.

Deep tow sidescan sonar and multichannel seismic streamer data were recorded with the following operational settings for the main recording parameters:

DTS-1 Sidescan Sonar	
Low sidescan sonar center frequency:	75 kHz
Low sidescan pulse:	7.5 kHz bandwidth, 14 ms duration
Low sidescan sonar range:	750 m
Low sidescan sonar data window:	26000 samples
High sidescan sonar center frequency:	410 kHz
High sidescan pulse:	40 kHz bandwidth, 2.4 ms duration
High sidescan sonar range:	150 m
High sidescan sonar data window:	23000 samples
Subbottom profiler pulse:	2-10 kHz bandwidth, 20 ms duration
Subbottom profiler data window:	6000 samples
Trigger mode:	coupled (75 kHz sidescan was master trigger)
Ping repetition rate:	0.98 s
Multichannel seismic streamer	
Sample interval:	0.25 ms
Record length:	3.072 s
Delay:	0, 1 or 2 s on profiles, depending on the survey area, variable in curves
Filter.	2nd order high-pass filter
Pre-amplifier gain:	24 dB

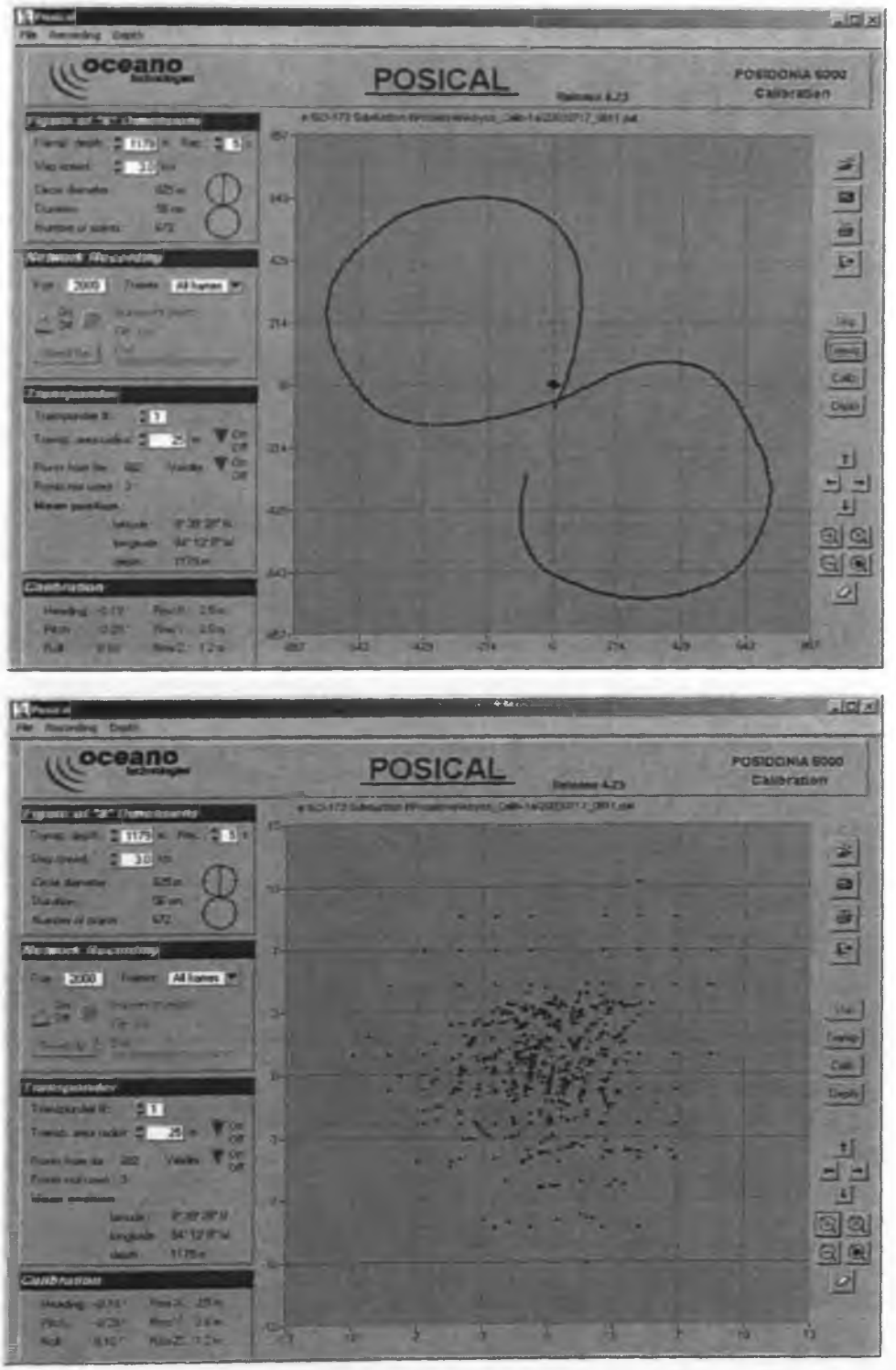

Fig. 5.5.6: *POSIDONIA calibration on July 17th, 2003. Two figures of eight were sailed, and the final resolution is +/- 7 m.*

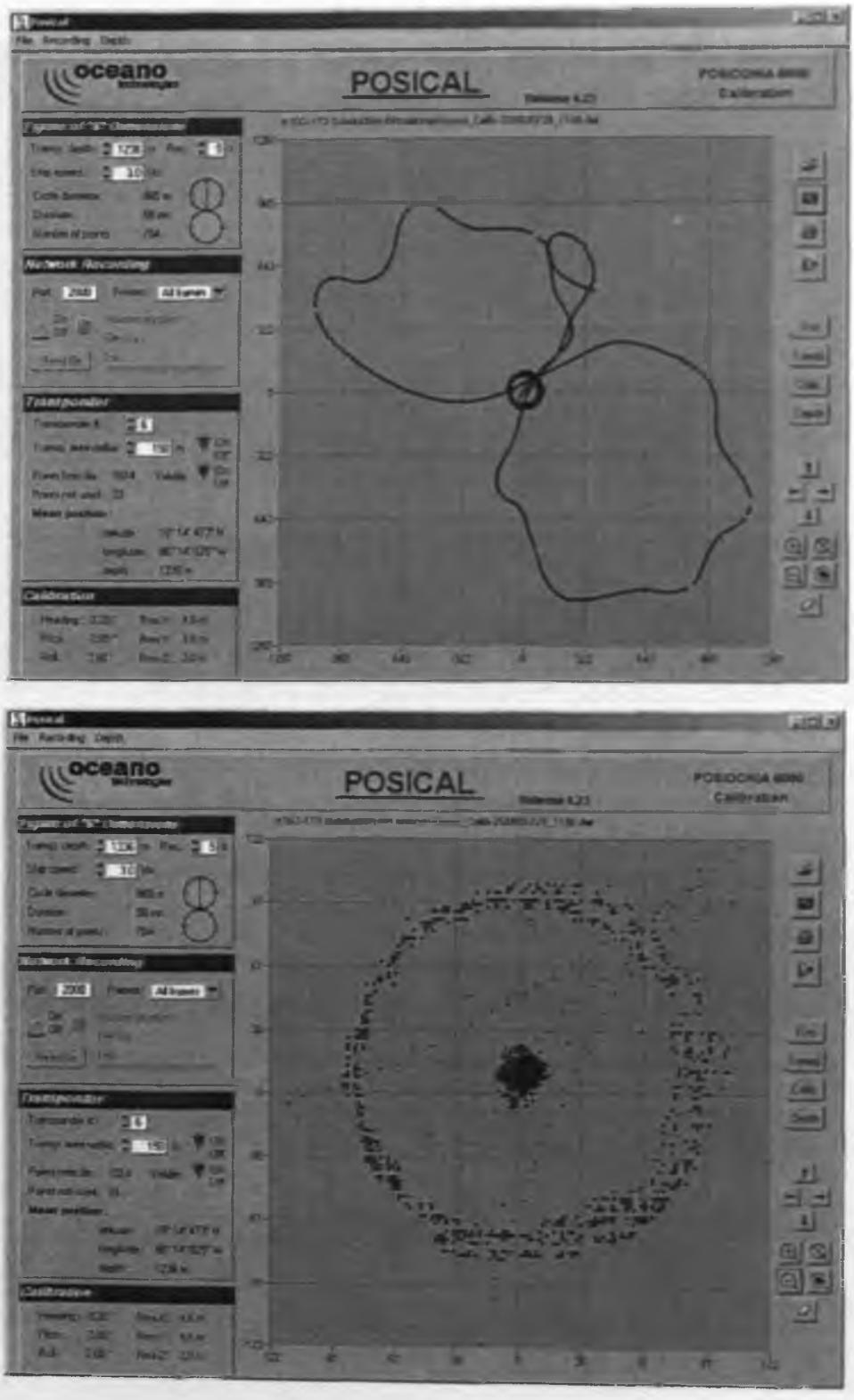

Fig. 5.5.7: POSIDONIA calibration on July 25th, 2003. One figure eight was sailed, the final resolution is +/- 12 m.

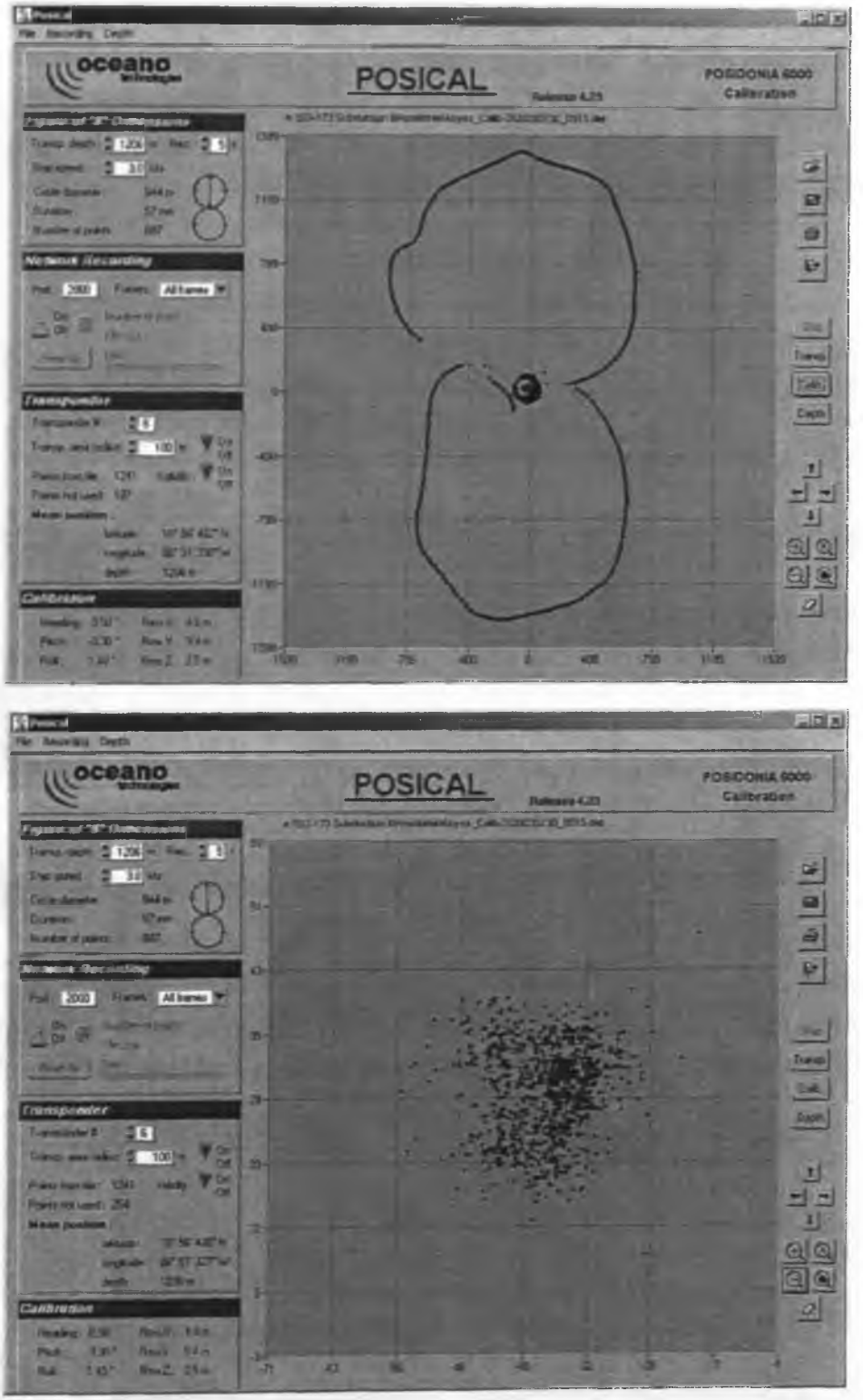

Fig. 5.5.8: *POSIDONIA calibration on July 31st, 2003. One figure eight was sailed, the final resolution is +/- 12 m.*

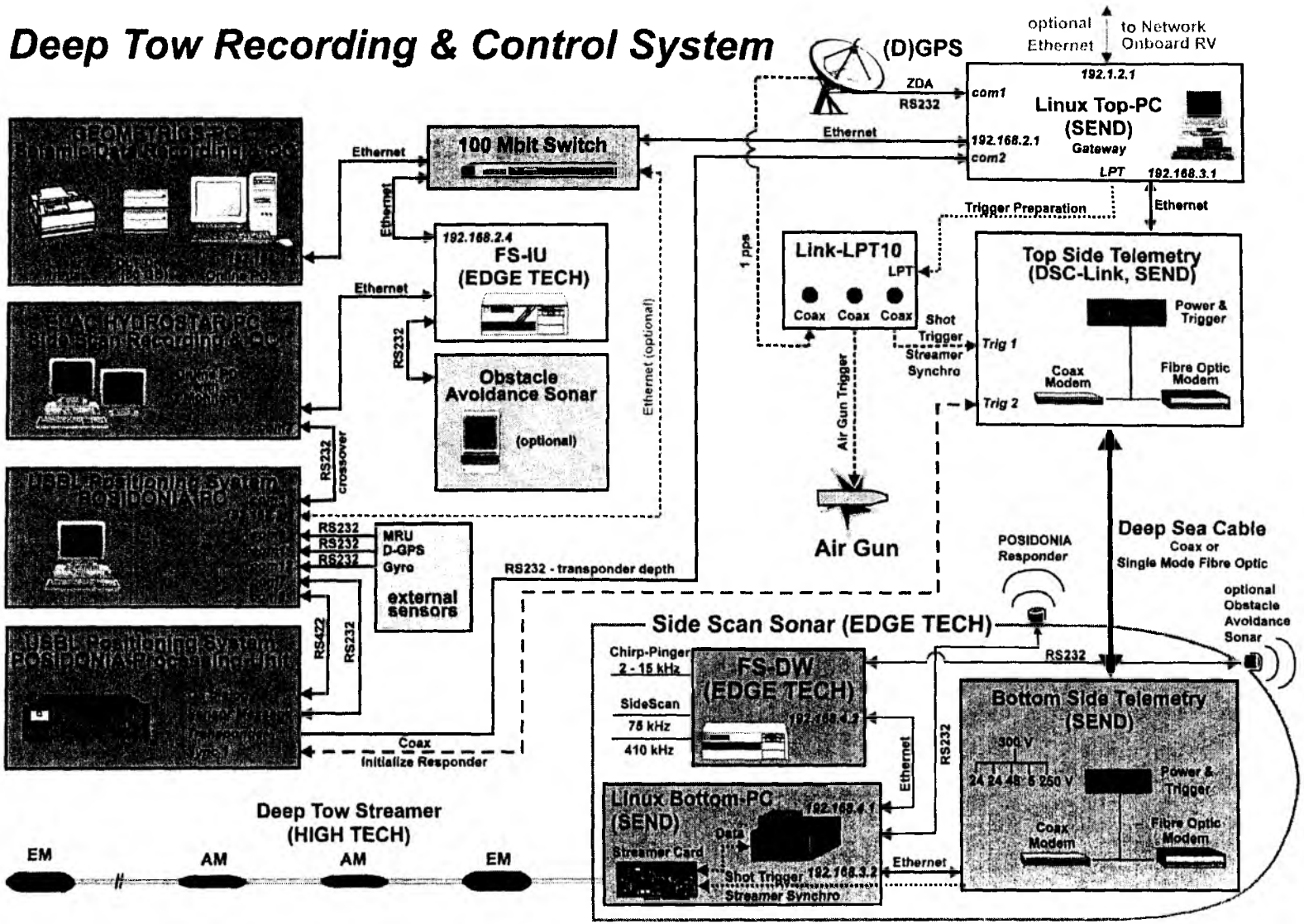

Fig. 5.5.9: Laboratory and underwater components of the recording and control system for the complete deep tow sidescan sonar and streamer system.

5.6 Seafloor observations

5.6.1 OFOS

H. Sahling, S. Echeverría Sáenz, E.M. Corrales Cordero, E. Soeding, E. Suess

OFOS (Ocean Floor Observation System) is equipped with the following instruments: two video cameras (color camera: Deep Sea Power and Light, black and white camera: Photosea), a stereo still camera system (Photosea), and halogen lights (Deep Sea Power and Light), CTD (Seabird), a compass, pitch and roll sensor, and a Simrad SSBL responder.

The sled is towed behind the ship at a speed of about 0.8 knots (kn). The distance of about 1.5 m to the seafloor is adjusted manually by the winch operator. For this purpose, a ground weight is suspended below the sled on a rope of 2 m in length. Two laser pointers can be used to scale the video image and the still camera images. The laser pointers are parallel and 20 cm apart, while a third one points at an oblique angle. The still camera is loaded with a slide film (Kodak Ectachrom 200) allowing a maximum of 800 shots. The still cameras were set with an aperture of 4 and a focus depth of 1.5 m. The images were taken manually. The video signal and the images are overlaid with the date and time (UTC). Introducing a novel technique, the black-and-white video signal was digitized in real time and stored as a mpeg file in vcd format.

During the SO 173 cruise we were confronted with a variety of ship-based software problems. The data transfer from OFOS to the ship regularly caused data gaps in the central database DVS. During nearly every deployment the DVS had to be restarted. After the restart the communication between ship and OFOS could not be reestablished, therefore, neither CTD nor compass data were recorded in the database. Furthermore, due to problems with the data export, navigation data are oftenlimited to an hourly interval.

5.6.2 TV-Grab

V. Liebetrau, H. Sahling

The TV-guided grab (TVG) is a heavy tool to collect sediment, rock or biological samples from the seafloor. Its shovels can be closed hydraulically. It is powered by deep-sea batteries that allow closing and opening it about three times. The opening of the grab is about 1.8 m^2. The grab was equipped with a black-and-white camera and a color camera. Accurate positions can be acquired by a SSBL responder.

5.7 Sediment Sampling and Sedimentology

Several sediment cores of 1 to 12 m (total length of recovered sediment) were taken by gravity corer (GC) during cruises SO 173/3+4 in the Costa Rican and Nicaraguan forearc area. The gravity corer was equipped with a 2-t-weight attached to the top of a 6- to 12-m-long steel tube enclosing an inner PVC tube. As soon as the cores arrived on deck, they were cut into approx. 1-m-long segments and the segments were sampled at both ends for gas-geochemical investigations. The core segments were then stored in a container cooled to 4°C, until core logging was performed using a GEOTEK Multi Sensor Core Logger. Logged sediment cores were split into archive and working halves and working halves were immediately sampled for further geochemical analyses and determination of physical properties . The archive halves were described by means of sedimentological characteristics based on Rock Color Chart and ODP lithology classification. Photographs of 1-m-long sediment segments and close-up photographs of particular features were taken with a Nikon Coolpix 995. Color scans of selected archive halves were made with a Minolta Color-Scanning System.

106 m of sediment were recovered by gravity coring during cruise SO 173/3.

5.8 Pore Water Geochemistry of Surface Sediments

E. Corrales-Cordero, B. Domeyer, C. Hensen, K. Nass, U. Schacht, K. Wallmann, U. Westernströer

Investigations of the geochemical composition of pore waters provide information to investigate the forces and impacts driving redox and mineralization processes within the upper sediment column. During cruises SO 173/3 and 4 the pore water composition of surface sediments was investigated at more than 60 locations to characterize and quantify sediment diagenetic processes and fluid geochemistry along the active continental margin off Costa Rica. Concentration vs. depth profiles of pore waters were determined for major nutrients, total alkalinity, chloride, hydrogen sulfide, and methane to identify locations influenced by seepage and to assess the effect of methane formation and decomposition processes.

Below we first give a short overview on the procedures of sediment retrieval, pore water processing, and geochemical laboratory methods followed by some of the major results.

5.8.1 Sampling, Processing, and Analyses

Sediments were generally retrieved by a TV-guided multicorer (TV-MUC) and a gravity corer (GC). Additional sediment samples were obtained from Fluid Flux Observatory as well as Benthic Chamber Landers and TV-Grab deployments.

To prevent a warming of the sediments after retrieval all cores were immediately placed into a cooling room and kept at a temperature of about 4°C. Supernatant bottom water of the multicorer cores was sampled and filtered for subsequent analyses. Multicorer cores were processed immediately after recovery, most of them in a glove box in an argon atmosphere. For cores with high amounts of methane and/or gas hydrates a faster sampling procedure outside the glove box was preferred, sub-samples for methane analysis were taken. Each core was cut into slices for pressure filtration with a minimum depth resolution of 0.5 cm. Gravity cores were cut lengthwise after recovery. On the working halves pH and Eh were determined and sample intervals between 10-50 cm were taken for pressure filtration. At sampling locations where methane was expected to be present, syringe samples were taken on deck from every cut segment surface. Occasionally, higher resolution sampling for methane analysis was carried out in the cooling laboratory immediately after storage by sawing rectangles of 4×4 cm into the PVC liner and taking syringe samples of 3 ml sediment every 30-40 cm which were injected into 24-ml septum vials containing 9 ml of a concentrated NaCl solution. After closing and subsequent shaking methane becomes enriched in the headspace of the vial. One replica was taken and poisoned with a saturated NaOH solution for subsequent isotopic analyses.

Each sample depth for pore water squeezing was additionally sampled for (1) the calculation of sediment density and (2) for determination of redox-sensitive elements. Porosity sub-samples were filled into pre-weighed plastic vials and redox samples were kept in specific gas-tight containers under argon atmosphere for subsequent analyses in the home laboratory.

For pressure filtration Teflon- and PE-squeezers were used. The squeezers were operated with argon at a pressure gradually increasing up to 5 bar. Depending on the porosity and compressibility of the sediments, up to 30 ml of pore water were received from each sample. The pore water was retrieved through 0.2 µm cellulose acetate membrane filters.

Pore water analyses of the following parameters were carried out during both cruises: nitrate, ammonia, phosphate, alkalinity, ferrous iron, hydrogen sulfide, chloride, methane, fluoride, silicate, calcium, Eh, and pH. The analytical techniques used on board to determine the various dissolved constituents are listed in

Table 5.8.1. Modifications of some methods were necessary for samples with high sulfide concentrations. Detailed descriptions of the methods are available on

http://www.geomar.de/zd/labs/labore_umwelt/Analytik.html.

Table 5.8.1: Techniques used for pore water analyses.

Constituent	Method	Reference
Nitrate	Autoanalyer / Spectrophotometry	Grasshoff et al. (1997)
Alkalinity	Titration	Ivanenkov and Lyakhin (1978)
Silicate	Spectrophotometry	Grasshoff et al. (1997)
Phosphate	Spectrophotometry	Grasshoff et al. (1997)
Ammonium	Spectrophotometry	Grasshoff et al. (1997)
Chloride	Titration	Gieskes et al. (1991)
Hydrogen sulphide	Spectrophotometry	Grasshoff et al. (1997)
Methane	Gas chromatography	Niewöhner et al. 1998
Ferrous iron	Spectrophotometry	http://www.geochemie.uni-bremen.de/links/links.html
Fluoride	Ion-sensitive electrode	http://www.geochemie.uni-bremen.de/links/links.html
Calcium	Titration	Grasshoff et al. (1997)
pH	Electrode	Dickson (1993)
Redox potential (Eh)	Electrode	-

Nitrate, ammonium and phosphate were measured photometrically (with the help of an autoanalyser in case of nitrate) using standard methods described by Grasshoff et al. (1997). Samples of the sediment pore water for total alkalinity measurements were analyzed by titration of 0.5-1 ml pore water according to Ivanenkov and Lyakhin (1978). Titration was finished until a stable pink color appeared. During titration the sample was degassed by continuously bubbling nitrogen to remove the generated CO_2 or H_2S. The acid was standardized using a IAPSO seawater solution. The method for sulfide determination according to Grasshoff et al. (1997) has been adapted for pore water concentrations of S^{2-} in the range of millimolar amounts. For reliable and reproducible results, an aliquot of pore water was diluted with appropriate amounts of oxygen-free artificial seawater; the sulfide was fixed by immediate addition of zinc acetate gelatin solution immediately after pore water recovery. After dilution, the sulfide concentration in the sample should be less than 50 µmol/l. Chloride was determined by titration with $AgNO_3$ standardized against IAPSO seawater. High concentrations of H_2S (> 1mM) in the sample affect the measurements. Therefore, these samples were pre-treated with a 1:1 dilution of 0.01 N suprapure HNO_3 and stored for 1-2 days, without lid, in a cool room. For the analysis of iron concentrations sub-samples of 1 ml were taken within the glove box, immediately complexed with 20 µl of Ferrozin and afterwards determined photometrically. Fluoride was determined in 1.5 ml sub-samples by an ion-sensitive electrode.

Acidified sub-samples (35µl suprapure HCl + 3 ml sample) were prepared for ICP analyses of major ions (K, Li, B, Mg, Ca, Sr, Mn, Br, and I) and trace elements. Sulfate, DIC, $d^{18}O$ and $d^{13}C$ of CO_2 will be determined on selected sub-samples in the shore-based laboratories.

5.9 Water Column Studies

5.9.1 CTD/ADCP

S. Mau, G. Rehder, K. Stange, M. Inthorn

The CTD/rosette available on R/V SONNE was deployed during cruise SO 173/3-4 to measure physical oceanographic parameters and to collect water samples. The CTD unit consists of a deck unit (SBE 11*plus*) which supports the underwater unit (SBE 9*plus*) and a SBE 32 carousel water sampler equipped with 24*10 l Niskin bottles. The CTD system supplies a modular temperature sensor (SBE 3 plus), a conductivity sensor (SBE 4), a Digiquartz pressure sensor, and an oxygen sensor (SBE 13). An external pump (SBE 5) maintains an optimum and constant water flushing speed for temperature, conductivity, and oxygen sensor via a TC Duct, thus guaranteeing that all sensors measure the same water.

The deck unit provides DC power to the sea cable, decodes the serial data stream arriving from the underwater unit and passes the data to a companion computer. Binary data from the sensors are transmitted serially 24 times a second. The deck unit has a separate communication channel for controlling the Seabird carousel and an audible bottom contact alarm. Acquired data are stored on the computer where post-processing is achieved with the software provided by Seabird.

The CTDunit worked well throughout cruise SO 173/3, but at the beginning of SO 173/4 the data records showed remarkable fluctuations. The sea cable had to be fixed and the sensors exchanged. Due to the latter, a new configuration file was compiled to process the data from the new sensors.

ADCPs (Acoustic Doppler Current Profilers) were deployed in addition to the moorings (see below). A downward-looking 330 kHz ADCP was attached to the carousel water sampler with a clamp (Fig. 5.9.1), recording data while the water column was sampled at vent sites. The data will be post-processed together with navigation data of the ship using software by M. Visbeck (IFM Kiel). These results will be very valuable for methane flux calculation, because water samples and oceanographic parameters were collected exactly at the same time.

5.9.2 BWS

The BWS (Fig. 5.9.2) is a new sampling device which was particularly designed to collect water samples from different levels above the seafloor which are out of reach of a standard rosette water sampler. It consists of a three-footed frame with an additional central axis which is revolvable against the frame. Five 5-liter Niskin bottles are attached to this axis horizontally and can be shifted between 10 and 120 cm above ground. For deployment the whole device is attached to a rope via a revolvable connector. Both the frame and the inner axis have current-sails which turn the Niskin bottles directly into the current. This is necessary to avoid any influences of turbulences developing from parts of the frame on the particle-flow. A burn wire system connected to a timer which is programmed before deployment closes the Niskin bottles at a specified time after bottom contact. We set a waiting time of 45 minutes to ensure that all the material which had been resuspended during deployment of the device was redeposited or had drifted away.

A pinger was attached to the rope 30 m above the BWS. The signal of the pinger made it possible to stop the BWS for a couple of minutes 5 to 10 m above the seafloor (depending on the wave and wind conditions) to give it some time to adjust to the current conditions close to the seafloor.

Another 20 m above the pinger, two floats were attached to the rope, which made it possible to let the

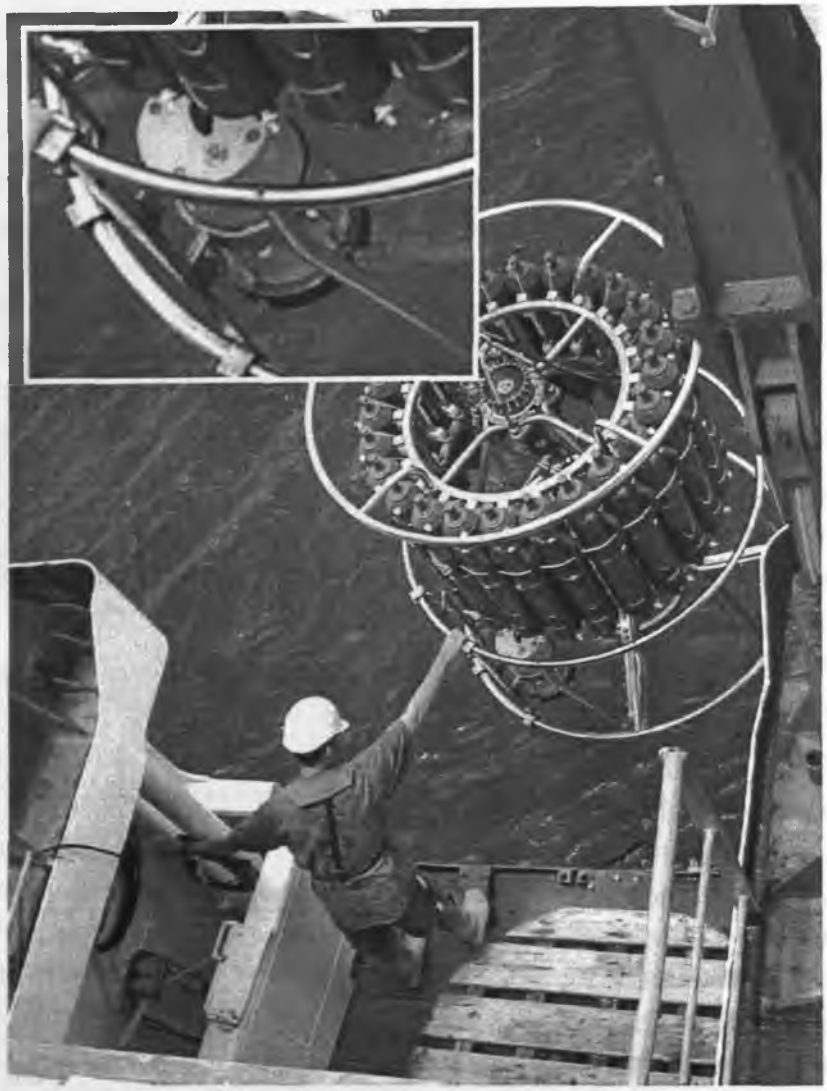

Fig. 5.9.1: CTD/rosette aboard R/V SONNE equipped with a 300-kHz ADCP (Acoustic Doppler Current Profiler, RDI).

rope hang loosely in the water without the risk of the slack rope winding around the BWS. This way it is ensured that ship movements will not directly result in movement of the BWS, which would involve artificial sediment resuspension.

5.9.3 CH_4 and O_2 analyses

Water for methane and oxygen analyses was sampled by the CTD/rosette and the BWS provided by RCOM Bremen. The ship's own SSBL transponder was attached to the cable about 30 m above the instruments, which allowed exact positioning and water sampling above seepage sites.

In addition to the oxygen sensor of the CTD, the Winckler titration (Grasshoff et al., 1997) was used for determination of the oxygen content. Usually, three Niskin bottles were sampled twice to control reproducibility of the measurements. The data of the oxygen sensor and the measured data display a linear correlation expressed by the formula y=1.11x+0.12 (x=sensor data, y=measured data). If no data were available from titration, the sensor data were corrected using this formula.

For CH_4 analysis aboard, a modification of the vacuum degassing method described by Lammers and Suess (1994) was used (Rehder et al., 1999). 1600 ml of water were injected into pre-evacuated 2200-ml

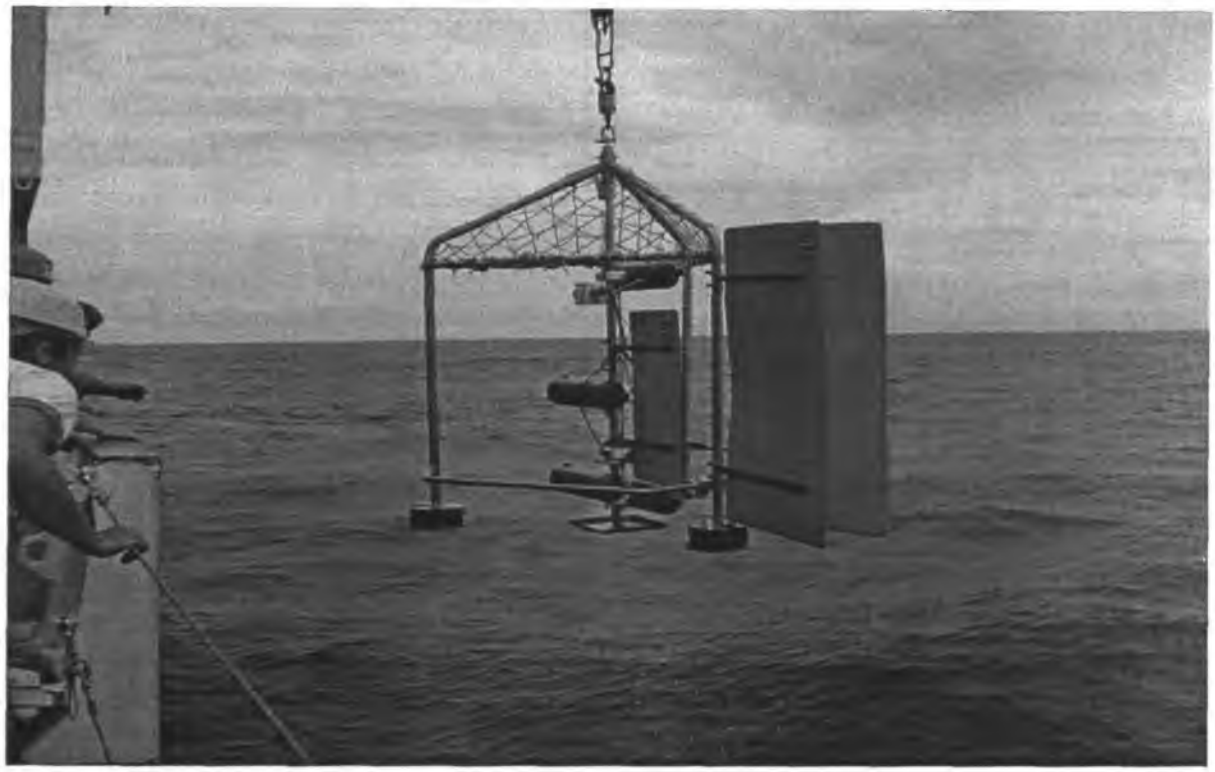

Fig. 5.9.2: *Bottom Water Sampler (BWS) deployment.*

glass bottles, which leads to almost quantitative degassing. The gas phase was subsequently recompressed to atmospheric pressure and the CH_4 mole fraction of the extracted gas was determined by gas chromatography. A Shimadzu GC14A gas chromatograph equipped with a flame ionization detector was used in connection with a Shimadzu CR6A integrator. Nitrogen was used as carrier gas. Separation was achieved using a 4 m 1/8' SS column packed with Porapack Q (50/80 mesh) run isothermally at 50 °C. The total gas content of the sample was calculated from the measured dissolved oxygen concentration assuming that N_2 and Ar are 100% saturated relative to their atmospheric partial pressures (Weiss, 1970). The dissolved methane concentration was estimated as the product of the mole fraction in the extracted gas phase and the amount of total gas (STP) in the sample. For calibration, mixtures of 1.936 ± 0.003 ppm and 9.854 ± 0.006 ppm of synthetic air (Deuste Steininger, calibrated against NOAA/CMDL standards at the Institute for Environmental Physics, Heidelberg) were used.

At newly discovered vent sites, two sets of 250-ml water samples were filled into crim cap glass bottles sealed with a butyl rubber septum and poisoned with 0.5 ml of a saturated Hg(II)Cl solution. These samples will be transported to Kiel at 4 °C for further analyses. One set will be used to measure methane concentrations with a standard purge and trap technique for intercomparison. The other will be used for the analysis of the stable carbon isotopic ratio of methane ($\delta^{13}C$) using the new MAT 253 Mass Spectrometer.

5.9.4 Moorings

Moorings were deployed in the vicinity of geological structures that showed signs of active seepage to obtain ocean current velocity and direction in order to calculate the methane flux of these sites. Each mooring was equipped with an anchor, two Aanderaa-current meters (RCM 8) provided by IFM Kiel, two acoustic releaser devices and subsurface floating units (Fig. 5.9.3). Benthos spheres were attached to

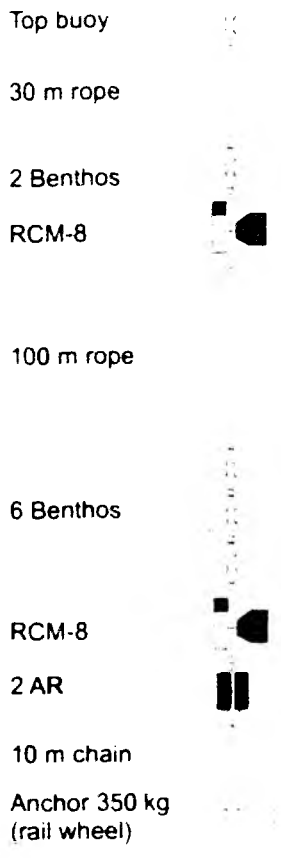

Fig. 5.9.3: Mooring used during SO 173/3-4 with its components (rope - METEOR nylon string, RCM - Aanderaa Recording Current Meter, AR - Oceano Acoustic Releaser). The total length is about 140 m

METEOR ropes above each instrument to keep the mooring straight in the water column during deployment. At each location current meters measured at about 10 m and 120 m above seafloor.

The current meters are self-recording instruments, obtaining and recording the vector-averaged speed and direction. The current direction sensor is a magnetic compass and the current speed sensor is a rotor with a magnet at its lower end. The energy for the current meter is provided by a battery, which must be non-magnetic due to its vicinity to the compass. A built-in quartz clock triggers the measuring cycle at regular, programmable intervals. During this cruise, there was always used a one-minute interval. The data are recorded internally in a removable and reusable solid-state Data Storage Unit (DSU) (Operating Manual of Aanderaa Instruments, 1995).

Five moorings were deployed in the area of mud extrusions (Mound Culebra and Mound 12) and scarps created by seamount subduction (Jaco Scarp). Two of them were positioned SE and NW of Mound Culebra and one NW of Mound 12, because ADCP data collected during 2002 suggest that SE is luff and NW is lee of the mounds. Instead of a further mooring SE of Mound 12, a lander device equipped with a 75-kHz ADCP was deployed. The moorings stayed at Mound Culebra from September 12th to 14th, and the one at Mound 12 from September 23rd to 27th. Two more moorings were placed in Jaco Scarp, one close to the head wall of the scarp and one on its south-eastern rim, from September 16th to 23rd. During the time of deployment methane was analyzed in water samples at these sites.

5.9.5 Equilibrator

The methane concentration in surface waters and the overlying marine air was continuously surveyed during the entire cruise using a fully automated, semi-continuous seawater-air equilibrator (Rehder et al., 2001). The equilibration system is equipped with an additional temperature sensor to record the temperature within the equilibration chamber. The survey was performed during the complete cruise. Interruptions data gaps only occured during the first days due to analytical problems, and for some hours during which the clean seawater pumping system had to be exchanged. All accompanying data, including ship's thermosalinograph data, meteorological data, ship's position, time, and nautical data, were extracted in real time from the DVS data. Some hours lacking the accompanying data resulted from a complete breakdown of the ship's DVS system. All data were recorded and merged automatically, using a new software developed by J. Greinert within the EU project CRIMEA.

For the determination of the atmospheric mole fraction of CH_4 in marine air and surface water CH_4, we used a fully automated, semi-continuous system based on gas chromatography, adapted to shipboard operation [Rehder et al., 2001; Bange et al., 1994; Weiss, 1981]. Samples of either calibration gas, marine air continuously pumped from the ship's bow, or air equilibrated with a continuous flow of seawater are sequentially shunted into a thermostated, 10-port valve via a flowmeter and Sicapent™ drying agent. About 80 ml of gas sample are flushed through the sample loop (2 ml) before the sample valve is rotated. N_2 is used as carrier, gas separation is provided by a 4 m 1 8-inch stainless steel-packed column filled with Porapack QS (mesh 50/80), and methane is detected using an FID. The sequence used for the analysis of the gas is in general CG1-E-A-E-CG2-E-A-E, where CG1 and CG2 are the calibration gases, E is the air equilibrated with surface seawater, and A is the atmospheric air sample. Two calibration gases were used, containing 9.8392 ± 0.003 ppmV CH_4 in N_2 and 1.9333± 0.003 ppmV CH_4 in N_2, respectively. The time for a single measurement is 10 min, which yields atmospheric values every 40 min and values for the equilibrated air every 20 min. The reproducibility was 0.01 ppmV for methane, based on multiple measurements of the certified calibration gases. Integration is performed using a Shimadzu CR6A integrator, and data of GC measurements. The integrated peak area, temperature in the equilibration system, GPS data and CTD data were stored in one file.

The determination of CH_4 in surface seawater is based on the equilibration of a re-circulating gas phase with a counter-current flow of continuously renewed seawater. The gas enters the equilibration vessel (about 2 l) from the bottom at a flow rate of about 1.5 l/min and is dispersed into small gas bubbles through a coarse glass frit. A 45-cm glass column is mounted on top of the equilibration vessel. The seawater inlet is installed on the top of the column, providing a laminar flow along the inner walls of the column (about 2,5l/min). The air leaves the equilibration chamber at the top of the column and is re-circulated via a backpressure regulator and a flowmeter. A vent to the atmosphere assures equilibration at ambient pressure. The entire glass apparatus follows a design described by Körtzinger et al. [1996] and is a combination of a 'bubble type' and 'laminar flow' equilibrator. However, the volume of both water and air phase in the system is larger by about a factor of 2, as the detection by gas chromatography requires the consumption and replacement of a part of the gas phase. When a sample of equilibrated air is taken from the system, an electronic valve closes the vent to avoid immediate replacement of the sampled air. This results in a slight underpressure in the system, which can be seen as an increase of the water level in the chamber, which however is less than 0.4 mm (i.e. the pressure drop is less than 0.4 ‰ of the total). In addition, the equilibration time is long compared to the flushing time of the sample loops. Hence, the effect has a negligible influence on the quantity measured. The valve opens after the sample is taken, and the

time between two measurements of the equilibrated air (20 min) is sufficient to allow replacement of the removed air via the vent and re-equilibration of the gas phase

Gas chromatographic analysis provides the mole fractions of CH_4 in dry air, x_{CH4}. The concentration of dissolved methane and the expected equilibrium values derived from the ambient air partial pressure will be calculated according to the equation of Wiesenburg and Guinasso, [1979]

$$\ln C = \ln f_{CH4} + A_1 + A_2(100/T) + A_3 \ln(T/100) + A_4(T/100) + S[B_1 + B_2(T/100) + B_3(T/100)^2] \quad (1)$$

where C is the equilibrium solubility in nmol l^{-1}, f_{CH4} the partial pressure in the gas ($P \cdot x_{CH4}$), T the absolute temperature, S the salinity, and A_n and B_n are constants. The equation allows the calculation of the CH_4 concentration from the mole fraction in dry air under the assumption that the ambient air is 100% water vapor-saturated. The same equation will be used to account for the solubility change due to the temperature shift between the sea surface and the equilibrator. To determine the saturation state of the surface waters, the oversaturation is calculated as

$$OS = (C_w - C_{air}) / C_{air} \cdot 100 \quad (2)$$

where C_w and C_{air} are the gas concentrations of the seawater and the calculated concentration in equilibrium with the ambient atmospheric partial pressure, respectively.

5.10 Kiel in-situ Pump (KISP)

The KISP system allows the in-situ filtration of suspended matter in depths of up to 3000m. It was used to sample the benthic boundary layer for methane oxidizing bacteria. For better sampling results the KISP was attached to a TV-guided multicorer.

The main parts are the filter holder (1 in Fig. 5.10.1), the battery pack (2), the electronic unit (3), the resin column (was not used), the pump (5) and the flow controller meter (6).

A pressure compensation technique is used, allowing constant flow rates with depth. The operation of the unit is controlled by software (PC) and all essential data are recorded for later evaluation. The built-in computer controls and records flow rates and the times and duration of pumping. The energy is supplied by battery packs. The number of battery packs determines how much water can be filtered. Filter clogging may be the limiting factor in turbid waters.

The details of the system are as follows:

Frame and housing of pump, electronics and power packs are made of stainless steel. The total weight is 70 kg in air, about 60 kg in water.

Pump motor and pump head form a separate unit. The pump motor is situated in a glass-reinforced PVC housing that is filled with turpentine oil. It is separated from the surrounding water by a diaphragm to keep it at in-situ pressure at all times.

The pump head is a three-step gear motor made of Ryton. It is magnetically connected to the pump motor within the housing. It produces a pressure of 3.5 bar at 4000 ml/min.

The pumping rate can be selected and kept constant between 1 and 200 dm^3/h. The filter used was a 0,4µm glass fiber filter with a diameter of 14 cm.

Electronic control: the software calibrates and controls the pumping rate, the times of start and end of pumping, records the volume sampled, the flow in user-selected time intervals and documents the battery condition at all times (Petrick at al. 1996).

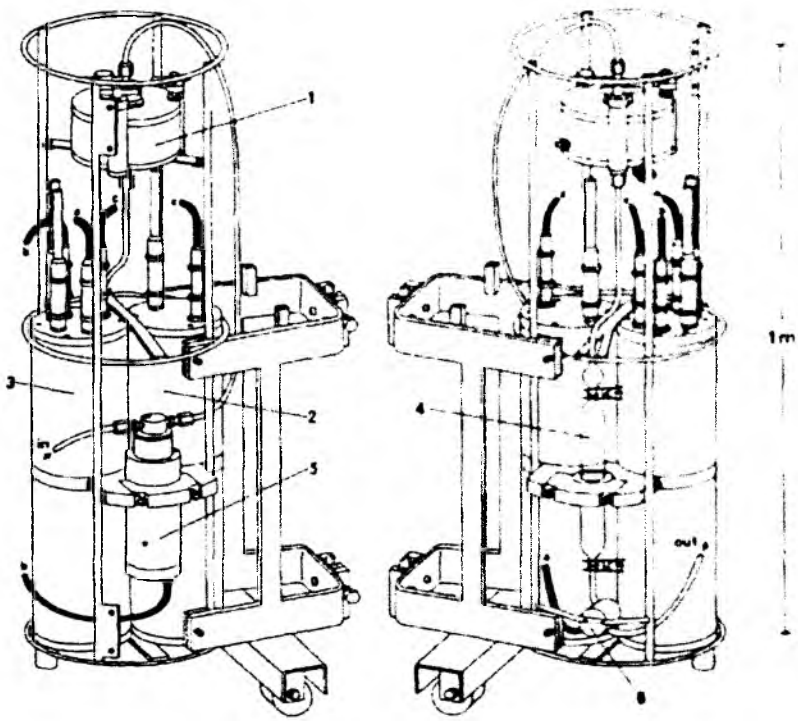

Fig. 5.10.1: *In-situ pump. 1 = filter holder; 2 = standard power pack housing; 3 = housing for electronics, 4 = resin holder (was not used); 5 = pump; 6 = flow rate counter a, b, c = cable connections*

5.11 Radionuclide Measurements: ^{222}Rn

As a contribution to fluid flux estimations for the recent venting activity, the on-board analyses of short-lived isotopes were continued in a refined sampling approach, integrating new lander technology and pore water profiles. Radioisotopes of the natural uranium-thorium decay chains are supplied to vent fluids and pore waters by water sediment-, water rock-interaction and by alpha recoil. Apart from the chemical composition of the sources the concentration of the radionuclides in the vent fluids depends to a larger extend on the transit time between the reaction zone and the discharge zone at the sediment surface. By measuring e. g. ^{224}Ra ($T_{\frac{1}{2}}$ = 3.6 d), ^{222}Rn ($T_{\frac{1}{2}}$ = 3.8 d), ^{223}Ra ($T_{\frac{1}{2}}$ = 5.7 a) and ^{226}Ra ($T_{\frac{1}{2}}$ =1600 a), information on vent fluid residence times and discharge rates can be estimated. Based on experiences from cruise M54 3a, where measurements of ^{224}Ra and ^{226}Ra suggested that fluid venting at the investigated sites was too low to be quantified by the applied Ra methods, the on-board radioisotope program of So 173 3-4 was focussed on the ^{222}Rn method with sampling extending from bottom water towards pore water profiles.

During SO 173 3-4 samples for on-board radionuclide measurements were obtained by means of CTD, BWS, TV-MUC, FLUFO and BCL. The lack of the VESP sampling system, due to electronic communication problems between former and state-of-the-art control devices, was partially compensated by FLUFO and BCL deployments. In contrast to FLUFO and BCL the bottom time of the towed VESP sytem is in general restricted to 90 minutes, providing 10-l samples of up to 5 different time intervals of fluid enrichment. However, results of cruise M54 3a have shown, that the enrichment factor at over 90 min was very close to the detection limit at the sites investigated. The time-resolved syringe sampling system of FLUFO and BCL could not provide the required sample amount due to the size of the syringes and the established preferences in aliquot strategy for the different subprojects. Nevertheless, the FLUFO and BCL lander were recovered with their main chambers containing for the first time enough material for ^{222}Rn analyses of 20 hours enriched bottom water from active vent sites off Costa Rica, including several centimeters of the underlying sediment.

For ^{222}Rn analysis of bottom water samples one liter of water was filled into an extraction apparatus and a water-immiscible scintillation cocktail (MaxiLight) was added. The sample was shaken for 1.5 hours and the organic phase was transferred into a low diffusive LS-vial which was stored three hours for isotope equilibration. Pore water sampling was performed parallel to the procedure carried out by the pore water group in the low-temperature lab container. Approximately 25 ml of soft sediment were transferred into a 50-ml beaker and immediately covered with 23 ml of the water-immiscible scintillation cocktail (MaxiLight). The beaker was closed tightly and sealed. This procedure was directly followed by centrifuge phase separation over 15 min at 3000 rpm. Scintillation cocktail and water were transferred into low diffusive vials by a layering technique which always keeps a layer of scintillation cocktail on top the sample. From that point on the procedure follows the description for 1-l bottom water samples.

Two liquid scintillation counters (Guardian and Triathler) were available for on-board ^{222}Rn measurements. Samples were counted for six hours. In order to determine $^{222}Rn_{excess}$ concentrations the samples must be back-measured in the home lab after the decay of unsupported ^{222}Rn is finished. Last measurements, final method calibrations and data reduction are topics of the actual laboratory routine.

5.12 Lander Deployments

P. Linke, M. Pieper, M. Poser, W. Queisser, S. Mau, K. Stange

Landers, as autonomous instrument carrier systems, are used to study processes at the benthic boundary layer. They are usually deployed on the seafloor at depths of several hundred to 6,000 meters beyond the reach of remote sensing and conventional systems. After a lander has reached the seafloor in free-fall mode an onboard command system starts a deep-sea experiment. At the end of the mission an acoustic command releases the ballast weights and the lander rises to the sea surface by virtue of its positive buoyancy.

Whereas landers are typically deployed in conventional free-fall mode, many scientific objectives addressing specific geomorphological features such as cold seeps, mud mounds or particular benthic communities require a targeted and soft lander deployment. For these requirements the concept of a targeted lander deployment with a special launching device connected to the ship's coaxial or hybrid fibre optical cable was developed. This launcher carries the telemetry, cameras, lights and an electric release to separate the GEOMAR Modular Lander (GML) from the launcher.

The GML itself provides the platform for various research activities and addresses integrated benthic boundary layer current measurements, quantification of particle flux, quantification of gas flow by acoustic bubble size imaging, monitoring of mega-benthic activity, fluid and gas flow measurements at the sediment-water interface, biogeochemical fluxes at the sediment-water interface (oxidants, methane nutrients), experiments with deep-sea sediment and organisms (food enrichment, tracer addition, change of physical and chemical environmental parameters) and gas hydrate stability experiments (Pfannkuche & Linke, 2003). The basic frame of the GML is a stainless steel or titanium tripod that carries a number of Benthos glass spheres for buoyancy on top and ballast attached by release toggles to each of the three legs. The ballast is controlled by two acoustic release units that provide parallel redundancy; a radio beacon and strobe aid in relocation at the surface, and an ARGOS system helps in tracking the lander in case of a premature release.

During cruise SO 173/4 three landers were used. Whereas the Benthic Chamber Lander (BCL) and the Fluid Flux Observatory (FLUFO) were deployed in video-guided mode with a launcher connected to the ship's coaxial cable, the LongRanger (LORA) was deployed in the conventional free-fall mode.

5.12.1 Long Ranger (LORA)

The Long Ranger Lander (LORA) was equipped with an upward-looking 75 kHz ADCP (RD Instruments) and a 3-axis MAVS current meter (NOBSKA). The lander was partly used in combination with or instead of a current meter mooring since the low frequency ADCP can cover a depth range of hundreds of meters in contrast to current meters which cover just one depth. LORA was deployed SE of Mound Culebra over a period of one day and SE of Mound 12 over a period of three days.

5.12.2 Benthic Chamber Lander (BC-L)

In-situ flux measurements were performed with a benthic chamber lander (BCL, Witte and Pfannkuche, 2000). On cruise SO 173/4 the frame was equipped with three squared Delrin chambers (20 x 20 cm) sitting in a stainless steel frame that was attached to the lander. Each chamber is an autonomous module with its own control unit and power supply with rechargeable NiCd-battery packs (6 V, 10 Ah) integrated in a Benthos glass sphere. The chambers are driven slowly into the sediment by a motor approx. 1 h after deployment in order to allow any resuspension plume to be swept away and/or settle. After

implementation of the chamber the lid is closed; each lid carries a central stirrer. At the end of each incubation a shutter at the bottom is closed by a second motor to retrieve the incubated sediment. Once the shutter is closed the chamber is slowly heaved out of the sediment by the first motor and the lander is ready for recovery. During each incubation, a syringe water sampler is attached to each chamber. It is equipped with seven glass syringes which obtain water samples of 50 ml each from the overlying water at pre-set intervals. The volume drawn by each syringe is replaced by ambient bottom water.

Oxygen concentrations were determined with two replicated Winckler titrations (Grasshoff et al., 1997) of each syringe water sample when a sufficient sampling volume was available.

Methane concentrations were analysed by adding 12 ml of water from the syringe sampler to 1.5 g of salt into 24-ml septum vials. The crim cap vials were closed and shaken for several minutes to allow a complete dissolution of the salt and transfer of the dissolved gases into the air headspace. The methane mole fraction in the headspace was determined by injecting a sample of the gas into a Shimadzu GC 14 A GC equipped with an FID and a 4m 1/8' Poraplot Q (mesh 50/80) packed column. 3 blanks were analysed by injecting water previously degassed under vacuum. The blank is basically introduced by the air phase with an atmospheric mole fraction of 1.8 ppmV. Methane concentrations of the water were calculated from the mole fraction of methane in the headspace gas.

As the chambers retrieved the sediment, the sediment depth and the height of the overlying water were measured to determine the volume of the enclosed water body. Push corers were used to subsample the retrieved sediments in the chambers of the lander. All sediment cores were immediately placed in a cooling room and kept at a temperature of about 4°C to prevent warming after retrieval.

5.12.3 Fluid Flux Observatory (FLUFO)

FLUFO was designed to quantify the different types of fluxes at the benthic boundary layer of sediments overlying near-surface gas hydrates and monitoring relevant environmental parameters such as temperature, pressure and near-bottom currents. The development and application of the FLUFO-System were part of the LOTUS project. Responsibilities for construction and application of the technical sub-systems were shared by Geomar (FLUFO-lander / FLUFO- peripherals) and TUHH / MT1 (FLUFO chamber units). FLUFO is equipped with two large (30 cm in diameter) circular benthic chambers.

The first (FLUFO) chamber unit separates the gas phase from the aqueous phase and measures their individual contribution to the total fluid flux including the flow direction. By switching a central valve, the FLUFO Chamber Unit can operate in 4 different modes:

1. Leakage test of the chamber / measurement of permeability of the sediment
2. High-resolution fluid flux measurement (0,1 – 60 ml/min)
3. Average resolution fluid flux measurement (50 – 1000 ml/min)
4. Simulation of the external current regime

The second chamber served was not equipped with such a system and is referred to as "control chamber". Each chamber was equipped with a syringe water sampler with seven glass syringes which obtain water samples of 50 ml.

Furthermore, FLUFO was equipped with a storage CTD (SBE 16plus SEACAT) and an upward-looking 1,200-kHz ADCP to monitor the environmental parameters.

6 Work Completed and First Results

6.1 Hydroacoustic Work - Multibeam Swathmapping

J. Bialas

The Simrad EM120 multibeam system was operated throughout SO 173/1. During transit and along the wide-angle profiles the beam angle was set to 120° in order to cover the widest range. During deep tow surveys the dense line grid was used to reduce the beam width to 45° or even 30°. Together with a slow speed of max. 3 kn this choice enabled a high-resolution coverage in the areas of Mound 11&12, the BGR slide, mound Culebra, and offshore Nicaragua, which provides a good complement to the existing data sampled less densely. Due to a limited availability of manpower these data have not been processed further onboard. The figures displayed have been provided by the WTD of R/V SONNE.

Bathymetry data of mounds 11&12 (Fig. 6.1.1) reveal that the smaller mound, mound 11, is surrounded by a slight depression. Two small mound-like structures are imaged on the southern flank of mound 11. The more pronounced mound, mound 12, rises some 130 m above the surrounding seafloor. No seafloor depression is recognized in the vicinity of mound 12. Both mounds cover an area of about 0.1 by 0.1 nm .

The BGR slide was traversed by several slope-parallel lines (Fig. 6.1.2). The slide covers an area of 0.1 by 0.3 nm. The headwall scarp, located at a water depth of about 600 m, does not form a unique circle but is separated into three parts. Each of them is located at a different depth, the shallowest, along the western rim, extends almost 100 m further upslope. The top of the sliding mass is offset about 75 m downslope from the scarp. Its outer border maintains the scarp morphology across both the center and eastern rim.. The western part of the slide did not preserve the finger-like shaped outline. Moreover the ridge-like western rim abruptly terminates at the height of the central headwall scarp, giving room for potentially following slumps to drain material to the west. This suggests that material from the finger-shaped part of the western margin slumped prior to the central and eastern part of the BGR slide.

A NW-SE trending deep tow survey was undertaken above the Culebra Mound (Fig. 6.1.3). This high-resolution survey provides a much clearer map of the Culerbra area than was available from METEOR M 54 Hydrosweep data collected prior to this cruise. Toby sidescan data suggested a NW-SE trending fault SE of mound Culebra; high-resolution Simrad EM 120 multibeam data collected on this cruise were able to clearly resolve the image.

The final 6 days of SO 173/1 were dedicated to a survey off Nicaragua (Figs. 6.1.4 - 6.1.7). Again, the swath width was reduced and additional Simrad system filter routines were applied. In this region an earlier survey during SO 163 had revealed several mound-like structures and two large slide areas. Due to the limited resolution of the Hydrosweep system and uncovered patches the interpretation of these features remained questionable. With the new deep tow system many possible mound structures could be identified and covered by Simrad and sidescan observation. The largest feature ("mound") was found to rise about 250 to 350 m above the surrounding seafloor, much higher than mound Culebra, the highest mound imaged in Central America. If the tentatively identified mound-like structures recognized offshore Nicaragua are confirmed by later processing, then this area will have a greater mound density than that recognized off Costa Rica.

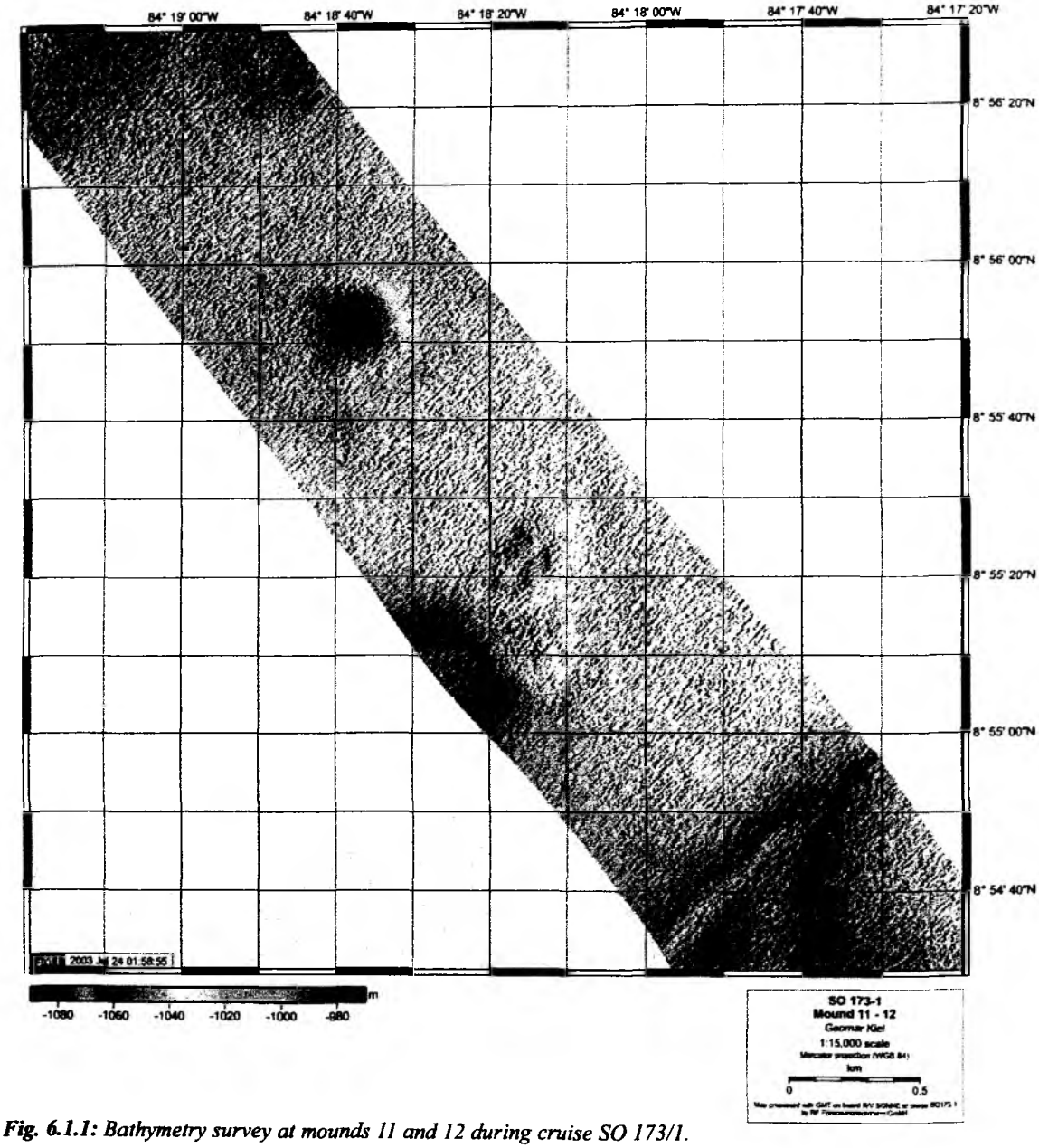

Fig. 6.1.1: Bathymetry survey at mounds 11 and 12 during cruise SO 173/1.

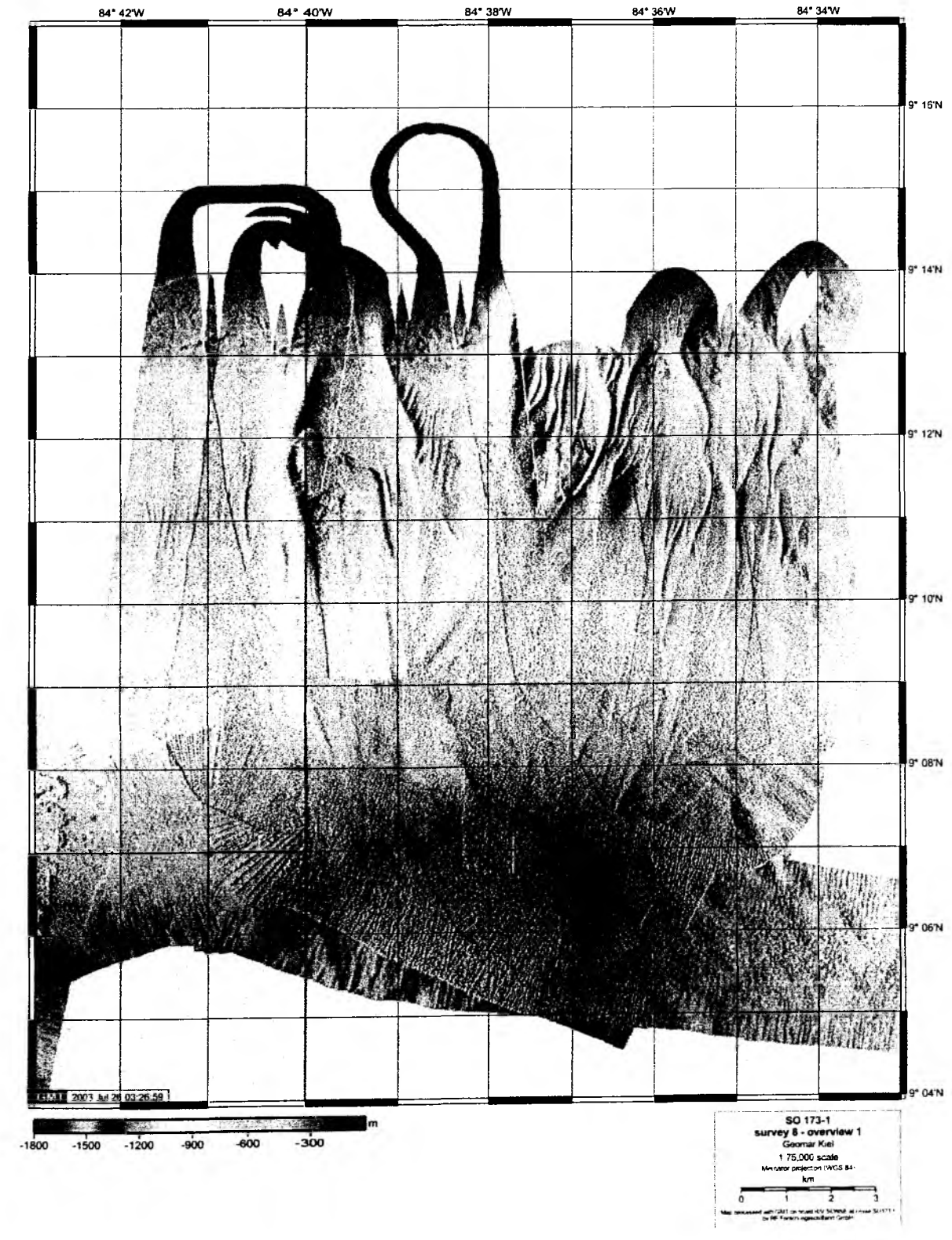

Fig. 6.1.2: *Bathymetry survey at BGR and GEOMAR slides during cruise SO 173/1.*

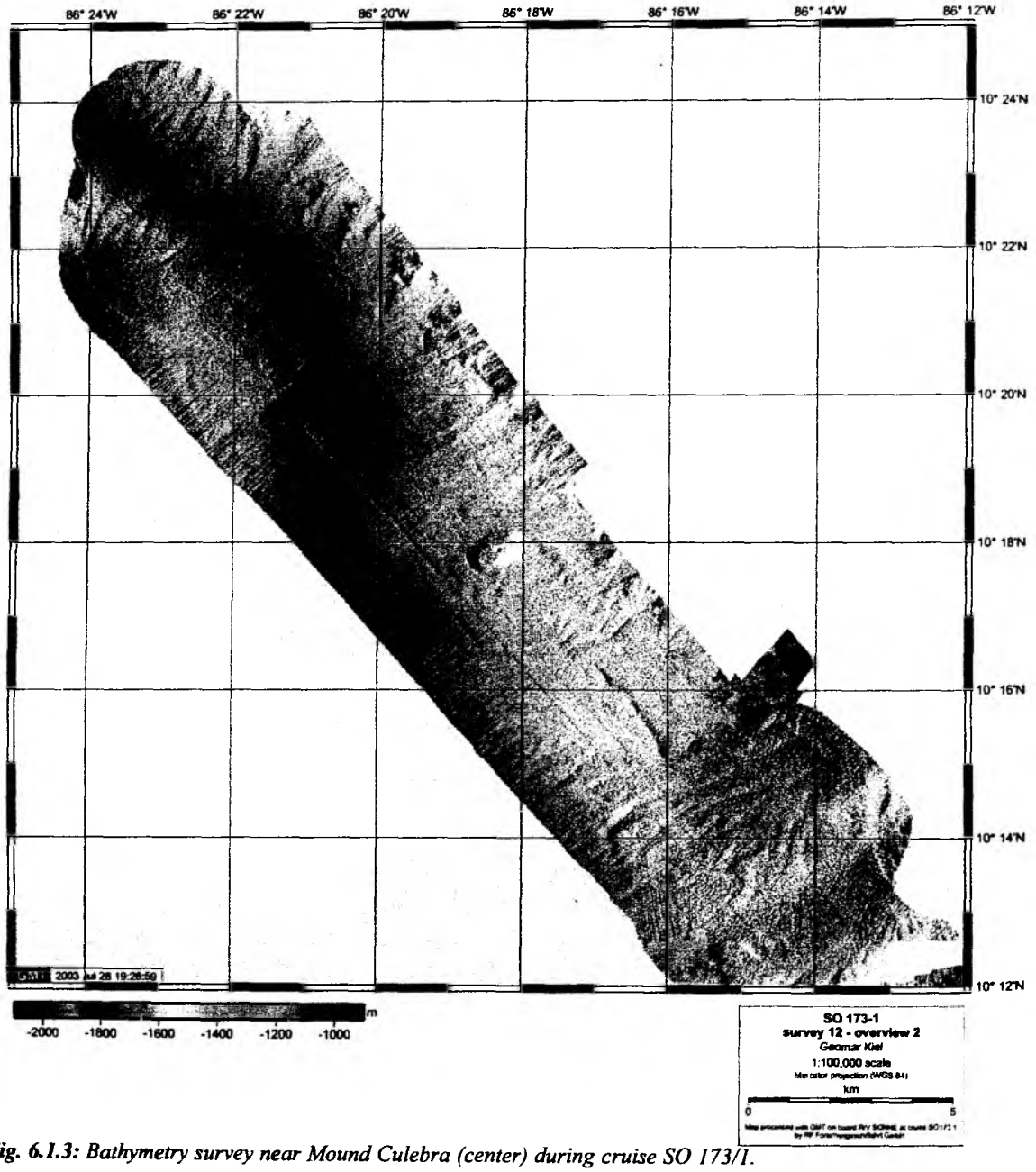

Fig. 6.1.3: Bathymetry survey near Mound Culebra (center) during cruise SO 173/1.

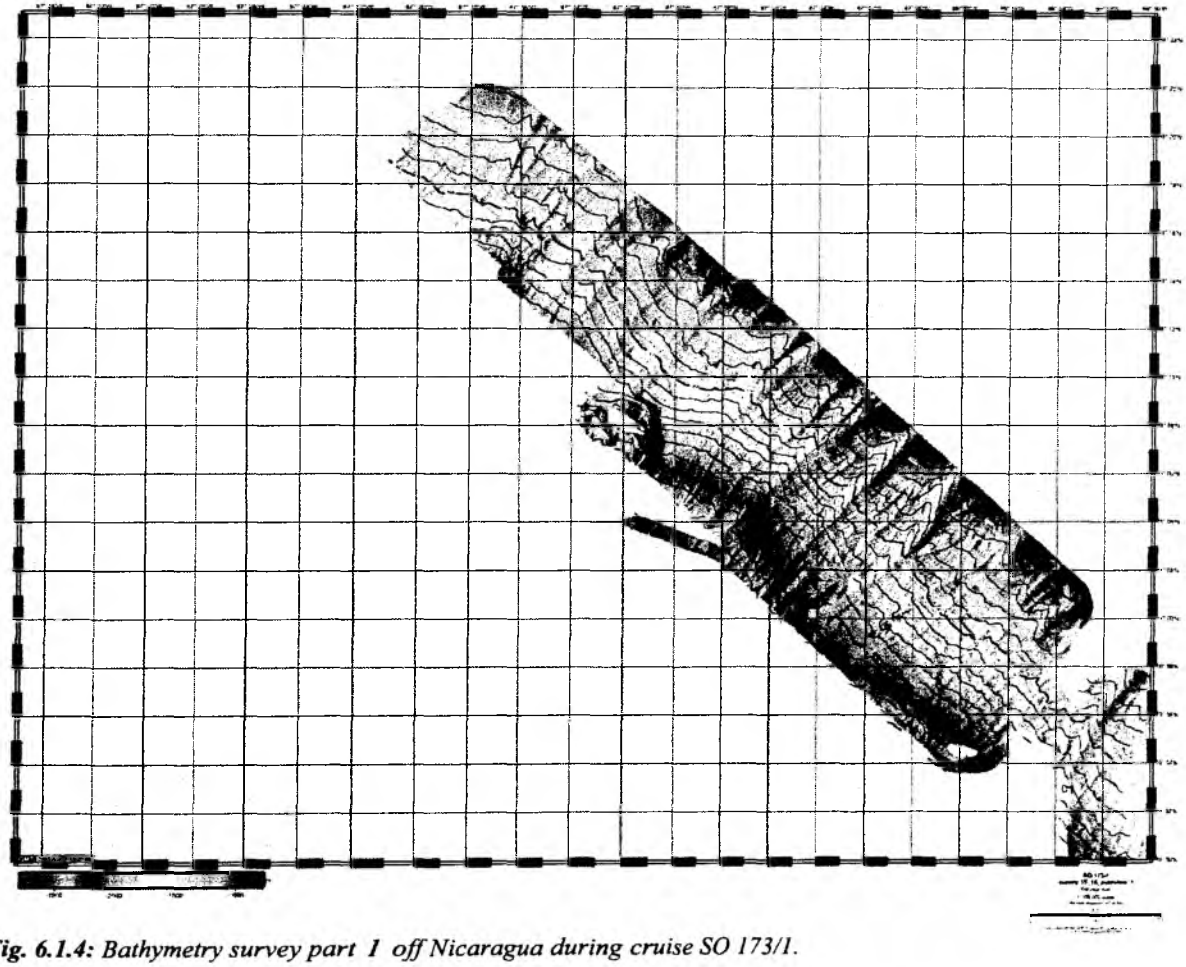

Fig. 6.1.4: Bathymetry survey part 1 off Nicaragua during cruise SO 173/1.

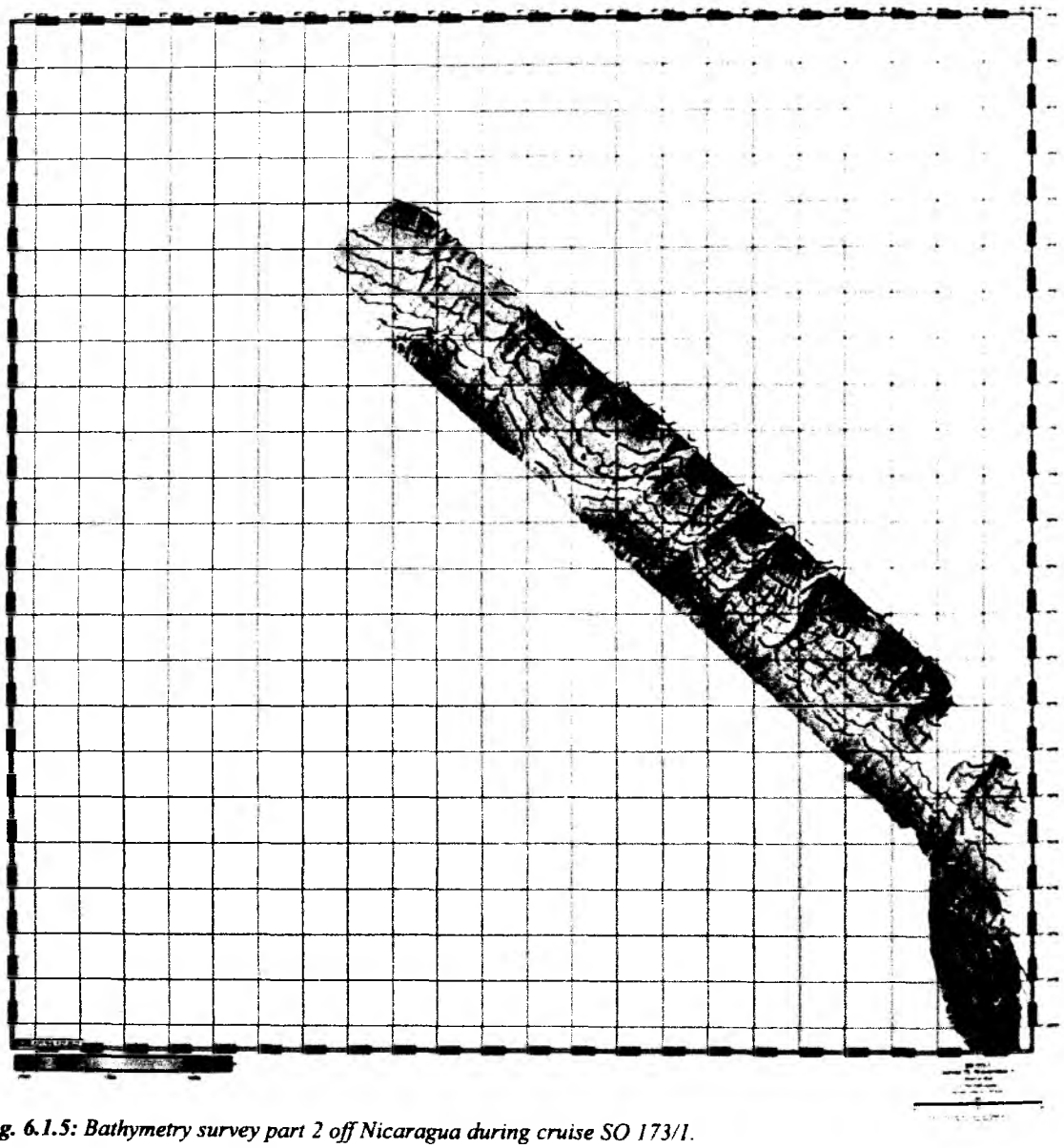

Fig. 6.1.5: Bathymetry survey part 2 off Nicaragua during cruise SO 173/1.

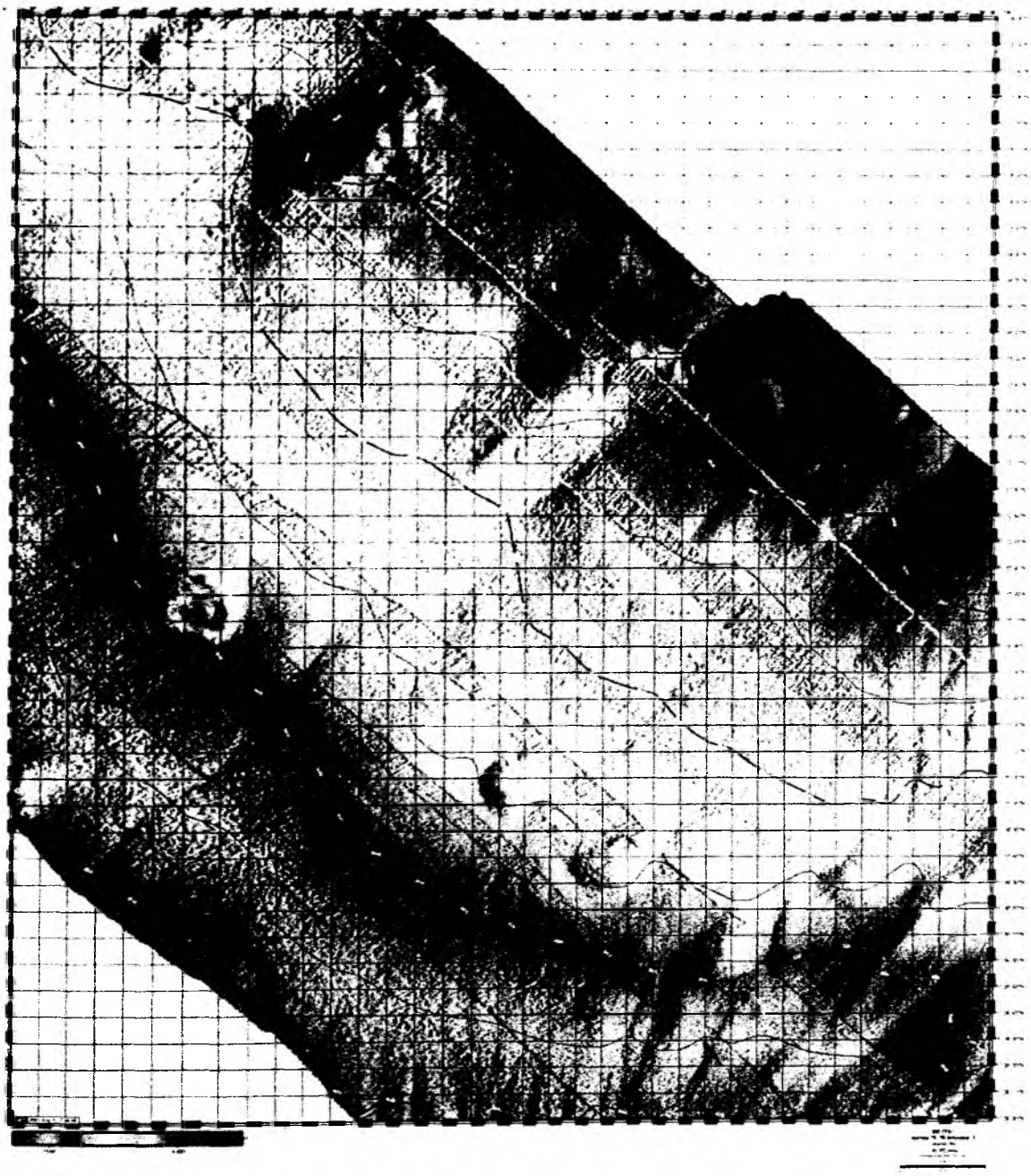

Fig. 6.1.6: *Close-up with mounds Baula, Quetzal, Buho, Hormiga and Iguana from the bathymetry survey off Nicaragua during cruise SO 173/1 (see chapter 6.5. for descriptions of the mounds).*

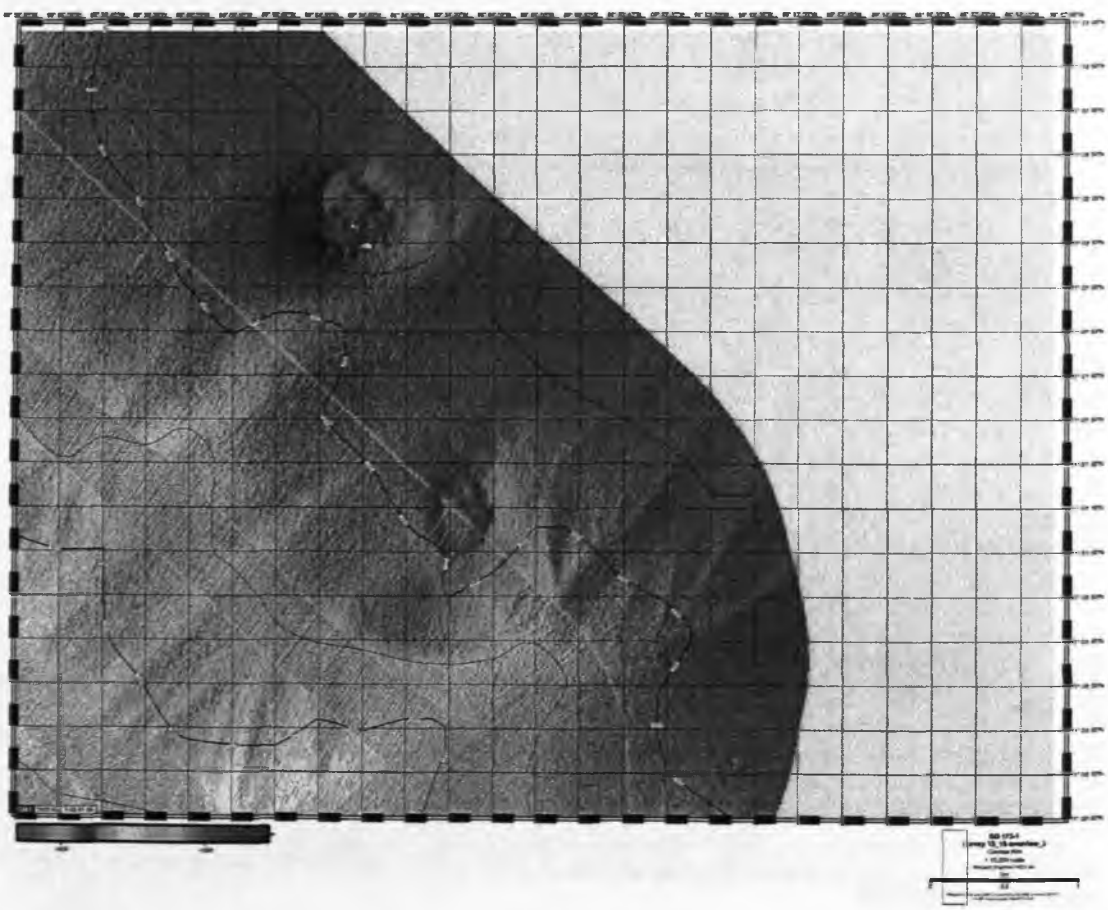

Fig. 6.1.7: Close-up of an unnamed mound from the bathymetry survey off Nicaragua during cruise SO 173/1.

6.2 Deep Tow Acoustic and Seismic Investigations

The deep towed sidescan sonar and seismic streamer system was deployed six times during R/V SONNE cruise SO 173/1. These deployments lasted from a few hours to 5.5 days and had some rather different objectives, including imaging of the decollement, detailed mapping of mounds, identifying the relationship between the limit of the gas hydrate stability zone and sediment failure on the upper slope, and surveying a large part of the Nicaraguan continental slope looking for new fluid escape-related features.

6.2.1 DTS-1 Sidescan Sonar Imagery

I. Klaucke, J. Bialas, M. Breitzke, D. Buerk, N. Fekete, E. Flueh, C. Papenberg, C. Ranero

6.2.1.1 Deployment 1: Decollement

The main purpose of this first deployment of the DTS-1 system was seismic imaging of the decollement offshore Costa Rica near 8°35'N, 84°20'W, Sidescan sonar imaging was only a by-product. However, the opportunity of this deployment lasting from July 18, 2003, 23:19 to July 19, 2003, 13:05 was welcome in order to search for features on the seafloor that might be related to fluid escape structures. Three strike-parallel and two dip-parallel profiles were covered(Fig. 6.2.1).

Most of the sidescan sonar data show numerous structures that are related to bathymetric ridges and depressions. They are part of the deformation front. In some places they are cut by canyons and gullies. Peculiar backscatter patches that could hint at fluid escape structures have been found in only a few places and there is also one area showing returns from within the water column (Fig. 6.2.2.). At this stage one can only speculate that these features might represent fluid flow from the underlying sediments, but only direct observation and measurements can confirm or refute this idea. In theory, the water should be too deep here in order for bubbles to form and persist in the water column, but highly concentrated brines would also be visible by 75-kHz sidescan sonar.

6.2.1.2 Deployment 2: Mounds 11 & 12

The second deployment of DTS-1 was designed to study in more detail two mounds (mounds 11 and 12) situated in the southern part of the study area between 8° 55' and 8°57'N and 84°18' and 84°20'W (Fig. 6.2.3.). These mounds had already been studied extensively for their geochemistry during cruise METEOR M 54/2-3, but their precise structure and geological setting was hitherto unknown. The mounds only extend a few hundreds of meters across and are less than 25 m high. The original plan was to run several parallel profiles crossing the mounds together with profiles perpendicular to the first set of profiles. This would allow to map the entire mounds with 410-kHz sidescan profiles. The DTS-1 system was deployed on July 20, 2003 at 01:20. However, the deep towed seismic streamer stopped working properly after only a few hundred shots. Following this failure, it was decided to use the DTS-1 for 75 kHz only and three profiles plus one large turn were run. On July 20, 2003 at 14:43 the DTS-1 system was taken up again to repair the streamer.

During the deployment mounds 11 and 12 were crossed three times and spectacular data of the distribution of high-backscatter patches on the mounds were registered. It turned out that mound 11 consists of two distinct areas (or summits) with a very patchy distribution of high-backscatter areas (Fig. 6.2.4). In addition, to the northwest of mound 12, another, yet unknown area with similar backscatter facies but lacking morphological expression, has been identified.

6.2.1.3 Deployment 3: Slide

The third deployment of the DTS-1 system lasted from July 21, 2003, 01:22 to July 21, 2003, 14:51. The purpose of this deployment was to map shallow sediment slides that occur on the upper continental slope at a water depth of about 580 m. One of these slides (the BGR slide) had already been identified previously and additional slides were suspected to the east of the BGR slide. These slides might be related to the limit of the stability of gas hydrates at a water depth of 580 m and the site where the BSR pinches out was an additional target of this deployment. Unfortunately, the deep towed seismic streamer stopped responding again shortly after the deployment. The whole layout of the deployment consisted of 12 parallel tracks up and down the continental slope between 9°05'N – 9°15'N and 84°33'W – 84°42'W (Fig. 6.2.5). After six profiles the DTS-1 system was brought on deck to repair the streamer.

The sidescan sonar data gained from the area east of the BGR slide are of little interest. There are no additional slides in the area and the sidescan data mainly show the traces of gullies and canyons crossing the cruise track in an oblique direction. A few areas at water depths of less than 500 m show high backscatter patches (Fig. 6.2.6.), but they are clearly too shallow to be related to the pinching out the BSR. From our first interpretation of the data, there are no particular features related to the lower limit of the gas hydrate stability zone in this area.

6.2.1.4 Deployment 4: Highmounds 11 & 12

For the fourth deployment we returned to the area of mounds 11 and 12 in order to obtain very detailed images of the mounds using 410-kHz sidescan sonar. This was attempted between July 22, 2003, 12:55 and July 22, 2003, 17:48 using two parallel tracks with adjustments made to the ship's course depending on the positioning information given by POSIDONIA (Fig. 6.2.7). Still, with a range of only 150 m we missed mounds 11 and 12 during the first run, when we passed close to these mounds, but did not cross the summit. We obtained, however, really spectacular images from the previously discovered fluid-escape features northeast of mound 12. During the second profile, we managed to pass right over mounds 11 and 12 and obtained superb images from these mounds. Unfortunately, processing of the 410-kHz sidescan sonar images onboard was not possible and pictures of these mounds could not be included in this report. This deployment showed that online USBL positioning with POSIDONIA is an essential requisite if highest-resolution profiles are to be located on top of such small-scale features.

6.2.1.5 Deployment 5: Mound Culebra

Mound Culebra, situated at 86°18'W and 10°18'N, was the target of a combined sidescan sonar and seismic study. This mound was well known from previous TOBI sidescan sonar imagery and had been studied with conventional multi-channel seismics, video observation and sediment coring. Mound Culebra turned out to be a complex feature whose origin might be related to deep-rooted faults that are possible pathways for deep-sourced fluids. While the mound was known to be active in terms of seeping fluids, the distribution of these sources was hitherto not well constrained. Sidescan sonar imagery was meant to fill this gap. The deployment of the DTS-1 on Mound Culebra was performed in two parts lasting from July 26, 2003, 16:18 to July 29, 2003, 04:58. The deployment had to be interrupted for about five hours for additional checks and repairs of the deep towed seismic streamer and the POSIDONIA positioning system. Six strike-parallel and eight dip-parallel lines across the mound and its immediate vicinity were collected and some very interesting data obtained (Fig. 6.2.8).

In contrast to mounds 11 and 12, the high-backscatter patches on Mound Culebra are not restricted to the summit of the mound (Fig. 6.2.9). If our interpretation is correct that these high backscatter areas

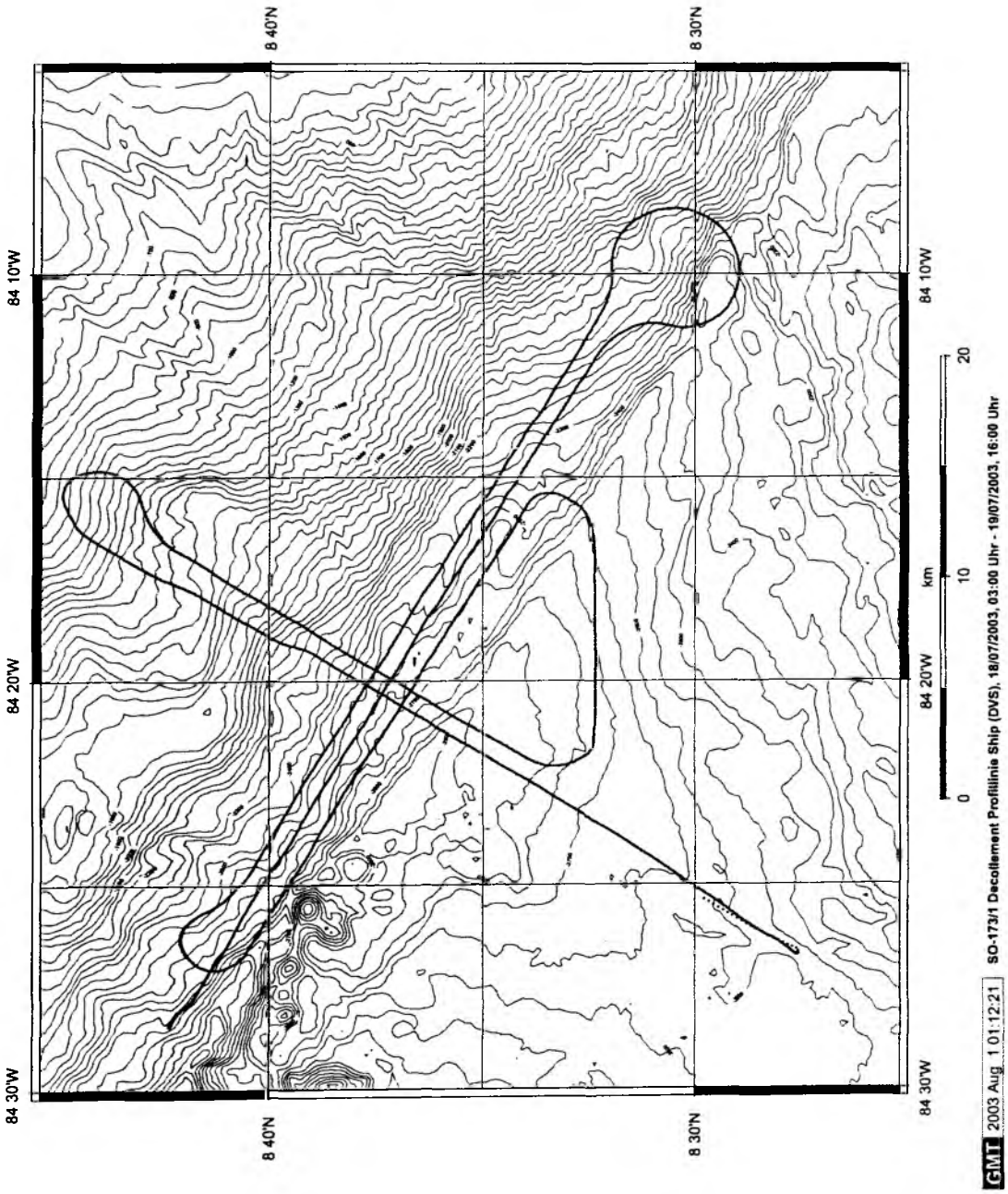

Fig. 6.2.1.: SO 173/1 Decollement Profile Ship (DVS), 18/07/2003, 03:00 Uhr - 19/07/2003, 16:00 Uhr.

represent carbonates resulting from fluid venting, then fluid venting is also active on the flanks of mound Culebra. The vicinity of mound Culebra, however, does not show signs for additional fluid venting in the area, except for one very small location to the northeast of the mound.

6.2.1.6 Deployment 6: Nicaragua

The sixth and final deployment of the DTS-1 system lasted for a full 5.5 days from July 31, 2003, 09:41 to August 5, 2003, 21:13. It consisted of 12 profiles along the continental slope off southern Nicaragua between 11°00'N and 11°20'N and ranging in water depth from 900 to 2500 meters. Eight of these profiles extended over 28 miles, while the lowermost four profiles had to be cut to only 12 miles due to time constraints (Fig. 6.2.10). The main purpose of these sidescan sonar profiles was to map and image domes and elevations that had been identified on previous bathymetric surveys. They were expected to represent mounds and mud diapirs such as those already studied further to the south off Costa Rica. In addition, the geometry and depositional environment of large submarine slides on the lower continental slope as well as sediment pathways and processes within submarine canyons that cut the Nicaraguan slope constituted additional objectives for this deployment.

The sidescan sonar images as well as the subbottom profiler data from this deployment are of very good quality and show many interesting features. A number of mounds have been mapped, and it appears as if many of the smaller mounds are covered with high-backscatter patches at seep carbonates on the seafloor (Fig. 6.2.11). The larger mounds (some of them over 200 m in relief height) seem to be less active, but this impression might also be related to viewing angles that were far from ideal (instrument height too shallow or below the actual summit of the mound). In any case, the data collected will allow to map the distribution of depositional facies on these mounds, if some ground truth becomes available in the future.

Many canyons cut the continental slope off Nicaragua. They all leave an expression on sidescan sonar images. Some of them are only mere gullies with less than 10 m in relief height, but some are deeply-cut canyons that are several tens of metres deep and hundreds of metres wide. They generally show deposits on the canyon floor with sometimes a braid-like distribution of high backscatter areas (Fig. 6.2.11). This figure also shows the trace of a major slump scar in the north-western part of the survey. Inter-canyon areas, on the other hand, are relatively smooth.

Fig. 6.2.2: *Screenshot of DTS-1 75-kHz sidescan sonar data from the "Decollement" deployment showing possible fluid vents in the water column. Height above seafloor is about 100 meters and high backscatter is dark.*

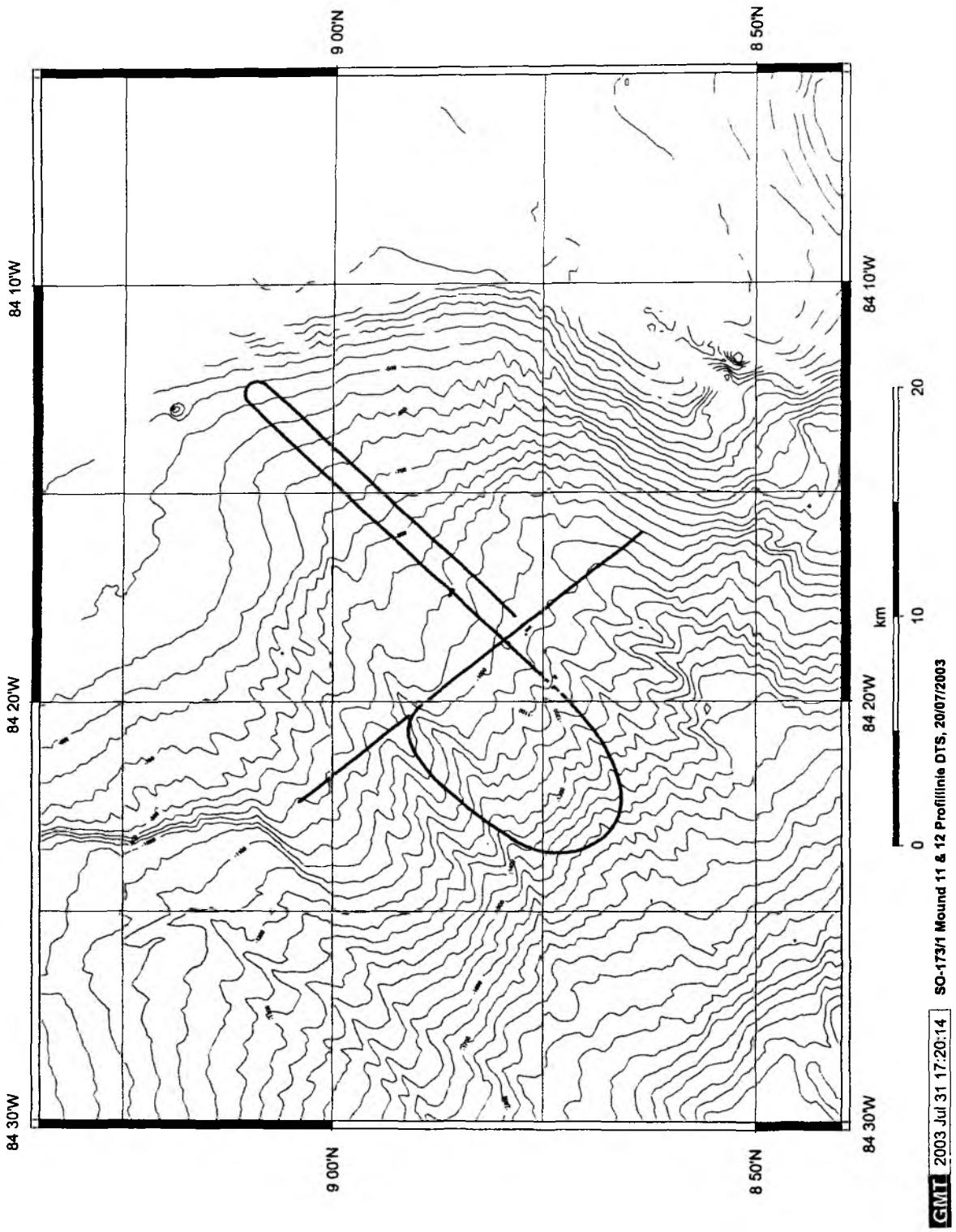

Fig. 6.2.3: SO 173/1 Mound 11 & 12 Profile DTS, 20/07/2003.

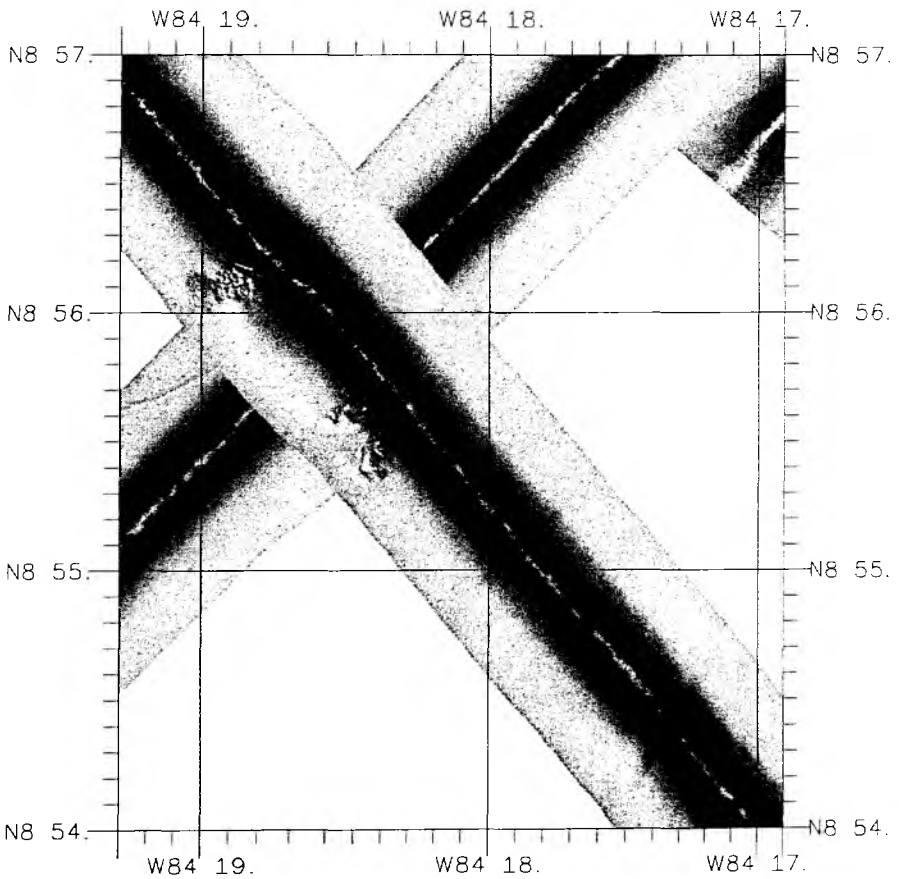

Fig. 6.2.4: *DTS-1 75-kHz sidescan sonar mosaic crossing the mounds 11 and 12 on the continental slope. High backscatter is dark.*

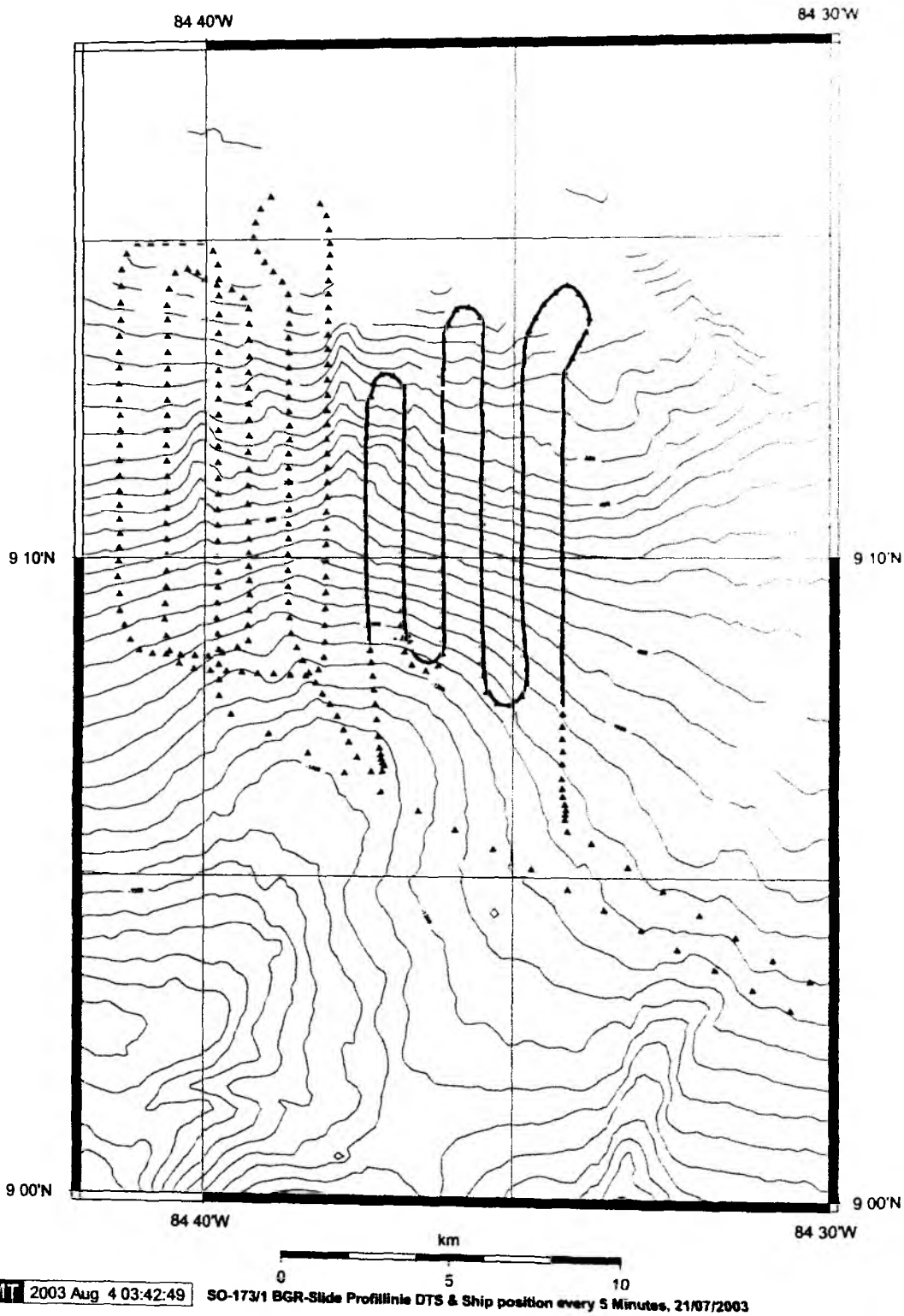

Fig. 6.2.5: SO 173/1 BGR slide Profile DTS & ship's position every 5 minutes, 21/07/2003.

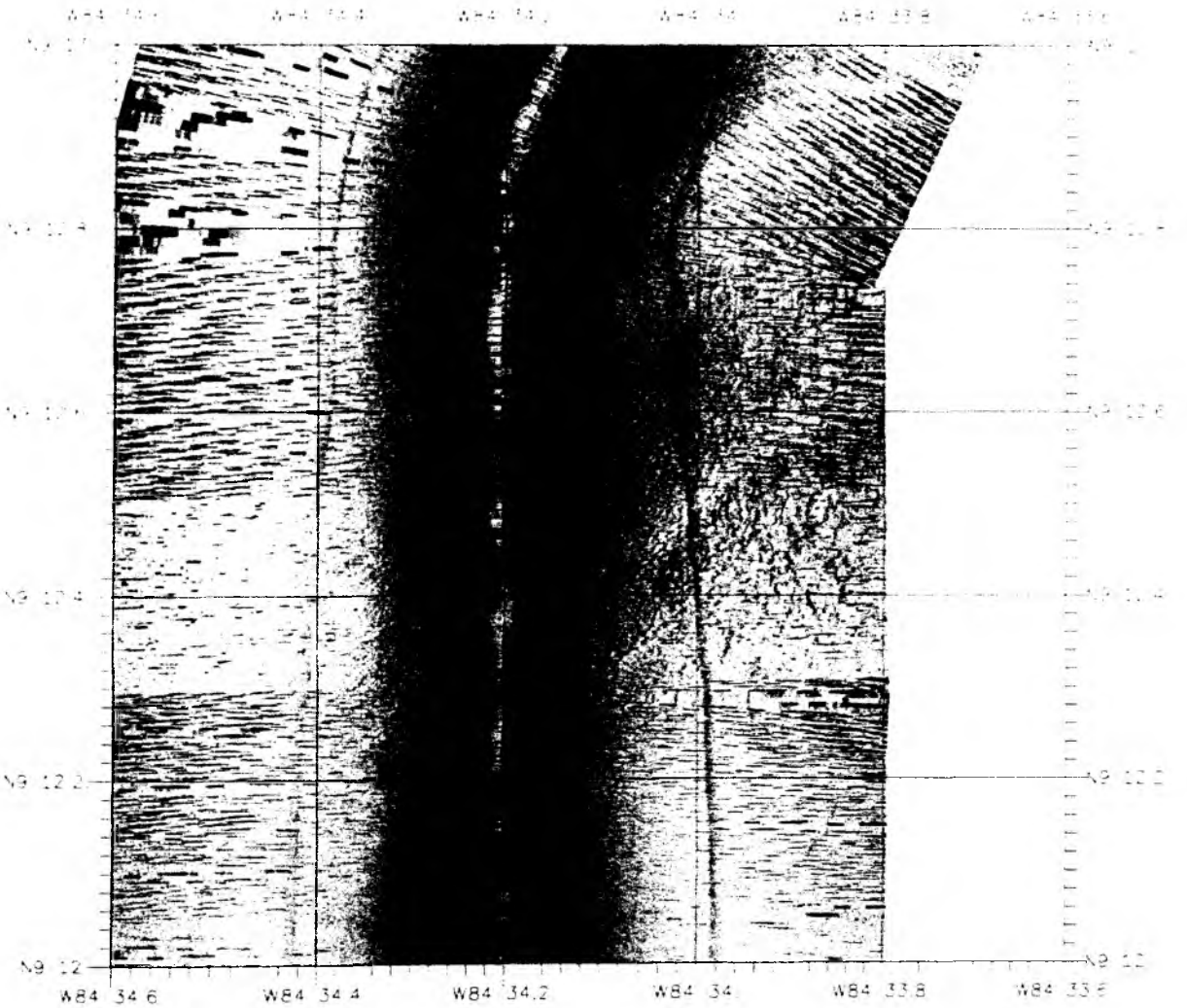

Fig. 6.2.6: *DTS-1 75-kHz sidescan sonar profile from the uppermost continental slope in the area of the BGR and GEOMAR slides showing a yet unidentified patch of high backscatter (= dark patch).*

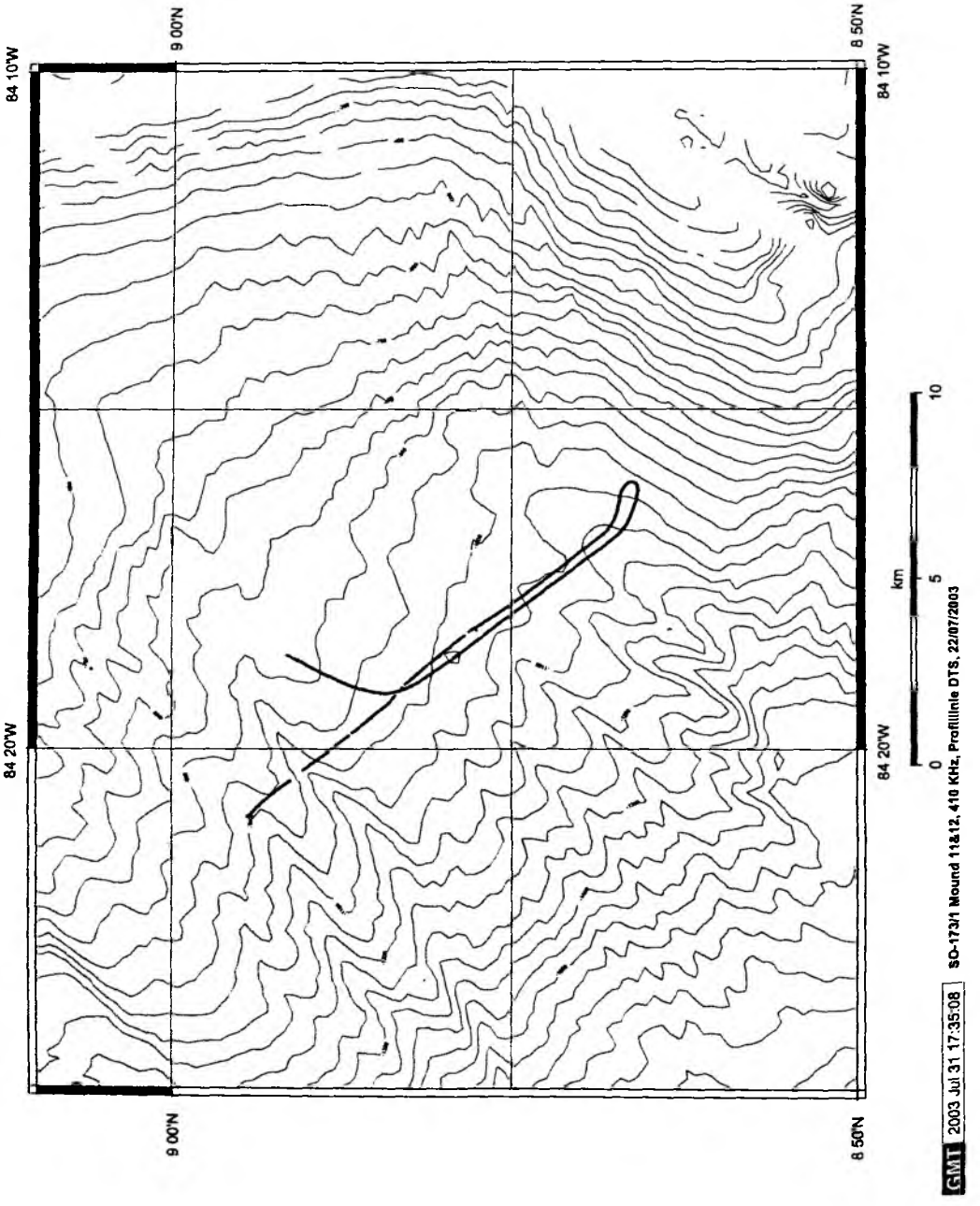

Fig. 6.2.7: SO 173/1 Mound 11&12, 410 KHz, Profile DTS, 22/07/2003.

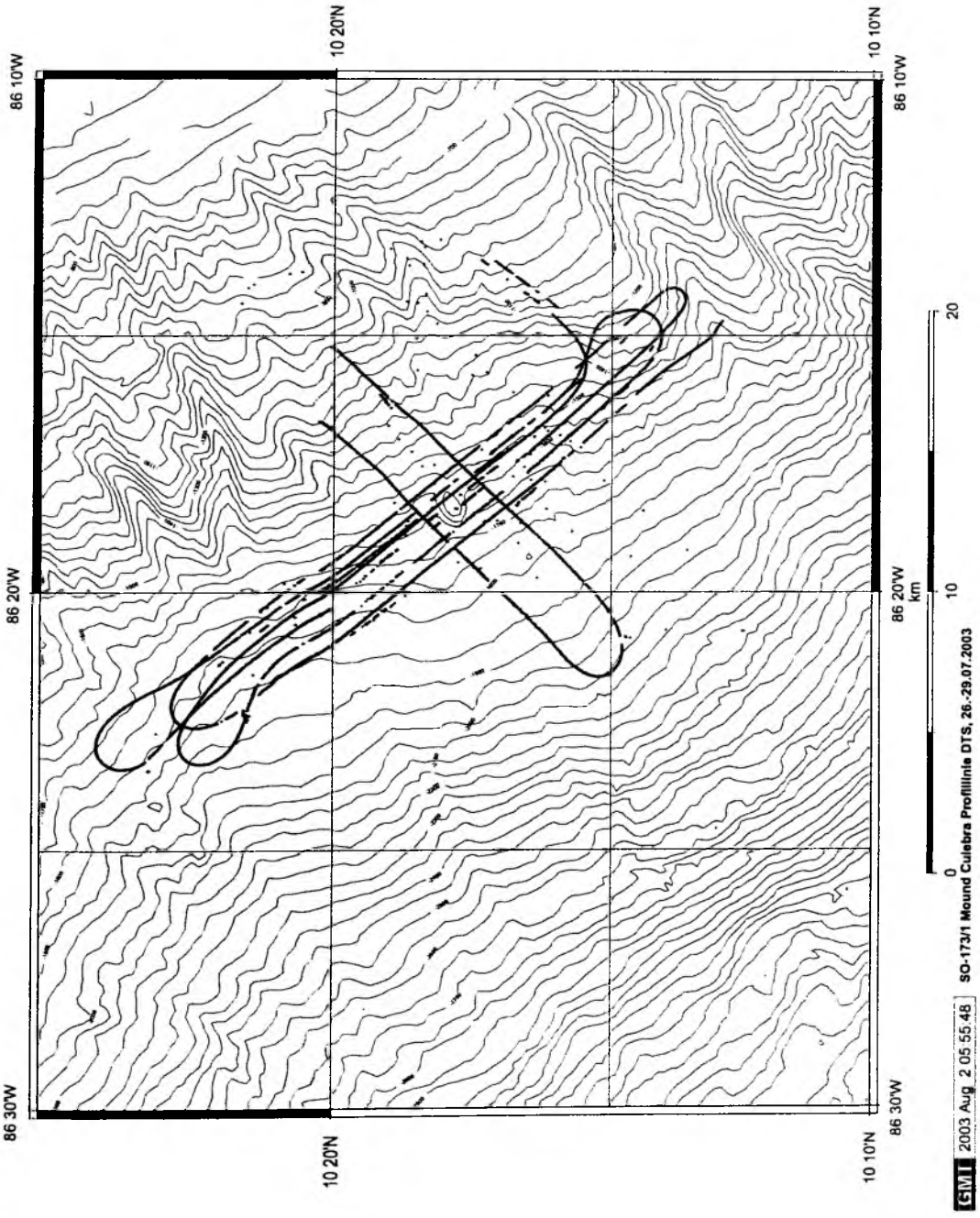

Fig. 6.2.8: SO 173/1 Mound Culebra Profile DTS, 26.-29.07.2003.

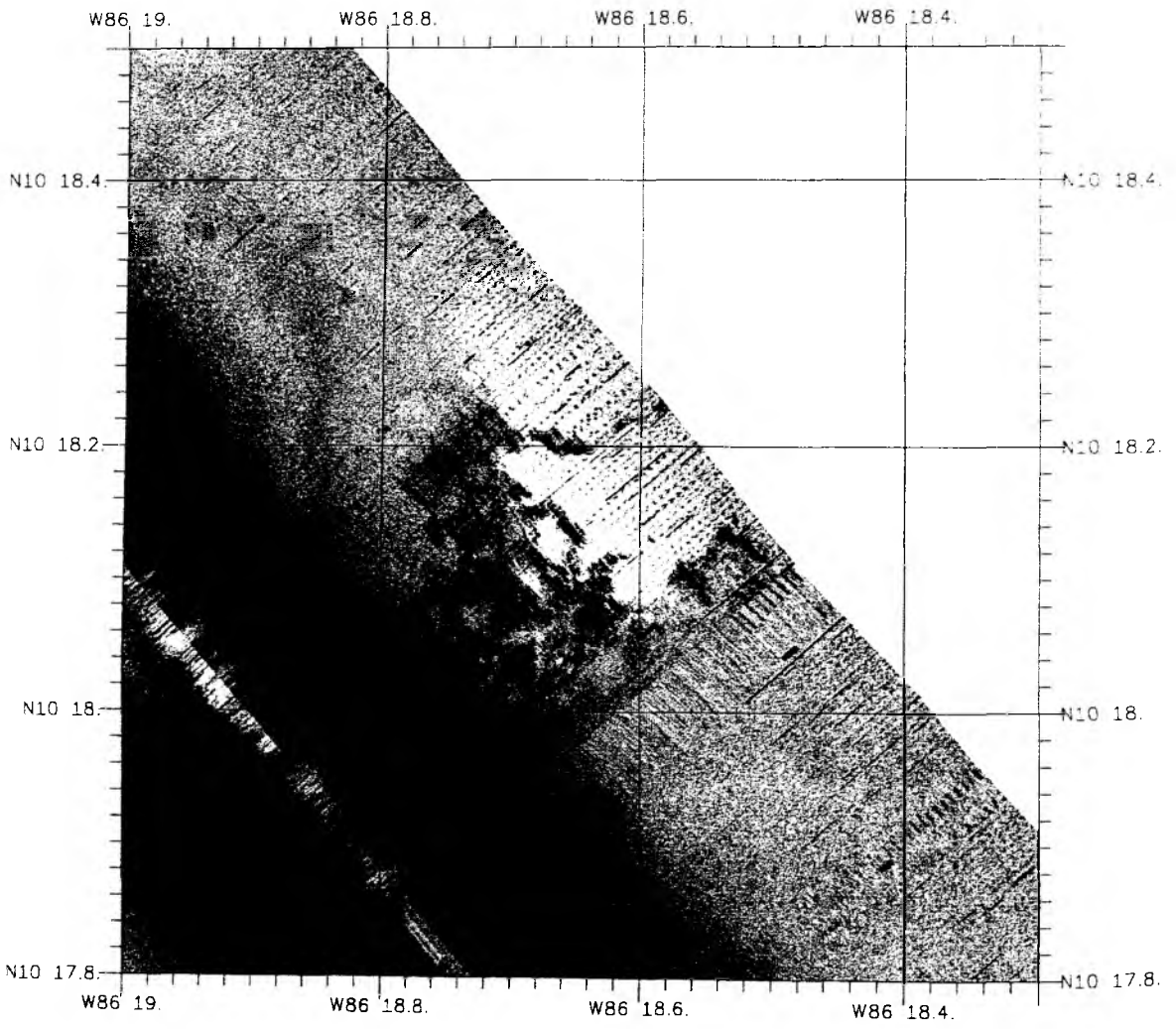

Fig. 6.2.9: *Part of DTS-1 75-kHz sidescan sonar profile touching Mound Culebra. High backscatter is dark.*

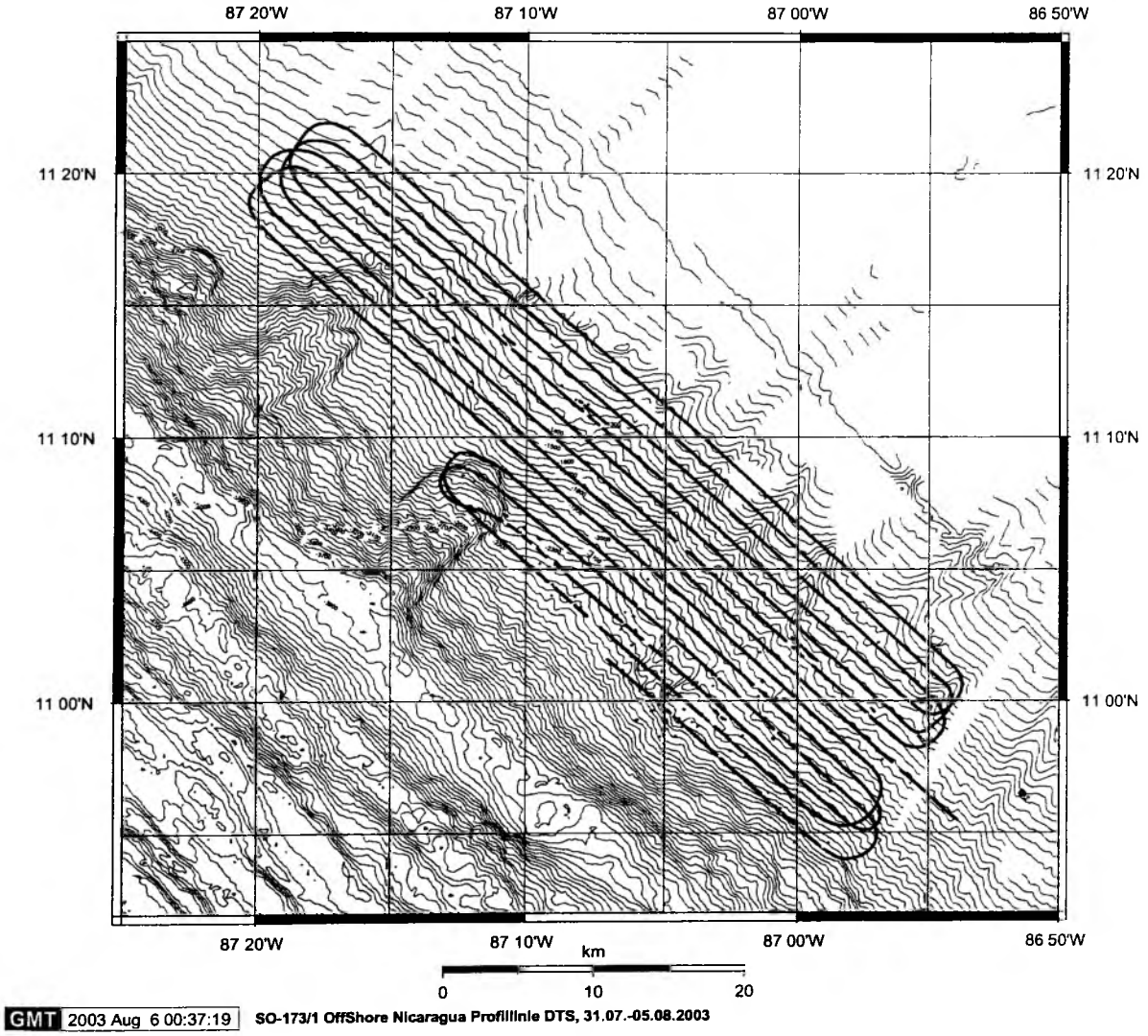

Fig. 6.2.10: SO 173/1 OffShore Nicaragua Profile DTS, 31.07.-05.08.2003.

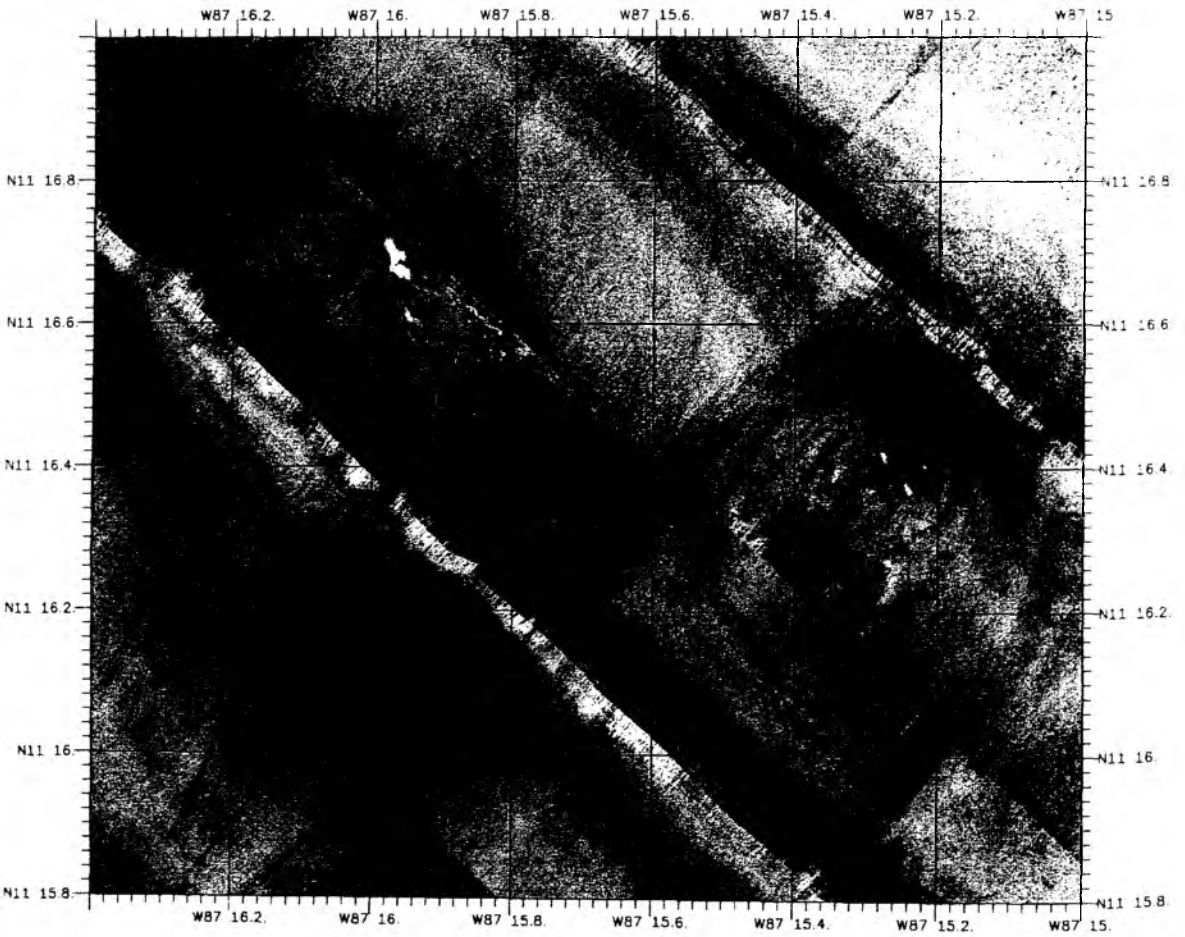

Fig. 6.2.11: DTS-1 75-kHz sidescan sonar mosaic from the continental slope off Nicaragua showing two prominent mounds and the scar of a major slump. High backscatter is dark.

6.2.2 Deep tow Streamer Seismogram Sections

M. Breitzke, J. Bialas, D. Buerk, N. Fekete, E. Flueh, I. Klaucke, C. Papenberg, C. Ranero

There were only three successful deployments of the deep tow streamer because of contact, corrosion and leakage problems at the pins and within the plugs of the cables and hydrophones causing short cuts within the streamer nodes. Hence, the streamer configuration varied from one deployment to the other because broken or leaking cables, plugs and/or hydrophones had to be changed or removed. Atotal of 86, 985 GI-gun shots were fired during R/V SONNE cruise SO173/1 to collect 421 nm of deep tow multichannel seismic data . The seismogram sections presented here as examples of the deep tow seismic data are raw brute stacks of three traces stacked without preceding NMO-correction and bandpass-filtered afterwards. No corrections for varying streamer depths were applied. The resulting trace spacing is equal to shot point spacing and on average it amounts to 10 m for an average ship velocity of 3 kn. Date, time and main objective of each deployment are described in the corresponding chapters for the sidescan sonar imagery (cf. sect. 6.2.1).

6.2.2.1 Deployment 1: Decollement

During the first deployment the streamer was composed of 25 nodes, connected by 1-m-long cables and attached to the sidescan sonar tow fish by a 50-m-long lead-in cable (Tab. 6.2.1). Six profiles of 58 nm in total length were recorded, three of them running parallel to the strike of the slope and trench, two of them running parallel to the dip of the slope and perpendicular to the trench, and one connecting the strike- and the dip-parallel profiles in east-west direction and towed about 1000 m above the sea floor, in contrast to all other profiles that were towed 100 - 130 m above the sea floor (Tab. 6.2.2, Fig. 6.2.12). The three strike-parallel profiles DTS03-002, DTS03-001 and DTS03-003 and the dip-parallel profile DTS03-006 are presented as data examples (Figs. 6.2.13 - 6.2.16). For the brute stacks traces 10 - 12 of each shot gather with an offset of 63 - 65 m to the sidescan sonar fish were stacked and bandpass-filtered between 50/100 - 500/1000 Hz. The towing rope lengths varied between about 4000 and 5000 m resulting in a rather low angle of incidence of approximately 55° - 60° for the seismic rays and leading to a vertically rather condensed wide-angle reflection seismogram section as a function of two-way travel time compared to a conventional normal incidence seismogram section (Breitzke et al., in press).

Generally, all deep tow streamer seismogram sections show the direct wave between GI-gun and streamer as strong first arrival, followed by a weak bubble and subsequent sea floor and subsurface reflections (e.g. Fig. 6.2.13). Variations in the arrival times of the direct wave indicate the different towing rope lengths due to variations in the sea floor topography, whereas variations in the arrival time difference between direct wave and sea floor reflection indicate changing towing depths above the sea floor. All these depth variations will be corrected later in a post-processing step taking into account the data of the engineering nodes.

The seismogram sections of all profiles in this survey area show rather incoherent scattered subsurface reflections. The most prominent feature is a BSR in the northeastern part of the strike-parallel lines DTS03-002 and DTS03-003 (Figs. 6.2.13, 6.2.14) and in the upslope northeastern part of the dip-parallel lines (Fig. 6.2.16). Reflections from the decollement which should appear about 400 ms TWT below sea floor in this wide-angle seismogram section (corresponding to about 800 ms TWT in a conventional normal incidence seismogram section) can only be vaguely distinguished along line DTS03-003, which is closest to the trench. These reflections have a dominant frequency of 50 - 70 Hz, which is close to the low-cut

frequency of the applied bandpass-filter. So, future post-processing of the data has to prove if similar reflections from the decollement also exist along the other lines. Similarly, future post-processing of the dip-parallel line(s) particularly with respect to the depth correction has to show the exact location of the trench crossed by the profiles DTS03-005 and DTS03-006.

6.2.2.2 Deployment 2: Mounds 11 & 12

The contact to the streamer was lost at a depth of about 800 - 900 m below sea surface at a rope length of about 1000 m. Only sidescan sonar data was collected during the first night and the whole system was brought on deck again the next morning for repair, so that no seismic data were collected in the survey area of mound 11 and 12.

6.2.2.3 Deployment 3: Slide

The deep tow streamer was still under repair during the third deployment, so that no deep tow seismic data were collected in the survey area of the BGR slide.

6.2.2.4 Deployment 4: Highmounds 11 & 12

The deep tow streamer was still under repair during the fourth deployment, so that again no deep tow seismic data were collected in the survey area of mound 11 and 12.

6.2.2.5 Deployment 5: Mound Culebra

During the first part of the fifth deployment the streamer was composed of 21 nodes, connected by both 1-m and 6.5-m cables and attached to the sidescan sonar tow fish by a 6.5-m cable, because the standard 50-m lead-in cable was broken (Tab. 6.2.3a). Due to further contact, corrosion and leakage problems with the pins, plugs, cables and hydrophones the number of nodes was reduced to 17 during the second part of the fifth deployment and another 1-m cable was replaced by a 6.5-m cable (Tab. 6.2.3b). A closely spaced grid of 15 crosswise profiles of 89 nm in total length were recorded in this survey area (Tab. 6.2.4, Fig. 6.2.17). Nine of them have an offset of 600 m each and cover Mound Culebra as major target. They were collected with the objectives of imaging the internal structures of Mound Culebra and - by wide-angle undershooting - answering the question if a BSR observed in conventional surface streamer data collected earlier in the vicinity of the mound is continuous or interrupted beneath the mound. The additional lines with an offset of 1000 m mainly run up- and downslope and cover the area adjacent to Mound Culebra revealing some smaller mounds and pronounced NW-SE-striking steps or faults in the sea floor bathymetry. As data examples three profiles running parallel to the strike of the continental slope northeast (DTS03-010, DTS03-012) and across Mound Culebra (DTS03-009) and five profiles running up- or downslope southeast (DTS03-014, DTS03-018), across (DTS03-017) and northwest of Mound Culebra (DTS03-019, DTS03-021) are presented. The brute stacks displayed in Figures 6.2.18 - 6.2.24 are stacks from traces 10 -12 of each shot gather with an offset of 21 - 23 m to the sidescan sonar fish, whereas traces 8 - 10 with an offset of 24.5 - 26.5 m to the sidescan sonar fish were stacked for the seismogram section in Figure 6.2.25. A bandpass filter between 70/140 - 500/1000 Hz was applied to each seismogram section. Depending on water depth, towing rope lengths varied between about 1000 and 3000 m, resulting in slightly steeper angles of incidence of approximately 50° - 55° for the seismic rays compared to the survey at the decollement (cf. sect. 6.2.2.1). Therefore, the recorded and displayed wide-angle deep tow seismogram sections are vertically less condensed than those collected in the decollement area.

The seismogram sections of the three strike-parallel profiles clearly show the diffraction hyperbolae from Mound Culebra (Figs. 6.2.18 - 6.2.20). For lines DTS03-010 and DTS03-012 northeast of the mound these

Table 6.2.1: Deep tow streamer and source geometry for the survey area 'Decollement' (deep tow seismic profiles DTS03-001 - DTS03-006). EM = engineering module, AM = acoustic module.

Streamer Node Position	Streamer Node No.	Node Type	Cable Length to Preceding Node [m]	Total Streamer Length (incl. Lead-in) [m]
25	26	EM	50.0[1)]	50.0
24	25	AM	1.0	51.0
23	24	AM	1.0	52.0
22	23	AM	1.0	53.0
21	22	AM	1.0	54.0
20	21	AM	1.0	55.0
19	20	AM	1.0	56.0
18	19	AM	1.0	57.0
17	17	AM	1.0	58.0
16	16	AM	1.0	59.0
15	15	AM	1.0	60.0
14	14	AM	1.0	61.0
13	08	EM	1.0	62.0
12	12	AM	1.0	63.0
11	11	AM	1.0	64.0
10	10	AM	1.0	65.0
09	13	AM	1.0	66.0
08	07	AM	1.0	67.0
07	06	AM	1.0	68.0
06	05	AM	1.0	69.0
05	04	AM	1.0	70.0
04	03	AM	1.0	71.0
03	02	AM	1.0	72.0
02	18	AM	1.0	73.0
01	01	EM	1.0	74.0

[1)] Length of Lead-in Cable

SEISMIC SOURCE

Type: GI-Gun **Volume:** 2 x 1.7 l **Pressure:** 150 bar

Delay between Generator and Injector: 58 ms

Towing Depth: 1.6 - 1.7 m

Position behind the ship: towed at starboard side,
ca. 10 m behind the ship's stern, ca. 3 m to starboard side

Table 6.2.2: Deep tow multichannel seismic lines collected in the survey area 'Decollement'.

	Start					End							
Profile	Latitude	Longitude	Date	Time [UTC]	Shot No.[1]	Latitude	Longitude	Date	Time [UTC]	Shot No.[1]	Course	Number of shots	Length [nm]
DTS03-001	8°40.89'N	84°26.31'W	18/07/2003	04:12:24	309	8°32.38'N	84°12.00'W	18/07/2003	10:07:10	3340	120°	3032	16.1
DTS03-002	8°32.86'N	84°11.97'W	18/07/2003	14:00:53	5340	8°40.35'N	84°24.54'W	18/07/2003	19:00:21	7900	300°	2561	12.8
DTS03-003	8°40.42'N	84°26.46'W	18/07/2003	20:40:03	8753	8°34.56'N	84°16.69'W	19/07/2003	00:30:59	10730	120°	1978	5.9
DTS03-004[2]	8°32.46'N	84°16.58'W	19/07/2003	01:39:56	11320	8°33.24'N	84°22.09'W	19/07/2003	03:39:45	12340	270°	1021	5.0
DTS03-005	8°34.11'N	84°21.83'W	19/07/2003	03:58:27	12500	8°40.91'N	84°17.62'W	19/07/2003	06:44:07	13920	30°	1421	6.8
DTS03-006	8°43.75'N	84°16.58'W	19/07/2003	09:00:03	15083	8°33.66'N	84°22.65'W	19/07/2003	13:02:20	17160	210°	2078	11.6
											Total	12091	58.2

[1] Geometrics Controller
[2] Towed 1000 m above sea floor

diffraction hyperbolae are side echoes which increase in height above the sea floor the closer the streamer passes the mound. Additionally, due to the asymmetric source-streamer geometry the diffraction hyperbolae are much more pronounced when the streamer approaches the mound than passed the mound. The slope sediments adjacent to Mound Culebra are more or less faulted and distorted. Signal penetration reaches about 400 ms TWT corresponding to depths of 300 - 350 m. A BSR of varying signal strength is visible at both sides of the mound. However, the question if it can be traced continuously underneath the mound or if it is interrupted cannot be answered from the raw brute stacks but has to be left to the finally processed data.

The dip-parallel lines southeast, across and northwest of Mound Culebra also show faulted and distorted slope sediments adjacent to the mound (Figs. 6.2.21 - 6.2.25) as well as pronounced diffraction hyperbolae from Mound Culebra and from another smaller mound northeast of Mound Culebra (Fig. 6.2.22). A BSR of varying signal strength can also be recognized to both sides of Mound Culebra and the other smaller mound, but again final data processing has to prove if it is continuous or interrupted underneath the mounds. Some indication for a larger-scale fault which can be traced from one line to the other is possibly visible in lines DTS03-019 and DTS03-021 (Figs. 6.2.24 and 6.2.25). Nevertheless, final data processing has to show if the feature marked as potential fault in these lines appears to be an actual fault associated with a step in the sea floor bathymetry or another sedimentary feature.

6.2.2.6 Deployment 6: Nicaragua

During the sixth and last deployment the streamer was still composed of 17 nodes, connected by both 1-m and 6.5-m cables and attached to the sidescan sonar tow fish by a 6.5-m cable (Tab. 6.2.5). However, during this survey the pressure sensor of the engineering node in the middle of the streamer was defective, so that depth values were only measured at the beginning and the end of the streamer. 13 NW-SE striking profiles (DTS03-022 - DTS03-024) of 274 nm in total length running parallel to the continental slope off Nicaragua with an offset of 1300 m were recorded at water depths between 1000 and 2300 m, and cover an area of approximately 700 km^2 (Tab. 6.2.6, Fig. 6.2.26). As data examples lines DTS03-027, DTS03-025 and DTS03-023 (Fig. 6.2.27 - 6.2.29), collected in the northeasternmost part of the survey area at the shallowest water depths, and lines DTS03-026 (Fig. 6.2.30) and DTS03-029 (Fig.6.2.31), collected in the middle of the survey area, are presented. For the brute stacks traces 8 - 10 of each shot gather with an offset of 24.5 - 26.5 m to the sidescan sonar fish were stacked and bandpass-filtered between 30/100 - 500/1000 Hz. Depending on the water depth towing rope lengths varied between about 1000 and 4500 m, resulting in angles of incidence of approximately 45° in shallower and 60° in deeper water.

Both bathymetry and seismic lines show that the continental margin off Nicaragua is dominated by deeply incised canyons and numerous mound structures, as well as slides at the lower slope in the northwestern part of the survey area (Fig. 6.2.26). For instance, line DTS03-027 crosses the most prominent mounds on the upper continental slope, which rises up to about 300 m above the surrounding sea floor (Fig. 6.2.27), line DTS03-026 crosses three smaller adjacent mounds further downslope (Fig. 6.2.30) and line DTS03-029, among other features, crosses the scar of the large slide on the lower continental slope in the north-western part of the survey area (Fig. 6.2.31). Furthermore, all deep tow seismogram sections show well stratified, slightly deformed and distorted sedimentary layers of 400 - 500 ms TWT(about 300 - 400 m) in thickness. They are bounded by a band of strong reflections which seem to form the recent base for the deeply incised canyons. At some locations the canyon incision has stopped some meters above the high-reflectivity band, at other locations canyons have cut into these high-reflectivity layers and provide a potential location to sample these sediments, but none of the canyons have cut through this reflection band.

Table 6.2.3a: Deep tow streamer and source geometry for the survey area 'Mound Culebra', part 1 (deep tow seismic profiles DTS03-007 - DTS03-019). EM = engineering module, AM = acoustic module.

Streamer Node Position	Streamer Node No.	Node Type	Cable Length to Preceding Node [m]	Total Streamer Length (incl. Lead-in) [m]
21	26	EM	6.5[1)]	6.5
20	25	AM	1.0	7.5
19	24	AM	1.0	8.5
18	22	AM	6.5	15.0
17	21	AM	1.0	16.0
16	20	AM	1.0	17.0
15	17	AM	1.0	18.0
14	16	AM	1.0	19.0
13	15	AM	1.0	20.0
12	08	EM	1.0	21.0
11	11	AM	1.0	22.0
10	10	AM	1.0	23.0
09	13	AM	1.0	24.0
08	07	AM	1.0	25.0
07	06	AM	1.0	26.0
06	05	AM	1.0	27.0
05	04	AM	1.0	28.0
04	03	AM	1.0	29.0
03	02	AM	1.0	30.0
02	18	AM	1.0	31.0
01	01	EM	6.5	37.5

[1)] Length of Lead-in Cable

SEISMIC SOURCE

Type: GI-Gun **Volume:** 2 x 1.7 l **Pressure:** 150 bar

Delay between Generator and Injector: 58 ms

Towing Depth: 1.6 - 1.7 m

Position behind the ship: towed at starboard side,
ca. 10 m behind the ship's stern, ca. 3 m to starboard side

Underneath there is a less reflective zone in which a BSR is visible in most parts of the survey area. This BSR varies in strength along the profile lines and from one line to the other and appears to be locally discontinuous along the profile lines and beneath mounds. Final data processing has to show at which locations this BSR actually occurs, where it is interrupted, and where it disappears.

Table 6.2.3b: Deep tow streamer and source geometry for the survey area 'Mound Culebra', part 2 (deep tow seismic profiles DTS03-020 - DTS03-021). EM = engineering module, AM = acoustic module.

Streamer Node Position	Streamer Node No.	Node Type	Cable Length to Preceding Node [m]	Total Streamer Length (incl. Lead-in) [m]
17	26	EM	6.5[1)]	6.5
16	25	AM	1.0	7.5
15	24	AM	1.0	8.5
14	22	AM	6.5	15.0
13	21	AM	1.0	16.0
12	20	AM	1.0	17.0
11	16	AM	6.5	23.5
10	08	EM[2)]	1.0	24.5
09	11	AM	1.0	25.5
08	10	AM	1.0	26.5
07	07	AM	1.0	27.5
06	06	AM	1.0	28.5
05	05	AM	1.0	29.5
04	04	AM	1.0	30.5
03	02	AM	1.0	31.5
02	18	AM	1.0	32.5
01	01	EM	6.5	39.0

[1)] Length of Lead-in Cable
[2)] Pressure (depth) sensor defect

SEISMIC SOURCE

Type: GI-Gun **Volume:** 2 x 1.7 l **Pressure:** 150 bar
Delay between Generator and Injector: 58 ms
Towing Depth: 1.6 - 1.7 m
Position behind the ship: towed at starboard side,
ca. 10 m behind the ship's stern, ca. 3 m to starboard side

Table 6.2.4: Deep tow multichannel seismic lines collected in the survey area 'Mound Culebra'.

	Start					End							
Profile	Latitude	Longitude	Date	Time [UTC]	Shot No.[1]	Latitude	Longitude	Date	Time [UTC]	Shot No.[1]	Course	Number of shots	Length [nm]
DTS03-007	10°13.31'N	86°15.20'W	26/07/2003	15:23:55	68	10°21.62'N	86°22.43'W	26/07/2003	19:18:59	2082	320°	2015	8.6
DTS03-008	10°22.27°N	86°21.44'W	26/07/2003	20:16:02	2571	10°14.27'N	86°14.39'W	27/07/2003	00:00:58	4499	140°	1929	10.0
DTS03-009	10°14.11'N	86°15.02'W	27/07/2003	00:50:33	4924	10°21.52'N	86°21.58'W	27/07/2003	04:03:35	6810	320°	1887	7.5
DTS03-010	10°22.94'N	86°21.89'W	27/07/2003	06:16:38	7719	10°15.55'N	86°15.84'W	27/07/2003	09:39:45	9460	140°	1742	8.4
DTS03-011	10°15.57'N	86°16.69'W	27/07/2003	11:17:45	10300	10°20.31'N	86°20.85'W	27/07/2003	13:02:59	11202	320°	903	5.9
DTS03-012	10°20.81'N	86°20.68'W	27/07/2003	15:27:11	12438	10°15.60'N	86°16.08'W	27/07/2003	17:59:54	13747	140°	1310	5.4
DTS03-013	10°15.60'N	86°16.08'W	27/07/2003	18:00:01	13748	10°18.41'N	86°14.49'W	27/07/2003	20:14:41	14898	40°	1151	3.2
DTS03-014	10°18.41'N	86°14.50'W	27/07/2003	20:14:48	14899	10°13.96'N	86°19.06'W	27/07/2003	22:32:56	16083	225°	1185	4.5
DTS03-015	10°16.33'N	86°19.66'W	28/07/2003	00:05:13	16874	10°20.53'N	86°15.31'W	28/07/2003	02:22:46	18053	45°	1180	5.0
DTS03-016	10°19.02'N	86°14.88'W	28/07/2003	04:00:52	263	10°14.47'N	86°19.40'W	28/07/2003	06:24:56	1052	225°	790	5.6
DTS03-017	10°16.13'N	86°20.13'W	28/07/2003	07:28:59	1601	10°20.53'N	86°15.50'W	28/07/2003	09:47:42	2790	45°	1190	6.4
DTS03-018	10°19.38'N	86°15.12'W	28/07/2003	10:46:51	3297	10°15.31'N	86°19.38'W	28/07/2003	12:43:11	4294	225°	998	5.9
DTS03-019	10°16.55'N	86°19.97'W	28/07/2003	14:19:12	5117	10°20.87'N	86°15.48'W	28/07/2003	16:35:20	6269	45°	1153	6.0
DTS03-020	10°16.64'N	86°18.68'W	29/07/2003	00:48:07	402	10°15.61'N	86°19.77'W	29/07/2003	01:17:24	653	225°	252	1.1
DTS03-021	10°15.48'N	86°21.83'W	29/07/2003	02:10:41	1364	10°20.28'N	86°16.58'W	29/07/2003	04:47:17	2452	45°	1089	5.3
											Total	18774	88.8

[1] Geometrics Controller

Table 6.2.5: Deep tow streamer and source geometry for the survey area 'Nicaragua' (deep tow seismic profiles DTS03-022 - DTS03-034). EM = engineering module, AM = acoustic module.

Streamer Node Position	Streamer Node No.	Node Type	Cable Length to Preceding Node [m]	Total Streamer Length (incl. Lead-in) [m]
17	26	EM	6.5[1)]	6.5
16	25	AM	1.0	7.5
15	24	AM	1.0	8.5
14	22	AM	6.5	15.0
13	21	AM	1.0	16.0
12	20	AM	1.0	17.0
11	16	AM	6.5	23.5
10	08	EM[2)]	1.0	24.5
09	11	AM	1.0	25.5
08	10	AM	1.0	26.5
07	07	AM	1.0	27.5
06	06	AM	1.0	28.5
05	05	AM	1.0	29.5
04	04	AM	1.0	30.5
03	02	AM	1.0	31.5
02	18	AM	1.0	32.5
01	01	EM	6.5	39.0

[1)] Length of Lead-in Cable
[2)] Pressure (depth) sensor defect

SEISMIC SOURCE

Type: GI-Gun **Volume:** 2 x 1.7 l **Pressure:** 150 bar

Delay between Generator and Injector: 58 ms

Towing Depth: 1.6 - 1.7 m

Position behind the ship: towed at starboard side,
ca. 3 - 5 m behind the ship's stern, ca. 1 - 2 m to starboard,
depending on surface currents

Table 6.2.6: Deep tow multichannel seismic lines collected in the survey area 'Nicaragua'.

	Start					End							
Profile	Latitude	Longitude	Date	Time [UTC]	Shot No.[1)]	Latitude	Longitude	Date	Time [UTC]	Shot No.[1)]	Course	Number of shots	Length [nm]
DTS03-022	10°56.24'N	86°54.78'W	31/07/2003	09:14:31	39	11°18.89'N	87°19.59'W	31/07/2003	20:48:34	5987	315°	5949	23.8
DTS03-023	11°20.46'N	87°17.36'W	31/07/2003	22:26:27	6826	11°00.05'N	86°54.81'W	01/08/2003	09:04:16	12293	135°	5468	26.6
DTS03-024	10°59.26'N	86°57.04'W	01/08/2003	10:29:05	13020	11°18.95'N	87°18.82'W	01/08/2003	20:43:49	18289	315°	5270	22.9
DTS03-025	11°20.05'N	87°15.84'W	01/08/2003	22:41:46	1	11°00.60'N	86°54.34'W	02/08/2003	08:43:24	5156	135°	5156	28.9
DTS03-026	10°59.60'N	86°56.42'W	02/08/2003	09:57:22	5790	11°19.45'N	87°18.34'W	02/08/2003	20:11:45	11054	315°	5265	20.3
DTS03-027	11°20.81'N	87°15.64'W	02/08/2003	22:04:04	12015	11°01.21'N	86°53.96'W	03/08/2003	08:12:01	17226	135°	5212	29.1
DTS03-028	11°00.05'N	86°55.83'W	03/08/2003	09:18:17	17794	11°19.87'N	87°17.75'W	03/08/2003	19:30:28	23040	315°	5247	28.4
DTS03-029	11°19.40'N	87°20.21'W	03/08/2003	20:33:28	23568	10°57.18'N	86°56.88'W	04/08/2003	07:49:07	29360	135°	5793	30.8
DTS03-030	10°56.15'N	86°59.95'W	04/08/2003	09:22:41	30162	11°05.86'N	87°10.59'W	04/08/2003	14:18:51	32700	315	2539	14.4
DTS03-031	11°04.77'N	87°06.36'W	04/08/2003	16:52:56	34011	10°56.55'N	86°57.25'W	04/08/2003	22:57:59	37138	135°	3128	12.3
DTS03-032	10°56.76'N	86°59.62'W	05/08/2003	00:42:24	38032	11°06.11'N	87°09.86'W	05/08/2003	05:30:27	40498	315°	2467	11.0
DTS03-033	11°07.99'N	87°10.93'W	05/08/2003	08:11:56	41879	10°56.03'N	86°57.72'W	05/08/2003	14:11:12	44952	135°	3074	17.8
DTS03-034	10°55.88'N	87°00.74'W	05/08/2003	16:26:24	46109	11°01.97'N	87°07.41'W	05/08/2003	19:28:38	47660	315°	1552	7.9
											Total	56120	274.3

[1)] Geometrics Controller

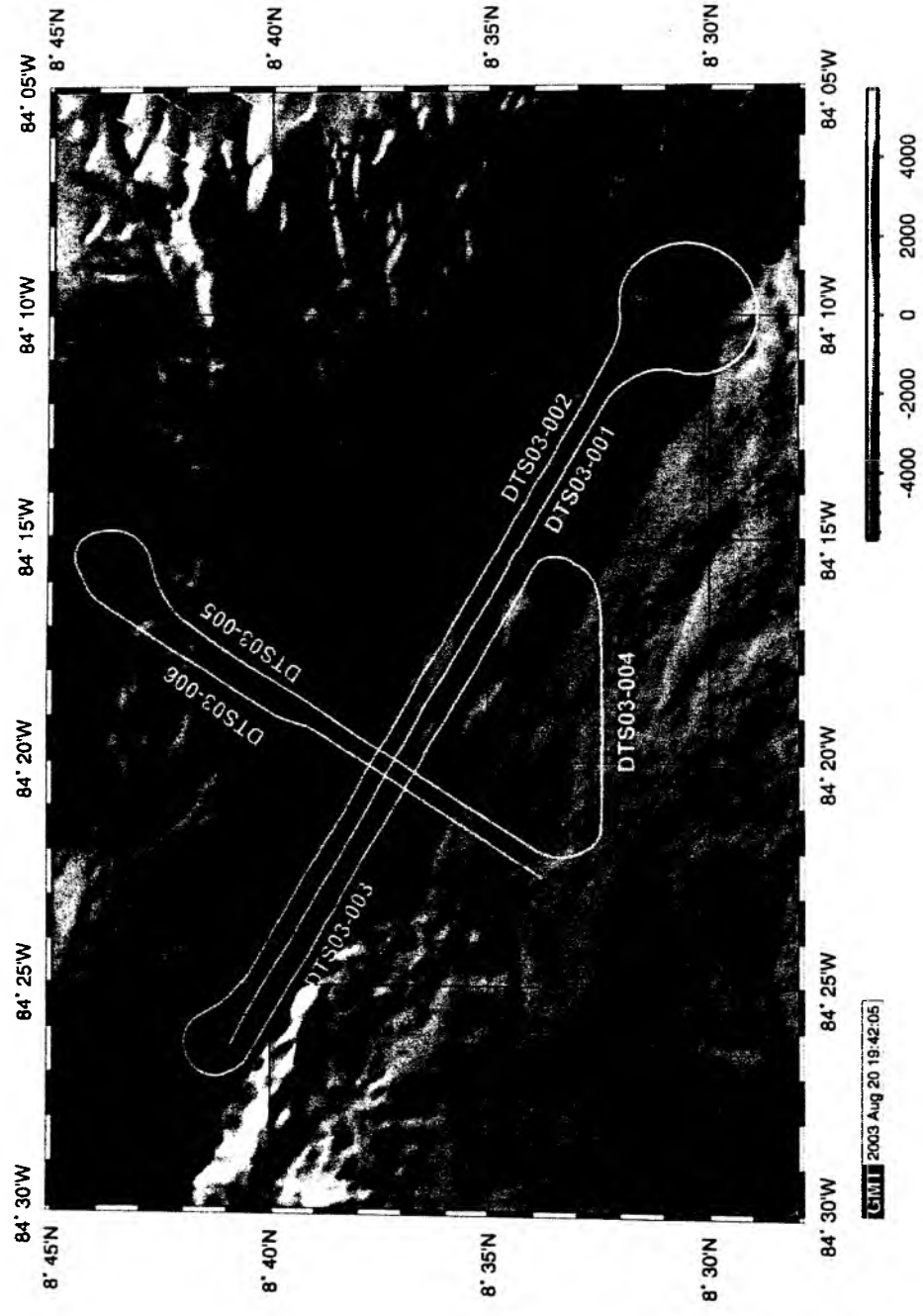

Fig. 6.2.12: Bathymetry and ship's track in the deep tow seismic and sidescan sonar survey area 'Decollement'.

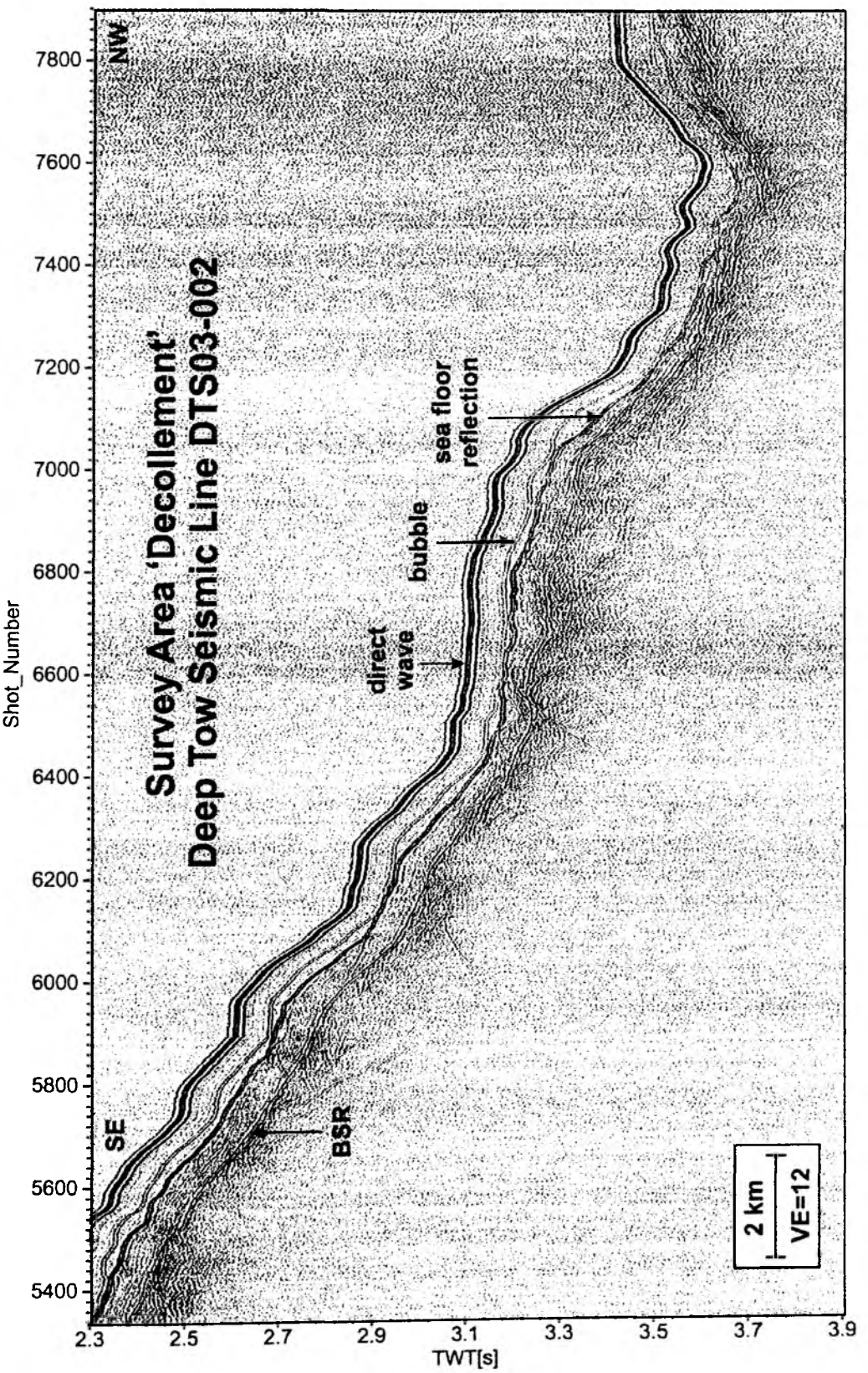

Fig. 6.2.13: *Brute stack of deep tow seismic profile DTS03-002 collected in the survey area 'decollement' parallel to the trench. Traces 10 - 12 from each shot gather were bandpass-filtered (50/100 - 500/1000 Hz) and stacked without NMO correction. No depth corrections were applied. Trace spacing (= shot point spacing) is about 10 m. VE = vertical exaggeration computed for a velocity of 1500 m/s.*

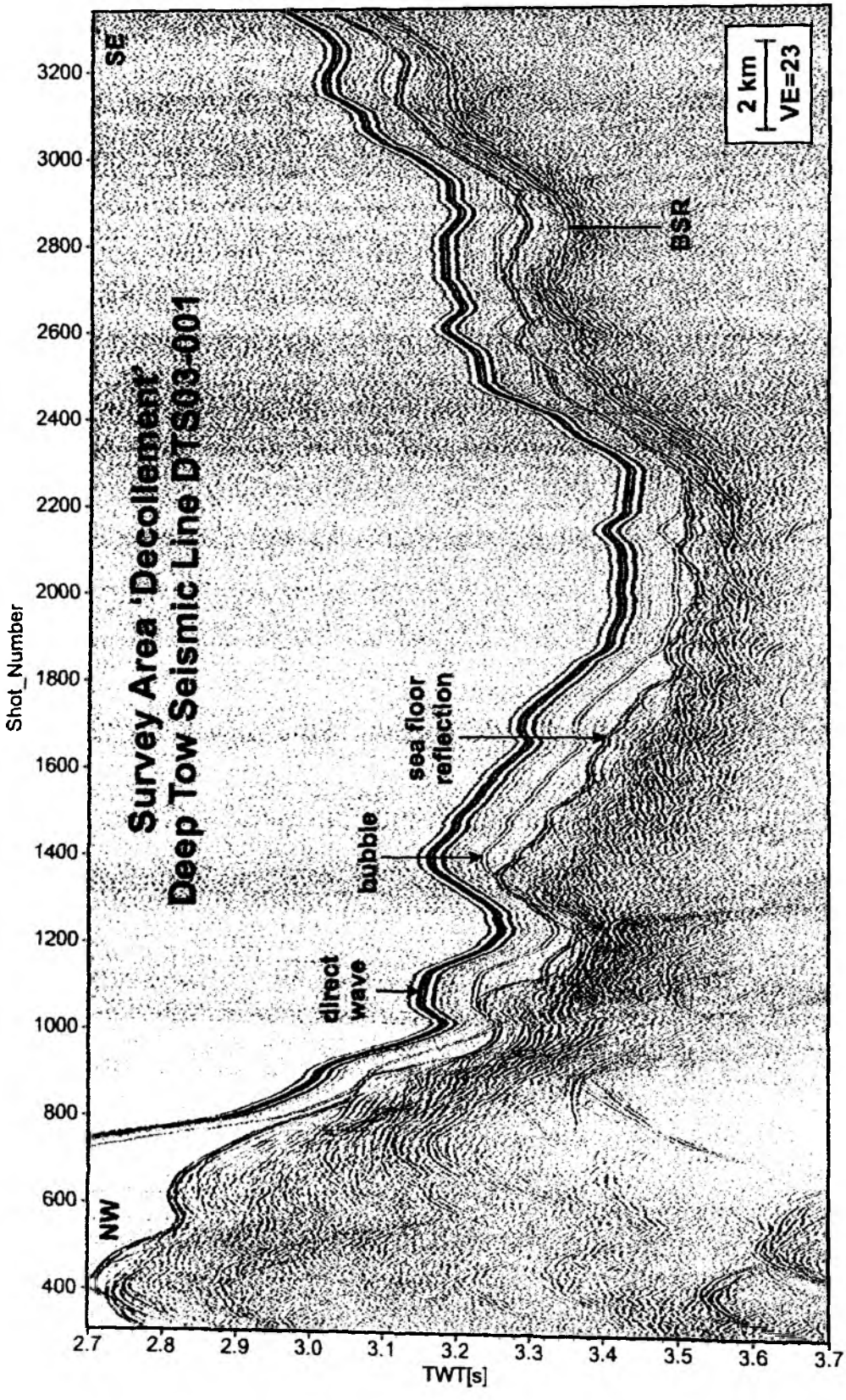

Fig. 6.2.14: *Brute stack of deep tow seismic profile DTS03-001 collected in the survey area 'decollement' parallel to the trench. Traces 10 - 12 from each shot gather were bandpass-filtered (50/100 - 500/1000 Hz) and stacked without NMO correction. No depth corrections were applied. Trace spacing (= shot point spacing) is about 10 m. VE = vertical exaggeration computed for a velocity of 1500 m/s.*

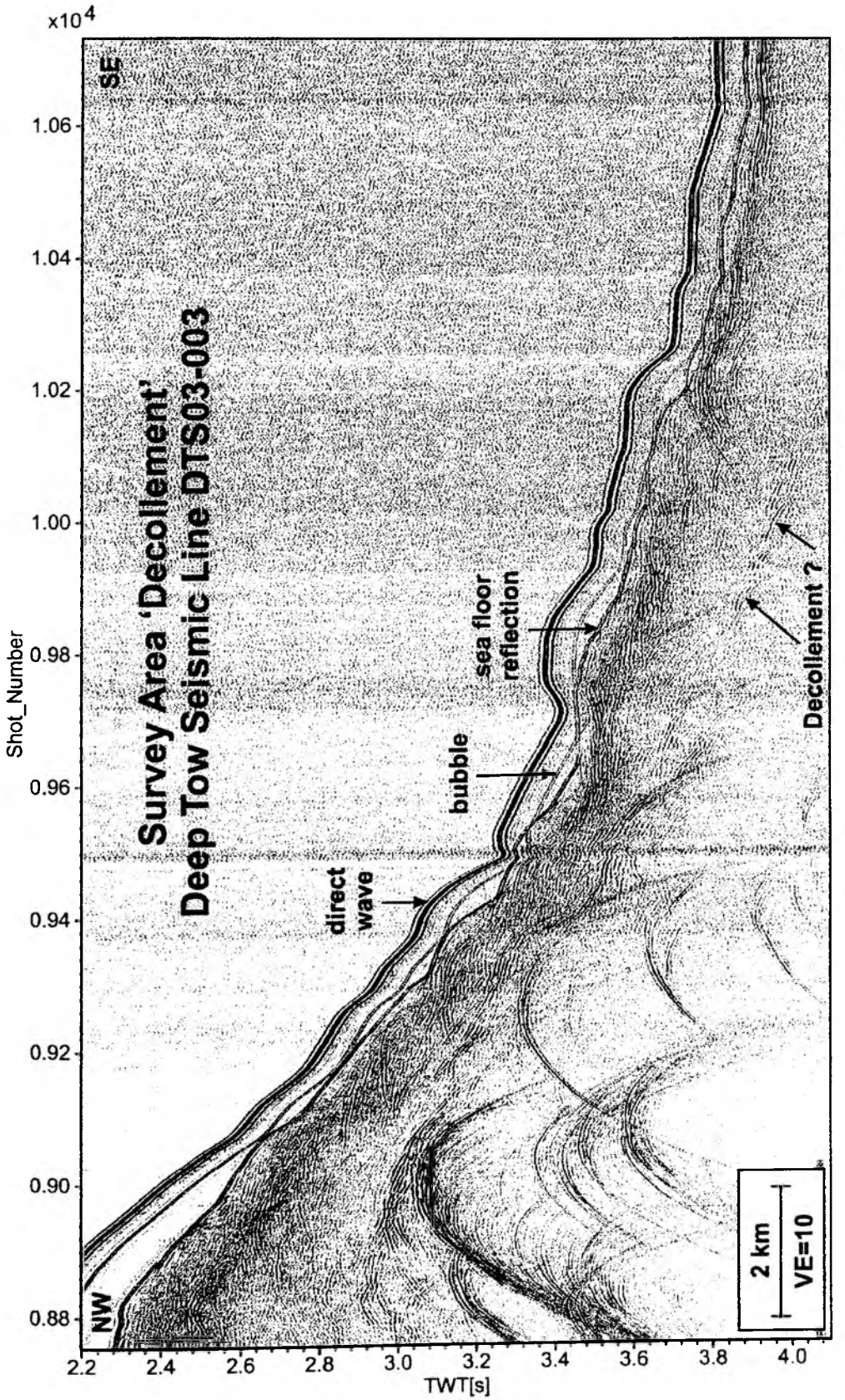

Fig. 6.2.15: *Brute stack of deep tow seismic profile DTS03-003 collected in the survey area 'decollement' parallel to the trench. Traces 10 - 12 from each shot gather were bandpass-filtered (50/100 - 500/1000 Hz) and stacked without NMO correction. No depth corrections were applied. Trace spacing (= shot point spacing) is about 10 m. VE = vertical exaggeration computed for a velocity of 1500 m/s.*

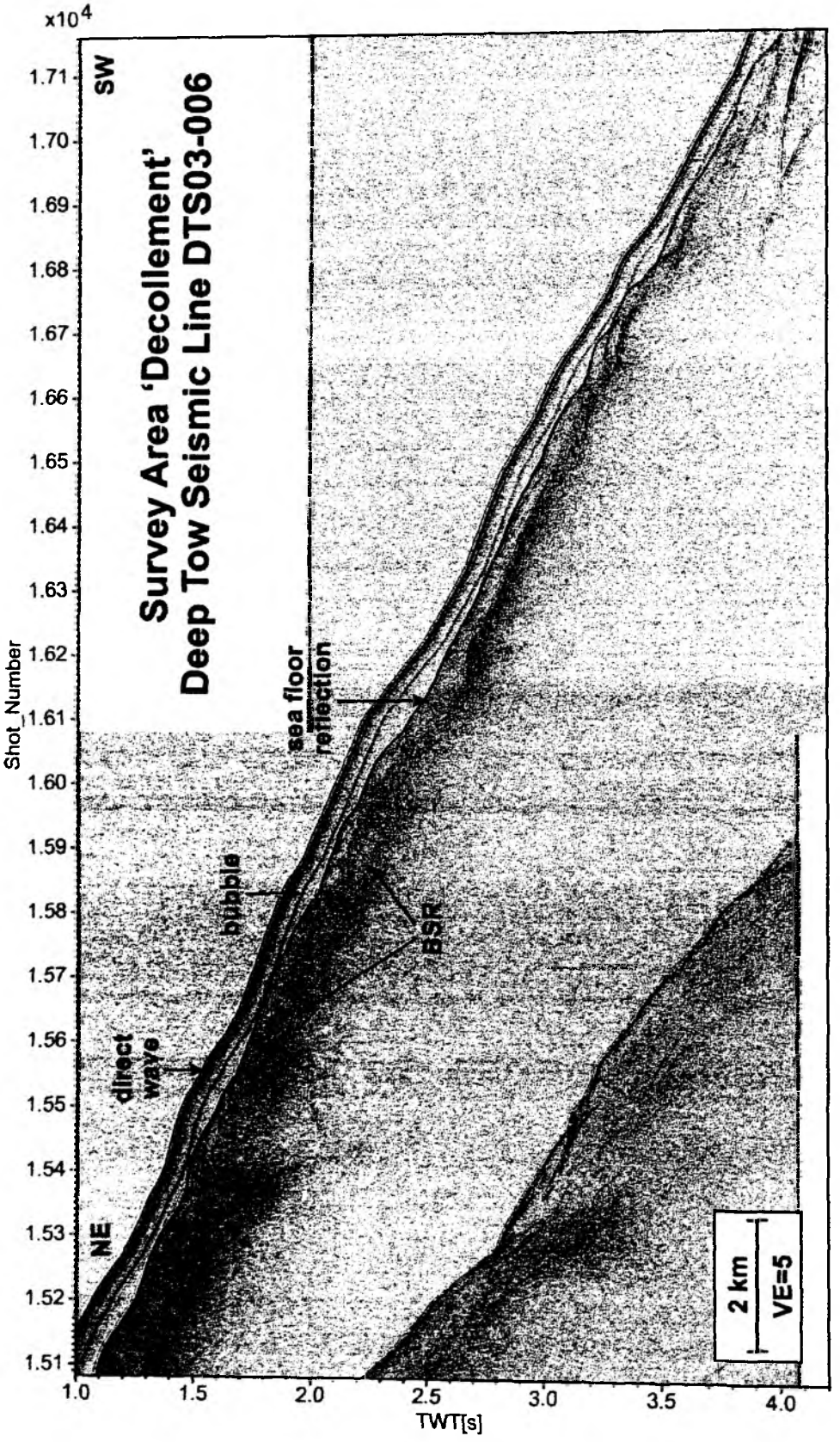

Fig. 6.2.16: *Brute stack of deep tow seismic profile DTS03-006 collected in the survey area 'decollement' perpendicular to the trench. Traces 10 - 12 from each shot gather were bandpass-filtered (50/100 - 500/1000 Hz) and stacked without NMO correction. No depth corrections were applied. Trace spacing (= shot point spacing) is about 10 m. VE = vertical exaggeration computed for a velocity of 1500 m/s.*

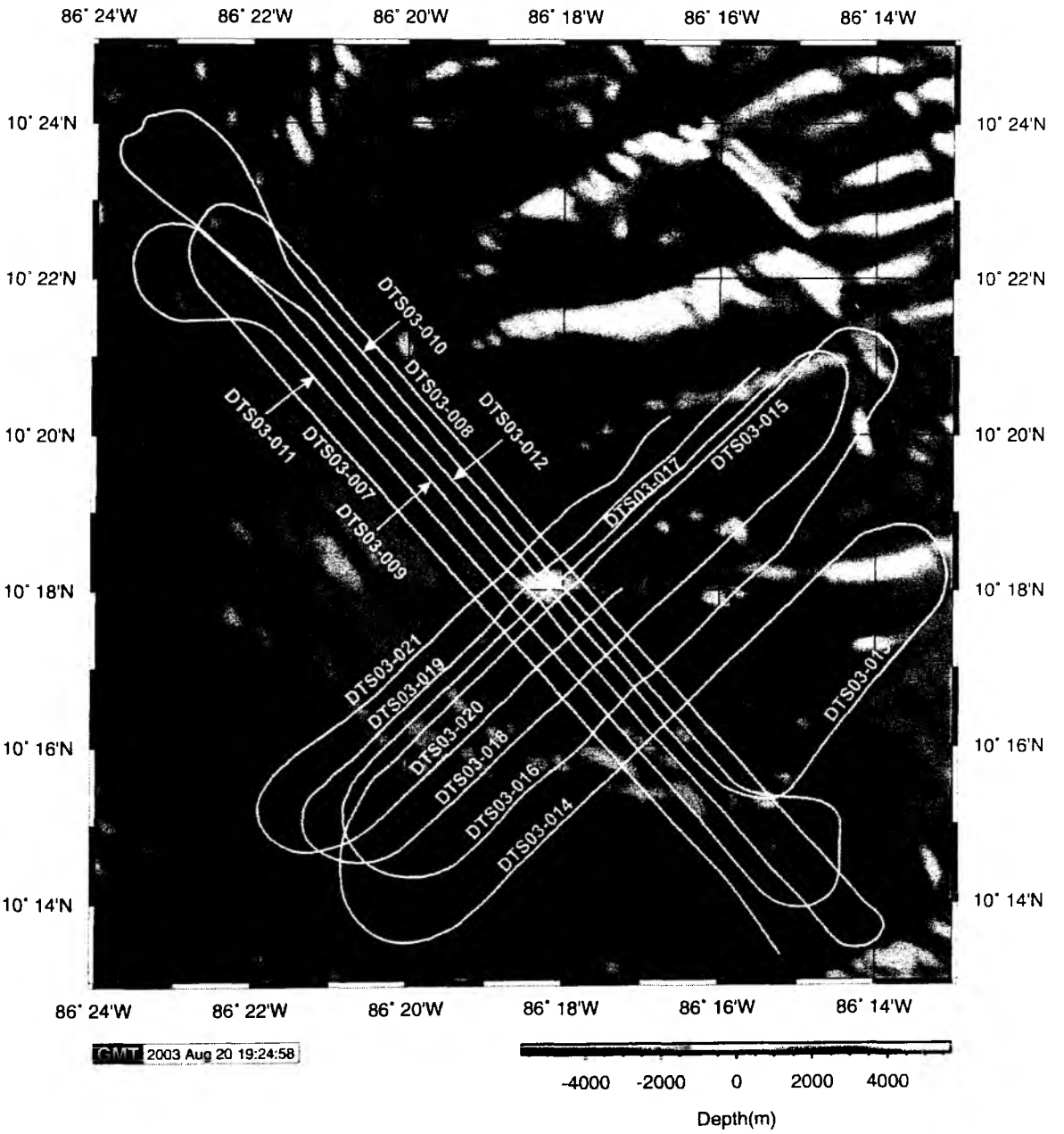

Fig. 6.2.17: Bathymetry and ship's track in the deep tow seismic and sidescan sonar survey area 'Mound Culebra'.

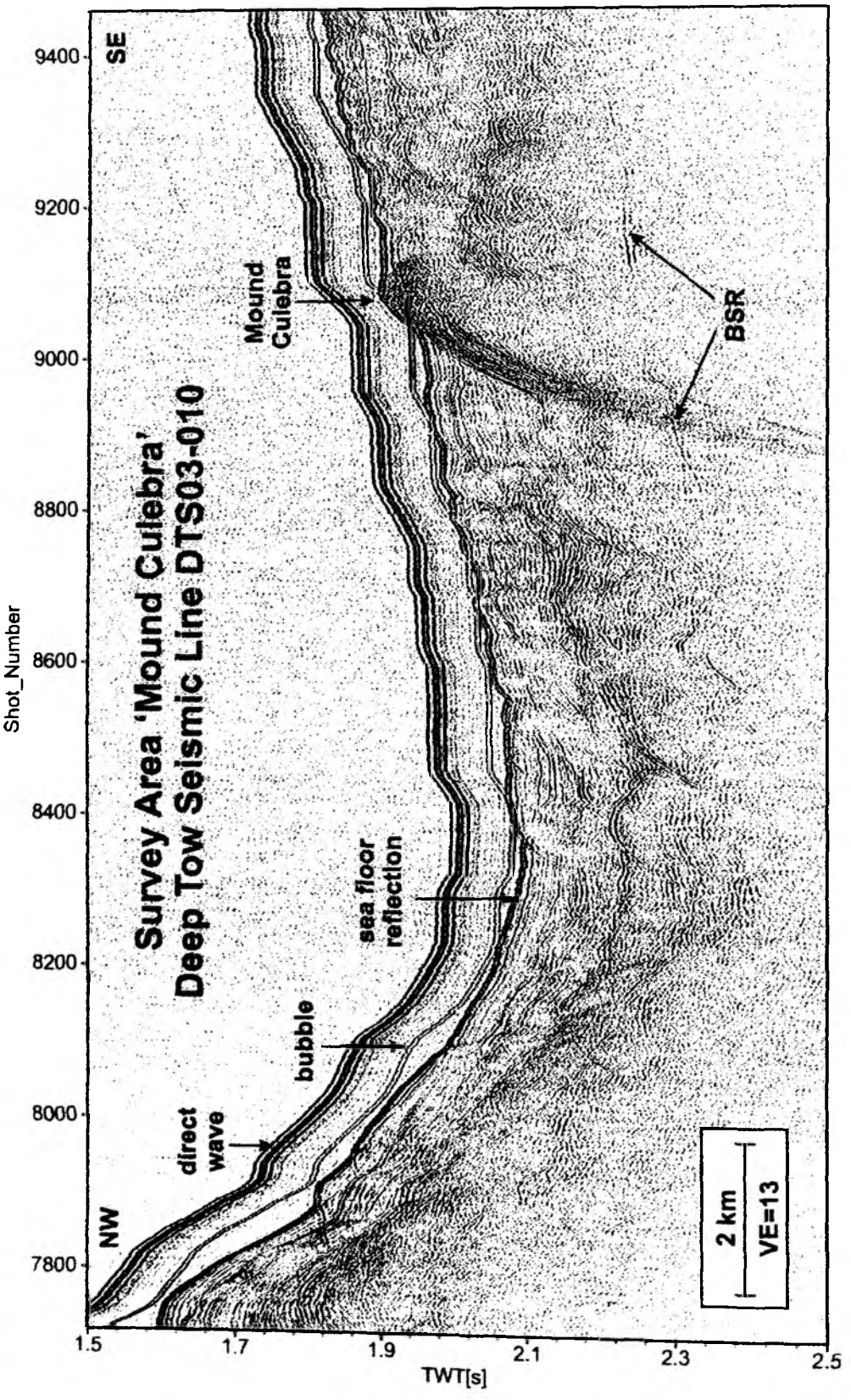

Fig. 6.2.18: *Brute stack of deep tow seismic profile DTS03-010 collected in the survey area 'Mound Culebra' parallel to the strike of the slope. Traces 10 - 12 from each shot gather were bandpass-filtered (70/140 - 500/1000 Hz) and stacked without NMO correction. No depth corrections were applied. Trace spacing (= shot point spacing) is about 10 m. VE = vertical exaggeration computed for a velocity of 1500 m/s.*

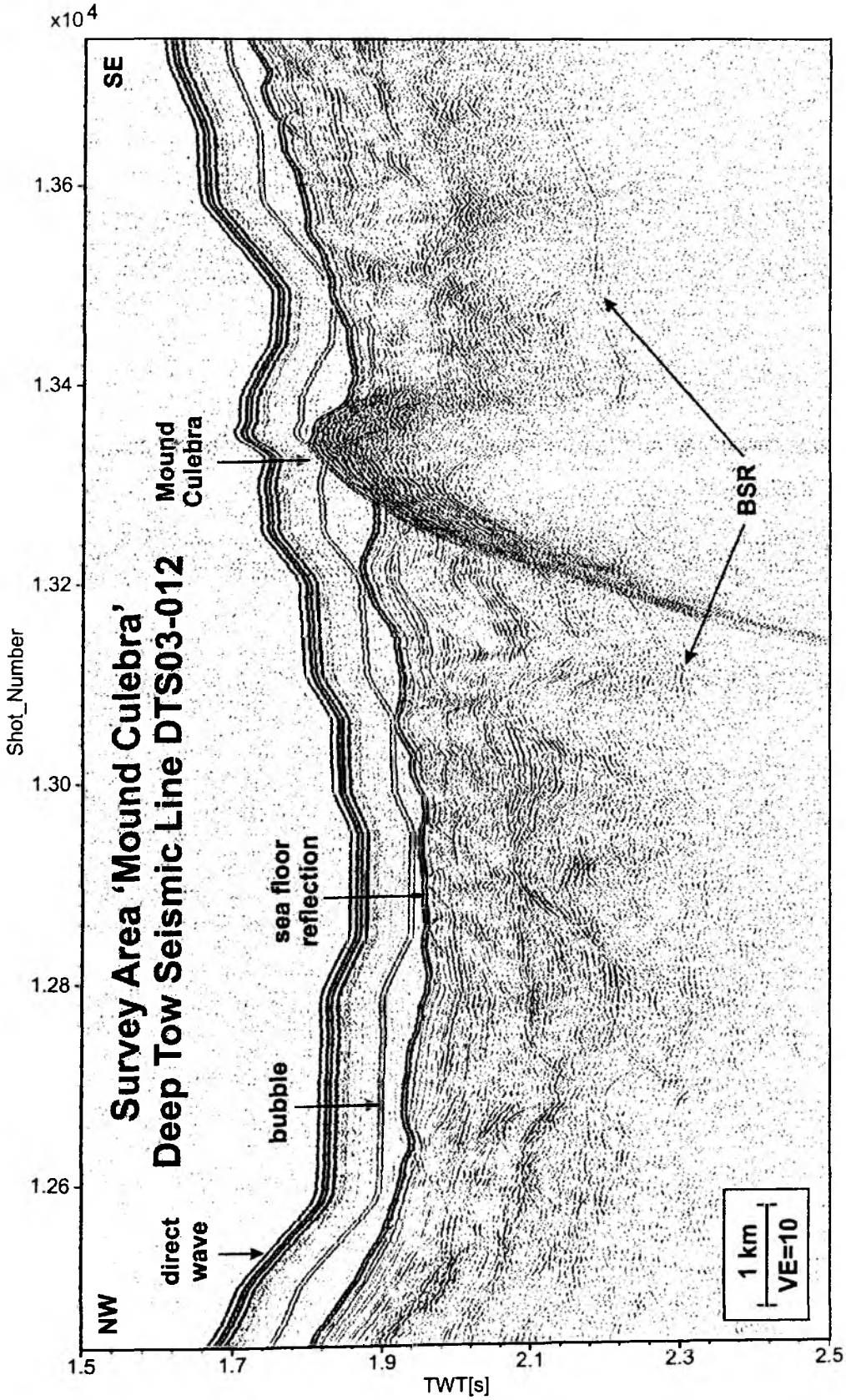

Fig. 6.2.19: *Brute stack of deep tow seismic profile DTS03-012 collected in the survey area 'Mound Culebra' parallel to the strike of the slope. Traces 10 - 12 from each shot gather were bandpass-filtered (70/140 - 500/1000 Hz) and stacked without NMO correction. No depth corrections were applied. Trace spacing (= shot point spacing) is about 10 m. VE = vertical exaggeration computed for a velocity of 1500 m/s.*

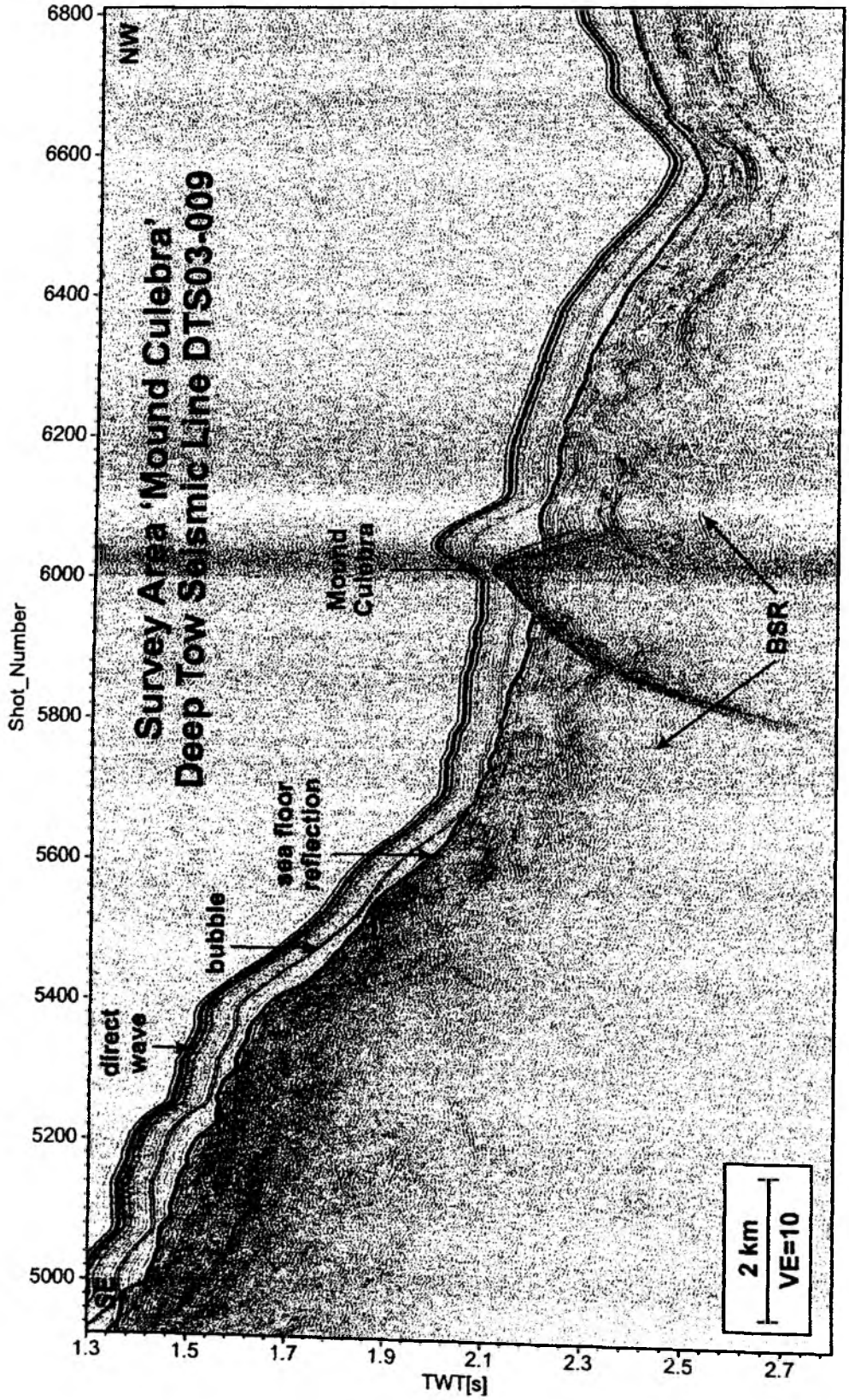

Fig. 6.2.20: *Brute stack of deep tow seismic profile DTS03-009 collected in the survey area 'Mound Culebra' parallel to the strike of the slope. Traces 10 - 12 from each shot gather were bandpass-filtered (70/140 - 500/1000 Hz) and stacked without NMO correction. No depth corrections were applied. Trace spacing (= shot point spacing) is about 10 m. VE = vertical exaggeration computed for a velocity of 1500 m/s.*

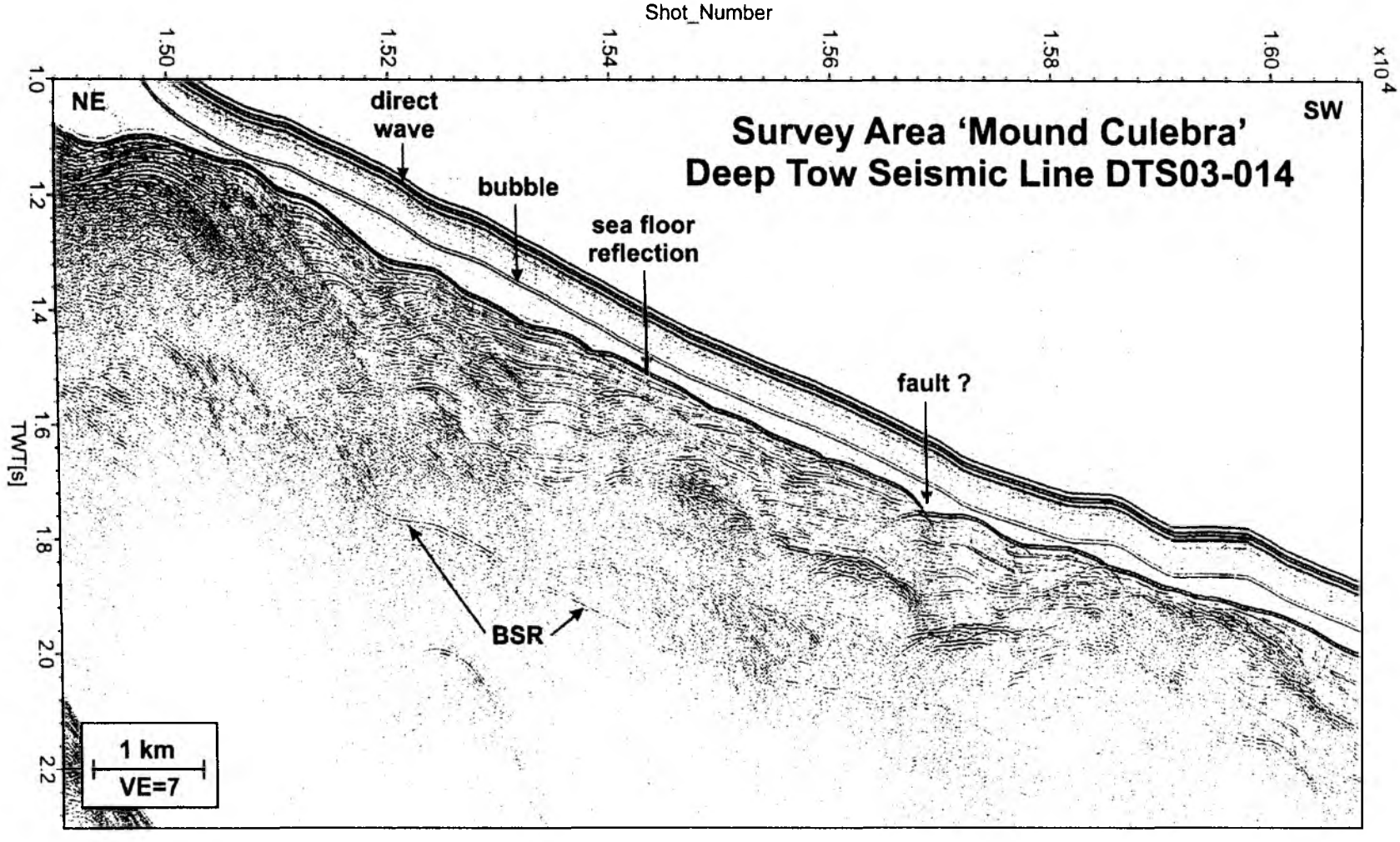

Fig. 6.2.21: *Brute stack of deep tow seismic profile DTS03-014 collected in the survey area 'Mound Culebra' parallel to the dip of the slope (downslope). Traces 10 - 12 from each shot gather were bandpass-filtered (70/140 - 500/1000 Hz) and stacked without NMO correction. No depth corrections were applied. Trace spacing (= shot point spacing) is about 10 m. VE = vertical exaggeration computed for a velocity of 1500 m/s.*

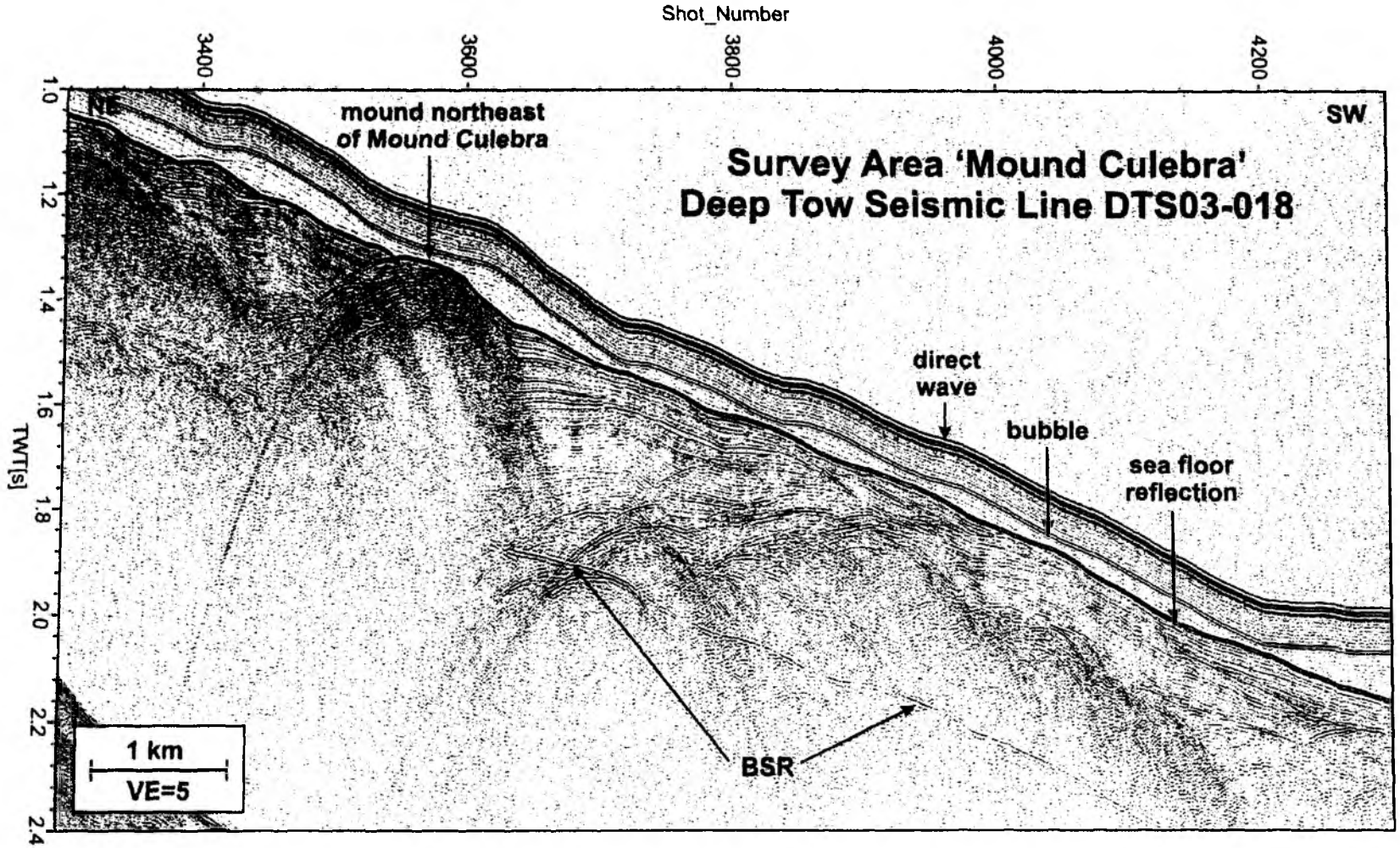

Fig. 6.2.22: *Brute stack of deep tow seismic profile DTS03-018 collected in the survey area 'Mound Culebra' parallel to the dip of the slope (downslope). Traces 10 - 12 from each shot gather were bandpass-filtered (70/140 - 500/1000 Hz) and stacked without NMO correction. No depth corrections were applied. Trace spacing (= shot point spacing) is about 10 m. VE = vertical exaggeration computed for a velocity of 1500 m/s.*

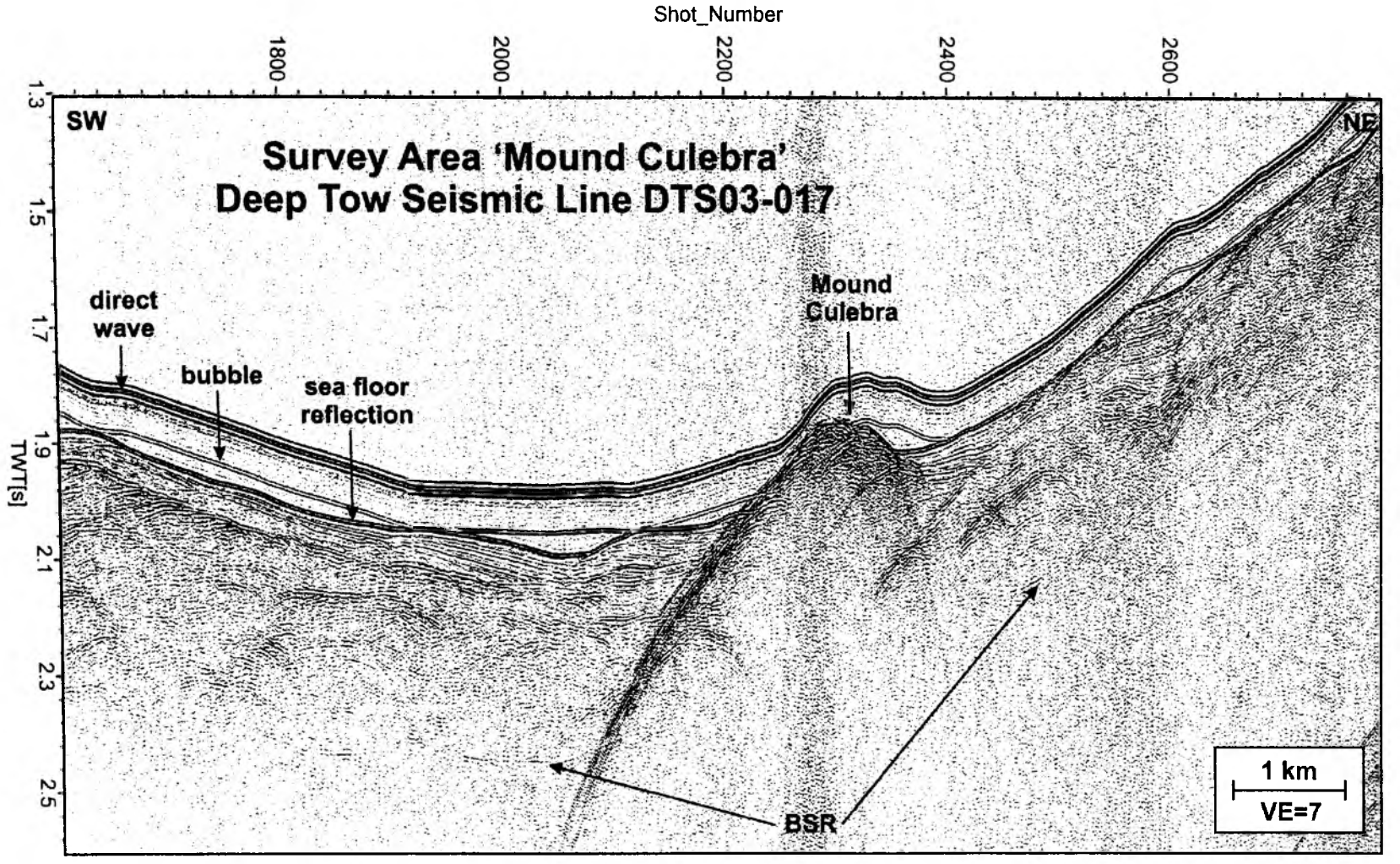

Fig. 6.2.23: *Brute stack of deep tow seismic profile DTS03-017 collected in the survey area 'Mound Culebra' parallel to the dip of the slope (upslope). Traces 10 - 12 from each shot gather were bandpass-filtered (70/140 - 500/1000 Hz) and stacked without NMO correction. No depth corrections were applied. Trace spacing (= shot point spacing) is about 10 m. VE = vertical exaggeration computed for a velocity of 1500 m/s.*

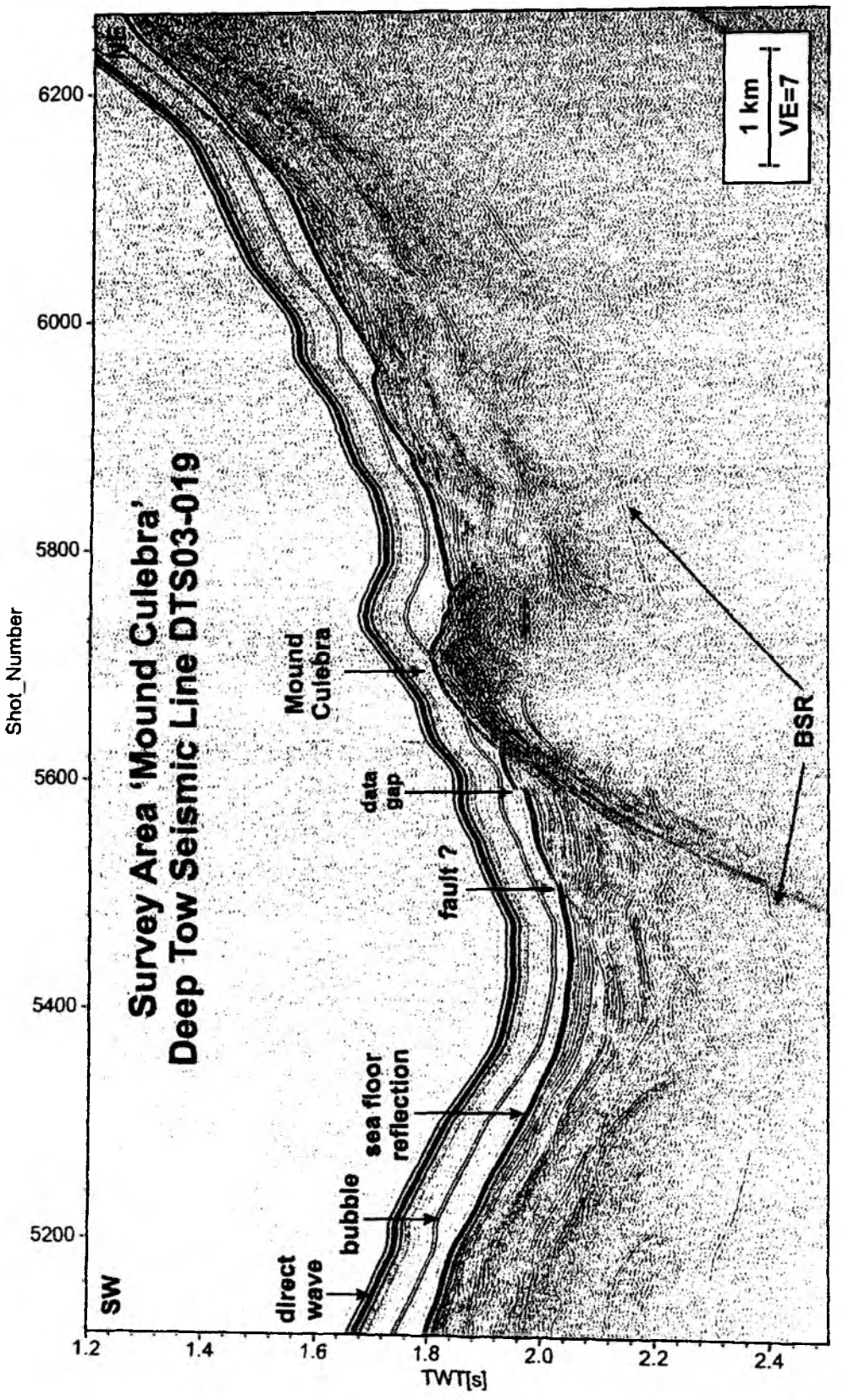

Fig. 6.2.24: *Brute stack of deep tow seismic profile DTS03-019 collected in the survey area 'Mound Culebra' parallel to the dip of the slope (upslope). Traces 10 - 12 from each shot gather were bandpass-filtered (70/140 - 500/1000 Hz) and stacked without NMO correction. No depth corrections were applied. Trace spacing (= shot point spacing) is about 10 m. VE = vertical exaggeration computed for a velocity of 1500 m/s.*

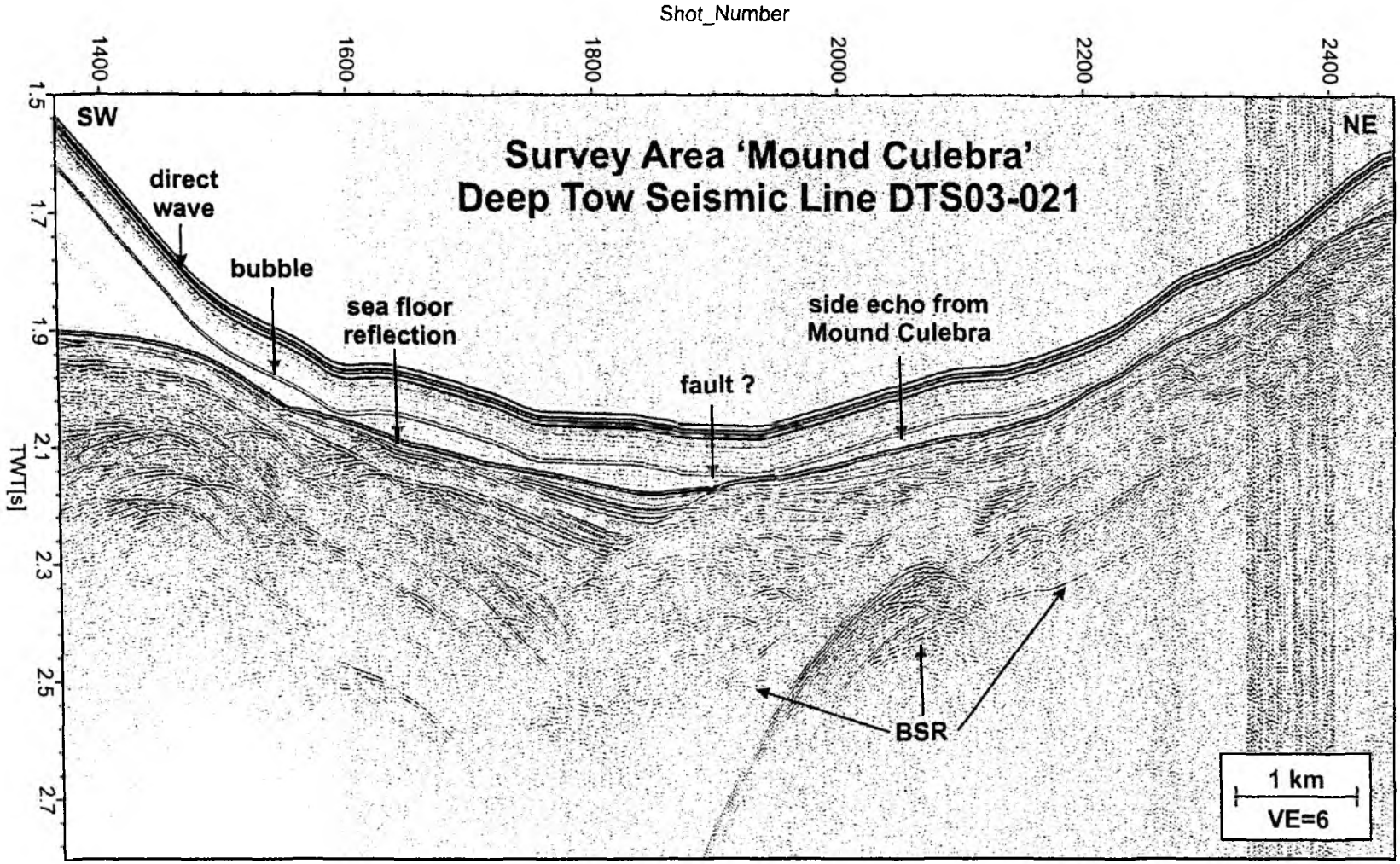

Fig. 6.2.25: *Brute stack of deep tow seismic profile DTS03-021 collected in the survey area 'Mound Culebra' parallel to the dip of the slope (upslope). Traces 8 - 10 from each shot gather were bandpass-filtered (70/140 - 500/1000 Hz) and stacked without NMO correction. No depth corrections were applied. Trace spacing (= shot point spacing) is about 10 m. VE = vertical exaggeration computed for a velocity of 1500 m/s.*

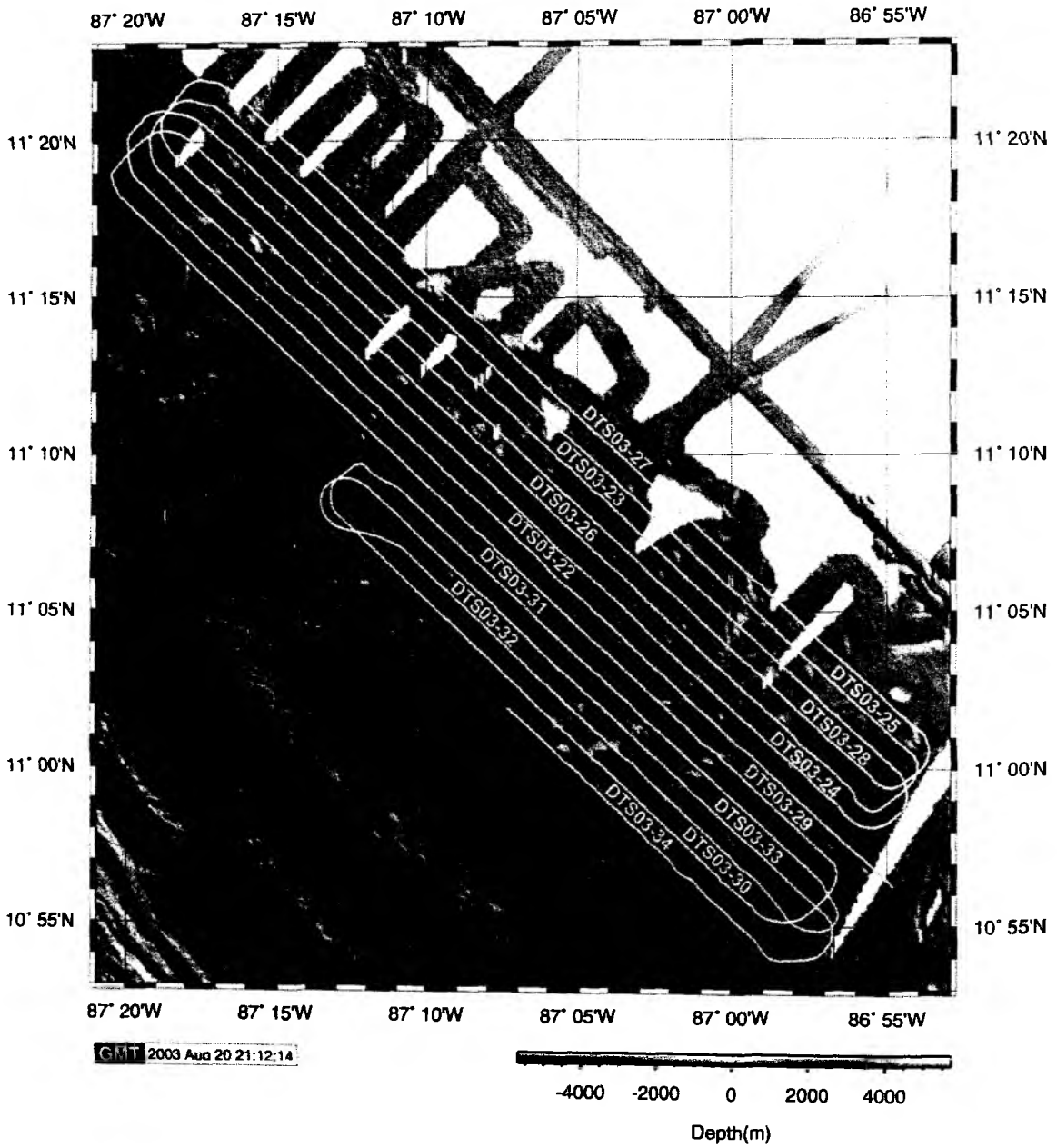

Fig. 6.2.26: Bathymetry and ship's track in the deep tow seismic and sidescan sonar survey area 'Nicaragua'.

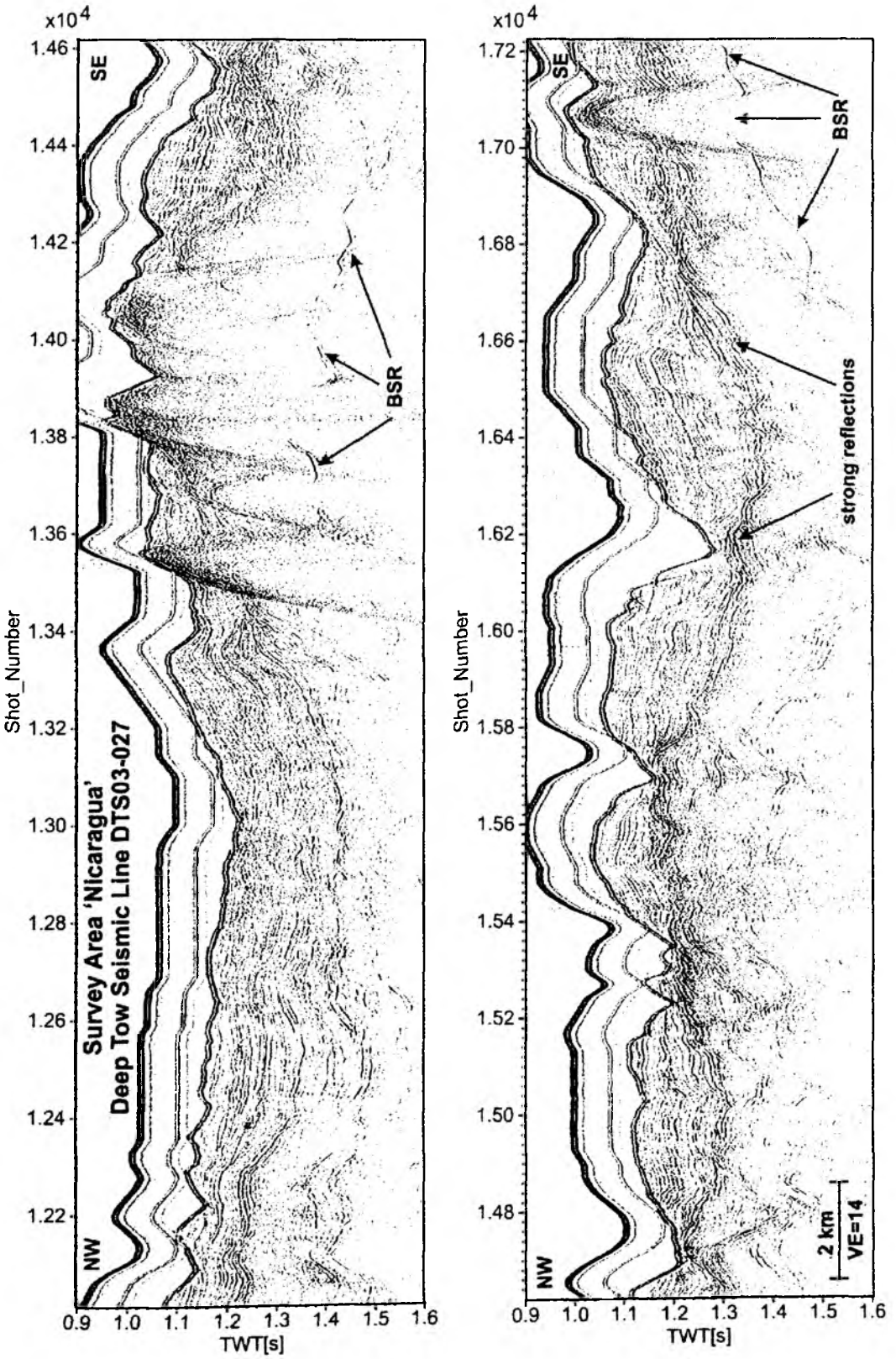

Fig. 6.2.27: *Brute stack of deep tow seismic profile DTS03-027 collected in the survey area 'Nicaragua' parallel to the strike of the slope. Traces 8 - 10 from each shot gather were bandpass-filtered (30/100 - 500/1000 Hz) and stacked without NMO correction. No depth corrections were applied. Trace spacing (= shot point spacing) is about 10 m. VE = vertical exaggeration computed for a velocity of 1500 m/s.*

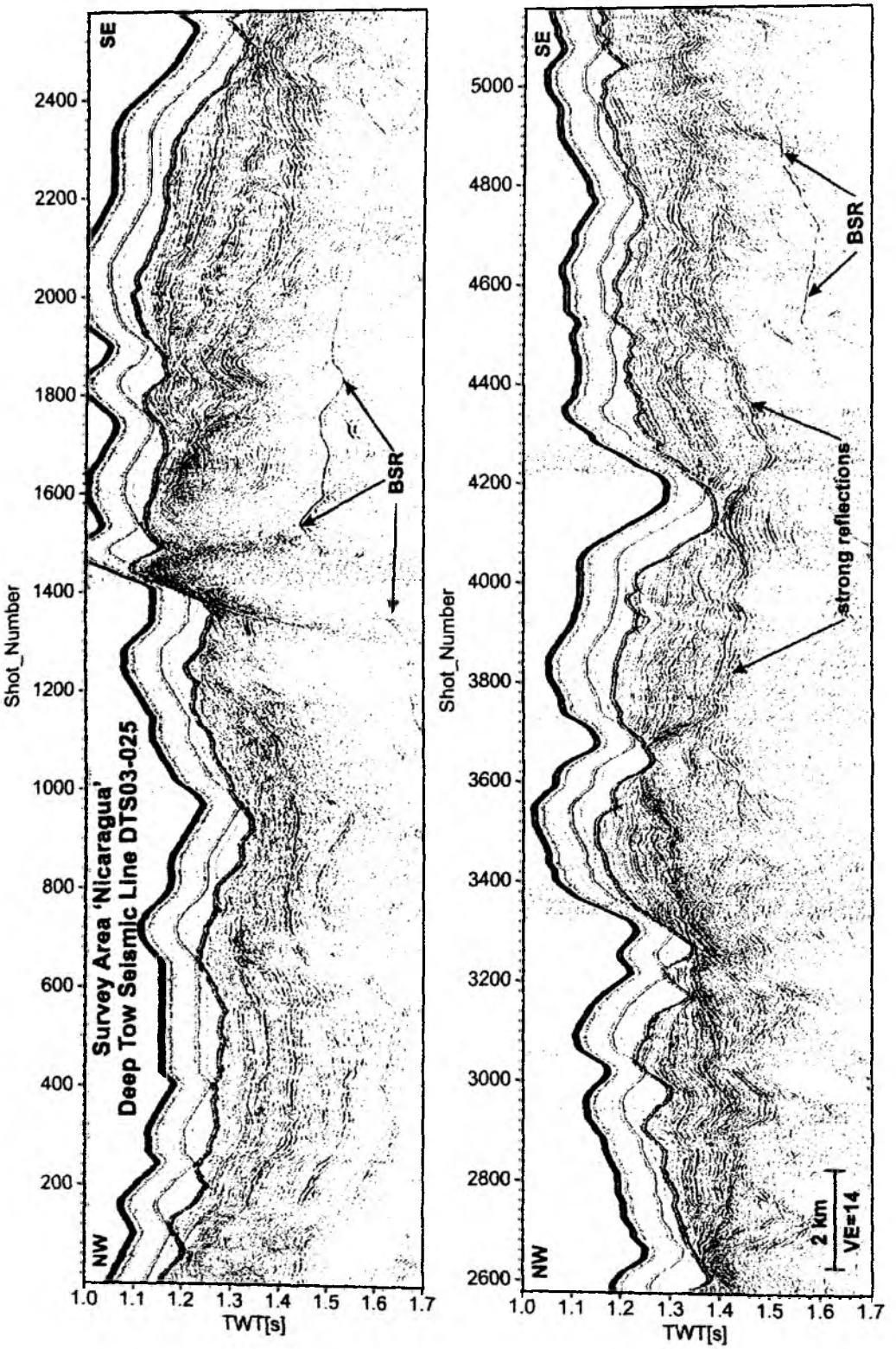

Fig. 6.2.28: *Brute stack of deep tow seismic profile DTS03-025 collected in the survey area 'Nicaragua' parallel to the strike of the slope. Traces 8 - 10 from each shot gather were bandpass-filtered (30/100 - 500/1000 Hz) and stacked without NMO correction. No depth corrections were applied. Trace spacing (= shot point spacing) is about 10 m. VE = vertical exaggeration computed for a velocity of 1500 m/s.*

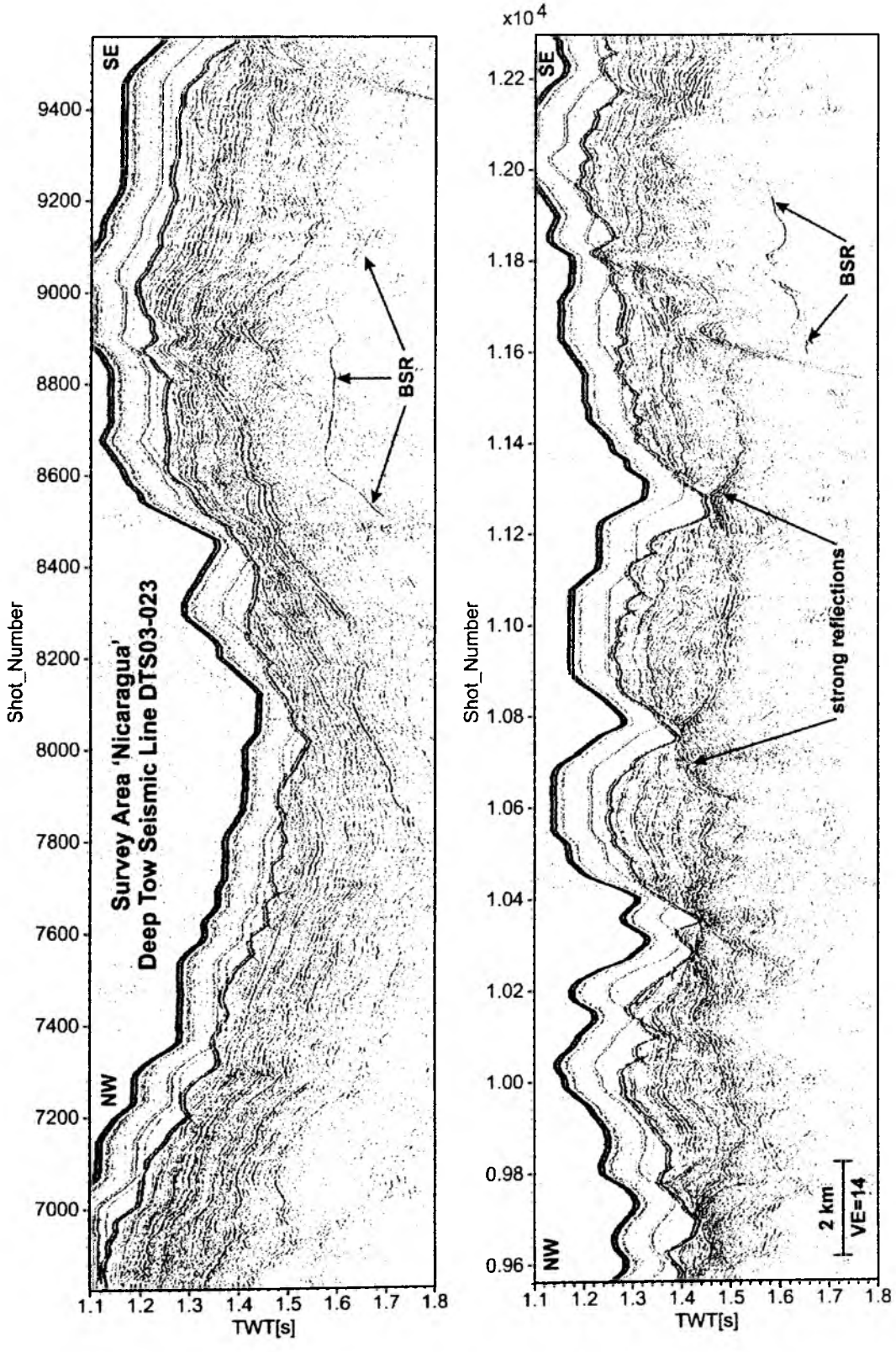

Fig. 6.2.29: *Brute stack of deep tow seismic profile DTS03-023 collected in the survey area 'Nicaragua' parallel to the strike of the slope. Traces 8 - 10 from each shot gather were bandpass-filtered (30/100 - 500/1000 Hz) and stacked without NMO correction. No depth corrections were applied. Trace spacing (= shot point spacing) is about 10 m. VE = vertical exaggeration computed for a velocity of 1500 m/s.*

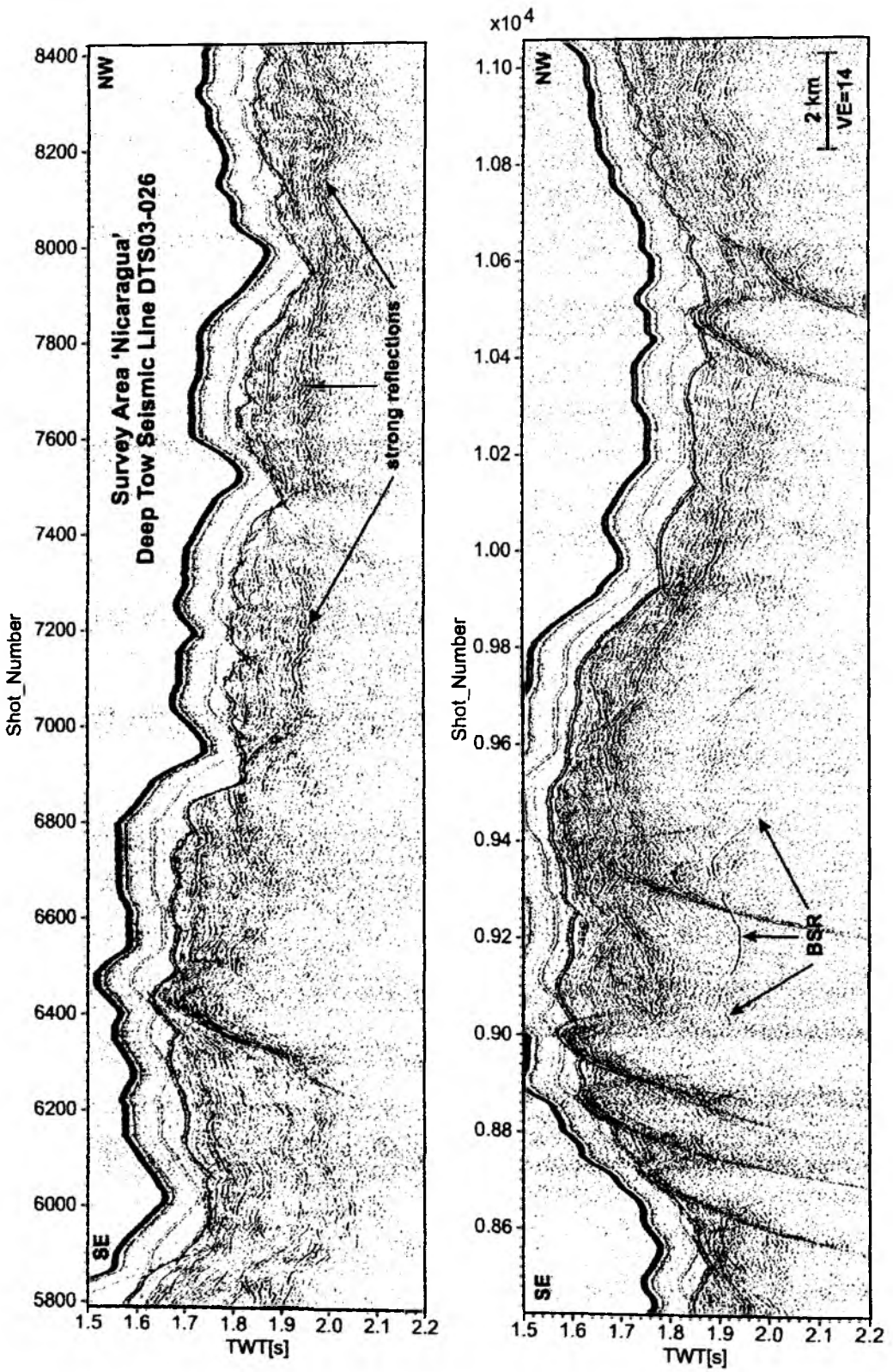

Fig. 6.2.30: *Brute stack of deep tow seismic profile DTS03-026 collected in the survey area 'Nicaragua' parallel to the strike of the slope. Traces 8 - 10 from each shot gather were bandpass-filtered (30/100 - 500/1000 Hz) and stacked without NMO correction. No depth corrections were applied. Trace spacing (= shot point spacing) is about 10 m. VE = vertical exaggeration computed for a velocity of 1500 m/s.*

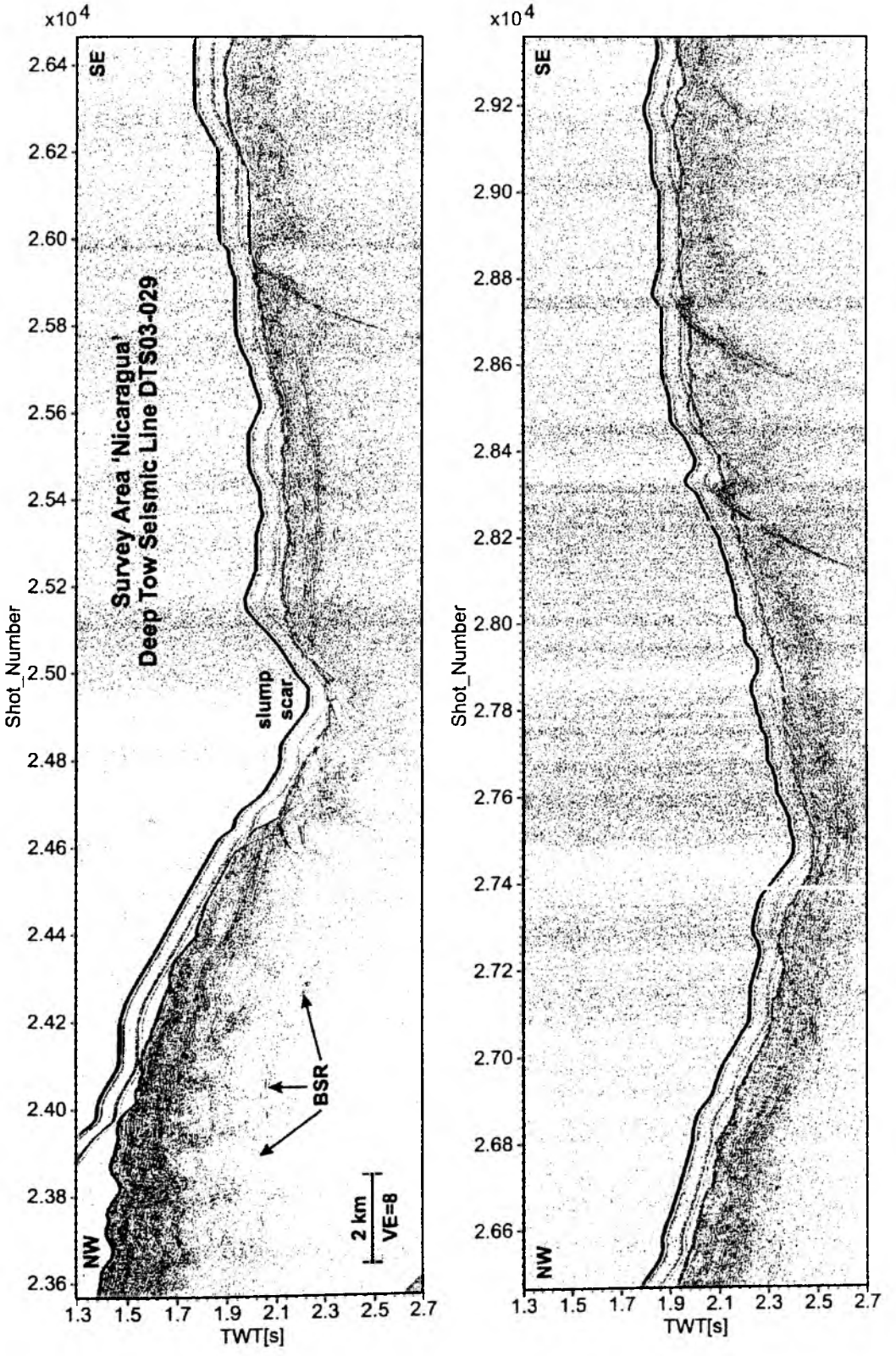

Fig. 6.2.31: *Brute stack of deep tow seismic profile DTS03-029 collected in the survey area 'Nicaragua' parallel to the strike of the slope. Traces 8 - 10 from each shot gather were bandpass-filtered (30/100 - 500/1000 Hz) and stacked without NMO correction. No depth corrections were applied. Trace spacing (= shot point spacing) is about 10 m. VE = vertical exaggeration computed for a velocity of 1500 m/s.*

6.3 Magnetic Data

6.3.1 SO173-1

During R/V SONNE cruise SO 173/1 2 magnetic profiles were collected. The magnetometer was deployed during transit between different working areas. Due to the technical parameters of the GeoMetrics G801/3 Marine Proton Magnetometer system, its maximum working depth is limited to 70 meters below the sea surface.

The measurement of the natural magnetic field requires that the influence of other, artificial magnetic fields is minimized. Consequently, a minimum distance between the vessel and the sensor is required. In the case of R/V SONNE this distance is 180 meters. To maintain a sensor depth of less than 70 meters below sea surface, the ship's velocity must exceed 4 nm per hour.

The total field magnetic raw data has been interpreted. No corrections such as daily variations or latitude correction were applied. Therefore, the resulting interpretations are preliminary.

The magnetic profiles obtained are shown in Figure 6.3.1 and 6.3.2. Both profiles are mostly on the

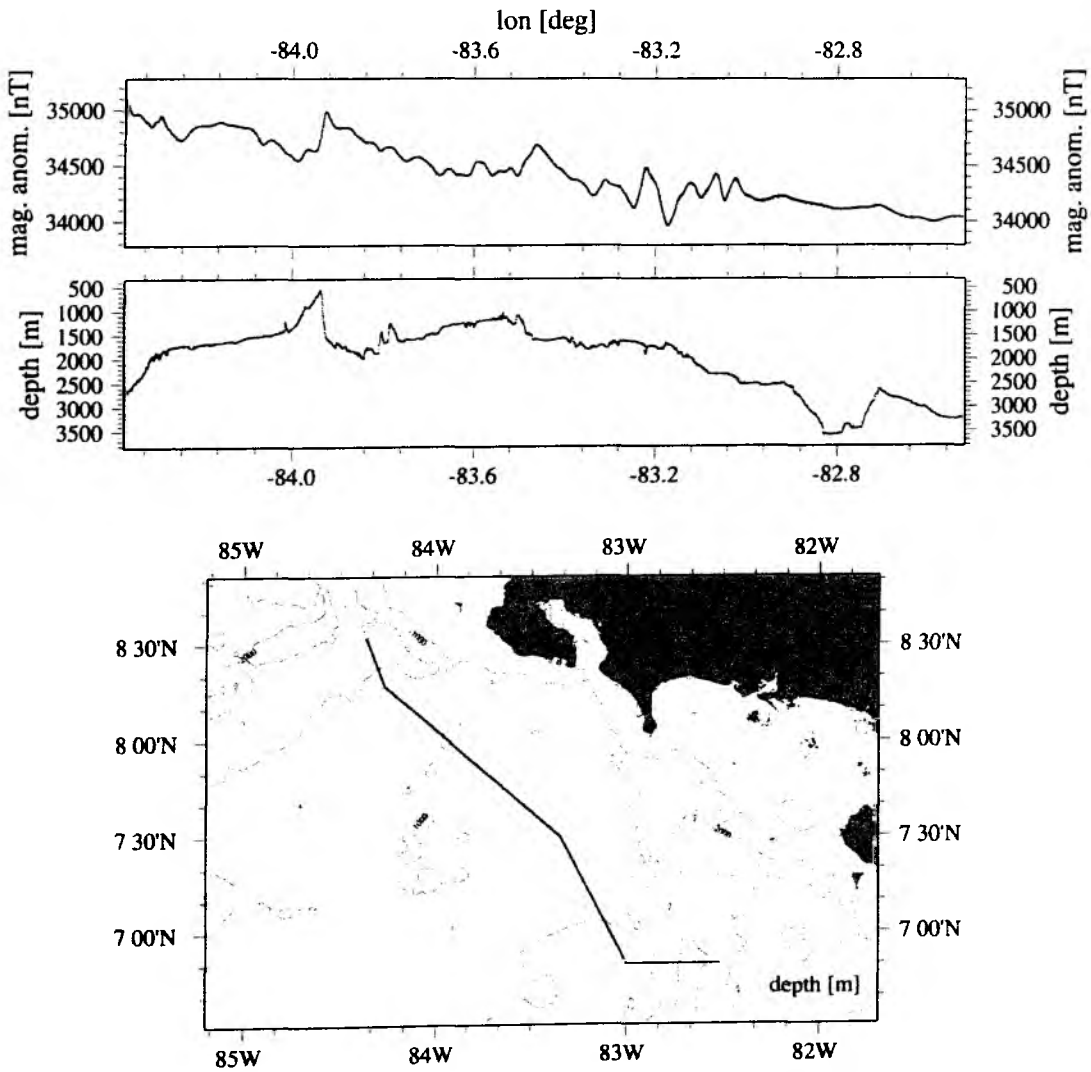

Fig. 6.3.1: Magnetic field strength, bathymetry and track of magnetic profile SO 173, Profile 1.

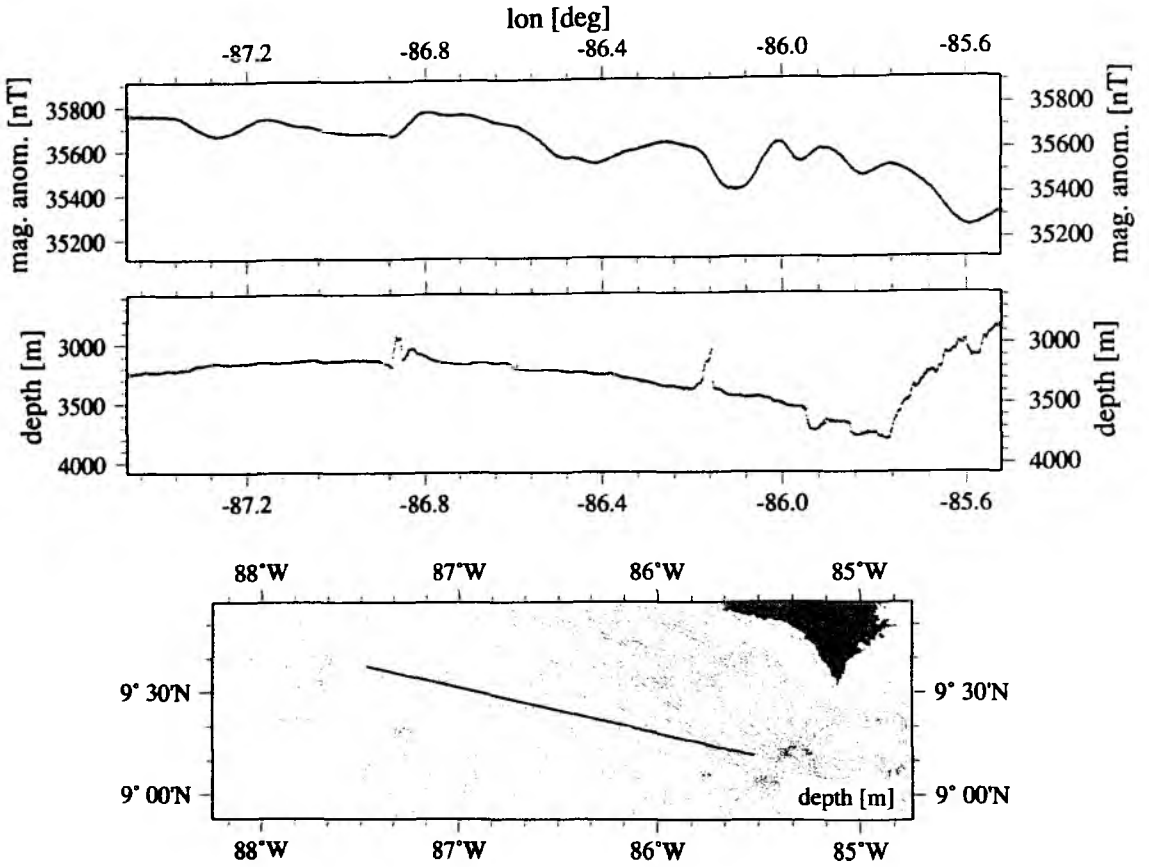

Fig. 6.3.2: Magnetic field strength, bathymetry and track of magnetic profile SO 173, Profile 2.

oceanic plate. Profile 1 strikes about 320° offshore Osa peninsula, with a length of approximately 180 nm, roughly paralleling the Costa Rican coastline. The magnetic data show a gradual decrease of about 1000 nT in magnetic field strength, with relatively higher values in the north-northwest. A correlation to topographical variations can be observed (e.g. between approximately 84° W and 83.5° W) as well as a series of abrupt changes between 83.3° W to 83° W, before the values continue smoothly towards the southwest.

Profile 2 trends approximately 290°, starting west of the Nicoya Slump, and extends about 120 nm. The overall variation is about 500 nT, with values gradually decreasing trenchwards. Topographic highs correlate to magnetic anomalies. Local variations seem to increase at the eastward end of Profile 2 (86.1° W to 85.6° W).

6.4 Seismics and Seismological Investigations

During cruise SO 173/1 numerous seismic profiles were collected, using ocean bottom recorders, a four-channel streamer and a deep tow streamer. Two different seismic sources were used. All instruments are described in chapter 5.3 and 5.5, details of the profiles can be found in Appendices 9.2, 9.3 and 9.4. In addition, seismological investigations were made (Chapter 6.4.2). In the following, the data processing and archiving is described.

6.4.1 Seismic Processing: OBH/OBS Wide-Angle Data and MCS Reflection Data

D. Klaeschen, C. Papenberg & Seismic and Seismological Working Group

6.4.1.1 The Processing Scheme

The OBH/S data recorded in continuous mode on the MLS and MBS units have to be converted into standard trace-based SEG-Y format for further processing. The necessary program structure was mainly taken from the existing REFTEK routines and modified for the OBH requirements and GEOMAR's hardware platforms.

The flow chart shown in Figure 6.4.1 illustrates the processing scheme applied to the raw data. A detailed description of the main programs follows below:

send2pas: For the PC cards used with the MBS and MLS recorders, data expansion and format conversion into REFTEK data format is performed using a DOS/Windows-based PC. The program send2pas reads data from the flashcards used during recording. Decompressed data are written onto the PC's hard disk using PASSCAL data format. Either 16- or 32-bit storage is available. After ftp transmission to a SUN workstation, ref2segy and all other software can be used to handle and process the data files and store them as SEG-Y traces.

While processing the MLS recordings, many time slips of one sampling interval were detected by the send2pas software, typically at a rate of one time slip every 1-2 hours. The time slips are caused by mismatch of the actual sampling rate of the MLS recorder compared to the desired sampling rate. This mismatch arises because the clock rate of the crystal oscillator in the MLS recorder is temperature-dependent (Klaus Schleisiek, SEND GmbH, pers. comm.). The temperature dependence is known and corrected in the determination of the system time, but for performance reasons the sampling pulses are directly generated from the oscillator signal without any time correction. The send2pas routine detects when the accumulated inaccuracies of the sample rate cause an effective timing error of one sample, but only reports and does not correct the „time slip".

The resulting total time error was 200 to 400 ms on average for the wide-angle profiles and up to several tens of seconds for the seismology network, showing clearly the necessity of a special time slip correction for the MLS data. After careful analysis of the problem, we concluded that the best way to address the time slip timing error in the wide-angle data is to add the time slips reported in the send2pas log file, and regard the time slip total as an extra skew contribution which is corrected within the dat2segy program later in the processing flow (see below, note that the signs of skew and time slips are opposed to each other, i.e., a negative sum of time slips corresponds to a positive skew). As each trace is at most a few tens of seconds long (vs. 1 hour and more between non-cancelling time slips), the corrected time is expected to be highly accurate with uncertainties well below one sample length.

ref2segy: The ref2segy program converts the output of send2pas into a pseudo SEG-Y trace consisting of one header and a continuous data trace containing all samples, as used by the PASSCAL suite of

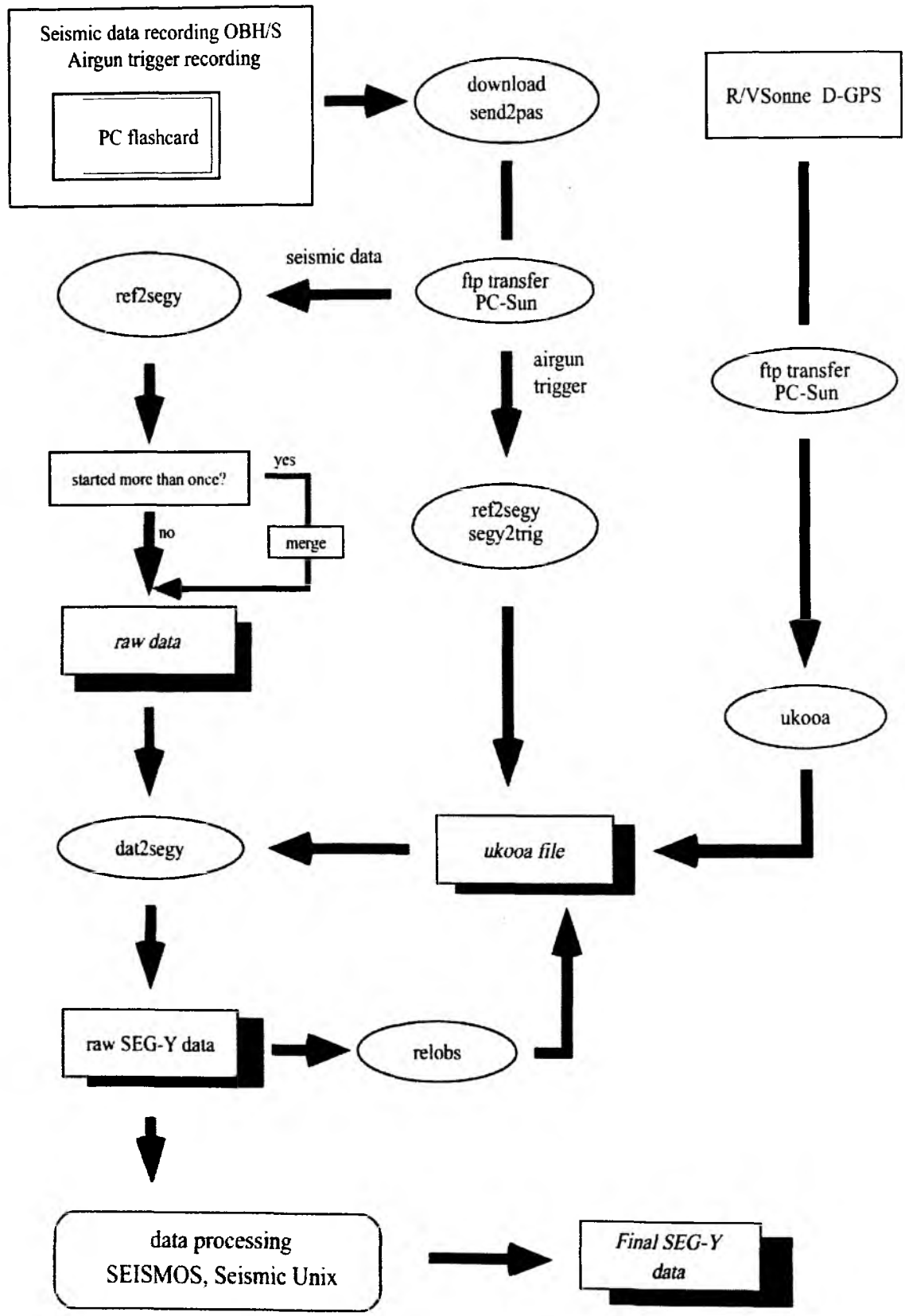

Fig. 6.4.1: Processing of OBH/OBS data from raw data to SEG-Y records.

seismic utility programs. For each channel (normally pressure, vertical velocity, and velocity along two mutually perpendicular horizontal directions for OBS; pressure for OBH) one file is created with the name derived from the start time, the serial number of the Methusalem system, and the channel number. The file size of the pseudo-SEGY file is directly related to the recording time. For instance, a recording time of one hour sampled at 200 Hz (16 Bit) will produce a file size of 1.44 MB per channel. A record with two channels and a recording time of two days will produce a total data volume of 70 MB.

merge: If an error occurs during the download process, the ref2segy program has to be restarted. This may lead to several data files with different start times. Merging these files into a single file is performed by the merge program. Gaps between the last sample and the first sample of the consecutive data traces are filled with zeros. Overlapping parts are cut out.

pql: pql (Passcal Quick Look) is a simple display program for continuous seismic data. Its interactive zooming capability allows a rapid inspection of data quality.

segy2trig: The trigger signal, provided by the airgun control system, is recorded on an additional MBS unit during the shooting period. The trigger data are treated similarly to regular seismic data and downloaded to the hard disk via the send2pas and ref2segy programs. Then, the segy2trig program detects the shot times in the data stream by identifying the trigger signal through a given slope steepness, duration and threshold of the trigger pulse. The output is an ASCII table consisting of the shot number and the shot time. Accuracy of the shot time is one of the most crucial matters in seismic wide-angle work, and must be reproduced with a precision of a few ms. Due to this demand the shot times have to be corrected with the shift of the internal recorder clock. Additionally, the trigger file contains the profile number, the start/ end time of the profile and the trigger recording. The shot times are part of the ukooa file, which links them with the coordinates of the source and the hydrophones.

ukooa: The ukooa program is used to establish the geometric database by calculating the positions of sources at any given shot time and offset from the ship. The source is placed on the ship track using simple degree/meter conversions and then written to a file in UKOOA-P84/1 format. Corrections for offsets between antenna and airguns as well as consistency checks are included. This file will be used when creating a SEG-Y section via the dat2segy program. The program requires the trigger file to contain the shot times, the ship's navigation (see Chapter 5.1.1), and a parameter file containing information for the UKOOA file header as basic input information.

dat2segy: The dat2segy program produces standard SEG-Y records either in a 16- or 32-bit integer format by cutting the single SEG-Y trace (the ref2segy output) into traces with a defined time length based on the geometry and shooting time information in the ukooa file. In addition, the user can set several parameters for controlling the output. These parameters are information about the profile and the receiver station, number of shots to be used, trace length, time offset of the trace and reduction velocity (to determine the time of the first sample within a record). Also the clock drift of the recorder (skew) is taken into account and corrected for. For the MLS data the total time error resulting from the observed time slips described above was subtracted from the clock drift value. The final SEG-Y format consists of the file header followed by the traces. Each trace is built up by a trace header followed by the data samples. The output of the dat2segy program can be used as input for further processing with GEOSYS, SEISMOS or Seismic Unix (SU).

relobs: Because of drifting of the OBH and OBS instruments during deployment and errors in the ship's GPS navigation system, the OBH positions may be mislocated by up to several 100 m. Since this error

leads to asymmetry and incorrect travel time information in the record section, it has to be corrected. This is accomplished with the program relobs.

For input, the assumed OBH location, shot locations and the picked travel times of the direct wave near to its apex are needed. To simplify the picking a static correction with a hyperbolic equation was performed to flatten the direct wave. This yields a much more coherent direct arrival which would normally suffer from strong spatial aliasing in the uncorrected section making it difficult to track. By shifting the OBH position, relobs minimizes the deviation between computed and real travel times using a least mean square fitting algorithm (assuming a constant water velocity).

Fortunately, wide-angle profiles 301/302, 33/34 and 50/51 were shot forth and back during the cruise giving us the opportunity to adjust the source offset, i.e. the distance from the research vessel's GPS position to the center of the airgun array, which was calculated to be 84 m for the Bolt-gun and 66 m for the GI-gun, respectively. Thus, an accuracy in receiver position determination of about 10 m was possible.

Beside these main programs for the regular processing sometimes additional features are needed for special handling of the raw data:

divide: The program divide cuts the raw data stream into traces of a given length without offset and time information, storing the output in SEG-Y format. The routine is useful for a quick scan of the raw data or if a timing error has occurred.

segyhdr: The routine segyhdr prints all the header values of the raw data on the screen.

segyshift: Segyshift modifies the time of the first sample, allowing the whole raw data trace to be shifted by a given value. This is very useful when shifting the time base from Middle European Time to Greenwich Mean Time or any local time. Because of recording problems, the data sometimes show a constant time shift, which can be corrected as well with segyshift.

castout: The program castout allows the user to remove a specified time window from the raw data stream. When the shooting window is much smaller than the recording time, one can reduce the data volume by cutting out only the useful information. This will reduce the demand for disk space.

6.4.1.2 OBH/OBS-Data Analysis and Processing with Source Signals of 32 Liter Bolt-Guns

Raw data: As an example, the OBH record section 01 for profile 302 shot with an Bolt-gun is shown in Figure 6.4.2. For the analysis, offset ranges between 0-12 km and 44-55 km southwest are presented in detail.

Frequency filter analysis: To determine the frequencies of the seismic energy, filter panels with narrow frequency band passes for the offset range 0-12 km and 44-55 km, respectively, are shown in Figures 6.4.3 and 6.4.5. In the lower section of the figure the amplitude spectra of the corresponding filter panels are appended. The amplitude spectra of the used Ormsby frequency filter operators are characterized by linear slopes. The filter applied, which is minimum delay, is described by four corner frequencies: Lower stop/pass band boundary and upper pass/stop band boundary. The frequencies on the filter panels correspond to the lower and upper pass frequencies. The main energy for the reflected phases between 3.0 and 4.5 s in the offset range from 0-12 km is between 3-21 Hz and for the direct wave up to 111 Hz. The main energy of the phase between 2.5 and 3.5 s in the offset range from 44-55 km is between 3-13 Hz. As a broad frequency range is contained in the data, time and offset dependent filtering was applied (see below).

Deconvolution analysis: To improve the temporal resolution of the seismic data a deconvolution is applied to compress the basic seismic wavelet. The recorded wavelet has many components, including the source signature, recording filter, and hydrophone/geophone response. Ideally, deconvolution should compress the wavelet components and leave only the earth's reflectivity in the seismic trace. We applied Wiener deconvolution in successive trace segments, based on the following assumptions:

1. The earth's reflectivity is 'white'.
2. The wavelet shows the minimum-delay phase behavior.

As in this wide-angle data the amplitude spectra of the seismic traces vary with time and offset (e.g. reflected, refracted pp phases and reflected ps and ss phases), the deconvolution must be able to follow these time and offset variations. For the single trace deconvolution each trace is therefore divided into 3-s data gates with 1-s overlaps, in which time-invariant deconvolution operators are computed from the autocorrelation function of the data segment and applied to account for the nonstationarity of the seismic signals. The overall deconvolved trace results from a weighted merging of the independently deconvolved gates.

To improve especially the spatial resolution of the seismic data a multi-trace deconvolution also called roll-along deconvolution which uses autocorrelograms averaged over a number of traces is tested to compress the basic seismic wavelet. Here,each trace is divided into 3-s data gates with 1-s overlaps, in which time invariant deconvolution operators are computed from the average autocorrelation function of 101 traces. The operator is recalculated for every trace in each data segment and applied. The overall deconvolved trace results from a weighted merging of the independently deconvolved gates.

Input for the deconvolution process is raw data. As several recordings were influenced by a DC shift, a 1-3-Hz high-pass minimum delay Kaiser frequency filter with 60 dB attenuation between the pass and reject zone was applied prior to deconvolution in order to center the amplitudes around zero. The deconvolution test panels are shown in Figures 6.4.4 and 6.4.6 for the offset ranges 0-12 km and 44-55 km respectively. In the lower section of the figure the autocorrelation function is appended. Constant operator lengths of 300 ms (predictive length included) and a variation of the predictive length from 20 to 180 ms is displayed for a single trace deconvolution (avere=1) and for a multi-trace deconvolution (avere=101).

The undeconvolved data in Figure 6.4.4 show a strong energy of up to 400 ms behind the zero lag and in Figure 6.4.6 a strong energy of over 1 s behind the zero lag is dominating in the autocorrelation function. The best resolution is obtained for a predictive length of 20 ms. The multi-trace deconvolution is showing less noise compared to the single trace deconvolution. An increase of the prediction length also increases the signal-to-noise ratio, best seen in the near-offset traces in Figure 6.4.4. A predictive length of 140 ms and a multi-trace deconvolution was chosen for this data set which is a compromise between temporal resolution and signal-to-noise ratio.

After deconvolution an offset- and time-variant Ormsby filter with minimum delay characteristic was applied. As the seafloor depth changes along the seismic lines, each trace was statically corrected to a fixed seafloor travel time of 11 s based on the water depth before filtering. This information is available in the trace headers. After this filter was applied, the data were shifted back to their original travel times.

Processed data: At comparison of the preprocessed data in Figure 6.4.7 to the unprocessed data in Figure 6.4.2 shows a clear reduction of the low and mono-frequency noise in the near and far offset traces and moderate compression of the wavelet signal. For the picking of events and model building by

raytracing both sections were used to keep all available seismic information.

Final processing sequence

- Input: SEGY-data, 2, 4 ms or 5 ms sampling rate with complete geometry information.
- Tapering the first 0.5 s to zero to reduce the response of the debias filter operator.
- Kaiser highpass (debias).
- Gated Wiener deconvolution with autocorrelation average of 101 traces: gate length 3 s, overlap 1 s length of merge region 1 s, operator length 300 ms (prediction interval included), prediction interval 140 ms.
- Static correction to a fixed seafloor traveltime of 11 s.
- Time and offset-dependent Ormsby frequency filter.

On time-shifted traces with a reduced time scale of 6 km/s the following filter parameters were used:

lower stop/pass	upper pass/stop (Hz)	offset(m)	beginfull(s)	endfull(s)
3/5	55/75	0	0	12.8
	8000	0	12.6	
	48000	0	0	
2/4	35/50	0	13.7	14.3
	8800	13.5	14.4	
	13200	13.0	13.9	
	52000	1.0	5.0	
	107000	0	0	
2/4	20/30	0	15.3	16.8
	11700	15.1	16.6	
	19200	14.8	16.3	
	61700	7.0	10.1	
	114000	2.0	3.0	
	152000	0	0	
2/4	10/20	0	19.0	trace length
	20000		18.4	trace length
	130000		3.5	trace length

6.4.1.3 OBH/OBS-Data Analysis and Processing with Source Signals of 1.7-l GI-Gun

Raw data: As an example, the hydrophone and the vertical component of OBS record section 09 of profile 301 are shown in Figure 6.4.8 and 6.4.12 respectively. For analysis, the hydrophone and the vertical component in offset ranges between 0-7 km southwest are presented in detail.

Frequency analysis: To determine the frequencies of the seismic energy, filter panels with narrow frequency pass bands for the hydrophone and the vertical component are shown in Figures 6.4.9 and 6.4.13 respectively. In the lower section of the figure the amplitude spectra of the corresponding filter panels are appended. The amplitude spectra of the Ormsby frequency filter operators used are characterized by linear slopes. The filter applied with minimum delay characteristic is described by four corner frequencies:

Lower stop/pass band boundary and upper pass/stop band boundary. The frequencies on the filter panels correspond to the lower and upper pass frequencies. The main energy for the reflected phase between 2.8 and 4.0 s is between 3-57 Hz and for the direct wave and shallow reflection phases more than 111 Hz. The main energy of the possibly converted shear wave phases on the vertical component between 4.8 and 6.0 s is between 3-31 Hz. Since a broad frequency range is contained in the data, time and offset dependent filtering is applied (see below).

Deconvolution analysis: The input for the deconvolution process is raw data. As several recordings were influenced by a DC shift especially the three component OBS recordings show low-frequency noise, a 3-5-Hz high-pass Kaiser frequency filter with minimum delay characteristic and 60db attenuation between the pass and reject zone was applied prior to deconvolution in order to center the amplitudes around zero. The deconvolution test panels are shown in Figures 6.4.10 and 6.4.14 for the hydrophone and the vertical component respectively. In the lower section of the figure the autocorrelation function is appended. Constant operator lengths of 300 ms (predictive length included) and a variation of the predictive length from 20 to 180 ms are displayed for a single trace deconvolution (avere=1) and for a multi trace deconvolution (avere=101).

On the undeconvolved data in Figures 6.4.10 and 6.4.14 a strong energy of up to 300 ms behind the zero lag is clearly visible in the autocorrelation function. The best resolution is obtained for a predictive length of 20 ms and a multi-trace deconvolution but with a reduction of signal-to-noise ratio and a change in the shape of the signal (phase error). An increase of the prediction length also increases the signal-to-noise ratio, as is best seen on the vertical component in figure 6.4.14 for the low-frequent phases between 4.8 and 6 s. A predictive length of 80 ms and an multi-trace deconvolution was chosen for this data set which is a compromise between temporal resolution and signal-to-noise ratio.

After deconvolution an offset- and time-variant Ormsby filter with minimum delay characteristic was applied. As the seafloor depth changes along the seismic lines, each trace was statically corrected to a fixed seafloor travel time of 11 s based on the water depth before filtering. This information is available in the trace headers. After this filter was applied, the data were shifted back to their original travel times.

Processed data: Comparison of the preprocessed hydrophone data in Figure 6.4.11 to the unprocessed data in Figure 6.4.8 and of the preprocessed vertical component data in Figure 6.4.15 to the unprocessed data in Figure 6.4.12 shows a clear reduction of the low- and mono-frequency noise and a moderate compression of the wavelet signal.

Final processing sequence

- Input: SEGY data, 2-4 ms sampling rate with complete geometry information.
- Tapering the first 0.5 s to zero to reduce the response of the debias filter operator.
- Kaiser highpass applied twice (debias).
- Gated Wiener deconvolution with autocorrelation average of 101 traces: gate length 3 s, overlap 1 s, length of merge region 1 s, operator length 300 ms (prediction interval incl.), prediction interval 80 ms.
- Static correction to a fixed seafloor travel time of 11 s.
- Time and offset-dependent Ormsby frequency filter.
- Resampling to 2 ms sample rate.

On time-shifted traces with a reduced time scale of 6 km/s the following filter parameters were used:

lower stop/pass	upper pass/stop (Hz)	offset(m)	beginfull(s)	endfull(s)
3/5	65/85	0	0	12.8
		8000	0	12.6
		48000	0	0
3/5	45/60	0	13.7	14.3
		8800	13.5	14.4
		13200	13.0	13.9
		52000	1.0	5.0
		107000	0	0
3/5	30/40	0	15.3	16.8
		11700	15.1	16.6
		19200	14.8	16.3
		61700	7.0	10.1
		114000	2.0	3.0
		152000	0	0
3/5	20/30	0	19.0	trace length
		20000	18.4	trace length
		130000	3.5	trace length

6.4.1.4 MCS Processing

The Bolt-gun and GI-gun shots were also registered by a 4-channel mini-streamer. The group spacing is 50 m and the first offset was calculated to approximate 118 m. Due to the different shot intervals from 8 to 60 s (approx. 10 to 100 m) and the variable data quality, the processing sequence was adjusted for each profile after a check of the raw data. The bad traces are degraded by high-amplitude noise and a low signal-to-noise ratio, especially the near trace or far trace. Problems with streamer depth variations between thefirst and last channel were nearly eliminated by attaching a buoy at the tail of the streamer. A residual static correction for the individual channels was determind for each profile manually.

A standard processing job was created with some variable modules (*), depending on the profile parameters and the data quality.

- Input: SEGY data, 0.4 ms sampling rate with complete geometry information.
- * Resampling from 0.4 ms to 0.8 ms for the GI-gun and 0.4 ms to 2 ms for the Bolt-gun.
- Kaiser highpass (debias).
- Static correction to a fixed seafloor travel time of 5.5 s.
- NMO correction with 1495 m/s.
- Time-variant single trace predictive deconvolution: gate from 5 to 8 s.

  Bolt-gun: operator length 300 ms prediction interval 100 ms.

  GI-guns: operator length 80 ms prediction interval 20 ms.
- Time dependent Ormsby frequency filter.

On time-shifted traces the following filter parameters were used:

	Time interval [s]	lower stop/pass[Hz]	upper pass/stop[Hz]
Bolt-guns:	0 .0 – 5.5	3/5	100/140
	6.0 – 6.5	3/5	60/80
	10.0 – trace length	3/5	20/40
GI-guns:	0 .0 – 5.5	3/5	300/350
	6.0 – 6.5	3/5	250/300
	10.0 – trace length	3/5	150/200

- Trace normalization:
  Bolt-gun: at 6.4 s gate length 2 s and at 8 s gate length 3 s.
  GI-gun: at 5.5 s gate length 1 s and at 7 s gate length 2 s.
- Remove static correction.
- Random noise attenuation by f-x prediction filtering.

* Trace interpolation by f-x prediction filtering for empty bins.
* Frequency-wavenumber antialiasing filtering (fk).

- Binning of traces, depending on the desired output spacing.
- Stolt migration with 1495 m/s.
- Output: SEGY data.

The MCS profiles are displayed in the individual chapters of the wide-angle profiles.

6.4.1.5 BGR99-41 MCS Processing

The MCS profile BGR99-41, which is coincident with the wide-angle profiles SO 173-301 and SO 173-302, was processed up to DMO-stack and post-stack time migration. The MCS profile is displayed in chapter 6.4.38.

6.4.1.6 Data Archiving

Data recorded on flash discs with the MBS/MLS recorder were transferred to a SUN workstation via a PC. On the workstation they were transformed into a so-called PSEUDO-SEGY format.

After navigation data had been merged in and SEGY-formatted traces with the appropriate header words had been created, the data were also archived. Finally, a third set was stored and archived after the shipboard processing, as described above, had been applied. All final processed SEGY data were archived on tapes.

6.4.1.7 Data Exchange

For exchange of the OBH/OBS data, the SEGY format on disk with a Sun tar-format was chosen. The raw SEGY data are in Integer2 format with trailer bytes between the record structure of SEGY. The processed data is in IBM-floating point without trailer bytes between the records.

This is the definition of the SEGY trace header for the GEOMAR OBS wide-angle reflection data. The

extension of the standard SEGY header from 181 to 240 bytes is a layout in order to process the data on the GEOSYS/SEISMOS software system. Reading bytes directly into this header will allow access to all of the fields.

BytePos	Bytes	Information	Comments (note: not all headers available in processed data)
1-8	(2x4)	lineSeq, reelSeq;	/* Sequence numbers within line and reel, resp.*/
			/* here station and shot number Def: 1, 1 */
9-12	(4)	profNumber;	/* Original field record number */
			/* Here profile number */
13-16	(4)	traceNumber;	/* Trace number within the original field record.*/
			/* Here station (receiver) Number */
17-20	(4)	energySourcePt;	/* Energy source (shot) point numbe */
			/* Def: 0 */
21-24	(4)	cdpEns;	/* CDP ensemble number: shot number */
			/* Def: 0 */
25-28	(4)	traceInEnsemble;	/* Trace number within CDP ensemble */
			/* Here azimuth in seconds of arc for unprocessed data*/
29-30	(2)	traceID;	/* Trace identification code:
			1=seismic data (Def) 4=time break 7=timing
			2=dead 5=uphole 8=water break
			3=dummy 6=sweep 9..., optional use */
31-34	(2x2)	vertSum, horSum;	/* Def: 1, 1 */
35-36	(2)	dataUse;	/* 1=production (Def), 2=test */
37-40	(4)	sourceToRecDist;	/* Distance in (m) */
41-44	(4)	recElevation;	/* Elevation in (m), Def: 0 */
45-48	(4)	sourceSurfaceElevation;	/* Def: 0 (m) */
49-52	(4)	sourceDepth;	/* Def: 0 (m) */
53-60	(2x4)	datumElevRec, datumElemSource;	/* Def: 0, 0 (m) */
61-68	(2x4)	sourceWaterDepth, recWaterDepth;	/* Def: 0, 0 (m) */
69-70	(2)	elevationScale;	/* Scale elevations Def: 0 (10**0) */
71-72	(2)	coordScale;	/* Scale coordinates
	Def: -2, means coordinates multiplied by 10**(-2) to get real value for unprocessed data.		
		NOTE: for processed data -100 means to divide by 100 to get the real value */	
73-80	(2x4)	sourceLongOrX, sourceLatOrY;	/* Either Cartesian or geographic */
81-88	(2x4)	recLongOrX, recLatOrY;	
89-90	(2)	coordUnits;	/* 1= meter or feet; 2=sec of arc */
91-92	(2)	weatheringVelocity; /* Def: 0 (m/s) */	
93-94	(2)	subWeatheringVelocity;	/* Reduction velocity, Def: 6000 m/s) */
95-96	(2)	sourceUpholeTime; /* Def: 0 (ms) */	
97-98	(2)	recUpholeTime;	/* Def: 0 (ms) */
99-102	(2x2)	sourceStaticCor, recStaticCor;	/* Def: 0, 0 (ms) */
103-104	(2)	totalStatic;	/* Def: 0 (ms) */
105-106	(2)	lagTimeA;	/* T(shottime) - T(first sample) */

```
107-108   (2)     lagTimeB;              /* Def: 0 (ms) */
109-110   (2)     delay;                 /* Def: 0 (ms) */
111-114   (2x2)   muteStart, muteEnd;    /* Def: 0, 0 (ms) */
115-116   (2)     sampleLength;          /* Number of samples in this trace */
                                         /* ( > 32767 )? = 32767
                                         set long samp_rate in 185-188 byte */
117-118   (2)     deltaSample;           /* Sampling interval in microseconds. */
119-120   (2)     gainType;              /* 1=fixed (Def), 2=binary,
                                         3=floating, 4... opt.*/
121-122   (2)     gainConst;                          /* Gain of recording channel */
123-124   (2)     initialGain;                        /* Gain of preamplifier in db */
125-126   (2)     correlated;                         /* 1=no (Def), 2=yes */
127-130   (2x2)   sweepStart, sweepEnd;              /* min. and max. amplitude of trace */
131-132   (2)     sweepLength;           /* Here defined as fraction of second of shot time */
133-134   (29)    sweepType;             /* Source type:
                                         1=linear, 2=parabolic, 3=exponential, 4=others
                                         5=bohrhole explosive, 6=water explosive, 7=airgun (Def)
                                         or fraction of microsecond of shot time for high resolution data
135-138   (2x2)   sweepTaperAtStart, sweepTaperAtEnd;   /* Start and end of trace (ms)
                                                          relative to Tred(0) */
139-140   (2)     taperType;             /* scaling factor for last two values Def: 1 (x10) */
141-144   (2x2)   aliasFreq, aliasSlope;            /* Def: 0, 0 */
145-148   (2x2)   notchFreq, notchSlope;            /* Def: 0, 0 */
149-152   (2x2)   lowCutFreq, hiCutFreq;            /* Def: 0, 0 */
153-156   (2x2)   lowCutSlope, hiCutSlope;          /* Def: 0, 0 */
157-166   (5x2)   year, day, hour,       /* Source (shot) time, the fraction of sec */
                  minute, second;        /* is set in millisec between 131-132 byte
                                         is set in microsec between 133-134 */
167-168   (2)     timeBasisCode;         /* 1=local, 2=GMT, 3=MET (GMT + 1 hour) (Def) */
169-170   (2)     traceWeightingFactor;                /* */
171-172   (2)     phoneRollPos1;         /* Component: 1=time code, 2=radial, 3=transverse
                                         4=vertical, 5=hydrophone (Def) */
173-174   (2)     phoneFirstTrace;       /* Methusalem instrument number in YYNN */
175-176   (2)     phoneLastTrace;        /* Channel number */
177-178   (2)     gapSize;               /* Source charge in cubic inches (airgun)
                                         or kg (explosives) */
179-180   (2)     taperOvertravel;       /* Def: 0=meaningless 1=up, 2=down */
/* !!! Following is extension !!! */
181-182   (2)     compNo;                /* 1=time code, 2=radial, 3=transverse
                                         4=vertical, 5=hydrophone (Def) */
183-184   (2)     samplingRate;          /* samples/sec */
185-188   (4)     numberSamples;         /* ( <= 32767) ? sampleLength : ( > 32767) */
189-190   (2)     shotPointNo;
191-192   (2)     ADCoeff;               /* Coefficient of A/D converter in mv/digit */
```

```
193-194   (2)   receiverCoeff;      /* Conversion coefficient of receiver,
                                     pascal/cm2 for hydrophone, velocity(m/s)/volt for geophone */
195-196   (2)   receiverType;       /* 1=hydrophone (Def), 2=geophone, 3...*/
197-200   (4)   lengthData; /* Def: 0 (ms), not used here */
201-204   (4)   distance;     /* Source to receiver distance in (m) */
205-208   (4)   (float) scaleFactor;   /* Scale factor same as in <segy.h>
                      Here azimuth in second of arc for processed data */
209-210   (2)   azimuth;      /* Orientation of the component in min */
211-212   (2)   eigenperiod; /* Eigenperiod of geo- or hydrophone in (ms) */
213-216   (4)   minAmpl;     /* Min. peak amplitude within trace  */
217-220   (4)   maxAmpl;     /* Max. peak amplitude within trace */
221-222   (2)   stationNo;    /* Station number */
223-224   (2)   channelNo;   /* Channel number (Default: 1) */
225-228(4)      sourceCharge;  /* Charge in kg (explosive) or cc (airgun) */
229-230(2)      redVelocity;   /* reduction velocity in (m/s);
                Def: 0 if no reduction velocity se */
231-232(2)      timeOffset;    /* Time offset in (ms) of first sample
                               relative to reduced source time:
                               positive if earlier than reduced time */
233-236(4)      redTime;       /* Reduced time in (ms) = distance/redVel */
237-238(2)      unused2;
239-240   (2)   instNo;       /* Methusalem instrument number */
```

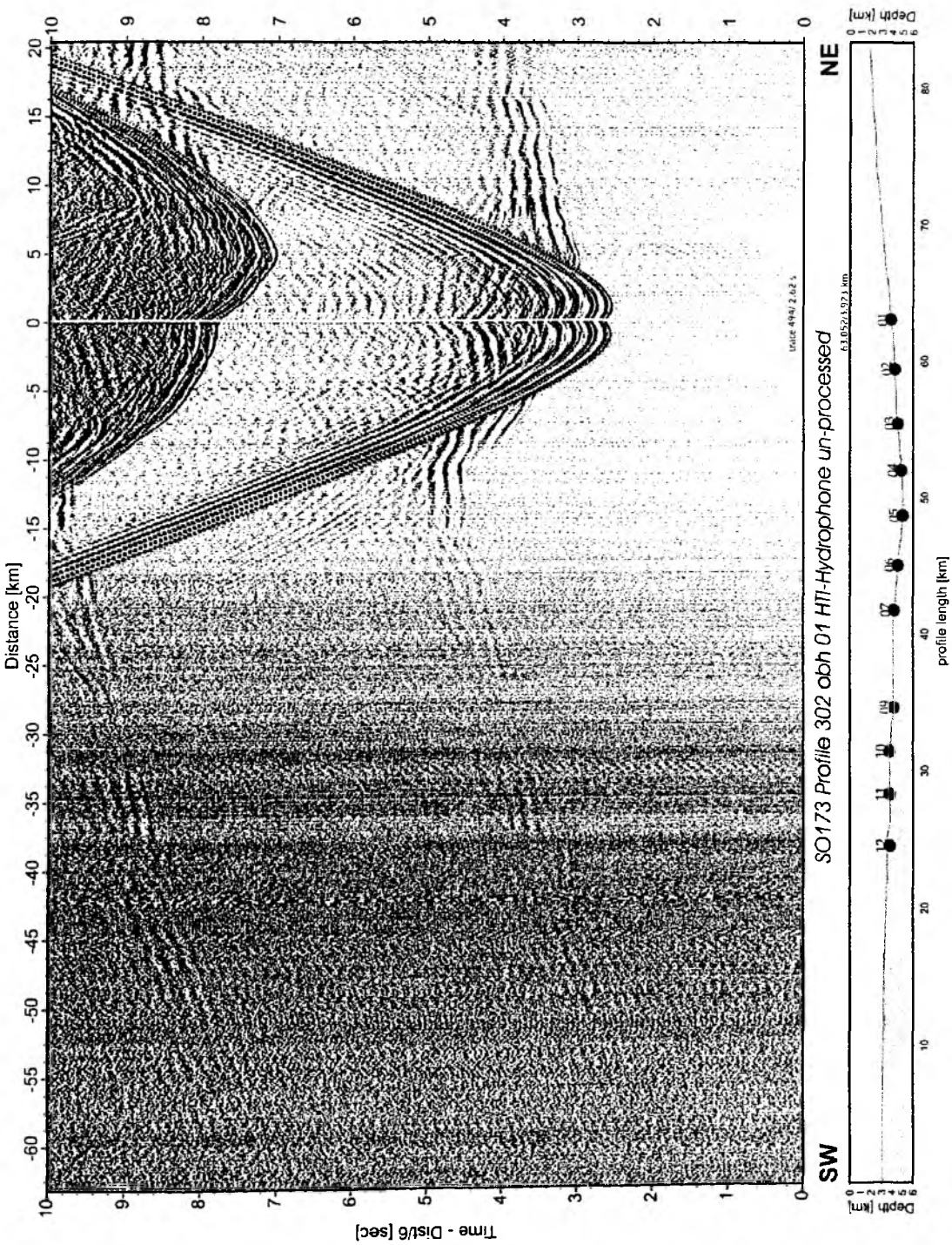

Fig 6.4.2: Record section from obh 01 HTI-Hydrophone un-processed.

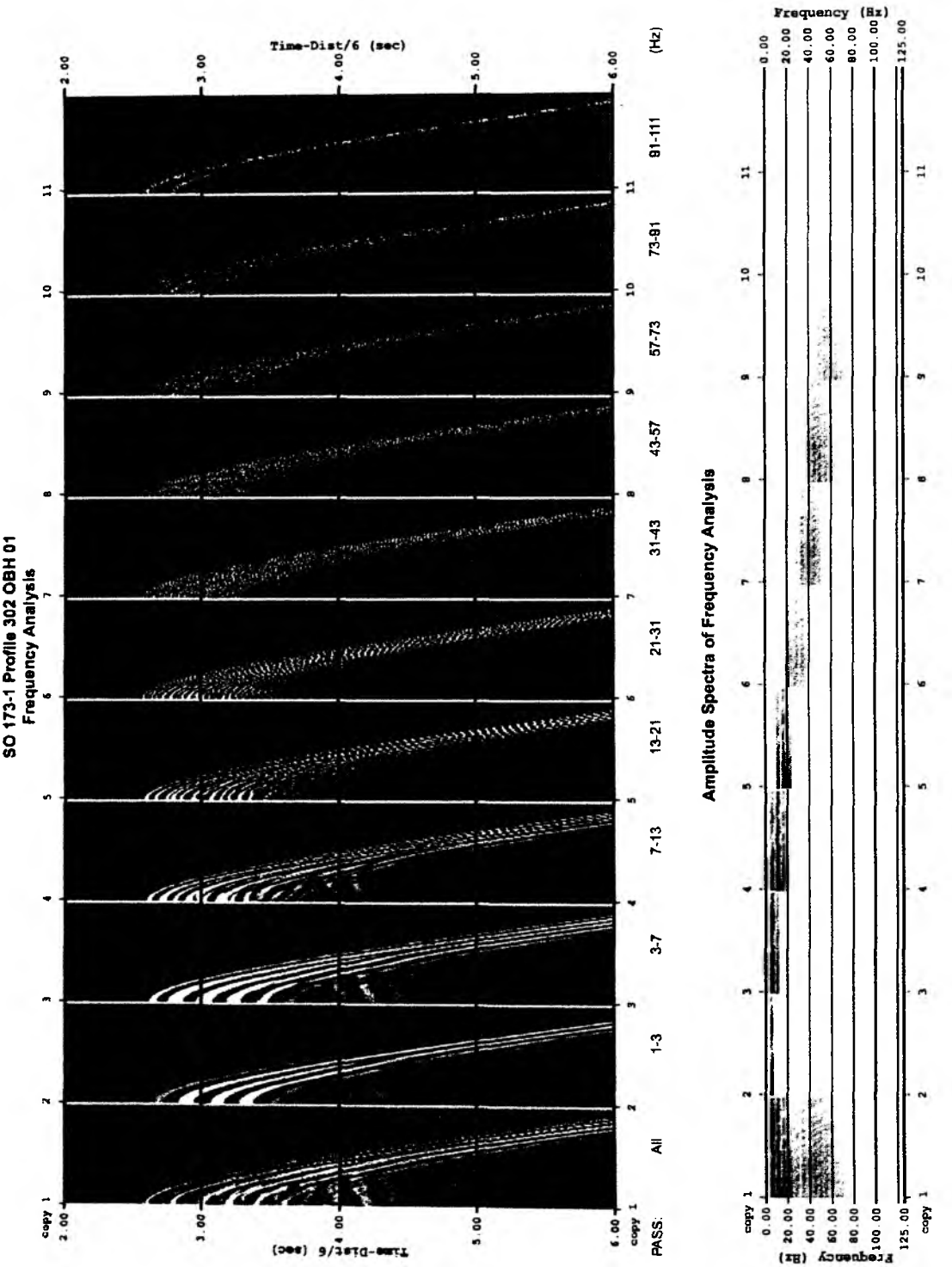

Fig. 6.4.3: Frequency analysis in the offset range 0-12 km.

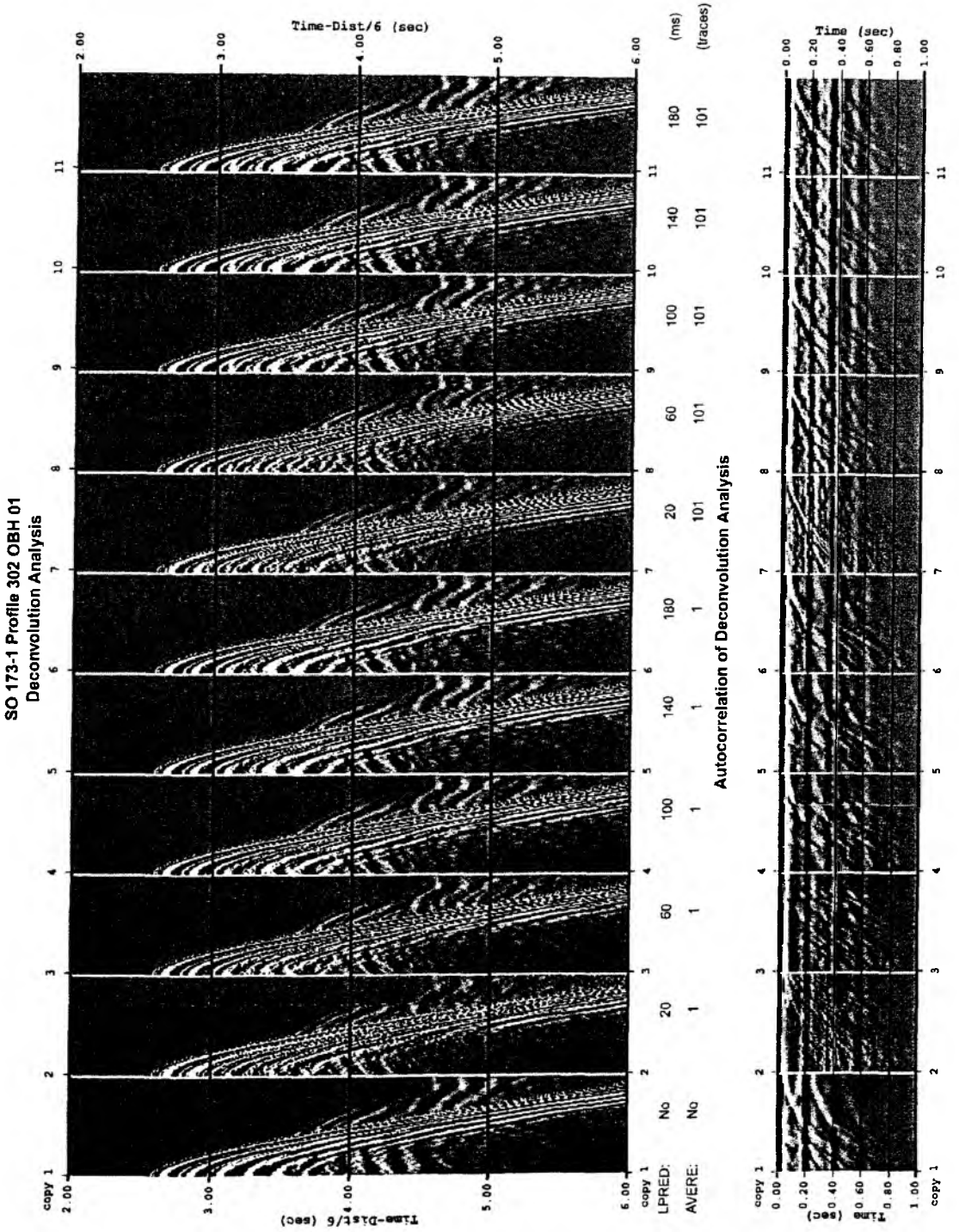

Fig. 6.4.4: Deconvolution analysis in the offset range 0-12 km with operator length 300 ms.

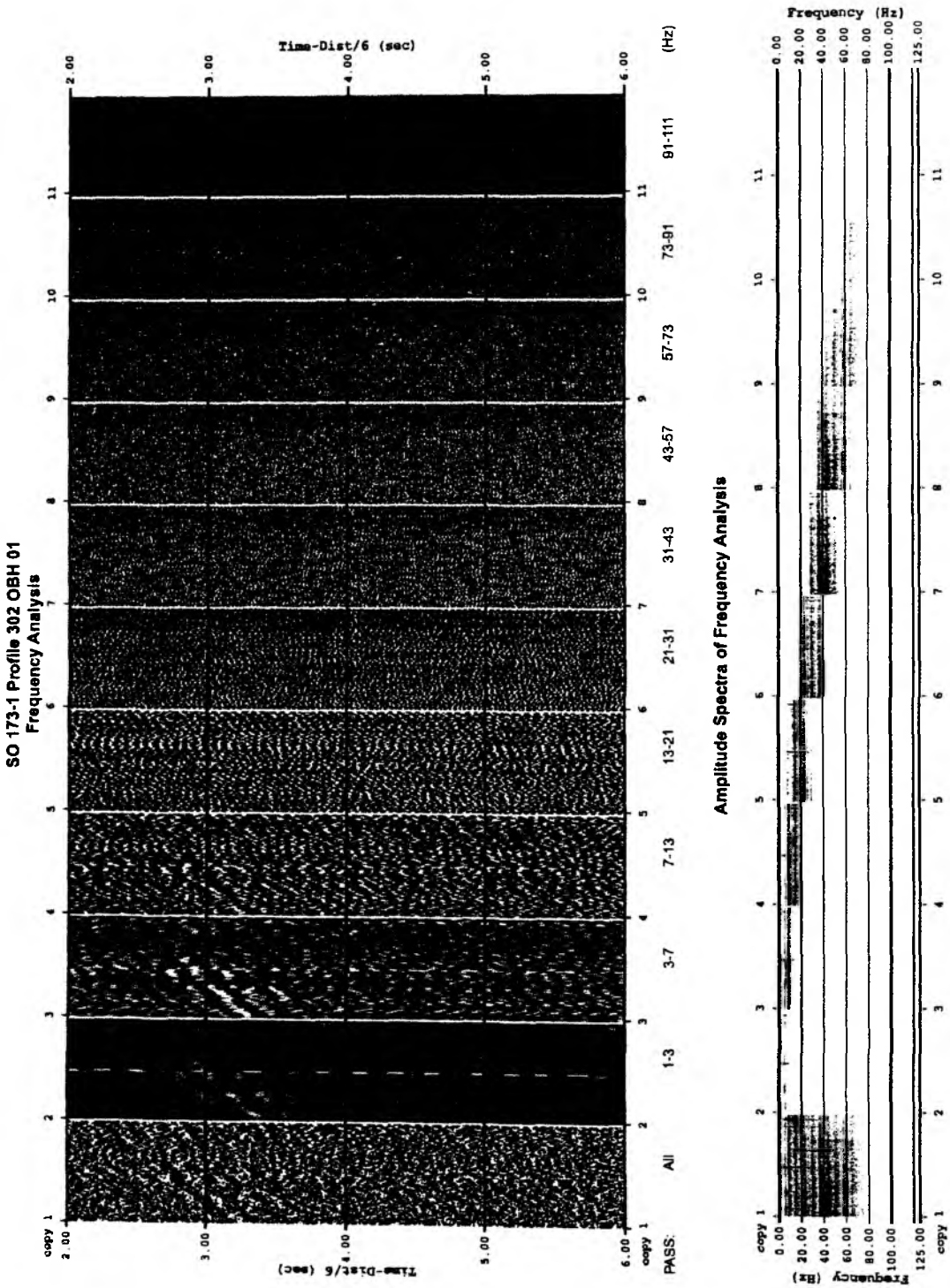

Fig. 6.4.5: Frequency analysis in the offset range 44-55 km.

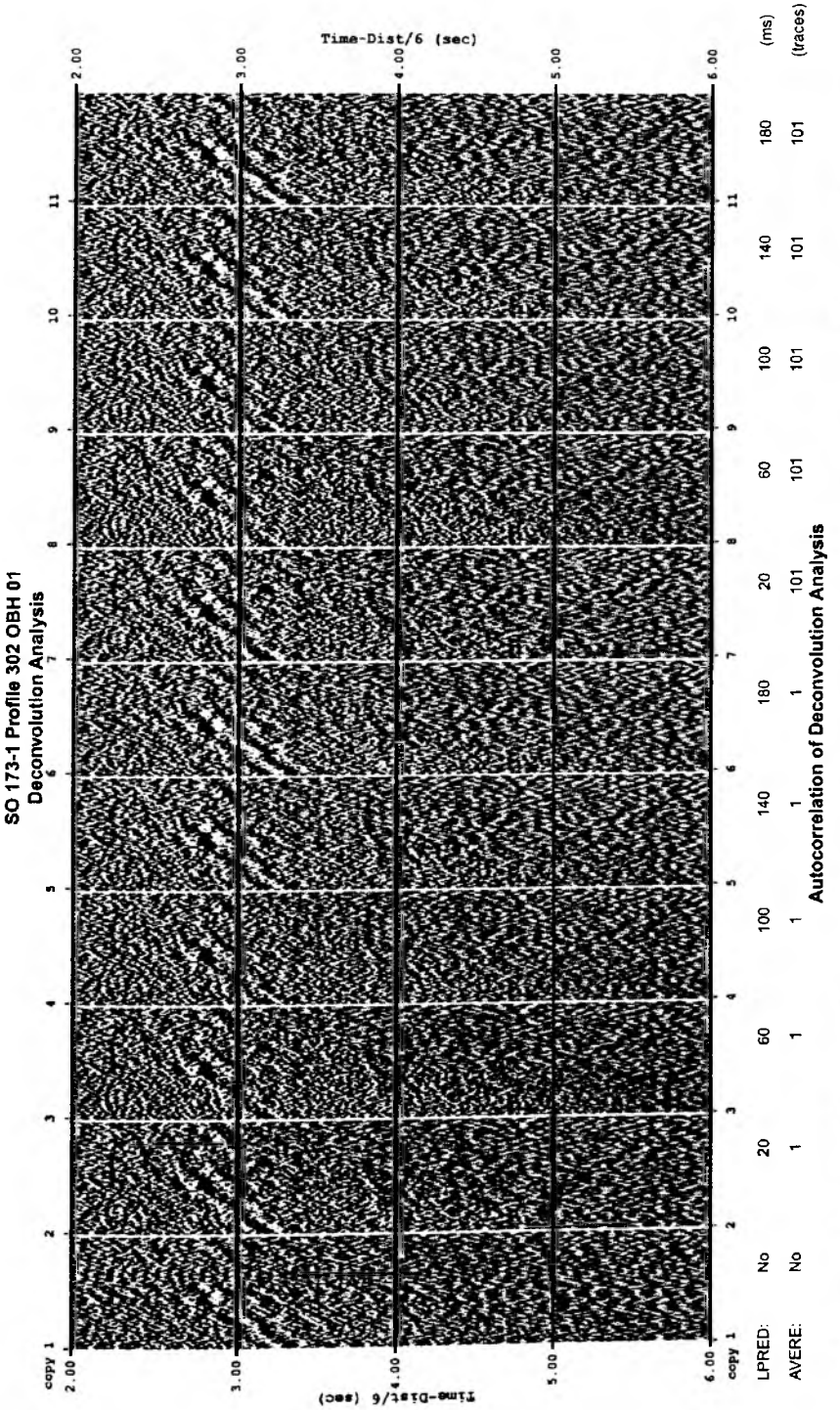

Fig. 6.4.6: Deconvolution analysis in the offset range 44-55 km with operator length 300 ms.

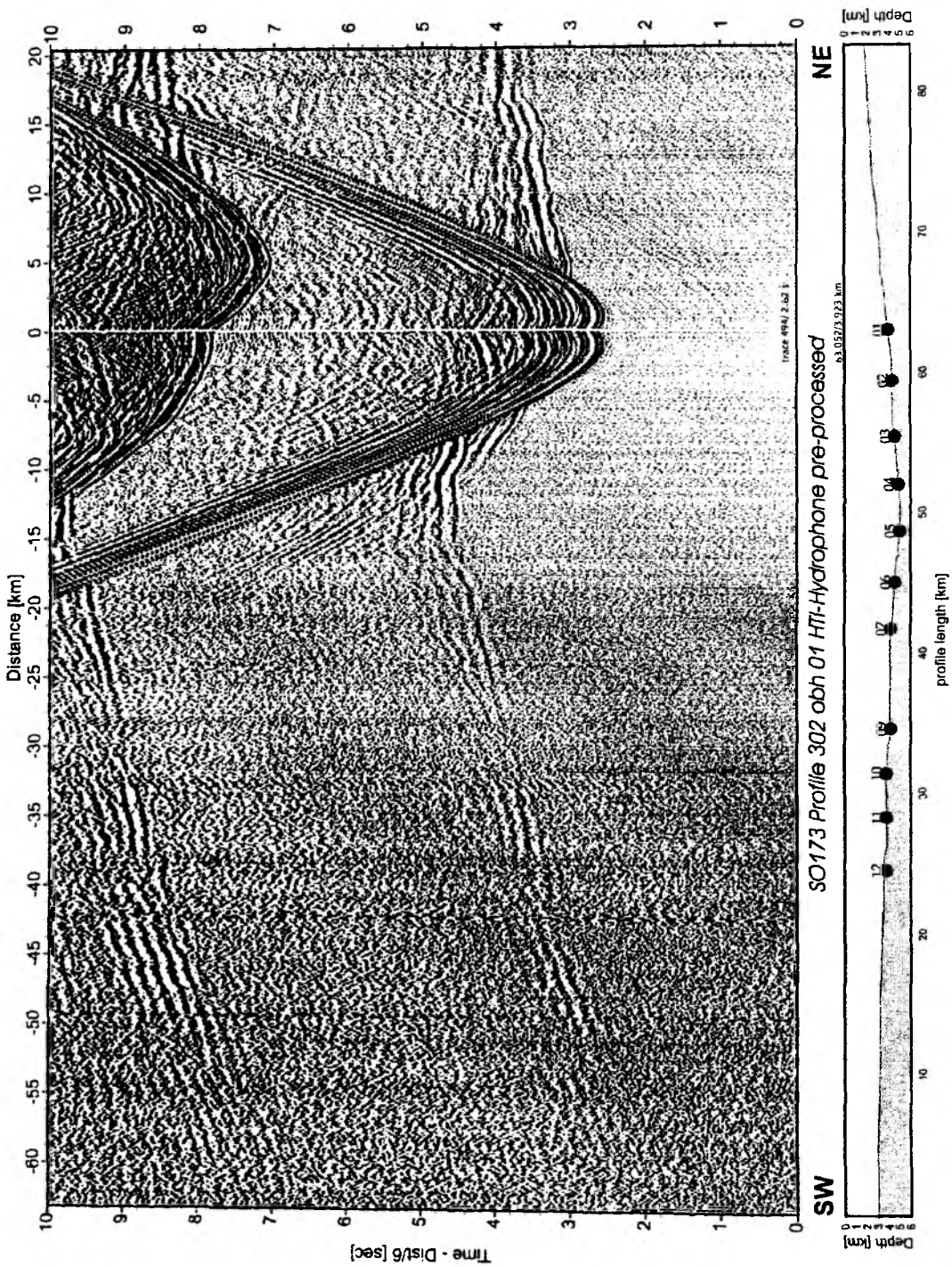

Fig. 6.4.7: Record section from obh 01 HTI-Hydrophone pre-processed.

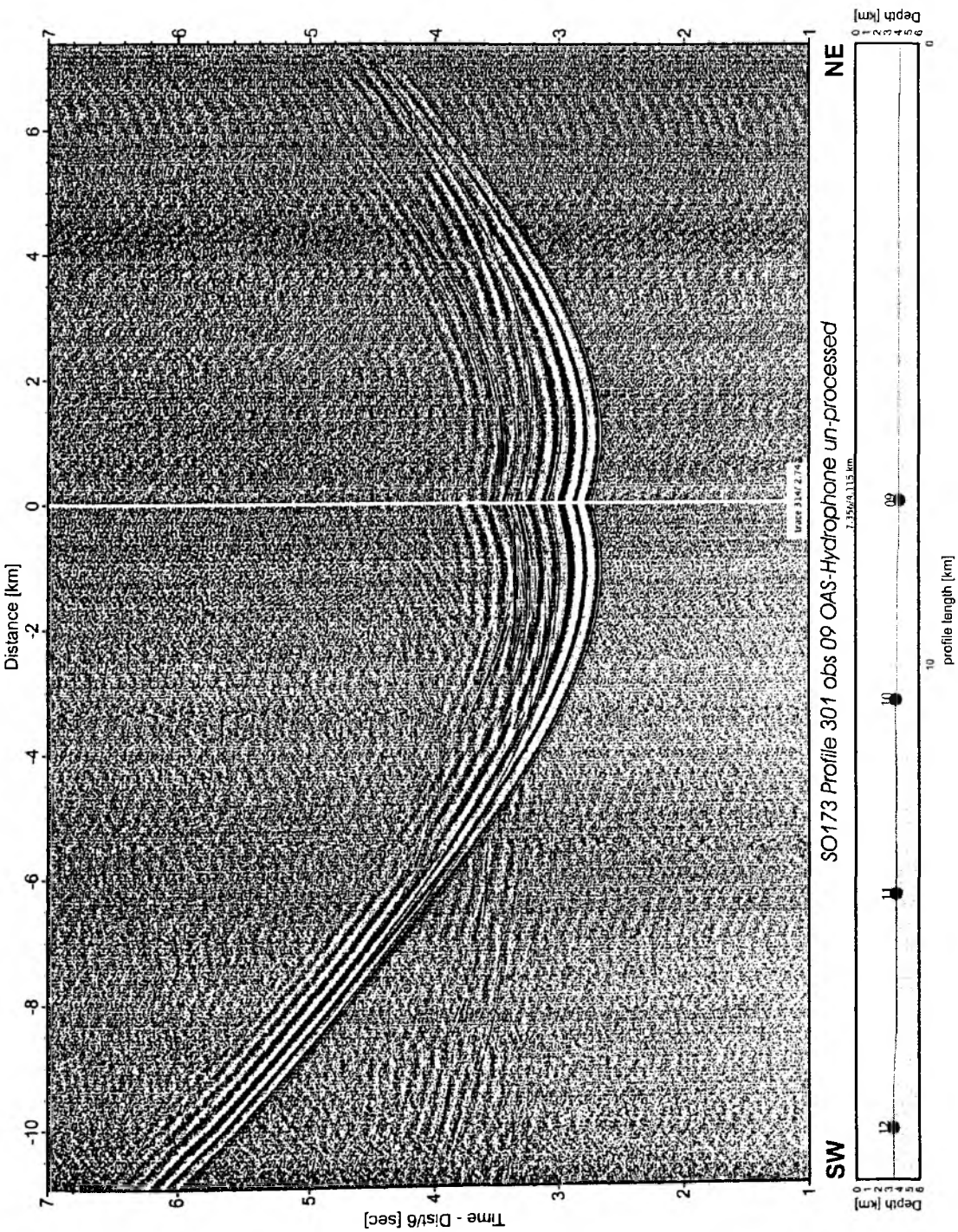

Fig. 6.4.8: Record section from obs 09 OAS-Hydrophone un-processed.

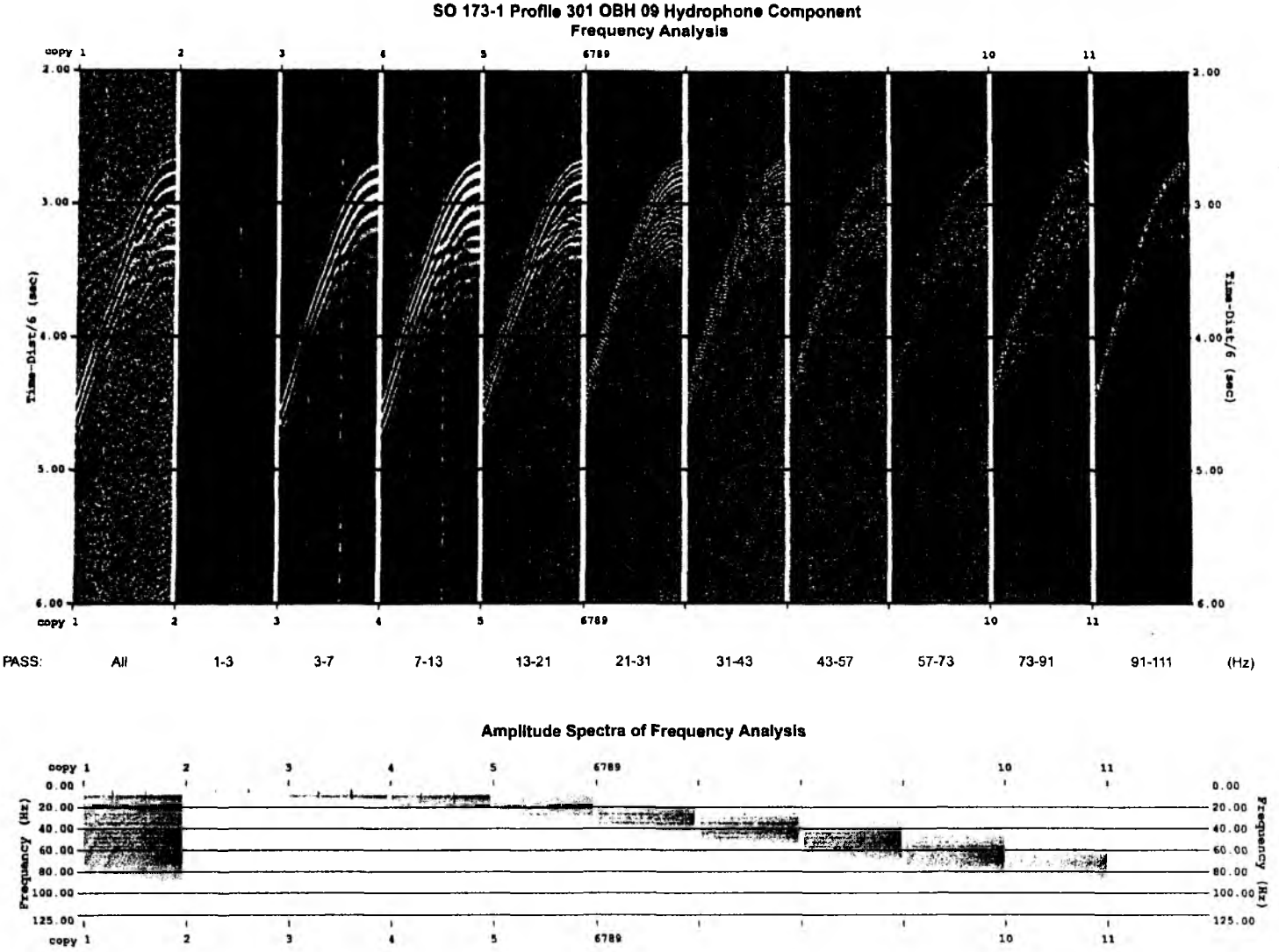

Fig. 6.4.9: Frequency analysis in the offset range 0-7 km.

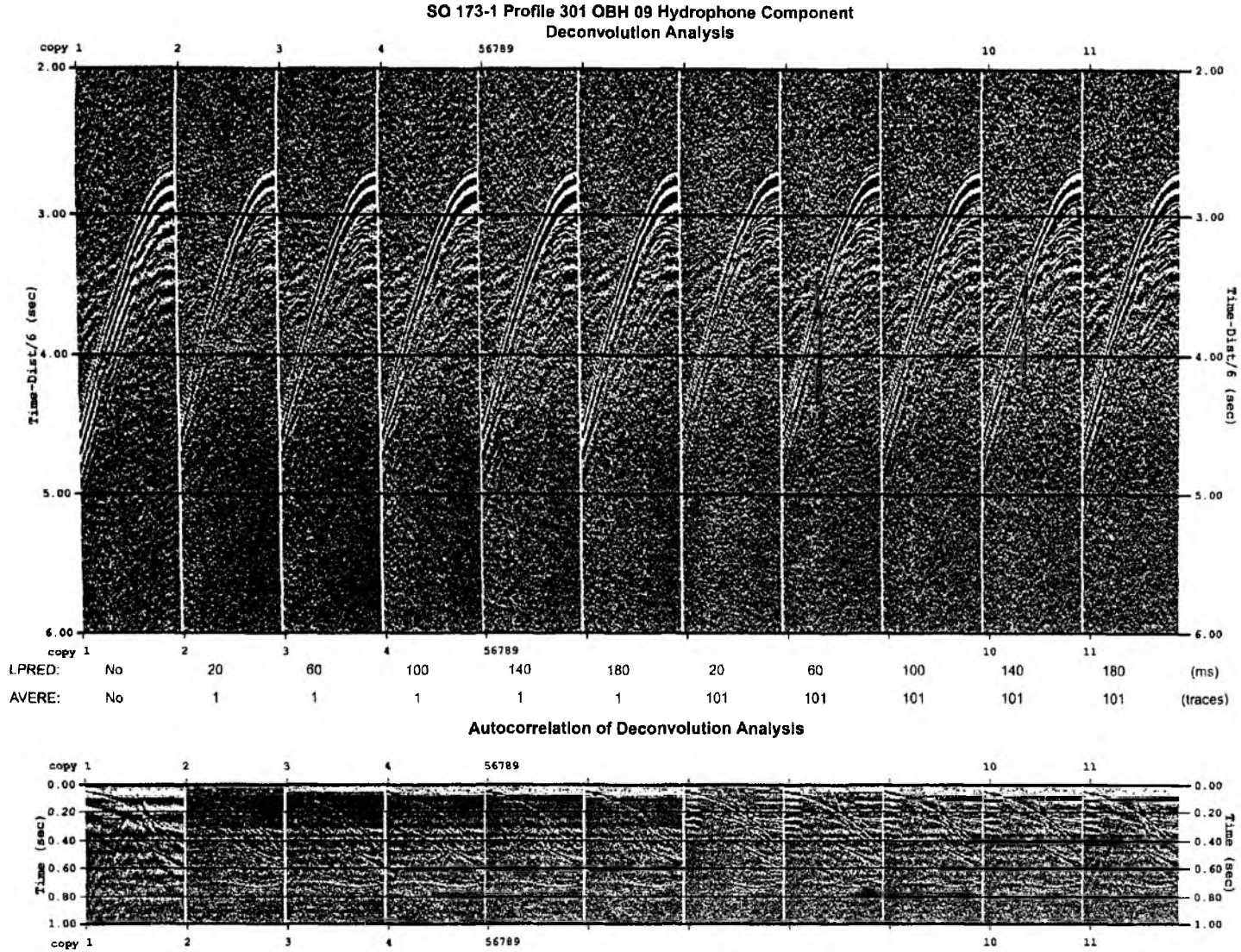

Fig. 6.4.10: Deconvolution analysis in the offset range 0-7 km with operator length 300 ms.

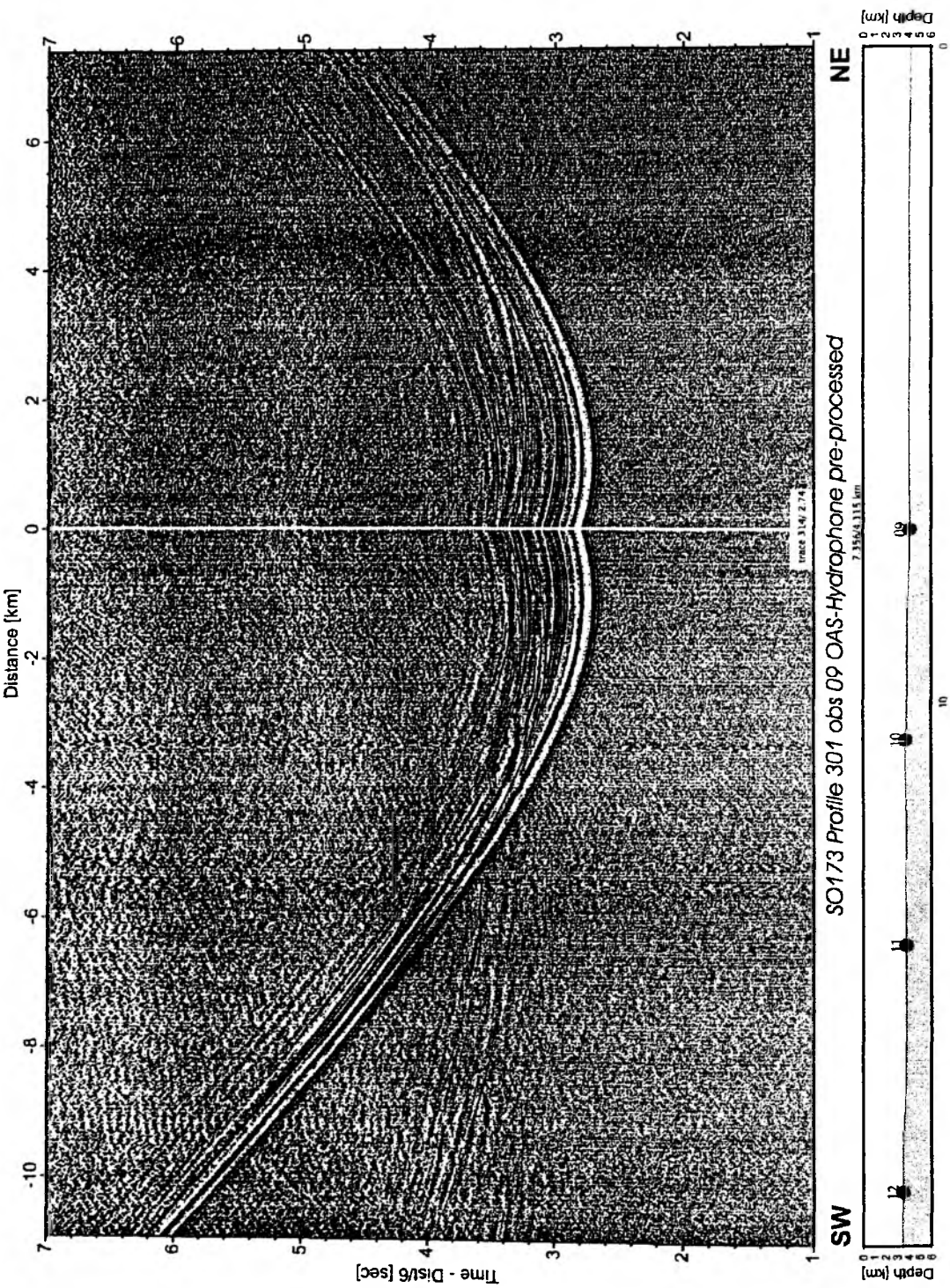

Fig. 6.4.11: Record section from obs 09 OAS-Hydrophone pre-processed.

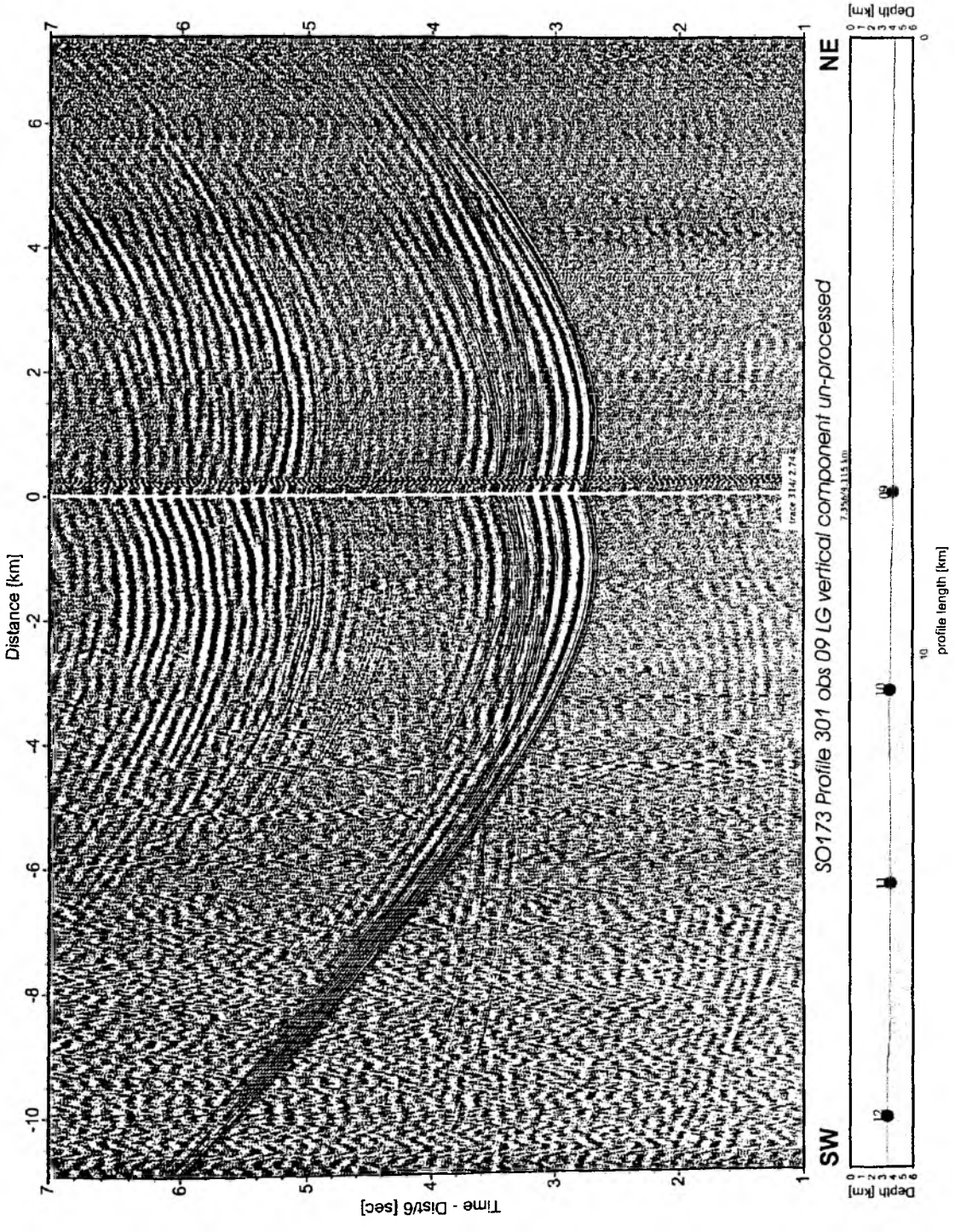

Fig. 6.4.12: Record section from obs 09 LG vertical component un-processed.

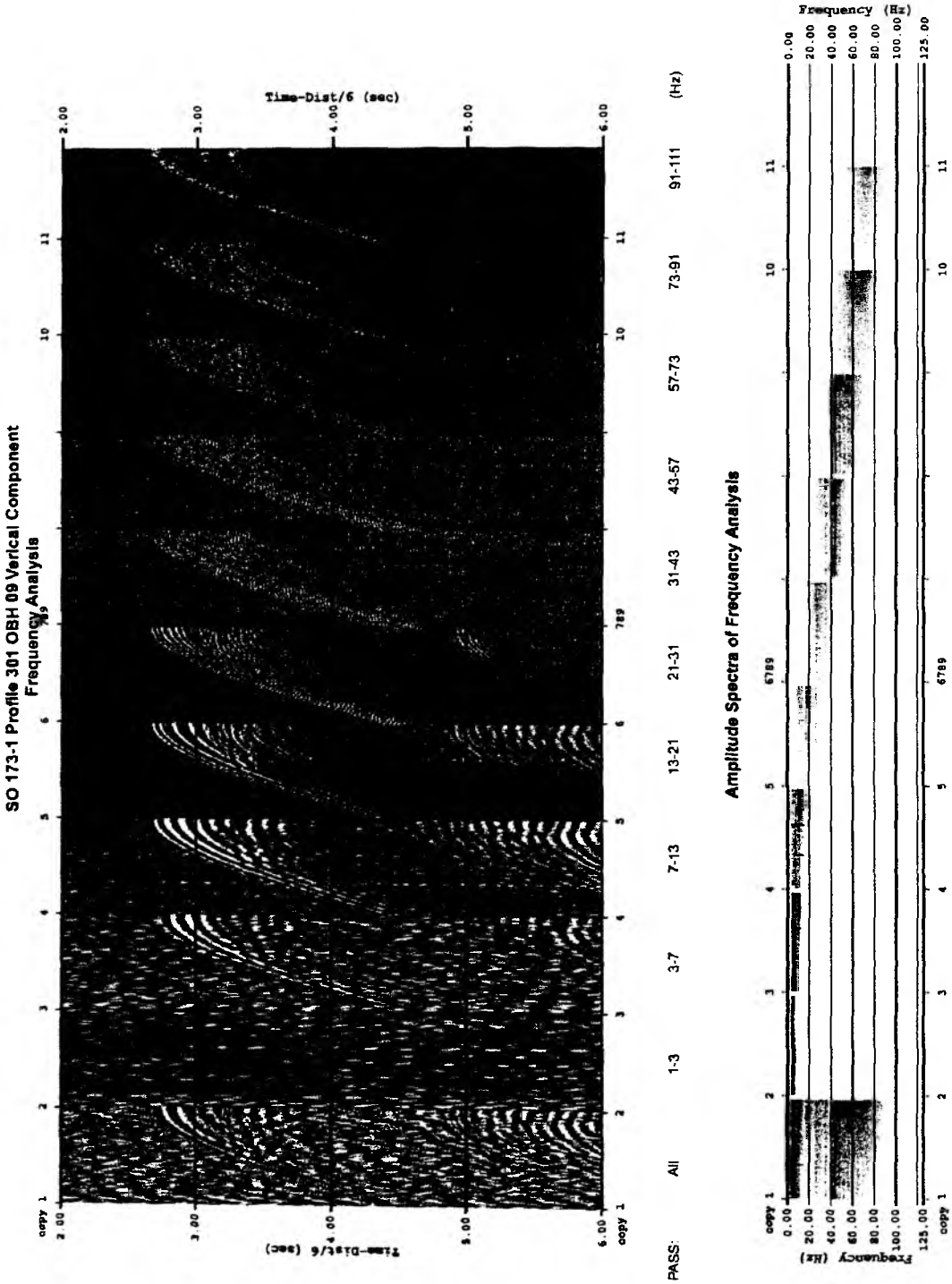

Fig. 6.4.13: Frequency analysis in the offset range 0-7 km.

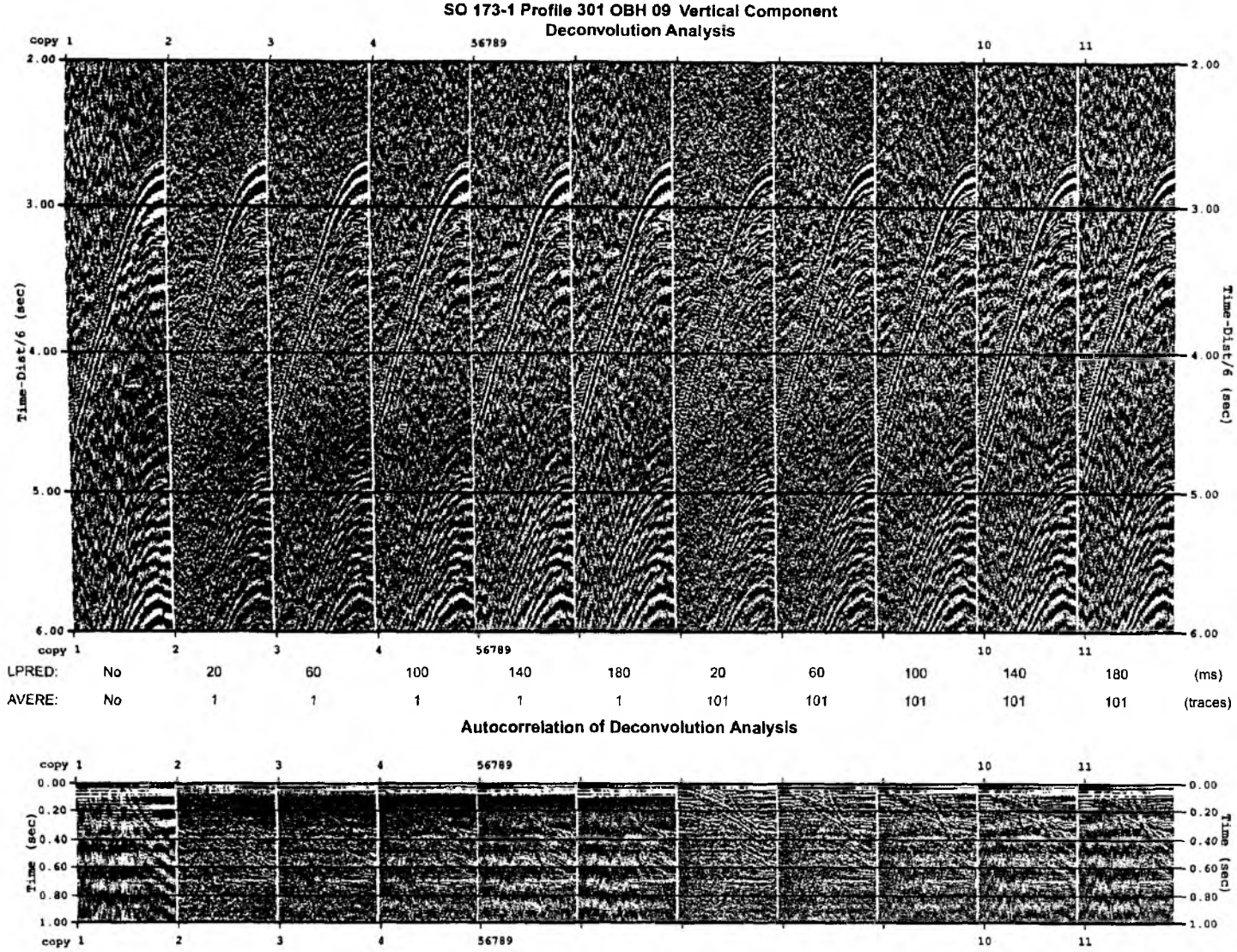

Fig. 6.4.14: Deconvolution analysis in the offset range 0-7 km with operator length 300 ms.

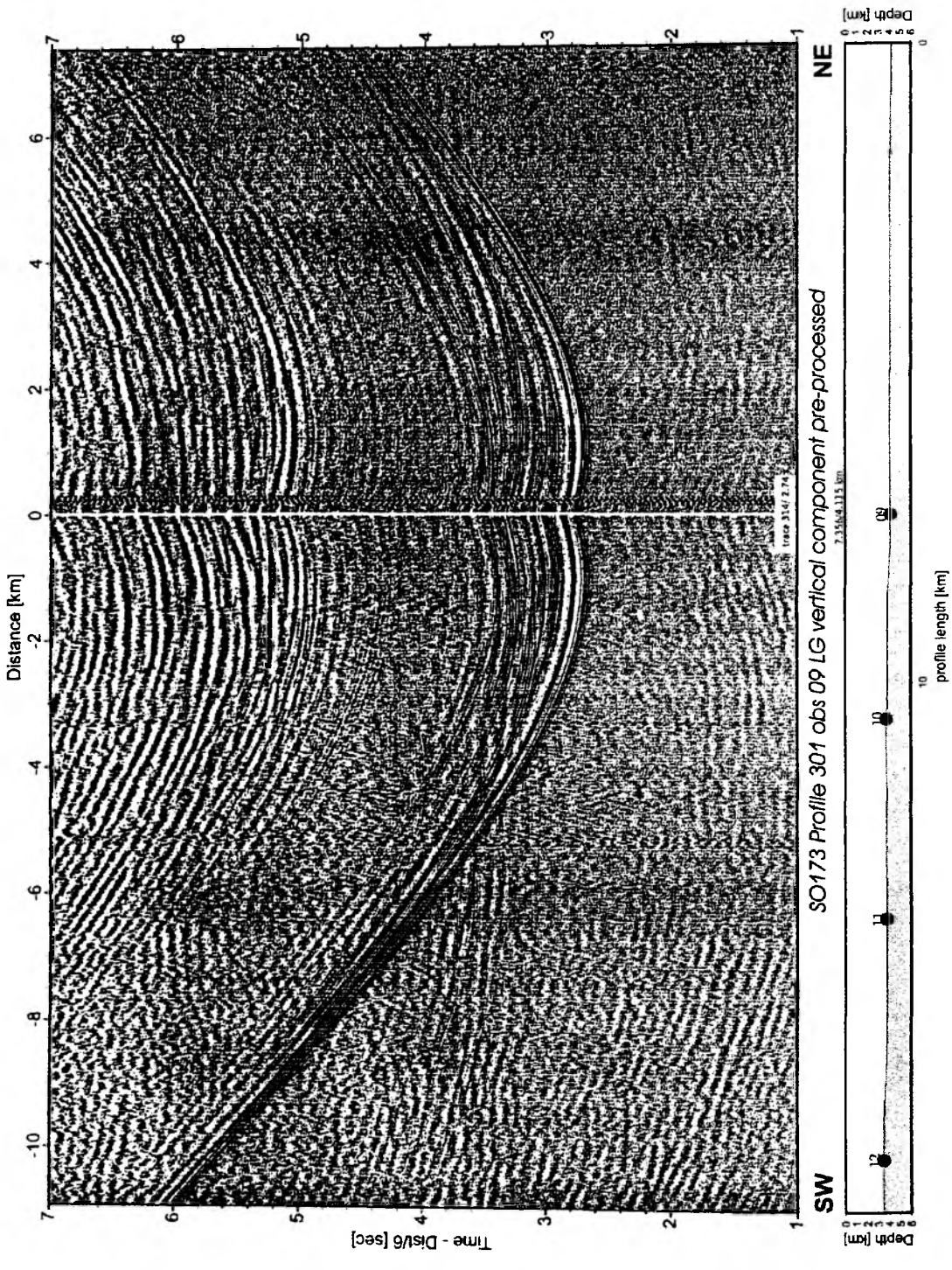

Fig. 6.4.15: Record section from obs 09 LG vertical component pre-processed.

6.4.2 Processing of Earthquake Data (QUEPOS NET)

I. Arroyo, I. Boschini, J. Gossler, M. Mora

The initial data processing is identical to the processing sequence for wide-angle data described in the previous section (i.e., reading of the flashcards, conversion into the PASSCAL Reftek format, and further on into a pseudo SEGY format (PASSCAL SEGY)). Following this step, the processing sequence of the earthquake data diverges from that of the wide-angle data.

Because of large file sizes the PASSCAL Reftek data output is written into multiple files of 518400 kbytes each for OBH stations, corresponding to a time period of 30 days of registration (1 channel with 100 Hz sample rate), and 691200 kbytes each for OBS stations, which corresponds to 10 days of registration time (1 hydrophone and 3 seismometer channels sampled with 100 Hz). Routine for all above-mentioned processing steps: transfer_obh/s (DOS batch file, running SEND2PAS and FTP).

Given the long, ~9 month, duration of the deployment most of the stations lost power. A power loss results in timing mismatchs and corruption of the data recorded during the last days whn there was still some power left. To avoid problems with wrong multiplexed data this part of the data must be removed manually from each affected station. For future long-term experiments it may be helpful to know that only the OBS stations equipped with lithium battery packs operated continuously without (power) problems until recovery.

After conversion the raw data files are compressed by gzip to save disk space and a backup is made on magnetic DLT tapes.

The occurrence of time slips (extra or missing samples) due to a mismatch of the desired and actual sample rates (see previous section for a more detailed discussion of time slips) has to be corrected for. The approach for a correction of time slips differs from the approach used for the wide-angle data because seismological analysis needs to refer back to the continuous data stream throughout. The occurrence time of all time slips is read out from the SEND2PAS log and the PASSCAL error file. The time slips before the beginning of the record are disregarded because the start time of the multiple PASSCAL Reftek files is correct, if they are directly produced by SEND2PAS (Figure 6.4.16). For time slips during the record a sample is added (positive time slips) or removed (negative time slips) at the

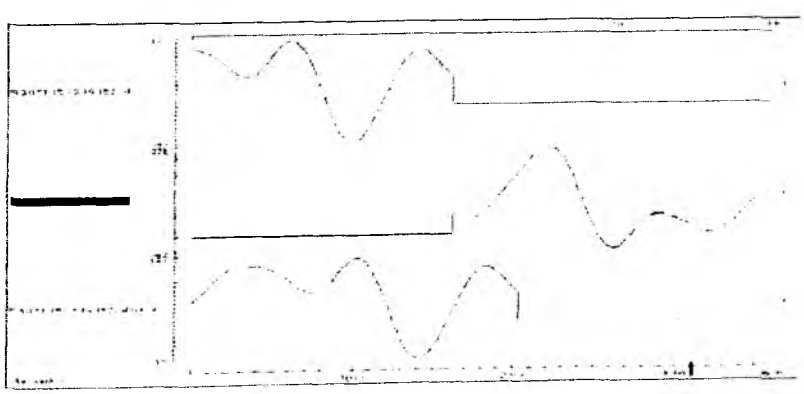

Fig. 6.4.16: *Seismogram example that shows how the unslip process works. While the uncorrected trace (bottom) does not fit to the adjacent trace (center), the unslipped trace (top) fits exactly. Missing samples are filled in by zeros (straight lines).*

appropriate time. This procedure is only approximate (a correct treatment would require resampling of the whole record, fraught with its own difficulties), and in general the apparent time of a sample can be off by up to half a sample length due to this approximation. Relative times within the same record can be off by up to one sample length if the time span straddles a time slip.

Routine for time slip correction: unslip:

After unslipping, the PASSCAL SEGY files have to be cut into 25-hour records with one hour of overlap between adjacent records, such that each record begins at 0:00:01 (except on the first day of recording, of course). This cutting makes file sizes smaller (more manageable) and enables time corrections to be applied on a daily basis.

Routine for cutting: split_segy.pl:

The registration period of the QUEPOS earthquake network stretches over New Year's eve which causes problems with the splitting routine. In the SEGY data the days are simply counted forward ignoring the year change. We fix this bug by splitting the primary PASSCAL SEGY file at midnight on December 31, and modifying the header entries for year and day of the resulting SEGY file.

Routine to fix New Year problem: fix_newyear.sh

Another small step is to merge the files of the days where the original PASSCAL Reftek files that had been split due to file size exceed the specified file size limits into 25-hour files.

Routine for merging: merge_splitfiles.sh:

Next, the timing of each 25-hour SEGY record has to be corrected. Timing errors occur because of the slow drift of the internal clock relative to GPS time. The system time is compared with GPS time at the beginning and the end of the deployment, and a linear drift rate is inferred from the observed difference (skew). The time of each 25-hour record is corrected by applying the shift appropriate for the time 12.5 hours after the beginning of the record. The underlying assumption is that the system clock does indeed drift linearly, and that the drift over a given 24-hour period is negligible (i.e. much less than one sample length) which is usually the case. Unfortunately, a skew value could only be determined for 4 stations. For the stations that ran out of power before the instruments were recovered, no skew values could be determined. Therefore we introduced an artificial skew averaged from previous deployments, noted in the recorder booklet (Table 6.4.1). Since with many recorders the historical skew value increases the longer the station was deployed, we used a time-weighted average to correct the drift. However, timing uncertainties for these stations accumulate at a rate of 1 ms per day, starting with the first day of deployment. This can be easily obtained by comparing the observed skew value of those stations that delivered a skew with their historical weighted average.

Routine for linear clock drift correction: clock_cor.pl.

Over longer time intervals the daily data is quality controlled using the PQL (PASSCAL Quick Look) seismogram viewer. A station status protocol is also prepared (Table 6.4.2).

A short-term-average versus a long-term-average (STA/LTA) trigger algorithm is then applied to the data to search for seismic events. Unfortunately, we must apply a 5-20-Hz bandpass filter prior to triggering, because of strong long-period noise around 0.2-0.5 Hz that shows up not only on broad-band sensors like DPG pressure sensors and PMD seismometers, but also on many OBH stations equipped with a hydrophone (Figure. 6.4.17). Because the filter cannot be applied directly to the SEGY data files, the files

Tab. 6.4.1: 1-D-velocity model for earthquake localisation based on offshore refraction profile 100 of R/V SONNE cruise SO 81 (Ye et al., 1996).

Vp (km/s)	Depth (km)
1.7	0.0
2.4	1.5
4.9	3.0
5.5	12.0
6.0	14.5
8.1	20.5

must first be converted into SAC format, then filtered and triggered. This results in a very long processing time, because some of the 25-hour files need up to 2 hours to be treated, and the whole procedure took almost one week. The trigger parameters are length of the short term (s) and long term (l) time window, the mean removal window length (m), the trigger (t) and detrigger ratio (d), minimum number of stations (S) and the network trigger time window length (M). The trigger parameters must be defined for each data set. The trigger parameters used for shipboard processing are shown in Table 6.4.2. These values are the same values as used for the nearby JACO network. Data have been checked visually for the first 10 days of registration. The selected trigger values yield good results. Only a few trigger signals have been obtained which did not belong to seismic activity. Therefore, we canceled the visual data check at this processing step and combined it with the phase picking, to be performed later on.

Routine for triggering: trig_all.csh (uses PASSCAL reftrig trigger algorithm):

After event triggers have been found the events have to be cut from the 25-hour files and stored into subdirec-tories, one per event. Because we are investigating local earthquakes, the appropriate length of the time window for the events is 3 minutes, starting 60 s prior to trigger time. Usually the events have to be quality-checked again and bad triggers sorted out. Events are also inspected for traces, that are unusable for a particular event because they contain only noise. In this experiment we omitted these steps after a quality check of the events of the first 10 days of registration had been done, because of the good trigger results, the time delay caused by the filtering prior to trigger, and due to the large number of events (> 12,000 events).

Routine for event cutting: collate_ev.pl:

The SEGY traces in the event directories are converted first into SAC, and then into SEISAN waveform format, which makes it possible to store all traces associated with an event in a single file. After conversion the data are registered into the SEISAN database (Havskov and Ottemöller, 2001).

Routines for conversion: segy2sac_all.csh, sac2sei.sh, seisei.sh, autoreg

At last, P and where possible S phases are picked and events are preliminarily located with the program HYP, which employs an iterative solution to the nonlinear localization problem (Lienert and Havskov, 1995). Care must be taken when picking S phases on hydrophone channels because there is a high probability of picking another prominent (non-S) phase (Figure 6.4.20). For the sake of simplicity for the

Tab. 6.4.2: Trigger parameters as defined in the text to search the continous recordings for seismic events.

Parameter	s	l	m	t	d	S	M
Value	0.5 s	60 s	500 s	2.8	0.8	4	30 s

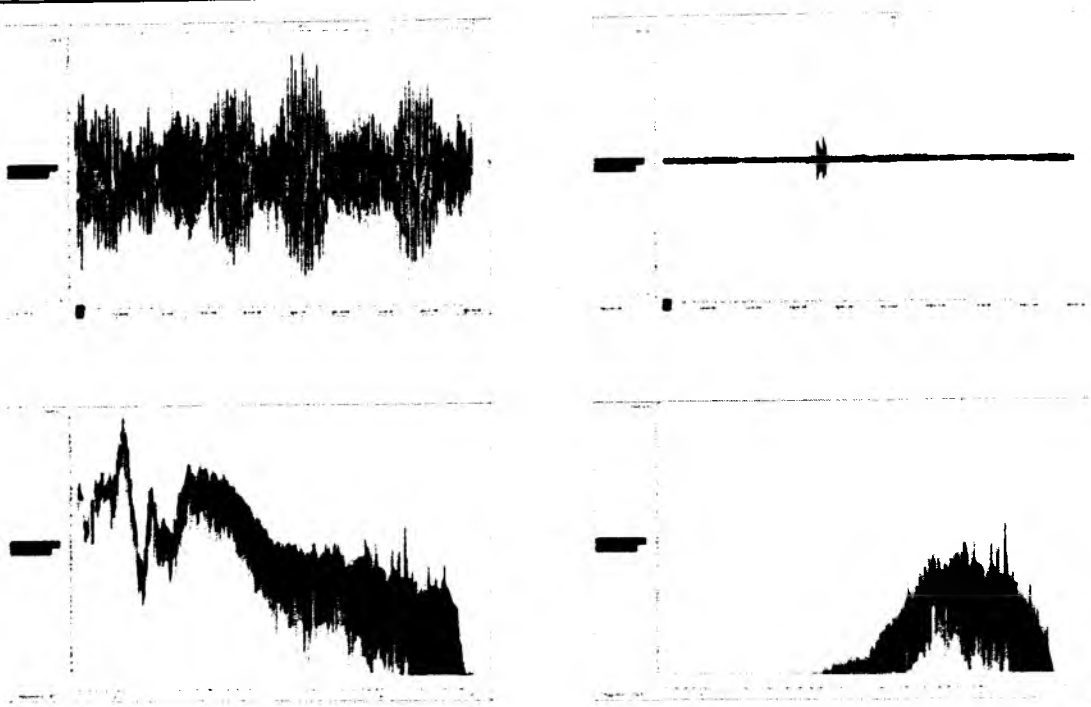

Fig. 6.4.17: Seismogram example from best quality hydrophone station OBH321 from October 18, 2002 starting at 0:00. The raw seismogram (upper left) contains strong long-period noise covering all higher frequencies. The noise frequency of ~ 0.1 Hz produces a large dominating peak in the raw spectrum (lower left). On the 5 – 20 Hz band pass filtered seismogram (upper right) a small earthquake can be identified, that can only be detected by the trigger routine if a prefilter is applied. The filtered seismogram spectrum (lower right) does not contain lower frequencies.

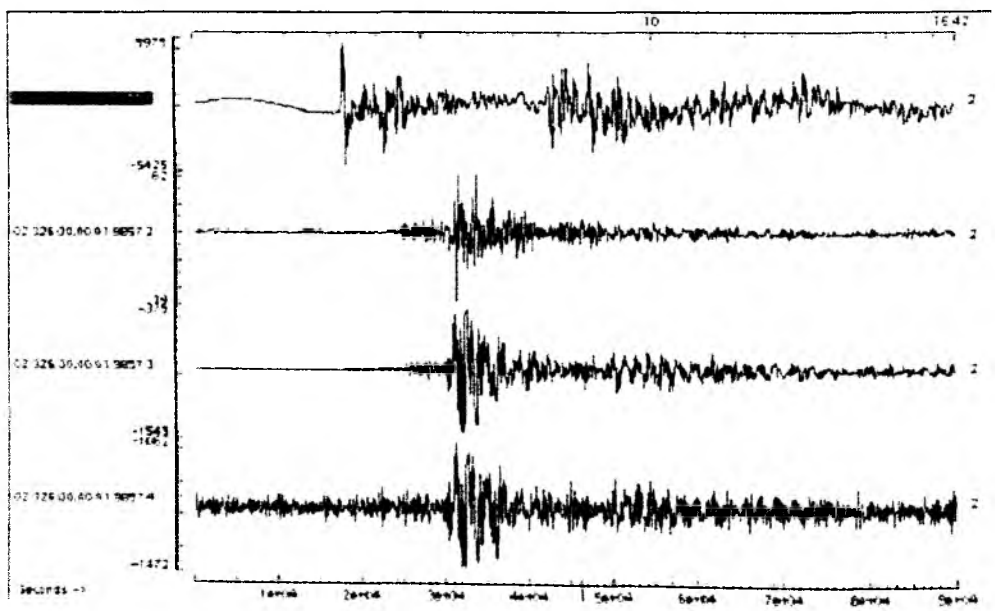

Fig. 6.4.18: Seismogram example of station obs307 that shows that the prominent phase on the hydrophone channel (top) at about 8 seconds (upper scale) is not S. The S-phase can be clearly identified on the seismometer channels (2-4) and occurs at about 5.5 seconds.

onboard processing, a one-dimensional velocity model (Table 6.4.1) is assumed based on offshore refraction profile line 100 of R/V SONNE cruise SO 81 (Ye et al., 1996).

6.4.3 The QUEPOS Earthquake Network

I. Arroyo, I. Boschini, J. Gossler, M. Mora

6.4.3.1 Introduction

The main theme of SFB 574 „Fluids, Volatiles, Hazards" subproject A2 is to understand the nature of coupling and mass transfer between upper and lower plate of the subduction zone in central Costa Rica.

With the passive seismic experiment, we are investigating the local seismicity in two adjacent regions for 6 months each. A combined on- and offshore seismic network, consisting of 23 ocean bottom and 15 land stations, was deployed in the coastal Pacific region of central Costa Rica near Jaco in April 2002 and was moved south-east to near Quepos in October 2002. The land stations were removed in March 2003 and at the beginning of this cruise the marine network was recovered.

Standard investigation of the local seismicity (i.e. the determination of hypocenter, magnitudes, polarity and focal mechanism) will shed insights into the seismogenic zone and the deeper content of the subducting slab (Benioff zone). Our previous results from the nearby JACO network suggest that the lateral coverage with hypocenters should be sufficient for seismic tomography studies. Detailed initial velocity models are available from the active seismic experiments carried out on- and offshore Costa Rica in the last decade (i.e. Ye et al, 1996 and others).

The main objective of the passive seismological experiment is to detect and register the local seismicity induced by the convergent dynamics between the subducting oceanic lithosphere and the Caribbean plate. The spatial dimensions of the joined marine and land networks are designed to register local tectonic events associated with the downgoing plate.

6.4.3.2 Description of the JACO and QUEPOS Marine Seismic Networks

Twenty-three ocean bottom instruments operated from April 28 until October 3, 2002 in a seismic network centered about the Jaco Scar (JACO network). Five additional OBH operated east of the network on Quepos Mound until they were recovered in July 2002. The stations in the vicinity of the Quepos Mound are part of the JACO network. From October 1 to 3, 2002 the ocean bottom instruments were recovered and redeployed in the Quepos area to establish the QUEPOS network.

At the same time as the ocean botton deployment of the OBH, the Instituto Costaricense de Electricidad (I.C.E.) ran a land-based local earthquake network together with GEOMAR and the University of Kiel. Both data sets can be used to further constrain earthquake locations and should provide additional data for focal mechanism analysis of events located in between the marine ocean bottom array and the land network. While the onshore network was removed earlier in March 2003, the marine part of the QUEPOS network was not removed before July 2003. Instrument locations for both the on- and offshore components of the network are shown in Figure 6.4.19.

6.4.3.3 Operating Details of the QUEPOS Network

The 23 ocean bottom instruments in the QUEPOS network comprise 19 OBH (i.e. hydrophone or DPG pressure sensor) and 4 OBS (ocean bottom seismometer plus pressure sensor). Site details for each of the marine stations are shown in Table 6.4.3. A detailed map of the marine station locations in the QUEPOS seismic network is shown in Figure 6.4.20. Most of these stations were deployed on the continental margin east of Parrita scar in the megalense area.

Tab. 6.4.3: The stations of the QUEPOS marine seismic network. Location, depth and sensor types are indicated.

Station	Latitude (N)	Longitude (W)	Depth (m)	Sensors
OBH301	9 15.56	84 30.03	311	DPG 93
OBH302	9 15.71	84 21.48	326	OAS 318
OBH303	9 08.36	84 23.15	656	OAS 30
OBH304	9 01.81	84 24.81	1156	OAS 02
OBS305	9 05.01	84 30.40	1038	DPG 86 + PMD 509
OBH306	9 07.06	84 42.99	1157	OAS 27
OBS307	8 50.03	84 49.96	3488	DPG 78 + Webb 2352
OBH308	8 39.20	84 32.78	2167	OAS 22
OBS309	8 34.80	84 22.79	2840	OAS "dnu" + PMD 539
OBH310	8 45.81	84 23.16	1849	DPG 91
OBH311	8 46.26	84 30.60	2550	OAS 29
OBH312	8 52.81	84 34.81	2613	DPG 92
OBH313	8 53.05	84 28.29	1993	OAS 38
OBH314	8 57.66	84 27.84	1617	OAS 06
OBH315	8 52.55	84 20.60	1312	HTI 802
OBS316	8 57.88	84 19.04	909	DPG 74 + PMD 540
OBH317	9 03.60	84 16.80	519	DPG 77
OBH318	9 10.53	84 15.27	354	HTI 302
OBH319	9 03.16	84 11.74	283	OAS 01
OBH320	9 00.08	84 10.89	220	HTI 902
OBH321	8 53.69	84 12.20	284	HTI 002
OBH322	8 47.41	84 15.60	796	HTI 102
OBH323	8 47.72	84 09.89	206	DPG 87

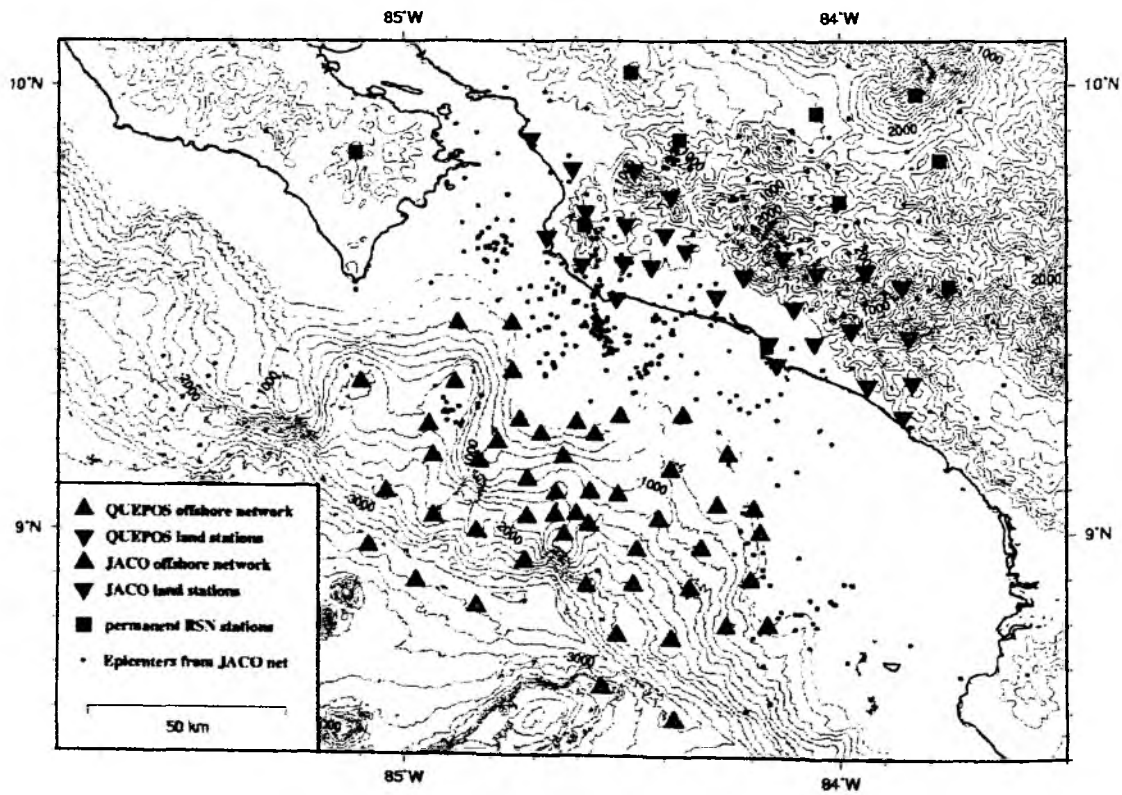

Fig. 6.4.19: Station locations for the temporary seismic networks: JACO (black triangles) and QUEPOS (gray triangles). Permanent Costa Rican national seismic network (RSN) stations (black squares). Epicenters of earthquakes located with the JACO land stations network from April to June 2002 are shown as black dots.

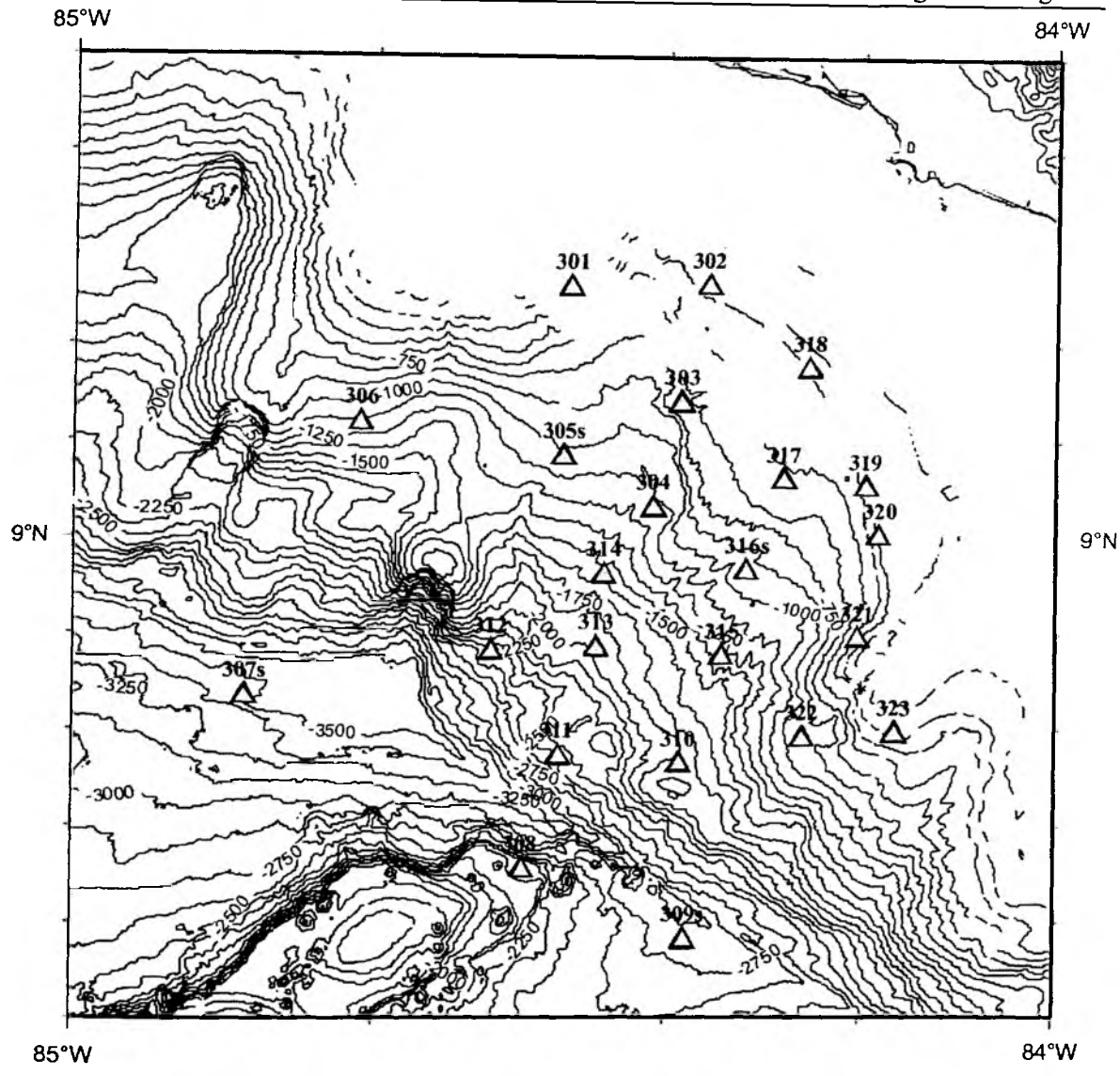

△ **QUEPOS ocean network**

Fig. 6.4.20: *The QUEPOS ocean bottom network, consisting of 19 OBH and 4 OBS stations operating from October 1, 2002 until July 15, 2003. Note that the suffix „s" after a station number denotes an OBS.*

Unfortunately, most of the stations ran out of power before recovery. Only the OBS stations equipped with lithium battery packs operated well throughout the whole registration period from October 1, 2002 until July 15, 2003. Most of the OBH stations stopped registering in April or May 2003. The loss of power results in many problems with the data. The most significant problem is that all OBH stations, except OBHs 309, 316 and 321, could not receive a time signal properly after recovery to determine the clock drift troughout the registration period (skew). Therefore the skew values have to be determined from historical records for each instrument. Skew values reported for each instrument on previous deployments are noted in the recorder booklet. However, it is worth noting that a comparison the historical skew values with the true values for the OBS stations shows that the historical skew can be off by as much as a factor of 2, resulting in an uncertainty of ~1 ms/day. By the end of April this translates into as much as 200 ms,

Tab. 6.4.4: Determination of the time-weighted average time drift for stations which did not receive a time skew after recovery because of power failure. Stations that obtained a skew are listed to test the averaging method.

Station Rec.	Date of recovery	Days	Hours	Skew (ms)	Skew (ms/h)	Average (ms/h) Weight. av. (ms/h)	Depl. Days hours	Tot. Skew (ms)	Deployed Recovered
OBH301	02.12.01	50	1200	61	0,051	0,068	288	466,65	01.10.2002
000713	25.04.02	40	960	85	0,089	**0,065**	6912	**447,74**	15.07.2003
	01.10.02	157	3768	238	0,063				
OBH302	09.10.00	32	768	-67	-0,087	-0,114			
000707	05.01	160	3840	-305	-0,079	**-0,119**			
	06.01	15	360	-30	-0,083				
	02.12.01	50	1200	-157	-0,131				
	25.05.02	40	960	-133	-0,139				
	02.10.02	139	3336	-548	-0,164				
OBH303	18.01.00	36	864	-102	-0,118	-0,088	288	-607,18	01.10.2002
991256	06.01	15	360	-22	-0,061	**-0,100**	6912	**-688,11**	15.07.2003
	01.12.01	50	1200	-95	-0,079				
	24.04.02	40	960	-62	-0,065				
	02.10.02	139	3336	-388	-0,116				
OBH304	25.04.02	39	936	51	0,054	0,045	286	309,68	01.10.2002
991247	17.07.02	61	1464	48	0,033	**0,045**	6864	**310,72**	13.07.2003
	01.10.02	143	3432	165	0,048				
OBH305									03.10.2002
000712				**376**					13.07.2003
OBH306	02.12.01	50	1200	-90	-0,075	-0,066	286	-455,12	01.10.2002
991238	20.12.01		57	-2	-0,035	**-0,093**	6864	**-639,60**	13.07.2003
	09.05.02	16	384	-19	-0,049				
	02.10.02	140	3360	-355	-0,106				
OBH307									02.10.2002
010407									13.07.2003
OBH308	01.12.01	49	1176	-62	-0,053	-0,060	285	-412,08	02.10.2002
000711	10.12.01		69	-4	-0,058	**-0,078**	6840	**-533,91**	13.07.2003
	20.12.01		55	-3	-0,055				
	09.05.02		410	-18	-0,044				
	01.10.02	138	3312	-305	-0,092				
OBH309	M47-2	11	264	21	0,080	0,061	283	413,57	02.10.2002
991243	Darwin	30	720	45	0,063	**0,056**	6792	**377,10**	11.07.2003
	05.01	160	3840	227	0,059				
	02.12.01	50	1200	82	0,068				
	09.05.02	16	384	20	0,052				
	01.10.02	139	3336	146	0,044				
	11.07.03	**285**	**6840**	**551**	**0,081**	**not used for av.**			
OBH310	M47-2	11	264	-9	-0,034	-0,076	283	-518,54	02.10.2002
991237	07.12.01	57	1368	-111	-0,081	**-0,095**	6792	**-646,86**	11.07.2003
	25.04.02	40	960	-79	-0,082				
	02.10.02	158	3792	-409	-0,108				
OBH311	06.12.01		39	-2	-0,051	-0,040	285	-275,86	02.10.2002
010402	10.12.01		49	-1	-0,020	**-0,040**	6840	**-274,97**	13.07.2003
	13.12.01		46	-2	-0,043				
	20.12.01		65	-3	-0,046				
OBH312	01.12.01	49	1176	125	0,106	0,099	286	679,01	02.10.2002
991250	10.12.01		51	5	0,098	**0,124**	6864	**854,13**	14.07.2003
	13.12.01		48	3	0,063				
	20.12.01		52	5	0,096				
	01.10.02	157	3768	496	0,132				

Tab. 6.4.4 (contd)

OBH313	05.01	160	3840	-76	-0,020	-0,054	286	-370,55	02.10.2002
991246	20.12.01		72	-2	-0,028	-0,055	6864	**-375,03**	14.07.2003
	17.07.02	61	1464	-128	-0,087				
	02.10.02	139	3336	-270	-0,081				
OBH314	01.12.01	49	1176	-10	-0,009	-0,005	284	-37,22	03.10.2002
010405	09.05.02		409	5	0,012	**-0,015**	6816	**-100,53**	13.07.2003
	01.10.02	143	3432	-69	-0,020				
OBH315	03.12.01	50	1200	66	0,055	0,056	282	378,21	03.10.2002
990701	01.10.02	138	3312	188	0,057	**0,056**	6768	**381,00**	11.07.2003
OBH316	M47-2	11	264	-15	-0,057	-0,054	283	-363,98	03.10.2002
991242	Darwin	31	744	-29	-0,039	**-0,048**	6792	**-322,62**	12.07.2003
	05.01	160	3840	-89	-0,023				
	01.12.01	50	1200	-58	-0,048				
	25.04.02	40	960	-43	-0,045				
	02.10.02	158	3792	-279	-0,074				
	12.07.03	**286**	**6864**	**-614**	**-0,089**	**not used for av.**			
OBH317	history not								03.10.2002
010409	available								12.07.2003
OBH318	30.08.01		103	-11	-0,107	-0,117	283	-793,76	03.10.2002
010401	09.09.01		74	-6	-0,081	**-0,178**	6792	**-1211,77**	12.07.2003
	10.12.01		63	-6	-0,095				
	01.10.02	139	3336	-615	-0,184				
OBH319	M47-2	11	264	-36	-0,136	-0,056	283	-383,59	03.10.2002
991236	01.12.01	49	1176	-51	-0,043	**-0,061**	6792	**-415,10**	12.07.2003
	12.10.01		50	-1	-0,020				
	14.12.01		50	-1	-0,020				
	02.10.02	139	3336	-209	-0,063				
OBH320	02.12.01	49	1176	42	0,036	0,033	283	223,50	03.10.2002
010403	10.12.01		67	1	0,015	**0,035**	6792	**237,10**	12.07.2003
	13.12.01		47	0	0,000				
			40	1	0,025				
	20.12.01		45	4	0,089				
OBH321	13.10.01		50	3	0,060	0,098	283	667,91	03.10.2002
000706	10.12.01		68	6	0,088	**0,147**	6792	**996,65**	12.07.2003
	15.12.01		42	4	0,095				
	02.10.02	139	3336	500	0,150				
	12.07.03	**286**	**6864**	**750**	**0,109**	**not used for av.**			
OBH322	M47-2	6	144	-20	-0,139	-0,110	282	-741,45	03.10.2002
991259	Darwin	7	168	-10	-0,060	**-0,123**	6768	**-834,83**	11.07.2003
	01.12.01	49	1176	-128	-0,109				
	02.10.02	140	3360	-440	-0,131				
OBH323	Darwin	7	168	14	0,083	0,120	283	816,73	03.10.2002
991249	05.01	160	3840	362	0,094	**0,130**	6792	**883,21**	12.07.2003
	25.04.02	40	960	131	0,136				
	02.10.02	157	3768	629	0,167				

which is 20 samples assuming a sampling rate of 100 Hz. Additional problems that occur when the internal recorder clock is interrupted include time resets and resync, often followed by time mismatches. Table 6.4.4 contains the historical skew values and recorder numbers of the instruments used in the QUEPOS network. Furthermore, premature power loss also results in data loss. The status of each station in the QUEPOS network as a function of date is shown in Figure 6.4.21. Given that only seven stations supply data significantly longer than April 30, we shut the network down on this day. The land network was removed at the end of March 2003, so there is a full overlap the marine and onshore parts of the network.

Another important point is the operating stability of the hydrophones and the DPG pressure sensors. For nine hydrophones (OAS and HTI type) the drift was strong enough to let the zero level go off-scale, so that no more signals were registered. The physical mechanism for hydrophone drift remains unclear. Three DPG sensors were very noisy and produced a lot of spikes, which results in a poor data quality, while one DPG sensor only produced instrument noise. The two PMD seismometers that were operating (one was not switched on (!)) show a good data quality, since they had been repaired before the cruise. The Webb seismometer had only one channel that delivered a fairly good quality. Table 6.4.5 summarizes more details about the individual stations.

6.4.3.4 Seismic Events Registered with the QUEPOS Marine Network

As described in the previous subchapter a LTA/STA trigger algorithm is applied to the data to search for seismic events. Prior to triggering a 5–20 Hz bandpass filter has to be applied to reduce the long-period noise between 0.03 and 0.5 Hz that often prevents the seismic events from being triggered (Figure 6.4.25). The results of the trigger procedure are very good. The first 10 days of data provide a bad trigger rate of less than 7 %, consequentely we canceled the quality check after event cutting. For each day we obtain a trigger file that contains the valid network trigger times. The event cutting is then based on these trigger times.

Initially, 9 stations (Table 6.4.6) that had produced fairly good data were selected for triggering, so that the number of bad triggers which are not related to seismic activity could be minimized. From November 5 to 23 the number of triggers increased strongly by as much as a factor of 10. After checking the numbers of single trace triggers of every station from the first 3 months, we found that station OBS316 produced 2/3 of the total amount of triggers compared to the other stations (Table 6.4.6). Since it is unlikely that the large number of trigger signals was caused by seismicity (especially as the DPG sensor is known to be spiky sometimes) we excluded station OBS316 from triggering.

After the single trace triggers from OBS316 had been removed and the network trigger had been applied again, the trigger numbers decreased significantly for the days mentioned, but they are still higher than the average, while the number for other days decreases only slightly. For the entire operating period of 211 days (until we closed the network on April 30), we obtained a total of 12.737 triggers. These triggers are not equally distributed over time. Half of the triggers (i.e. 6.416) were registered during a 15-day interval from April 9 to April 23, 2003.

The reason for the extremely high number of triggers between April 9 and 23 seems to be attributable to very high microseismic activity directly beneath the shallowest stations and not instrument-related noise. See also subchapter 6.4.3.7 about tremors for additional information.

On average, excluding the period from April 9 to April 23, we recorded 32 triggers per day. Figure 6.4.22 shows the number of network triggers on a daily basis. The increase on October 8 is attributed to a

magnitude 4.8 earthquake east of the network (9.101° N; 84.037 ° W) followed by ~100 aftershocks within 10 hours.

Until the end of the SO 173/1 cruise we evaluated the triggered events of the QUEPOS offshore network from October 2002. 330 earthquakes have been located within a total of 979 events. Histograms on a daily basis are shown in Figure 6.4.23. The peak on Oct 8 (DOY 281) is caused by the 4.8 earthquake and its aftershocks. 76 aftershocks were located very close east of the network until Oct 12(Figure 6.4.24). In this area a major 6.4 earthquake took place on June 2002. Other earthquakes are located close to the coastline of central Costa Rica. There were some earthquakes very close along the trench. Two events are located directly on Parrita Scar. Only few events have been observed beneath the oceanic plate, four of them are located on the Fisher seamount chain close to the Nicoya slide, where other earthquakes have been located by the JACO land network (Figure 6.4.30).

6.4.3.5 Seismogram Examples

Three earthquakes registered by the QUEPOS offshore network are presented as data examples. The most prominent one is the magnitude 4.8 event from Oct 8, 2002 (Figure 6.4.25). An aftershock with magnitude 3.3 from Oct 8 is shown as an example for filtering with the 5-20 Hz band pass (Figures 6.4.26, 6.4.27). Another magnitude 3.6 event from Oct 12 is presented to demonstrate the good data quality of the registrations of the QUEPOS network (Figure 6.4.28).

6.4.3.6 Magnitudes of JACO Land Stations Network

Before the events of the QUEPOS offshore network were prepared for phase picking, the magnitudes of the seismic events registered by the JACO onshore network from April to July 2002 had been determined. To calculate the local magnitude the maximum amplitude of an event has to be picked on the Wood-Anderson filtered traces (Gutenberg and Richter, 1954). For the JACO network this was done for 959 earthquakes from a total of 2134 events. Figure 6.4.29 shows the magnitude distribution of these events. The distribution peaks at magnitude ~2.2, which means that below that magnitude less events are detected by the network than there took place. This is due to a restricted resolution because of noisy environmental conditions. The stations were operated in densely populated areas. Figure 6.4.30 shows the epicenters of earthquakes located within the JACO onshore network from April to July 2002.

6.4.3.7 Non-volcanic Tremors Related to Subduction Zones in Front of Quepos?

Non-volcanic, tremor-like signals have recently been detected in Southwest Japan (Obara, 2002; Katsumata & Kamaya, 2003), where the Philippine Sea plate is subducting, and at the Cascadia subduction zone (Rogers & Dragert, 2003). The signals are described as very small-amplitude, long-period tremors with generally emergent onsets that last from a few minutes to a few days. Their frequency content is mainly between 1 and 10 Hz. By analyzing the signal envelope a propagation velocity of 4 km/s is estimated, suggesting S-wave velocity propagation (Obara, 2002). This seems to agree with the greater amplitudes recorded by the horizontal components of the seismometers as compared to the vertical ones.

Using cross-correlation and routine location techniques the tremor events are located along the strike of the subducting plates over lengths of hundreds of kilometers and at depths between 20 and 40 km, concentrated near the Moho discontinuity (30 km depth in Japan). The tremor activity migrates along the strike of the subduction zone with velocities from 5 to 15 km per day (Rogers & Dragert, 2003). In the Cascadia region Rogers & Dragert (2003) report a temporal and spatial correlation between the tremor activity and "silent" slip events at the plate interface based on GPS measurements from 1996 to the present. During the intervals between slips, tremor activity is minimal or non-existent.

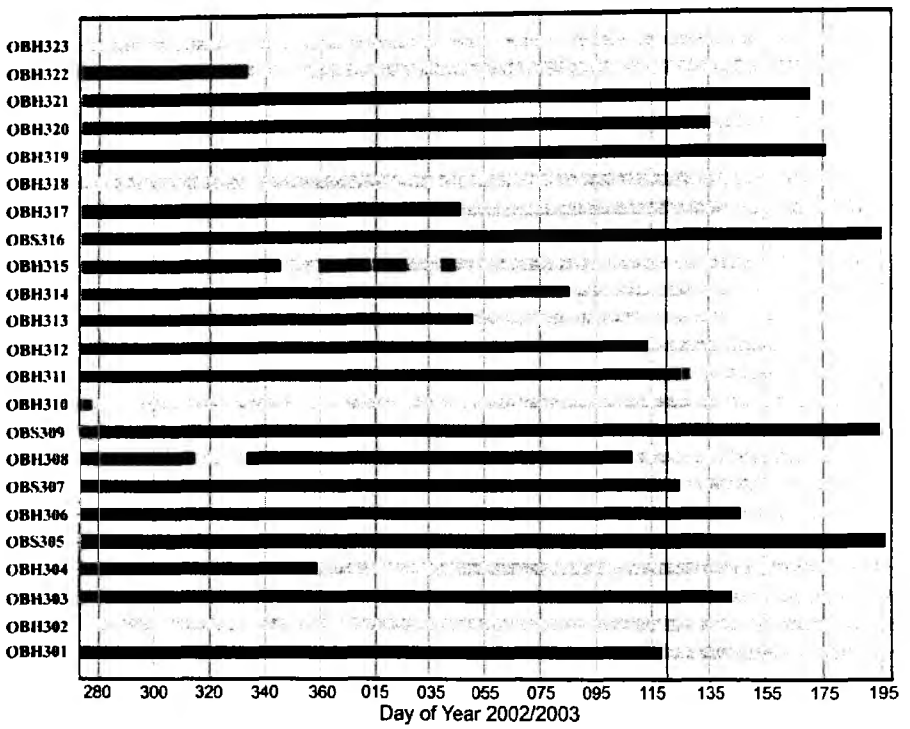

Fig. 6.4.21: *Station status of the QUEPOS offshore network. The days from which even a portion of data of the specified station can be used (i.e. at least from one channel of an OBS station) are marked black, while gray indicates stations deployed but the data (if any) cannot be used. April 30, 2003 (DOY 120) when the network is closed is marked by the vertical gray line.*

Obara (2002) points out that the generation of these tremors could be related to the movement of fluids in the subduction zone, liberated by dehydration of the slab, which move to the slab surface at the depth of the Moho. Laboratory experiments conducted by Dobson et al. (2002) seem to support this hypothesis. Katsumata and Kamaya (2003) consider the water produced by dehydration processes of chlorite and amphibole as likely sources for the fluid. On the other hand, based on correlation with slip events, Rogers & Dragert (2003) attribute these tremors to a shearing source in which the fluids may play an important role by regulating the shearing strength of rock.

The source processes of these non-volcanic tremors associated with subduction zones are poorly understood and lot of work must be done. Investigations of non-volcanic tremors from additional subduction zones will certainly yield greater insights into the governing processes. The recent seismological experiments carried out in the subduction zone in the Pacific region of Costa Rica by GEOMAR (Germany) in collaboration with the Instituto Costarricense de Electricidad (ICE, Costa Rica) provided a suitable setting to investigate if non-volcanic tremors are produced at the Central American subduction zone. This motivated a very first attempt to search non-volcanic tremors in the QUEPOS sea network, which was recovered during the SO 173/1 expedition. The network operated continuously from October, 2002 to April, 2003.

Tab. 6.4.5: Data quality check of the individual stations of the QUEPOS network.

Station	Sensor type	Data quality
OBH301	DPG	Poor quality, noisy
OBH302	OAS	Station lost
OBH303	OAS	Zero level off every few hours, quality ok
OBH304	OAS	Zero level off since Dec 23, sometimes spiky
OBS305	DPG + PMD	DPG: ok, sometimes very spiky Seismometer: ok
OBH306	OAS	Ok
OBS307	DPG + Webb	DPG: sometimes very spiky Seism.: only 1 horizontal component fairly ok
OBH308	OAS	ok, spikes every 2 hours
OBS309	OAS + PMD	OAS: out 320 Seismometer: ok
OBH310	DPG	Only 40 s of data(!)
OBH311	OAS	Zero level often off since March 24, quality ok
OBH312	DPG	Very poor
OBH313	OAS	Zero level off since February 17, poor
OBH314	OAS	Ok
OBH315	HTI	Zero level often off, disk full (4 chan. on)
OBS316	DPG + PMD	DPG: sometimes spiky Seismometer: channels switched off(!)
OBH317	DPG	Poor quality
OBH318	HTI	Recorder problem, produced only a straight line
OBH319	OAS	Zero level often off, quality ok
OBH320	HTI	Ok, sometimes spikes
OBH321	HTI	Zero level off since June 17, very good quality
OBH322	HTI	Zero level off since November 27, good quality
OBH323	HTI	Only instrument noise

Tab. 6.4.6: Numbers of single trace triggers of the first 3 month from all stations that had been used for triggering initially. Station OBH316 was excluded from triggering because of its extremely high trigger number compared to other stations.

Station	No. of triggers	Days	Triggers/day
OBH303	17865	91	196
OBH304	11662	83	141
OBH306	8806	91	97
OBH308	4478	69	65
OBH311	4574	87	53
OBS316	81382	90	904
OBH319	23356	90	260
OBH320	32262	90	358
OBH321	17578	90	195

6.4.3.8 Method

In order to search for examples of signals that could potentially be tremor-like events, a simple MATLAB code was developed during the cruise to compute the signal envelope at various stations. The estimation, based on the Hilbert Transform (*H*), is:

$$E(t) = \left| \sqrt{S^2(t) + H(S(t))^2} \right|$$

where *S(t)* is the input signal and *E(t)* is the envelope. This method produces a detailed envelope that can be smoothed afterwards using a moving average filter. Furthermore, it allows more accurate estimations of the correlation functions for eventual epicenter determinations.

6.4.3.9 Results

From figures 6.4.31 to 6.4.34 the analysis of two examples of possible tremor signals is shown. In the first case (Figure 6.4.31) the envelopes of a 10-minute record are shown. A flat envelope can be observed from 0 to 250 s, from this point the tremor onset varies from 250 s at OBH 313 to 290 s at OBH 321. The amplitude increases progressively to a maximum between 400 and 450 s (except for OBH 313), and then decreases in the same way to the end. At the seismometer OBS 305 the signal can be recognized, however it is strongly affected by low-frequency energy. From the spectra of the 5-minute signal (Figure 6.4.32) we can recognize that most of the energy of the tremor is concentrated between 2 and 10 Hz at all stations. However at the OBS 305 Z station the energy between 1 and 2.5 Hz is greater than that of the signal.

Like in the previous model, in the second example we observe that during the 10-minute record the envelope of the signal is similar at all OBH stations (figure 6.4.33). At OBS 305 the signal can be recognized mainly at the S3 horizontal component between 5 and 20 Hz. The high-amplitude spikes observed at around 150 s and 350 s are produced by electronic noise. In figure 6.4.34 the spectra of a 35-second slice of tremor indicated by an arrow in figure 6.4.33 is shown. Here, most of the energy of the signal is concentrated between 5 and 15 Hz as can be observed in all the OBH stations. However at OBS 305 3 the energy between 1 and 5 Hz masks the signal. Once this energy is filtered the signal frequency content is similar to that observed in OBH 305 (A and B spectra at figure 6.4.34).

6.4.3.10 Concluding Remarks and Future Work

Both examples presented in this report and others analyzed during the cruise match part of the characteristics of subduction related tremors reported in the literature: a common envelope at all stations and a frequency content that suggests a source effect rather than a propagation effect. As with the tremor-like events reported in the literature, most of the spectral energy is concentrated below 10 Hz. Although preliminary inspection suggests that these events are not the result of a teleseismic or regional signal, our results must be taken with caution. Additional, more rigorous processing will resolve some of these outstanding issues.

These signals are not only important because they may provide a link between different research fields, but because of a possible connection of this tremor activity with the occurrence of major earthquakes, as outlined by Obara (2003), and their coincidence with the so-called "slow earthquakes". In this connection, our results are encouraging and further investigation is needed.

Further analysis of the tremor signals must include a quantification of the semblance of the envelopes by cross-correlation estimates and delay estimations for location of the events. Time-frequency analysis (ex: pectrograms) could provide a more detailed description of the tremor and source evolution.

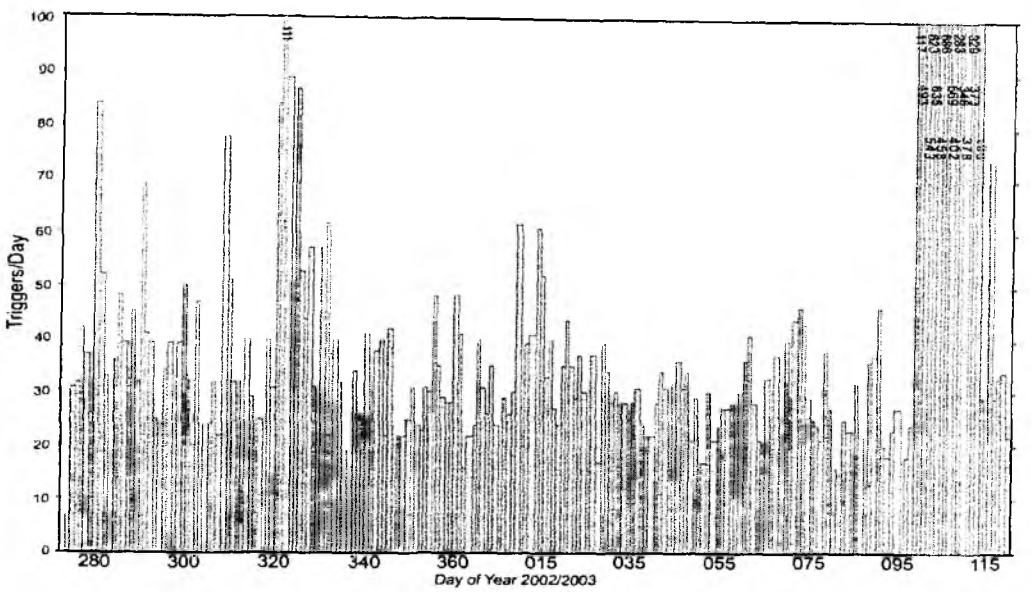

Fig. 6.4.22: *Trigger statistics of QUEPOS offshore network. The numbers of daily network triggers are shown in gray. From the first 10 days less than 7 % are bad triggers, all others are related to seismic activity. The peak on DOY 281 (Oct 8) is caused by a large earthquake and the associated aftershocks while the peak values around DOY 322 (Nov 18) and from DOY 99 to 113 (Apr 9-23) appear to correlate with microseismicity. Without taking into account DOY 99 to 113, the average number of triggers per day is 32.*

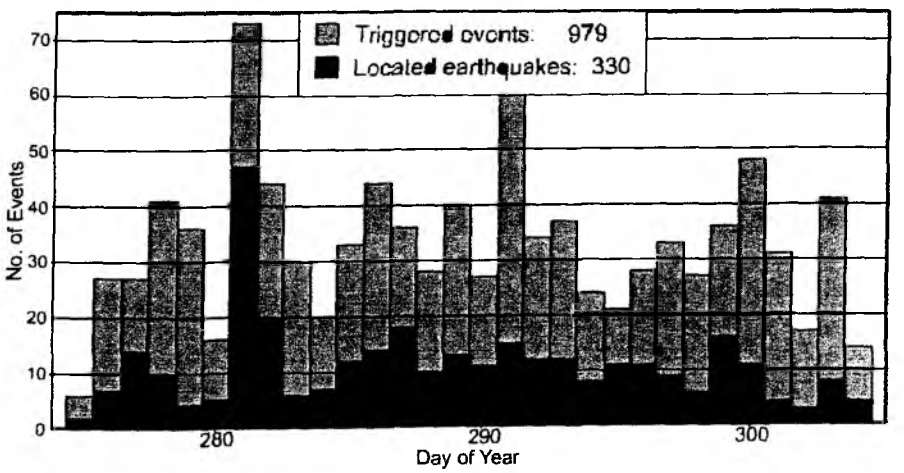

Fig. 6.4.23: *Daily number of triggered events (gray histrograms) and of located earthquakes (black) for october, 2002. The large number on DOY 281 (08.10.2002) is caused by a magnitude 4.8 earthquake and its aftershocks.*

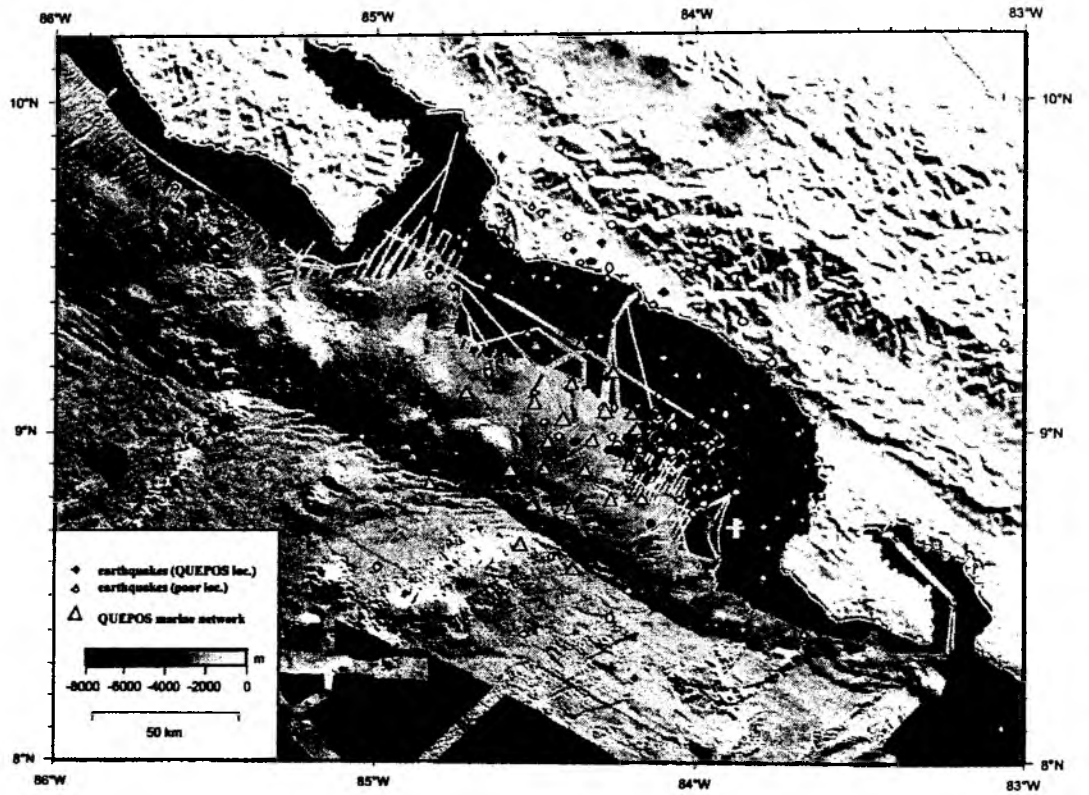

Fig. 6.4.24: Epicenters of 330 earthquakes from October 2002 located with the QUEPOS offshore network.

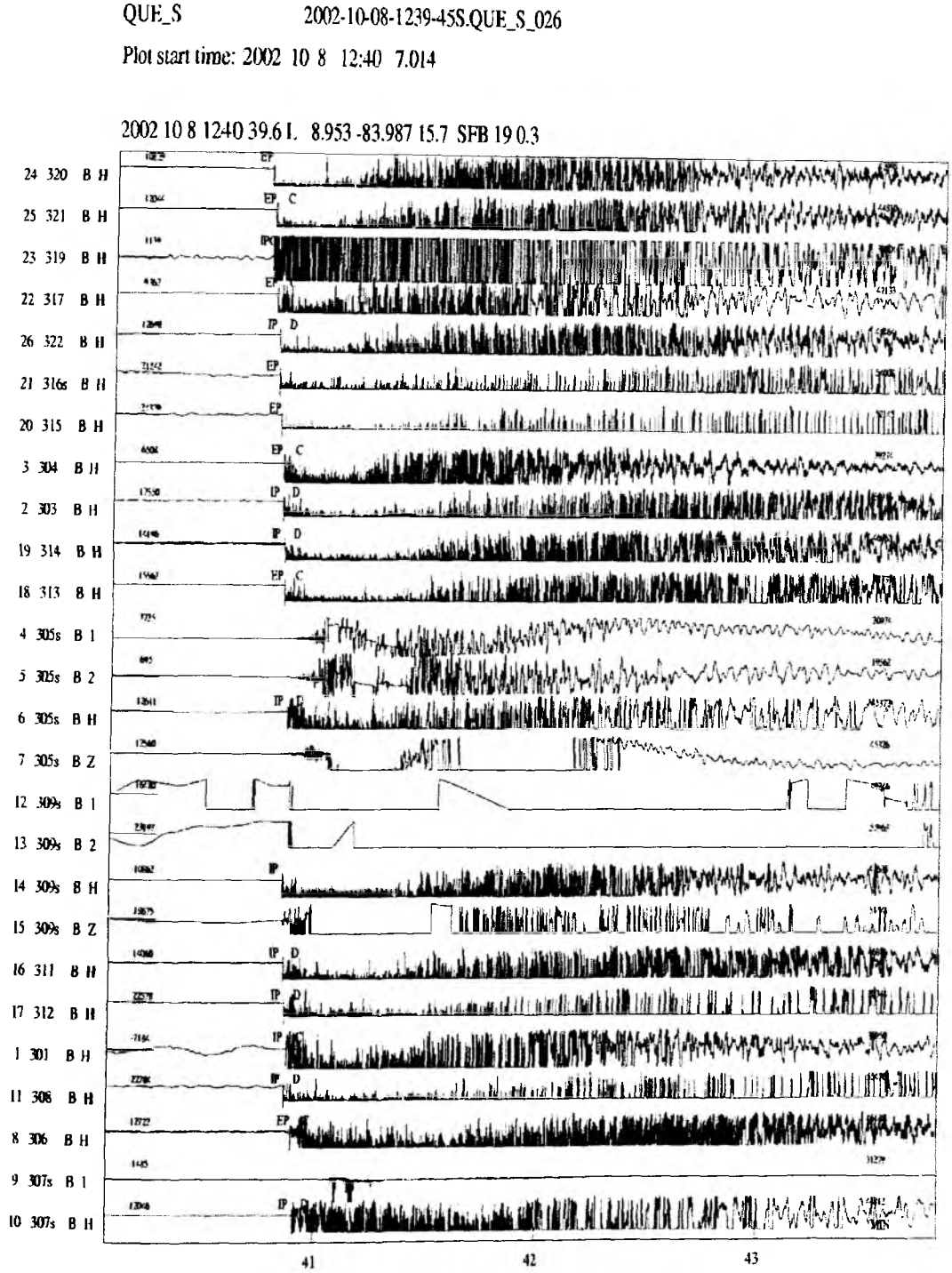

Fig. 6.4.25: *Magnitude 4.8 mainshock of a sequence of >77 earthquakes registered on Oct 8, 2002 12:40 with the QUEPOS network. All sensor components are clipped, so that only the first arrivals can be picked, which is often the case with strong earthquakes. The epicenter has been located at 8.953° N; 83.987° W with a focal depth of 15.7 km.*

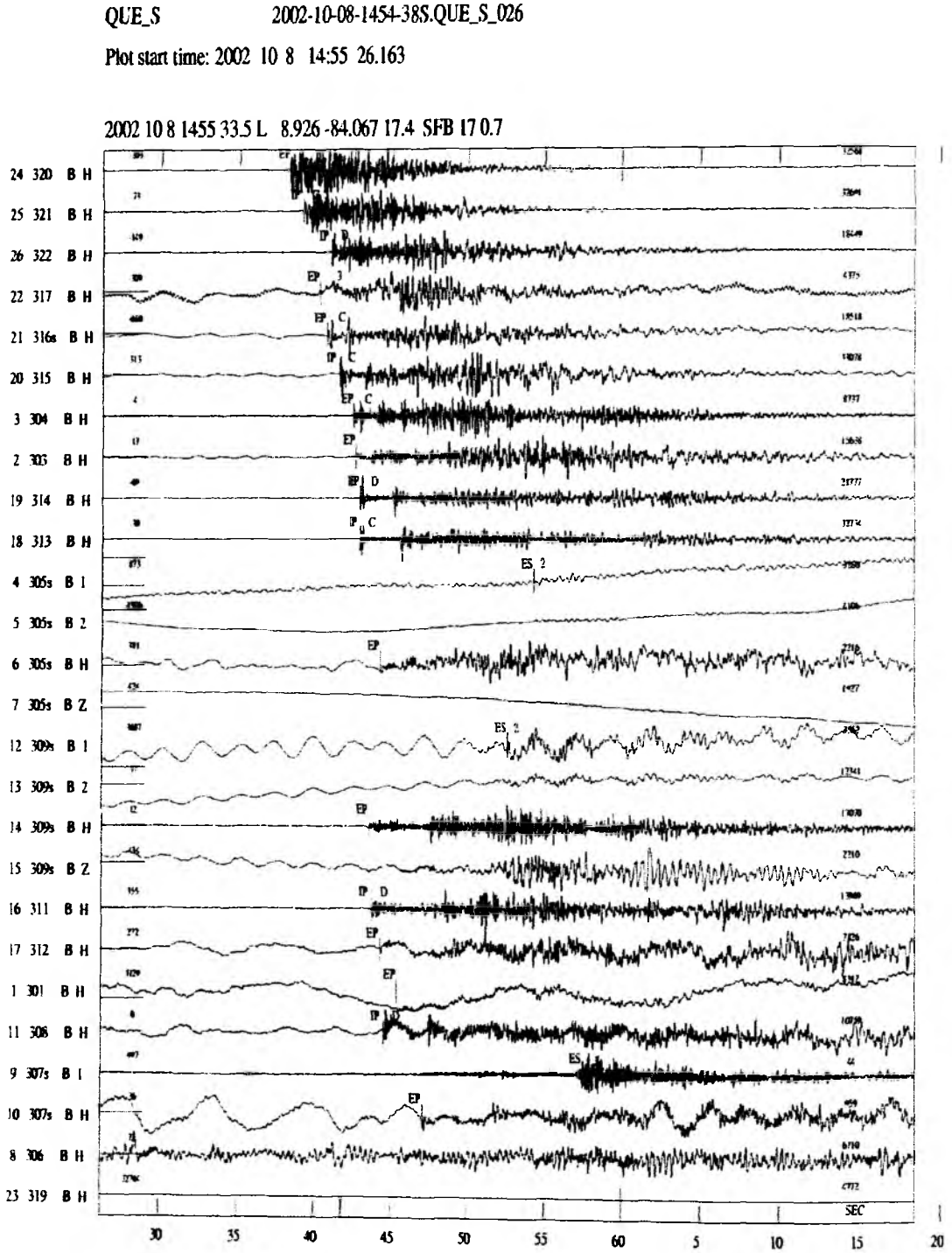

Fig. 6.4.26: Magnitude 3.3 aftershock of the previous earthquake from Oct 8, 2002 14:55, located at 8.926° N; 84.067° W at 17.4 km depth. Components have been clipped only at the closest station OBH320.

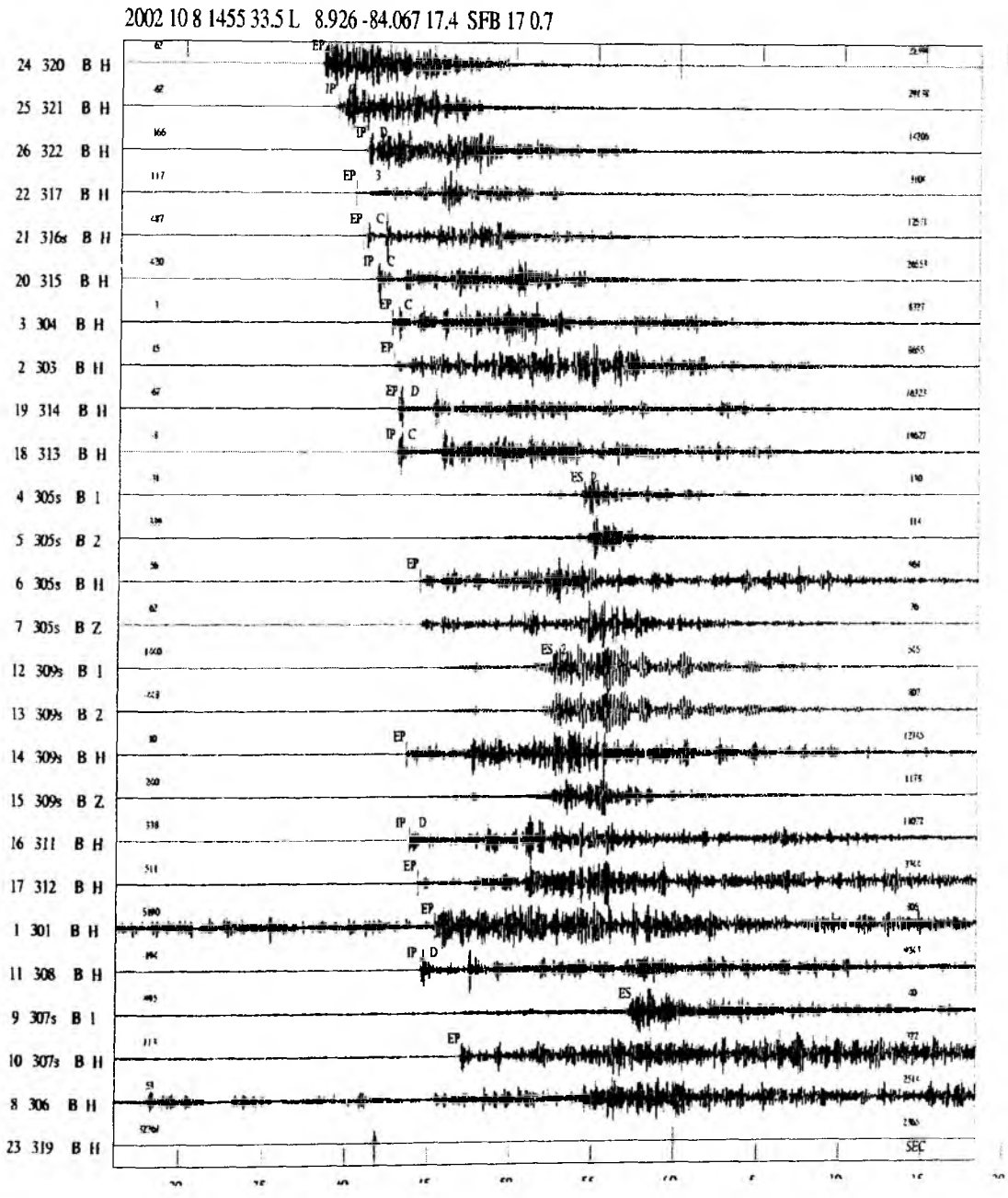

Fig. 6.4.27: *Same event as in Figure 6.4.26, but filtered by a 5-20 Hz band pass. Filtering strongly enhances the visibility of the S waves of OBS stations 305 and 309, as well as the P onsets of OBH301 and the pressure component of OBS307.*

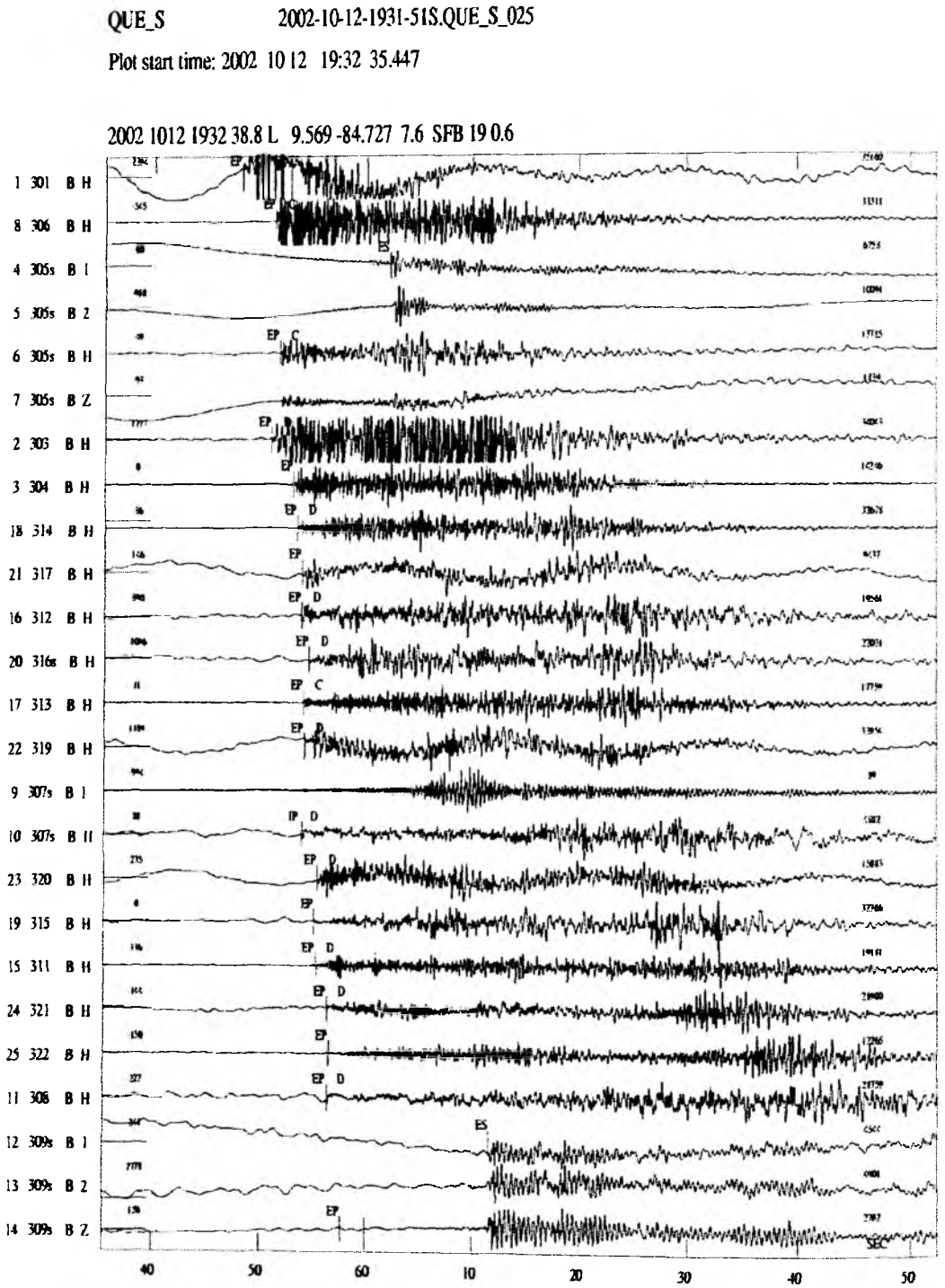

Fig. 6.4.28: Magnitude 3.6 earthquake from Oct 12, 2002 located beneath to the coastline at 9.569° N; 84.727° W at 7.6 km depth. Clear S waves can be seen on the horizontal seismometer components.

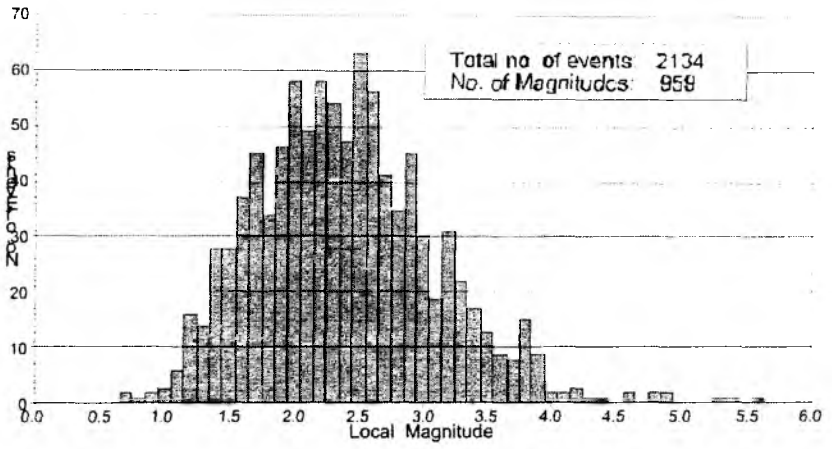

Fig. 6.4.29: *Local magnitude distribution of 959 earthquakes located with the JACO land network (April - June, 2002). The peak number of events is reached at magnitude 2.5.*

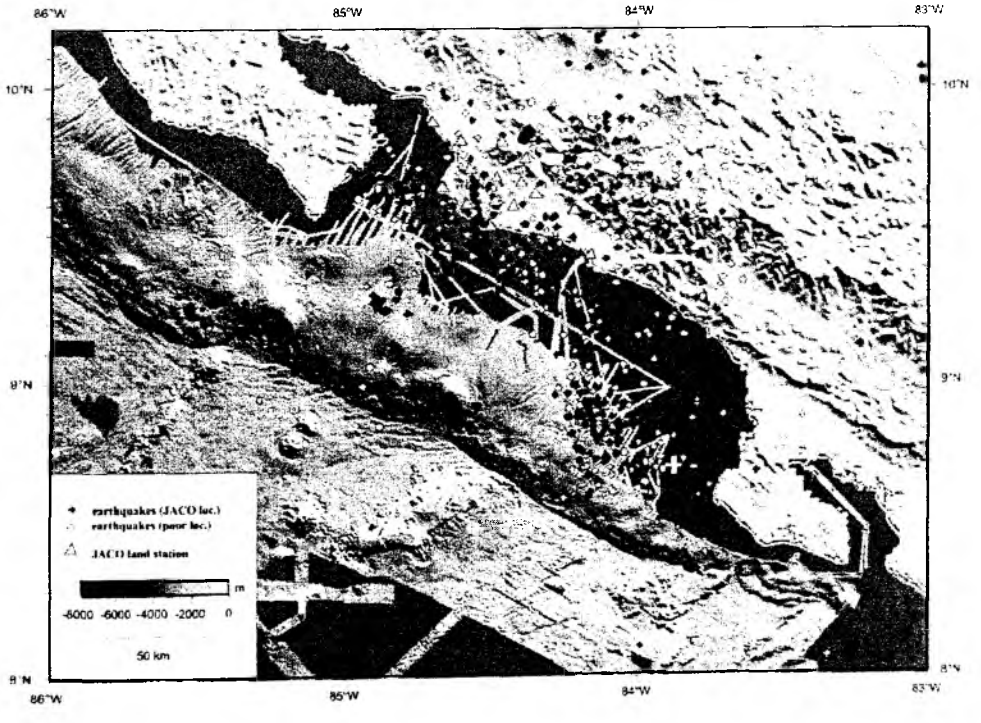

Fig. 6.4.30: *Earthquake epicenters located with the JACO land network from April to July 2002. The white cross marks the location of the mag. 6.4 earthquake of June 16, 2002 associated with many aftershocks. Interesting are the 15 events on Nicoya slide.*

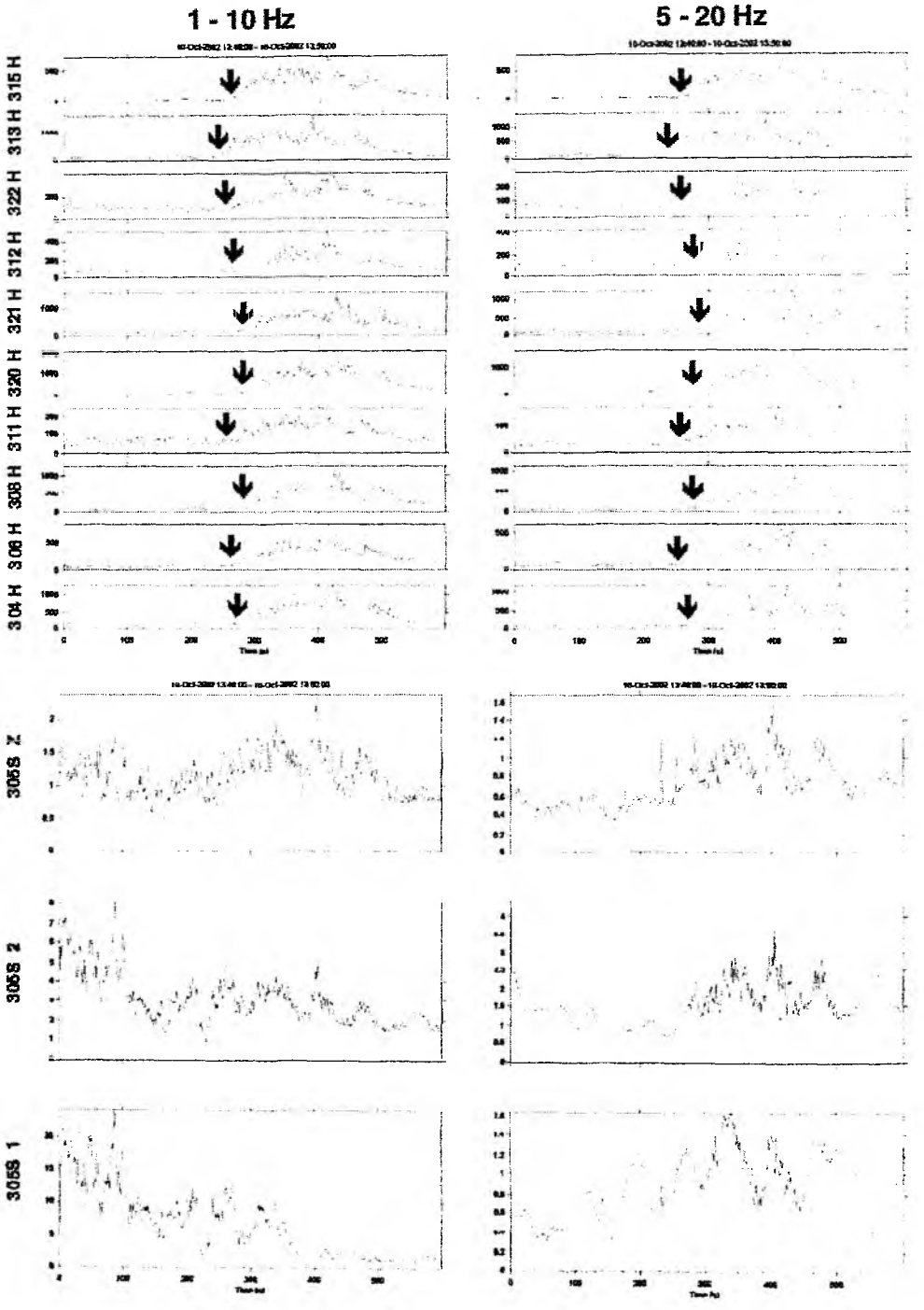

Fig. 6.4.31: Envelopes of a 10-minute record from 10 OBHs and one seismometer (3 channles, down) containing a possible tremor signal between 250 and 600 seconds. Input signals were filtered at two frequency bands: 1 - 10 Hz (left column) and 5 - 20 Hz (right column). The envelopes were smoothed using a 2-s wide moving average filter. The arrows point to the approximate onset of the signal.

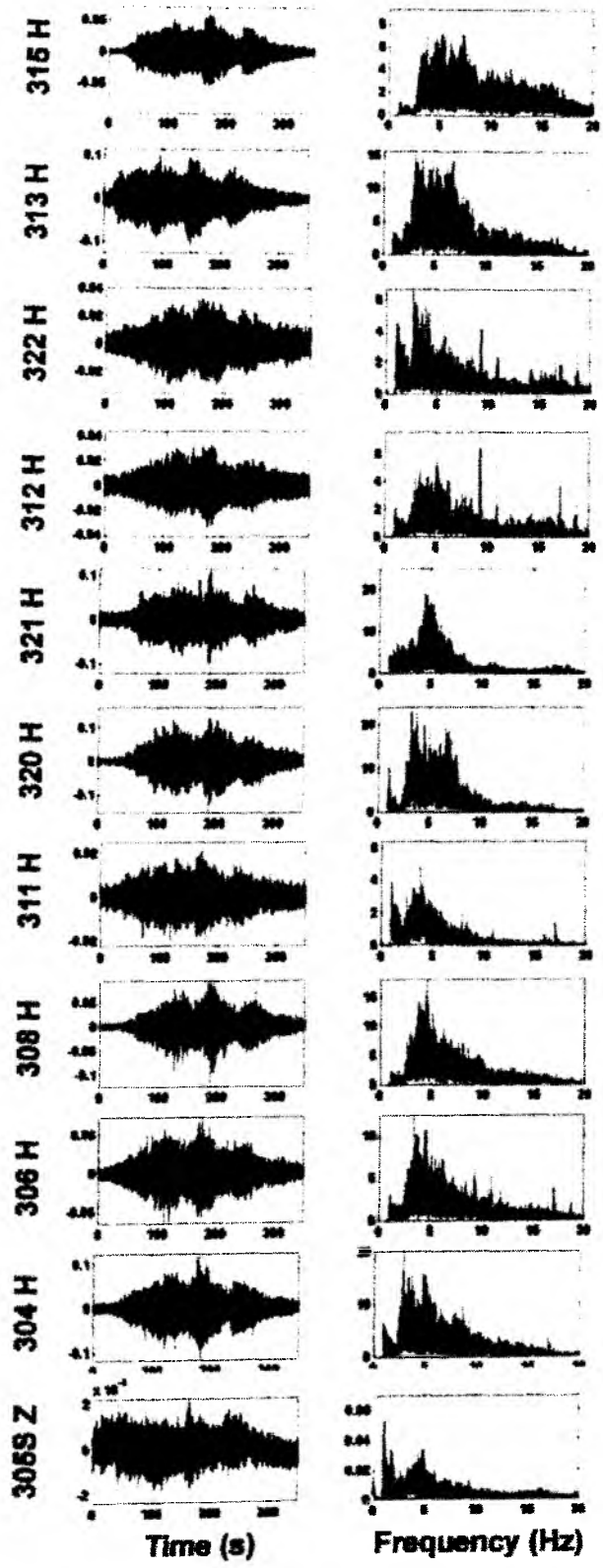

Fig. 6.4.32: Waveforms (left) and corresponding spectra (right) of the tremor signal between 250 and 600 seconds shown in figure 6.4.31. Most of the energy is concentrated between 2 and 5 Hz.

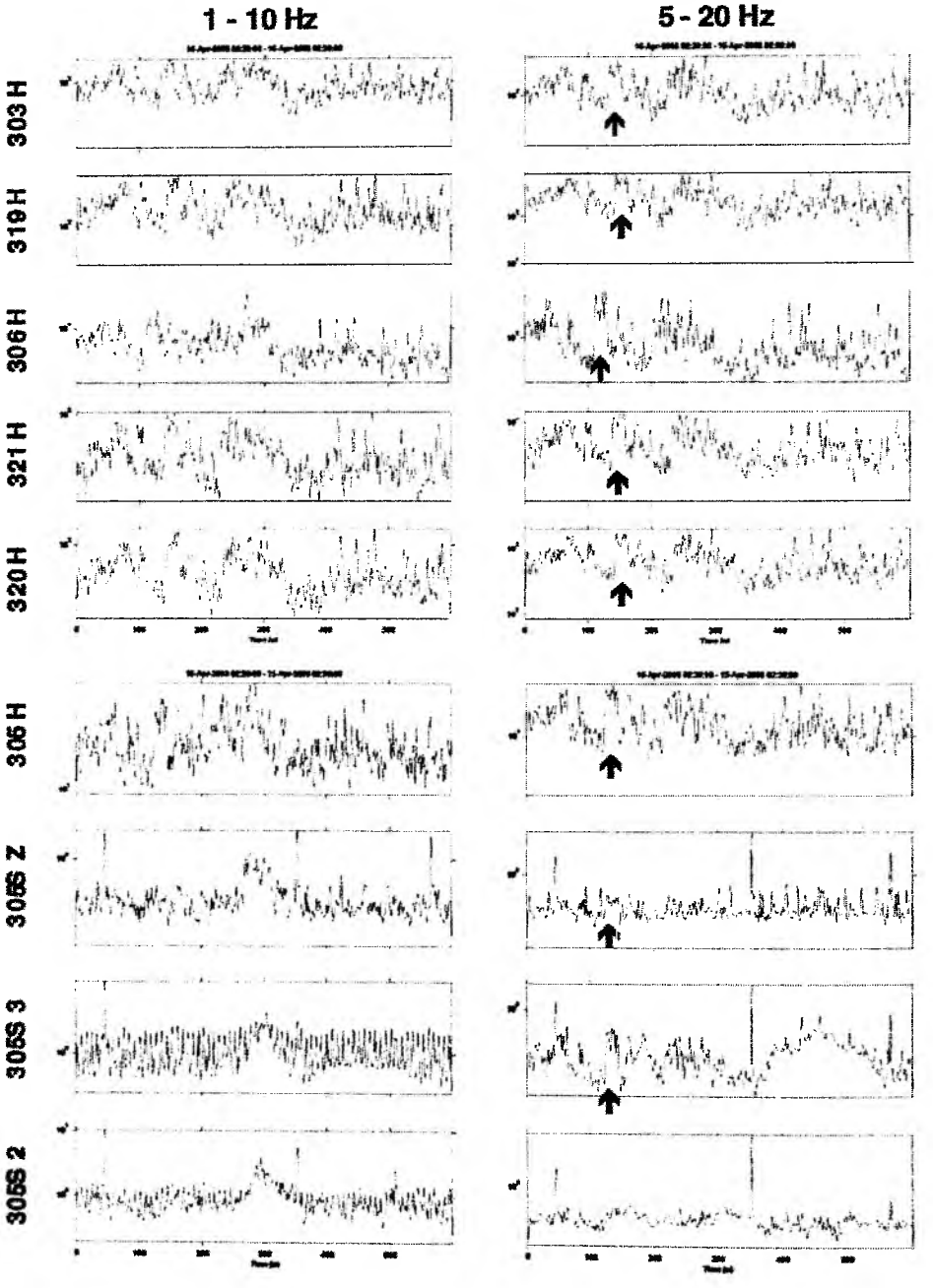

Fig. 6.4.33: Idem figure 6.4.31 for a 10-minute long tremor signal.

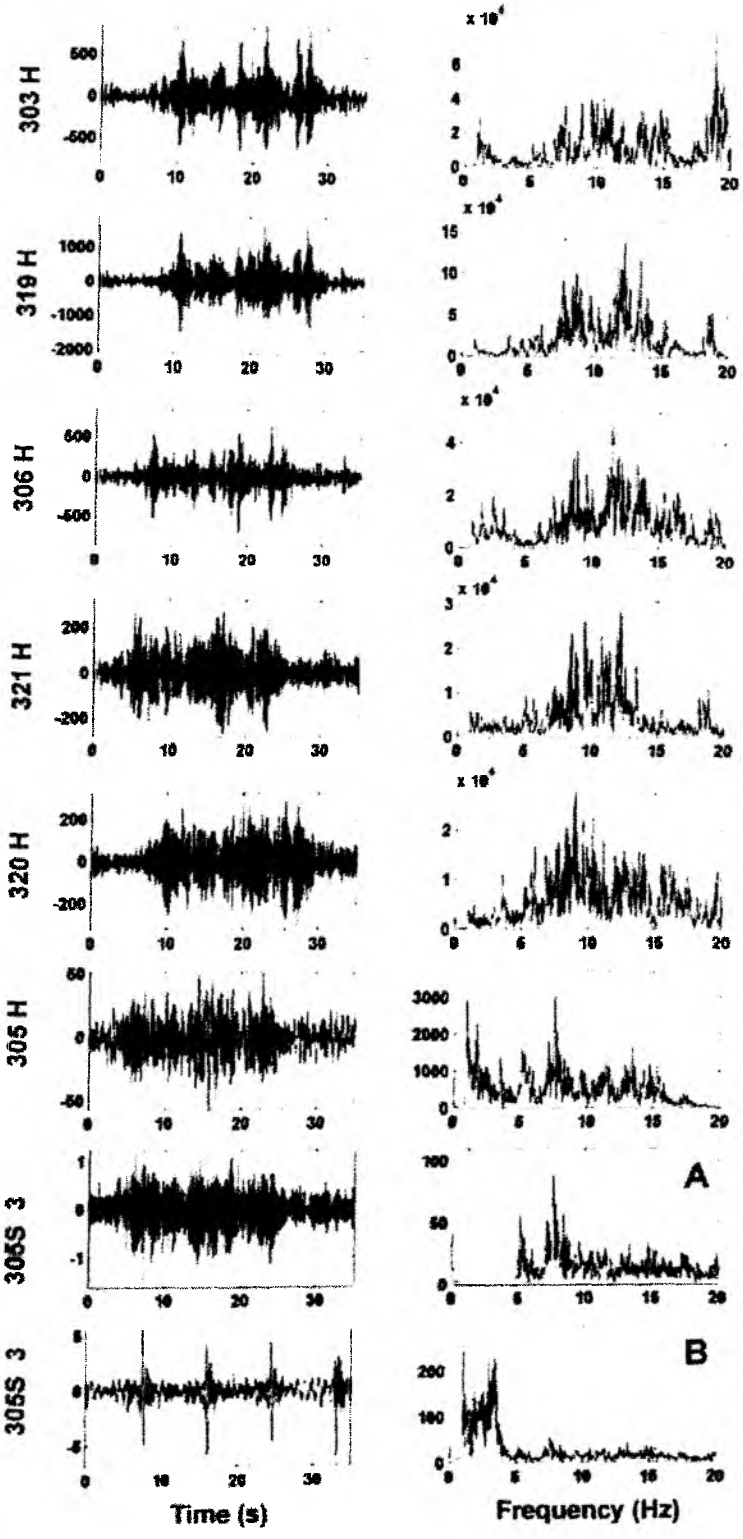

Fig. 6.4.34: Waveforms (left) and corresponding spectra (right) of a 35-s slice of tremor signal marked by black arrows in figure 6.4.33. Records were filtered between 5 and 20 Hz. In the case of the OBS 305 3 the signal was filtered at two frequency bands: (A) 5 and 20 Hz and (B) 1 and 5 Hz. Notice the energy content below 5 Hz which masks the tremor signal.

6.4.4 Oceanic Crust I

E. Flueh, D. Klaeschen, C. Papenberg, P. Sak

The objective of this experiment is to test the hypothesis that the subducting Cocos plate is serpentinized. Profile 302, shot across the MAT, was designed to test if the recorded mantle velocities are consistent with the presence of serpentinite. The recognition of low mantle velocities (<~ 7.9 km s-1) would be consistent with a serpeninized zone within the upper mantle.

Twelve instruments (OBH 1 to OBH 12) were deployed at a 2 nm spacing on July 14 along profile 302 to record an active seismic source (Figure 6.4.35). The source, two 32-l Bolt guns shot at a 60-s interval 8 m below the sea surface, yielded a ~100 m shot spacing. Instrumentation and profile details are presented in appendices C. At many of the instruments, a 1.7 liter GI gun was shot while the ship triangulated around the instrument in order to precisely orient the instrument. Some data examples are shown in Appendix B, figures B-1 to B-8.

All twelve instruments were recovered on July 15. The hydrophone of OBH 03 did not work correctly and the recording device of OBH 8 was a new prototype that we were unable to download while at sea. Consequently, only picks from the remaining 10 stations are available to constrain the shipboard seismic interpretation and velocity modeling.

A migrated section is used to constrain the gross geometry of the profile (Figure 6.4.36). In the migrated section, numerous steeply-dipping, small-scale, normal faults that displace the sedimentary package are resolvable. The apparent fault spacing density increases towards the trench where numerous shallow planar faults displace the sedimentary package. Several normal faults which penetrate to greater depth are recognized in the vicinity of the outer rise and appear to sole into the Moho. Several of the faults displace the seafloor demonstrating that they remain active. Across the trench, in the toe of the continental slope, fault orientations and apparent displacements change. In the upper plate, fault geometries are consistent with trench-vergent thrusting that juxtaposes upper slope sediments against sediments ponded in the trench axis.

General estimates of the velocity structure along profile 302 are constrained using MacRay 2.0 (Luetgert, 1992), an interactive conventional 2-D raytracing system. The models are developed using the interactive raytracing program and a trial and error approach. A layer-stripping strategy is applied to modeling from top to bottom, working towards the center of the profile from both ends. Layer thicknesses are further constrained by the preliminary analysis of the migrated section. Shipboard forward modeling suggests a thin (< 0.7 km) sedimentary veneer (1.6 – 1.7 km s^{-1}) underlain by ~ 5-km-thick oceanic plate with velocities ranging from ~ 4 km s-1 to 6.8 km s^{-1} (Figure 6.4.37). The best-fit shipboard model yields mantle velocities ranging from a minimum of 7.5 km s^{-1} at the Moho. The velocity structure indicated by the shipboard modeling efforts is then used to produce a new DMO stack and migrated section (Figure 6.4.38). The slow upper mantle velocities are consistent with a serpentinized zone.

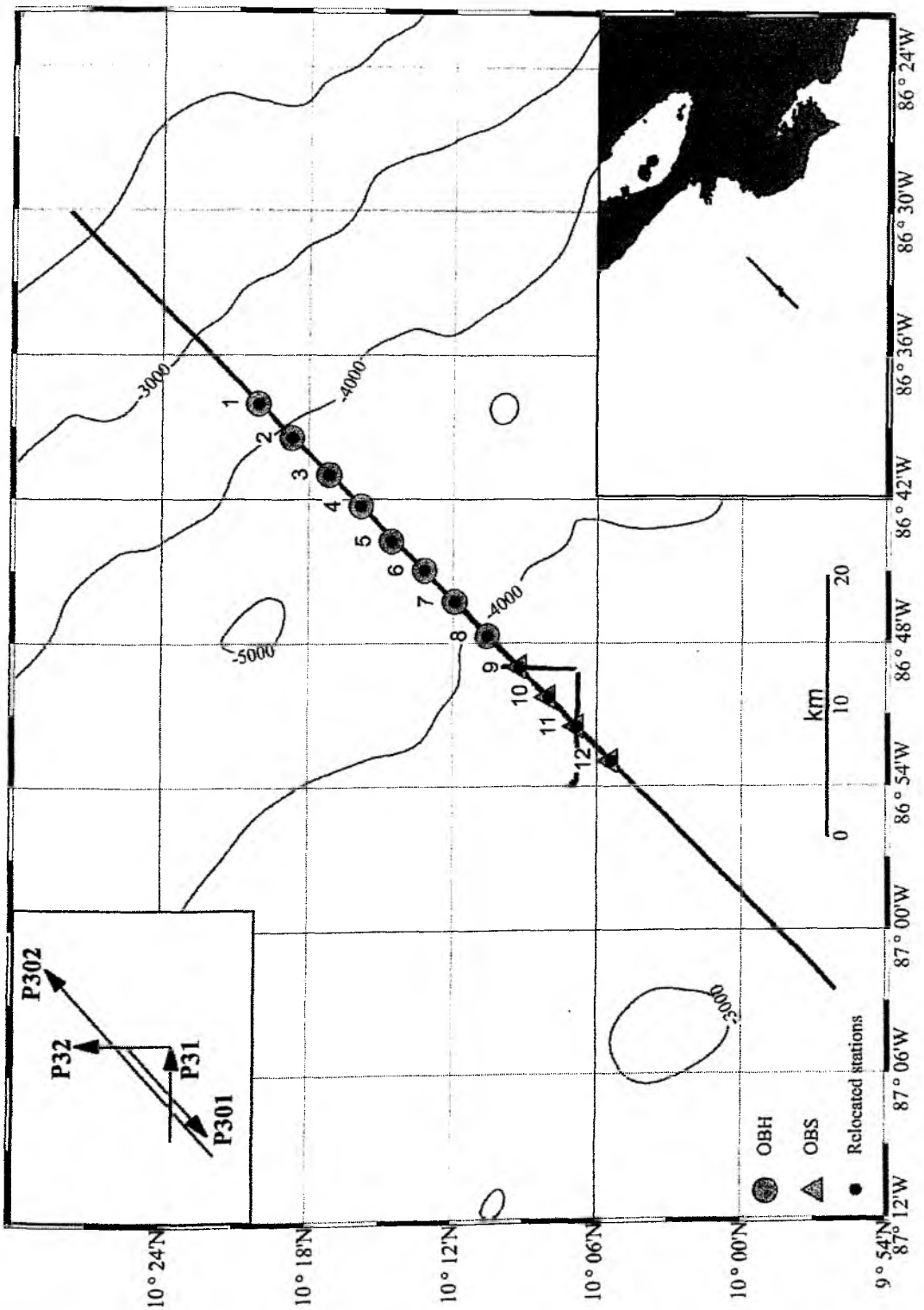

Fig. 6.4.35: Location of Profile 302 across the MAT.

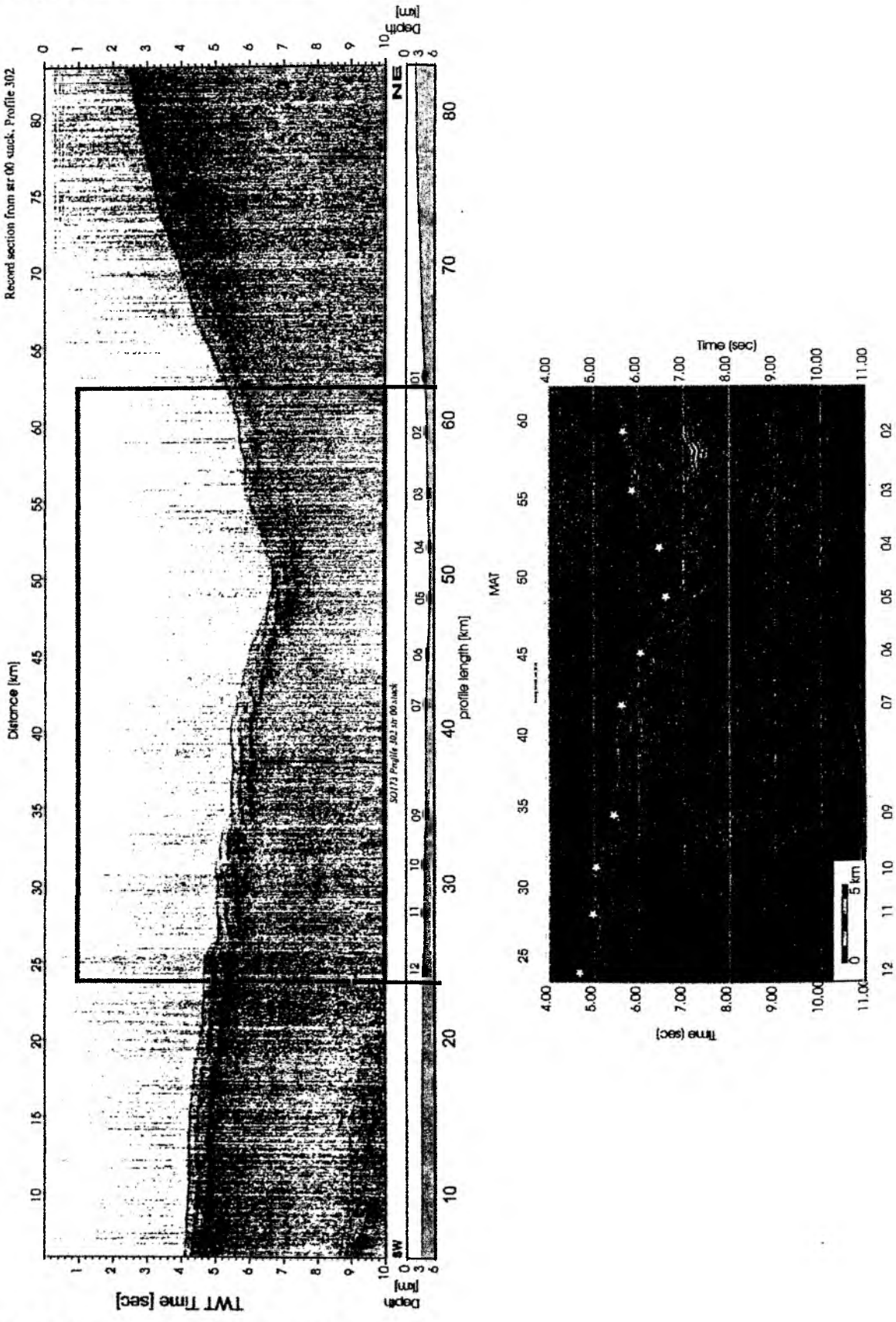

Fig. 6.4.36: Migrated section of profile 302.

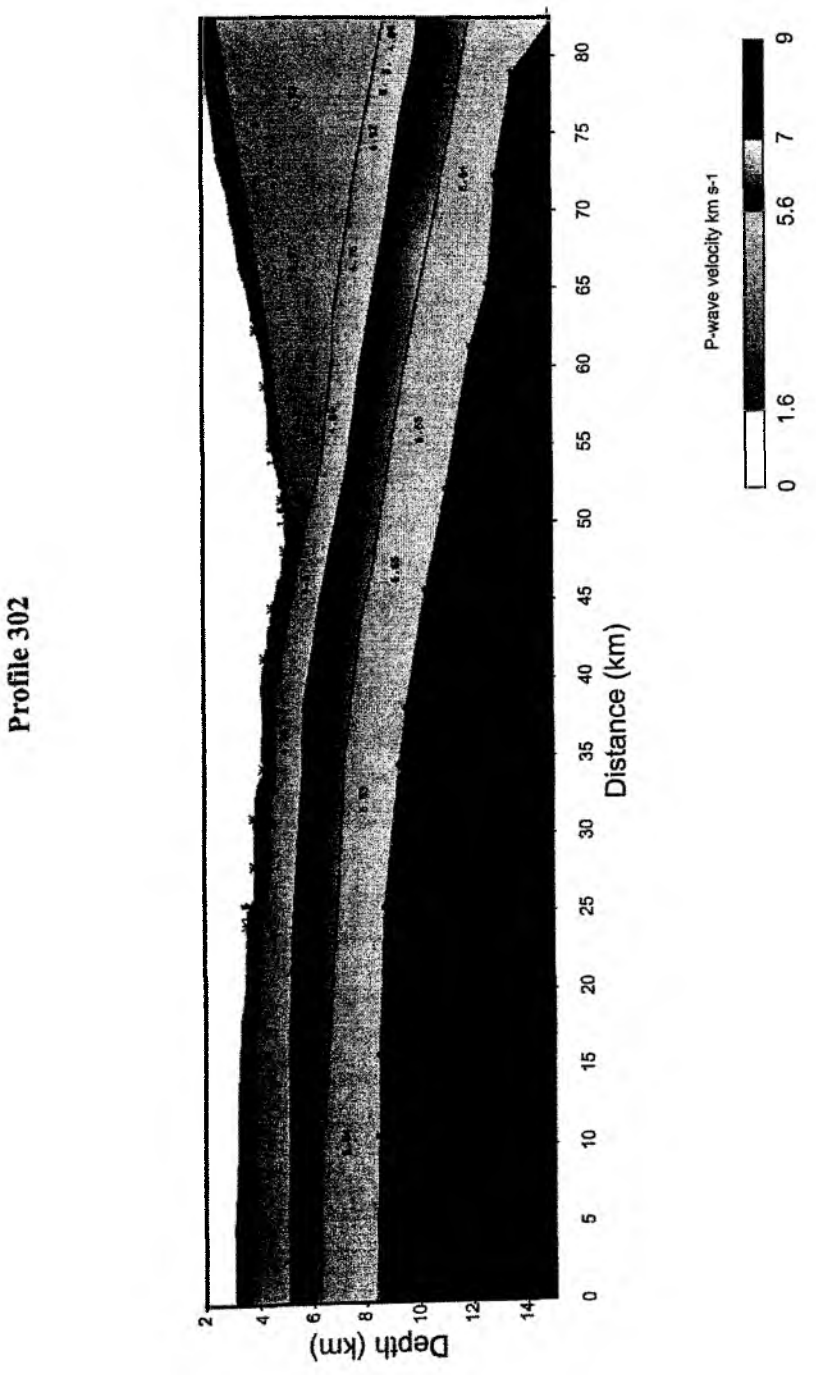

Fig. 6.4.37: Forward modelled velocitiy section of Profile 302.

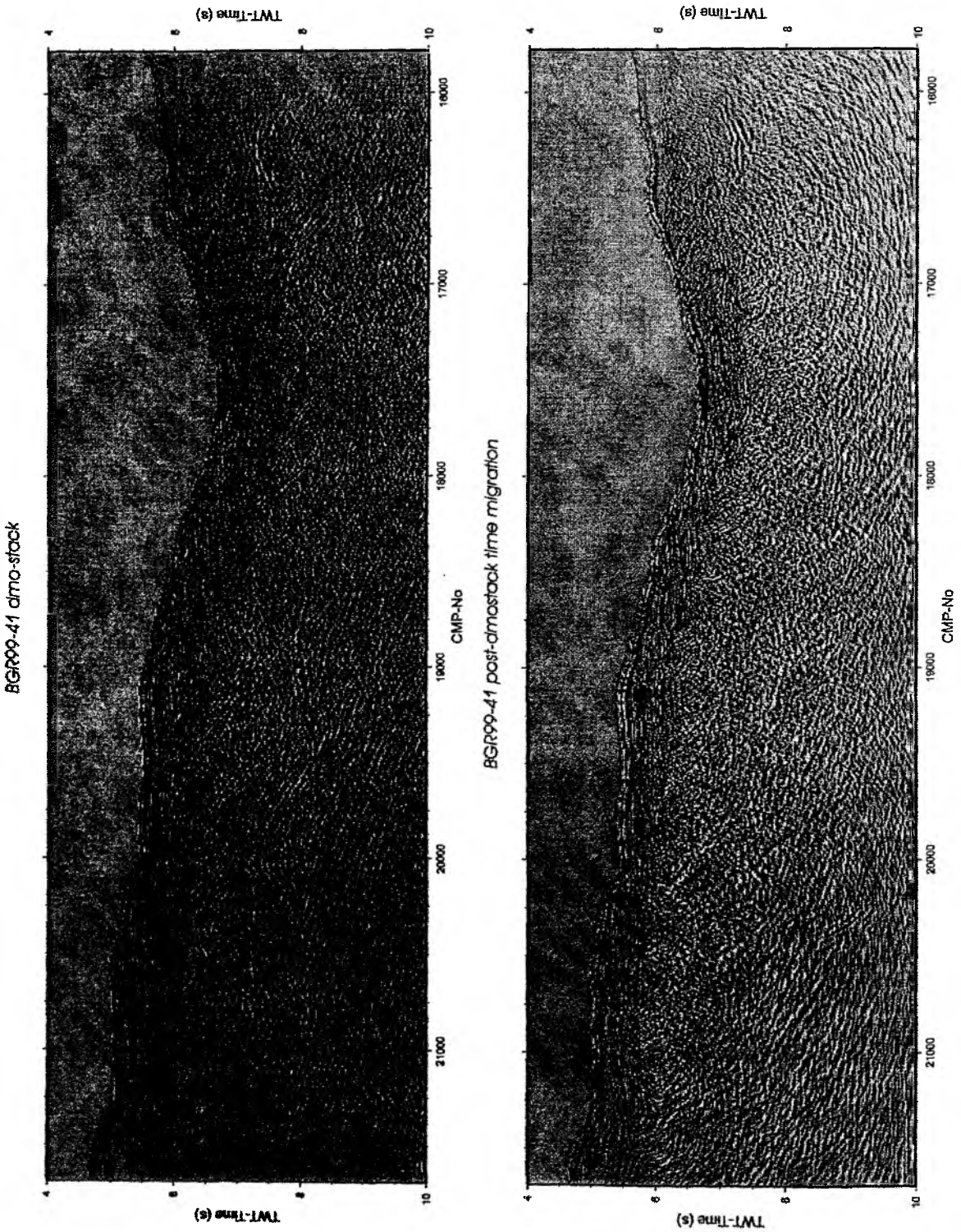

Fig. 6.4.38: dmo-stack and post-dmostack time migration.

6.4.5 The Décollement

M. Schnabel, E. Flueh, D. Klaeschen, C. Papenberg, N. Fekete

The main objectives pursued within the subproject A2 of the SFB 574 are to determine the key factors that lead to accretion or erosion at convergent margins. Coupling and mass-transfer between upper and lower plate are to be studied and seismic images of the resulting tectonic units will be provided. One target area is the décollement, which separates the upper and lower plate. We are especially interested in the lithological properties, which may be used to analyze and quantify the amount of sediment incorporated in the subduction channel and indicate potential locations of porosity changes and fluid losses.

The décollement zone plays an important role in the volatile budget of a subduction zone. It is the focus of mechanical compaction, which releases pore water. New volatile reservoirs are generated by alteration of sediments. Off Costa Rica, the décollement has in places a high reflectivity, which implies a massive dewatering within about 4 km of the deformation front (Shipley and Moore, 1986). In this zone, porosity decreases from perhaps 50% to 25%. Based on ODP Leg 170, Kimura et al. (1997) showed that the décollement reflection is a result of a very sharp boundary in physical properties, with higher porosities below than above, indicating marked mechanical decoupling. The plate boundary décollement off Costa Rica is structurally divisible into an upper brittle-fracture-dominated domain overlying a lower, ductile domain (Tobin et al., 2001).

As area of investigation we have chosen a part of the Central American Trench situated south of the Quepos Plateau. On the R/V SONNE Cruise SO 81, profile 5 showed one of the strongest reflections of the décollement in this region (Hinz et al., 1996). During SUBDUCTION I (SO 163), we collected new seismic wide-angle data along this line. Additionally, we measured two dip profiles. We found out that the reflection strength of the décollement varies considerably both across strike but even more pronounced along strike. To further investigate this along strike variability, we decided to conduct an additionally seismic survey with ocean bottom receivers at a very dense spacing.

On July 17, we deployed 8 OBH and 4 OBS at a spacing of 0.1 nm on average. First, we used the Bolt airgun to acquire a profile (P33) across this array, shooting one Bolt gun every 30 sec. Afterwards, several profiles (P34 to P36 along strike, P37 and P38 perpendicular to the trench) were acquired using the GI-gun, fired at 7-sec intervals. All instruments were recovered on July 19.

10 stations had proper recordings of the airgun shots. Concerning the GI gun shots, the amplitudes of the direct arrivals are not clipped and we can use this information for further processing. 3-D relocalization showed that the stations did not drift more than 50 m off the profile (figure 6.4.39, upper right).

Figure 6.4.40 shows the surface streamer recording of profile 33. The décollement (at 4.2 sec TWT) is quite well imaged below the OBH positions. Due to the signal strength of the Bolt gun we can also see deep faults in the oceanic crust (at 6 sec TWT). One example for a Bolt gun recording at the ocean bottom is shown in figure 6.4.41. Refracted waves within the sedimentary wedge as well as in the subducted oceanic crust can be identified. The following figure (6.4.42) is an example for a recording of the GI-gun. The data show a sharp reflection from the décollement (at 800 ms zero-offset-TWT behind the direct wave).

The result of a preliminary velocity modelling is shown in figure 6.4.43. We used the real bathymetry of the seafloor, but the other layers are assumed to be horizontal. As sound velocity in water, we used 1494 m/s. This value was obtained by a previous CTD on SO 163 in this area. Within the sedimentary wedge,

we obtained velocities from 1730 m/s at the seafloor to 1900 m/s at the bottom of this layer. For the thin layer of subducted oceanic sediment, we used a velocity of 1680 m/s. This corresponds to a layer thickness of about 220 m. However, the sensitivity is limited. The reflection of the top of the oceanic crust can also be fitted with vp=1850 m/s within a 240-m-thick sedimentary layer. These values will be refined during the AVA analysis, because the reflection amplitude of wide angles (greater than 30 degrees) relate only relates to the contrast in v_p (Shuey, 1985). The P_g phases indicate velocities of 4500 m/s at the top of the oceanic crust. Additional data examples are given in Appendix B, figures B-9 to B-23.

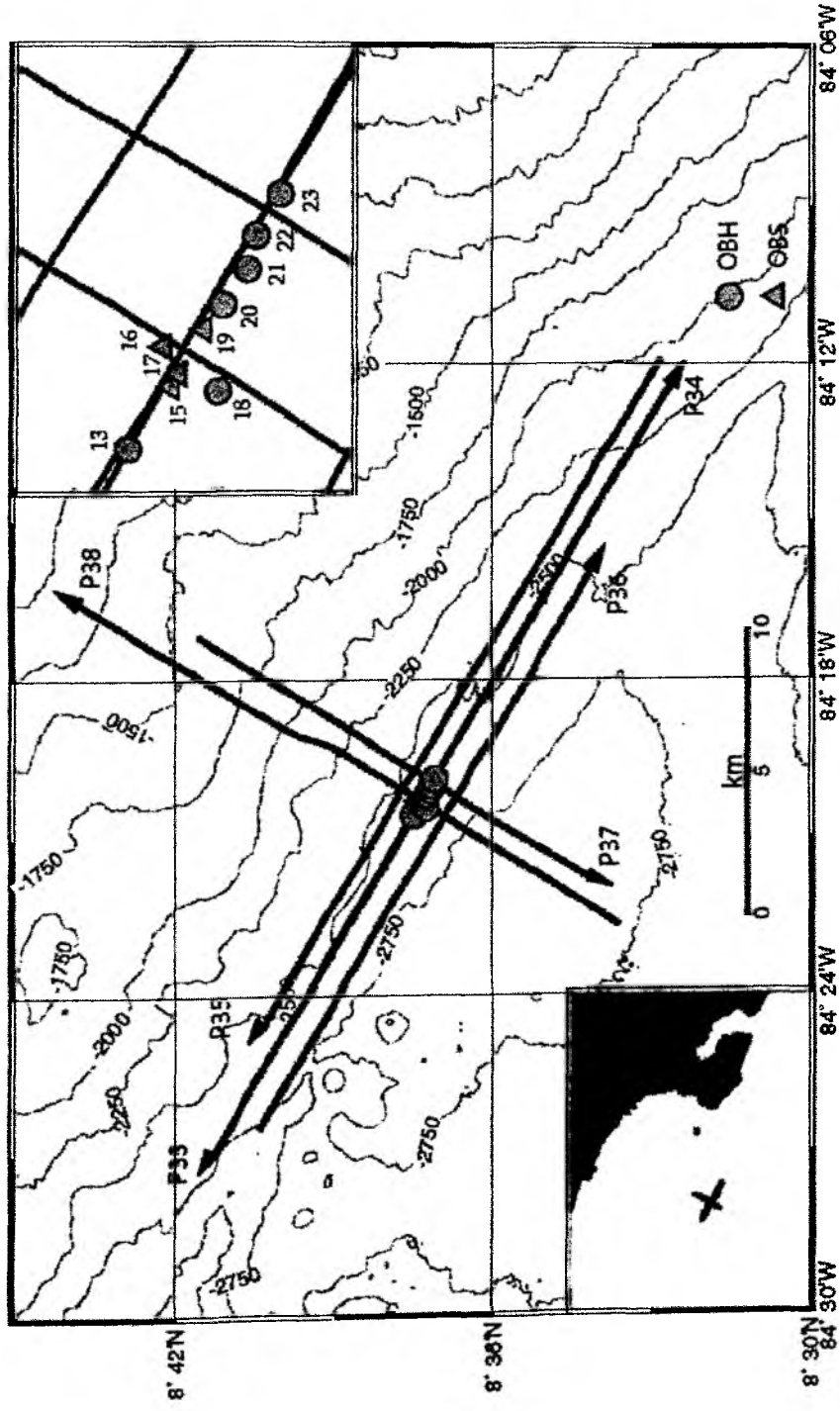

Fig. 6.4.39: Location map of profile 33 (Boltgun) and 34 - 38 (GI gun).

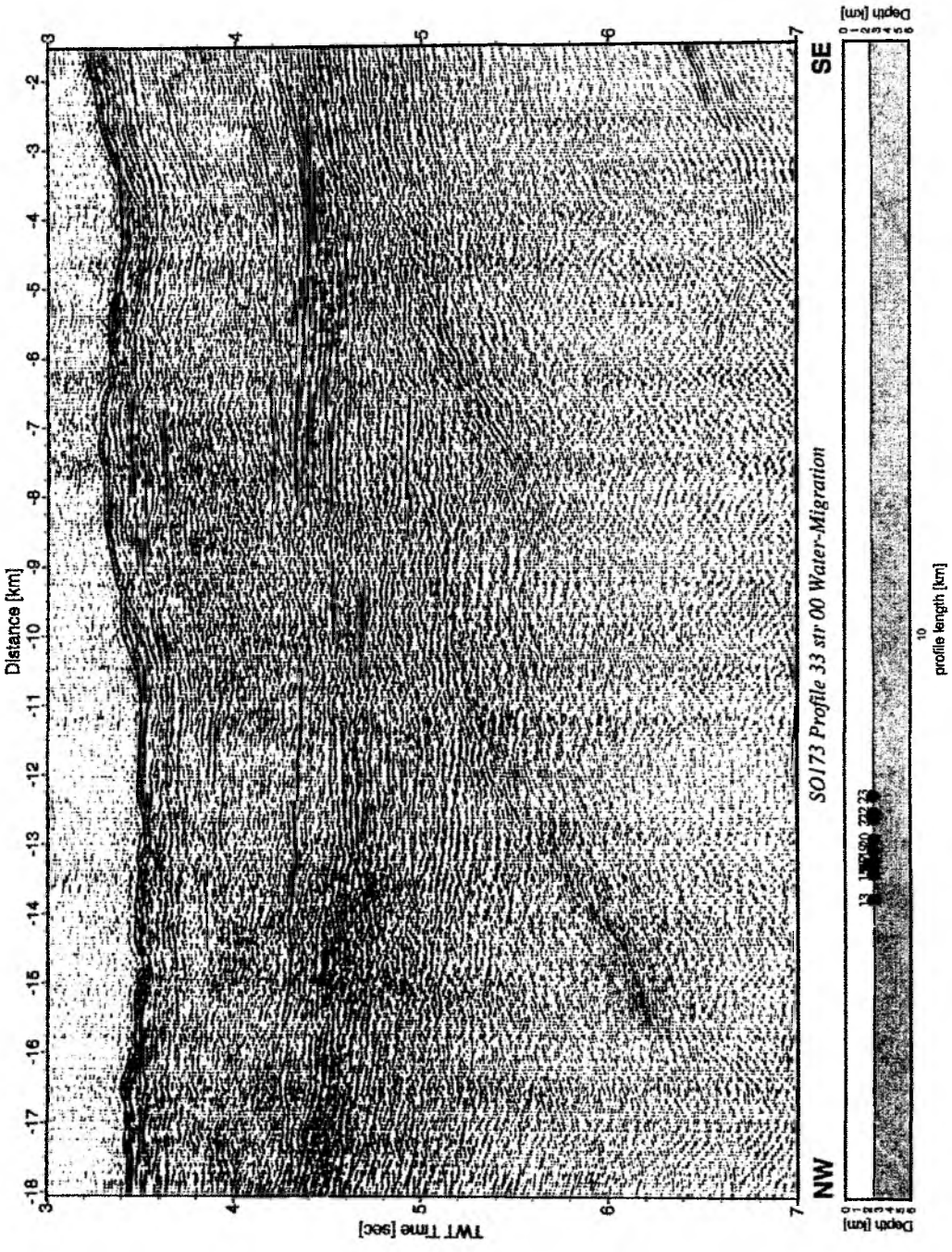

Fig. 6.4.40: Record section from str 00 Water- Migration Profile 33.

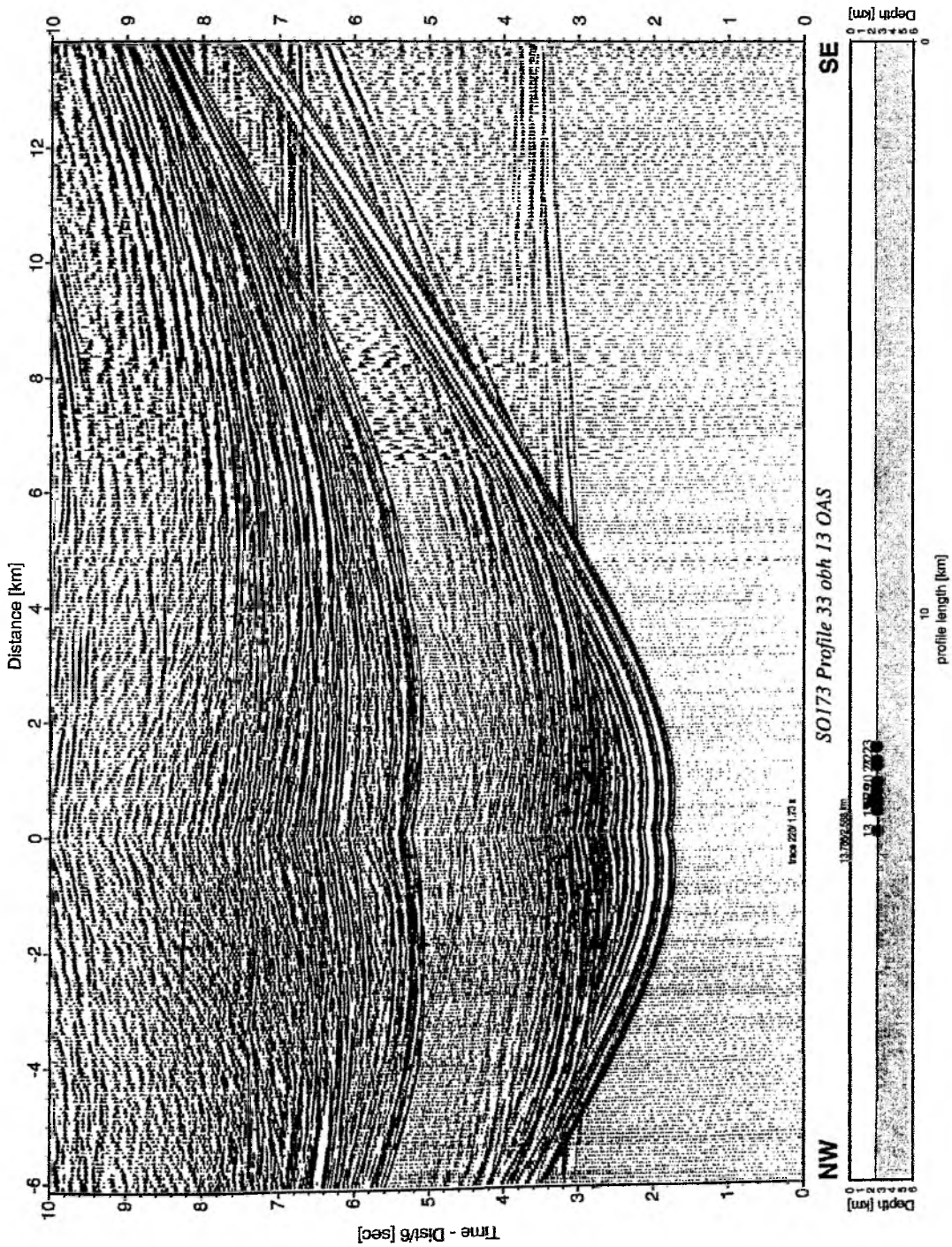

Fig. 6.4.41: Record section from OBH 13 OAS Profile 33.

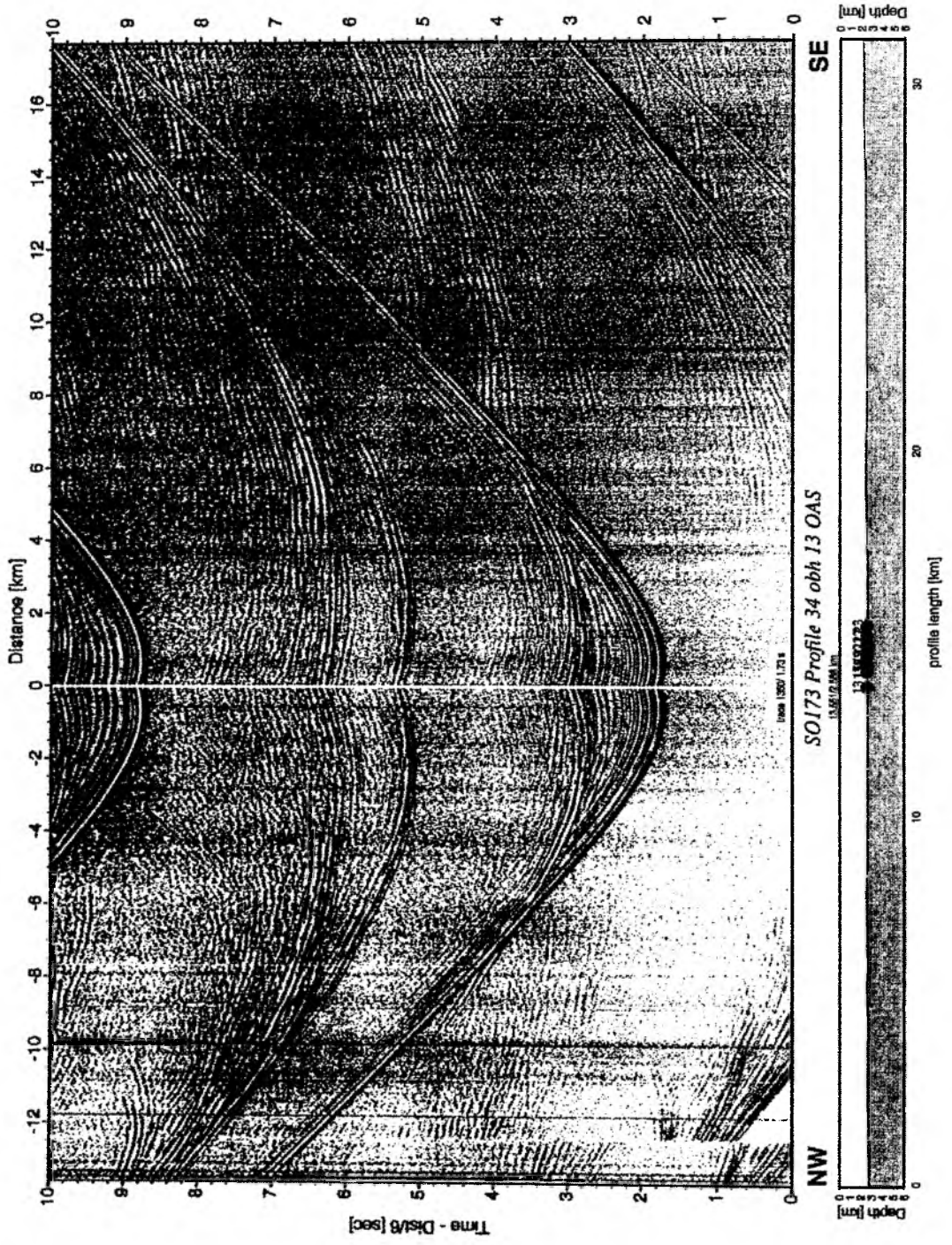

Fig. 6.4.42: Record section from OBH 13 OAS Profile 34.

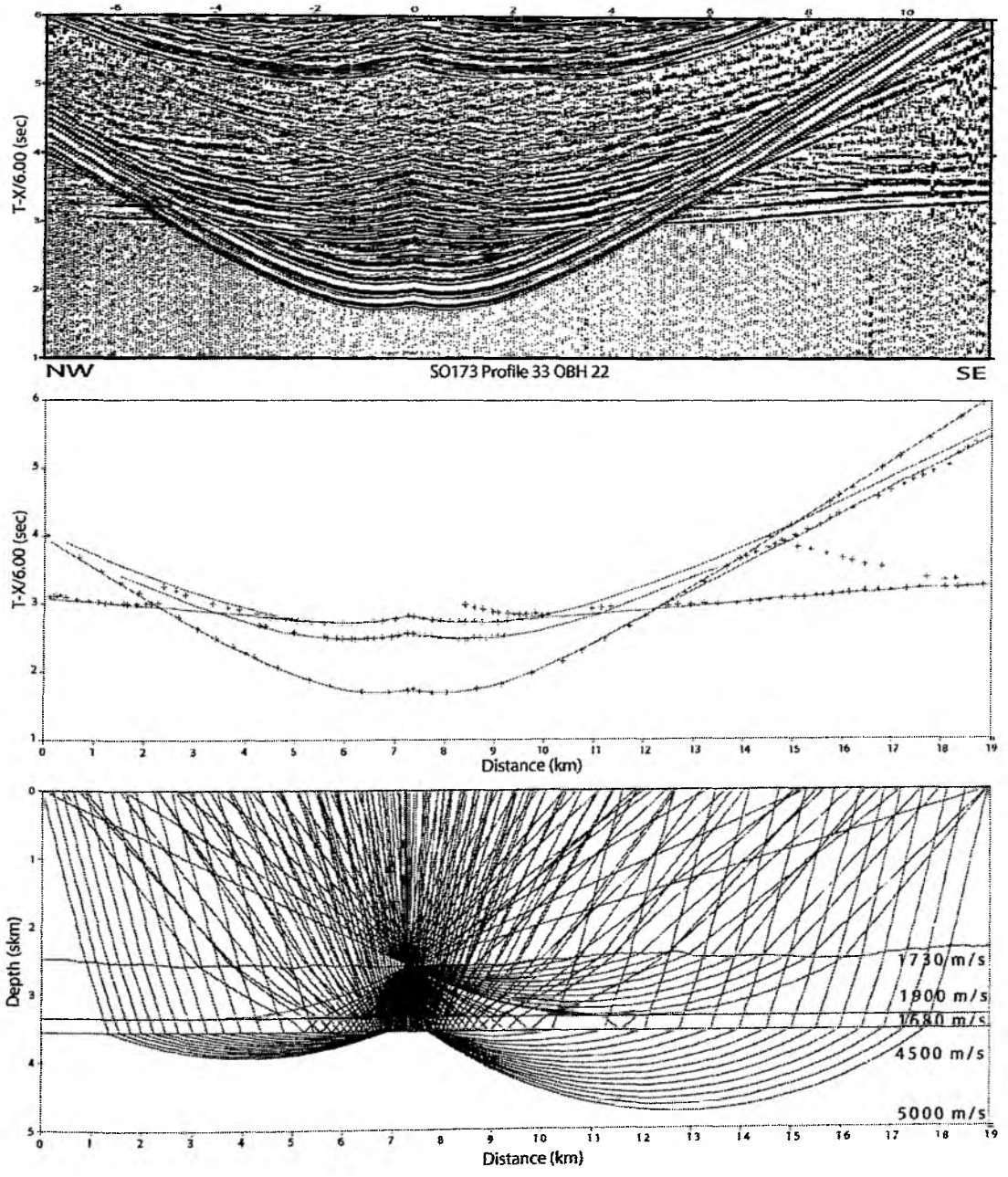

Fig. 6.4.43: *Top: seismic data, recorded at OBH22. Middle: Observed (crosses) and calculated (lines) travel times. Bottom: seismic rays in the earth model.*

6.4.6 Mound 11 and 12

The aim of these seismic profiles was to map velocity variations near the seafloor related to the mounds detected here in earlier years. Eight OBH/S were deployed on July 17th at a spacing of 0.1 nm on average. Since we encountered problems with the deep tow streamer, only one seismic line was shot across the array using the GI-Gun.

A location map of the profile is shown in Figure 6.4.44. An example of data from the streamer and the OBH/S is shown in Figures 6.4.45 and 6.4.46. More examples are given in Appendix B, figures B-24 to B-27.

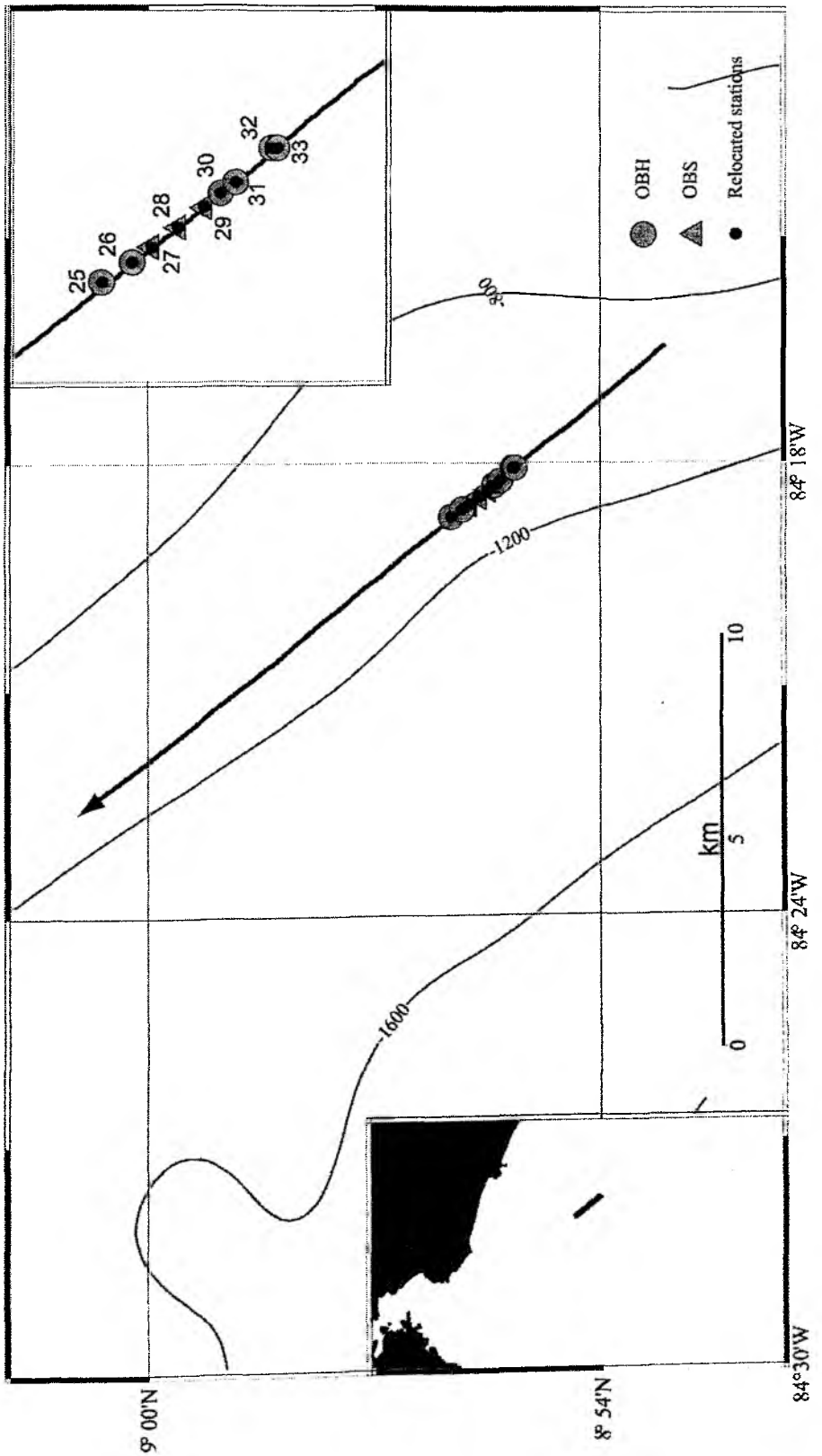

Fig. 6.4.44: Location map of profile 40 (GI-gun).

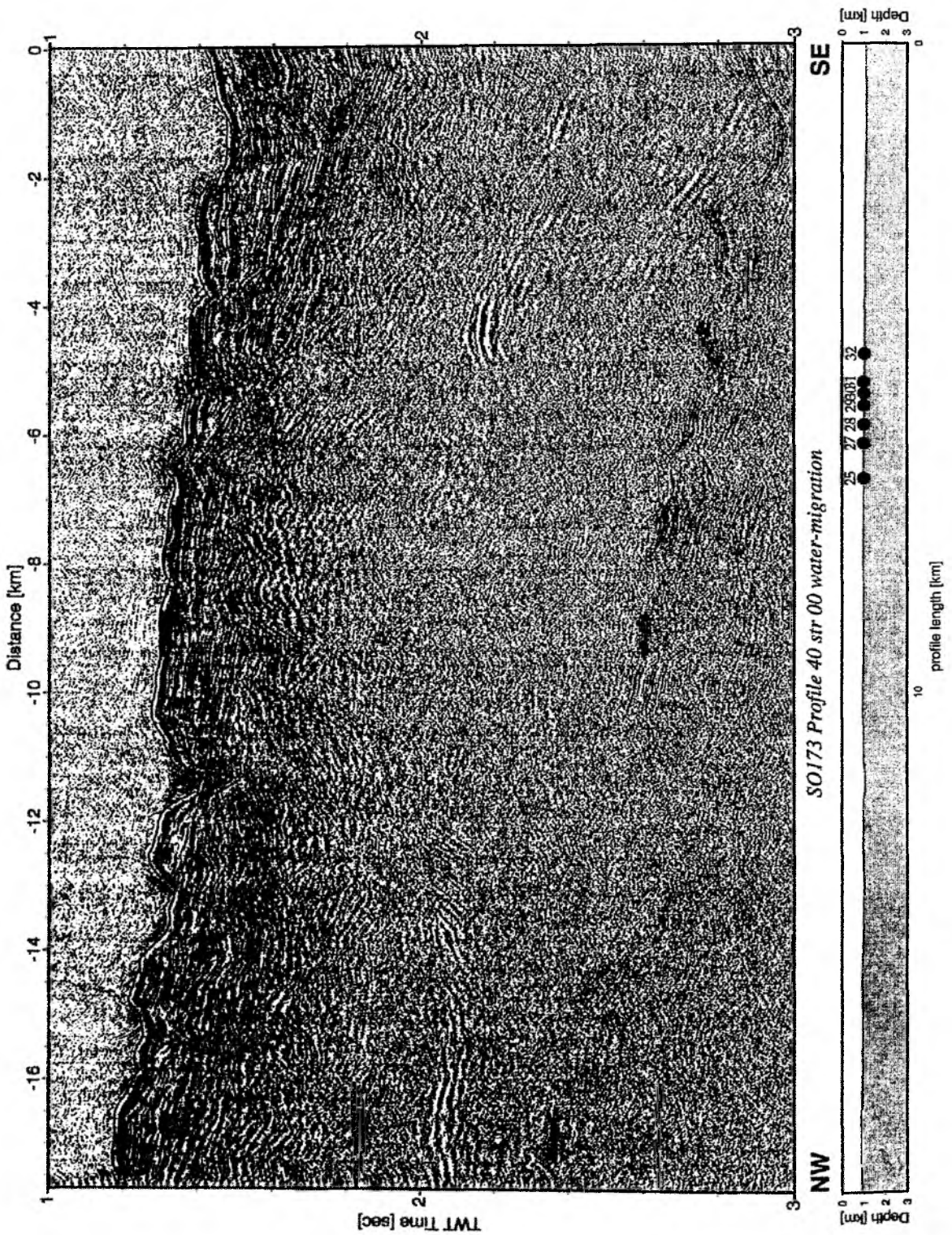

Fig. 6.4.45: Record section from str 00 water-migration Profile 40.

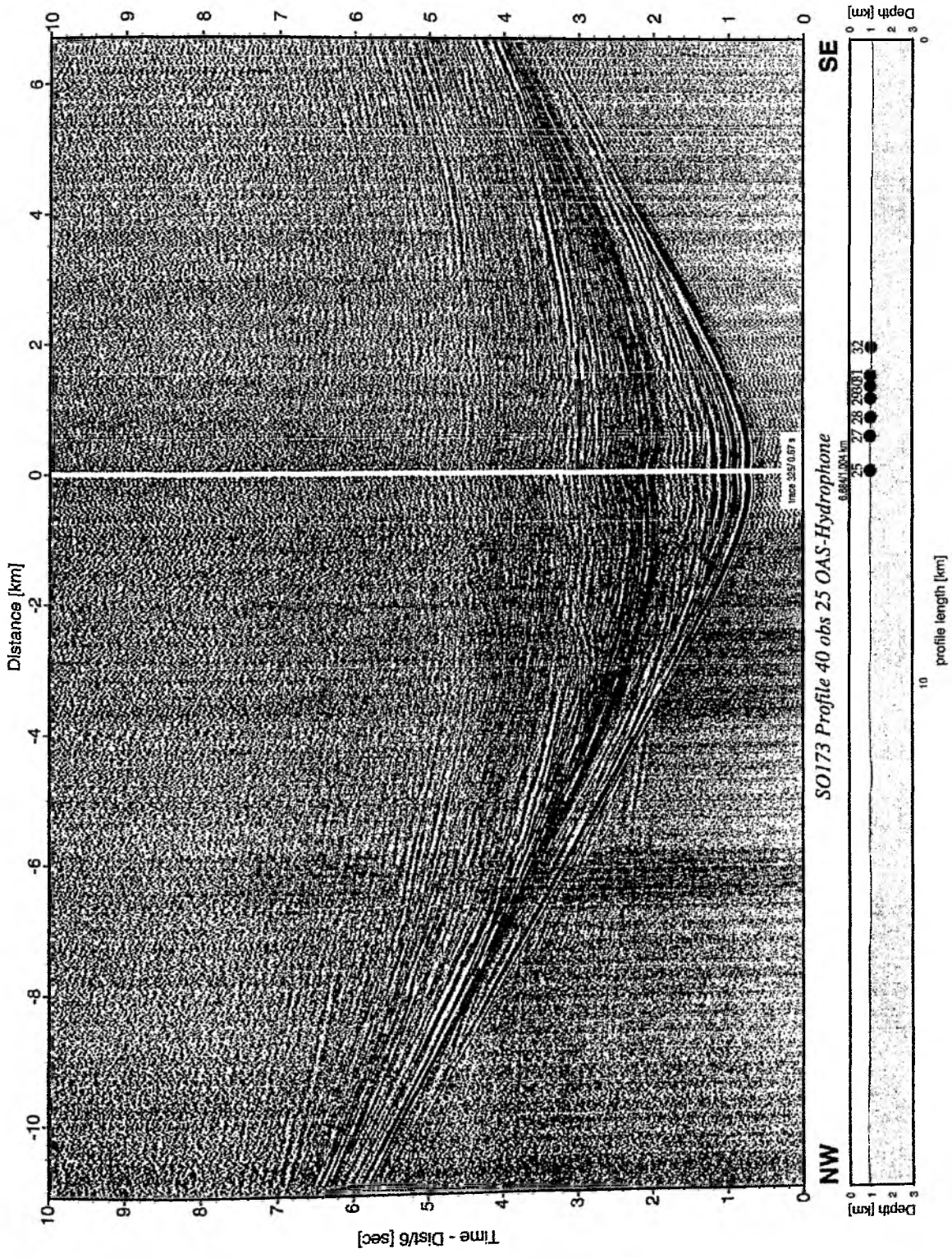

Fig. 6.4.46: Record section from OBS 25 OAS-Hydrophone, Profile 40.

6.4.7 BGR Slide

A small scar had been mapped during previous cruises and is clearly visible on one the the MCS lines collected by BGR in earlier years. This scar is located very close to the gas hydrate stability field, where the BSR reaches the seafloor. To further investigate this and to map the extent of this structure, a set of 6 profiles was shot and recorded by the surface streamer (Fig. 6.4.47). A high-resolution map collected by the Simrad system is shown in Figure 6.4.48, a data example from the six profiles is shown in Figure 6.4.49. More examples are given in Appendix B, figures B-28 to B-30.

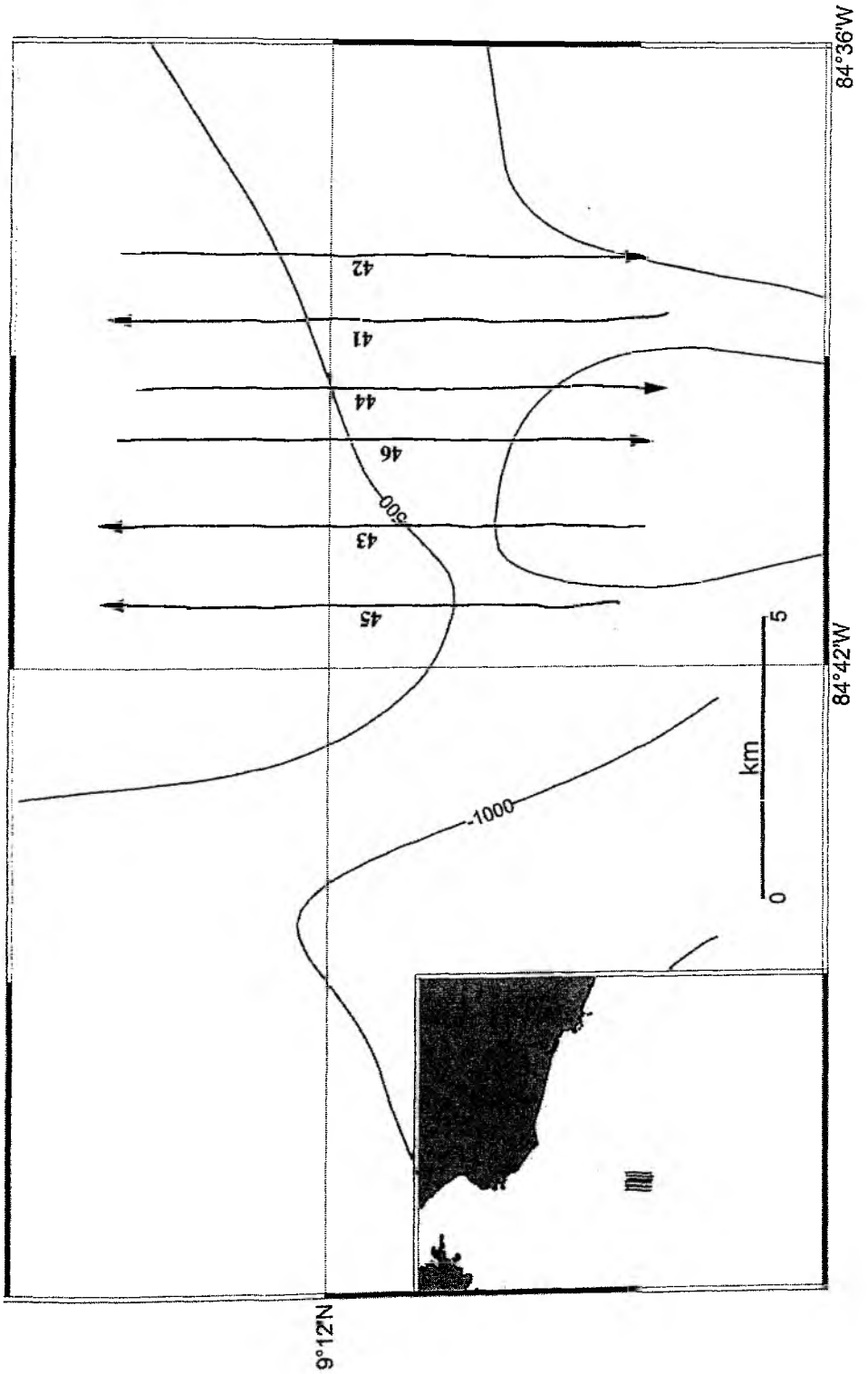

Fig. 6.4.47: Location map of profile 41 - 46 (GI-gun).

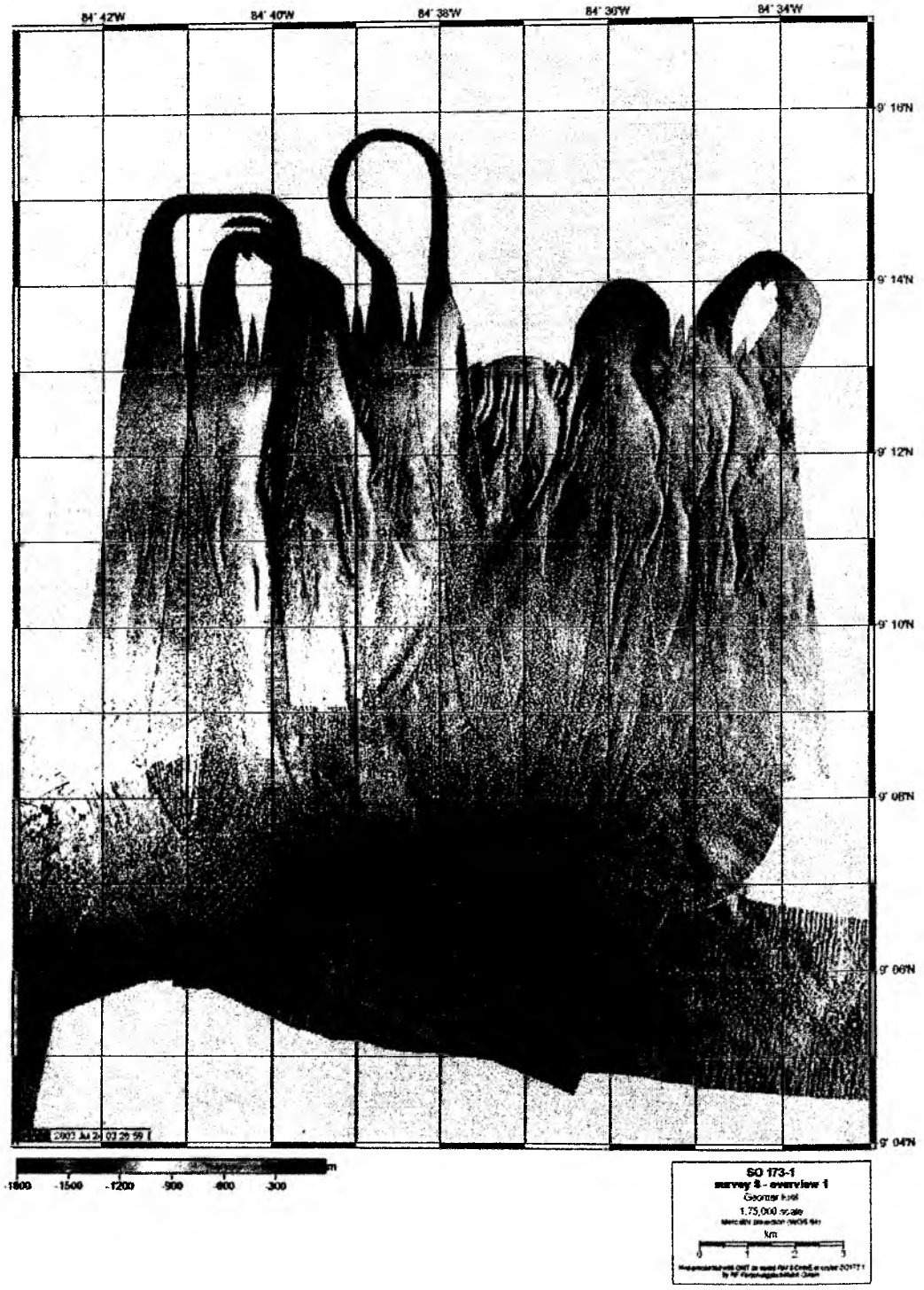

Fig. 6.4.48: Bathymetry at BGR and GEOMAR slides recorded during cruise SO 173/1.

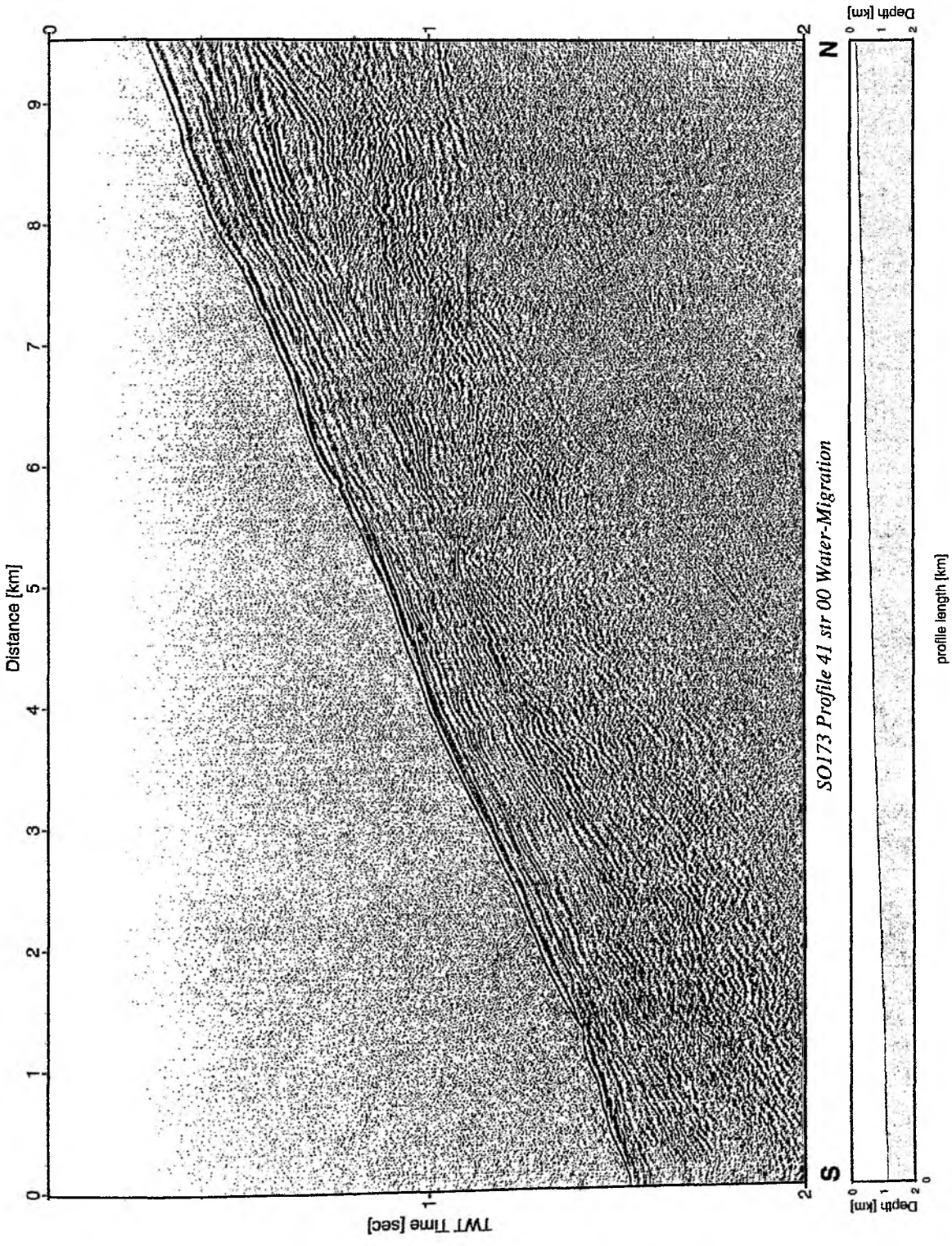

Fig 6.4.49: *Record section from str 00 Water-Migration, Profile 41.*

6.4.8 Oceanic Crust II

E. Flueh, D. Klaeschen, C. Papenberg, P. Sak

In order to study the possible inflow of water into the oceanic crust and upper mantle during plate bending, which could potentially alter the composition of the lithosphere, an 80-nm-long profile (Fig. 6.4.50) was acquired from the outer rise to the trench northwest of the Nicoya Peninsula. This location was chosen because many normal faults are seen in the bathymetric map, and a large portion of the profile is coincident with an MCS line collected by R/V MAURICE EWING in 1999, including some wide-angle data close to the trench and on the margin.

17 instruments altogether (OBS34 to OBH50) were deployed at intervals between 2.5 and 3.5 nm. Three Bolt guns of 32 l each were used to shoot along this line. They were fired at intervals of 60 s, which at a speed of 3.5 kn results in an average shot spacing of 100 m. All of the four outermost instruments were OBSs, and to be able to orient the horizontal components, three short profiles (P51,52, and 53) were shot using the GI-Gun, which were recorded simultaneously by our four-channel streamer. Further details on instrumentation and shooting can be found in appendices C. A location map, together with other data of interest is shown in Figure 6.4.50, examples of the seismic data are shown in Figures 6.4.51 to 6.4.53. More examples are given in Appendix B, figures B-31 to B-41.

General estimates of the velocity structure along profile 50 are constrained using MacRay 2.0 (Luetgert, 1992), an interactive conventional 2-D raytracing system. The models are developed using the interactive raytracing program and a trial and error approach. A layer-stripping strategy is applied to modeling from top to bottom, working towards the center of the profile from both ends. Shipboard forward modeling suggest a thin (< 0.7 km) sedimentary veneer (1.6 – 1.7 km s^{-1}) underlain by ~ 5-km-thick oceanic plate with velocities ranging from ~ 4 km s^{-1} to 6.8 km s^{-1}. The best-fit shipboard model yields mantle velocities ranging from a minimum of 7.5 km s^{-1} at the Moho. These slow upper mantle velocities are consistent with a serpentinized zone.

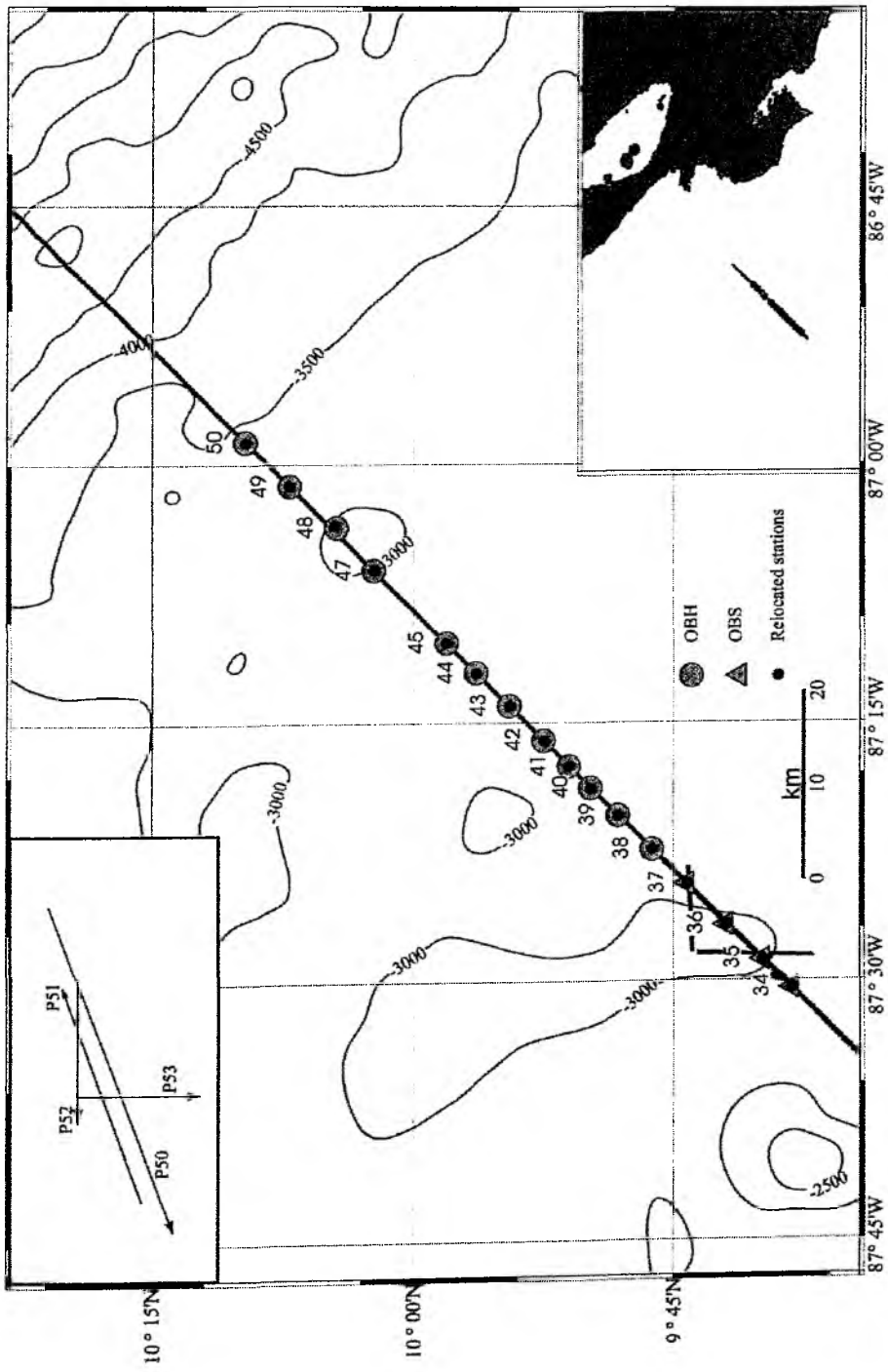

Fig. 6.4.50: Location map of profile 50 (Boltgun) and 51 - 53 (GI-gun).

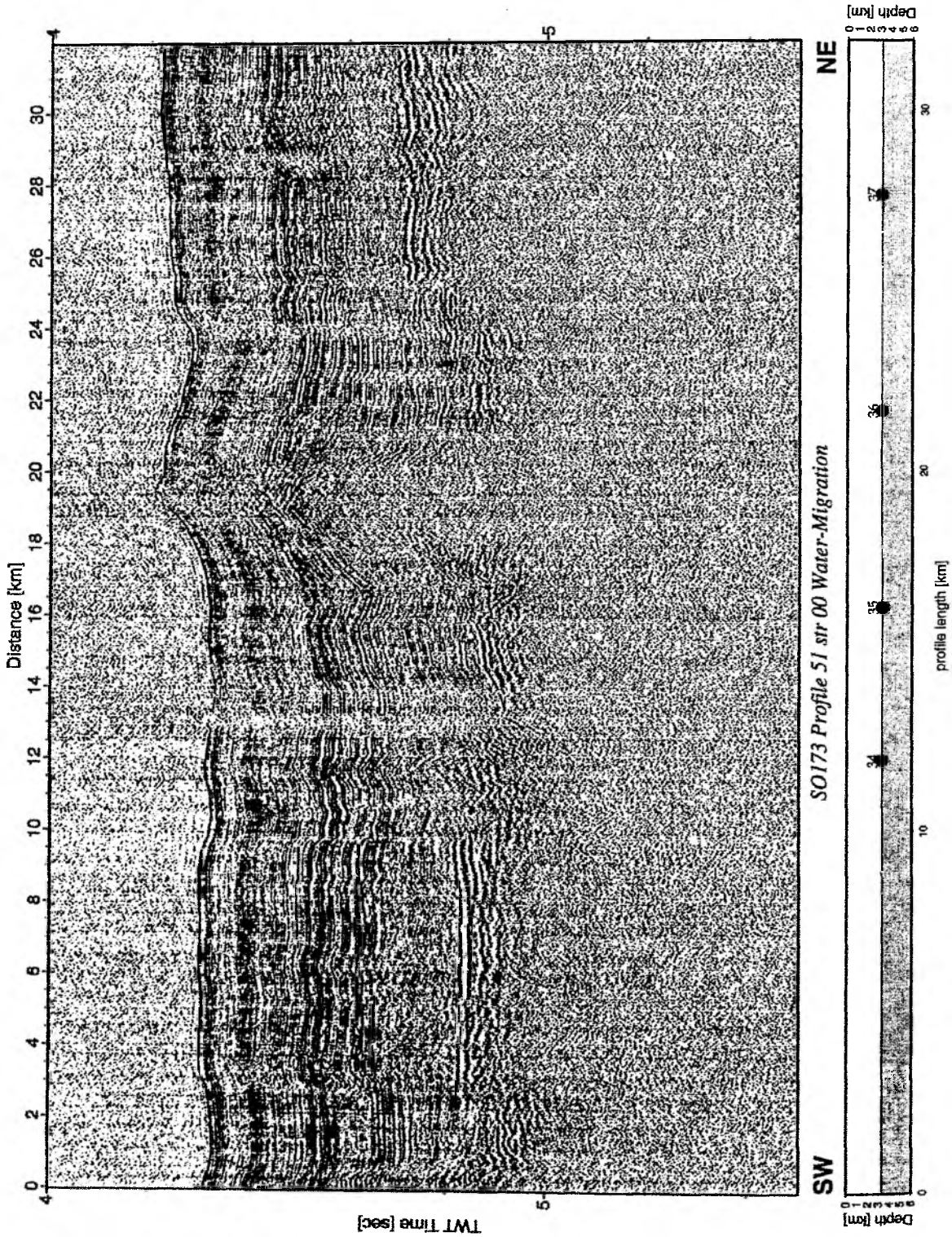

Fig. 6.4.51: Record section from str 00 Water-Migration, Profile 51.

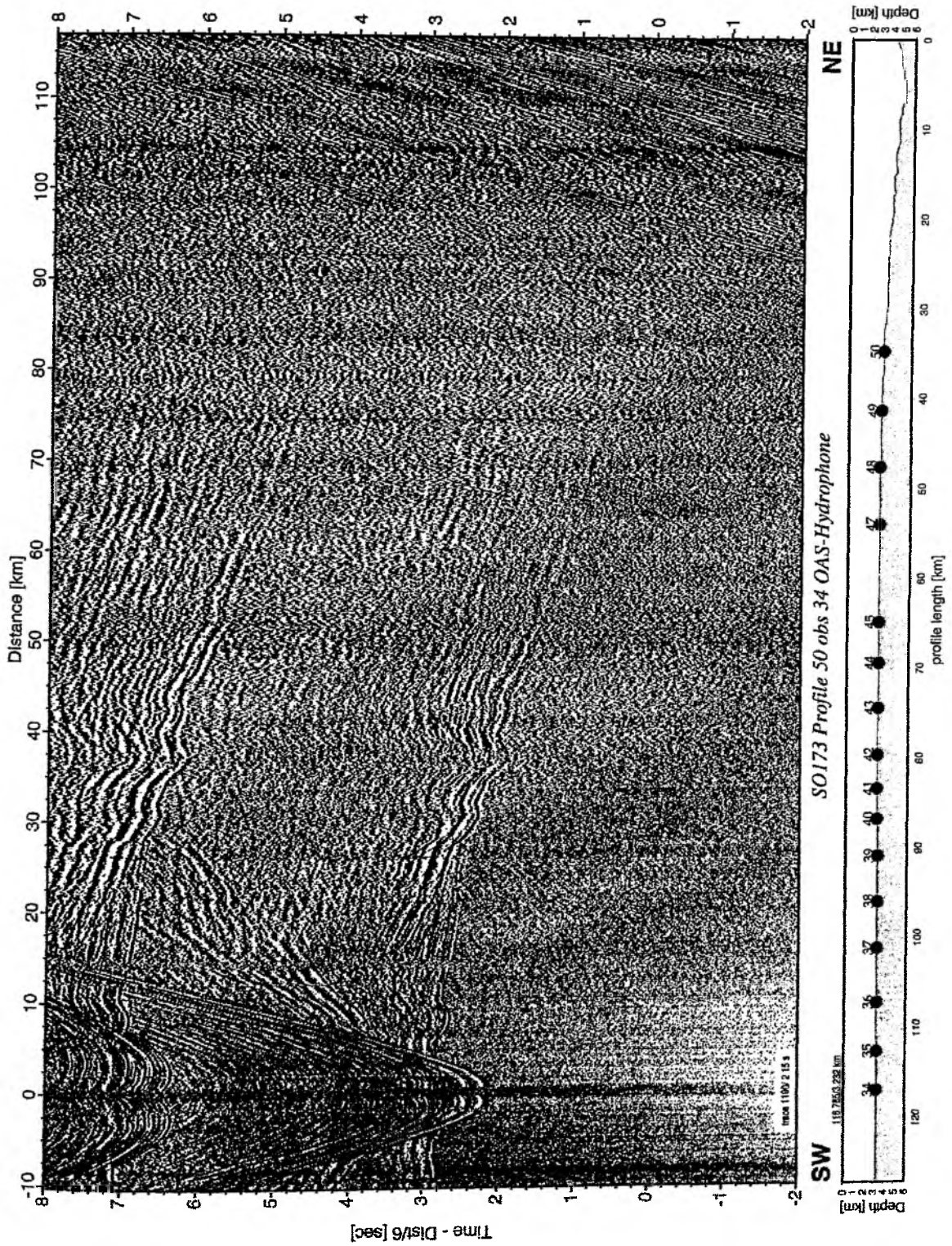

Fig. 6.4.52: Record section from OBS 34 OAS-Hydrophone, Profile 50.

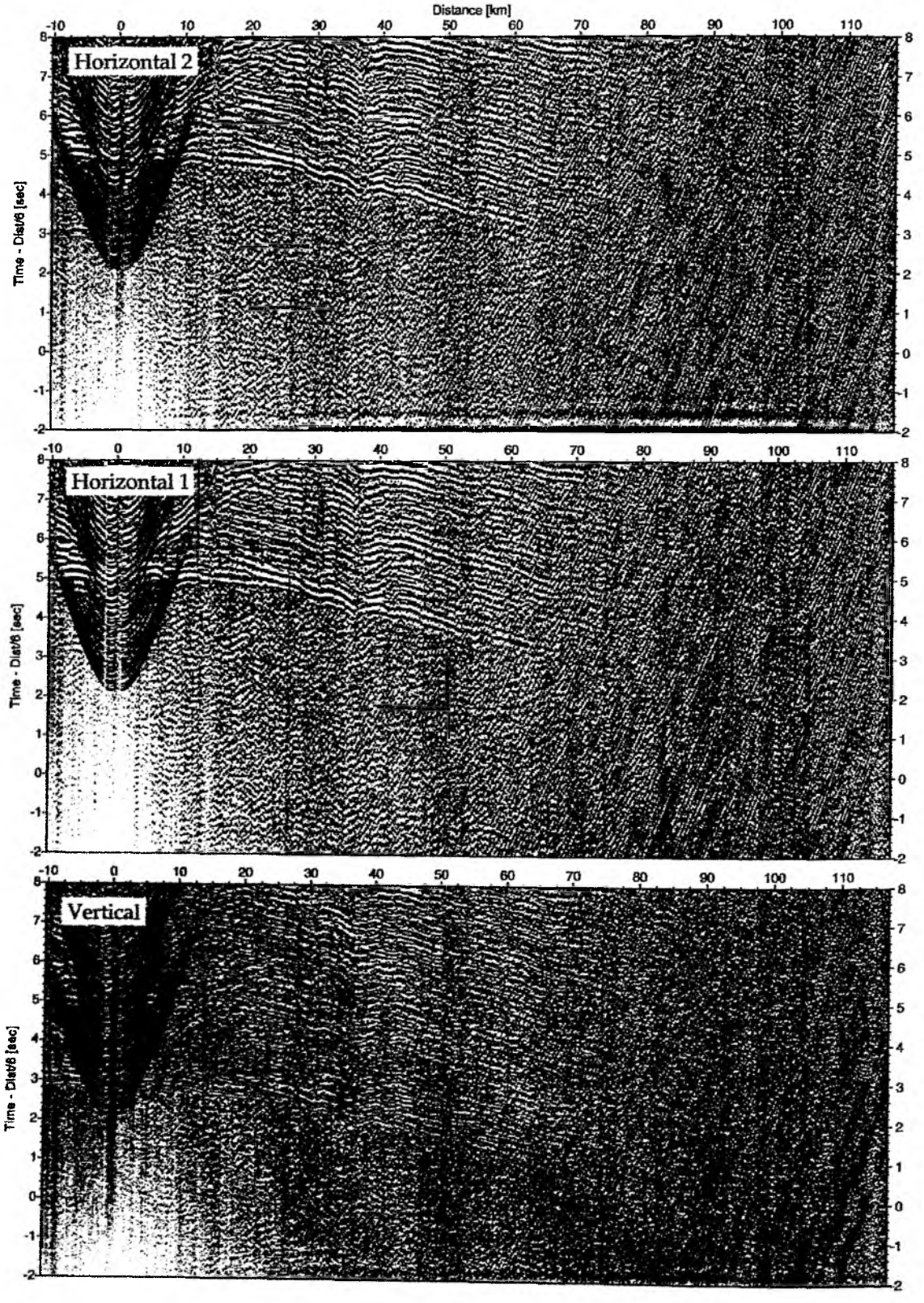

Fig. 6.4.53: Record sections from OBS 34 OAS/LG, SO 173 Profile 50.

6.4.9 Seismology Outer Rise

I. Grevemeyer

During the cruise SO 173/1a seismological network of four ocean bottom differential pressure gauges (DGP) was recovered. The deployment of the ocean bottom seismological stations was a pilot experiment to detect the local and regional earthquake activity off southern Central America. The results will be used to design a future SFB574 "outer rise seismological experiment" proposed to yield the depth of faulting in the incoming plate. Faults are re-activated or created while the brittle lithosphere is bent during subduction (Ranero et al., 2003). The centroid depth of these earthquakes can be used as proxy to assess the depth down to which fluids may migrate and hence at which alteration and perhaps serpentinization occurs. In addition, waveforms of deep earthquakes may provide important information about the properties of the lithosphere at greater depth (e.g., Abers et al., 2003). The instruments had been on the seafloor four a period of 34 days, they had been deployed during leg SO 173/ 1 of R/V SONNE.

A first assessment of the quality of data recorded during this time interval was accomplished by cutting out earthquakes with a magnitude of $m_b > 4$. Event origin times and geographical locations were obtained from the National Earthquake Information Center (NEIC) in Boulder, Colorado. Six events were reported by NEIC for the period of deployment. The earthquakes had magnitudes of 4.1 to 6.0 and had occurred between July, 30 and August 26, 2003 (Fig. 6.4.54). Examples of the recorded events are shown in Figs 6.4.55 to 6.4.58. The regional earthquakes occurred at epicentral distances of ~90 to ~620 km. The nearest event was located off Nicoya Peninsula near the trench axis and was perhaps related to bend faulting in the down-going lithosphere. The event furthest away occurred at a depth of 60 km depth under the coastline of Guatemala.

In general, high-quality waveforms were obtained from all large events and clear *P*-onset times and polarity of first motion can be reported for all events, even for magnitude m_b=4 earthquakes at D=400-600 km. However, the m_b=6.0 earthquake at D=605 km from the center of the network overloaded the recording systems. The *P*-onset and polarity of the first wave train is well recorded, though. A common feature of all events is a prominent second arrival, which is in good agreement with the multiple in the water column at the site of deployment. A more refined analysis of the $m_b > 4$ events and a search for local earthquakes below the teleseismic detection level will be done in the post cruise phase.

Event times and locations for the $m_b > 4$ events were provided by e-mail for onboard investigation by R. Herber from the Geophysical Observatory of the University of Hamburg.

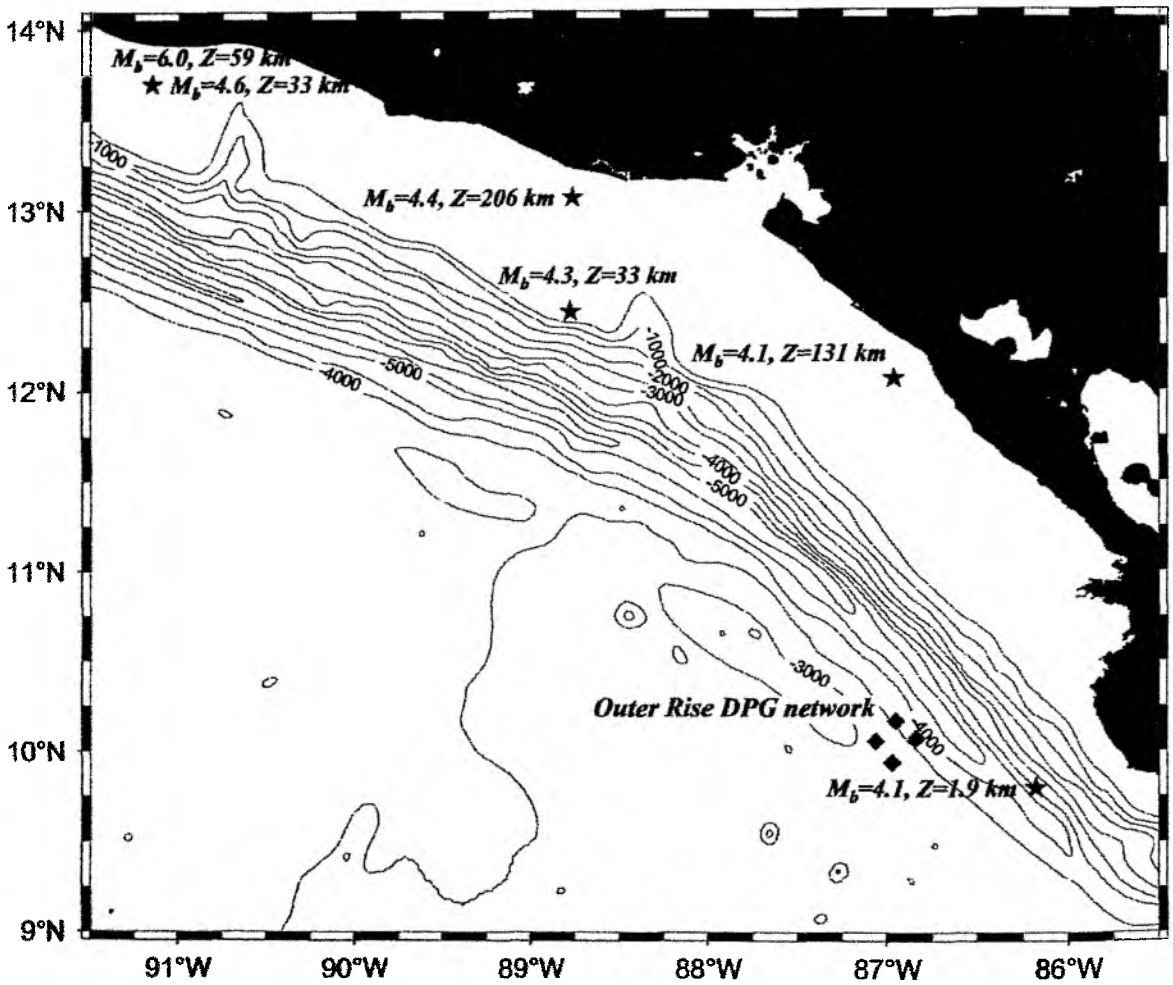

Fig. 6.4.54.: Network of ocean bottom stations (diamonds) deployed for a pilot "outer rise" seismological experiment. Earthquake locations with magnitude m_b> 4 are shown by stars. Six events have been reported by the National Earthquake Information Center (NEIC) for the 34 days of network operation.

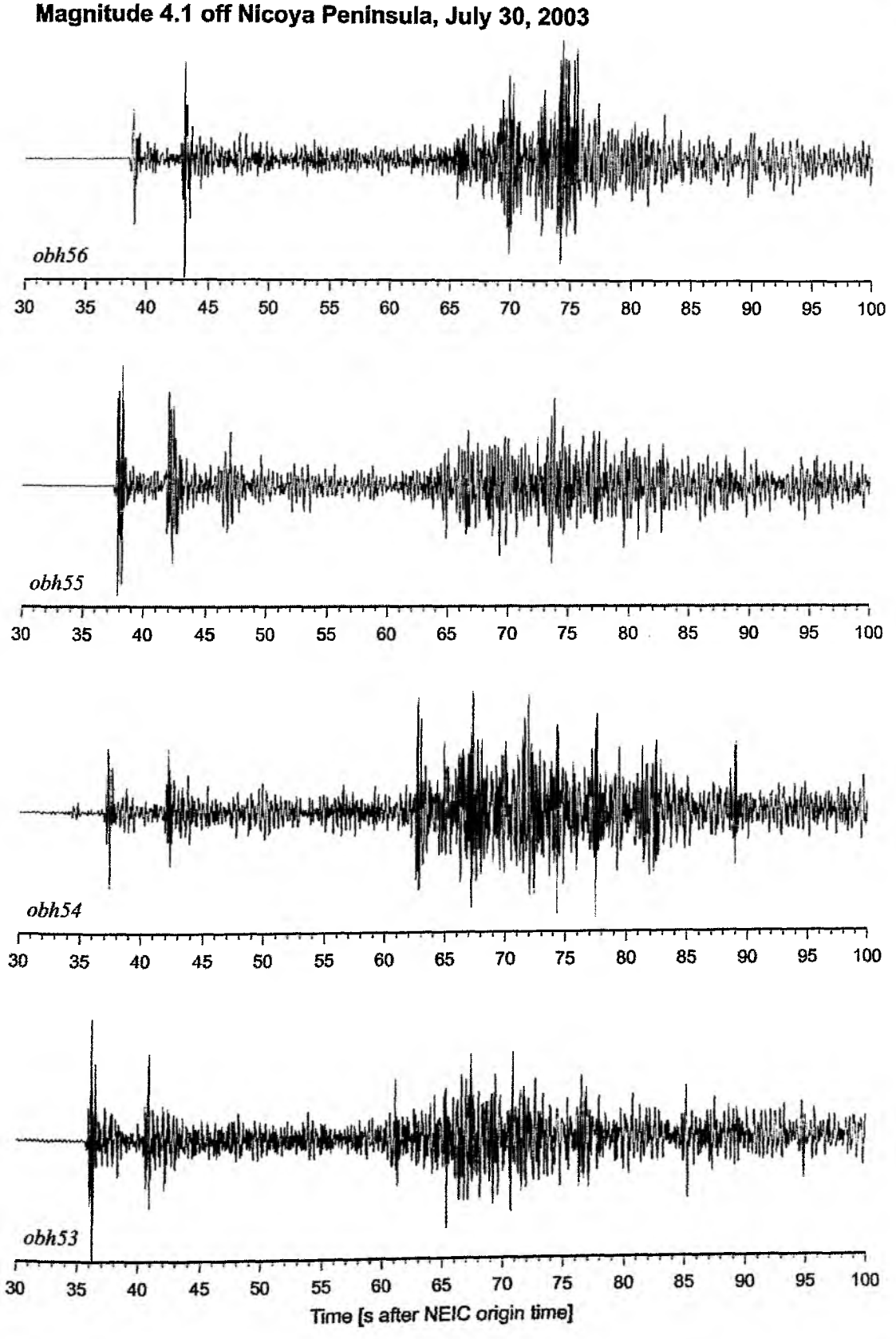

Fig. 6.4.55: Waveforms from all four instruments for an event near the trench axis offshore Nicoya Peninsula (D ~ 90 km, depth ~ 2 km).

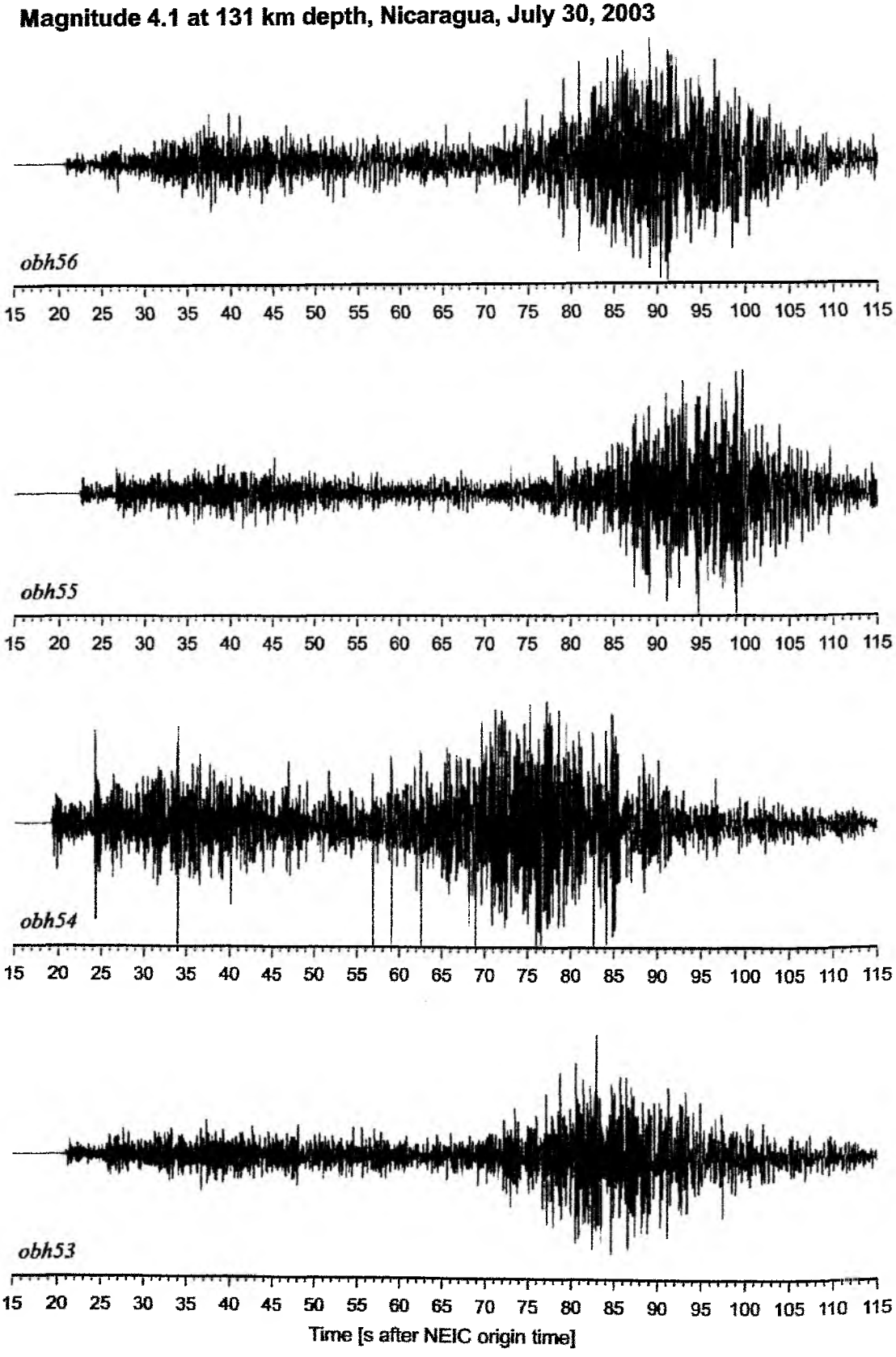

Fig. 6.4.56: Waveforms from all four instruments for an event at 130 km depth off Nicaragua.

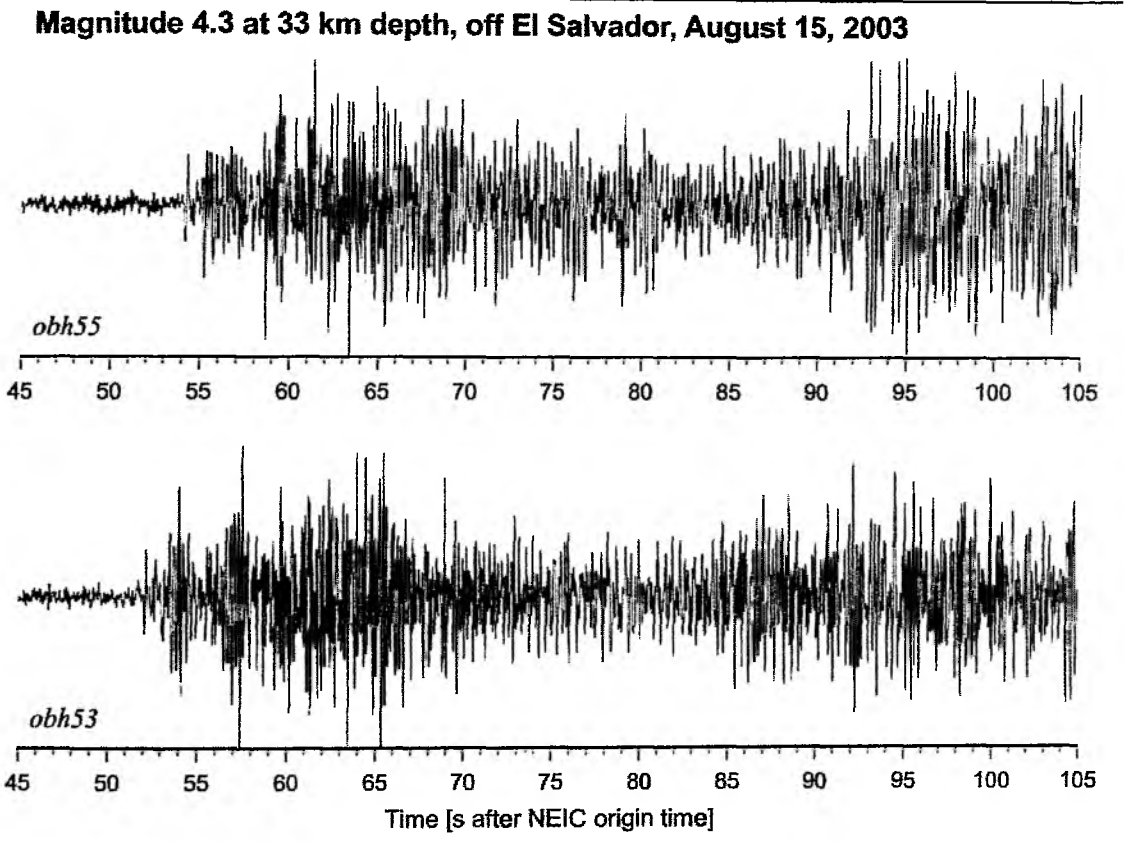

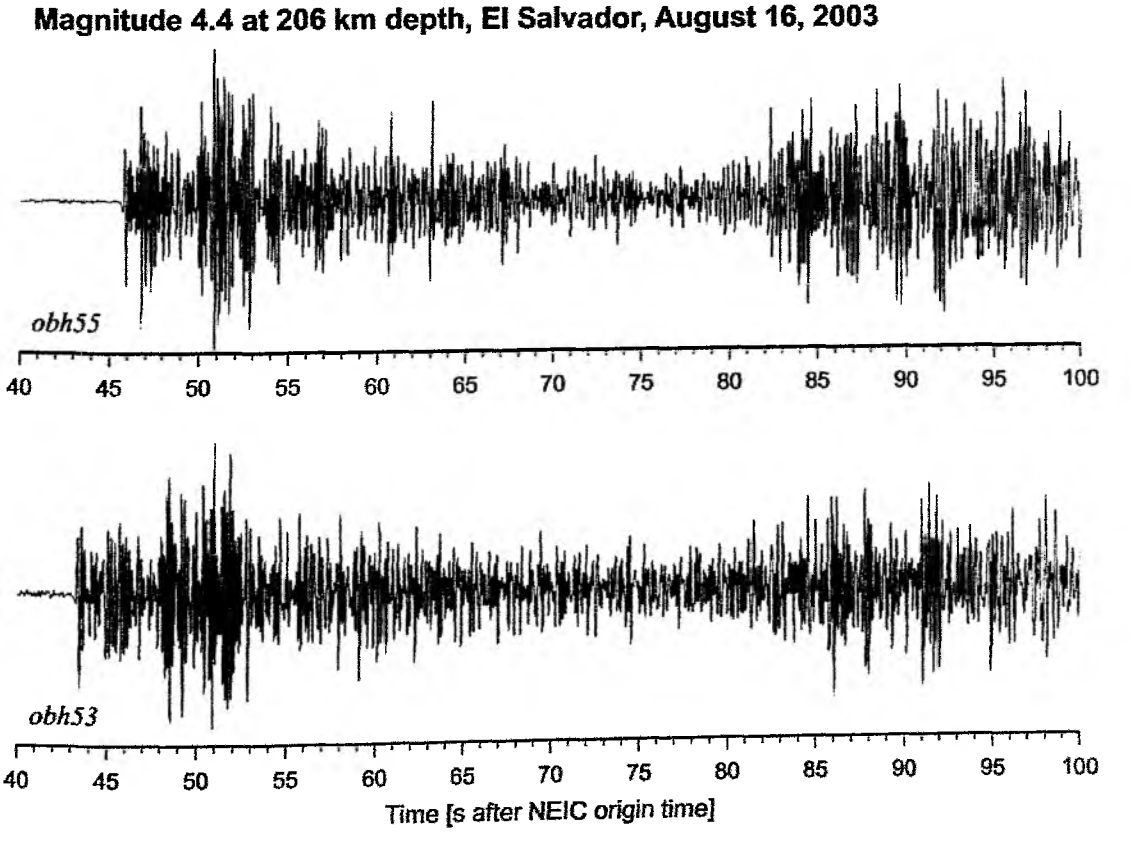

Fig. 6.4.57: Waveforms from two events off El Salvador recorded on OBH53 and OBH55.

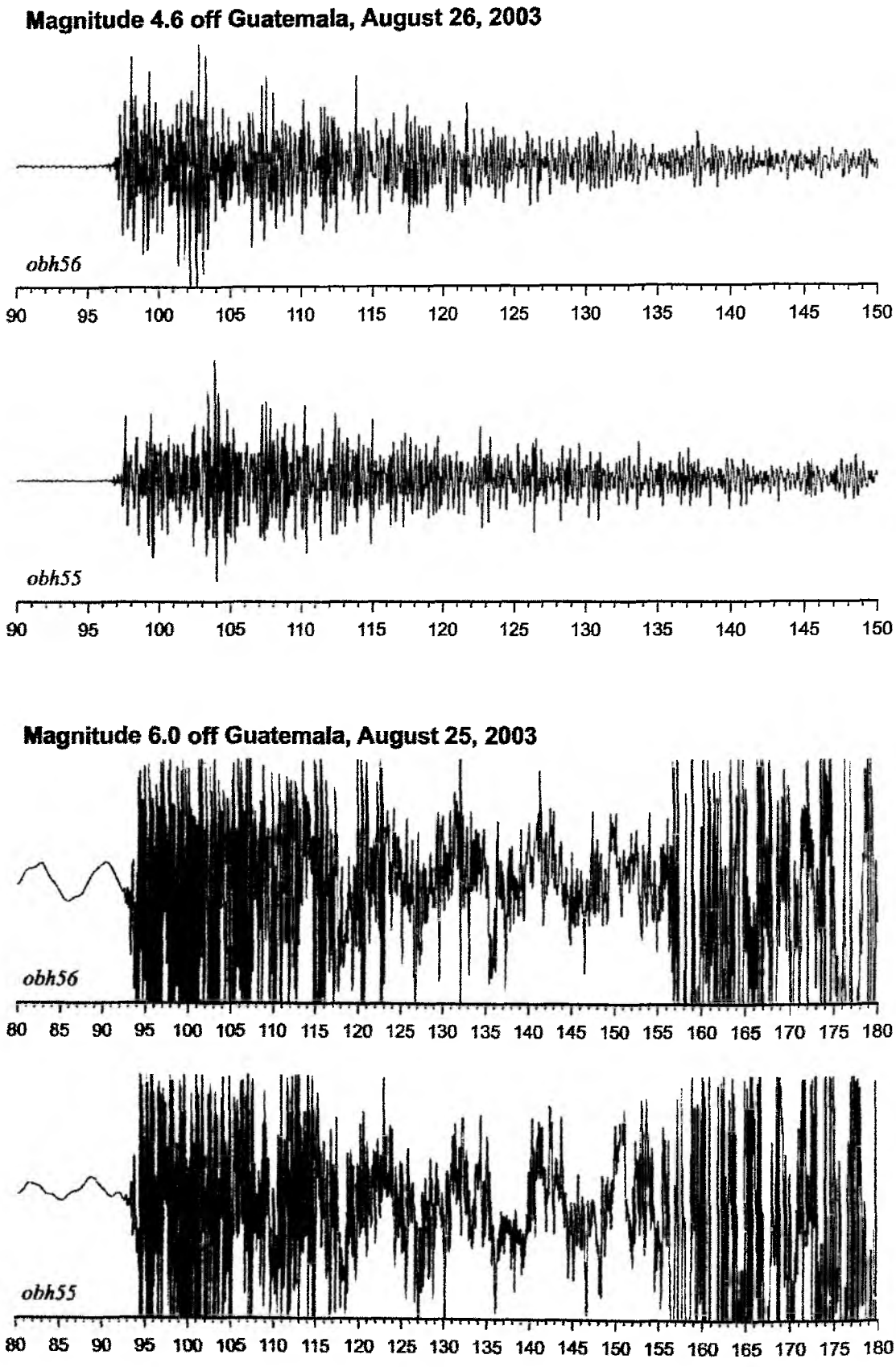

Fig. 6.4.58: Waveforms from two events off Guatemala recorded on OBH55 and OBH56. The m_b=4.6 event (top) is well recorded while the m_b=6.0 event (bottom) overloaded the recording system.

6.5 Seafloor Observations by OFOS

H. Sahling, S. Echeverría Sáenz, E.M. Corrales Cordero, E. Soeding, E. Suess

6.5.1. Objectives

On previous cruises methane seeps had been discovered at mounds, slides and seamount subduction scarps along the continental margin off Costa Rica and Nicaragua. During this cruise the main objective was to search for evidence of methane seepage in areas that had not been surveyed before: (1) Mounds at the continental margin off Nicaragua surveyed by the Deep-Towed Sidescan Sonar System (DTS) during SO 173/1, (2) backscatter anomalies that are not associated with mounds, imaged by TOBI sidescan, (3) slides at depths close to the gas hydrate stability limit for which new high-resolution swath bathymetry is available. Furthermore, we conducted detailed mapping of known mounds (Fig. 6.5.1).

6.5.2. Results

A summary of all OFOS deployments performed during cruise SO 173/3 and 4 is given in Table 6.5.1. A summary of all mounds and other structures observed and sampled is compiled in Table 6.5.2. Detailed maps of the mounds, stations and OFOS tracks covered during SO 173/3 and 4 can be found in chapter 2.3.

6.5.3. Discussion

The mounds off Nicaragua are generally larger than those off Costa Rica further south. In general, they appear to be similar to Mound Culebra: they are conical and have steep flanks, in the top area there are authigenic carbonates, vesicomyid clams and vestimentiferan tubeworms. Some mounds vary from the "Mound Culebra type" in having, e.g., only weak morphology or by being inhabited by mytilid mussels or bacterial mats. However, the variation can be explained by erosion and deposition at the continental slope, e.g., Mound Iguana is nearly completely buried by slope sediments. Only the seaward flank is exposed and collapsed which probably caused more vigorous venting here: mytilid mussels and bacterial mats were observed.

Several TOBI backscatter anomalies were observed in order to get some ground-truth on what had caused the acoustic anomalies. We found that backscatter anomalies at faults and at mounds are caused by authigenic carbonates. In most cases, chemosynthetic communities were also present.

Table 6.5.1: OFOS deployments during SO 173-3&4.

Station No.	Target	Date	At seafloor	Off seafloor	Pictures	Videos	Observation/Comments
OFOS 2	Mound Baula	6. Sept. 2003	-	-	-	-	Abandoned due to technical problems
OFOS 4	Mound Quetzal Mound Buho Mound Hormiga	6. Sept. 2003	3:15:50	11:55	~400	3	3 profiles at Mound Quetzal, 1 profile over Mound Buho and Hormiga
OFOS 9	Mound Baula	7. Sept. 2003	01:59:50	04:15:58	~ 200	1	2 profiles
OFOS 19	Mound Iguana	9. Sept. 2003	17:31:06	20:02:50	190	1	4 profiles
OFOS 21	Mound Carablanca	10. Sept. 2002	00:01:13	03:07:20	285	1	4 profiles
OFOS 24	Mound Morpho	10. Sept. 2003	13:13:45	14:39:10	73	1	1 profile, no SSBL
OFOS 45	Backscatter triplet	13. Sept. 2003	01:01:09	02:20:30	103	1	1 profile
OFOS 46	Culebra spur	13. Sept. 2003	04:27:15	11:37:54	245	2	Various profiles
OFOS 50	Mound Culebra	13. Sept. 2003	20:23:07	21:17	62	1	1 profile
OFOS 57	"BGR Slide"	15. Sept. 2003	02:22:48	04:21:09	301	1	3 profiles at headwall, no navigation data
OFOS 62	E of Quepos Slide	15. Sept. 2003	20:45:10	22:21:20	110	1	1 profile, DVS with data gaps
OFOS 70	Quepos Slide	18. Sept. 2003	14:09:50	17:03:12	510	1	Various profiles, DVS with data gaps
OFOS 77	Hongo Mound Area	19. Sept. 2003	14:26:22	18:41:40	92	2	1 profile at fault, 3 profiles over Mound Jaguar
OFOS 80	Mound 10	20. Sept. 2003	06:04:01	11:33:09	416	2	Various profiles, DVS with data gaps
OFOS 107	Mound 11 Backscatter anomaly Grillo	24. Sept. 2003	04:08:40	11:50	~ 520	2	Various profiles, no DVS protocol
OFOS 113	Backscatter anomaly in canyon	25. Sept 2003	06:41:50	07:55	117	1	1 profile, no DVS protocol, no Frontend data
OFOS 114	Backscatter anomaly pulga Backscatter anomaly luciernaga	25. Sept. 2003	09:10:15	11:19:43	~ 200	1	3 profiles, no DVS protocol, no Frontend data

Table 6.5.2: Names, stations and observations at mounds and other seafloor structures during SO 173-3&4.

Name Location Depth	Stations	Descriptions
Mound Quetzal 11° 12.36' N 87° 10.85 'W 1315 m	OFOS 4 GC 5, 5-1, 6, 6-1 CTD 7 TVG 8	Circular mound with depression which is probably caused by slumping of the SW flank (DTS No. 29, 13). Top of mound with massive sometimes fractured carbonates surrounded by areas with less extensive carbonate coverage. Here, vesicomyid clams and pogonophoran tubeworms occur. In the depression massive carbonates, carbonate talus and sediments occur. North of top sediments with clamshells and clams and fewer carbonates were observed. A carbonate boulder was grabbed. *Quetzal: Famous Middle American bird*
Mound Buho 11° 11.12' N 87° 09.10' W 1260 m	OFOS 4	The Mounds Buho and Hormiga are part of a linear series of mounds above a landslide. Mound Buho (DTS No. 28) was surveyed by only one OFOS profile which crossed the southern flank. Carbonate talus with dark Fe/Mn coating and scattered shells occurred in patches. *Buho: Owl*
Mound Hormiga 11° 10.65' N 87° 08.38' W 1260 m	OFOS 4	The Mounds Buho and Hormiga are part of a linear series of mounds above a landslide. Widespread occurrence of carbonates at top of Mound Hormiga (DTS No. 27). Only few clamshells. *Hormiga: Ant*
Mound Baula 11° 15.3' N 87° 09.9' W 890 m	OFOS 9	Largest mound in SO 173 survey area off Nicaragua (DTS No. 37, 20). At top two summits. Top area largely covered by a continuous carbonate layer. At the top carbonates massive and fractured showing that they are several meters thick. At E side transition between carbonates and sediments 2-3 clam clusters of 1-2 m size were observed during both OFOS profiles. *Baula: Leather back turtle*
Mound Iguana 11° 12.25' N 87° 9.25' W 1200 m	OFOS 19 CTD 22	Mound without typical mound-like seafloor morphology but with backscatter anomaly (DTS No. 49). OFOS survey indicate that the mound is buried by slope sediments on its landward side and, thus, is hidden in the slope morphology. At seaward base of the mound massive carbonates are exposed; in fractures mytilid mussels and pogonophoran tubeworms were present. At sediments that probably covered recently these fractures bacterial mats occurred. Individual bacterial patches were small (~20 cm). *Iguana: Iquana*
Mound Carablanca 11° 16.4' N 87° 15.25' W 1430 m	OFOS 21 TV-MUC 26, 28, 29 TVG 27 CTD 31 BWS 32 GC 33, 34, 35,36	The sidescan image of Mound Carablanca (DTS No. 31) shows circular alternations between high and low backscatter. The OFOS survey did not reveal evidences that could obviously explain this sidescan pattern. At the top of the mound 5 small sidescan "shadows" occur. In these areas carbonate pave the seafloor. In between the pavement and between the different spots many 1-m-size clusters of vesicomyid clams occur. A grab in this habitat recovered about 50 living vesicomyid clams and 2 solemyid bivalves as well as cemented sediments that appear to be first stages in the formation of large, solid carbonates. TV-MUC samples were taken close to clam clusters. 4 gravity corer were taken. Mud clasts and scaly clays were found. Increasing concentrations of methane towards the seafloor were found in the CTD and BWS, but maximum values were generally low. *Carablanca: White face monkey*

Mound Morpho 11° 00.1' N 87° 00.55' W 1670 m	OFOS 24 TVG 37 TV-MUC 38, 39	Mound Morpho (DTS No. 58) is characterised by high backscatter and steep small-scale morphology that cause "shadows" in the sidescan image. At the entire top area carbonates were exposed with few areas of soft sediments in between. 1-m size clam clusters occurred in between carbonates partly in sediments. 2 TV-MUCs were deployed at clam clusters but did not recover living specimens or fluid-influenced porewater. A grab-recovered carbonates that elevated about 1 m above the surrounding sediments. They were cemented sediments with large holes and openings. *Morpho: Blue morpho butterfly*
Backscatter triplet 10° 18.8' N 86° 11' W 600 m	OFOS 45	The backscatter triplet are three backscatter anomalies without seafloor morphology imaged by TOBI sidescan (Id # 860008-10). The areas at two anomalies were surveyed. Nothing observed was at the seafloor that could explain the anomalous backscatter.
Culebra Spur 10° 15.95' N 86° 16.6' W 1530 m	OFOS 46 GC 49, 97	Culebra spur is the south-western part of a 8 nautical miles long fault system that strikes along the slope and cuts through Mound Culebra. The fault can be traced morphologically and in TOBI sidescan images. Methane seepage was found in an area of complex morphology where the fault is intercepted by a small depression. Clams clusters and one bacterial mat were present in soft sediments. The extant of communities were too little to be sampled by TV-MUC. Two gravity corer revealed that chlorite-depleted fluids slowly seep through the sediments.
Mound Culebra 10° 17.9' N 86° 18.3' W 1500 m	OFOS 50 GC 51, 87, 98 TV-MUC 52, 52-1, 94, 95, 96 CTD 83, 84, 86, 93	The top and the southern flank of Mound Culebra were surveyed by OFOS. No indications for seepage or mud extrusion were found at the southern slope. TV- MUCs were taken at the Northern slope. A living large vesicomyid clam was recovered. Porewater composition indicates strong heterogeneity in methane seepage. *Culebra: Snake*
Mound 10 10° 00.45' N 86° 11.45' W 2270 m	OFOS 80 TVG 90 TV-MUC 78, 79 BWS 91 CTD 92 GC 81	Small scale mapping of Mound 10 revealed that in addition to the known seep sites a second site exists with carbonates, pogonophoran tube worms and vesicomyid clams. A TVG grabbed next to a vesicomyid clam cluster and recovered carbonates and living *Acharax* specimens.
Mound Jaguar 09° 39.5' N 85° 53.0' W 2000 m	OFOS 77	The objective of OFOS 77 was to survey backscatter anomalies at a fault as well as on the mound which was surveyed during the SO 144 cruise with OFOS 10. Areas with carbonates discovered but the main active seep site was not found. *Jaguar: Jaguar*
BGR Slide 09° 11.4' N 84° 39.8' W 550 m	OFOS 57 GC 59, 59-1, 61, 61-1 CTD 58, 60 BWS 65	Survey of the headwall of the BGR slide did not reveal any evidence for methane seepage. Gravity cores were taken and sampled both, the slide mass and the consolidated sediments that formed the slide plane.
Quepos Slide 08° 51 ' N 84° 13' W 400 m	OFOS 62, 70 TV-MUC 63, 64, 71, 73 GC 74 BWS 65, 75, 103 CTD 72 BCL 102 FLUFO 108	OFOS surveys during previous cruises revealed the presence of bacterial mats at the base of the headwall of Quepos Slide. This area was mapped in detail with OFOS 70 in order to confirm the limits of the bacterial mats. Bacterial mats occur at a small ridge that An additional survey (OFOS 62) was conducted east of the main slide but did not reveal any evidence for methane seepage.
Mound 11 08° 55.35' N 84° 18.2' W 1015 m	OFOS 107 TV-MUC 127 TVG 128 BCL 130	Mound 11 is a complex structure with two summits. Seep activity is present at both summit areas. Bacterial mats and carbonates occur.

Backscatter anomaly Grillo 08° 56.3' N 84° 18.88' W 1000 m	OFOS 107 GC 117	Backscatter anomaly north-west of Mound 12. 2-3 small patches with bacterial mats in area where Parasound shows hard reflector. *Grillo: Grasshopper*
Backscatter anomaly in canyon 08° 57.55' N 84° 20.65' W 1050 m	OFOS 113	OFOS survey revealed that a high circular backscatter anomaly at the canyon floor is caused by outcropping compacted sediment strata. No indication for methane seeps.
Backscatter anomaly Luciernaga 08° 58.60' N 84° 17.95' W 855 m	OFOS 114	TOBI backscatter anomaly. Exposed fractured massive carbonate blocks. No seep fauna. Probably fault related. *Luciernaga: Firefly*
Backscatter anomaly Pulga 08° 58.40' N 84° 18.15' W 870 m	OFOS 114	TOBI backscatter anomaly. 3 clam cluster and a bacterial mat in gentle slope. Probably fault related. *Pulga: Sandfly*

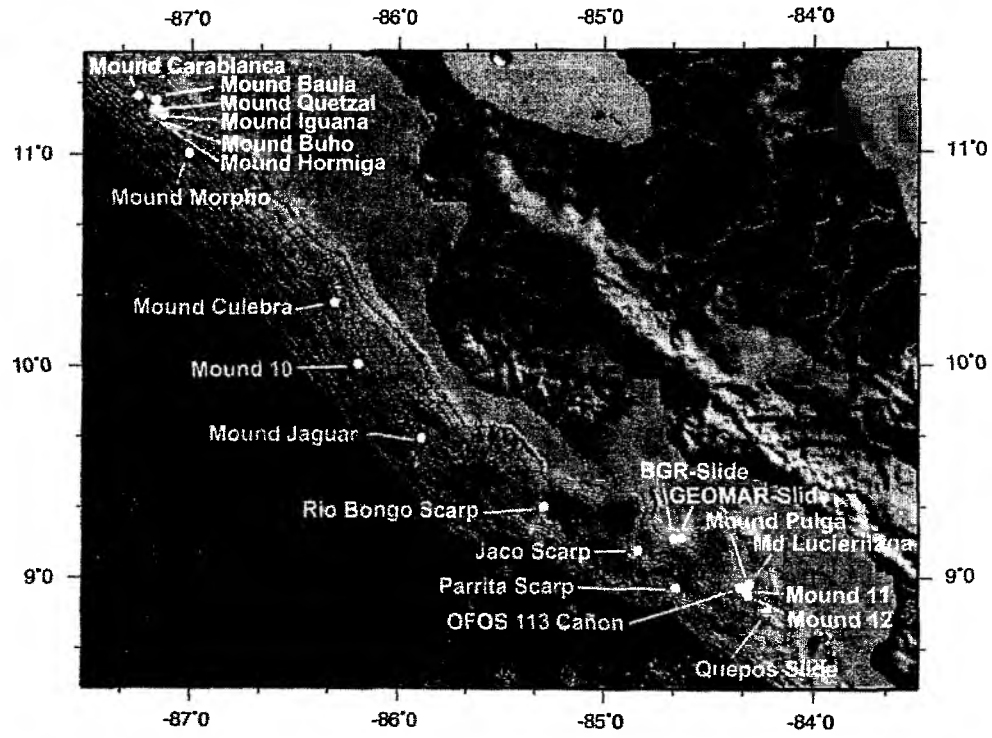

Fig. 6.5.1: Overview of sampling locations visited during SO 173/3 and 4.

6.6 Sediment Sampling and Sedimentology

S. Kreiter, S. Kutterolf, R.. Mejias Chaves, T. Moerz, W. Queisser, M. Schmidt, E. Steen

6.6.1 Core descriptions

New mound area off Nicaragua

SO 173/3-5-1 (11°12.50'N, 87°10.86'W, 1334 mbs)

Total core recovery: 337 cm. The matrix mainly consists of sandy clay, and fluid channels were indicated in the whole core. Shell fragments were found in the core and bioturbation was indicated. Two cm-sized ash layers could be made out. The core was taken at northern slope of Mound Quetzal. A massive fishbone ring (1.5 cm) was found at a depth of 178 cm.

SO 173/3-6-1 (11°12.26'N, 87°10.83'W, 1330 mbs)

This station is located on top of Mound Quetzal. The total core length is 392 cm. The sediment mainly consists of carbonate mud mixed with carbonate concretions.

SO 173/3-33 (11°16.33'N, 87°15.11'W, 1479 mbs)

The core was located on the eastern slope of Mound Carablanca. 77 cm of consolidated clay mixed with silty clay and carbonate mud clasts were recovered.

SO 173/3-34 (11°16.42'N, 87°15.32'W, 1432 mbs)

4.5 m of sediment were recovered at station 34 located at the southern slope of Mound Carablanca. The sediment mainly consists of scaly clay, carbonate mud and clay clasts.

SO 173/3-35 (11°16.51'N, 87°15.37'W, 1479 mbs)

The station is located on the northwestern slope of Mound Carablanca. The core recovery was about 90 cm. The sediment mainly consists of carbonate concretions, carbonate and clay clasts. One felsic ash layer was identified at the base of the core.

SO 173/3-36 (11°16.51'N, 87°15.37'W, 1479 mbs)

Station 36 was located on top of Mound Carablanca. 121 cm of reworked /mixed clay and carbonate clasts were recovered. A black ash layer was identified at 6 cm and scaly clay was found in the core catcher. Bioturbation was indicated.

Mound 10

SO 173/3-40 (10°00,47'N, 86°11,45'W, 2263 mbs)

563 cm of sediment could be recovered at Mound 10. About 40 cm of surface sediment was lost in the weight of the GC. The core mainly consists of silty clay at its top and of carbonate mud mixed with carbonate concretions at its base. Consolidated clay was found in the core catcher.

SO 173/4-81 (10°00.50'N, 86°11.40'W, 2272 mbs)

192 cm of sediment were recovered. The upper 92 cm consist of silty clay mixed with carbonate mud and carbonate concretions and clay clasts. The lower part mainly consists of scaly clay and clay clasts. Mm-sized carbonate layers are present. A strong H_2S smell was noted from the whole core.

Mound 12

SO 173/4-110-1 (08°55.75'N, 84°18.79'W, 1006 mbs)

120 cm of sediment were recovered at the western slope of Mound 12. The upper part consists of silty clay mixed with ash lenses and diffuse ash layers. The lower part consists of firm clay with a high gas content (H_2S smell, degassing bubbles).

SO 173/4-115 (08°55.67'N, 84°18.62'W, 1008 mbs)

The station is located at the southern slope of Mound 12. 560 cm of sediment were recovered. The core is dominated by numerous turbidite sequences mixed with ash. Degassing was observed in the lowest segment.

Mound 13

SO 173/4-117 (08°56.30'N, 84°18.88'W, 986 mbs)

The core was taken on top of Mound 13. The core length was about 610 cm. The sediment consists of bioturbated silty clay, and turbidites with sandy ash bases are indicated.

Mound Culebra

SO 173/3-51 (10°17.66'N, 86°18.32'W, 1617 mbs)

238 cm of sandy clay mixed with mm- to cm-sized volcanic (?) clasts were recovered. Carbonate mud and carbonate concretions were found at the lower part of the core.

SO 173/4-87 (10°17.92'N, 86°18.46'W, 1524 mbs)

The core was taken from a small depression on Mound Culebra. About 185 cm of core were recovered. The upper 60 cm consist of silty clay mixed with carbonate mud and concretions. The lower part is dominated by mud breccia and clay clasts. 20 cm of consolidated clay were recovered from the core catcher.

SO 173/4-98 (10°17.79'N, 86°18.59'W, 1567 mbs)

460 cm of sediment were recovered mid-slope southwest of Mound Culebra. 2 discrete white ash layers and several diffuse black ash layers could be identified. The matrix is mixed with slightly more consolidated clay clasts in the lower 260 cm of sediment.

Ash cores

SO 173/3-11 (12°00.00'N, 88°09.00', 1646 mbs)

The area is located on the slope off northern Nicaragua. 565 cm of core were recovered. The core matrix mainly consists of silty clay and 6 ash layers (felsic and mafic) could be identified.

SO 173/3-11-1 (12°00.00'N, 88°09.00'W, 1650 mbs)

The core is 1150 cm long. 12 ash layers were identified.

SO 173/3-13-1 (11°26.37'N, 88°28.00'W, 4134 mbs)

The core was sampled at the oceanic plate off Nicaragua. The core is 555 cm long. 14 ash layers were defined in the silty clay matrix. Strong bioturbation is indicated.

SO 173/3-15 (10°43.16'N, 88°54.09'W, 3288 mbs)

The sampling station is located on the incoming oceanic plate off Nicaragua. 626 cm of core were recovered. 7 ash layers (felsic and mafic) were identified. Strong bioturbation is indicated.

SO 173/3-17 (11°15.80'N, 88°12.60'W, 3716 mbs)

9 ash layers were found. 235 cm of core were recovered. The area is located on the oceanic plate off Nicaragua.

SO 173/3-18 (11°36.00'N, 87°36.00'W, 1606 mbs)

The station is at the slope off Nicaragua. 11 ash layers were identified. Bioturbation is indicated. The core is 844 cm long.

Canyon

SO 173/3-25 (11°08.30'N, 87°02.80'W, 1229 mbs)

The station is located in a deep sea canyon on the slope off Nicaragua. The core is characterized by rip-up clasts, discordances, turbidites and firm/consolidated silty clay at the base. The total core recovery is 284 cm. Two reworked ash layers could be identified.

Mound Culebra Fault

SO 173/3-49 (10°15.94'N, 87°16.60'W, 1530 mbs)

The core was recovered southeast of Mound Culebra in a fractured area. The total core recovery was 841 cm and the sediment mainly consists of olive gray silty clay. A dark gray ash layer was identified at 640 cm. The sediment had a strong H_2S smell and pore water degassing was indicated by small gas bubbles rising to the sediment surface between 170 cm and 841 cm.

SO 173/4-97 (10°15.93'N, 87°16.61'W, 1531 mbs)

603 cm of sediment was recovered near the Mound Culebra Spur. Normal background sedimentation is indicated in the upper 3 m of sediment. Strong H_2S smell, degassing bubbles and vertical carbonate mud-filled conduits are found between 300 and 600 cm.

BGR Slide

SO 173/3-59 (09°11.76'N, 84°40.00'W, 559 mbs)

The corer was penetrated into slided sediment at the base of the head wall. The total core recovery was 348 cm. Reworked silty clay dominating the upper part of the sediment changes to consolidated firm silty clay at 116 cm. A dark gray ash layer was also found at 116 cm. A second ash layer (white) is located at 225 cm. Sulfides are frequent between 254 and 314 cm.

SO 173/3-59-1 (09°11.83'N, 84°39.7'W, 554 mbs)

The station was planned to be located above the head wall of the BGR slide but the measured rope length was about 590 m. 418 cm of sediment were recovered. The sediment is dominated by numerous turbidite sequences and laminated and tilted structures.

SO 173/4-122 (09°11.65'N, 84°39.10'W, 567 mbs)

The station was located on top of the BGR slide. The core was about 614 cm long. The upper 455 cm of sediment consist of silty clay. Four light gray ash layers were identified. The lower part consists of laminated clay with discordances.

GEOMAR Slide

SO 173/3-61-1 (09°11.80'N, 84°37.24'W, 654 mbs)

570 cm of sediment were recovered at the base of the head wall of the GEOMAR slide. Reworked ash, clay lenses, rip-up clasts and turbidites dominate the whole sediment core. A possible change between the slided sediment and old ground mass is indicated by a change of density at about 530 cm.

Quepos Slide

SO 173/4-74 (08°51.19'N, 84°13.15'W, 405 mbs)

550 cm of sediment were recovered at the base of the head wall. About 18 turbidite sequences were identified in the core. Carbonate concretions and bioturbation channels are abundant.

6.6.2 Marine Tephras Offshore Nicaragua and Costa Rica – Preliminary Results from SO 173/3

S. Kutterolf, U.Schacht, T. Moerz, M. Schmidt

6.6.2.1 Introduction

In Central America and other regions on Earth, highly explosive, plinian volcanic eruptions generate buoyant eruption columns penetrating 20-40 km high into the atmosphere up to the level of neutral buoyancy where they spread laterally (Kutterolf et al. 2004). Eruption clouds drift with the wind prevailing at any altitude and gradually drop their ash load over areas larger than 10^5 km^2. Ash layers are best preserved in non-erosive marine or lacustrine environments and therefore provide the most complete record of volcanic activity. In Central America, volcanoes rest fairly narrow to marine regions, therefore prevailing south-easterly surface- and north-westerly upper level winds (Carey and Sigurdsson, 2000) disperse ash erupted at the volcanic arc across marginal areas of the Pacific and Caribbean basin.

Wide aerial distribution across sedimentary facies boundaries, near-instantaneous emplacement, chemical signatures facilitating stratigraphic correlations, and the presence of minerals suitable for radiometric dating make ash layers excellent stratigraphic marker beds for marine geoscience. Marine tephrostratigraphy provides constraints on the temporal evolution of both, the volcanic source region and the ash-containing sediment facies, and is a good feature to correlate different sediment successions from on-land and marine environments of the whole Central American region with each other (Kutterolf et al. 2004).

6.6.2.2 Methods

As piston and gravity cores only reach depths of up to 20 m in soft sediments our tephrostratigraphy is limited to ages of less than 10^6 years. Visual identification of ash layers is easy when the ash forms mm- to cm-thick distinct and undistorted layers. In slope settings, however, mass wasting processes redistribute ashes and therefore visual recognition in core sections can be difficult. Core logging techniques allow to identify both distinct layers and dispersed ashes in marine sediment cores, prior to core description. Standard core logging parameters include P-wave velocity, density from gamma attenuation and magnetic susceptibility. Magnetic susceptibility is the degree to which a material can be magnetized by an external magnetic field. It is expressed as the intensity ratio of sediment magnetization to an external magnetic

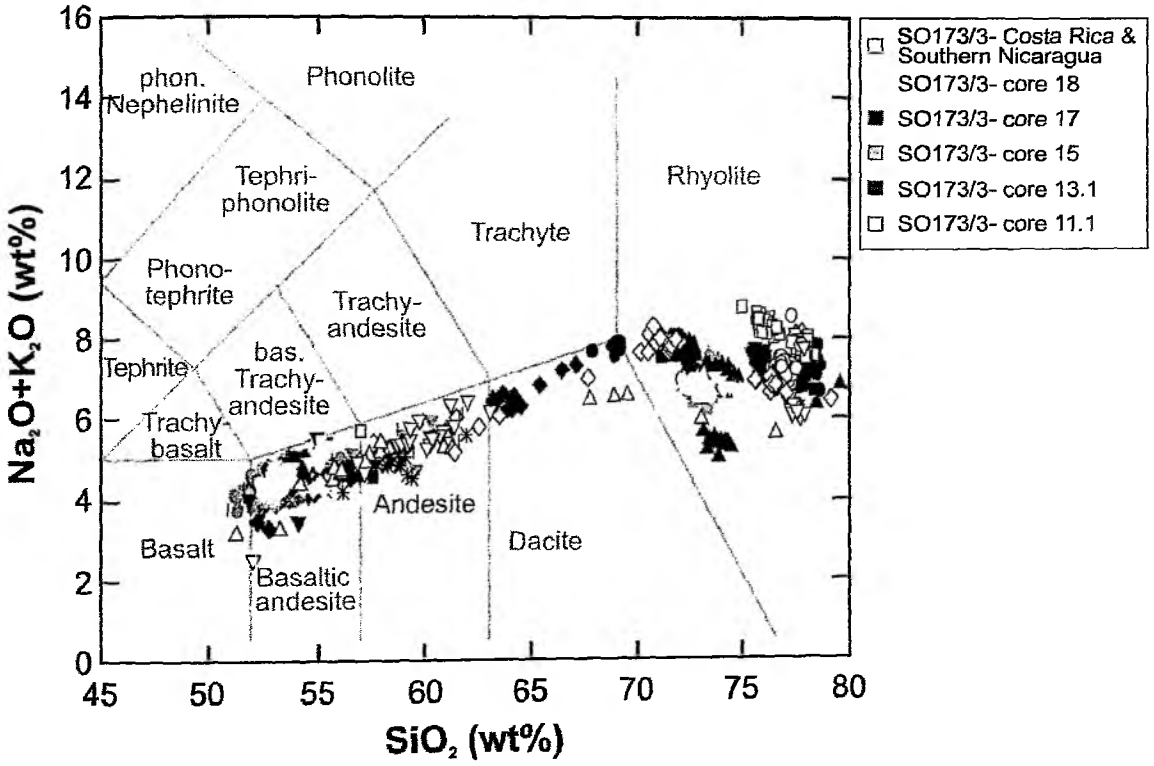

Fig. 6.6.1: TAS-diagram of marine tephras from cruise SO 173/3

field. The Magnetic susceptibility value of a natural sample is proportional to the volume fraction of magnetic minerals (Blum 1997). Through logging, the magnetic susceptibility of ashes can be closely linked to density values of marine ashes. Bulk slice samples are easily cut from ash layers with thicknesses in the cm-range whereas samples from very thin ash layers are usually mixed with sediment. Even primary fallout layers usually contain some biogenic and clastic debris. Thus Laboratory techniques need to be employed to separate the volcanic material before geochemical bulk analyses.

Petrographic and structural studies combined with geochemical analyses are the most powerful tools in marine tephrostratigraphic work. Compositional data, including mineral assemblages, mineral and glass compositions obtained by electron microprobe, as well as bulk rock chemistry, are used for correlations between marine and land tephras. Microanalytical methods eliminate the need for tedious mineral grain and glass shard separation as necessary for bulk analyses, unless prior enrichment is required when ash is dispersed in the sediment. Moreover, microanalyses of glass shards may allow to detect components of compositional zoning of magma chambers or of ash beds containing material from different eruptions mixed by reworking. Many volcanic deposits have distinct chemical characteristics at major element levels which can be determined by electron microprobe analysis of the glass shards. When variations in major elements are not sufficiently diagnostic, the trace element composition of glass shards can be determined by Laser Ablation ICP-MS or ion-probe (e.g. Clift and Blusztajn 1999; Ukstins Peate et al. 2003; Schmincke 2003). Potassium-bearing minerals are used for single-crystal $^{40}Ar/^{39}Ar$ dating at ages greater than 10^4 years. Dating of younger ash layers is based on constraints from the interbedded sediments, or ^{14}C-ages as determined from organic material of correlated tephra on land.

6.6.2.3 Results

Sediment cores were collected during R/V SONNE Cruise SO 173/3 by gravity coring offshore Nicaragua and Costa Rica between 9°11'N / 84°37'E and 12°00'N / 88°09'E on the lower continental

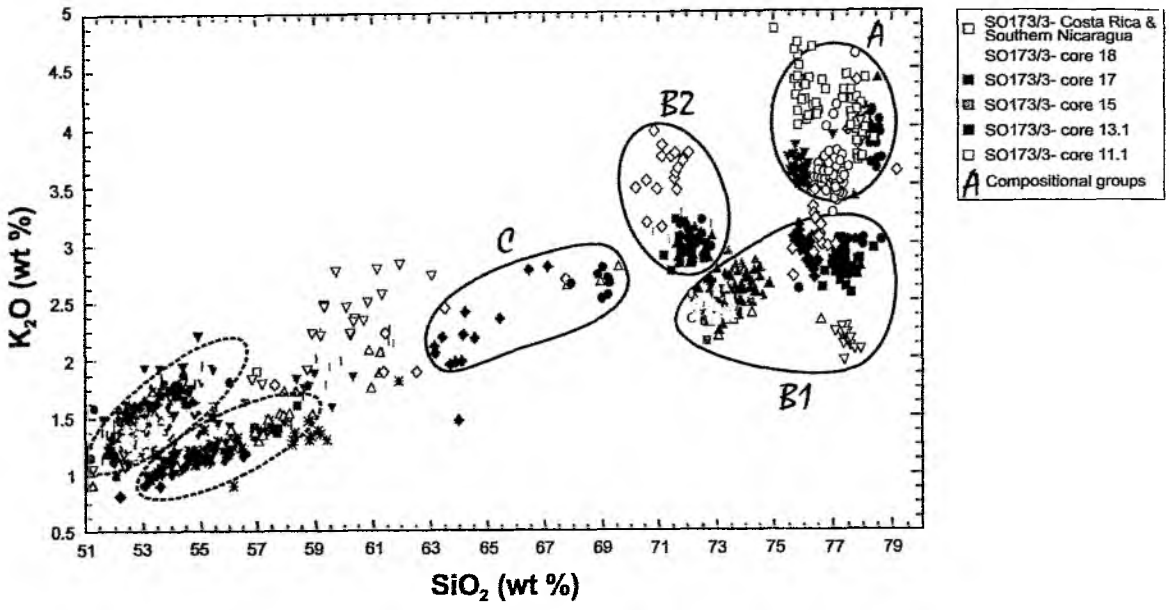

Fig. 6.6.2: Discrimination of magmatic composition groups with K2O vs. SiO2 diagram.

slope (1200 m water depth), and on the opposite flank of the trench (3300 m water depth), i.e. at distances of 200-350 km from the Central American Volcanic Front. Core lengths generally extended to 3.5-11 m below seafloor. Cores SO 173-11, SO 173-11.1, SO 173-18, SO 173-25, SO 173-35, SO 173-49, and SO 173-59.1 were situated at the Nicaraguan and Costa Rican slope and core SO 173-13.1, SO 173-15 and SO 173-17 were taken from the incoming plate, where average sedimentation rates are lower. Ten cores of SO 173/3 together contain 57 ash layers intercalated with terrigenous and pelagic sediments. The core logging shows, that the mafic ash layers are characterized by high magnetic susceptibility and high density values. Felsic ashes show low or negative magnetic susceptibility values and also high densities. Cores SO 173/3-13.1 and 17 have 13 and 12 ash layers respectively, contained within 5 or 2.5 m sediment recovered whereas the other cores taken in front of Nicaragua have an average of 7 ash layers in 2 to 11 m of sediment. The cores taken in front of Costa Rica only contain sporadic ash layers and are stratigraphically situated deeper in the cores.

Most of the ash layers are white to grayish pink or dark gray to pink light gray in color. From the petrographic analysis (Tab. 6.6.1) on board, 15 black layers of basaltic, 18 grey layers of intermediate or mixed and 24 pinkish-white layers of rhyolitic composition can be distinguished. Ash layer thicknesses range from 0.5 to 23 cm. Most of them appear to be primary fallout deposits but some are reworked. Discontinuous ash lenses occur in the sediment sequence as well as reworked pumice clasts. The contact between sediment and ash at the bottom of the ash layer is usually sharp, whereas the contact at top of the horizons frequently show a gradual change from ash to deep marine sediment. In some cores, thin ash layers have been disturbed by bioturbation. Additionally, admixtures of are frequent within terrigenous and pelagic sediments.

Microscopic examination of white ash shows mostly clear, colorless, volcanic glass shards. Dark gray ash layers, consisting predominantly of "smoked" shards and black vitreous glass, are also found in many of the cores. The typical grain size of the shards and pumice remnants in the ash layers varies in the range of medium silt to about coarse sand (<1000µm). The mineral assemblages comprise plagioclase, pyroxene, hornblende, olivine, and occasionally biotite in the most evolved felsic layers. Most of the glass shards in

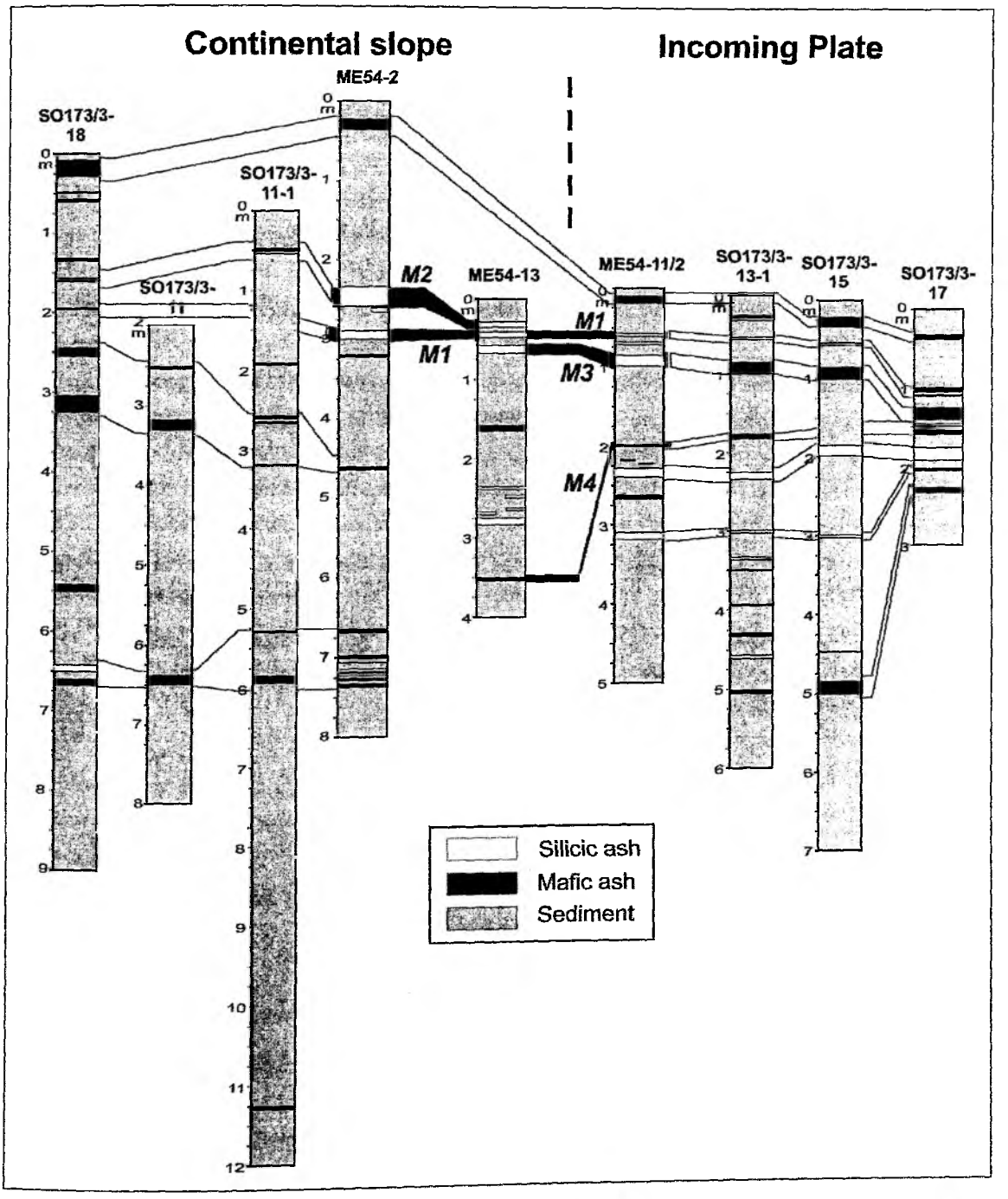

Fig. 6.6.3: Preliminary stratigraphic correlation of SO 173/3 cores with cores from METEOR 54/2 recovered in 2002. Correlations are based on petrographical investigations of ash layers performed onboard.

the basaltic layers have blocky shapes, are poorly to non-vesicular, and constitute up to 70 vol%. Glass-shard contents are high (>80 vol%) in the rhyolitic layers, and the shards have a highly vesicular, pumiceous texture of commonly elongated bubbles.

First preliminary results of major element analysis with electron microprobe yield compositions ranging from basalt to rhyolite (51-79 wt% SiO_2), measuring *c.* 1100 glass shards from 48 ash layers of 10 cores (Fig. 6.6.1). Silicic ashes can be divided into four compositional groups (Fig. 6.6.2). Group A ash is high-

silica rhyolite (76-80 wt% SiO_2), rich in potassium (3.5-4.7 wt% K_2O), and commonly biotite-bearing. Group B1 and B2 ash are calc-alkaline rhyolites (72-78 wt% SiO_2) that are commonly found in many arc settings. They have typical low potassiumcontents (2.0-2.7 wt% K_2O) contents in group B1 and high-potassium contents (2.7-4 wt% K_2O) concentrations in group B2. Finally, group C ash has dacitic compositions (63-69 wt% SiO_2). Overall, the chemical variations show a pattern consistent with fractional crystallization from a range of parental compositions as the major differentiation processes. These results are nearly similar to the analysis of the ashes from the METEOR M 54/2 cruise with the exception of group B2, which is mostly found in the slope area in front of Costa Rica. Two major differentiation trends can also be seen in the mafic ash layers are also recognized (Fig. 6.6.2) , which are inexistent in the results of the M54/2 cruise (Kutterolf et al. 2004, Soeding et al., 2003).

Similar to the results of the METEOR M 54/2 cruise, the first chemical analysis of the glass shards suggests that some of the ash layers are contaminated with material from older and stratigraphically deeper ash layers. The reworked ash material mostly appears in the form of rip-up clasts which can be diagnostically hardened compared to their host sediment or in lenses within the newly emplaced ash. We interpret intra-clasts and ash lenses as a result of mass wasting at nearby fault scarps that took place while a deposition of primary, new fallout ash through the water column was in progress. In some cases the reworking effect can be so strong that primary-like ashes can be originated. This has to be considered when correlations are made between the cores and the tephra on land. The first attempts to correlate the cores by means of stratigraphical, modal compositional and textural features show good correlations between the cores of the slope – including the METEOR M 54/2 cores – and on the other side between the cores of the incoming plate (Fig. 6.6.3) These correlations have to be verified by chemical analysis of the glass shards in the next step.

According the sedimentation rates, first preliminary assumptions can be made by these correlations using the ages of on-land tephras, their associated marine tephra layers and the differences in pelagic sedimentation between these marine ashes. Therefore, the average sedimentation rate of the incoming plate is *c.* 8 –10 cm per thousand years and increases up to 30-40 cm per thousand years on the slope area. First results also show, that there are different changes in the amount of sedimentation rates probably according to modified erosive and depositional processes.

6.6.3 TV-Guided Grab (TVG) Deployments

V. Liebetrau, H. Sahling

Five TV-grab stations were performed during SO 173/3 and 4. The locations, targets and recovery are summarized in table 6.6.2.

6.6.3.1 TVG 8 at Mound Quetzal

TVG 8 was towed up the southern slope of Mound Quetzal to the top area. Three grabbing attempts were abandoned as the grab could not be prevented from tilting. Finally, a collection of different carbonates was grabbed together with sediments and clam shells. Carbonate blocks with venting channels, chimney structures, downward layered carbonates, green dolomite pebbles with white matrix and coating, as well as fragile structures of active vent paths were recovered. The grab position was at the transition from consolidated carbonate platform to sediments with living clam shells as a tracer for active fluid venting.

6.6.3.2 TVG 27 at Mound Carablanca

TVG 27 was towed over the top area of Mound Carablanca. This area is characterized by a widespread occurrence of carbonates that are not significantly elevated over the seafloor and form a nearly continuous pavement. In between the carbonates there are sediment pockets with living vesicomyid clams. With TVG 27 this habitat was sampled. 2/3 of the grab was filled with relatively undisturbed sediments, carbonates and biota and 1/3 with water hat slowly ran out on deck. In one localized area within the grab about 50 living vesicomyid clams and two solemyid bivalves (*Acharax* sp.) were found. Below the clams there were blackish, soupy sediments with a strong sulfide odour. The porewater group did not want to squeeze these soupy sediments as they were afraid that the flushing of the grab could have altered the chemistry. However, as the clams reached exactly into this layers we believe that this are the fluid conduits. After the opening of the grab a mixture of black, soupy sediments, grey, sticky sediments and carbonates were looked through. The pore water group squeezed central parts of large chunks of the grey, sticky sediments. The carbonates showed a special feature of flowstone-like structures in open pore space near the sediment surface. Fine carbonate cementation of granulates with top-bottom criteria and dolomitic pseudomorphs were recovered. The observed structures imply active venting rather through a dispersed system than focussed through isolated and massive carbonate channels.

6.6.3.3. TVG 37 at Mound Morpho

TVG 37 was deployed close to the top area of Mound Morpho. It grabbed carbonates that were elevated about 1 m above the surrounding seafloor. One carbonate piece was caught between the jaws of the grab which therefore did not close completely. The carbonates were flushed with water during the ascent through the water column. Four pieces of carbonate came on deck and two of them resembled a structure with isolated vent channels. The recovered blocks showed a high degree of alteration, but some of the channels were coated with a thin skin of white carbonate as an implication for a recent, if probably reduced, vent activity.

6.6.3.4. TVG 90 at Mound 10

TVG 90 was deployed close to the top area of Mound 10 in search of specific biota communities accompanied by recent carbonate precipitation. It grabbed sediments with 1 living Acharax, several shell remnants and small carbonates with tube structures.

6.6.3.5. TVG 128 at Mound 10

TVG 90 was deployed close to the top area of Mound 10 in search of gas hydrate. Sediment with dense and heavy concentrical carbonate concretions, but without gas hydrate was grabbed. The concretions showed inclusions of wood and tube structures.

Table 6.6.1: Smear slide tephra samples from SO 173/3.

	Comment	Size	Glass cont. %	Crystal cont. %	Mafic/ felsic glass	Pumice fragments	Fluidal structures in pumice fragments	Crystals: ● = many ○ = abundant ? = few			
								Green hbl	px	Biotit	ol
SO173/3-11_255	A lot of altered clasts, mafic and felsic. The felsic ones are mostly altered, whereas the altered part of the mafic ones is only 20%. Plag with nice melt inclusions 5768 mafic, 5769 mafic with little elongated bubbles, altered 5770+5771, 5772+5773 altered felsic, group of felsic and mafic shards, overview 5779-5782	middle	50-60 40 maf 20 fels	10-20	50/50	Few mafic and abundant felsic	Some fluidal structures in mafic and elongated bubbles. Most of altered felsic shards have fluidal structures		● (aug, hyp)		?
SO173/3-11_563	Felsic layer, with a lot of plag (plag/heavy 80/20), nice glass shard only little altered Pics of felsic shards 5783+5784; 5785 elongated bubbles in felsic.	Fine-middle	50	40	15/85	abundant	In felsic and in mafic shards abundant; in felsic shards elongated bubbles	○	●		
SO173/3-11.1_48	Mafic ash, a few altered felsic and some fresh. Mafic mostly fresh. plag/heavy =50/50 Pics overview 5786+5787	Middle-fine	50-60	10	90/10		Mafic only with some mostly round bubbles		● (aug)		○
SO173/3-11.1_53	Felsic ash layer with a lot of small glass shards; most crystals are plag (plag/heavy: 90/10); pics 5842-5846	fine	80	20	10/90	abundant	Some fluidal structures but mostly only glass shards with typical y-structure; some elongated bubbles	?	●		?
SO173/3-11.1_187-191	Not very well exposed felsic ash, a lot of plag, (plag heavy:70:30). The bigger glass fragments are mostly altered. So is it really an ash?	Very fine	60	30	5/95	few	Only little small glass shards, only some y-structures and nearly no pumice and elongated structures	○	○		
SO173/3-11.1_261	Very nice mafic ash; a lot of spinell, only altered felsic shards, medium plag cont. (plag/heavy:50/50) Pics: 5847-5848	coarse	70	20	95/5	absent	Elongated bubbles, nearly scoria clasts. Some fluidal structures		●		○
SO173/3-11.1_318-325	Mafic-intermediate and felsic ash, both compositions are in the ash. Fresh material. Plag is the most common mineral (Plag/heavy: 80/20)	Fine-middle	50	30	50/50	absent	Nice y-structures; only a few elongated bubbles; no fluidal structures		●		○
SO173/3-11.1_1130	Mafic and felsic ash, both compositions are in the ash. Fresh and altered material. Plag is the most common mineral (Plag/heavy: 80/20)	fine	50	30	50/50	Few big	Only little small glass shards only some y-structures and one or two pumice clasts with tubular bubbles and elongated structures		○		○
SO173/3-13.1_13	Mafic; lot of glass an a lot of magm. Spinell, mostly mafic glass and altered felsic; altered /fresh: 70/30; Plag/heavy:80/20	Fine-middle	60	30	90/10	None	Most fresh glass shards with y, some fluidal structures (altered), some bubble remnants		● ti-aug, cpx		

SO173/3-13.1_32	Mafic; altered/ fresh: 50/50; Plag/heavy:60/40; Plag with melt incs; abundant magm. spinell	Fine-middle	70-80	10-20	90/10	Few felsic/abundant mafic	Glass shards mostly with y; some fluidal strucs in glass, not altered, some big shards with elongated bubbles and fluidal strucs (little altered)		● aug		o
SO173/3-13.1_43	Felsic, partly altered clasts; mafic strong altered; Plag/heavy:70/30; nearly no magm. Spinell; carbonated cemented?	Coarse	60	10	10/90	Many 50/50 structure/structureless	A lot of fluidal strucs; bubble relicts, elongated bubbles	?	● cpx, opx		
SO173/3-13.1_60	Felsic, partly altered clasts; Plag/heavy:90/10; carbonated cemented matrix	Fine-middle	30	10	5/95	Few	Most glass shards with y	o	●		?
SO173/3-13.1_89	Mafic and intermediate mixture; mix between more mafic and less mafic; altered more strongly; Plag/heavy:90/10; + abundant Apatite	Fine-middle	20	10	60/40	Some small each composition	Some y, some elongated bubbles	o	●		
SO173/3-13.1_100	Felsic, a lot of very small glass shards and some bigger fluidal struc pumice remants; 2 fractions (fine+middle); Plag/heavy:70/30; abundant magm. Spinell; very fresh ash; aug + ol with melt incs mafic	Fine+middle	80	10-20	10/90	Abundant-many with very elongated bubbles → Röhrenbims	In small fract. only y; clasts with a lot of elongated, tabular bubbles	?	● cpx, opx		o
SO173/3-13.1_130	Felsic and some mafic shards; Plag/heavy:90/10	Middle	60	10	20/80	Few-abundant	Mostly y, + some luidal strucs in bigger clasts	o	●		
SO173/3-13.1_181	Mafic, very fresh; Plag/heavy:70/30;	Fine	70	20	90/10	Few mafic, none felsic	Mostly glass without, some bubble remanants and y; some elongated bubbles		●		o
SO173/3-13.1_234	Mixed layer of felsic + mafic shards but altered more strongly;	Fine	40	20	80/20	Few - none	Round bubbles on shards; y-strucs, seldom elongated or fluidal bubbles		●		
SO173/3-13.1_300	Felsic, a lot of very small glass shards and some bigger fluidal struc pumice remnants; 2 fractions (fine+middle); Plag/heavy:95/5; abundant magm. Spinell; some altered mafic clasts, bigger clasts are more altered, little clasts very fresh; Plag with nice incs	Fine+middle	70-80	10-20	10/90	Abundant	Many y; pum with elongated bubbles; few with fluidal struc		●		
SO173/3-13.1_349	Felsic fresh ash, a lot of Plag, some mafic; Plag/heavy:95/5	Middle	80	15-20	20/80	Abundant	Nice fluidal and tabular and elongated strucs of bubbles		● (cpx, opx)		o
SO173/3-13.1_478	Mafic, only little altered but more intermediate composition?; abundant magm. Spinell; Plag/heavy:80/20	Fine-middle	50	20	80/20	Few	Only a few fluidal and elongated struc. In bubbles; abundant y		●		?
SO173/3-13.1_509	Mafic ash layer, little altered; a lot of plag; Plag/heavy:80/20	fine-middle	40	10	90/10	Few	Little clasts with fluidal strucs; mostly shards without strucs		●		?
SO173/3-15_23	Mixture of mafic and felsic shards; Plag/heavy:70/30	Fine	50	10-20	50/50	few	Abundant nice y and some clasts with nice bubbles		● (cpx, opx)		?
SO173/3-15_60	Mixture of mafic and felsic shards; Plag/heavy:60/40	Fine	40	10	50/50	abundant	Some fluidal strucs		●		

SO173/3-15_98	Very fine mafic + middle mafic shards; big clasts all with fluidal struics; small are very fresh; Plag/heavy:70/30; seems that are transition compositions; abundant magmatic spinell	Very Fine + Middle	60	20	70/30	abundant	Strong elongated bubbles and strong fluidal strucs in big clasts, small clasts without struc		● (cpx)		?
SO173/3-15_195	Felsic ash layer; fresh; Plag/heavy:90/10	Fine-middle	90	10	5/95	abundant	A lot of y-strucs; some pum. With nice fluidal strucs		●		?
SO173/3-15_498	Mafic layer, transition in composition from mafic to intermediate; two fractions; Plag/heavy:80/20	Fine	60-70	10-20	80/20	abundant	Abundant fluidal and elongated; a lot of y; and few round bubbles in matrix;		●		?
SO173/3-17_31	Felsic, fresh, Plag/heavy:90/10	Fine	70	10	5/95	Few-abundant	A lot of y; some fluidal	o	o		?
SO173/3-17_37	Mafic felsic micture, a lot of magm. Spinell; fresh/altered: 50/50; Plag/heavy:80/20	Fine	60	20-30	80/20	Few	Some elongated		●		o
SO173/3-17_42	Fresh felsic layer; probably a intermediate clast population too; 2 fractions; Plag/heavy:90/10	Fine + coarse	60-70	10	10/90	Abundant	Nice fluidal; a lot of y		●		?
SO173/3-17_53	Mixture between felsic and mafic + intermediate; a lot of magmatic spinell: Plag/heavy:90/10 All is fresh	Fine-middle	40	30	50/50	few	Some fluidal struc in mafic + felsic; little are without struc.; some y → overall mostly without strucs	o	o		?
SO173/3-17_106	Mafic; no felsic but some intermediate glass shards wich are fresh Plag/heavy:70/30	Fine	40-50	20-30	70/30	none	Only some round bubble remnants; only little bubbles; very dense shards → some y		●		
SO173/3-17_117	Mafic; no felsic but some intermediate glass shards wich are fresh Plag/heavy:70/30	Fine	50-60	10-20	70/30	Abundant	Only some round bubble remnants; only little bubbles; very dense shards → some y		●		?
SO173/3-17_136	Mafic; no felsic but some intermediate glass shards wich are fresh Plag/heavy:70/30	Fine	60-70	10-20	50/50	Abundant	Only some round bubble remnants; only little bubbles; very dense shards → some y		●		
SO173/3-17_147	Felsic fresh; Plag/heavy:90/10	Fine	70	10	20/80	Abundant	A lot of y; abundant fluidal	●	o		
SO173/3-17_160	Mafic; no felsic but some intermediate glass shards wich are fresh Plag/heavy:70/30	Fine-middle	60-70	10-20	60/40	few	Only some round bubble remnants; only little bubbles; very dense shards → some y; some elongated bubbles in bigger clasts		●		?
SO173/3-17_186	Felsic fresh; only the bigger are little altered; Plag/heavy:80/20	Middle	90	5-10	10/90	Abundant	A lot of nice y + abundant fluidal strucs and elongated bubbles	●	o		o
SO173/3-17_207	Felsic fresh; a lot of pumice remnants; Plag/heavy:80/20	Middle-coarse	80	5-10	10/90	A lot of	A lot of fluidal, elongated and tabular and y	●	●		
SO173/3-17-core	Mafic layer with a lot of magm. Spinell; very coarse scoria clasts; Plag/heavy:80/20	Very coarse	70	10-20	90/10	Nearly only	Only pumice/scoria clasts; some small fragments of dense glass; fluidal?; more little elongated clasts and bubbles; no fluidal strucs; only moderate bubbles content		● (cpx, ti-aug)		o
SO173/3-18_163	Mafic ash in carbonate matrix; little altered + some nice plag in same size wit a lot of incs; prob. Primary Plag/heavy:80/20	Coarse	30	20	80/20	No scoria are abundant	No fluidals; mostly dense glass with only a few round bubbles		●		

SO173/3-18_243	Mixture of fresh mafic and felsic glass; crystal rich; Plag/heavy:40/60	Middle-coarse	40	30	70/30	Few	Elongated bubbles in mafic; + fluidal strucs in felsic		● (cpx, opx)		o
SO173/3-18_251	Mafic layer; fresh; Plag/heavy:70/30	Fine-middle	50	30	90/10	None	Dense shards nearly no bubbles or bubble remnants		●		?
SO173/3-18_255	Two fractions of felsic ash; Plag/heavy:80/20	Very fine-fine + Coarse	80-90	10	0/100	Coarser are all pumice remnants with a lot of bubbles	In pim clasts strong fluidal strucs and elongated bubbles; in finer fraction y-strucs		● (cpx, opx)(Hypersthen)		?
SO173/3-18_307	Mafic and felsic mixture; Plag/heavy:90/10	Fine-middle	20	30	70/30	Abundant felsic and mafic	Mixture between dense, bubble-free shards and shards with round bubbles and shards with elongated bubbles and fluidal stucs (mafic + felsic)	?	● (cpx, opx)		
SO173/3-18_550	Mostly mafic glass shards; Plag/heavy:90/10	Fine-middle	10	20	80/20	None	Few, only bubble remnants with round bubbles. In felsic shards fluidal strucs		● (cpx, opx)		
SO173/3-18_650	Felsic ash layer; very fresh; a lot of heavy min crystals; Plag/heavy:70/30	Middle	90	10	5/95	A lot of (50/50 pum/glass stucs)	Abundant; nice elongated bubbles; a lot of y; tabul strucs are abundant	●	o		
SO173/3-18_666	Mafic / intermediate ash; a lot of heavy min crystals; Plag/heavy:60/40; a lot of magmatic spinell	Middle	60	10+10 spinell	50/50	Abundant	Mixture of nice strucs (fluidal and elongated clasts)		●	●	?
SO173/3-25_42	Mafic? More a concentration of minerals and base of turbidite; 50 % strongly altered	Middle	20-40	30-40	80/20	Few felsic	Felsic pum all with fluidal strucs; mafic mostly only round bubbles		● (cpx, opx)		●
SO173/3-25_138	Felsic ash layer; Plag/heavy:90/10	Middle	70-80	5-10	5/95	abundant	Mostly glass shards without bubbles; a lot of y; pum with strong fluidal strucs but plenty of bubbles	?	o	?	
SO173/3-25_143	Felsic ash layer with some mafic shards; Plag/heavy:80/20	Fine	60-70	10-20	15/85	few	Mostly y; and pum with strong fluidal strucs.	●	●		
SO173/3-35_80	Felsic-intermediate; fresh; Plag/heavy:90/10	Very coarse	90	5-10	5/95	A lot of with long bubbles	Very strong elongated bubbles in pum; clast are tabular; some y	●	●	?	
SO173/3-35_85	Felsic; fresh; a lot of heavy min crystals Plag/heavy:70/30	Fine	80-90	10-20	0/100	Few	Only glass shards with y; only a few bubbles	●	o		
SO173/3-36_0-7	Mafic; fresh; reworking is possible; Plag/heavy:70/30	Fine-middle	20-30	40	90/10	None	No fluidal strucs only round bubbles and remnants; mostly dense material	●	●	?	?
SO173/3-49_692	Felsic + mafic mixture Plag/heavy:80/20	Fine-middle	30-40	10	20/80	abundant	Small ones without strucs only some y; bigger mostly with fluidal strucs	o	●	o	?
SO173/3-49_640	Mafic/intermediate mixture; fresh shards; a small fraction lower than 50µ is abundant; a lot of heavy min crystals; Plag/heavy:50/50	Middle-coarse	50	20	60/40	Mostly	Abundant fluidal strucs + some elongated bubbles		●	?	

SO173/3-59_114	Intermediate – mafic – felsic layer; Plag/heavy:60/20	Fine-middle	60	20	30/30/30	Abundant	Fluidal and elongated strucs all over the compositions	o	●	o	
SO173/3-59_225	felsic layer; Plag/heavy:90/10	Fine	80	10-20	5/95	Few	Mostly dense; little glass shards without any struc; some y; the big ones have no fluidal but some elongated bubbles	●	o	?	
SO173/3-61.1_175	Felsic ash layer; Plag/heavy:80/20	Fine	40	20	20/80	none	Some round bubbles, but mostly dense glass	●	o	?	

Table 6.6.2: TVG deployments during SO 173/3&4.

Station No.	Target	Date	Lat	Long	Depth	Comments	Recovery
TVG 8	Mound Quetzal	6. Sept. 2003	11° 12.374' N	87° 10.775' W	1320 m		Carbonates, clam shells
TVG 27	Mound Carablanca	10. Sept. 2003	11° 16.46' N	87° 15.20' W	1430 m	No SSBL	Carbonates, living clams, sediment
TVG 37	Mound Morpho	11. Sept. 2003	11° 00.244' N	87° 00.475' W	1660 m		Carbonates
TVG 90	Mound 10	22. Sept. 2003	10° 00.3' N	86° 11.35' W	2278 m		1 living *Acharax*, shells & carbonates
TVG 128	Mound 11	25. Sept. 2003	8° 55.32' N	84° 18.24' W	1013 m		Sediment, carbonate concretions

6.7 Pore Water Geochemistry

E. Corrales-Cordero, B. Domeyer, C. Hensen, K. Nass, U. Schacht, K. Wallmann, U. Westernströer

6.7.1. Introduction

Investigations of the geochemical composition of pore waters provide information to investigate the forces and impacts driving redox and mineralization processes within the upper sediment column. During cruise SO 173/2 the pore water composition of surface sediments was investigated at more than 60 locations to characterize and quantify sediment diagenetic processes and fluid geochemistry along the active continental margin off Costa Rica. Concentration vs. depth profiles of pore waters were determined for major nutrients, total alkalinity, chloride, hydrogen sulfide, and methane to identify locations influenced by seepage and to assess the effect of methane formation and decomposition processes.

Below we first give a short overview on the procedures of sediment retrieval, pore water processing, and geochemical laboratory methods followed by some of the major results.

The major goals of the pore water geochemistry working group on SO 173/2 were to get an overview of the general pore water system within the slope sediments off Nicaragua (i.e. changes along the shelf to deep-sea transects) and to refine the knowledge on the geochemical characteristics of methane-rich fluids at a number of mound locations on the upper slope off Nicaragua and Costa Rica.

6.7.2. Shelf to Deep-Sea Transects (Ash Cores)

A total of six stations (SO 173/: 11, 11-1, 13-1, 15, 17, and 18) were sampled by gravity corer along two transects perpendicular to the coastline off Nicaragua (see Figure 2.3.1, chapter 2.3). The overall pattern for the whole area is that the mineralization intensity decreases from the upper continental slope into the deep-sea, which can be observed best for the parameters alkalinity, methane, and ammonia. Representatively, this is displayed for three stations in Figures 6.7.1-6.7.3. E.g. alkalinity levels decrease

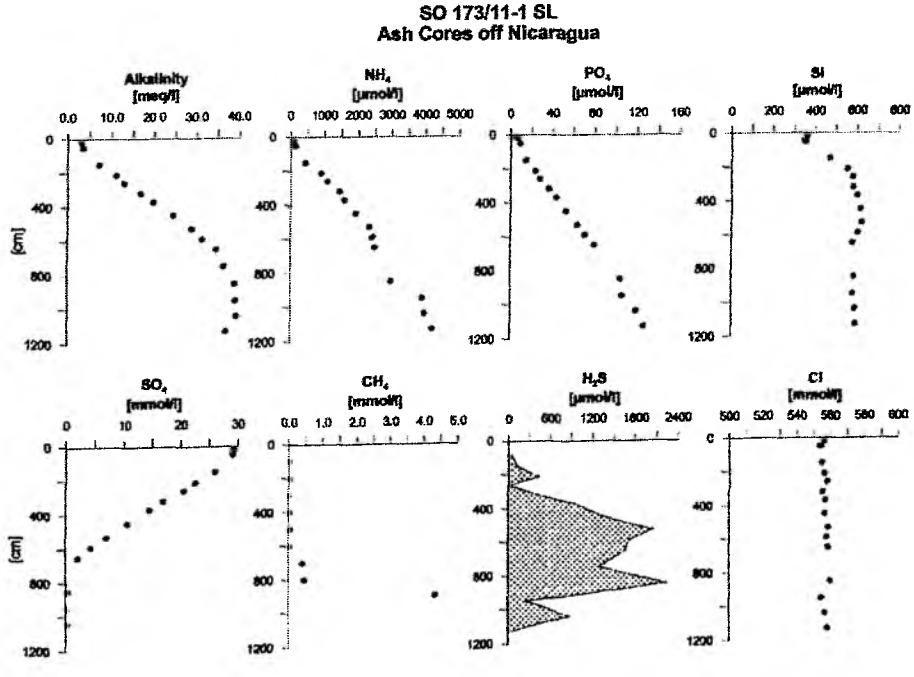

Fig. 6.7.1: Pore water profiles of gravity core SO 173/11-1.

from nearly 40 meq/l at depth at station SO 173/11-1 (Figure 6.7.1) to about 8 meq/l at the other two stations. Obviously, the major part of the reactive organic material is deposited at the upper slope, which is in contrast to findings of cruise M 54/2, suggesting that the downslope transport of sediment is not as important as off S-Nicaragua and Costa Rica.

6.7.3. Slides

Two slide areas were investigated and sampled during SO 173/3 off southern Costa Rica, the BGR/ GEOMAR slides (stations 59, 59-1, 61-1) and Quepos slide (stations 63, 64, 71, 73, 74; see location map on Figures 2.3.11, 2.3.15 and 2.3.16, chapter 2.3).

The cores in the BGR/GEOMAR slide area were taken in order to explore mechanisms of the slides in relation to the outcrop of the BSR and possible changes in gas hydrate stability at this site. Figure 6.7.4 shows the pore water profiles of core SO 173/59 taken below the headwall off the BGR slide. It shows a marked change in gradients for a number of parameters at about 1 mbsf, which is the boundary between the old, consolidated sediment below and more recent deposits on top. Pore water profiles will be used to constrain the timing of the slide events in this area and their importance for methane release into the water column.

An extensive sediment and pore water sampling program was carried out at the Quepos slide, where a large area below the headwall is densely covered by bacterial mats. Figures 6.7.5-6.7.7 show results obtained from two TV-MUC and one gravity corer deployment. All pore water profiles show that methane-rich and chloride-depleted fluids reach the sediment surface forcing intense anaerobic oxidation of methane (AOM) and carbonate precipitation. In contrast to the chloride-depleted fluids at the mound locations (see below), it is assumed that a freshwater outflow following a steep hydrostatic gradient from the mountainous hinterland is triggering the processes at this site. High flow rates are indicated by the

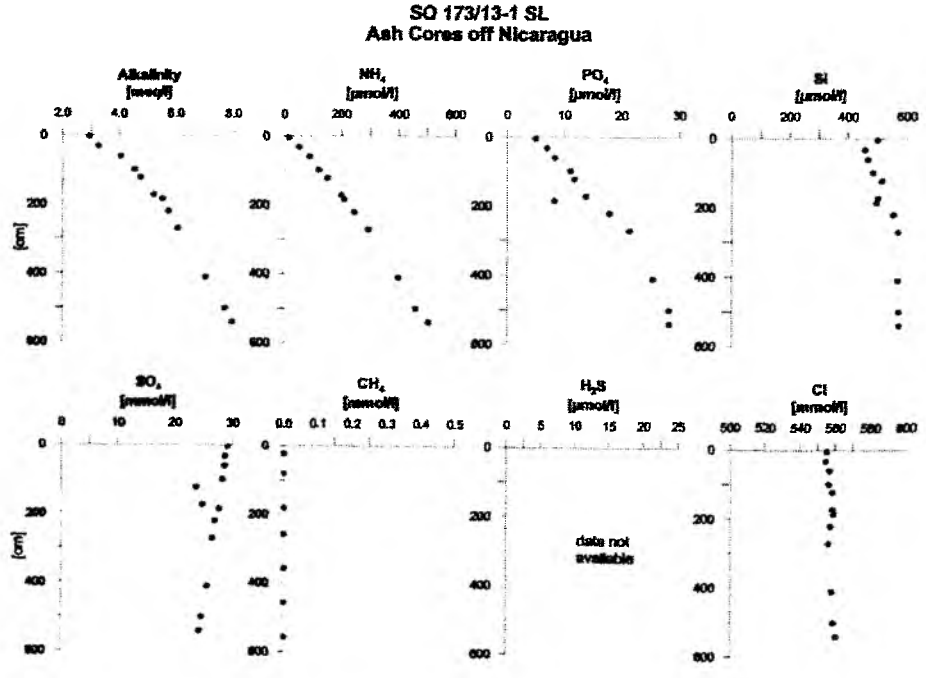

Fig. 6.7.2: Pore water profiles of gravity core SO 173/13-1.

steep concentration gradients close to the sediment-water interface (Figure 6.7.5) and by the uniformity of the profiles in the gravity core (Figure 6.7.7).

6.7.4. Mound Areas off Nicaragua and Costa Rica

6.7.4.1. New Mounds

The so-called "new mounds" comprise all mounds that had not been investigated in detail by use of seafloor observation and sediment sampling devices on cruises preceding SO 173. Cores for pore water investigations were taken at Mound Quetzal (stations 5-1, 6-1), Mound Carablanca (stations 26, 28, 29, 33, 34), and Mound Morpho (stations 38, 39). Sea floor observation by OFOS revealed only rare indications for active venting. In agreement with these observations, the mineralization processes are not significantly different from background diagenesis. Only one active vent site could be sampled at Mound Carablanca (station 34; Figure 6.7.8), where advection of slightly chloride-depleted, methane-rich fluids shifts the zone of AOM close to the sediment surface. Another slightly fluid-affected site was sampled by TV-MUC at Mound Morpho (station 39; Figure 6.7.9). Unfortunately, the venting activity at this site was too low for us to really obtain a significant amount of deep fluid.

6.7.4.2. Mound Culebra and Mound 10

Mound Culebra (stations 49, 52, 52-1, 81, 87, 95, 96, 97, 98) and Mound 10 (stations 40, 78) had been locations of cruise M 54/2 and 3 and were revisited in order to get pore water samples that would provide a purer fluid chemistry, preferentially by TV-MUC sampling. This goal could only be fulfilled partly since it was very difficult to obtain MUC samples from active sites. One example is shown in Figure 6.7.10a,b (stations 52a,b), which represents pore water results of two MUC cores from the same deployment. The difference is that a large specimen of a living Calyptogena was sitting on top of core 52a, whereas there were no active vent organisms in core 52b. Although there are significantly increased concentrations of

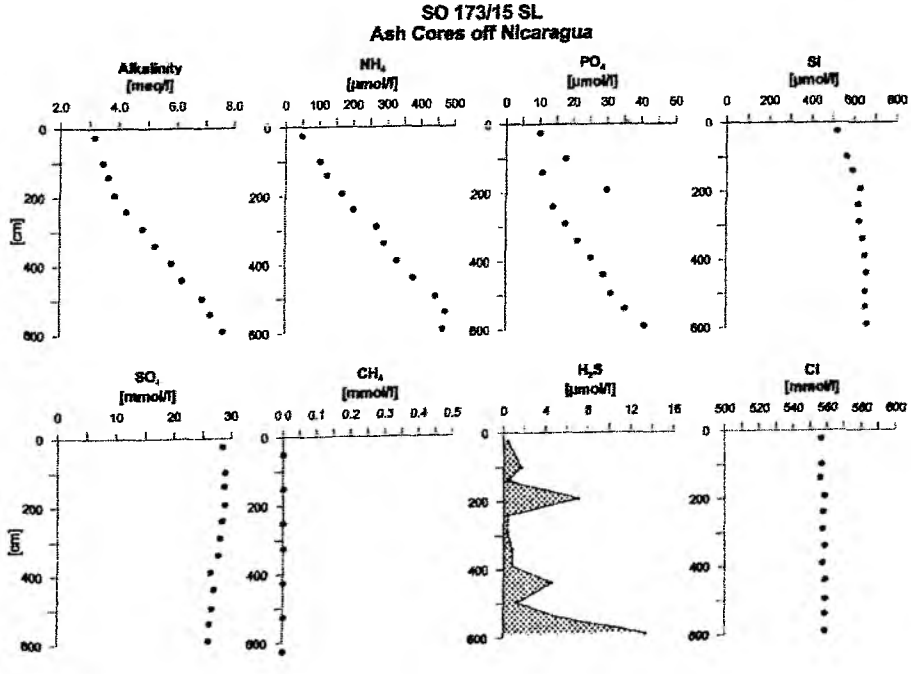

Fig. 6.7.3: Pore water profiles of gravity core SO 173/15.

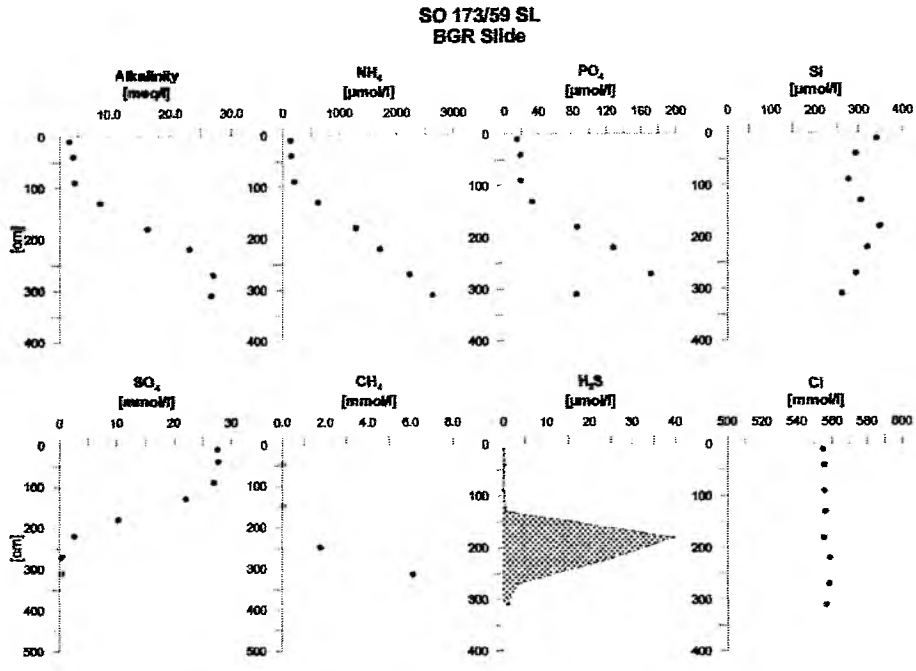

Fig. 6.7.4: Pore water profiles of gravity core SO 173/59.

methane and hydrogen sulfide (which are needed by Calyptogena) flow rates do not seem to be very high at this site, thus further information on fluid geochemistry could not be obtained. Some gravity corer deployments at Mound 10 (SO 173/ 81; Figure 6.7.11) and at the southeast prolongation of Culebra Fault (SO 173/: 49, 97; Figures 6.7.12 and 6.7.13) were more successful in this regard. Both locations show advection of chloride-depleted methane-rich fluids. The increase of the sulfate penetration depth from station SO 173-49 to SO 173-97 by about one meter may be due to the larger distance to the fluid conduit at the latter site.

6.7.4.3. Mound 10, 11 and 13

Mound 11 (SO 173/127) and Mound 12 (stations 110-1, 115, 118, 120, 135-1) had also been locations of cruise M 54/2-3 that were revisited. One core was taken from Mound 13 (station 117), a small elevation nearby. As expected from the results of M 54/2-3 these sites are characterized by active venting. TV-MUC SO 173-127 (Figure 6.7.14) was taken from a bacterial mat patch and shows nearly the same depth distribution of pore water profiles as observed at station M 54-138. Due to the high advection rates deep-seated, strongly freshened fluids reach the seafloor and accelerate AOM and related processes. The same type of fluid could be sampled at station SO 173-115 (Figure 6.7.15) at Mound 12, although flow rates are much lower in this case. Whereas only chloride depleted fluids were found at Mound 11 (on this cruise and on M 54/2-3), different fluid compositions were retrieved from Mound 12. Two examples for this are shown in Figures 6.7.16 and 6.7.17. These fluids do not show a chloride anomaly and have very high concentrations of hydrogen sulfide within the entire core depth. However, station SO 173-118 (Figure 6.7.17), also from a bacterial mat patch, indicates flow rates comparable to site SO 173-127 (Figure 6.7.14).

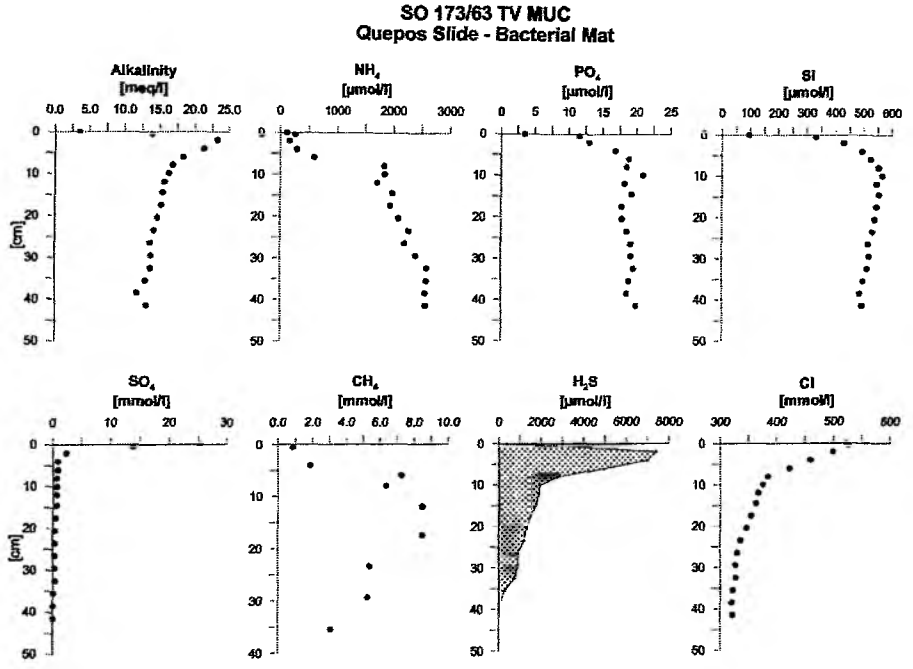

Fig. 6.7.5: Pore water profiles of TV-MUC SO 173/63.

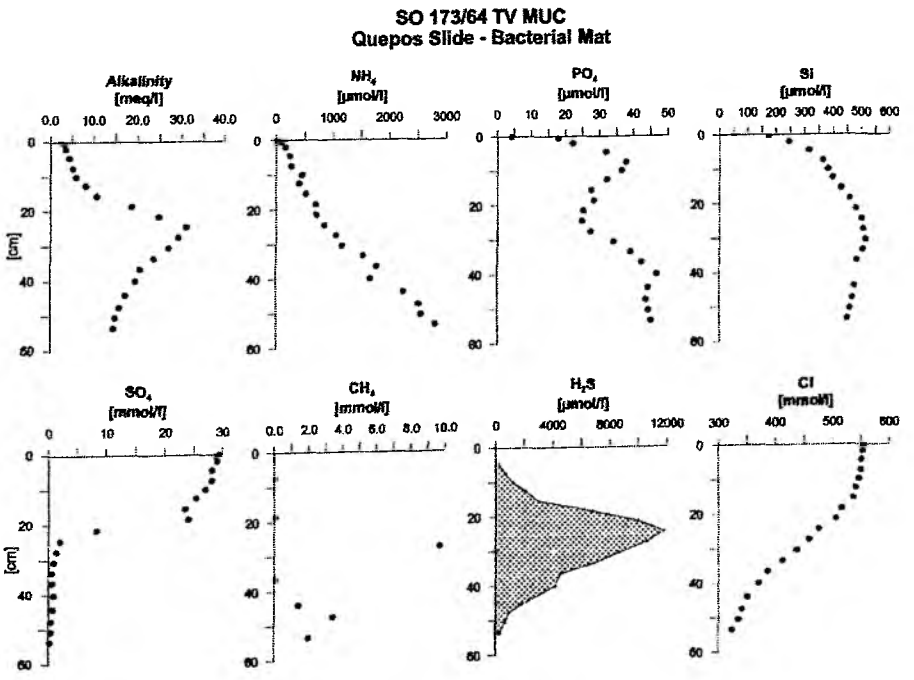

Figure 6.7.6: *Pore water profiles of TV-MUC SO 173/64.*

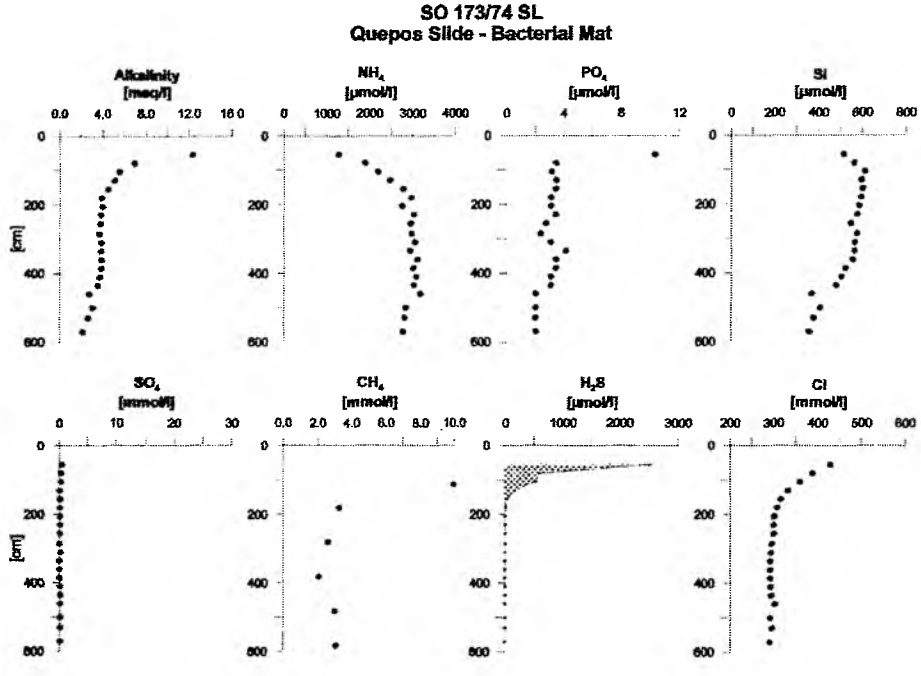

Fig. 6.7.7: Pore water profiles of gravity core SO 173/74.

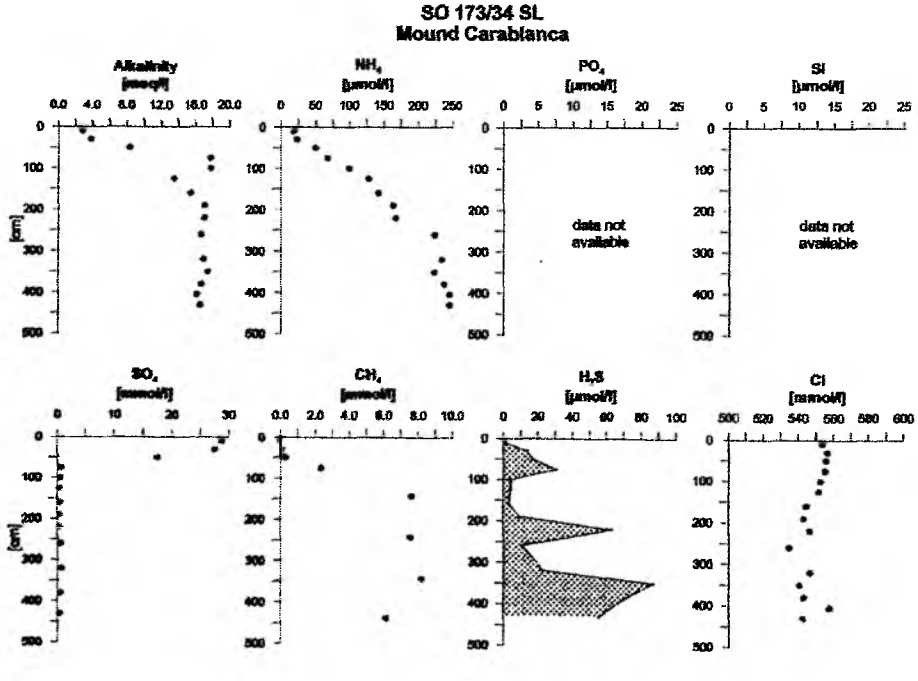

Fig. 6.7.8: Pore water profiles of gravity core SO 173/34.

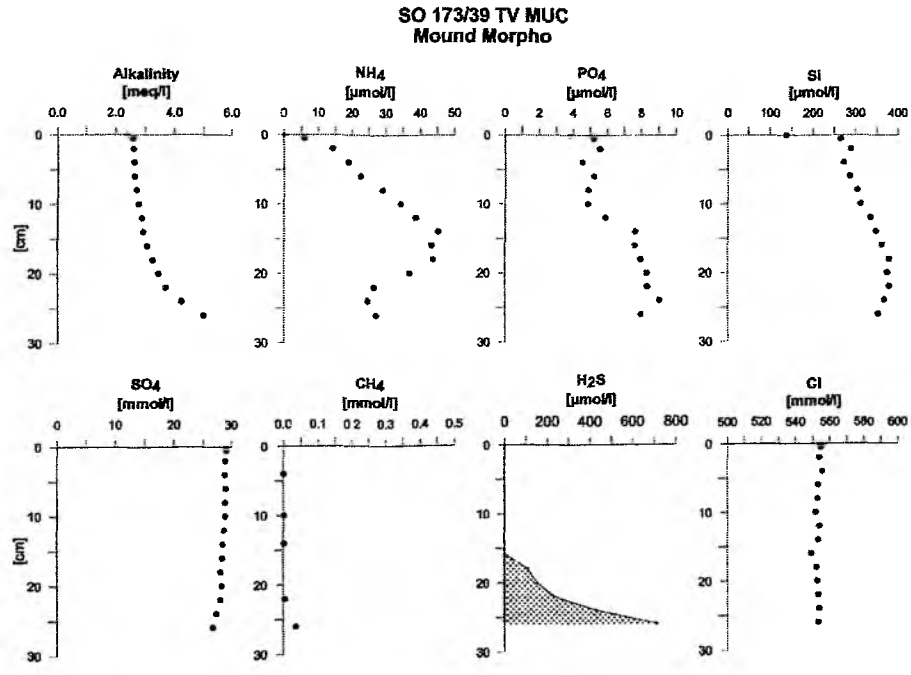

Fig. 6.7.9: Pore water profiles of TV-MUC SO 173/39.

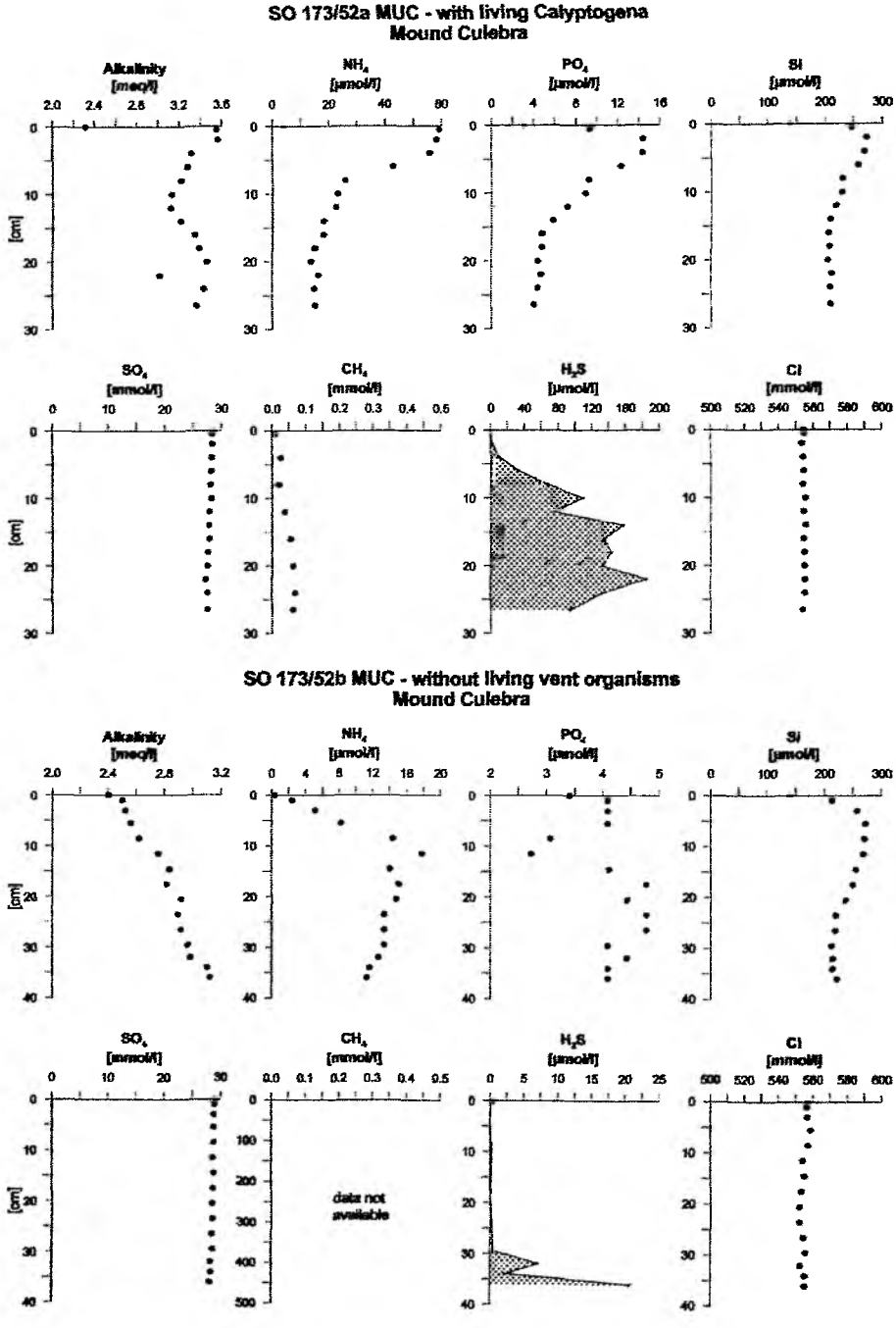

Fig. 6.7.10: Pore water profiles of TV-MUC SO 173/39. (a) with living Calyptogena on top, (b) without visible vent organisms.

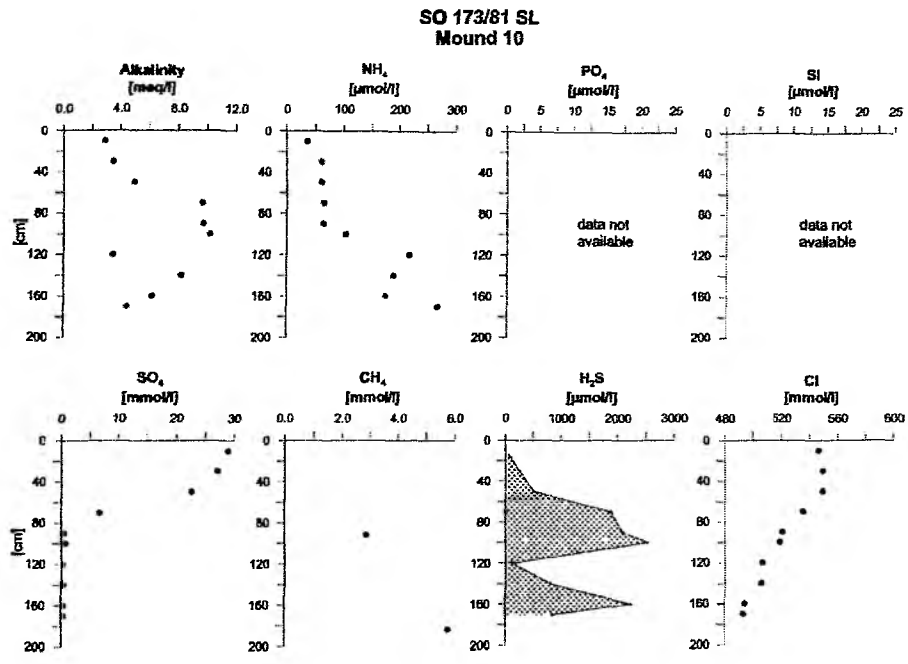

Fig. 6.7.11: Pore water profiles of gravity core SO 173/81.

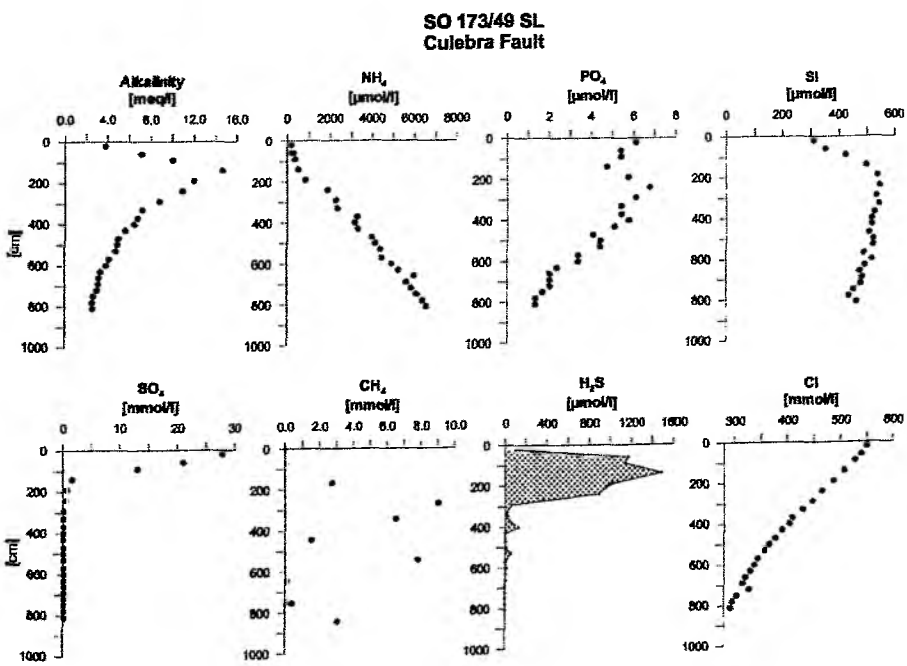

Fig. 6.7.12: Pore water profiles of gravity core SO 173/49.

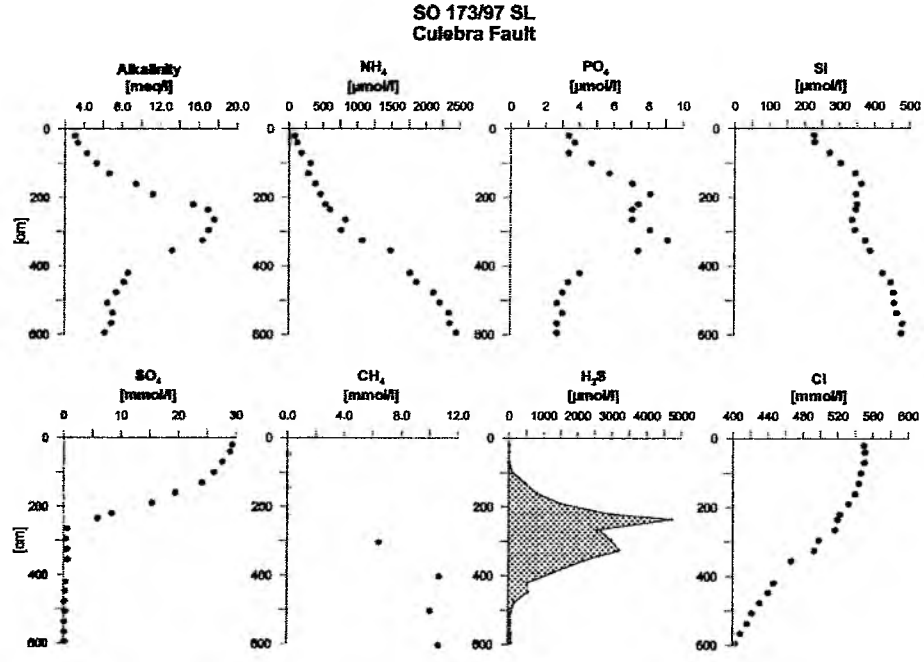

Fig. 6.7.13: Pore water profiles of gravity core SO 173/97.

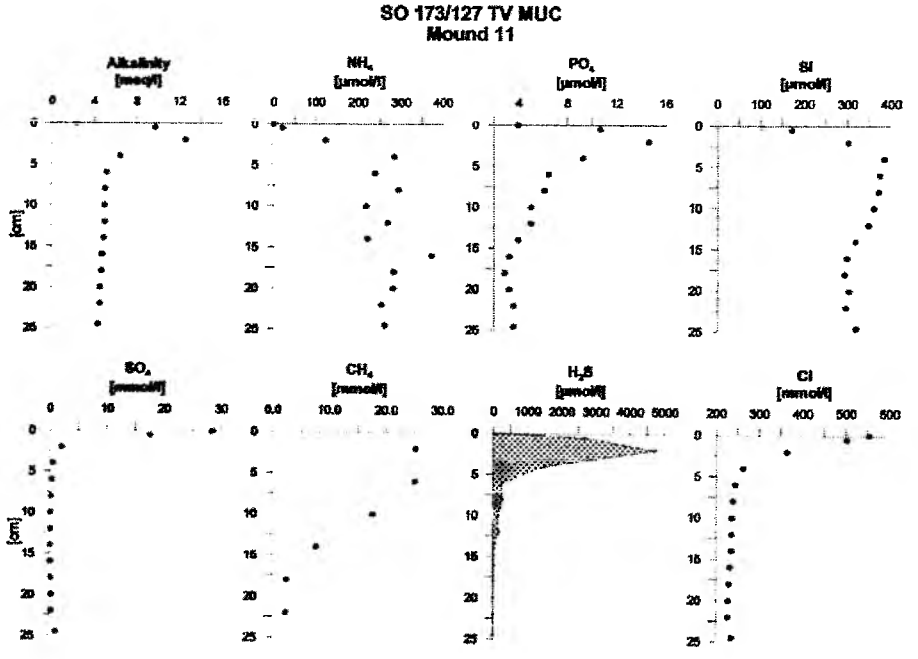

Fig. 6.7.14: Pore water profiles of TV-MUC SO 173/127.

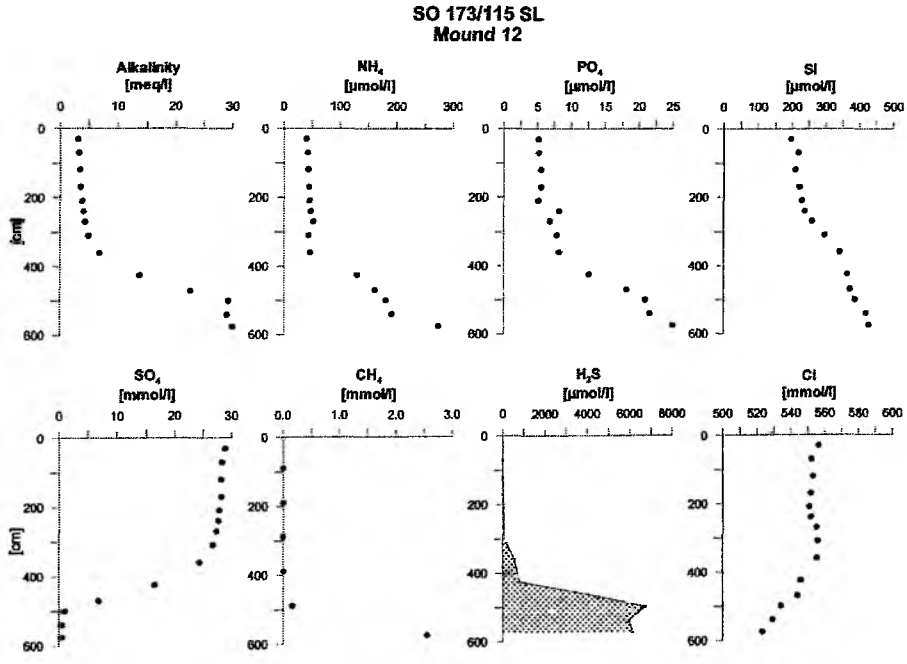

Fig. 6.7.15: Pore water profiles of gravity core SO 173/115.

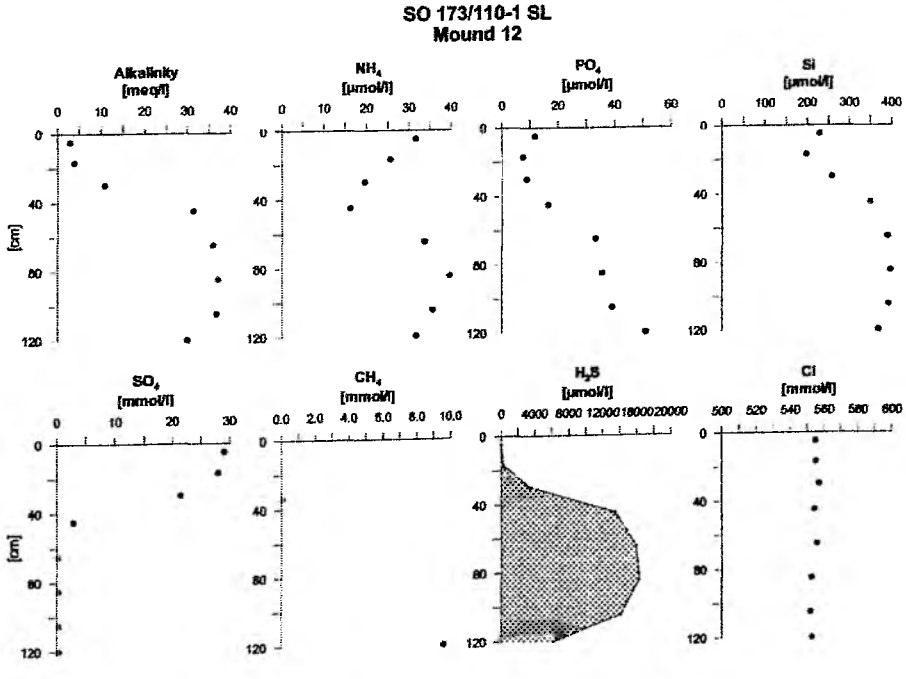

Fig. 6.7.16: Pore water profiles of gravity core SO 173/110-1.

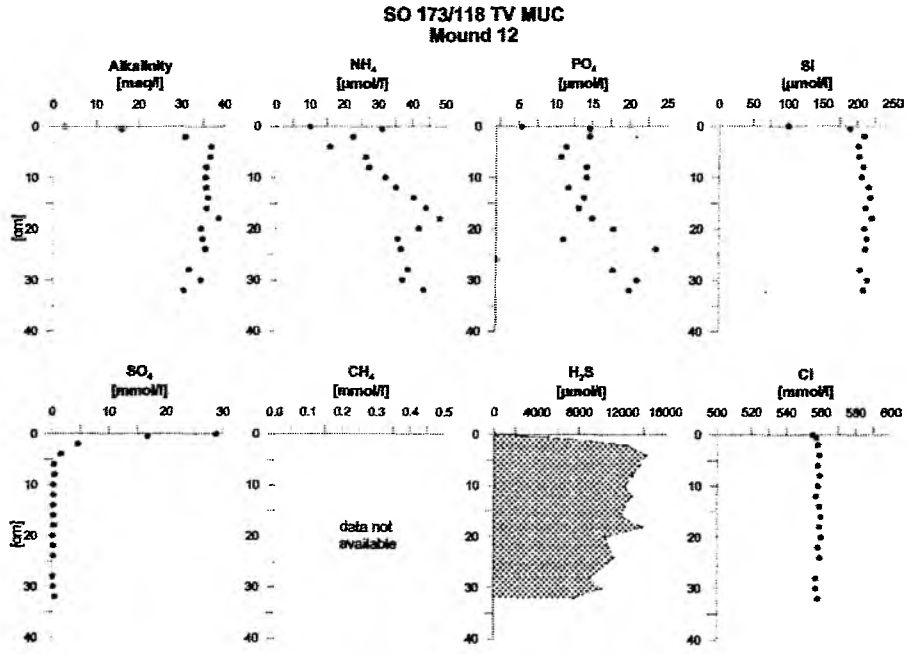

Fig. 6.7.17: Pore water profiles of TV-MUC SO 173/118.

6.8 Water Column Studies

S. Mau, G. Rehder, K. Stange

6.8.1 Introduction

The investigation of methane in the water column provides valuable insight in the processes of dewatering at active continental margins, because methane belongs to the cycled key components. Methane injection into the water column is just one process of the carbon cycle at active seep sites. Due to its relatively short lifetime and its generally low background in deep waters this injected methane is ideally suited to locate currently active vent sites and the dimensions of the generated methane plumes. Methane concentration in the water column and investigations of its isotopic composition will yield information about the formation and further development of it in the water column.

The results of the cruises SONNE 163-2 and METEOR 54-2/3 showed that four mud extrusions, two slides, and Jaco Scarp are active seepage sites. Methane plumes above Mound Culebra (a mud diapir) and Mound 12 (a mud volcano) have been mapped in detail and agree with seafloor observations by OFOS. That is, methane anomalies occur above areas covered by vent fauna. In the vicinity of Jaco Scarp the source area of a widespread methane anomaly was located at the NW edge of the slide and CH_4 distribution has been investigated and mapped throughout the scarp. Moreover, it could be shown that slides at water depths of 400-600 m are also actively venting, in this connection the latter depth correlates with the upper level of the stability field of gas hydrates.

After having located cold seeps and mapped methane plumes in different geological settings (mud extrusions, scarps, slides) in 2002, we put more emphasis on the following points during cruise SO 173-3/4:

- Investigation of mud extrusions which are situated offshore Nicaragua to extend our studies of mud extrusions along the continental slope of Central America. Stations offshore Nicaragua were chosen from results of OFOS observations and DTS raw data.
- Collection of physical, oceanographic data at known vent sites in addition to water sampling along transects which are positioned perpendicular to current flow. ADCP data from cruise METEOR 54 in 2002 indicated bottom water velocity and direction. The data of current meters/ADCP and CH_4 concentration will be used to calculate excess methane at these seepage sites.
- Examination of vent signs at slides which are located at the upper level of the stability zone of gas hydrate.
- Analysis of CH_4 concentration at revisited locations to observe variations with time.

6.8.2 Mud Extrusions Offshore Nicaragua

Three mud extrusions were investigated offshore Nicaragua (Fig. 6.8.1) in order to continue the mound survey along the Pacific continental margin of Central America. In 2002, mud extrusions or mounds were observed and sampled offshore Costa Rica. The results are now to be compared and extended into the new area. The new mud extrusions are located at depths ranging from 1430 m to 1230 m at a distance of about 33 km to the Central American trench. For a better understanding and distinction between the single mud extrusions they are referred to as Mound Carablanca, Mound Quetzal, and Mound Iguana (from north to south). At all extrusions signs of active venting have been found.

Water from atop Mound Carablanca was investigated using the CTD/rosette and the BWS. The results indicate venting of CH_4 in fluid form with values increasing towards the seafloor (Fig. 6.8.2). The

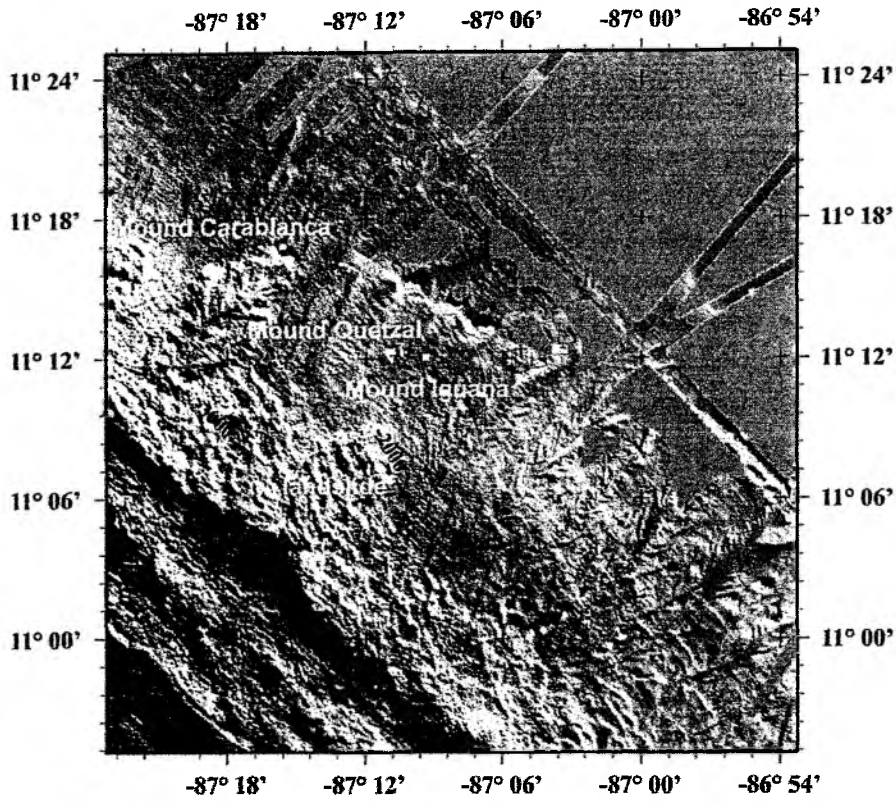

Fig. 6.8.1: Bathymetric map showing mud extrusions and a slide sampled offshore Nicaragua.

lowermost sample taken by the CTD/rosette reaches a value of 4.3 nmol/l whereas the bottom water samples show values as high as 24.2 nmol/l (Fig. 6.8.2). The former originates from about 9 m above ground and the latter was sampled only centimeters from the seafloor. Thus, methane concentration strongly decreases in the first few meters above ground.

The station at Mound Quetzal was located in the area of a slump which is positioned SE of the mound. CH_4 concentration increases with depth reaching a maximum of 31.5 nmol/l at a depth of 1345 m (17 m above seafloor), and decreasing again towards the seafloor (Fig. 6.8.2). Therefore, no bottom source was found at this location, but the source area could be located along the head wall of the slump. Background values of 1-2 nmol/l were measured at 1325 m and atop which is 37 m above ground and about 12 m above the top of the mud extrusion. At a water depth of 1340 m a value of 15.7 nmol/l was found, this is about the depth of the rim of the headwall. Hence, it seems as if the top of the mud extrusion does not emit any methane.

Mound Iguana was investigated because of its strong backscatter anomaly indicating abundant carbonates. But the methane concentration in the water above the mound is low, ranging between 1 and 2.4 nmol/l with a slight enrichment in the samples closest to the ground (Fig. 6.8.2). These samples were taken 19 to 21 m above seafloor. The results from Mound Carablanca show clearly that most methane becomes diluted and/or oxidized in the first few meters above ground. Hence, a further increase of CH_4 concentration towards the ground at Mound Iguana can not be excluded.

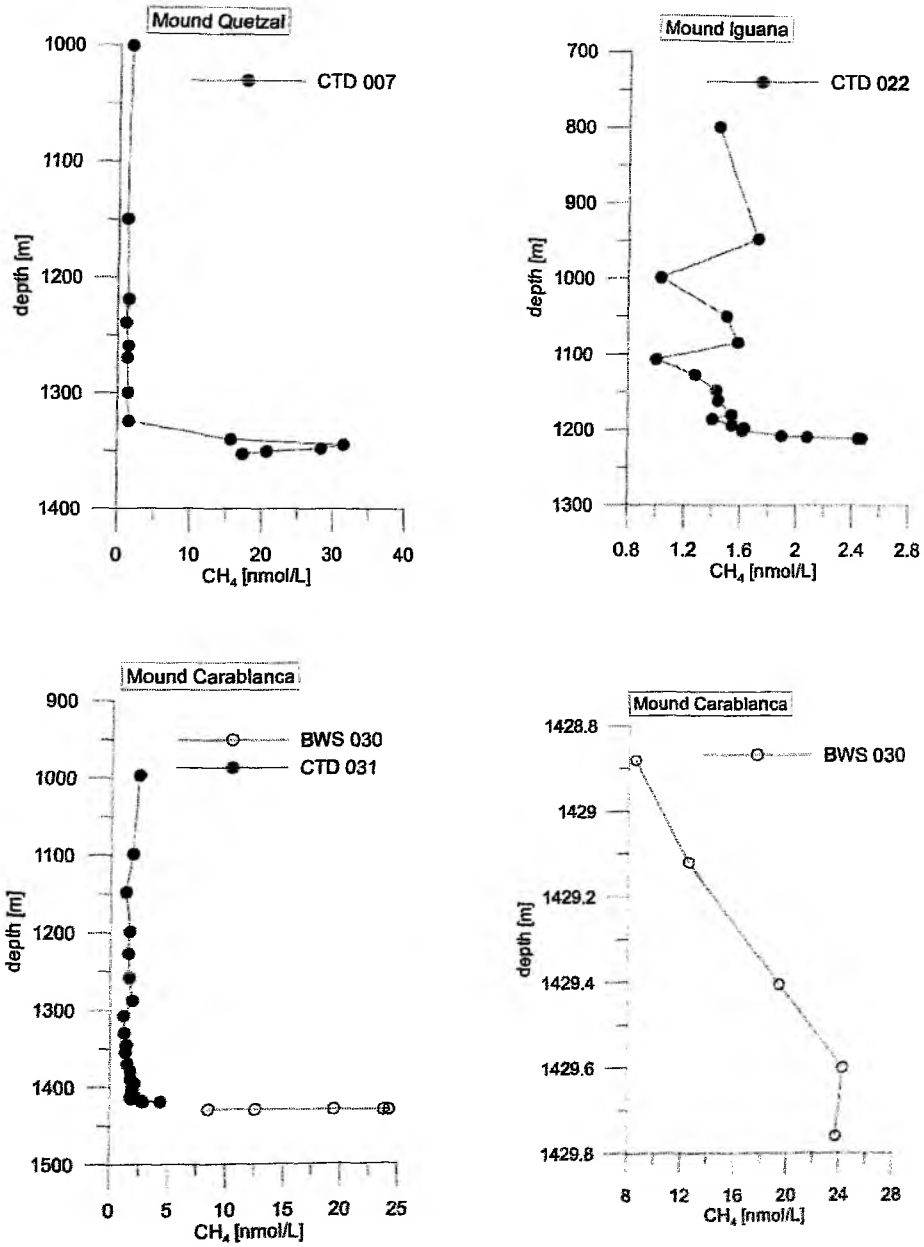

Fig. 6.8.2: *CH_4 concentration in the water column above mud extrusions offshore Nicaragua. Bottom water samples (BWS) and CTD/rosette samples at Mound Carablanca are collected at the same location. The diagram in the lower right represents the BWS data of Mound Carablanca on a larger scale.*

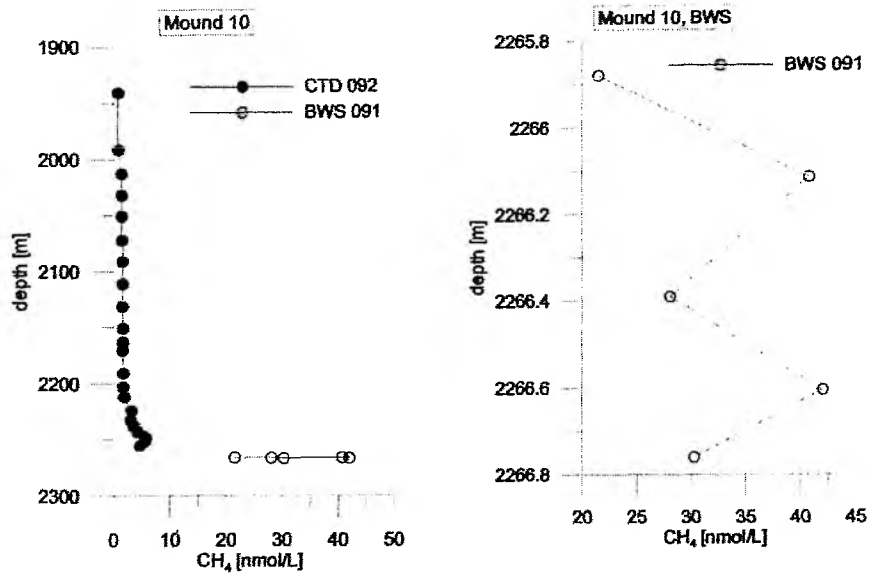

Fig. 6.8.3: CH_4 versus depth profiles at Mound 10. Bottom water samples (BWS) and CTD/rosette samples were collected at the same location (10°0.47 and –86°11.44). The diagram on the right represents the BWS data on a larger scale.

6.8.3 Mud Diapir - Mound 10

Bottom water and the water column were sampled at the same location at Mound 10 as during cruise METEOR 54-2/3. Even though data of the water column above Mound 10 indicate a decline of vent activity (see 6.8.6 Time variability), the bottom water is enriched in methane (Fig. 6.8.3). CH_4 concentrations vary between 42 nmol/l and 21.5 nmol/l at 40 cm and 112 cm above ground, respectively, that is one order of magnitude higher than the regional background of 1 to 2 nmol/l. The decrease from the bottom water values to 4.7 nmol/l at 5 m above seafloor (lowermost sample by CTD/rosette) suggests that the methane is strongly diluted and/or oxidized in the first few meters above ground.

6.8.4 Methane and Current Flow Measurements at Mound Culebra, Mound 12, and Jaco Scarp

Three transects directed from NE to SW were carried out at Mound Culebra (Fig. 6.8.4). Two of them consist of three stations, and the third of two stations at which the water column was sampled from about 10 m above ground to 1300 m. Methane concentrations were only slightly enriched with values of 1-4 nmol/l compared to the regional background of 1-2 nmol/l except for two profiles (Fig. 6.8.5). These showed methane values of up to 7 nmol/l and 12 nmol/l and are situated to the south and southeast of the mud diapir, respectively. However, these concentrations were measured at 107 m and 39 m above seafloor, and the values decreased towards the ground indicating no bottom source at these locations. Furthermore, revisited stations point to a decline of vent activity over the last year (see 6.8.6. Time variability). Obviously venting shifted from the top of the diapir to its south-eastern side. If the fault striking NW-SE is the pathway for mud and fluids, the fault could have been activated closing old fluid pathways and opening new ones.

Flow measurements were carried out at stations SE and NW of Mound Culebra using a 75 kHz ADCP attached to a lander device and current meters deployed over a period of 2 days. The data from the ADCP indicate a current direction to the NNW at depths from 20 to 100 m above seafloor and an average

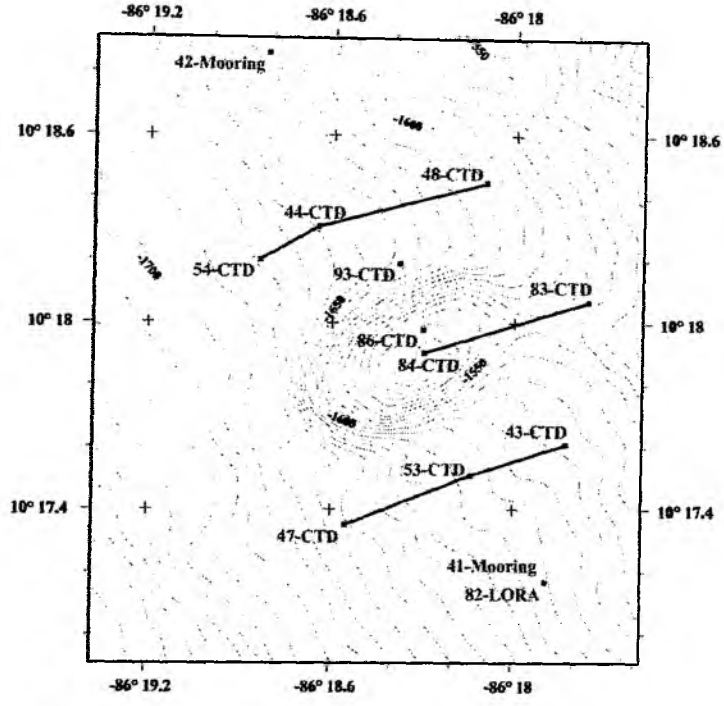

Fig. 6.8.4: Bathymetric map of Mound Culebra with station. Locations where moorings were deployed at the luff and lee sides of the mound and the transects are oriented perpendicular to the flow direction as suggested by ADCP data collected in 2002. CTD 86 and 93 are revisited sites.

current speed of 3.8 cm/s (Fig. 6.8.6). Data of current meters from about 10 m above ground show a NW-ward flow at the station SE of the mound, twisting with hardly any movement at the station NW of the mound (Fig. 6.8.7). Hence, the SE side is the luff and the NW side the lee of the mound and the transects are oriented perpendicular to the current direction. Beyond 100 m the current direction turns to the SE as illustrated by ADCP and current meter data (Fig. 6.8.6 and Fig.6.8.7).

At Mound 12, which was the most active mud extrusion investigated in 2002, we measured CH_4 concentrations along two transects directed from NE to SW again (Fig. 6.8.8). Like at Mound Culebra, the transects consist of three stations each and water from about 5-10 m above the seafloor to 850 m was sampled and analyzed. To save precious time, we took 12 water samples at e.g. station 111a, then went to the new location (in this case 111b) while towing the CTD/rosette and started sampling again. This operation could only be accomplished due to the short distances between the locations. Methane concentration increased towards the ground at each of the sites ranging from 7.5-13.5 nmol/l (Fig. 6.8.9). Apart from that, a second methane plume was found to be centered at water depths of 950-975 m at the stations of the southern transect and the CH_4 profile at station 131 shows an enrichment of 21.1 nmol/l at 873 m. The other two stations of the northern transect indicate bottom sources of methane at these sites, but no further anomalies were observed in the water column above. In bottom water (BWS 112) sampled SW of the mound we measured 20.6 to 29.4 nmol/l. In summary, venting at Mound 12 occurs in an area of ca. 650 m in diameter, thus in a much larger area than previously assumed.

Flow measurements of bottom water were taken by an ADCP attached to a lander device SW of Mound 12 (FLUFO in Fig.6.8.8). Like the results from 2002 the new data indicate a flow towards the NW from ca. 1-8 m above ground (Fig. 6.8.10). In 2002 the velocities ranged from 5.2 to 6.8 cm/s at 4 and 7 m,

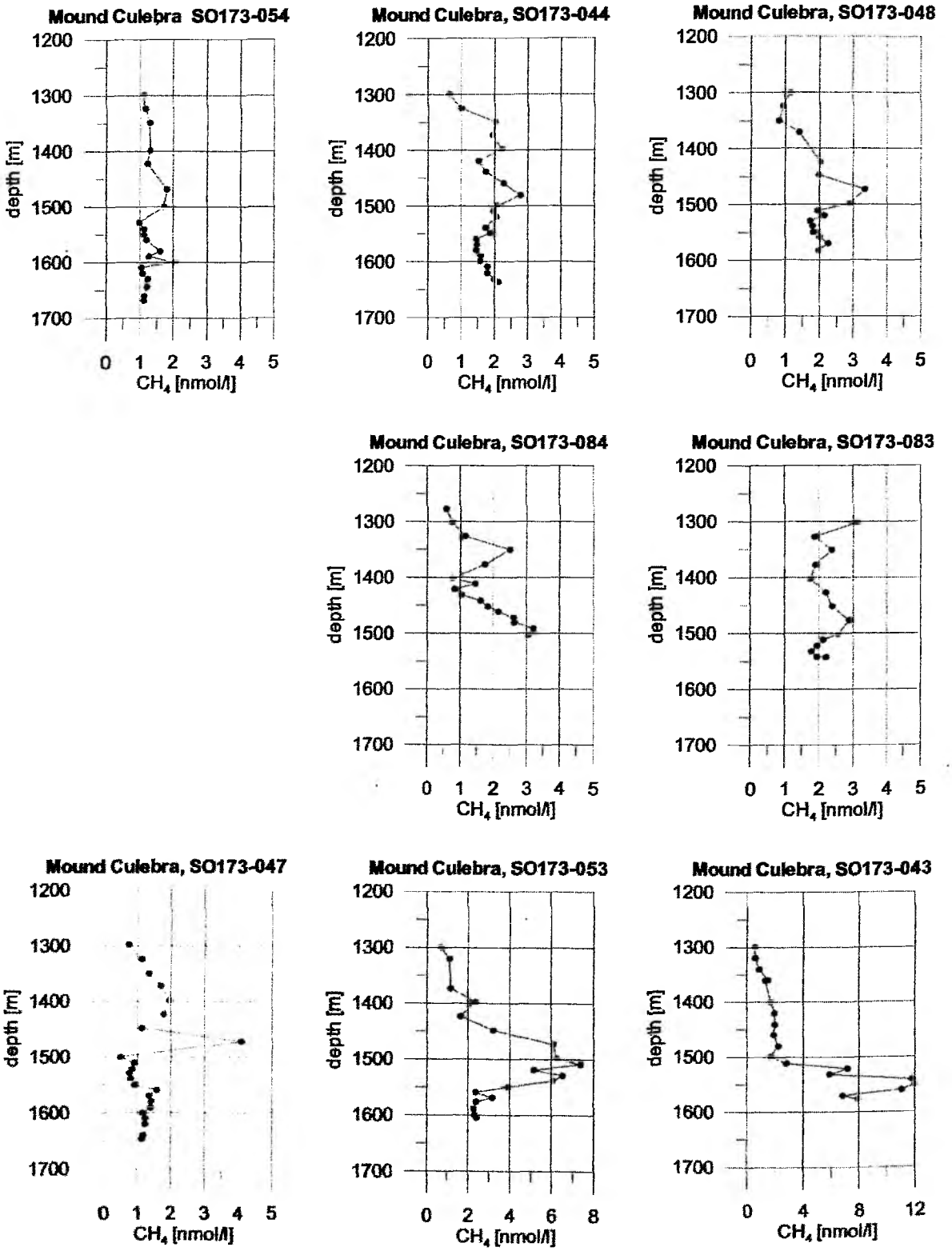

Fig. 6.8.5: Mound CulebraCH_4 profiles of transects directed from SW (left on page) to NE (right on page). The upper three profiles are from the northern transect, the two in the middle are from the one crossing the mound, and the lower one from the southern transect (Fig. 6.8.4). Note different scale of diagrams SO173-053 and SO173-043 at which the highest methane concentrations have been observed of the mound.

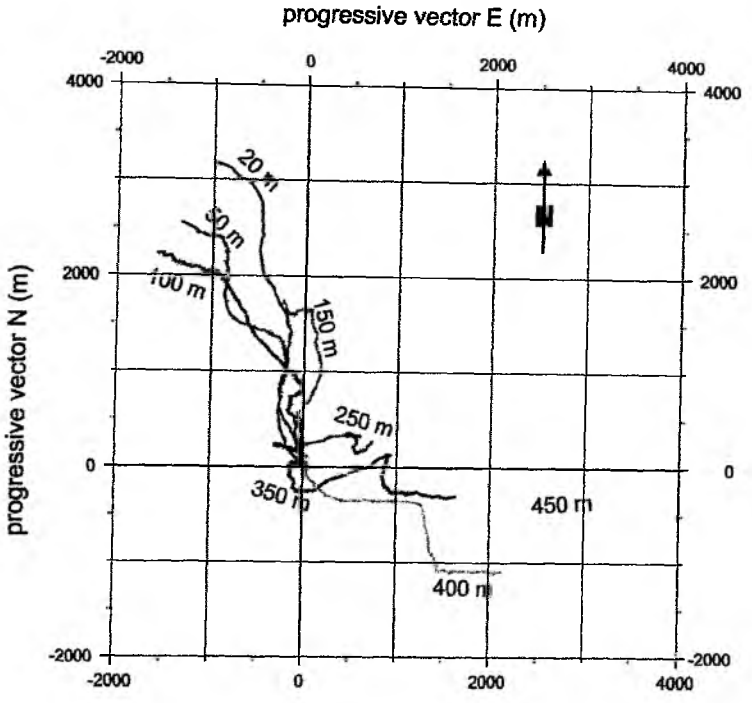

Fig. 6.8.6: Progressive vector plots of ADCP data at depths indicated above ground at Mound Culebra. Measurements were taken from 03/09/20 03:27 to 03/09/21 22:31 indicating a north-west current at 20-100 m above seafloor turning to a south-east current at 350-450 m above seafloor.

respectively, whereas in September 2003 the velocity was 2.6 and 3.8 cm/s at 1 and 8 m. A 75-kHz ADCP was positioned between Mound 12 and Mound 11 to investigate the current velocity and direction at 20 to ca. 450 m above seafloor. These results show a great diversity (Fig. 6.8.11). At 20 m above ground, the flow is directed to the SW probably due to topography. Then the current flows S at 50 m, turning SE at 100 m and W at 175 m. At 200 m, the current flows to the NW. This could be related to the phenomena of the Ekman spiral. Current meter measurements from station 104 (Fig. 6.8.8) located NW of the mound at 10 m and about 120 m above seafloor both indicate a final SW-ward movement even though the flow was directed to the SE at 10 m above ground in the first half of the deployment period of 3.5 days (Fig. 6.8.12). Still, this agrees well with the ADCP data from the other side of the mound.

Two sites in the vicinity of Jaco Scarp were reinvestigated during R/V SONNE cruise SO 173/4. One is situated at the edge of the slide and the other at the SE rim (Fig. 6.8.13). Methane concentrations had changed at both sites over the last year, but the plumes observed are centered at about the same depth as in 2002 (Fig. 6.8.14). CH_4 anomalies were found at 1835 m with 64 nmol/l and at 1724 m with 110.8 nmol/l at the station at the edge of the slide. Values of 1 to 2 nmol/l, the regional background, were measured at 1377 m. In contrast to the CH_4 concentrations of last year the plume decreased at about 1840 m whereas the plume did not change at 1720 m. The methane profile at the SE rim of Jaco Scarp shows an anomaly centered at 1921 m with 29.7 nmol/l and one at 1742 m with 68.8 nmol/l. In September 2002 the bottom plume was not observed and the methane value at 1700 m was 99.3 nmol/l (see 6.8.6. Time variability). However, Jaco Scarp is still one of the most active vent sites along the Central American margin showing a stronger enrichment of methane than found at other scarps and at the mounds.

Moorings were deployed at the same two sites over a period of seven days. The results of mooring 68 situated in the north-western corner of the scarp (Fig. 6.8.13) indicate a strong turbulence with rapidly

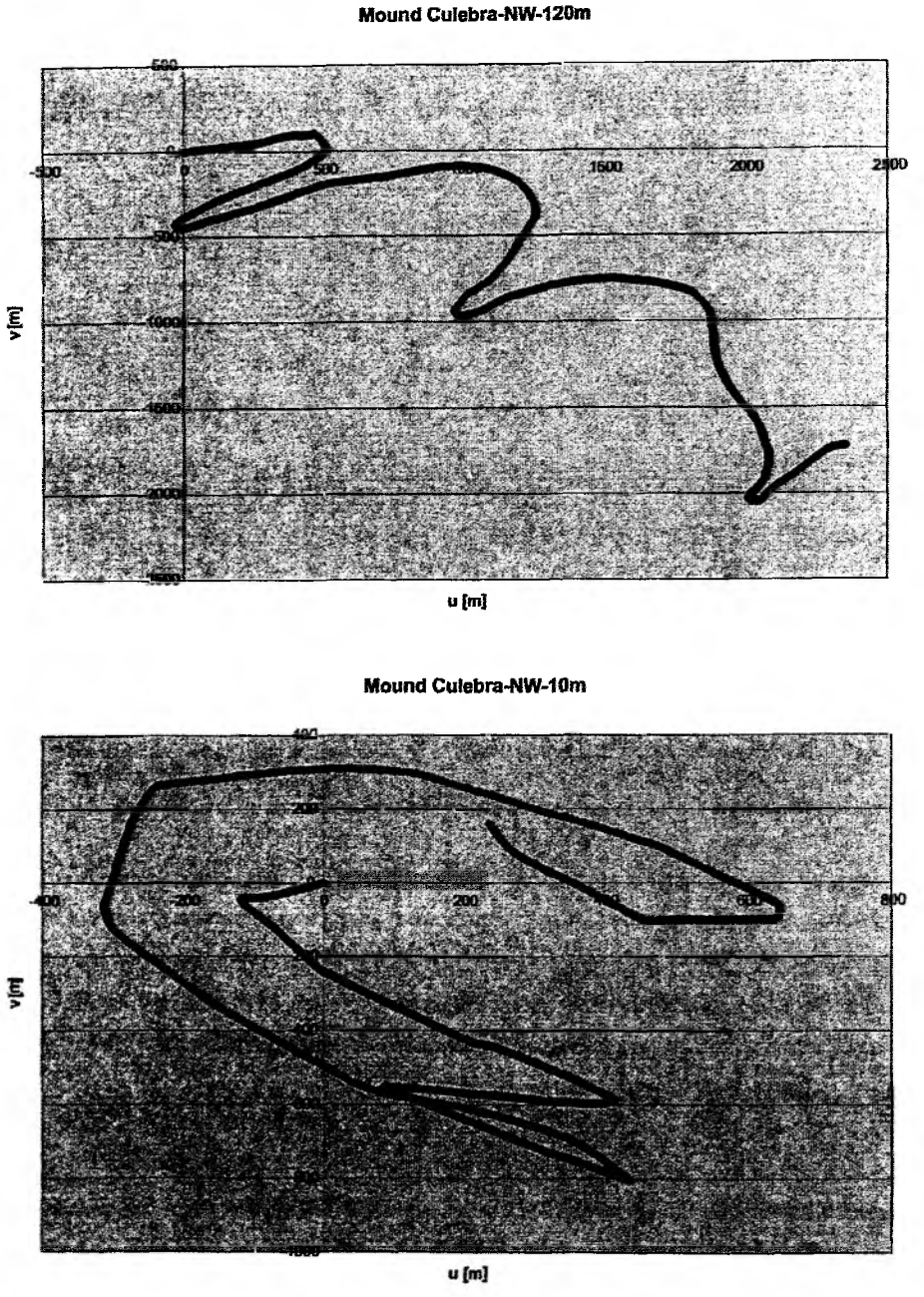

Fig. 6.8.7: Progressive vector plots of current meter data. The current meters were located NW of Mound Culebra at station 42 (Fig. 6.8.4) from September 12th to 14th 2003. The vector plots indicate a SE-ward flow at 120 m and almost no movements except of those caused by tidal forces at 10 m above seafloor.

changing directions at about 10 m above ground (Fig. 6.8.15). Directions change less frequently 120 m above ground and the velocities are increased compared to the ones measured at 10 m above seafloor. LADCP measurements collected during water sampling point to a flow direction to SW (Fig. 6.8.16). This correlates with the mooring results, because they display a southward flow at that time. The data of current meters located at the SE rim of Jaco Scarp illustrate a predominantly NW current at 10 m above ground and a predominantly SE-ward flow at about 120 m above ground. This agrees well with LADCP data from CTD station 99 indicating a northward flow at 1900 m water depth turning towards the SE about 100 m above (Fig. 6.8.16). The velocities of all measurements to ca. 150 m above seafloor range

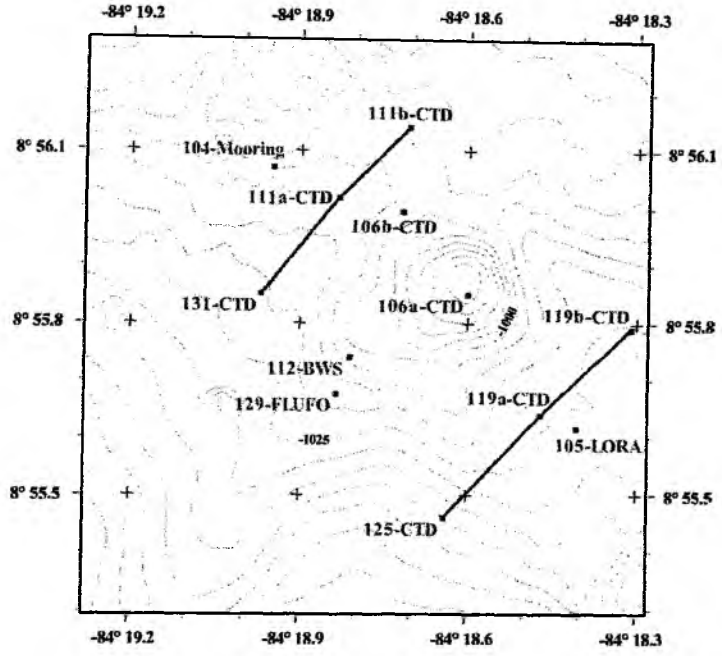

Fig. 6.8.8: Bathymetry of Mound 12 with sampling locations. CTD 106 a and b are revisited sites and the transects are oriented perpendicular to the current direction which was indicated to be NW flowing in 2002. ADCPs were attached to different lander devices (LORA and FLUFO).

mostly from 0-10 cm/s, and tidal influences can be seen in all diagrams presenting Aanderaa data (Fig. 6.8.15).

6.8.5 Slides

Different slides have been explored along the continental slope offshore Nicaragua and Costa Rica (Fig. 6.8.1 and Fig. 6.8.17). They are situated at water depths varying from 2300 to 400 m and show diverse results. CH_4 concentrations measured at the slide offshore Nicaragua at a water depth of 2300 m were as low as the regional background of 1-2 nmol/l (Fig. 6.8.18). This indicates no venting at all. In contrast, maximum CH_4 concentrations of 11.1 and 18.1 nmol/l were found at the much smaller BGR slide and GEOMAR slide, respectively. The methane plume at the BGR slide is centered at 600 m and decreased from 18.5 to 11.1 nmol/l over the last year (Fig. 6.8.18). The CH_4 profile from the GEOMAR slide displays a bottom source at the sampling location. Both slides are situated at water depths of about 600-650 m, that is the upper level of the stability field of gas hydrates. Thus venting at these sites could be associated to dissolving gas hydrate.

The Quepos slide is located at an even shallower depth, at about 400 m. The depth range from about 50 m to 1100 m is characterized by its low O_2 content (less than 1 ml/l), which defines the oxygen minimum zone. In this zone the background methane concentration is increased to up to 20 nmol/l at 400 m. Hence, methane anomalies of up to 20 nmol/l can be the result of this zone and/or of seepage. At Quepos slide we mainly sampled bottom water for biomarker analyses in addition to methane measurements, because last years' biomarker samples had only been useful at sites where high CH_4 concentrations were found. Abundant bacterial mats were discovered in the northern corner of the slide's scarp indicating strong methane input in the water column. Therefore, BWS 065 was positioned right in this corner and CH_4 concentrations ranged from 42.1 to 9.3 nmol/l at 24 and 90 cm above ground, respectively (Fig. 6.8.18 and

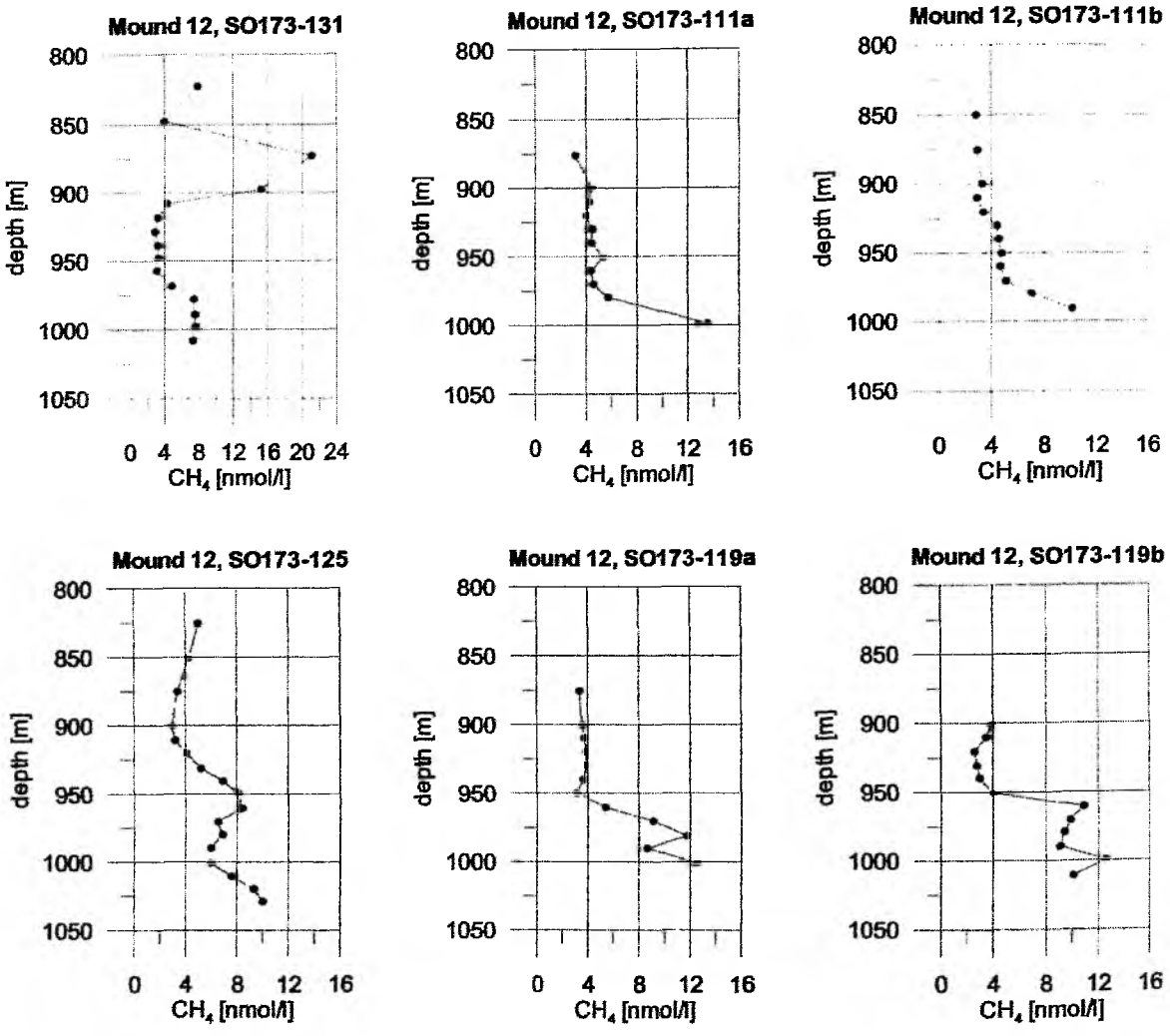

Fig. 6.8.9: CH_4 versus depth profiles of the transects aligned from SW (left on page) to NE (right on page) at Mound 12. The stations of the northern transect are shown in the upper row and the ones of the southern transect are shown in the lower row. All profiles indicate active venting in the vicinity of ca. 650 m around the mound.

Fig. 6.8.19). Bottom water was also sampled on the talus of the slide and showed increasing values with increasing distance to seafloor, but methane was only slightly enriched. Reinvestigating the water column in the northern corner, we measured CH_4 concentrations of up to 489 nmol/l in CTD/rosette samples and up to 679.7 nmol/l in bottom water samples at a station close by. The varying results of three BWS deployments indicate local, small vent sites. However, these methane values are the highest observed of all vent sites offshore Costa Rica and Nicaragua.

6.8.6 Time variability

Changes of methane concentration in the water column over time were observed at different cold vent sites offshore Costa Rica. The cold vent sites are situated at mud extrusions, slides and scarps (Fig. 6.8.17), the latter being produced by seamount subduction (Ranero and von Huene, 2000). Measurements were taken in October - November 1999 (Bohrmann et al., 2002), in April – May 2002, in August-September 2002, and in September 2003. Figures 6.8.20, 6.8.21, 6.8.14, and 6.8.18 illustrate that during this time the methane values decreased at the different sites. The methane concentrations found in 2003 are up to 94% lower than the concentrations of the year before. The values above the NW flank of

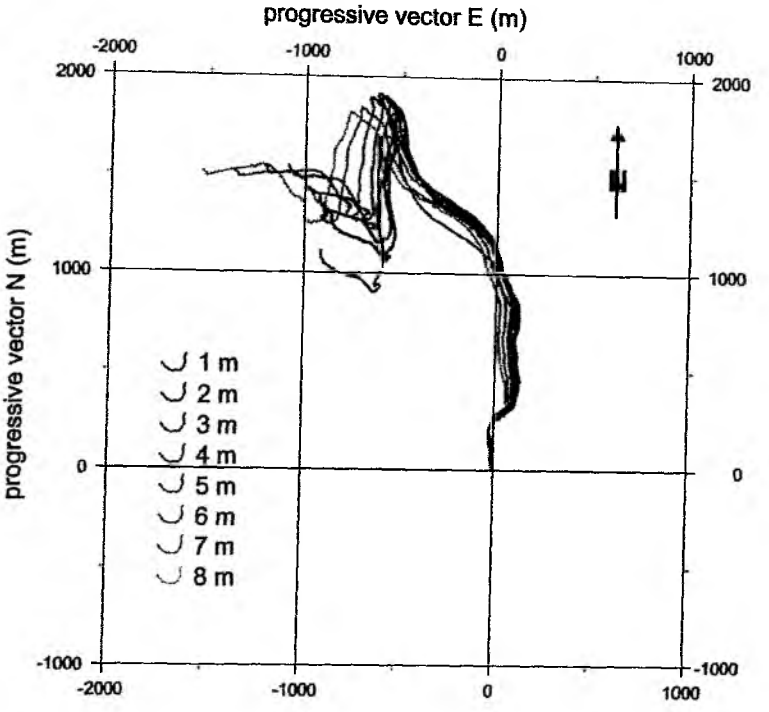

Fig. 6.8.10: Progressive vector plot of ADCP data at 1-8 m above ground showing a north-westward flow whose velocity increased with increasing distance from the seafloor (that is, the end point from the 8-m line is further off the 0/0 point than the one from the 1-m line). Data were collected from 03/09/26 21:59 to 03/09/27 18:33 SW of Mound 12 (FLUFO in Fig. 6.8.8).

Mound Culebra which showed an increase from May 2002 to August 2002 from 15,9 nmol/l to 42,3 nmol/l dropped to 2,4 nmol/l. At the top of this mud diapir the methane concentration decreased from 21,4 nmol/l to 4,04 nmol/l during the last year. The values above Mound 10 (another mud diapir) and Mound 12 (mud volcano) show the same trend (Fig. 6.8.20). Methane concentrations at the upper edge of the talus in Jaco Scarp seem to vary greatly with time, however, from August 2002 to September 2003 the maximum value decreased from 178,5 nmol/l to 63,9 nmol/l. Measurements at the SE rim of the Scarp indicate a drop by 30% (Fig. 6.8.14). Lower methane concentrations were also found at the Rio Bongo Scarp (from 21,1 nmol/l to 16,8 nmol/l), at the Parrita Scarp (from 33,9 nmol/l to 19,7 nmol/l; Fig. 6.8.21), and at the BGR slide. (from 18.5 to 11.1 nmol/l; Fig. 6.8.18).

The decline in methane concentration could be related e.g. to methane oxidation, changes in ocean currents or seismic activity. If aerobic oxidation plays a major role in the observed decrease of CH_4 this would suggest that no further methane would is added from the vent sites. Analyses of $\delta^{13}C$ will provide a better insight into this matter. The ocean currents of this area are not well known. Thus, we collected ADCP data and deployed moorings to gain more information on the current system and on how it is effecting the methane plumes above cold seeps. To date, the results indicate a strong tidal influence. It is known that tides cause pressure differences which in turn affect outflow rates at vent sites. However, this does not explain the decline in methane concentration which we observed, mainly because of the different time scales. A group of geophysicists within the SFB 574 work on recording local seismicity induced by convergent dynamics between the subducting oceanic plate and the Caribbean plate. Two temporary seismic networks in the area of Jaco Scarp and Quepos reported two major earthquakes in June 2002 and

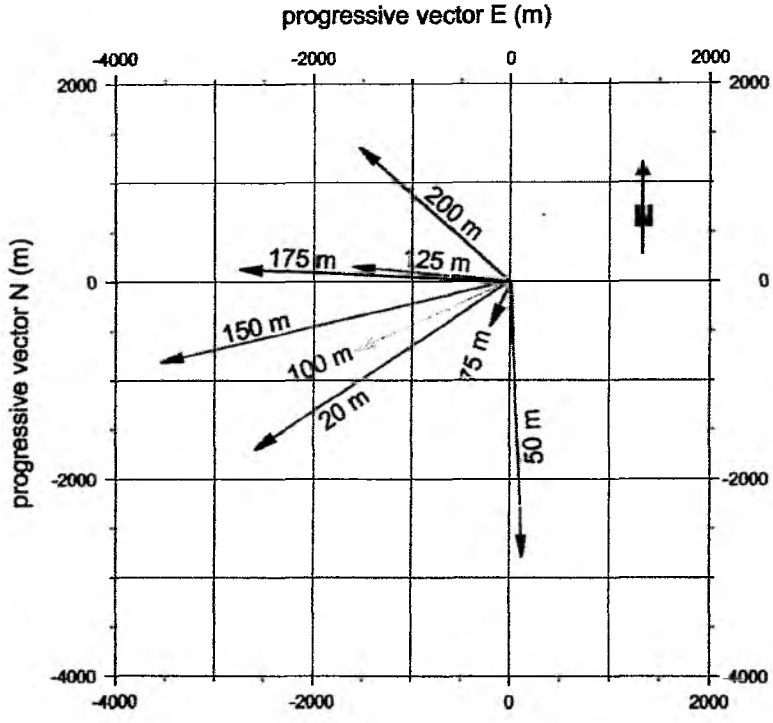

Fig. 6.8.11: Simplified progressive vector plots of ADCP data at labeled depths at Mound 12 (LORA in Fig. 6.8.8). The arrows mark the start and the end point of the vector plots excluding tidal forces for a better overview of flow direction and speed (lengths of arrow) at the different depths. The flow directions could be related to turbulence due to topography and/or the Ekman spiral.

October 2002 with magnitudes of 6.4 and 4.8, respectively, and a very high microseismic activity from April 9th to 23rd. All recorded events are locally bound and may play a role for one or two of the vent sites, but none would induce a decrease of the outflow rates along the whole margin. Therefore, we will look at data of a broader seismic network on land and large-scale oceanographic changes like El Niño in order to identify the reason for the decreasing activity.

6.8.7 Surface Methane Concentrations

First uncalibrated data confirm a relatively high saturation state (above 150 %) for the surface waters within the SFB target area, with increasing concentrations towards the shelf. The high oversaturation is consistent with the observation of high methane concentrations in the subsurface waters, presumably as a result of in situ production in the lower, already strongly oxygen-depleted part of the photic zone.

The results of these investigations will illustrate the amount of methane which reaches the surface water and the atmosphere. Together with water column data of the methane concentrations and their isotopic signal, and the meteorological data, they will be used to assess the methane flux from the ocean to the atmosphere and to constrain the sources responsible for this flux within the SFB target area.

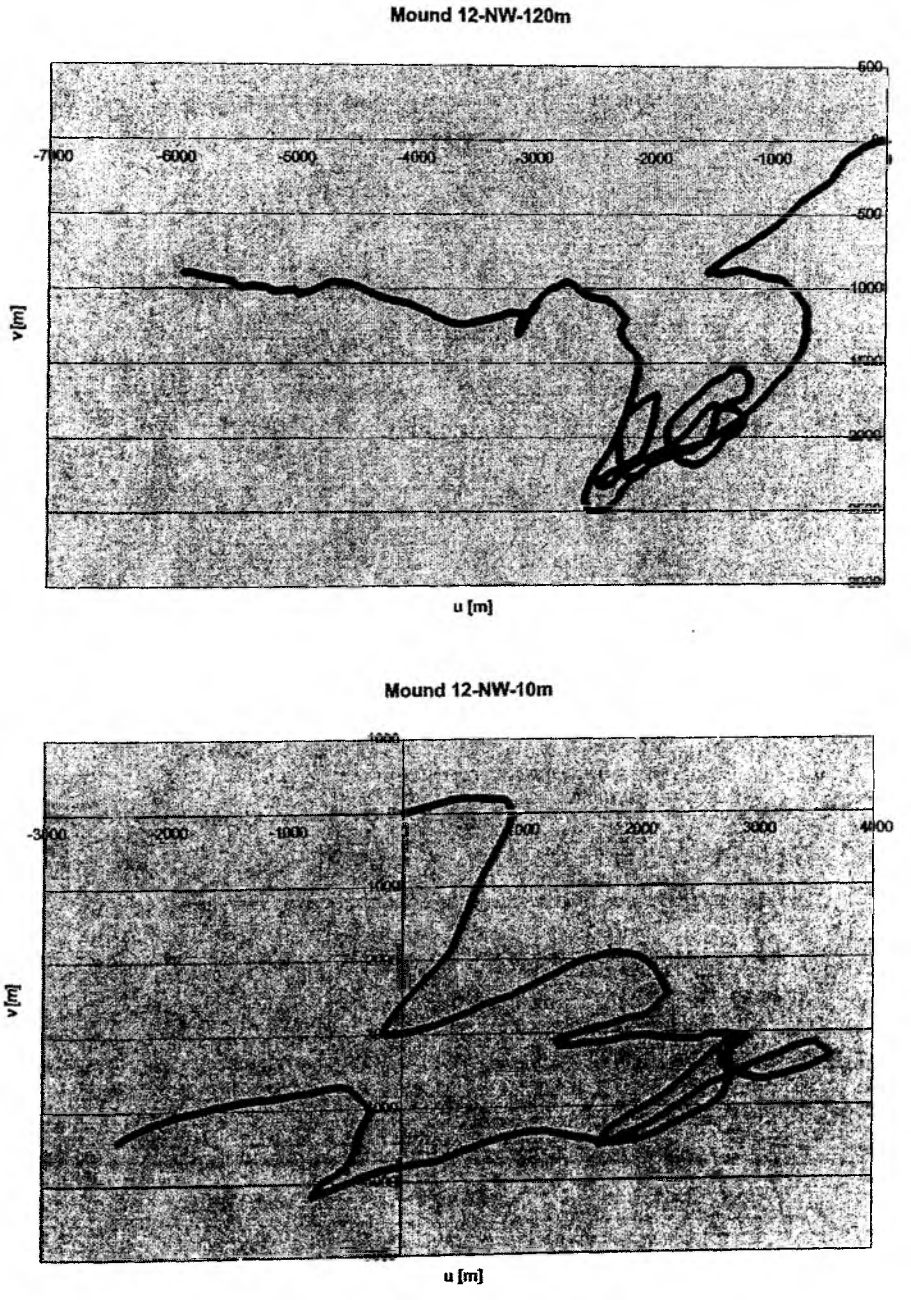

Fig. 6.8.12: *Progressive vector plot of current meter data from station 104, NW of Mound 12 (Fig. 6.8.8). Data were collected from September 24th to 27th 2003. The measurements from 10 m above ground show a SE-ward flow in the first half of the deployment period which then turns to the SW and the data from ca. 120 m above seafloor indicate a SW-ward movement turning further to the WSW in the second half of the deployment period.*

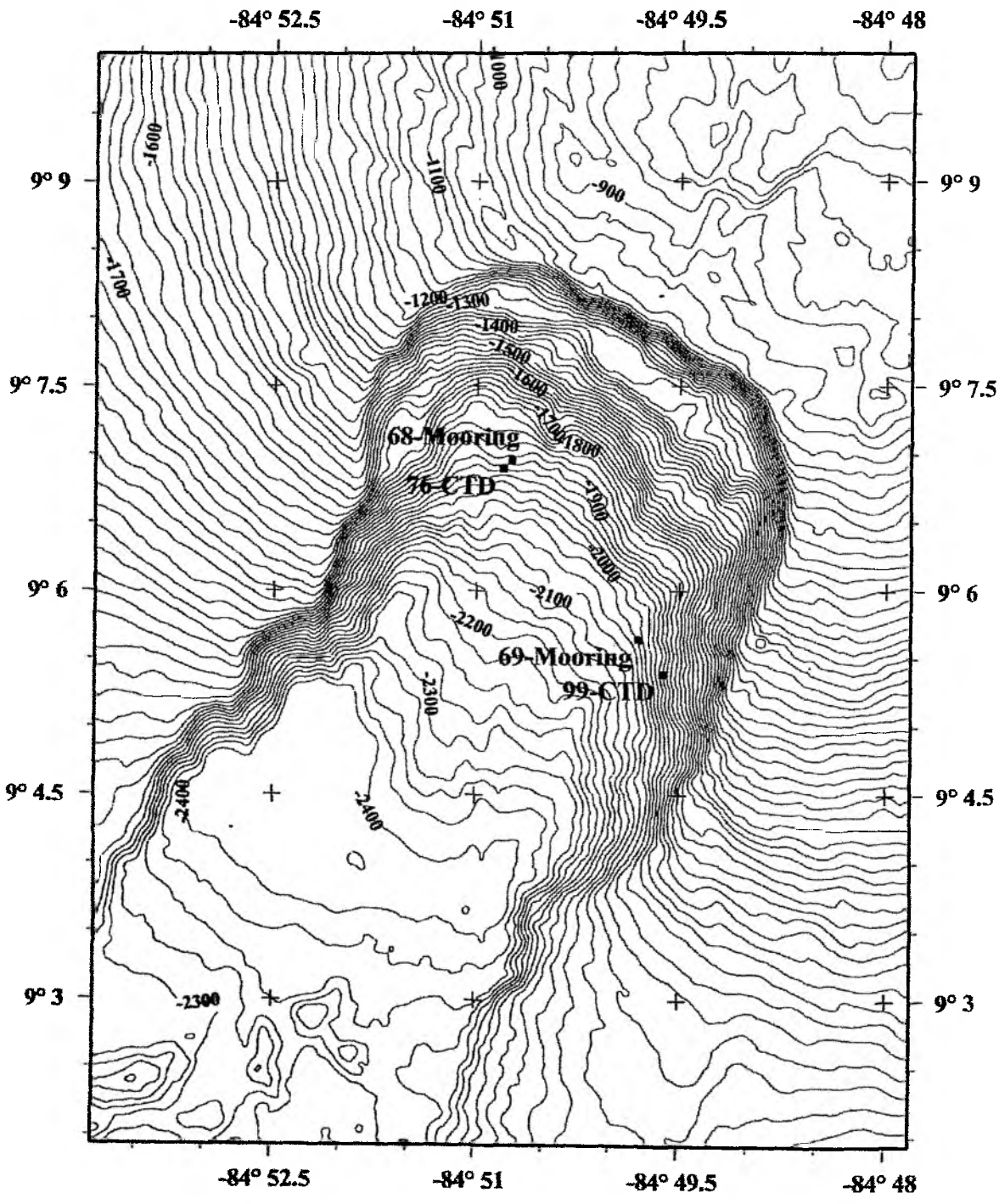

Fig. 6.8.13: Bathymetric map of Jaco Scarp with locations of moorings and CTD stations.

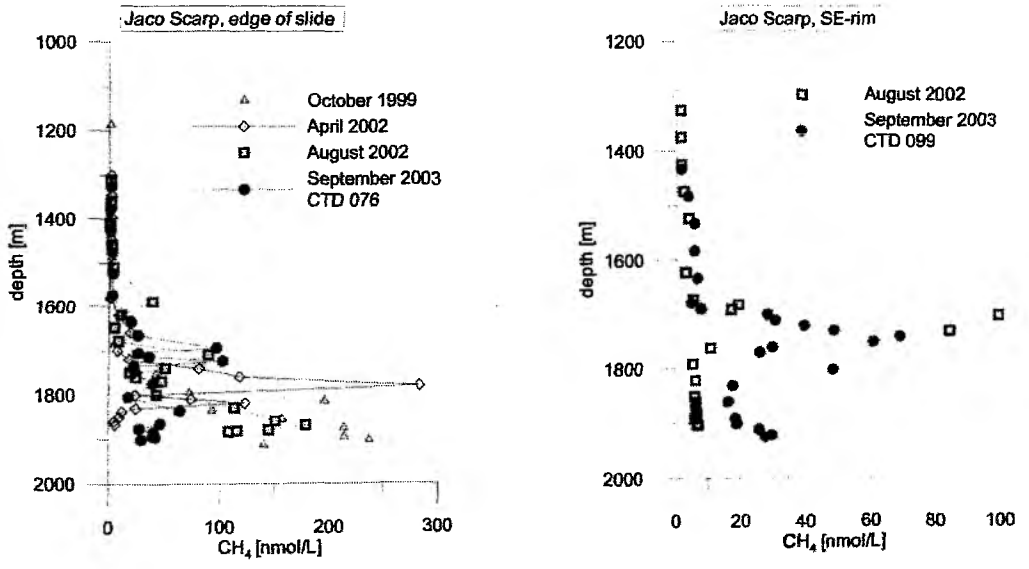

Fig. 6.8.14: CH_4 profiles at Jaco Scarp, which is a highly active seepage site offshore Costa Rica. The two sites have been revisited and indicate changing methane content over the years.

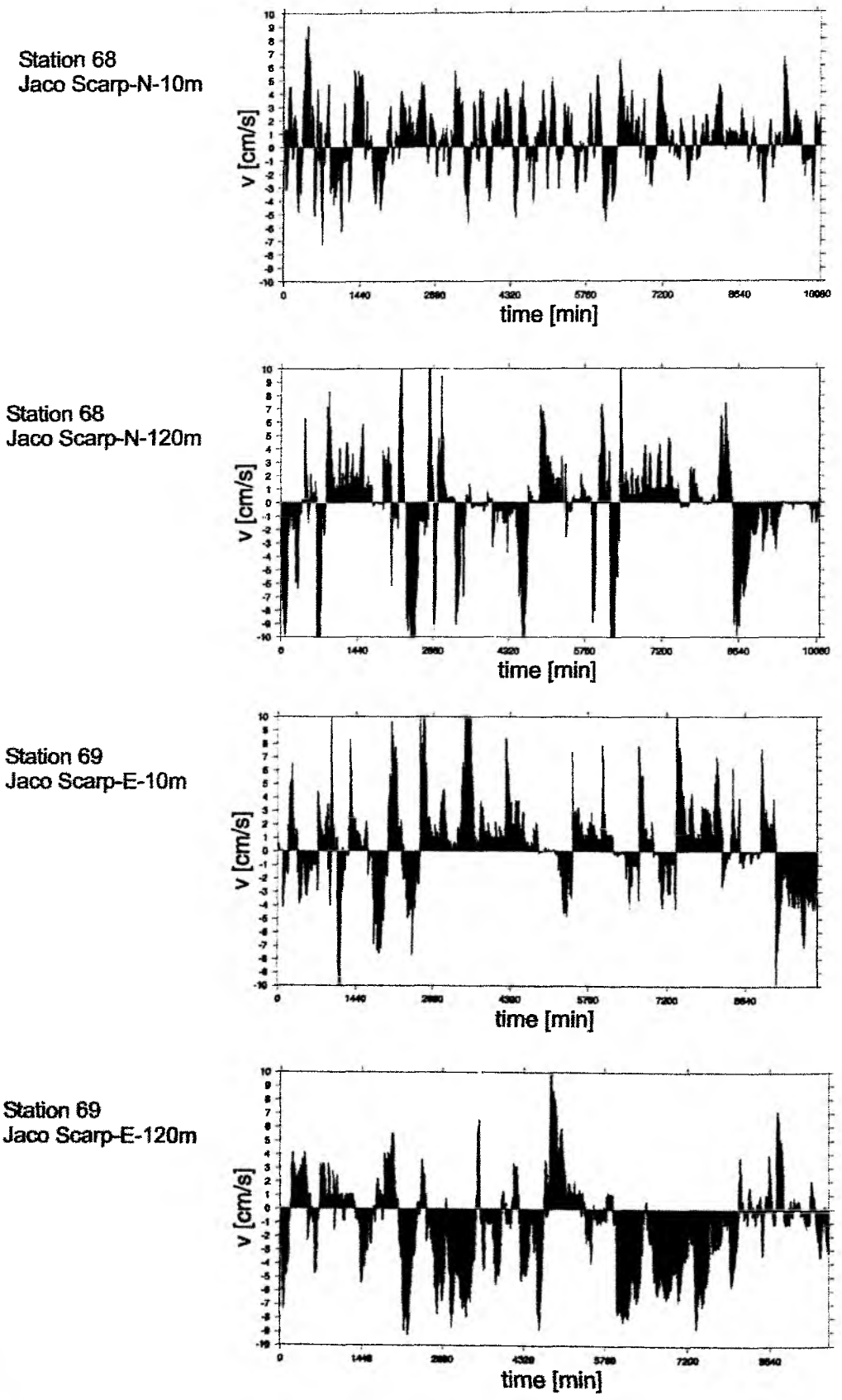

Fig. 6.8.15: *Current meter data of station 68 and 69 (Fig. 6.8.13). Measurements were taken at ca. 10 m and 120 m above seafloor over a period of seven days.*

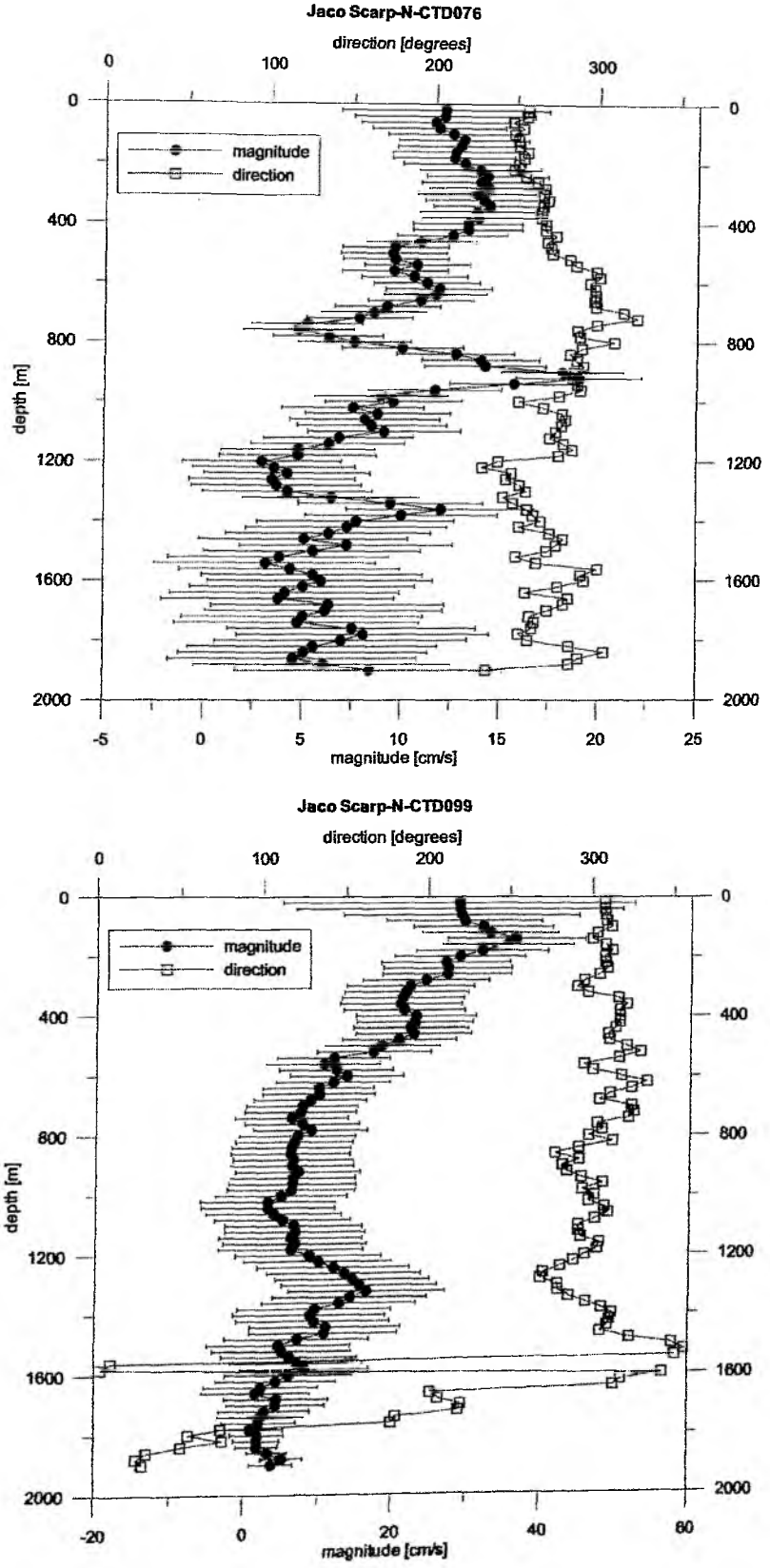

Fig. 6.8.16: *LADCP data of CTD-stations 76 and 99 (Fig. 6.8.13). LADCP data were collected by an ADCP attached to the CTD/rosette and processed using software by M. Viesbeck (IFM Kiel). Note different scale of plots.*

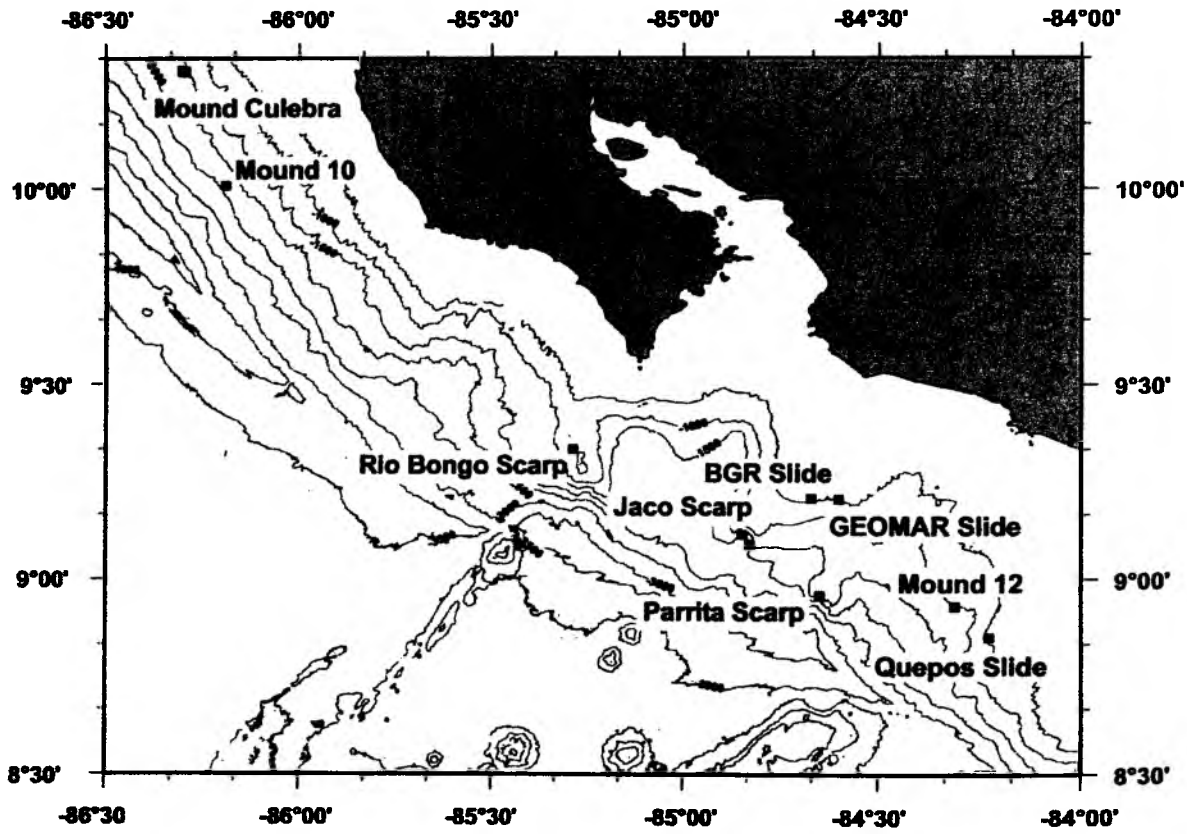

Fig. 6.8.17: Bathymetry of the research area offshore Costa Rica with locations of observed vent sites.

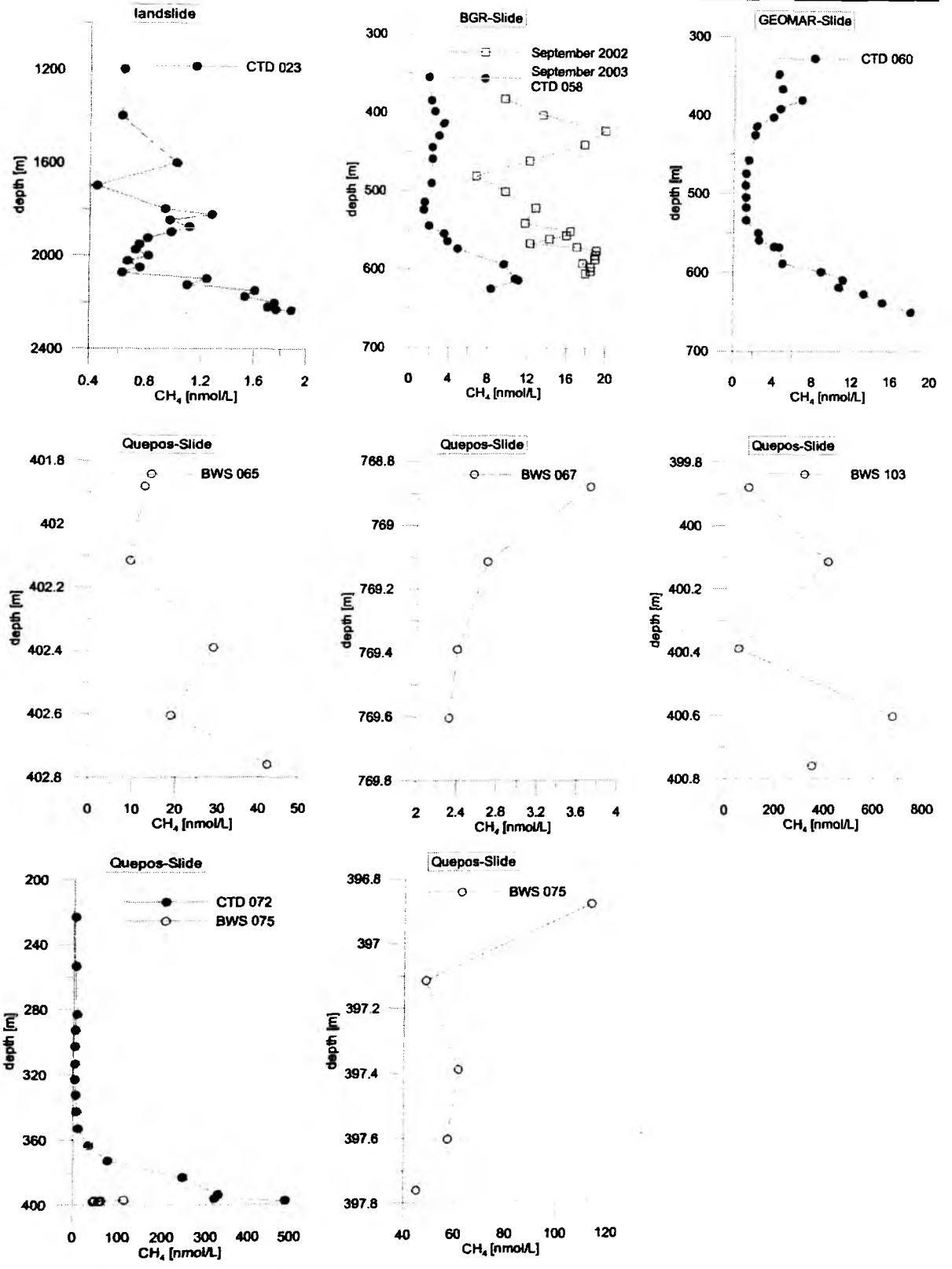

Fig. 6.8.18: *CH_4 concentration versus depth at different slides (note different scales). Water samples were collected by CTD/rosette and Bottom Water Sampler (BWS), samples of CTD 072 and BWS 075 are from the same location. For positions of stations see Fig. 6.8.1, Fig. 6.8.17, and Fig. 6.8.13*

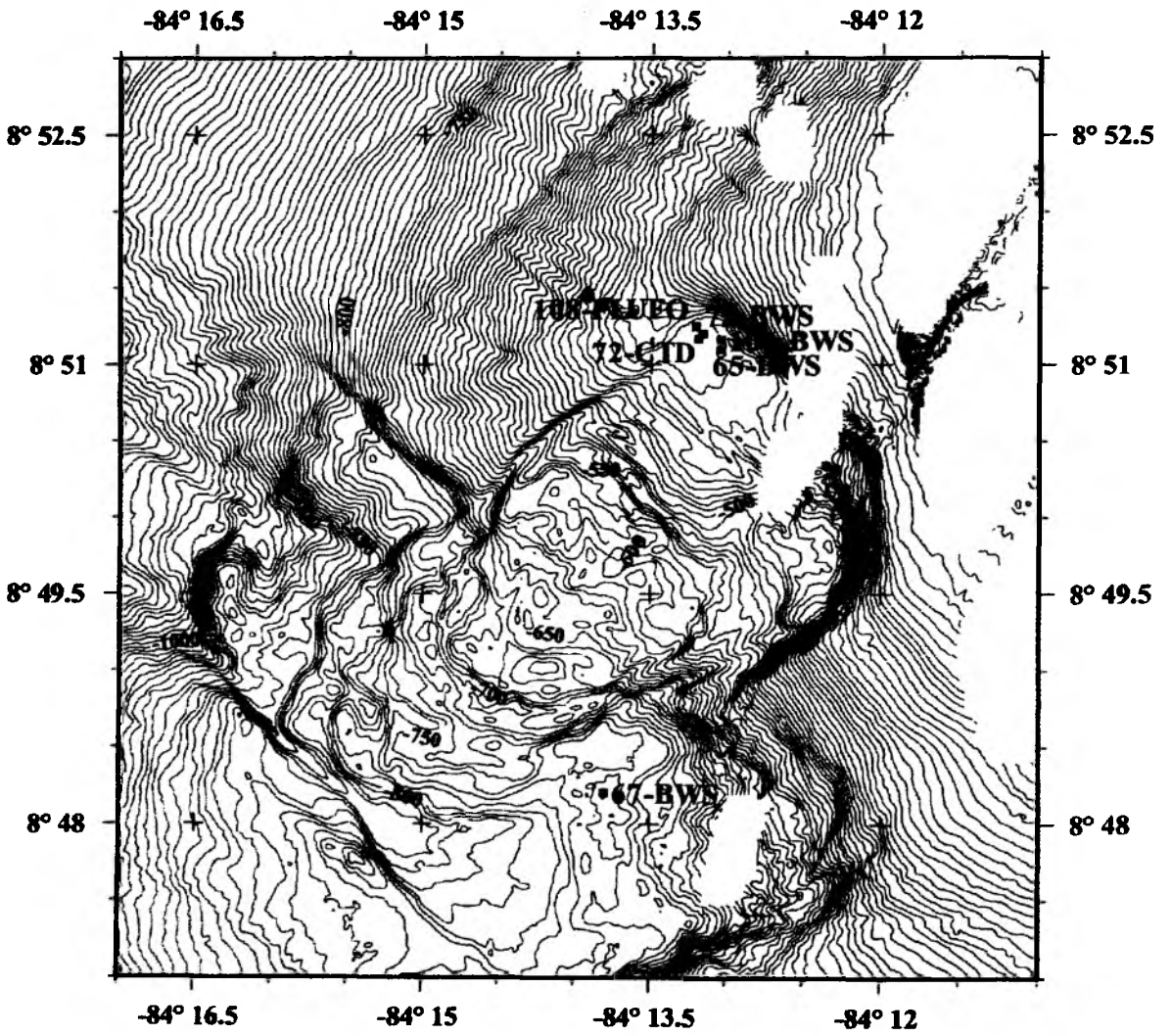

Fig. 6.8.19: Bathymetric map of Quepos slide with water sampling locations.

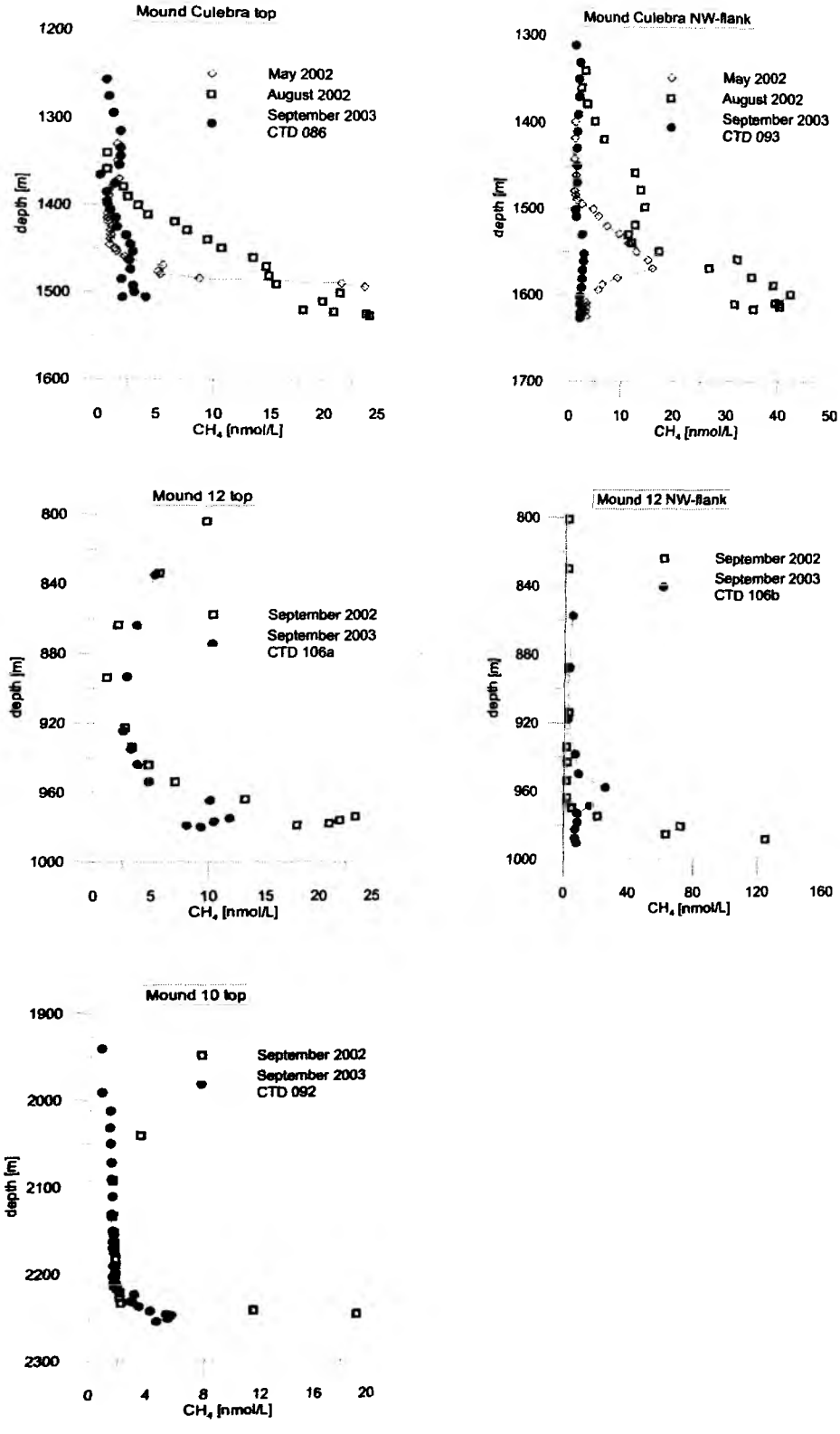

Fig. 6.8.20: Profiles of methane versus depth of Mound Culebra, Mound 12, and Mound 10. Mound Culebra and Mound 10 are mud diapirs whereas Mound 12 is a mud volcano; all of them show declining methane concentrations since 2002. Decreasing values were also observed at different sites of the same mound (Mound Culebra and Mound 12).

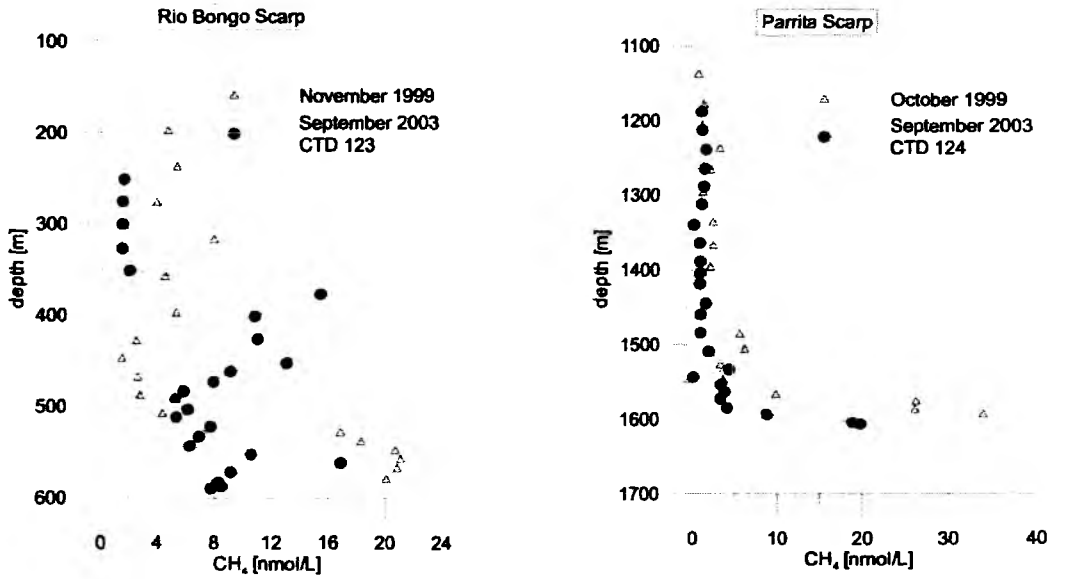

Fig. 6.8.21: Methane concentration versus depth at different scarps that were created by seamount subduction. The methane content in Rio Bongo Scarp and Parrita Scarp changed over the last year as well as the CH_4 concentration at the revisited locations in Jaco Scarp (Fig. 6.8.14). Data of October/November 1999 is derived from R/V SONNE cruise 144.

6.9 Biomarkers

B. Manzke

The biomarkers used in this study are lipid biomarkers, which are molecules that are indicative for a specific group of organisms. Fatty acids are particularly useful biomarkers since they are essential components of bacteria with the exception of archaebacteria. Analysis of fatty acids is used to indicate the presence and relative abundance of the microorganisms in a given environment. The analysis of phospholipid ester-linked fatty acids (PLFA) is one of the more sensitive chemical methods to determine the microbial biomass and community structure.

Isoprenoids are used to indicate the presence of archaea bacteria.

Previous results indicate that methane oxidation goes on well into the benthic boundary layer. Therefore the sediment and the directly (1m) overlying water were extensively sampled, preferably sites with bacterial mats.

Two sampling "devices" were used:

1. Bottom Water Sampler (BWS, Fig.6.9.1) to measure the vertical concentration and carbon isotopic gradients of the bacteria. The sampling procedure was as follows: first a methane sample was taken and depending on the concentration measured the remaining water was then filtered using a 0,4 µm pre-cleaned GF-Filter.

2. A TV-guided Multicorer with an attached Kiel In-Situ pump (Fig. 6.9.2) was used to obtain sediment samples and water samples at the same time and spot. One core was taken, the supernatant used for methane analysis and the remaining material filtered as described above. The pump was programmed to pump a certain time while on ground, thereby getting a filter sample from the vent site at the height of about 1m.

Some carbonate, sediment, and water samples were taken from selected Lander and TV-Grab stations.

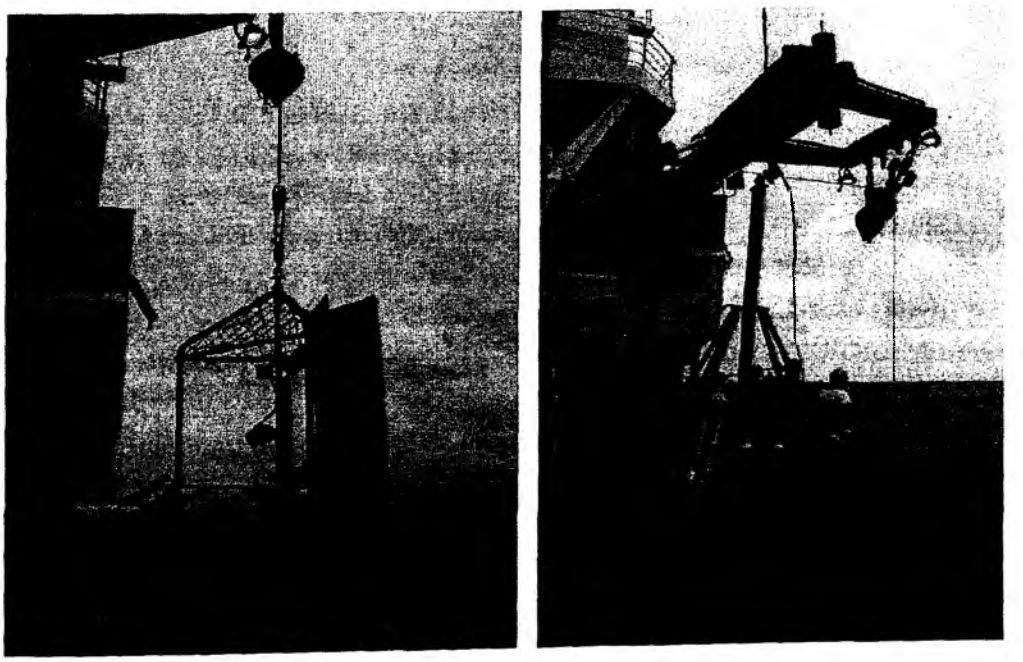

***Fig 6.9.1 & 6.9.2:** Bottom-water-sampler (BWS) (left). TV-guided multicorer with attached Kiel-in-situ-pump (right)*

6.10 Trace Elements and Isotope Geochemistry

D. Garbe-Schönberg, V. Liebetrau, J. Scholten, U. Westernströer

6.10.1. Introduction

The chemical composition of the fluids sampled during leg SO 173/3 - pore water, vent fluid, bottom seawater, normal seawater – is the result of variable mixtures of fluid components from different sources and origins, e.g.,: (i) low-salinity/ high alkalinity fluids rich in sulfide and methane assumed to represent ascending fluids originating from the dewatering of clays at the top of the subducted slab, (ii) fresh water from *in-situ* gas hydrate destabilization, (iii) a local fluid source, essentially pore water that has interacted with local sediment; (iv) normal seawater. The distribution of selected trace elements is characteristic for the different fluid components and can be used for the identification and differentiation of fluid components and their sources. Redox reactions that take place while ascending fluids mix with infiltrating seawater overprint the concentrations of a number of trace elements. Another aspect is the identification and quantification of trace elements in the water column above active vents which can be used as a conservative fluid tracer for mass balance calculations.

The fluid sampling program of leg SO 173/3 focused on re-sampling of known carbonate mounds (Mound Culebra, Mounds # 10, 11, and 12) as well as surveying newly discovered structures where active venting of fluids was manifested by bacteria, vent communities, and chemical anomalies (methane) in the bottom water. The mud-diapiric origin of at least some of the mounds has been evidenced by over-solidified clay as well as basaltic clasts in the sediments. *In-situ* destabilization of gas-hydrates plays a role in the pore water composition at Mound 11. In contrast, fluids that probably come from shallower depths are released at Jaco Scar. Again, fluids of markedly different chemical compositions,probably originating from contrasting sources and depths, could be sampled during leg SO 173/3.

6.10.2 Methods

Fluid samples were obtained by means of (i) pressing pore water from sediments obtained with the gravity corer (GC, see table 1), multi-corer (TV-MUC), and TV-guided grab sampler (TV-G) ; (ii) bottom water sampler (BSW), (iii) Niskin sampling rosette (CTD), and (iv) FLUFO sampler. In addition, time-series samples were taken from incubation experiments with the Benthic Chamber Lander (BCL). The pore water was pressed through 0.2µm cellulose acetate membrane filters in all-Teflon devices pressurized with Argon. Immediately after filtration, all samples (1-2 ml) were acidified with a few drops of subboiled concentrated nitric acid. Water samples with larger volumes (bottom seawater (BSW), normal seawater (SW), vent fluids mixed with seawater (VF)) were pressure-filtrated through 0.2 µm Nuclepore PC membrane filters in Sartorius filtration units and acidified with 100 µl subboiled concentrated nitric acid per 50 ml. Procedural blanks were processed at regular intervals. All work was done in a class 100 clean bench (Slee, Germany) using plastic labware. The rinse water was ultrapure (>18.2 Mohm), dispensed from a Millipore Milli-Q system.

A total of 587 pore water and 142 water samples were taken (Table 6.10.1). After our return to the home labs in Kiel, selected samples will be analyzed for trace element composition (e.g., I, Br, B, Li, Al, Ti, Cs, Ba, Sr, Y-REE, Fe, Mn, Cr, V, Cu, Co, Ni, Pb, U, Mo, As, Sb, W) by ICP mass spectrometry using both collision-cell quadrupole (Agilent 7500cs) and high-resolution sector-field (Micromass PlasmaTrace 2) based instrumentation.

6.10.3 Isotope Geochemistry

In order to get time series information about past venting activity, fluid origin and fluid mixing, vent-related carbonates were sampled by TV-G, TV-MUC and GC for U-Th disequilibrium geochronology, Sr isotope composition and light stable isotope analyses to be performed at the IFM-GEOMAR in Kiel. A complete sample list is given in table 6.10.2.

As a contribution to fluid flux estimations for recent venting activity, the on-board analyses of short-lived isotopes were continued in a refined sampling approach, integrating new lander technology and pore water profiles. Radio isotopes of the natural uranium-thorium decay chains are supplied to vent fluids and pore waters by water/sediment-, water/rock-interaction and by alpha recoil. Apart from the chemical composition of the sources, the concentration of the radionuclides in the vent fluids depends to a larger extent on the transit time between the reaction zone and the discharge zone at the sediment surface. By measuring e. g. ^{224}Ra ($T_{½}$ = 3.6 d), ^{222}Rn ($T_{½}$ = 3.8 d), ^{228}Ra ($T_{½}$ = 5.7 a) and ^{226}Ra ($T_{½}$ =1600 a), vent fluid residence times and discharge rates can be estimated. Based on experiences from cruise M54/3a, where measurements of ^{224}Ra and ^{226}Ra suggested that fluid venting investigated at the sites was too low to be quantified by the applied Ra methods, the on-board radioisotope program of So 173/3-4 was focussed on the ^{222}Rn method with sampling extended from bottom water towards pore water profiles.

During So 173/3-4 samples for on-board radionuclide measurements were obtained by means of CTD, BWS, TV-MUC, FLUFO and BCL. The lack of the VESP sampling system, due to electronic communication problems between older and state-of-the-art control devices, was partially compensated for by FLUFO and BCL deployments. In contrast to FLUFO and BCL the bottom time of the towed VESP sytem is in general restricted to 90 minutes, providing 10-liter samples from up to 5 different time intervals of fluid enrichment. However, the results of cruise M54/3a have shown, that an enrichment factor over 90 min war very close to the detection limit at the sites investigated. The time-resolved syringe sampling system of FLUFO and BCL could not provide samples of the required volume due to the size of the syringe and the established preferences in aliquot strategy for the different subprojects. Nevertheless, the FLUFO and the BCL lander were for the first time able to recover enough material for ^{222}Rn analyses of 20 hours' enriched bottom water from active vent sites off Costa Rica, including several centimeters of the underlying sediment.

For ^{222}Rn analysis of bottom water samples one liter of water was filled into an extraction apparatus and a water-immiscible scintillation cocktail (MaxiLight) was added. The sample was shaken for 1.5 hours and the organic phase was transferred into a low diffusive LS-vial which was stored three hours for isotope equilibration. Pore water sampling was performed parallel to the procedure by the pore water group in the low temperature lab container. Approximately 25 ml of soft sediment were transferred into a 50ml beaker and were immediately covered with 23 ml of the water-immiscible scintillation cocktail (MaxiLight), the beaker was closed tightly and sealed. This procedure was directly followed by centrifuge phase separation for 15 min at 3000 rpm. Scintillation cocktail and water were transferred into low diffusive vials by a layering technique which always keeps a layer of scintillation cocktail on top of the sample. From that point on the procedure follows the description for one liter bottom water samples.

Two liquid scintillation counters (Guardian and Triathler) were available for on-board ^{222}Rn measurements. The samples were counted for six hours. In order to determine $^{222}Rn_{excess}$ concentrations the samples have

to be back-measured in the home lab after the decay of unsupported ^{222}Rn is finished. Some preliminary results of $^{222}Rn_{excess}$ concentrations from Mound Culebra, Quepos Slide and Mound 12 are given in figures 6.10.1 - 610.3. Last measurements, final method calibrations and data reduction are subject of the current laboratory routine.

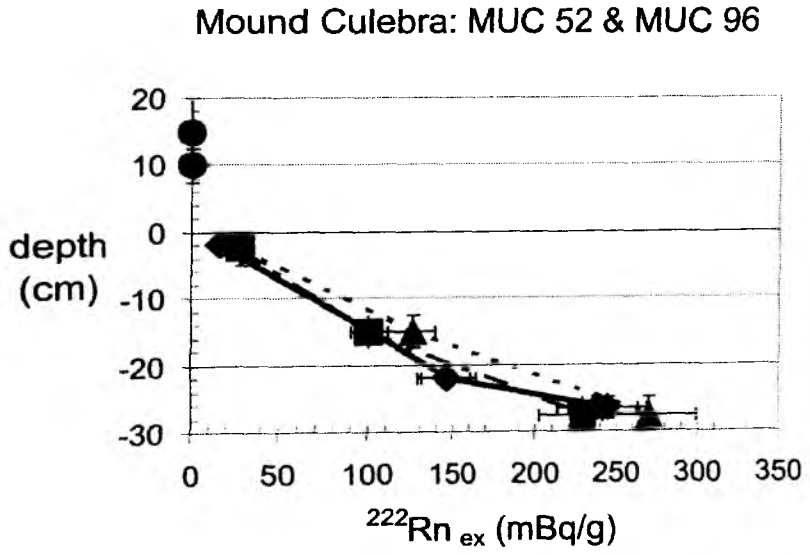

Fig. 6.10.1: *$^{222}Rn_{excess}$ concentration of MUC pore water and bottom water samples from Mound Culebra in mBq/g (station depth: 1550 m). The pore water profiles show comparable results for different sampling techniques (squares: syringe technique; triangles: spoon technique) of MUC 96 and for different sites at Mound Culebra (diamonds: spoon technique on MUC 52). The circles represent bottom water samples of MUC 96.*

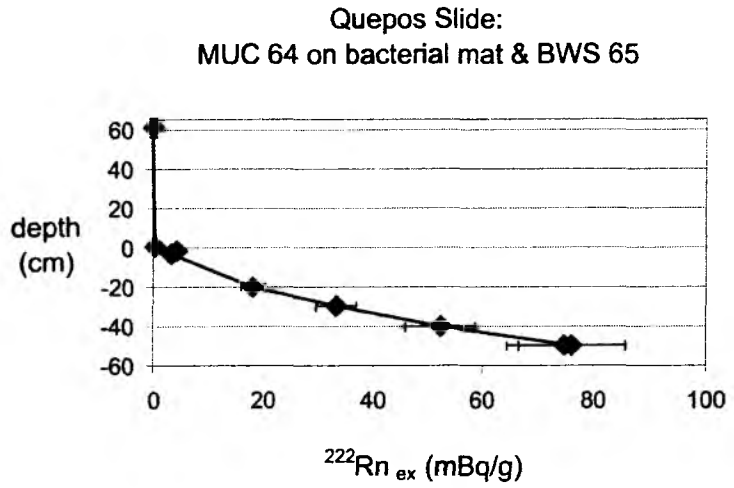

Fig. 6.10.2: *$^{222}Rn_{excess}$ concentration of pore water (MUC 64) and bottom water samples (BWS 65) from Quepos Slide in mBq/g. The pore water profiles show significantly lower values with a steeper slope than measured on Mound Culebra. Both observations would correlate with lower primary ^{222}Rn production due to lower $^{230}Th_{excess}$ enrichment in sediments from shallow water (approx. 400 m) and with increased fluid flux at Quepos Slide.*

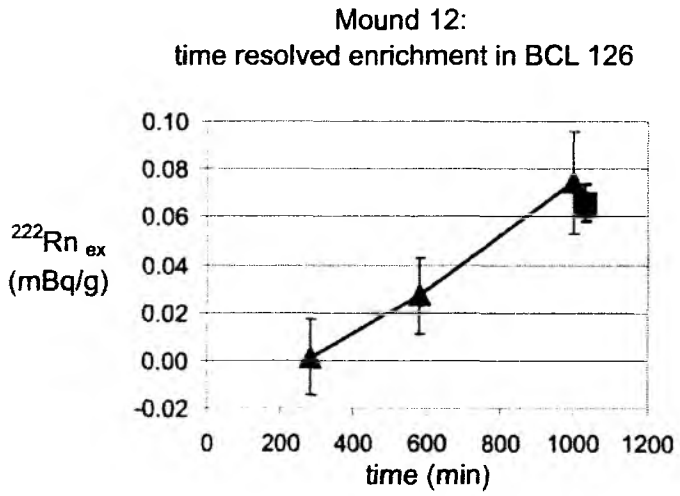

Fig. 6.10.3: *$^{222}Rn_{excess}$ concentration of bottom water samples recovered with a time-resolving syringe system of a benthic chamber lander (BCL 126) at Mound 12. The triangles are 40 ml in situ samples and the squares represent the results of 1-l samples taken on board after lander recovery from the remaining reservoir with established extraction techniques. The errors reflect that the syringe sample size is close to the detection limit. Larger samples and a modified sample timing are required for future approaches. The slope of the syringe samples and the overlap between the last syringe and the final 1-l water sample of this first approach opens promising perspectives for a combination of ^{222}Rn studies with BCL deployments in the future. From this first approach a $^{222}Rn_{excess}$ flux of about 1.85 mBq cm^{-2} d^{-1} could be determined.*

Table 6.10.2: So173/3-4 list of carbonate, sediment and water samples

station	area	sample type	code extension So173-	preliminary on-board description and comment
GC-5-1	Mound Quetzal	sediment	VL-1	170-cm-long chunnel in sediment, bottom to top with mud suspension
GC-5-1	Mound Quetzal	mud-suspens.	VL-2	upper 50 cm disperse distributed in overlying sediment. (VL-1&2)
GC-5-1	Mound Quetzal	carbonate	VL-3	carbonate in mud suspension (VL-2)
GC-5-1	Mound Quetzal	carbonate	VL-4	depth not reported
GC-6-1	Mound Quetzal	carbonate	VL-5	100 cm below sediment surface
GC-6-1	Mound Quetzal	carbonate	VL-6	141 cm below sediment surface
GC-6-1	Mound Quetzal	carbonate	VL-7	150 cm below sediment surface
GC-6-1	Mound Quetzal	carbonate	VL-8	156 cm below sediment surface
GC-6-1	Mound Quetzal	concretion	VL-9	190 cm below sediment surface
GC-6-1	Mound Quetzal	carbonate	VL-10	222 cm below sediment surface
GC-6-1	Mound Quetzal	carbonate	VL-11	271 cm below sediment surface
GC-6-1	Mound Quetzal	carbonate	VL-12	296 cm below sediment surface
GC-6-1	Mound Quetzal	carbonate	VL-13	301 cm below sediment surface
GC-6-1	Mound Quetzal	carbonate	VL-14	320 cm below sediment surface
GC-6-1	Mound Quetzal	carbonate	VL-15	352 cm below sediment surface
GC-6-1	Mound Quetzal	carbonate	VL-16	375 cm below sediment surface
TVG-8-1	Mound Quetzal	carbonate	VL-17-18	green dolomite pebbles
TVG-8-1	Mound Quetzal	carbonate	VL-19	1/2 chimney structure
TVG-8-1	Mound Quetzal	carbonate	VL-20-21	brownish secondary zoned dolomite
TVG-8-1	Mound Quetzal	carbonate	VL-22-24	green dolomite pebbles
TVG-8-1	Mound Quetzal	carbonate	VL-25	part of a ring-like structure, strongly altered
TVG-8-1	Mound Quetzal	carbonate	VL-26	block with closing (carb. precipitate) fluid flow channels
TVG-8-1	Mound Quetzal	carbonate	VL-27	block with sediment bearing open fluid flow channels
TVG-8-1	Mound Quetzal	carbonate	VL-28	block with vent structure, downside layered
TVG-8-1	Mound Quetzal	carbonate	VL-29	altered dolomite, drying structures, white overgrowth
TVG-8-1	Mound Quetzal	carbonate	VL-30-32	breccia and green pebbles with bright white filling
TVG-8-1	Mound Quetzal	carbonate	VL-33	channel or carbonate fossil
TVG-8-1	Mound Quetzal	carbonate	VL-34	breccia and green pebbles with bright white filling
TVG-8-1	Mound Quetzal	carbonate	VL-35	green dolomite with 1/2 tube (demonstration)
TVG-8-1	Mound Quetzal	carbonate	VL-36-38	porous carbonate on dolomite pebble
TVG-8-1	Mound Quetzal	carbonate	VL-39	big blocks of an inactive vent spot
TVG-8-1	Mound Quetzal	carbonate	VL-40	fragile green pebble, white altered matrix, vent holes
TVG-8-1	Mound Quetzal	carbonate	VL-41	tube carbonate in green pebbles
TVG-8-1	Mound Quetzal	carbonate	VL-42	shell remnants
TVG-27	Mound Carablanca	carbonate	VL-50	
TVG-27	Mound Carablanca	carbonate	VL-51	coating on hard sediment plus carb. split, very porous
TVG-27	Mound Carablanca	carbonate	VL-52	coating on hard sediment. plus carb split. very porous
TVG-27	Mound Carablanca	carbonate	VL-53	yellow coating on hard gray consolidated sediment and biota
TVG-27	Mound Carablanca	carbonate	VL-54	flat porous
TVG-27	Mound Carablanca	carbonate	VL-55	selection
TVG-27	Mound Carablanca	carbonate	VL-56	large pseudomorph
TVG-27	Mound Carablanca	carbonate	VL-57	block with flat top
TVG-27	Mound Carablanca	carbonate	VL-58	high density
TVG-27	Mound Carablanca	carbonate	VL-59	high density
TVG-27	Mound Carablanca	carbonate	VL-60	flowstone-like
TVG-27	Mound Carablanca	carbonate	VL-61	dark pseudomoprh block
TVG-27	Mound Carablanca	carbonate	VL-62	positive and negative pseudomorphs
TVG-27	Mound Carablanca	carbonate	VL-63	dark flowstone path inside block
TVG-27	Mound Carablanca	carbonate	VL-64	gray flowstone inside block
TVG-27	Mound Carablanca	carbonate	VL-65	fine carbonate cement
TVG-27	Mound Carablanca	carbonate	VL-66	fine carbonate cement
TVG-27	Mound Carablanca	carbonate	VL-67	flat surface carbonate cover (oriented)
TVG-27	Mound Carablanca	carbonate	VL-68	vent block (oriented)

TVG-27	Mound Carablanca	carbonate	VL-69	granulate top
TVG-27	Mound Carablanca	carbonate	VL-70	granulate and concretion bottom
TVG-27	Mound Carablanca	carbonate	VL-71	granulate top to bottom profile block
TVG-37	Mound Morpho	carbonate	VL-72	flat, porous
TVG-37	Mound Morpho	carbonate	VL-73	vent block
TVG-37	Mound Morpho	carbonate	VL-74	vent holes with bright carbonate coating
TVG-37	Mound Morpho	carbonate	VL-75	gray yellow skin on top
TV-MUC-94	Mound Culebra	carbonate	VL-127	altered, cone shape
TV-MUC-94	Mound Culebra	carbonate	VL-128	gravel collection and young clam remnants
TV-MUC-95	Mound Culebra	carbonate	VL-129	surface carbonate with white coating, barnacle on top
TV-MUC-95	Mound Culebra	carbonate	VL-130	gravel collection, gray
TV-MUC-95	Mound Culebra	carbonate	VL-131	gravel collection
BCL-109-k1	Quepos Slide	carbonate	VL-150	plates incl. up-down criteria (T.Moerz-collection)
BCL-109-k2	Quepos Slide	carbonate	VL-151	plates incl. up-down criteria (T.Moerz-collection)
BCL-109-k3	Quepos Slide	carbonate	VL-152	plates incl. up-down criteria (T.Moerz-collection)
Flufo-121	Quepos Slide	carbonate	VL-197	permeable layer between bacterial mat and sediment
TV-MUC-78	Mound 10	carbonate	VL-107	carbonate on top (T.Moerz-collection)
TV-MUC-78	Mound 10	carbonate	VL-108	bright to dark with increasing depth (T.Moerz-collection)
TVG-90	Mound 10	carbonate	VL-121	clam trace
TVG-90	Mound 10	carbonate	VL-122	clam and beginning carbonatization
TVG-90	Mound 10	carbonate	VL-123	1/2 pipe (E. Suess-collection)
TVG-90	Mound 10	carbonate	VL-124	2 x 1/2 worm tube
TVG-90	Mound 10	carbonate	VL-125	tube filling
TVG-90	Mound 10	carbonate	VL-126	split pieces
TVG-128	Mound 11	carbonate	VL-198	dense, sediment-rich, concretion including wood, tubes

^{222}Rn samples

station	area	extraction routine	code extension	comment
			So173-	
CTD-22	Mound Iguana	water	VL-43	1l, bottle 1
CTD-22	Mound Iguana	water	VL-44	1l, bottle 2
TV-MUC-26	Mound Carablanca	water	VL-45	1l, no wash volume
TV-MUC-29	Mound Carablanca	water	VL-46	1l with 1l wash
BWS 32	Mound Carablanca	water	VL-47	bottle 1, slight bubbling on top
BWS 32	Mound Carablanca	water	VL-48	bottle 3
BWS 32	Mound Carablanca	water	VL-49	bottle 5, slight bubbling
TV-MUC-52	Mound Culebra	pore water	VL-79	3 ml 21-23 cm, 25 ml sediment
TV-MUC-52	Mound Culebra	pore water	VL-80	8 ml, 1-3 cm, 12.5 ml sediment
TV-MUC-52	Mound Culebra	pore water	VL-81	1 ml, 25-28 cm, 35 ml sediment
TV-MUC-96	Mound Culebra	pore water	VL-110	0 - 5 cm
TV-MUC-96	Mound Culebra	pore water	VL-111	17.5 – 25.5 cm
TV-MUC-96	Mound Culebra	pore water	VL-112	25 - 30 cm
TV-MUC-96	Mound Culebra	pore water	VL-113	6 ml, 0 - 5 cm, 13,5 ml sediment
TV-MUC-96	Mound Culebra	pore water	VL-114	2.5 ml, 17,5 - 25.5 cm, 17 ml sediment
TV-MUC-96	Mound Culebra	pore water	VL-115	1 ml, 25 - 30 cm, 11 ml sediment
TV-MUC-96	Mound Culebra	pore water	VL-116	14 ml, 0 - 5 cm, 32 ml sediment
TV-MUC-96	Mound Culebra	pore water	VL-117	3 ml, 17,5 - 25.5 cm, 31 ml sediment
TV-MUC-96	Mound Culebra	pore water	VL-118	2 ml, 25 - 30 cm, 27 ml sediment
TV-MUC-96	Mound Culebra	pore water	VL-119	2 ml, 25 - 30 cm, 28 ml sediment
TV-MUC-96	Mound Culebra	water	VL-120a	1l
TV-MUC-96	Mound Culebra	water	VL-120b	200 ml
CTD-58	BGR-Slide	pore water	VL-82	1l, bottle 18
CTD-58	BGR-Slide	pore water	VL-83	1l, bottle 19
CTD-58	BGR-Slide	pore water	VL-84	1l, bottle 2
TV-MUC-64	Quepos Slide	pore water	VL-86	4.5 ml
TV-MUC-64	Quepos Slide	pore water	VL-87	13 ml
TV-MUC-64	Quepos Slide	pore water	VL-88	1.75 ml
TV-MUC-64	Quepos Slide	pore water	VL-89	1.5 ml

TV-MUC-64	Quepos Slide	pore water	VL-90	0.5 ml
TV-MUC-64	Quepos Slide	pore water	VL-91	0.25 ml
TV-MUC-64	Quepos Slide	pore water	VL-92	8 ml
BWS - 65	Quepos Slide	water	VL-93	II bottle 1
BWS - 65	Quepos Slide	water	VL-94	II bottle 2
TV-MUC-73	Quepos Slide	pore water	VL-95	7.25 ml, 0-1 cm
TV-MUC-73	Quepos Slide	pore water	VL-96	10.5 ml, 1-3 cm
TV-MUC-73	Quepos Slide	pore water	VL-97	15,5 ml, 3-5 cm
TV-MUC-73	Quepos Slide	pore water	VL-98	14 ml, 9-11 cm (free gas)
TV-MUC-73	Quepos Slide	pore water	VL-99	14 ml, 13-16 cm
TV-MUC-73	Quepos Slide	pore water	VL-100	11 ml, 19-22 cm
TV-MUC-73	Quepos Slide	pore water	VL-101	4.5 ml, 25-28 cm (granulate)
TV-MUC-73	Quepos Slide	pore water	VL-102	0.5 ml, 31-34 cm
TV-MUC-73	Quepos Slide	water	VL-103	100 ml
GC-74	Quepos Slide	pore water	VL-104	4.5 ml, 42-45 cm, coarse layer like end of MUC-73
GC-74	Quepos Slide	pore water	VL-105	3.7 ml, 275-280 cm
GC-74	Quepos Slide	pore water	VL-106	1.75 ml, 518-522 cm
BWS-103	Quepos Slide	water	VL-132	bottle 1 (high methane in bottle 2)
BWS-103	Quepos Slide	water	VL-133	bottle 3 (high methane in bottle 2)
BCL-109-k3	Quepos Slide	water	VL-134	200 ml (sediment and free gas rich)
BCL-109-k3	Quepos Slide	pore water	VL-135	3 ml, 1-2 cm, 7,5 ml sediment
BCL-109-k3	Quepos Slide	pore water	VL-136	1 ml, 3-4 cm, 5 ml sediment
BCL-109-k3	Quepos Slide	pore water	VL-137	2,25 ml, 5-7 cm, 7,5 ml sediment
BCL-109-k3-1	Quepos Slide	water	VL-138	2,5 ml, 0 min, syringe 1
BCL-109-k3-2	Quepos Slide	water	VL-139	2,5 ml, 10 min, syringe 2
BCL-109-k3-3	Quepos Slide	water	VL-140	2,5 ml, 40 min, syringe 3
BCL-109-k3-4	Quepos Slide	water	VL-141	2,5 ml, 130 min, syringe 4
BCL-109-k3-5	Quepos Slide	water	VL-142	2,5 ml, 370 min, syringe 5
BCL-109-k3-6	Quepos Slide	water	VL-143	2,5 ml, 670 min, syringe 6
BCL-109-k3-7	Quepos Slide	water	VL-144	2,5 ml, 1210 min, syringe 7
Flufo-121-K5-1	Quepos Slide	water	VL-166	4 ml syringe 1 sample plus 6 ml maxilight
Flufo-121-K5-2	Quepos Slide	water	VL-167	4 ml syringe 2 sample plus 6 ml maxilight
Flufo-121-K5-3	Quepos Slide	water	VL-168	4 ml syringe 3 sample plus 6 ml maxilight
Flufo-121-K5-4	Quepos Slide	water	VL-169	4 ml syringe 4 sample plus 6 ml maxilight
Flufo-121-K5-5	Quepos Slide	water	VL-170	4 ml syringe 5 sample plus 6 ml maxilight
Flufo-121-K5-6	Quepos Slide	water	VL-171	4 ml syringe 6 sample plus 6 ml maxilight
Flufo-121-K5-7	Quepos Slide	water	VL-172	4 ml syringe 7 sample plus 6 ml maxilight
Flufo-121-K4-1	Quepos Slide	water	VL-173	4 ml syringe 1 sample plus 6 ml maxilight
Flufo-121-K4-3	Quepos Slide	water	VL-174	4 ml syringe 3 sample plus 6 ml maxilight
Flufo-121-K4-5	Quepos Slide	water	VL-175	4 ml syringe 5 sample plus 6 ml maxilight
Flufo-121-K4-7	Quepos Slide	water	VL-176	4 ml syringe 7 sample plus 6 ml maxilight
Flufo-121-K4	Quepos Slide	pore water	VL-177	14 ml, 0-2 cm, 12 ml sediment
Flufo-121-K4	Quepos Slide	pore water	VL-178	11 ml, 2-4 cm, 12,5 ml sediment
Flufo-121-K4	Quepos Slide	pore water	VL-179	8 ml, 4-6 cm, 10 ml sediment
Flufo-121-K4	Quepos Slide	pore water	VL-180	13 ml, 8-10 cm, 15 ml sediment
Flufo-121-K4	Quepos Slide	pore water	VL-181	10 ml, 14-16 cm, 18 ml sediment
Flufo-121-K4	Quepos Slide	pore water	VL-182	3 ml, 18-20 cm, 8 ml sediment
Flufo-121-K4	Quepos Slide	water	VL-183	II
Flufo-121-K4	Quepos Slide	water	VL-184	II
Flufo-121-K5	Quepos Slide	water	VL-184 b	200 ml
GC-110-1	Mound 12	pore water	VL-145	2,5 ml, 5 cm, 25 ml sediment
GC-110-1	Mound 12	pore water	VL-146	0,5 ml, 30 cm, 23 ml sediment
GC-110-1	Mound 12	pore water	VL-147	0,5 ml, 45 cm (above carbonate layer), 23,5 ml sed
GC-110-1	Mound 12	pore water	VL-147	0,5 ml, 45 cm (below carbonate layer), 23,5 ml sed
GC-110-1	Mound 12	pore water	VL-148	1 ml, 65 cm (below carbonate layer), 22 ml sed.
GC-110-1	Mound 12	pore water	VL-149	0,5 ml, 120 cm, 24 ml sediment
GC-115	Mound 12	pore water	VL-153	0.6 ml, 30 cm, 27,5 ml sediment
GC-115	Mound 12	pore water	VL-154	1,2 ml, 120 cm, 27 ml sediment
GC-115	Mound 12	pore water	VL-155	1 ml, 210 cm, 34 ml sediment

GC-115	Mound 12	pore water	VL-156	1 ml, 310 cm, 37,5 ml sediment
GC-115	Mound 12	pore water	VL-157	0.75 ml, 425 cm, 34 ml sediment (slight smell)
GC-115	Mound 12	pore water	VL-158	0.75 ml, 575 cm. 37,5 ml sediment (strong smell)
MUC-118	Mound 12	pore water	VL-159	4,25 ml, 5-7 cm, 20 ml sediment (strong smell)
MUC-118	Mound 12	pore water	VL-160	1 ml, 15-17 cm. 32 ml sediment (strong smell)
MUC-118	Mound 12	pore water	VL-161	0.5 ml, 27-29 cm. 25 ml sediment (strong smell)
MUC-118	Mound 12	water	VL-162	1l, sediment- and gas-rich
MUC-120	Mound 12	pore water	VL-163	12,5-17,5 cm
MUC-120	Mound 12	pore water	VL-164	12.5-17.5 cm
MUC-120	Mound 12	pore water	VL-165	12,5-17.5 cm
BCL-126-K1-1	Mound 12	water	VL-185	40 ml syringe 1 sample plus 6 ml maxilight
BCL-126-K1-2	Mound 12	water	VL-186	40 ml syringe 2 sample plus 6 ml maxilight
BCL-126-K1-3	Mound 12	water	VL-187	40 ml syringe 3 sample plus 6 ml maxilight
BCL-126-K1-4	Mound 12	water	VL-188	40 ml syringe 4 sample plus 6 ml maxilight
BCL-126-K1-5	Mound 12	water	VL-189	40 ml syringe 5 sample plus 6 ml maxilight
BCL-126-K1-6	Mound 12	water	VL-190	40 ml syringe 6 sample plus 6 ml maxilight
BCL-126-K1-7	Mound 12	water	VL-191	40 ml syringe 7 sample plus 6 ml maxilight
BCL-126-K1	Mound 12	pore water	VL-192	12 ml, 0-2 cm, 20 ml sediment
BCL-126-K1	Mound 12	pore water	VL-193	9 ml, 2-4 cm. 20 ml sediment
BCL-126-K1	Mound 12	water	VL-194	200 ml plus 10 ml maxilight
BCL-126-K2	Mound 12	water	VL-195	200 ml, reserve, no scint.
BCL-126-K3	Mound 12	water	VL-196	1 l
Flufo 134	Mound 12	water	VL-199	1 l
GC-135-1	Mound 12	gashydrate	VL-200	some chips, molten in maxilight
GC-135-1	Mound 12	gashydrate	VL-201	some chips, molten in maxilight

Table 6.10.1: Samples for Trace Element Geochemistry

St. No. SO 173/3	Instrument	Latitude N°	Longitude W°	Water depth (m)	Sample Type	Sample depth SW in [m]; BSW, PW in [cm]; VP [Bottle No.]; INC in [min]																		Remarks
5-1	GC	11:12.50	87:10.86	1334	PW	60	90	120	150	180	210	240	270	300	330									Mound Quetzal
6-1	GC	11:12.25	87:10.83	1330	PW	10	40	70	105	130	160	190	220	250	280	310	340	370	VL					Mound Quetzal
10	CTD	12:00.00	88:09.00	1622	SW	1000	900	800	700	650	600	550	500	450	425	400	400	375	350	300	250	200	150	Background
						100	70	70	30	5	5	Blk	Blk	Blk										
11	GC	11:59.99	88:09.01	1636	PW	230	290	325	380	430	490	540	595	645	700	730								Asn layers
11-1	GC	12:00.00	88:09.0	1622	PW	20	48	50	150	213	260	320	370	450	530	590	650	750	850	950	1040	1130		Asn layers
12	CTD	11:28.00	88:27.0	4102	SW	1000	900	800	700	650	600	550	500	475	450	425	400	375	350	325	300	250	200	Background
						150	100	70	40	20	5													
13-1	GC	11:26.37	88:28.00	4134	PW	4	32	60	172	122	99	185	220	270	410	500	540	blk						Asn layers
14	CTD	11:04.00	89:18.00	3450	SW	1000	900	800	700	650	600	550	500	475	450	425	400	375	350	325	300	264	200	Background
						150	100	30	20	4														
15	GC	10.43.14	88.54.15	3288	PW	25	100	140	193	240	290	340	390	440	496	540	590							Asn layers
16	CTD	10.45.00	88.53.00	3200	SW	1000	800	700	650	600	550	500	475	450	425	425	400	375	350	325	300	250	200	Background
						150	100	60	30	4	4													
17	GC	11:15.79	88:12.60	3216	PW	10	30	80	210	160														Asn layers
18	GC	11:36.00	87:36.00	1606	PW	20	70	120	170	220	270	315	390	490	550	590	650	690	790					Asn layers
25	GC	11:08.30	87:02.80	1229	PW	25	44	110	155	210	260													Asn layers
26	MUC	11:16.38	87:15.12	1435	PW	0-1	-2	-3	-5	-7	-9	-11	-13	-16	-19	-21	-24	-27	-29	BW				Mound Carablanca
28	MUC	11:16.42	87:15.29	1425	PW	0-1	-2	-3	-5	-7	-9	-11	-13	-15	-17	BW								Mound Carablanca
29	MUC	11.16.44	87:15.30	1425	PW	0-1	-2	-3	-5	-7	-9	-11	-13	BW										Mound Carablanca
32	BWS	11:16.43	87:15.24	1430	BSW	24	39.5	61	88.5	112														Mound Carablanca
33	GC	11:16.33	87.15.11	1479	PW	20	40	60																Mound Carablanca
34	GC	11:16.42	87:15.32	1430	PW	10	30	50	75	125	160	220	320	380	405	430								Mound Carablanca
38	MUC	11.00.16	87.00.55	1670	PW	0-1	-2	-3	-5	-7	-9	-11	-13	-15	BW									Mound Morpho
39	MUC	11.00.11	87:00.60	1669	PW	0-1	-3	-5	-7	-9	-11	-13	-15	-17	-19	-21	-23	-25	-27					Mound Morpho
40	GC	10.00.47	86.11.46	2283	PW	30	90	130	200	230	260	300	340	390	420	450	490	520	550					Mound 10

Table 6.10.1: Samples for Trace Element Geochemistry (continued)

St. No. SO 173/3	Instrument	Latitude N°	Longitude W°	Water depth (m)	Sample Type	Sample depth SW in [m]; BSW, PW in [cm]; VF [Bottle No.]; INC in [min]																		Remarks
49	GC	10 15 94	86 16 61	1530	PW	20	60	90	140	190	240	290	330	370	400	430	470	500	530	570	600	630	660	Culebra Spur
						690	720	750	780	810														
52	MUC	10 18 00	86 18 32	1531	PW	0-1	-3	-5	-7	-9	-11	-13	-15	-17	-19	-21	-23	-25	-28	BW			w/ clam	Culebra N Slope
52 b	MUC	10 18 00	86 18 32	1531	PW	0-2	-4	-7	-10	-13	-16	-19	-22	-25	-28	-31	-35	-37	BW				wo clam	Culebra N Slope
52-1	MUC	10:17 91	86 18 32	1522	PW	0-2	-4	-6	-8	-10	-13	-16	-19	-22	-24	-26	-28	BW						Culebra N Slope
59	GC	9:11 76	84 40 00	559	PW	10	40	90	130	180	220	270	310											BGR Slide
59-1	GC	9:11 83	84 39 87	554	PW	20	70	110	160	270	310	370	410											BGR Slide
61-1	GC	9:11 80	84 37 24	654	PW	20	50	100	150	200	230	260	300	330	360	400	430	460	480	500	530			BGR Slide
63	MUC	8 51 14	84 13 03	408	PW	0-1	-2	-3	-5	-7	-9	-11	-13	-16	-19	-22	-25	-28	-31	-34	-37	-40	-43	Quepos Slide
						BW																		
64	MUC	8 51 12	84 13 04	407	PW	0-1	-3	-5	6-9	-11	-14	-17	-20	-23	-26	-29	-32	-35	-38	-42	-46	-49	-52	Quepos Slide
						-55	BW																	
65	BWS	8 51 10	84 13 04	403	SW	24	39.5	61	88.5	112														Quepos Slide
71	MUC	8:51 20	84 13 19	399	PW	0-5	-10	-15	-20	-25	-30	-35	-40	-45	-50	-55								Quepos Slide
73	MUC	8:51 18	84 13 13	404	PW	0-1	-3	-5	-7	-9	-11	-13	-16	-19	-22	-25	-28	-31	-34	BW				Quepos Slide
74	GC	8 51 19	84 13 15	405	PW	55	80	105	130	155	180	205	230	255	285	310	335	360	385	410	435	460	500	Quepos Slide
						530	570																	
75	BWS	8:51 17	84 13 19	398	SW	24	39 5	61	88.5	112														Quepos Slide
78	MUC	10:00 42	86 11 40	2264	PW	0-1	-3	-5	-7	-9	-11	-13	-15	BW										Mound 10
81	GC	10:00.51	86 11.39	2272	PW	10	30	50	70	90	100	120	140	160	170									Mound 10
87	GC	10:17.93	86 18.45	1524	PW	10	35	60	85	110	135	160												Mound Culebra
91	BWS	10:00.50	86:11.41	2267	SW	24	39.5	61	88.5	112														Mound 10
95	MUC	10:17 90	86.18.45	1555	PW	0-1	-3	-5	-8	-11	-14	BW												Mound Culebra
96	MUC	10:17.96	86 18.38	1554	PW	0-2	-4	-6	-8	-10	-12	-14	-16	-18	-20	-22	-24	-26	-29	BW				Mound Culebra
97	GC	10:15 93	86 16.61	1531	PW	20	40	70	100	130	160	190	220	235	265	295	325	355	385	420	447	477	507	Mound Culebra
						537	567	595																Area

Table 6.10.1: Samples for Trace Element Geochemistry (continued)

St. No. SO 173/3	Instrument	Latitude N°	Longitude W°	Water depth (m)	Sample Type	Sample depth SW in [m]; BSW, PW in [cm]; VF [Bottle No.]; INC in [min]																		Remarks
98	GC	10:17.79	86:18.59	1567	PW	30	90	120	150	190	220	250	290	303	320	350	390	420	450					Mound Culebra
103	BWS	8:51.16	84:13.04	401	SW	24	39.5	61	88.5	112														Jaco Scarp
109	BCL	8:51.24	84:13.16	391	SW	0	10	40	130	370	670	1210												Quepos Slide
109	BCL	8:51.24	84:13.16	391	PW	0-1	-2	-3	-5	-8	BW													Quepos Slide
110-1	GC	8:55.74	84:18.81	1006	PW	5	17	30	45	65	85	105	120											Mound 12
112	BWS	8:55.74	84:18.81	1011	SW	24	39.5	61	88.5	112														Mound 12
115	GC	8:55.68	84:18.62	1008	PW	30	70	120	170	210	240	270	310	360	425	470	500	540	575					Mound 12
117	GC	8:56.30	84:18.88	986	PW	80	150	190	250	290	350	390	450	490	550	590								Mound 12
118	MUC	8:55.69	84:18.84	1018	PW	0-1	-3	-5	-7	-9	-11	-13	-15	-17	-19	-21	-23	-25	-27	-29	-31	-33	BW	Mound 12
120	MUC	8:55.73	84:18.84	1011	PW	0-1	-3	-5	-7	-9	-11	-13	-16	-18	-22	-25	-28	-31	-32	BW				Mound 12
121	FLUFO	8:51.26	84:13.20	402	SW	0	10	40	130	310	610	1030												Quepos Slide
121	FLUFO	8:51.26	84:13.20	402	PW	0-2	-4	-6	-8	-10	-12	-14	-16	-17	BW									Kammer 4
121	FLUFO	8:51.26	84:13.20	402	PW	0-1	-3	-5	-7	-9	BW													Kammer 5
122	GC	9:11.65	84:39.10	567	PW	90	140	190	240	290	340	390	440	490	540	590	640							BGR-Slide
126	BCL	8:55.66	84:18.81	1004	SW	0	10	40	100	280	580	1000												Mound 12
126	BCL	8:55.66	84:18.81	1004	PW	0-1	-3	-5	-7	BW														Kammer 2
126	BCL	8:55.66	84:18.81	1004	PW	0-1	-2	-4	-8	BW														Kammer 3
127	MUC	8:55.32	84:18.25	1012	PW	0-1	-3	-5	-7	-9	-11	-13	-15	-17	-19	-21	-23	-26	BW					Mound 11
134	FLUFO	8:55.52	84:18.77	1021	SW	0	10	40	100	220	360	570												Mound 12
134	FLUFO	8:55.52	84:18.77	1021	PW	0-1	-3	-5	-7	-10	-13	-16	BW											Kammer 4
134	FLUFO	8:55.52	84:18.77	1021	PW	0-1	-3	-5	-8	-11	BW													Kammer 5
135-1	GC	8:55.69	84:18.81	1015	PW	40	80	105	140	180	205	250	280	315	340	365	415	440	465	515	540	565		Mound 12

CTD (Niskin Rosette Sampler) GC (Gravity Corer) VESP-L (Vent Lander) PW (Pore Water) VF (Vent Fluid)

TV-MUC (TV-Multicorer) TV-G (TV-Grab sampler) BC (Benthic Chamber lander) SW (Sea Water) INC (Incubation)

MUC (Multicorer) VESP (Vent Sampler) BWS (Bottom Water Sampler) BSW (Bottom Sea Water) FLUFO

6.11 Lander Results

P. Linke, M. Piper, M. Poser, T. Schott

During SO 173/4 the landers were deployed at three different locations (Tab. 6.11.1). The deployments at Quepos slide and Mound 12 yielded the most complete data sets, consisting of a time series of methane, and nutrient concentrations in the enclosed bottom water of the chamber, as well as the pore water composition of the sediments recovered. These data clearly show that at both stations, the lander was deployed on sediments that were influenced by fluid venting. Furthermore, the data show considerable variability between the different chambers of each deployment reflecting the patchy distribution of venting. Here, we are presenting the data of BCL1 chamber K3 as an example of vigorous chemical release and turnover at the vent sites (Fig. 6.11.1& Fig. 6.11.2).

As a part of an extensive sediment and pore water sampling program the BC and FLUFO Landers were deployed at Quepos slide, where a large area below the headwall is densely covered by bacterial mats. Figures 6.11.1 & 6.11.2 show results obtained from the BCL1 deployment. The changes of concentration in the chamber and the pore water profiles in the retrieved sediments show that methane-rich and chloride-depleted fluids reach the sediment surface forcing intense anaerobic oxidation of methane (AOM) and carbonate precipitation (see section 6.7.). In contrast to the chloride-depleted fluids at the mound locations, it is assumed that a freshwater outflow following a steep hydrostatic gradient from the mountainous hinterland is triggering the processes at this site. High flow rates are indicated by the steep concentration gradients close to the sediment-water interface in the chamber which are continued in the TV-MUC cores (SO 173/63 & 64) and by the uniformity of the profiles in the gravity core (SO 173/74).

Table 6.11.1: Summary of BCL and FLUFO deployments during SO 173/4.

Station No. Deployment / Recovery	Area	No.	Chamber sediment recovery	O_2	CH_4	Nutrients	PW
BCL1 102 / 109	Quepos slide						
		K1	8 cm	Anox.	x	x	
		K2	8 cm	x	x	x	
		K3	8 cm	Anox.	x	x	x
BCL2 116 / 126	Mound 12						
		K1	6 cm	n.d.	x	x	
		K2	8 cm	x	x	x	x
		K3	7 cm	x	x	x	x
BCL3 130 / 136	Mound 11						
		K1	-	-	-	-	-
		K2	-	-	-	-	-
		K3	-	-	-	-	-
FLUFO1 108 / 121	Quepos slide						
		K4	18 cm	Anox.	x	x	-
		K5 (ref)	18 cm,	increase	x	x	x
FLUFO2 129 / 134	Mound 12	K4	17 cm	x	x	x	x
		K5 (ref)	15 cm	increase	x	x	x

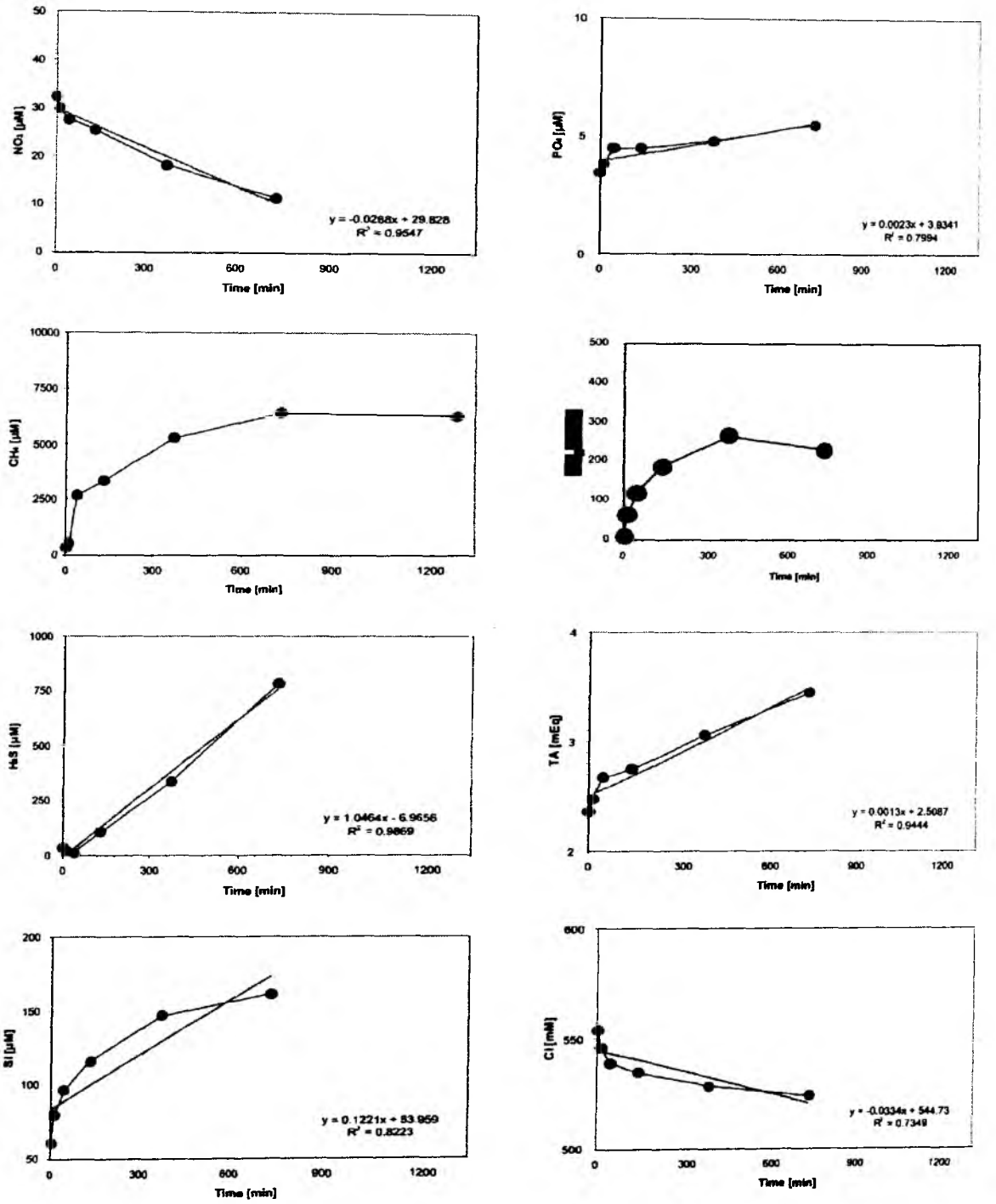

Fig. 6.11.1: *The concentration change of chemical constituents in the chamber water with time (BCL1 109, K3, Quepos slide). Oxygen was not detectable and the decrease in clorinity depicts the impact of freshened water. Alkalinity increase can be explained by vigorous methane oxidation.*

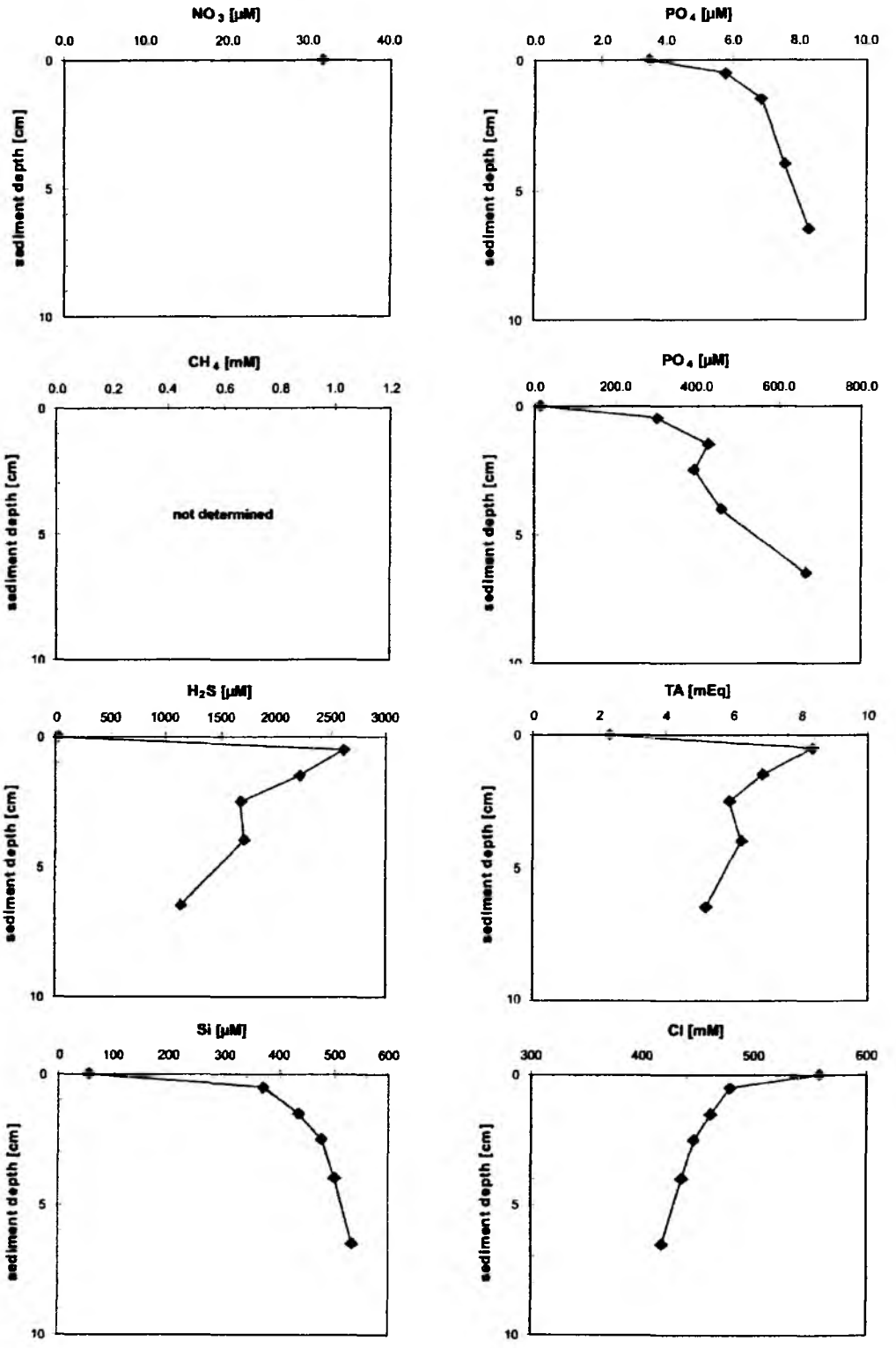

Fig. 6.11.2: The chemical composition of pore water in the sediments retrieved in chamber K1, BCL1 109 at Quepos slide. The sharp gradients indicate the release of a low-chlorinity sulphidic fluids.

6.12 Biological Samples

S. Echeverría Sáenz, H. Sahling

The marine fauna at the continental slope off Costa Rica is largely unknown. Thus, the primary objective was to collect all biological samples that came on board. The sediments that came with the geological samples (TV-MUC, TVG, Landers) were sieved to extract the macrofauna. Smaller organisms were hand-selected from the sediments using a dissecting microscope. All specimens were preserved in 10 % borax-buffered formaldehyde or frozen.

Seep species were taken back to the lab in Germany for further taxonomic and genetic studies. Non-seep species were collected from various stations (Tab. 6.12.1) and will be classified in the working group around Ingo Werthmann (ingowerthmann@gmx.de) at the Biological School of the University of Costa Rica. The samples will find their final depository at the Zoology Museum in San José.

Table 6.12.1: Biological non-seep samples collected during SO 173/4.

Date 2003	Station	Taxon
06 / Sep	TVG 8	Ophiuroidea (Associated with soft coral)
12 / Sep	TV-MUC 39	Ophiuroidea
14 / Sep	TV-MUC 52-1	Filaments (attached to Carbonate)
18 / Sep	TV-MUC 71	Polychaeta
18 / Sep	Attached to CTD 72	Jellyfish
18 / Sep	TV-MUC 73	Gastropoda (shallow water?)
19 / Sep	TV MUC 78	Bivalvia + Polychaeta
21 / Sep	TG 90	Polychaeta + Sipunculida
22 / Sep	TV-MUC 95	Cirripedia
22 / Sep	TV-MUC 96	Sediment small-sized fauna
24 / Sep	Lander BC-L 109	Decapoda + Polychaeta + Mollusca
26 / Sep	Lander BC-L 126	Bivalvia + polychaeta
26 / Sep	TV-MUC 127	Polychaeta
26 / Sep	TVG 128	Bivalvia/ Solemyidae
27 / Sep	Lander FLUVO 134	Gasteropoda + Polychaeta

7 Acknowledgements

Cruise SO 173 was funded by the German Ministry of Education and Research (BMBF) within the continued and generous most commendable support for marine sciences with an outstanding research vessel such as Sonne.

The cruise is part of SFB574 at Christian Albrechts University in Kiel, which is supported by the Deutsche Forschungsgemeinschaft (DFG).

We warmly thank masters M. Kull and H. Andresen and their crew for their excellent support in all the work done and for the splendid working atmosphere throughout the entire and ambitious working program.

And last but not least we thank Mrs. Silke Schenck and Mr. Wolf Semm for the valuable assistance reviewing and correcting the manuscript. Your efford to adjust everyones written english to a common standard was much appreciated.

8 References

Abers, G.A., Plank, T. and Hacker, B.R. (2003) The wet Nicaragua slab, Geophys. Res. Lett., 30(2), 1098, doi: 10.1029/2002GL015649.

Bange, H. W., Bartell, U. H., Rapsomanikis, S., Andreae, M. O. (1994) Methane in the Baltic and North Seas and a reassessment of the marine emissions of methane. Glob. Biogeochem. Cycl., 8, pp. 465-480.

Bialas J. and Flueh E.R. (1999) A new Ocean Bottom Seismometer (with a new type of data logger), Sea Technology, 40, p. 4.

Blondel, P. and Murton, B.J. (1998) Handbook of seafloor imagery. John Wiley and Sons Ltd, West Sussex, England. 314 pp.

Blum, P. (1997) Physical properties handbook: A guide to the ship board measurement of physical properties of deep-sea cores. ODP Technique Note, 26, vol. available from http://www.odp.tamu.edu/publications/tnotes/tn/INDEX.HTM.

Bohrmann, G., Jung, C., Heeschen, K., Weinrebe, W., Baranov, B., Cailleau, B., Heath, R., Hühnerbach, V., Hort, M., Masson, D. and Schaffer, I. (2002) Widespread fluid expulsion along the seafloor of Costa Rica convergent margin. Terra Nova, 14, pp. 69-79.

Breitzke, M., Bialas, J., Kostrov, A., Krabbenhöft, A., Planert, L. and Schott, T. (in press) Deep-towed seismic and acoustic investigations. In: V. Spieß and Cruise Participants, Report and Preliminary Results of Meteor Cruise M 56, Douala (Cameroun) - Libreville (Gabon), November, 11 - December 29, 2002. Berichte, Fachbereich Geowissenschaften, Universität Bremen.

Carey, S. and Sigurdsson, H. (2000) Grain Size of Miocene volcanic ash layers from Sites 998, 999, and 1000: Implications for source areas and dispersal. In: Leckie, R. M., Sigurdsson, H., Acton, G. D. and Draper, G., (eds): Grain Size of Miocene volcanic ash layers from Sites 998, 999, and 1000: Implications for source areas and dispersal. College Station, 165, pp. 101-113.

Clift, P. D. and Blusztajn, J. (1999) The trace-element characteristics of Aegean and Aeolian volcanic arc marine tephra. J. Volc. Geo. Res., 92, pp. 321-347.

Dobson, D.P., Meredith, P.G. and Boon, S.A. (2002) Simulation of Subduction Zone Seismicity by Dehydration of Serpentine. Science, 298, pp. 1407-1410.

Grasshoff, K., Ehrhardt, M. and Kremling, K. (1997) Methods of seawater analysis. Verlag Chemie, Gulf Publishing, Houston.

Gutenberg, B. and Richter, C.F. (1954) Seismicity of the earth and associated phenomena. Princeton University Press, pp. 310.

Flueh, E. R. and Bialas J., (1996) A digital, high capacity ocean bottom recorder for seismic investigations; Int. Underwater Systems Design 18(3), pp.18-20.

Flüh, E. R., Kukowski, N. and Reichert, C. (Ed.) (1997) FS SONNE, Fahrtbericht/Cruise Report SO 123: MAMUT (MAKRAN MURRAY TRAVERSE - Geophysik Plattentektonischer Extremfälle). Maskat-Maskat, 07.09 - 03.10.1997, GEOMAR Report 62, p. 292 .

Havskov, J. and Ottemöller, L. (Eds) (2001) SEISAN: The earthquake analysis software for Windows, Solaris and LINUX, version 7.2. Institute of Solid Earth Physics, University of Bergen, Norway.

Hinz, K., von Huene, R., Ranero, C.R. and the PACOMAR Working Group (1996) Tectonic structure of the converget Pacific margin offshore Costa Rica from multichannel seismic reflection data. Tectonics, 15, pp. 54-66.

Ivanenkov, V. N. and Lyakhin, Y. L. (1978) Determination of total alkalinity in seawater. In: Bordovsky, O.K. and Ivanenkov, V. N. (eds.): Methods of hydrochemical investigations in the ocean, Nauka Publ. House, Moscow, 11 0-1 14 (in Russian).

Katsumata, A. and Kamaya, N. (2003) Low-frequency continuos tremor around the Moho discontinuity away from volcanoes in the southwest Japan. Geophys. Res. Letters, v. 30, n. 1, doi: 10.1029/ 2002GL015891.

Kimura, G., Silver, E. and Shipboard Scientific Party (1997) Initial reports of the Ocean Drilling Program, Volume 170. College Station, Texas, Ocean Drilling Program, 458pp.

Knickmeyer, E.T. (1996) Hochgenaues Differential-GPS, Proc. 11th Annual Meeting of the German Hydrographic Society, Glücksburg, 3.-5.6.

Körtzinger, A. et al. (1996) At sea - intercomparison of two newly designed underway pCO2-systems - encouraging results. Mar. Chem., 52, pp. 133-145.

Kutterolf, S., Schacht, U., Wehrmann, H., Freundt, A. and Mörz, T. (2004) Onshore to offshore tephro-stratigraphy and marine ash layer diagenesis in Central America. In: Alvarado, G. and J., B. (eds): Onshore to offshore tephro-stratigraphy and marine ash layer diagenesis in Central America. Balkema, Lisse, Niederlande, Tokio, Japan.

Lammers, S. and Suess, E. (1994) An improved head-space analysis method for methane in seawater. Marine Chemistry, 47, pp. 115-125.

Lienert, B.R. and Havskov, J. (1995) A computer program for locating earthquakes both locally and globally. Seismological Res. Letters, 66, pp. 26-36.

Luetgert, J.H. (1992) RID One-Dimensional Seismic Travel Modeling: USGS Open File Report 43.

Obara, K. (2002) Nonvolcanic Deep Tremor Associated with Subduction in Southwest Japan. Science, 296, pp. 1679-1681.

Pfannkuche, O. and Linke, P. (2003) GEOMAR Landers as Long-Term Deep-Sea Observatories. Sea Technology, 44 (9), pp. 50-55.

Petrick, G., Schulz-Bull, D.E., Martens, V., Scholz, K., and Duinker, J.C. (1996) An in-situ filtration/ extraction system for the recovery of trace organics in solution and on particles tested in deep ocean water. Marine Chemistry, 54, pp. 97-105.

Ranero C. R., Phipps-Morgan, J., McIntosh, K. and Reichert, C. (2003) Bending, faulting and mantle serpentinization at the Middle America Trench. Nature, 425, pp. 367-373.

Ranero, C., von Huene, R. (2000) Subduction erosion along the Middle America convergent margin. Nature, 404, pp. 748-752.

Rehder, G., Keir, R., Suess, E. and Rhein, M. (1999) Methane in the Northern Atlantic controlled by microbial oxidation and atmospheric history. Geophysical Research Letters, 26, pp. 587-590.

Rehder, G. and Suess, E. (2001) Methane and pCO2 in the Kuroshio and the South China Sea during maximum summer surface temperatures. Mar. Chem., 75, pp. 89-108.

Rogers, G. and Dragert, H. (2003) Episodic Tremor and Slip on the Cascadia Subduction Zone: The Chatter of Silent Slip. Sciencexpress, report, 10.1126/science.1084783.

Schmincke, H.-U. (2003) Volcanism, Wissenschaftliche Buchgesellschaft, Darmstadt, ed. second.

Seeber, G. (1996) Stand und Einsatzmöglichkeiten von GPS - ein Überblick, Proc. 11th Annual Meeting of the German Hydrographic Society, Glücksburg, 3.-5.6.

Shipley, T.H. and Moore, G.F. (1986) Sediment accretion, subduction, and dewatering at the base of the trench slope off Costa Rica: a seismic reflection view of the décollement. J. Geophys. Res., 91, pp. 2019-2028.

Söding, E., Wallmann, K., Suess, E. and Flueh, E. R. (eds.) (2003) Cruise Report M 54/2+3: Fluids and Subduction Costa Rica 2002., vol. 111 (Geomar, Kiel).

Tobin, H., Vannucchi, P. and Meschede, M. (2001) Structure, inferred mechanical properties, and implications for fluid transport in the décollement zone, Costa Rica convergent margin. Geology, 29, pp. 907-910.

Ukstins Peate, I., Baker, J. A., Kent, A. J. R., Al-Kadasi, M., Al-Subbary, A., Ajylew, D. and Menzies, M. (2003) Correlation of Indian Ocean tephra to individual Oligocene silicic eruptions from Afro-Arabian flood volcanism. Earth Planet. Sci. Lett. 211, pp. 311-327.

von Huene, R., Ranero, C. R., Weinrebe, W. and Hinz, K. (2000) Quarternary convergent margin tectonics of Costa Rica, segmentation of the Cocos Plate, and Central American volcanism. Tectonics, 19, pp. 314-334.

Weiss, R. F. (1970) The solubility of nitrogen, oxygen and argon in water and seawater. Deep-Sea Research, 17, pp. 721-735.

Weiss, R. F. (1981) Determinations of carbon dioxide and methane by Dual Catalyst Flame Ionisation Chromatography and nitrous oxide by Electron Capture Chromatography. J. Chrom. Sci., 19, pp. 611-616.

Wessel, P. and Smith, W. H. F. (1995) New version of the Generic Mapping Tools released. EOS Trans. AGU, 76, p. 329.

Wiesenburg, D.A. and Guinasso, N. L. Jr. (1979) Equilibrium solubilities of methane, carbon monoxide, and hydrogen in water and seawater. J. Chem. and Engin. Data, 24, pp. 356-360.

Witte, U. and Pfannkuche, O. (2000) High rates of benthic carbon remineralisation in the abyssal Arabian Sea. Deep-Sea Res. II 47(14), pp. 2785-2804.

Ye, S., Bialas, J., Flüh, E.R., Stavenhagen, A., von Huene, R., Leandro, G., Hinz, K. (1996) Crustal structure of the Middle American Trench off Costa Rica from wide-angle seismic data. Tectonics, 15, 5, pp. 1006-1021.

Appendix A:
Seismic Profile Data Examples

ATTENTION

Appendix A is not included with this report. It can be downloaded and printed from the SFB574 website at http://www.sfb574.geomar.de /downloads/reports/so173/22_appendix_a.pdf

Appendix B:
Ocean Bottom Recorder Stations

Decollement

SUBDUCTION SONNE 173/1

INST.	LAT (N)	LON (W)	Distance to	DEPTH	REL.	ANT.	REC.	SKEW	SENSOR	Other Sensors	REMARKS
	D:M	D:M	next (nm)	(m)	CODE	CH.	REC.	(ms)	HYDRO.		
OBH 13	8:37.536	84:20.596	0.10	2590	3629	D	980905		HTI26		
OBH 14	8:37.440	84:20.497	0.12	2602	3674	C	991256		OAS22		
OBS 15	8:37.416	84:20.404	0.13	2600	03B8+0355	D	001006		HTI302	LG 07	
OBS 16	8:37.432	84:20.279	0.08	2607	3659	D	000611		OAS27	LG 06	
OBS 17	8:37.368	84:20.319	0.11	2626	03B5+0355	C	980403		HTI802	LG 05	
OBH 18	8:37.271	84:20.385	0.17	2657	3614	D	001001		OAS01		
OBS 19	8:37.305	84:20.205	0.10	2620	03B6+0355	B	000614		OAS29	Owen 10 (4,5 Hz)	
OBH 20	8:37.258	84:20.140	0.11	2634	03BB+0355	D	001002				
OBH 21	8:37.195	84:20.040	0.11	2602	3609	C	000612		HT01PCA		
OBH 22	8:37.141	84:19.945	0.14	2587	0386+0355	D	0613		S/N31200902		
OBH 23	8:37.068	84:19.819	0.14	2588	0387+0355	C	616		38		
OBH 24	8:36.998	84:19.703		2594	03B3+0355	C	990712		2		

MOUND 11-12

SO173 -1

INST.	LAT (N)	LON (W)	Distance to	DEPTH	REL.	ANT.	REC.	SKEW	SENSOR	Other Sensors	REMARKS
	D:M	D:M	next (nm)	(m)	CODE	CH.	REC.	(ms)	HYDRO.		
OBS 25	08:56.012	84:18.740	0.159	1008	03B8+0355	D	1006	0	HTI 22	LG 07	
OBH 26	08:55.878	84:18.654	0.156	993	03B3+0355	C	990712	-6	OAS 2		
OBS 27	08:55.756	84:18.557	0.144	1001	03B6+0355	D	614	-15	OAS 29	OWEN 10	
OBS 28	08:55.639	84:18.473	0.152	1020	03B5+3055	D	611	-8	HTI 802	LG 05	
OBS 29	08:55.519	84:18.379	0.606	1026	3659	D	980905	-9	OAS 27	LG 06	
OBH 30	08:55.999	84:18.749	0.789	1036	0386+0355	C	1001	-12	HTI 902 (28)		
OBH 31	08:55.375	84:18.266	0.259	1012	3609	B	1002	-4	HTI 30		
OBH 32	08:55.176	84:18.100	0.051	1044	03BB+0355	C	000612	-3	OAS 03		
OBH 33	08:55.136	84:18.069		1040	03B2+0355	C	20303			TILT 4949	

Oceanic Crust I — SUBDUCTION SO173 -1

INST.	LAT (N)	LON (W)	Distance to	DEPTH	REL.	ANT.	REC.	SKEW	SENSOR	Other Sensors	REMARKS
	D:M	D:M	next (nm)	(m)	CODE	CH.	REC.	(ms)	HYDRO.		
OBH 01	10:20.130	86:38.00	2.02	3926	03BD+0355	D	980905		HTI 26		
OBH 02	10:18.711	86:39.434	2.07	4266	03B3+0355	D	713		DPG 77		
OBH 03	10:17.197	86:40.979	1.94	4508	3609 or 3629		991256		1		
OBH 04	10:15.865	86:42.286	1.90	4900	0386+0355	C	1001		81200902		
OBH 05	10:14.69	86:43.661	1.82	4951	3609	D	613		HTI 01PCA		
OBH 06	10:13.199	86:44.982	1.81	4513	03BB+0355	D	1002		87		
OBH 07	10:11.959	86:46.274	1.92	4216	3614	D	990712		6		
OBH 08	10:10.587	86:47.702	1.87	4132	3674	C	30501		22		
OBS 09	10:9.217	86:49.016	1.75	4115	03B8+0355	D	614			LG 07	
OBS 10	10:8.002	86:50.277	1.68	3742	3659	D	1006		27	LG 06	
OBH 11	10:6.815	86:51.500	2.02	3793	03B6+0355	C	980403		99	Owen 10 (4,5 Hz)	
OBS 12	10:05.382	86:52.959		3491	03B5+0355	B	611		HTI 802	LG 05	

OCEANIC CRUST II — SUBDUCTION SO173 -1

INST.	LAT (N)	LON (W)	Distance to	DEPTH	REL.	ANT.	REC.	SKEW	SENSOR	Other Sensors	REMARKS
	D:M	D:M	next (nm)	(m)	CODE	CH.	REC.	(ms)	HYDRO.		
OBS 34	09:38.22	87:30.46	2.35	3234	03B5+3055	C	980905		HTI 27	LG 05	
OBS 35	09:39.87	87:28.79	2.93	3236	3659	D	000613		OAS 27	LG 06	
OBS 36	09:41.97	87:26.75	3.27	3186	03B8+0355	C	1006		HTI 22	LG 07	
OBS 37	09:44.21	87:24.37	2.86	3174	03B6+0355	D	614		OAS 29	OWEN 10	
OBH 38	09:46.25	87:22.36	2.77	3172	03BB+0355	C	990712		3		
OBH 39	09:48.20	87:20.39	2.24	3155	3609	C	1001		30		
OBH 40	09:49.77	87:18.79	1.80	3067	0386+0355	C	000616		28		
OBH 41	09:51.04	87:17.52	2.09	3090	03B3+0355	B	1002		2		
OBH 42	09:52.50	87:16.03	2.84	3064	3614	D	000612		6		
OBH 43	09:54.50	87:14.02	2.69	3116	3674	D	000611		22		
OBH 44	09:56.39	87:12.11	2.46	3110	3629	C	991259		HTI 26		
OBH 45	09:58.12	87:10.36	2.98	3068	03B9+0355	D	991238		OAS 30		
OBH 46	10:00.21	87:08.24	0.11	3070	0387+0355	C	991247		OAS 38		
OBH 51	10:00.21	87:08.35	3.06	3071	03B2+0355	D	020303			TILT 4948	
OBH 47	10:02.31	87:06.13	3.49	3078	03BD+0355	C	010401		HTI 30		
OBH 48	10:04.77	87:03.65	3.40	3098	3824	B	991242		DPG 91		
OBH 49	10:07.16	87:01.23	3.59	3177	03B7+0355	A	991250		DPG 74		
OBH 50	10:09.69	86:58.68		3369	03B4+0355	D	000713		DPG 86		

OUTER RISE SEISMICITY

SO173 -1

10:10.03	86:57.02	9.53	3398	03B7+0355	C	000713		DPG 74			
10:03:07	87:03.53	8.62	3048	3624	C	991242		DPG 91 71			
09:58.06	86:58.52	11.24	3120	03BD+0355	D	991237		DPG 78			
10:04.00	86:50.56	37.65	3551	03B4+0355	D	991250		DPG 86			
10:14.36	86:14.36		1239	03B8+03557	C	020303		tilt4948			

Appendix C: Airgun Profiles

Airgun - Pulserstation

Project: **SO 173-1** Line: ..... Gun-Array: ..**GI**..

Date	Time UTC	Latitude	Longitude	Speed [kn]	Course o.G/GPS	Guns	Depth [m]	Trigger Interval [s]	Remarks Operator
11.07.03	06:49	08°35	84°22	5		GI	1.7	8	1st Shot Profile 1
11.07.03	07:45	08°34.05	84°22.61	5		GI	1.7	8	Last Shot Profile 1
11.07.03	10:49	08°34.05	84°22.61	5		GI	1.7	8	1st Shot Profile 2
11.07.03	11:44	08°45 48	84°22.69	5		GI	1.7	8	Last Shot Profile 2
11.07.03	13:34	08°50.68	84°21.02	3		GI	1.7	8	1st Shot Profile 3
11.07.03	15:28	08°52.28	84°19.98	5		GI	1.7	8	Last Shot Profile 3
11.07.03	17:11	08°49.40	84°17.44	5		GI	1.7	8	1st Shot Profile 4
11.07.03	18:36	08°46.33	84°16.28	4.5		GI	1.7	8	After last shot Profile 4 (322)
12.07.03	00:00	08°48.77	84°10.59	2.5		GI	1.7	8	1st Shot Profile 5
12.07.03	01:00	08°48.3	84°10.5			GI	1.7	8	Last Shot Profile 5 (323)
12.07.03	02:12	8°52.02	84°12.36	4.9		GI	1.7	8	1st Profile Profile 7
12.07.03	03:17	8°54.13	84°13.25	4.9		GI	1.7	8	Last Shot Profile 7

Sheet - No.: .....1.....

Airgun - Pulserstation

Project: SO 173-1 Line: ..... Gun-Array: .....GI.....

Date	Time UTC	Latitude	Longitude	Speed [kn]	Course o.G./GPS	Guns	Depth [m]	Trigger Interval [s]	Remarks Operator
12.07.03	04:47	08°57.07	84°18.41	4.0		GI, 1.7I	1.7	8	1st Shot Profile 8
12.07.03	05:35	08°58.59	84°18.66	4.0		GI	1.7	8	Last Shot Profile 8
12.07.03	07:11	08°59.3	84°11.7	4.0		GI	1.7	8	Trace of bubbles along hose
12.07.03	08:06	08°59.35	84°10.50	4.0		GI	1.7	8	Last Shot Profile 9
12.07.03	09:03	09°02.00	84°11.42	5.0		GI	1.7	8	1st Shot Profile 10
12.07.03	09:34	09°04.15	84°12.13	5.0		GI	1.7	8	No trigger from ship
12.07.03	09:35	09°04.14	84°12.02	5.0		GI	1.7	8	Trigger back on
12.07.03	09:50	09°03.98	84°11.00	5.0		GI	1.7	8	Last shot Profile 10
12.07.03	11:13	09°02.89	84°16.36	5.0		GI	1.7	8	1st Shot OBH 317
12.07.03	11:57	09°04.79	84°16.66	5.0		GI	1.7	8	Last Shot OBH 317
12.07.03	13:10	09°09.22	84°15.51	4.2		GI	1.7	8	1st Shot OBH 318
12.07.03	14:08	09°10.07	84°15.07	3.5		GI	1.7	8	Last Shot OBH 318

Sheet - No.: .....2.....

Airgun - Pulserstation

Project: SO 173-1 Line: ..... Gun-Array: .....GI.....

Date	Time UTC	Latitude	Longitude	Speed [kn]	Course o.G/GPS	Guns	Depth [m]	Trigger Interval [s]	Remarks Operator
12.07.03	15:56	09°15.57	84°20.31	4.1		GI, I.7I	1.7	8	1st Shot Profile 12 OBH 302
12.07.03	16:46	09°16.44	84°20.96	2.2		GI	1.7	8	Last Shot Profile 12 OBH 302
12.07.03	19:36	09°16.40	84°28.29	3.4		GI	1.7	8	1st Shot Profile 14 OBH 301
12.07.03	20:28	09°15.62	84°30.82	3.4		GI	1.7	8	Last Shot Profile 14 OBH 301
12.07.03	22:35	09°08.89	84°22.38	2.9		GI	1.7	8	1st Shot Profile 15 OBH 303
12.07.03	23:08	09°07.98	84°23.89			GI	1.7	8	Last Shot Profile 15 OBH 303
13.07.03	00:32	09°01.87	84°24.06	4.4		GI	1.7	8	1st Shot Profile 16 OBH 304
13.07.03	01:03	09°01.58	84°25.49	4.4		GI	1.7	8	Last shot Profile 16 OBH 304
13.07.03	02:21	09°04.75	84°28.93	5.3		GI	1.7	8	1st Shot Profile 17 OBS 305
13.07.03	03:13	09°05.85	84°30.48	4.0		GI	1.7	8	Last Shot Profile 17 OBS 305
13.07.03	04:54	09°07.16	84°41.57	5.0		GI	1.7	8	1st Shot Profile 18 OBH 306
13.07.03	05:55	09°08.08	84°43.67	5.0		GI	1.7	8	Last Shot Profile 18 OBH 306

Sheet - No.: .....3.....

Airgun - Pulserstation

Project: SO 173-1 Line: ..... Gun-Array: .....GI.....

Date	Time UTC	Latitude	Longitude	Speed [kn]	Course o.G./GPS	Guns	Depth [m]	Trigger Interval [s]	Remarks Operator
13.07.03	08:16	08°09.90	84°48.80	4.7		GI, 1.7I	1.7	8	1st Shot Profile 18 OBS 307
13.07.03	09:09	08°51.11	84°50.20	3.4		GI	1.7	8	Last Shot Profile 18 OBS 307
13.07.03	12:14	08°38.83	84°34.08	5.0		GI	1.7	8	1st Shot Profile 19 OBH 308
13.07.03	13:00	08°39.91	84°32.36			GI	1.7	8	Last Shot Profile 19 OBH 308
13.07.03	14:16	08°44.95	84°30.72	4.8		GI	1.7	8	1st Shot Profile 21 OBH 311
13.07.03	14:57	08°46.67	84°30.25	3.1		GI	1.7	8	Last Shot Profile 21 OBH 311
13.07.03	16:42	08°51.56	84°34.25	4.0		GI	1.7	8	1st Shot Profile ?? OBH 312
13.07.03	17:19	08°53.55	84°34.85	3.8		GI	1.7	8	Last shot Profile ?? OBH 312
14.07.03	18:24	10°12.19	86°46.01	3.9		GI	1.7	10	1st Shot
14.07.03	19:11	10°09.68	86°48.58	4.6	224	GI	1.7	10	OK
14.07.03	19:25	10°08.92	86°49.39	4.4	223	GI	1.7	10	OK
14.07.03	19:37	10°08.28	86°50.00	4.7	225	GI	1.7	10	OK

Sheet - No.: .....4.....

Airgun - Pulserstation

Project: SO 173-1 Line: S-30 Gun-Array: GI

Date	Time UTC	Latitude	Longitude	Speed [kn]	Course o.G./GPS	Guns	Depth [m]	Trigger Interval [s]	Remarks Operator
14.07.03	20:02	10°06.88	86°51.44	4.8	221	GI, 1.7I	1.7	10	OK
14.07.03	20:31	10°05.27	86°53.10	4.6	224	GI	1.7	10	OK
14.07.03	20:37	10°05.72	86°30.13	2.2	224	GI	1.7	10	End of Line
14.07.03	22:28	09°56.11	87°02.46	4.2	051	BB Bolt	8	60	BB 1st Shot S-30 Bolt
14.07.03	22:44	09°56.84	87°01.67	4.1	045	SB Bolt	8	60	ST 1st Shot
14.07.03	23:02	09°57.76	87°00.70	4.4	043		6		Streamer into the water
14.07.03	23:50	10°00.10	86°58.33	4.1	046	BB + ST		60	OK
15.07.03	00:54			4.3	048	BB + ST		60	OK Monika
15.07.03	01:20	10°04.76	86°53.60	4.0	044	BB + ST		60	OK Monika
15.07.03	01:40	10°05.74	86°52.62	4.0	042	BB + ST		60	OK Monika
15.07.03	01:59	10°06.61	86°51.72	4.0	046	BB + ST		60	OK Monika
15.07.03	02:17	10°07.42	86°50.87	4.2	045	BB + ST		60	

Sheet - No.: 5

Airgun - Pulserstation

Project: **SO 173-1** Line: **S-20 S-30?** Gun-Array: **2+32L Bolt**

Date	Time UTC	Latitude	Longitude	Speed [kn]	Course o.G./GPS	Guns	Depth [m]	Trigger Interval [s]	Remarks Operator
14.07.03	02:46	10°08.80	86°49.46	4.1	045	BB+ST		60	STB not shooting, trigger OK, press OK
14.07.03	03:15	10°10.25	86°47.97	4.1	045	BB		60	STB gun on deck
14.07.03	03:30	Reduce Speed	Reduce Speed	3.0-3.5				60	BB OK
15.07.03	04:16	10°12.79	86°45.37	3.0	045	BB+STB			STB Gun 1st Shot
15.07.03	04:35	10°13.76	86°30.18	1.0	047	BB+STB		60	STB 1st Shot
15.07.03	05:01	10°15.08	86°43.06	4.4	047	BB+STB		60	OK
15.07.03	05:27	10°16.42	86°41.68	4.3	048	BB+STB		60	OK
15.07.03	05:49	10°17.56	86°30.18	4.4	047	BB+STB		60	OK
15.07.03	06:10	10°18.60	86°39.46	4.2	042	BB+STB		60	OK
15.07.03	06:30	10°19.58	86°38.47	4.3	048	BB+STB		60	
15.07.03	06:50	10°20.56	86°37.49	4.	045	BB+STB		60	
15.07.03		10°21.56	86°36.47	4.0	045	BB+STB		60	

Sheet - No.: 6

Airgun - Pulserstation

Project: SO 173-1 Line: S-30 Gun-Array: 2+32L Bolt

Date	Time UTC	Latitude	Longitude	Speed [kn]	Course o.G/GPS	Guns	Depth [m]	Trigger Interval [s]	Remarks Operator
15.07.03	07:21	10°22.07	86°35.94	4.1	047	BB+STB		60	
15.07.03	07:40	10°22.99	86°34.99	4.2	043	BB+STB		60	
15.07.03	08:00	10°23.94	86°34.03	4.2	044	BB+STB		60	
15.07.03	08:20	10°24.96	86°33.00	4.3	045	BB+STB		60	
15.07.03	09:21	10°27.93	86°29.94	3.2	041	BB+STB		60	End of Line

- No.: 7

Airgun - Pulserstation

Project: SO 173-1 Line: Gun-Array:

Date	Time UTC	Latitude	Longitude	Speed [kn]	Course o G/GPS	Guns	Depth [m]	Trigger Interval [s]	Remarks Operator
15.07.03	19:00	10°09.88	86°48.99	4.0	172	GI		10	1st Shot Profile 32 Quepos ??? OBS
15.07.03	20:56	10°06.82	86°53.32	5	270	GI		10	Last Shot Profile 32 Quepos ??? OBS
17.07.03	14:27	08°33.71	84°14.23	3.1	297	32 L Port	8	30	BOL
17.07.03	17:07	08°33.44	84°12.29		2.1	32	L Port 8	30	BOL
17.07.03	17:07	08°39.28	84°23.54	4	298	32 L Port	8	30	EOL

- No.: 8

Airgun - Pulserstation

Project: **SO 173-1** Line: **S33-GI/DTS** Gun-Array: **GI**

Date	Time UTC	Latitude	Longitude	Speed [kn]	Course o.G./GPS	Guns	Depth [m]	Trigger Interval [s]	Remarks Operator
18.07.03	03:56	08°41.26	86°26.90	2.3	120	GI	1.7	8	BOL
	04:10	08°40.92	86°26.37	2.3	123	GI	1.7	7	Change trigger interval
18.07.03	10:40	08°31.05	84°11.21	3.0	Turn	GI	1.7	7	
18.07.03	12:06	08°29.62	84°08.67	3.1	Turn	GI	1.7	7	
18.07.03	13:47	08°32.55	84°11.41	3.0	End Turn	GI	1.7	7	
18.07.03	14:40	08°33.79	84°13.57	2.8	306	GI	1.7	7	SOL 34
18.07.03	19:32	08°41.51	84°25.66	2.9	305	GI	1.7	7	Streamer on Deck
19.07.03	04:27	08°35.26	84°21.11	2.7	325	GI	1.7	7	SOL 36
19.07.03	12:06	08°36.04	84°21.16		8	11	GI 1.7	7	
19.07.03	13:00	08°33.74	84°22.60	3.0	212	GI	1.7	7	EOL 36

- No.: 9

Airgun - Pulserstation

Project: SO 173-1 Line: 40(?) Gun-Array: GI

Date	Time UTC	Latitude	Longitude	Speed [kn]	Course o.G./GPS	Guns	Depth [m]	Trigger Interval [s]	Remarks Operator
20.07.03	20:50	9°0.47	86°22.15	2.6	146	GI	1.7	7	BOL 40 (?)
20.07.03	21:46	8°58.5	84°21	2.9	145	GI	—	—	BOL
21.07.03	16:22	9°7.13	84°38.13	2.4	001	GI	1.2	7	Gi-Gun
21.07.03	18:36	9°13.98	84°38.66	2.8	170.4	GI	1.2	7	End Profile
21.07.03	20:19	9°13.98	84°38.01	2.6	183.9	GI	1.2	7	Begin Profile
21.07.03	22:03	9°13.95	84°38.04	3.1	181.9	GI	1.2	7	End Profile
21.07.03	22:50	9°8.21	84°39.68	3.0	273.9	GI	1.2	7	Problem with the trigger on ship (solved).
21.07.03	23:19	9°9.00	84°40.65	3.0	359.6	GI	1.2	7	Begin Profile
22.07.03	01:02	9°14.11	84°40.62	3.1	006.2	GI	1.2	7	End Profile (22->21)
22.07.03	01:47	9°13.82	84°39.33	3.0	179	GI	1.2	7	Begin Profile (17->18)
22.07.03	02:38	9°11.18	84°39.31	3.2	178	GI	1.2	7	Trigger off, then on
22.07.03	02:55	9°10.15	84°39.30	2.5	177	GI	1.2	7	Hydrosweep not working

Sheet - No.: 10

Airgun - Pulserstation

Project: SO 173-1 Line: ..... Gun-Array: .....GI.....

Date	Time UTC	Latitude	Longitude	Speed [kn]	Course o.G./GPS	Guns	Depth [m]	Trigger Interval [s]	Remarks Operator
22.07.03	03:27	9°08.70	84°39.30	2.7	193	GI	1.2	7	End Profile
22.07.03	04:26	9°09.25	84°41.38	3.1	000	GI	1.2	7	Begin Profile
22.07.03	04:33								Hydrosweep working again
22.07.03	05:11	9°11.34	84°41.40	2.9	000	GI	1.2	7	OK
22.07.03	05:37	9°12.64	84°41.41	2.9	000	GI	1.2	7	OK
22.07.03	06:06	9°14.05	84°41.38	3.1	000	GI	1.2	7	End Profile
22.07.03	07:07	9°13.99	84°39.80	3.4	179	GI	1.2	7	Begin Profile (5->6)
22.07.03	07:18	9°13.34	84°39.79	3.6	179	GI	1.2	7	OK
22.07.03	07:46	9°11.93	84°39.79	2.9	179	GI	1.2	7	OK
22.07.03	08:13	9°10.57	84°39.80	2.9	179	GI	1.2	7	OK

Sheet - No.:

Airgun - Pulserstation

Project: SO 173-1 Line: ..... Gun-Array: .....GI.....

Date	Time UTC	Latitude	Longitude	Speed [kn]	Course o.G./GPS	Guns	Depth [m]	Trigger Interval [s]	Remarks Operator
22.07.03	08:41	9°09.18	84°39.80	3.0	183	GI	1.2	7	OK, 5 minute to end
22.07.03	08:46	9°08.98	84°39.80	2.9	175	GI	1.2	7	End Profile
22.07.03	08:52	9°08.67	84°39.79	2.8	177	GI	1.2	7	Last shot

Sheet - No.: .....12.....

Appendix D:
Masters Report SO 173/1

FS SONNE **Reise SO 173.1** **Balboa 09.07.**
– Caldera 06.08.2003

Eingesetzte Geräte

Einsätze		
CTD-Sonde SIMRAD	CTD	1
Aufnahme/Auslage von OBH/OBS/OBT	76 / 59	135
Auslage Verankerung		1
Magnetik	Profile: 02 Profilzeit: 31 Std. Profildistanz: 436 sm	2
Side Scan Sonar	Profile: 43 Profilzeit: 186 Std. Profildistanz: 522 sm	43
Seismik	Profile: 41 Profilzeit: 98 Std. Profildistanz: 328 sm	41
Auslöser-Test	Gerätetest an W 6	3
Schlauchbooteinsätze		5

Simrad Fächerecholotsystem	im Dauerbetrieb
Thermosalinograph	im Dauerbetrieb
UKW-Peiler der Brücke	für Aufnahme/Auslage OBHs
Transducer im Lotschacht	für Akustik mit Bodengeräten
Posidonia-Antenne im Lotschacht	für DTS-Profilfahrt

Eingesetzte Winden :

Winde	D/M	. Typ	RF-Nr	SO 173.1 Einsatz	Gesamt Einsatz	SO 173.1 S'länge	Gesamt S'länge	Zust.
W 1	18,2	LWL	812001	0000 h	0000 h	000000 m	0000000 m	1
W 2	18,2	LWL	810001	0000 h	1659	000000	0966465	4-5
W 4	11,0	NSW	818045	0000 h	0034	000000	0036663	2
W 5	11,2	NSW	812106	0000 h	0012	000000	0008455	5 •
W 6	18,2	DRAKO	818238	0005 h	0743	007251	0730096	3

• ***EL-Kabel Winde W 5 spult sehr schlecht, erhebliche Zeitverluste bei Einsatz der Winde***

Winde	SO 173.1 gefierte max.Länge	jemals gefierte max.Länge	Seil-/Kabellänge Restlänge/Istlänge
W 1	0000 m	0000 m	8022 m
W 2	5699 m	7202 m	7603 m
W 4	0000 m	5489 m	8081 m
W 5	0000 m	4400 m	7000 m
W 6	4300 m	6400 m	7609 m

Geräteverluste : OBH Nr. 302 tauchte nicht auf und muss vorerst als Verlust verbucht werden.

Tiefseekabel

LWL W 2: Außenmantelschaden bei KL 3090-3095m (1 Litze gebrochen) die Stelle wurde am Anfang und am Ende der Schadstelle mit Tape versehen und laufend kontrolliert, bei Bedarf wurde die Stelle mit neuem Tape versorgt und somit erfolgreich eine Vergrößerung der Schadstelle vermieden. Die äußere Lage ist stark verrostet, das Kabel löst sich dort langsam auf. Zustand jetzt 4-5, sollte bei nächster Gelegenheit gegen ein neues Kabel gewechselt werden.
EL-Kabel W 4: Das Kabel wurde während der Reise SO 173.1 um 15m wegen Beschädigung am Kabelstopper aufgekürzt.
Tiefseeseil W 6: Das Seil wurde nach Einsatz mit Boltgun 32 Ltr. um 10m aufgekürzt, da aufgedreht.

Windenausfälle: keine

Abkürzungen im Stationsprotokoll:

z.W.	zu Wasser	a.D.	an Deck
KL max.	Kabellänge(maximale)	SL max	Seillänge (maximale)
WT	Lottiefe nach Simrad-Fächerecholotanlage		
W x	eingesetzte Winde	t / tw	Lufttemperatur / Wassertemperatur
PS	Parasound	SIMRAD	Simrad-Fächerecholotanlage

STATIONSPROTOKOLL **SO 173.1**

alle Zeitangaben in UTC

(LT = UTC - 5 Std.)

Mi., 09.07.2003
15:12 Abfahrt Balboa
16:00 Anfang der Seereise Revier 7sm 08 51,79 N 079 29,76 W

17:00 Sicherheitsmanöver mit Bootsmanöver 08 38,74 N 079 31,12 W
Wind: umlaufend 1, c 7/8, 1008,4 hPa, t 26,5 C, tw 28,4 C, RF 86% Dünung: nil

Do., 10.07.2003

00:10 Beginn der wissenschaftl. Datenaufzeichnungen SIMRAD 07 15,72 N 079 53,19 W
KüG 195° v13,0 kn WSW 4, c7/8,1008,8 hPa, t 26,2 c, tw28,5 C, Düng. 200° 6s 2m
02:07 ändern Kurs auf rw 270° v 13,0 kn 06 50,00 N 080 00,00 W
11:08 Magnetometer z.W. WT ..... m KüG 270° v 11,0 kn 06 50,00 N 081 53,33 W
17:35 ändern Kurs auf rw 332° WT 2525m KüG 332° v 11,0 kn 06 50,00 N 083 00,50 W
20:00 Einfahrt in die Gewässer Costaricas 07 14,47 N 083 12,86 W
22:12 ändern Kurs auf rw 311° WT 1593m KüG 311° v 4/5 kn 07 34,32 N 083 26,05 W
Airgun 1,7 ltr zum Test z.W.
22:44 Airgun 1,7 ltr a.D. v 11,0 kn 07 35,96 N 083 27,94 W

Fr., 11.07.2003
01:50 Borduhren 20 Min. zurückgestellt
04:33 ändern Kurs auf rw 339° v 11,0 kn 08 17,00 N 084 16,00 W
05:40 Borduhren 20 Min. zurück gestellt
06:06 Ende Magnetometerprofil WT 2746m v 4,0 kn 08 32,44 N 084 21,96 W
06:21 Magnetometer a.D. Profilzeit: 19,7 Std. Profillänge 315 sm 08 33,36 N 084 22,43 W
Wind: umlaufend 1, bedeckt, 1008,4 hPa, t 25,9 C, tw 27,8 C, RF 82% Dünung210°6s 1,5m

Profil 01 / OBH 309

06:29 Airgun 7,5 ltr z.W. v 2,0 kn
06:38 Beginn Profil 01 / OBS 309 WT 2830m v 4 / 5 kn 08 34,18 N 084 22,84 W
06:58 drehen über Bb. WT 2880m
07:26 drehen über Bb. WT 2840m
07:42 drehen über Bb. WT 2816m
07:44 Ende Profil 01 WT 2830m 08 34,05 N 084 22,71 W
07:55 Airgun a.D.
07:54 Hydrophon z.W. WT 2816m
07:58 OBH 309 ausgelöst WT dito 08 34,44 N 084 22,32 W
09:11 OBH 309 aufgetaucht und gesichtet / Anfahrt
09:37 OBH 309 an Deck 08 35,05 N 084 23,10 W
09:10 Ende Profil 01
10:00 Schiffsuhren 20 Min. zurückgestellt **(LT = UTC – 6 h)**

Profil Nr. 02 / OBH 310

10:50 Beginn Profil 02 Airgun 7,5 ltr 1.Schuss WT 08 44,60 N 084 23,15 W
11:10 drehen über Stb. WT 1928m
11:29 drehen über Stb. WT 1856m
11:44 Letzter Schuss WT 1746m 08 45,48 N 084 22,69 W
11:54 Hydrophon z.W. WT 1807m 08 45,25 N 084 22,79 W
11:56 OBH 310 ausgelöst WT 2100m
12:19 Hydrophon a.D. WT
12:35 OBH 310 aufgetaucht, opt./UKW-Peiler/Radar geortet 08 46,22 N 084 23,63 W
noch Fr., 11.07.2003

12:56 OBH an Deck WT 1531m 08 46,08 N 084 23,42 W
Wind: West 4, o/p, 1009,4 hPa, t 26,2 C, tw 27,4 C, RF 84% Dünung 230° 6s 1,5 m

Profil Nr. 03 / OBT 315

13:32 Beginn Profil 03 Airgun 7,5 ltr 1.Schuss WT 08 50,58 N 084 21,00 W
12:54 drehen über Stb. – Vollkreis und neuer Anlauf
15:10 drehen über Stb. 08 52,98 N 084 20,77 W
15:34 Letzter Schuss / Airgun a.D. 08 52,28 N 084 20,01 W
15:48 Hydrophon z.W. WT 1235m
15:49 OBT 315 ausgelöst WT 1235m
16:18 OBT 315 aufgetaucht, optisch/Radar geortet 060° 0,7 sm
16:30 OBT 315 a.D. WT 1386m 08 52,62 N 084 21,03 W
Wind:Nord 4, o/p, 1009,4 hPa, t 24,6 C, tw 27,4 C, RF 84% Dünung 240° 06s 1,5 m

Profil Nr. 04 / OBH 322

17:10 Beginn Profil 04 WT 1113m 1.Schuss 08 49,43 N 084 17,48 W
18:30 Letzter Schuss WT 0812mAirgun a.D. 08 46,30 N 084 15,54 W
18:53 Hydrophon z.W.
18:54 OBH 322 ausgel. WT 0800m steigt Abst. 850m
19:03 OBH aufgetaucht u. gesichtet/Radar/UKW i.O. 060° 0,2 sm
19:15 OBH 322 an Deck WT 0800m 08 47,59 N 084 15,87 W

Profil Nr. 05 / SIMRAD-Kalibrierung

19:15 Beginn Profil SIMRAD 05 KüG 250° v 11,0 kn 08 47,59 N 084 15,87 W
20:20 Aussetzposition CTD-SIMRAD erreicht W 4 08 45,70 N 084 23,93 W
20:30 CTD in Abgangsblock Seitengalgen gehievt / klarieren und wechseln auf W 6
20:40 CTD z.W. WT 2352m W 6 08 45,86 N 084 24,50 W
21:30 CTD SL 1951m WT 2369m hieven
22:12 CTD-Sonde a.D. WT 2382m 08 46,34 N 084 27,55 W

Wind:WSW 3, c 7/8, 1006,6 hPa, t 25,2 C tw 28,1 C RF 84,5 % Dünung 260° 05 s 1,5 m

Sa., 12.07.2003

Profil Nr. 06 / OBH 323

00:00 Beginn Profil 06 1.Schuss WT 171m rw 126° v 4 / 5 kn 08 48,78 N 084 10,60 W
00:37 drehen über Stb.
01:00 letzter Schuss, Airgun a.D. WT 380m 08 46,99 N 084 10,15 W
01:13 OBH 323 ausgelöst
01:15 OBH optisch gesichtet, Anlauf zur Aufnahme 060° 0,7 sm
01:31 OBH 323 an Deck WT 193m 08 48,08 N 084 10,18 W

Profil Nr. 07 / OBH 321

02:12 Beginn Profil 07 Airgun z.W. / 1. Schuss WT 145m 08 52,02 N 084 12,36 W
03:17 letzter Schuss, holen Airgun a.D. WT 617m 08 54,13 N 084 13,27 W
03:18 v 4,0 kn Transducer Lotschacht ausgefahren
03:20 Airgun a.D. / Anfahrt OBH-Position rw 110° 1,5 sm
03:35 OBH 321 ausgelöst
03:39 Transducer wieder hochgefahren
03:43 OBH 321 aufgetaucht, opt.ges./Radar- und UKW-Ortung
03:53 OBH 321 an Deck WT 377m 08 53,93 N 084 12,41 W
Wind:ESE 1-2, o/p, 1010,0 hPa, t 26,1 C, tw 27,6 C, RF 78 % Dünung 260° 05 s 1,5 m

Profil Nr. 08 / OBS 316

04:47 Beginn Profil 08, Airgun z.W. / 1.Schuss WT 945 m 08 57,09 N 084 18,57 W
05:20 Transducer Lotschacht ausgefahren
05:35 Ende Profil, letzter Schuss, WT 882, holen Airgun a.D. 08 58,60 N 084 18,65 W
05:39 Airgun a.D.
05:40 OBS 316 ausgelöst
05:55 OBS 316 aufgetaucht und gesichtet, rw 160° 0,5 sm ab
06:06 Transducer eingefahren
06:14 OBS 316 a.D. WT 935m /Anfahrt Profil 09 08 58,20 N 084 19,21 W

Profil 09 / OBH 320

07:11 Beginn Profil 09, Airgun z.W. 1. Schuss WT 945m 09 01,04 N 084 10,27 W
08:00 Transducer ausgefahren
08:06 Ende Profil, letzter Schuss, holen Airgun a.D. WT 210m 08 59,31 N 084 10,57 W
08:11 Airgun a.D.
08:13 OBH 320 ausgelöst
08:25 Transducer Lotschacht eingefahren
08:20 OBH 320 gesichtet / Anlauf
08:32 OBH 320 an Deck WT 250m / Anfahrt Profil 10 09 02,25 N 084 11,47 W
Wind:ENE 1, o, 1008,4 hPa, t 25,8 C, tw 27,8 C, RF 82% Dünung 210° 6s 1,5 m

Profil 10 / OBS 319

09:00 Beginn Profil 10 Airgun z.W. 1. Schuss WT 270m 09 01,84 N 084 11,34 W
09:30 drehen über Stb.
09:42 Transducer Lotschacht ausgefahren
09:50 Ende Profil 10, letzter Schuss, WT 150m 09 03,92 N 084 10,94 W
09:55 GI-Gun a.D. WT 149m
09:55 OBS 319 ausgelöst
10:00 OBS 319 opt. gesichtet / Anlauf WT 153m
10:40 OBS a.D. WT 361m 09 03,44 N 084 12,05 W

Profil 11 / OBH 317

11:08 Beginn Profil 11, Airgun z.W. 11:13 1. Schuss WT 536m 09 02,83 N 084 16,04 W
11:57 Ende Profil 11, letzter Schuss WT 498m 09 04,80 N 084 16,65 W
12:02 Airgun a.D. / Transducer Lotschacht ausgefahren
12:07 OBH 317 ausgelöst
12:13 OBH 317 optisch gesichtet, Anlauf zur Aufnahme
12:29 OBH 317 an Deck WT 517m 09 03,80 N 084 16,99 W
Wind:umlfnd 1, c 1/8, 1009,4 hPa, t 26,4 C, tw 28,1 C, RF 80% Dünung 210° 6 s 1,5 m

Profil 12 / OBH 318
13:07 Beginn Profil 12, Airgun z.W. 13:10 1. Schuss, WT 418m 09 09,06 N 084 15,35 W
13:50 Ende Profil
14:12 Airgun a.D. , Transducer ausgefahren 09 10,21 N 084 14,53 W
14:17 OBH 318 ausgelöst WT 337m Regenschauer mit wechselnder Sicht
14:24 OBH aufgetaucht und gesichtet, Transducer Lotschacht eingef.
14:54 OBH 318 a.D. 3 Anläufe z. Aufn. wegen starkem Strom 09 11,14 N 084 15,46 W

Profil 13 / OBH 302
15:50 Beginn Profil 13, Airgun z.W. 15:56 1.Schuss WT 284m 09 15,64 N 084 20,40 W
16:46 Transducer Lotschacht ausgefahren
16:46 Ende Profil, letzter Schuss, holen Airgun a.D. WT 219m 09 16,31 N 084 20,97 W
16:52 Airgun an Deck
16:53 OBH 302 ausgelöst, keine eindeutige Rückmeldung, starke Regenschauer

noch Profil 13
17:59 Transducher eingefahren
18:00 OBH taucht nicht auf, kann nicht gesichtet werden 09 15,49 N 084 22,12 W
wiederholtes Ansprechen über Transducer, keine eindeutigen Signale zu empfangen, Gerät kann auch nicht optisch gefunden werden. Vermutlich von Grundnetzfischerei verschleppt oder vorzeitig zum Auftauchen gebracht ?
18:50 Suche abgebrochen, OBH vorerst als Verlust notiert. 09 17,04 N 084 22,27 W
Wind:umlfnd 1, c 6/8, 1010,2 hPa, t 26,6 C, tw 28,4 C RF 79% Dünung: nil

Profil 14 / OBH 301
19:36 Beginn Profil 14, Airgun z.W. WT 139m 1. Schuss 09 15,22 N 084 29,39 W
20:10 Drehen über Stb. WT .... 09 14,40 N 084 30,17 W
20:24 Transducer Lotschacht ausgefahren WT 205m 09 15,26 N 084 30,70 W
20:28 Ende Profil 14, letzter Schuss, holen Airgun an Deck 09 15,63 N 084 30,82 W
20:32 Airgun a.D.
20:34 OBH 301 ausgelöst WT 200m
20:37 OBH akustisch aufgetaucht
21:07 OBH 301 optisch gesichtet, Anlauf zur Aufnahme
21:17 OBG 301 an Deck WT 215m 09 15,90 N 084 30,01 W

Profil 15 / OBH 303
22:32 Beginn Profil 15 Airgun z.W. WT 635m 22:35 1.Schuss 09 09.02 N 084 22,44 W
23:08 Ende Profil WT 734m hieven Airgun 09 07,98 N 084 23,88 W
23:14 Airgun an Deck, Transducer im Lotschacht ausgefahren
23:25 OBH 303 ausgelöst
23:30 OBH aufgetaucht und gesichtet rw 140° 0,3 sm
23:40 OBH 303 an Deck WT 679m 09 08,56 N 084 23,28 W
23:43 Transducer eingefahren, Anfahrt Profil 16
Wind:SWzS 2, c/o, 1008,2 hPa, t 24,7 C, tw 28,1 C, RF 87% Dünung : nil

So., 13.07.2003

Profil 16 / OBH 304

00:32 Beginn Profil 16 1.Schuss mit Airgun WT 1111m 09 02,30 N 084 23,85 W
00:47 drehen über Stb. 09 00,97 N 084 24,63 W
01:00 Transducer Lotschacht ausgefahren
01:03 Ende Profil letzter Schuss, holen Airgun ein, WT 1205m 09 01,59 N 084 25,48 W
01:12 OBH 304 ausgelöst
01:27 aufgetaucht und opt. gesichtet
01:32 Transducer im Lotschacht eingefahren
01:44 OBH 304 an Deck, Anfahrt Profil 17 WT 1145m 09 02,07 N 084 24,82 W
Wind:Süd 1, o, 1010,0 hPa, 25,4 C, tw 27,4 C, RF 87% Dünung: nil

Profil 17 / OBS 305

02:22 Beginn Profil 17 WT 1073m erster Schuss mit GI-Gun 09 04,68 N 084 29,12 W
03:13 Ende Profil 17 WT 0976m letzter Schuss 09 05,86 N 084 30,47 W
03:17 GI-Gun a.D. / Transducer im Lotschacht ausgefahren
03:20 OBS 305 ausgelöst
03:24 Transducer Lotschacht eingefahren
03:33 OBS 305 aufgetaucht opt. gesichtet und UKW-Signal empf.
03:44 OBS 305 an Deck WT 1016m 09 05,19 N 084 30,50 W
Wind:Nwlich 1, c/o, 1009,0 hPa, t 25,9 C, tw 27,8 C, RF 81% Dünung 210° 6 s 1,5 m

Profil 18 / OBH 306

04:54 Beginn Profil 18 WT 1177m 1. Schuss mit GI-Gun 09 07,12 N 084 41,76 W
05:38 Transducer Lotschacht ausgefahren
05:55 Ende Profil 18 WT 1043m letzter Schuss 09 08,10 N 084 43,67 W
05:58 Airgun a.D.
06:00 OBH 306 ausgelöst
06:10 OBH 306 aufgetaucht und opt. gesichtet WT 1080m
06:14 Transducer Lotschacht eingefahren
06:30 OBH 306 an Deck 09 07,17 N 084 43,26 W

Profil 19 / OBS 307

08:16 Beginn Profil 19 WT 3511m 1. Schuss mit GI-Gun 08 50,01 N 084 48,45 W
08:45 drehen über Stb. WT 3351m 08 49,36 N 084 50,80 W
09:07 Transducer im Lotschacht ausgefahren
Wind:varr. 1-3, o, 1007,0 hPa, t 25,7 C, tw 27,8 C, RF 86% Dünung 210° 6 s 1,0 m
09:09 Ende Profil 19 WT 3503m letzter Schuss 08 51,18 N 084 50,16 W
09:13 Airgun an Deck
09:14 OBS 307 ausgelöst WT 3505m
10:00 OBS 307 aufgetaucht und opt. / akustisch geortet
10:12 Transducer im Lotschacht eingefahren
10:25 OBS 307 an Deck 08 50,16 N 084 50,11 W

Profil 20 / OBH 308

12:12 Beginn Profil 20 WT 2055m 1. Schuss um 12:14 08 38,60 N 084 34,24 W
12:38 drehen über Stb. 08 39,97 N 084 32,62 W
12:55 Transducer im Lotschacht z.W.
13:00 Ende Profil 20 WT ... letzter Schuss ....
13:04 Airgun an Deck
13:05 OBH 308 ausgelöst WT 2157m 08 38,74 N 084 32,52 W
13:26 OBH 308 opt. gesichtet 08 39,35 N 084 32,75 W
13:35 OBH 308 an Deck WT 2142m
Wind:SSE 2, c 3/8, 1009,4 hPa, t 26,0 C, tw 27,6 C, RF 81% Dünung 140°210° 5s 1m

Profil 21 / OBH 311

14:16 Beginn Profil 21 WT 2446m 1. Schuss 08 44,95 N 084 30,73 W
14:46 Transducer im Lotschacht ausgefahren
14:57 Ende Profil 21 WT 2419m letzter Schuss 08 46,67 N 084 30,23 W
15:00 GI-Gun an Deck
15:02 OBH 311 ausgelöst
15:31 OBH 311 aufgetaucht opt./akustisch geortet rw 216° 0,3 sm 08 46,57 N 084 30,42 W
16:00 OBH 311 nach 2.Anlauf an Deck 08 46,45 N 084 30,68 W

Profil 22 / OBH 312
16:42 Beginn Profil 22 WT 2652m 1. Schuss 08 51,39 N 084 34,27 W
17:13 Transducer im Lotschacht ausgefahren
17:19 Ende Profil 22 WT 2414m letzter Schuss 08 53,58 N 084 34,83 W
17:25 OBH 312 ausgelöst
18:24 OBH aufgetaucht und gesichtet, Transducer Lotschacht eingefahren
18.39 OBH 312 an Deck WT 2572m 08 52,96 N 084 34,99 W

Profil 23 / OBH 313
19:28 Transducer Lotschacht ausgefahren Beginn WT 1950m 08 54,30 N 084 29,52 W
19:36 OBH 313 ausgelöst WT 1930m
20:06 OBH 313 aufgetaucht und gesichtet 08 53,81 N 084 28,46 W
noch Profil 23

20:08 Transducer eingefahren
20:32 OBH 313 an Deck 08 53,80 N 084 38,58 W

Profil 24 / OBH 314
21:05 Transducher im Lotschacht ausgefahren WT 1762m 08 56,42 N 084 28,82 W
21:16 OBH 314 ausgelöst WT 1686m
21:35 OBH 314 aufgetaucht WT 1568m opt. gesichtet
21:40 Transducer Lotschacht eingefahren
21:51 OBH 314 an Deck WT 1562m 08 57,84 N 084 28,07 W
Wind: Süd 3, c 6/8, 1006,8 hPa, t 26,7 C, tw 28,2 C, RF 78 % Dünung 210° 5s 1,0 m

---

Von 23 Geräten 22 wieder wohlbehalten an Bord, OBH 302 (Profil 13) tauchte nicht auf

---

Profil 25 / Test 1x 32 ltr Gun
22:00 Gun z.W. WT 1562m 08 57,84 N 084 28,07 W
22:13 Gun a.D. WT 1589m Test beendet 08 57,75 N 084 28,99 W

Profil 26 / SIMRAD-Kalibrierung Roll/Pitch
23:00 Profilbeginn WT 1782m rw 210° 8,0 kn 08 56,27 N 084 37,65 W
23:30 drehen Schweineohr über Bb. mit 5,0 kn
23:50 auf Gegenkurs 030° v 8,0 kn WT 3440m 08 52,77 N 084 39,91 W
Mo., 14.07.2003
00:25 Ende Kalibrierprofil D 10 sm WT 1546m 08 56,67 N 084 37,42 W
Anfahrt Arbeitsgebiet Nicoya D 124 sm mit rwK 305°

Profil 27 / SIMRAD-Vermessungsprofil
00:25 Beginn Vermessungsprofil rwK 305° 13,8 kn 08 56,67 N 084 37,42 W
11:30 Ende Vermessungsprofl Profilzeit: 11,1 Std. D 124 sm 10 20,12 N 086 38,00 W

Profil 28 / Auslage von 12 OBH/S (Absand 2sm Richtung 227°)
11:30 OBH 1 z.W. WT 3926m 10 20,12 N 086 38,00 W
11:54 OBH 2 z.W. WT 4267m 10 18,71 N 086 39,43 W

12:21 OBH 3 z.W. WT 4510m 10 17,18 N 086 40,95 W
12:46 OBH 4 z.W. WT 4880m 10 15,86 N 086 42,28 W
13:07 OBH 5 z.W. WT 4965m 10 14,49 N 086 43,66 W
13:35 OBH 6 z.W. WT 4511m 10 13,20 N 086 44,98 W
13:58 OBH 7 z.W. WT 4212m 10 11,96 N 086 46,27 W
14:28 OBH 8 z.W. WT 4137m 10 10,55 N 086 47,78 W
15:02 OBH 9 z.W. WT 4118m 10 09,21 N 086 49,02 W
15:58 OBH 10 z.W. WT 3740m 10 07,96 N 086 50,27 W
Wind: umlfnd. 2, c 7/8, 1009,8 hPa, t 26,5 C, tw 32,2 C, RF 82% Dünung 180° 8 s 1,0 m
16:28 OBH 11 z.W. WT 3794m 10 06,82 N 086 51,50 W
17:07 OBH 12 z.W. WT 3488m 10 05,38 N 086 52,95 W

Profil 29 Seismikprofil GI-Gun 1,7 ltr (227° von OBH 8 nach OBH 12)
18:20 GI-Gun 1x 1,7 L z.W. WT 4312m 10 12,32 N 086 45,92 W
18:24 Beginn Seismikprofil 29 WT 4300m rwK 225° v 5 kn 10 11,95 N 086 46,19 W
18:50 Lanleine quer im Kurs, mitgezogen und durchgerissen 10 10,84 N 086 47,03 W
20:37 Ende Seismikprofil WT 3481m Profileit: 2,3 h D 10 sm 10 05,04 N 086 53,31 W
20:40 GI-Gun a.D. / Anfahrt Seismikprofil 2x 32 L - Guns

noch Di., 15.07.2003

Profil30 S Seismikprofil 32-Ltr. Guns (045° 40 sm)
22:10 Airgun Stb. 32 Ltr z.W. WT 3005 m
22:28 Airgun Bb. 32 Ltr. z.W. WT 3003 m 09 56,14 N 087 02,43 W
22:43 Beginn Profil S 30 1. Schuss Trigger 60 sec v 4,0 kn 09 56,90 N 087 01,60 W
22:50 Streamer z.W. bis 23:00 KüG 045° v 4,0 kn
Di., 15.07.2003
02:51 Ausfall Stb. Airgun
04:07 Stb. Airgun z.W.
09:22 Ende Profil S 30 letzter Schuss WT 1786m 10 27,92 N 086 29,95 W
Profilzeit: 10,6 Std. Profildistanz: 40 sm
09:31 Stb.-Airgun a.D. WT 1651m
09:45 Bb. -Airgun a.D. WT 10 28,80 N 086 29,13 W
09:55 Streamer a.D. WT 1380m

Profil 31 Aufnahme OBHs 12 x
11:04 Transducer Lotschacht ausgefahren
11:06 OBH 1 ausgelöst WT 3410m
12:04 OBH 2 ausgelöst
12:24 OBH 1 an Deck WT 3966m 10 20,28 N 086 38,40 W
12:55 OBH 3 ausgelöst
13:11 OBH 2 an Deck WT 4288m 10 18,89 N 086 39,71 W
13:35 OBH 4 ausgelöst
14:03 OBH 3 an Deck WT 4577m 10 17,48 N 086 41,37 W
14:27 OBH 5 ausgelöst
14:40 OBH 4 aufgetaucht
14:50 OBH 4 an Deck WT4924m 10 16,10 N 086 42,41 W
15:12 OBH 6 ausgelöst
15:48 OBH 5 optisch gesichtet
16:00 OBH 5 an Deck WT 4940m 10 14,68 N 086 43,87 W
16:23 OBH 7 ausgelöst
16:27 OBH 6 optisch gesichtet ca. 1,0 sm ab
16:54 OBH 6 an Deck WT 4470m 10 13,39 N 086 45,58 W
17:15 OBH 8 ausgelöst

17:31 OBH 7 aufget. und gesichtet
17:50 OBH 7 an Deck WT 4206m 10 12,08 N 086 46,75 W
18:12 OBH 8 aufget. und gesichtet
18:35 OBH 8 an Deck WT 4142m 10 10,64 N 086 48,24 W
Transducer Lotschacht eingefahren

Profil 32 GI-Gun
18:46 GI-Gun z.W. WT 4092m KüG 180° v 4,0 kn 10 10,54 N 086 48,63 W
19:00 Beginn Profilaufzeichnungen, 1. Schuss Trigger 10 s
19:12 Streamer z.W. bis 19:41
20:05 ändern Kurs über Stb. auf 270° 10 06,78 N 086 49,43 W
20:20 Streamer an Deck WT 3788m 10 06,79 N 086 50,42 W
20:56 Ende Profil 32 – letzter Schuss WT 3750m 10 06,81 N 086 53,36 W
21:00 Airgun a.D. NzE 2, c 6/8, 1005,6 hPa, t 28,2 C, tw 33,0 C,Dünung 045° 5s 1,5m

Station 33 Auslösertest Winde W 6
21:10 Auslöser z.W. WT 3616m 10 07,00 N 086 53,83 W
21:30 SL max 1000m WT 3610m ausgelöst, hieven 10 07,00 N 086 53,90 W
21:51 Auslöser a.D. WT 3611m dito
noch Di., 15.07.2003

Fortsetzung Profil 31 - Aufnahme OBH
21:37 OBH 12 ausgelöst
22:14 OBH 11 ausgelöst
22:16 OBH 12 opt. gesichtet / Anlauf
22:36 OBH 12 an Deck WT 3490 m 10 05,36 N 086 53,28 W
22:58 OBH 10 ausgelöst
23:18 OBH 11 an Deck WT 3799m 10 06,00 N 086 51,82 W
23:35 OBH 09 ausgelöst
23:40 OBH 10 aufgetaucht und gesichtet
23:54 OBH 10 an Deck WT 3799m 10 08,09 N 086 50,53 W
Mi., 16.07.2003
00:23 OBH 09 aufgetaucht und gesichtet Wind NNE 3, c 7/8, 1005,8 hPa, t 28,6 C
00:30 Transducer im Lotschacht eingefahren
00:47 OBH 09 an Deck WT 4108m 10 09,49 N 086 49,56 W
Ende Profil 31 12x Aufnahme OBH / Anfahrt Verankerung rw 086° 31 sm

Station 34 / Verankerungsauslage TPB 3 Verankerungsspill+Schiebebalken+Beiholer
03:48 auf Auslageposition Verankerung TPB 3 WT 1607m 10 17,21 N 086 17,89 W
Wind: EzS 1-2, c 5/8, 1008,6 hPa, t 28,2 C, tw 27,7 C, Dünung aus 045° 6 s 1,5 m OMw + 3°
04:00 Auslagebeginn über Stb.-Seite: Ankerstein z.W. WT 1607m 10 17,19 N 086 17,90 W
04:10 Auslöser z.W. WT 1607m 10 17,22 N 086 17,92 W
04:34 Auftrieb mit Blitz und Sender „B" z.W. WT 1607m 10 17,20 N 086 17,90 W
04:36 Verankerung TPB 3 taucht ab WT 1607m SIM **Position: 10 17,17 N 086 17,89 W**

Profil 35 SIMRAD
04:36 Beginn Vermessungsprofil SIM 35 KüG 079° v 11,5 kn 10 17,17 N 086 17,89 W
05:20 ändern Kurs auf rw 137° v 11.5 kn D 7 sm 10 18,43 N 086 10,20 W
06:10 Ende Profil 35 gesamt Distanz: 16 sm 10 11,36 N 086 04,86 W
Wind:E 3, c 6/8, 1008,4 hPa, t 27,8 C, tw 30,2 C, Dünung 045° 6s 1,5 m

Profil 36 SIMRAD- Anfahrt Caldera
06:10 Beginn Vermessungsprofil SIM 36 KüG 137° v 11,0 knVV 10 11,36 N 086 04,86 W
11:23 ändern Kurs auf rw 090° D 59 sm 09 28,70 N 085 24,10 W
12:57 ändern Kurs auf rw 045° D 17 sm 09 28,60 N 085 07,00 W

16:00 Ende Vermessungsprofil SIM 36 D 22 sm gesamt D 98sm 09 37,04 N 084 58,41 W

16:18 Reiseunterbr. Caldera-Reede, fallen Bb.-Anker WT16m 09 54,91 N 084 44,27 W

Wind: SSW 2, c 7/8, 1010,7 hPa, t 27,5 C, tw 32,0 C, Dünung 180° 6s 1,0 m

17:58 Lotsenboot CECILIA Stb. längsseits Agent 1x mit Behörden 5x a.B. und Luftfracht

18:12 4 Kisten Luftfracht an Bord AWB .....

18:24 Schiff durch die Behörden einklariert

18:34 Agent und Behörden von Bord

18:40 hieven Anker

18:48 Fortsetzung der Reise/Reiseunterbrechung gesamt: 2,5 Std. Anker vor u. seefest

19:30 starker Gewitterschauer

Profil 37 SIMRAD-Vermessungsprofil

22:42 Beginn Vermessungsprofil 37 SIMRAD WT 200m 09 13,68 N 084 35,25 W

23:00 ändern Kurs auf rw 145° v 12,5 kn VV 09 10,13 N 084 33,80 W

Do., 17.07.2003

02:29 Ende Profilfahrt, Profilzeit: 3,8 Std. Profildistanz: 38 sm 08 39,82 N 084 12,00 W

noch Do., 17.07.2003

Profil 38 Kalibrierung Posidonia-Antenne im Lotschacht

02:29 OBH 01 z.W. WT 1190m 08 39,82 N 084 11,98 W

02:30 Posidonia-Antenne im Lotschacht ausgefahren dito

Warten auf Landung des OBH 01

02:50 Hydrophon z.W. WT 1190m / 02:55 Hydrophon a.D.

03:00 Beginn Kalibrierung Posidonia WT 1190m v 3.5 kn 08 39,82 N 084 12,00 W

2x2 Kreise mit Radius 0,59 sm über Stb. und über Bb. gefahren (eine 8 über OBG 01), anschliessend noch eine kleine 8

07:00 Ende Kalibrierung Posidonia 08 39,12 N 084 11,96 W

07:10 OBH 01 ausgelöst WT 1200m

07:28 OBH 01 aufgetaucht

07:43 OBH an Deck 08 39,03 N 084 12,04 W

07:49 Ende Profil 38 / Anfahrt Profil 39 rw 260° 9 sm

Profil 39 Auslage OBSs

09:23 OBS 01	z.W. WT 2590m	08 37,53 N 084 20,59 W
09:40 OBS 02	z.W. WT 2602m	08 37,46 N 084 20,49 W
10:10 OBS 03	z.W. WT 2610m	08 37,42 N 084 20,41 W
10:42 OBS 04	z.W. WT 2607m	08 37,43 N 084 20,28 W
11:16 OBS 05	z.W. WT 2615m	08 37,37 N 084 20,32 W
11:27 OBS 06	z.W. WT 2657m	08 27,23 N 084 20,38 W
11:39 OBS 07	z.W. WT 2621m	08 37,31 N 084 20,21 W
11:55 OBS 08	z.W. WT 2616m	08 37,26 N 084 20,13 W
12:16 OBS 09	z.W. WT 2598m	08 37,20 N 084 20,03 W
12:36 OBS 10	z.W. WT 2591m	08 37,14 N 084 19,94 W
12:49 OBS 11	z.W. WT 2600m	08 37,07 N 084 19,82 W
13:07 OBS 12	z.W. WT 2594m	08 37,00 N 084 19,70 W

Profil 40 S 32Ltr. Airgun Stb. + Streamer

14:27 Airgun 32 ltr Bb. z.W. WT 2344m Kurs 301° v 4,0 kn 08 33,53 N 084 14,83 W

Beginn Seismikprofil 40 1.Schuss Trigger 30 sec D 10 sm

14:31 Streamer z.W. WT 2372m 08 33,56 N 084 14,18 W
Wind:umlaufend 1, c2/8,1011,1 hPa, t 26,6 C, tw 28,2 C,RF 81% Dünung 180° 05 s 1,0 m
17:06 WT 2492 – Streamer an Deck, Position 08 39,35 N 084 23,64 W
17:07 Ende Profil – letzter Schuss WT 2543m 08 39,35 N 084 23,64 W
17:21 Bb.-Airgun 32 ltr an Deck,Anlauf Profilbeginn Profil 41 DTS

Profil 41 DTS Winde W 2
18:00 auf Startposition WT 2768 m 08 42,20 N 084 27,93 W
Treffen Vorbereitungen zum Aussetzten

18:15 Schlauchboot z.W. Einkauf Frischfisch von Fischerboot 08 42,20 N 084 27,92 W

19:06 Radartransponder im Boot aktiviert, Signal X-Band Radar i.O.

19:16 Schlauchboot mit 8 Thunfischen, frisch gefangen, zurück 08 42,49 N 084 28,67 W

20:41 DTS z.W. WT 2768m KüG 121° v 1,5 kn 08 42,26 N 084 28,53 W
20:47 Depressor z.W. fieren System mit 0,3m/sec Winde W 2 v 2,0 kn
21:39 DTS defekt, hieven System wieder a. D. 08 41,39 N 084 27,14 W
21:39 KL 1318m WT 2692m
22:24 Depressor a.D.
22:44 DTS zur Reparatur an Deck, drehen auf Aussetzposi. 08 40,73 N 084 25,89 W

23:06 Schlauchboot z.W. Übungsfahrt / 23:47 Schlauchboot a.D.

Fr., 18.07.2003
02:45 DTS z.W. WT 2818m KüG 121° v 1,0 – 1,5 kn 08 42,36 N 084 28,66 W

noch Fr., 18.07.2003

noch Profil 41 DTS Winde W 2 (DTS + 1x GI-Gun)
03:18 Depressor z.W. fieren mit 0,2 bis 0,5m/sec FüG 3,0 kn
Wind:umlfnd. 1-2, c 3/8, 1011,0 hPa, t 26,8 C, tw 29,0 C, RF72% Dünung 160° 08 s 1,5 m
03:46 GI-Gun 1,7 ltr z.W. Trigger 10 sec
04:00 Profilbeginn 1. Schuss 08 41,17 N 084 26,75 W
10:00 Ende Profil 41 Distanz: 10 sm KL 2784m drehen ü. Stb. 08 32,40 N 084 12,04 W

10:47 drehen über Bb. 08 30,70 N 084 11,26 W
11:14 drehen über Stb. in das neue Profil WT 1971m KL 2784m 08 32,03 N 084 09,86 W
11:31 Drehung beendet WT 1962m KL2784m 08 32,16 N 084 10,68 W

Profil 42 DTS Winde W 2 (DTS + 1x GI-Gun + Streamer)
15:00 Beginn Profil 42 DTS 08 34,31 N 084 14,43 W
KüG 301° FüG 3,0 kn WT 2416 m KL 4364 m
16:00 Streamer z.W. Wind varr.1, c 2/8, 1011,7 hPa, t 27,7 C 08 35,77 N 084 16,86 W

16:43 Schlauchboot zur Kontrolle Fisch mit Hydrophon z.W.

17:00 KL 4598m WT 2586m 08 37,21 N 084 19,30 W

17:28 Schlauchboot zurück a.D.

18:00 KL 5182m WT 2464m 08 38,83 N 084 21,96 W
18:08 Schiff passiert WP Profilende KL 5222m WT 2455m 08 39,03 N 084 22,28 W
18:58 Ende Profil 42 letzter Schuss Profildistanz: 10 sm 08 40,31 N 084 24,08 W
WT 2544m KL 4995m , Wind var.1, c2/8,1011,1 hPa, t 27,8 C, tw 29,0 C
19:28 Streamer an Deck WT 2483m KL 3772m
19:30 GI-Gun vorgehievt, beginn Drehen über Bb.

Profil 43 DTS Winde W 2 (DTS + 1x GI-Gun)
20:35 Drehung über Bb. beendetWT 2882m 08 40,54 N 084 26,67 W

20:37 Gl-Gun auf Länge gefiert WT 2669m KL 3544m 08 39,80 N 084 25,43 W
21:12 Start Profil 42 DTS KüG 121° FüG 3,0 kn 08 39,65 N 084 25,16 W
WT 2660m KL 3737m ,1. Schuss, Wind varr.1, c 4/8, 1008,6 hPa, t 28,2 C, tw 29,6 C
22:00 WT 2649m KL 4866m 08 38,49 N 084 23,23 W
23:00 WT 2300m KL 5140m 08 36,95 N 084 20,67 W
24:00 WT 2594m KL 5486m 08 35,39 N 084 18,08 W

Sa., 19.07.2003

00:30 Ende Profil 43 WT 2545m KL 5590m D 10,0 sm 08 34,56 N 084 16,69 W
00:48 drehen über Stb., hieven DTS WT 2473m KL 4842m 08 34,14 N 084 15,93 W

Profil 44 DTS Winde W 2 (DTS + 1x Gl-Gun)
01:36 auf Kurs / Anfahrt ProfilWT 2641m KL 2778m 08 32,48 N 084 16,41 W
02:00 WT 2670 m KL 2673m 08 32,43 N 084 17,58 W
03:00 WT 2733m KL 2673m 08 32,41 N 084 20,67 W
03:36 WT 2829m KL 2813m fieren Kabel 08 32,99 N 084 22,03 W
04:00 WT 2829m KL 3182m 08 34,19 N 084 21,77 W
04:34 Profil 44 DTS WT 2848m KL 3916m KüG 031° FüG 3,0 kn 08 35,24 N 084 21,13 W
05:00 WT2669m KL4815m, Wind S W1-2, c2/8,1010,0hPa t26,8 08 36,61 N 084 20,28 W
06:00 überlaufen Profilendpunkt WT 2242m KL 5169m 08 38,99 N 084 18,26 W
06:42 letzter Schuss WT 1677m KL 4474m **Distanz 6 sm** 08 40,85 N 084 17,64 W
Fischerei Langleine überfahren
07:08 Beginn Kursänderung über Bb. WT 1543 m KL 1648m 08 41,96 N 084 15,50 W
noch Sa., 19.07.2003

Profil 45 DTS Winde W 2 (DTS+1xGl-Gun+Streamer)
08:05 auf Gegenkurs 211° WT 1121m KL 1179m fieren Kabel 08 43,96 N 084 16,43 W
09:00 Beginn Profil 45 Gl-Gun fieren WT 1179m KL 1275m 08 43,76 N 084 16,58 W
10:00 WT 1598m KL 2297m KüG 211° FüG 3,0 kn 08 41,38 N 084 18,05 W
Wind:W 2-3, c 6/8, 1007,6 hPa, t 26,7 C, tw 28,5 C, RF 77% Dünung 245° 7s 1,5 m
10:15 Streamer z.W. WT 1829m KL 2575m 08 40,64 N 084 18,52 W
11:00 WT 2317m KL 3315m 08 38,69 N 084 19,50 W
12:00 WT 2782m KL 4466m 08 36,29 N 084 21,00 W
13:00 Profilende D 12,0 sm KL 5699m WT 2784m hieven 08 33,76 N 084 22,58 W
13:18 Gl-Gun an Deck WT 2728m KL 5058m hieven DTS 08 33,02 N 084 23,08 W
13:33 Streamer an Deck WT 2675m KL 4365m 08 32,32 N 084 23,54 W
14:00 WT 2658m KL 3274m 08 31,19 N 084 24,26 W
15:00 WT 2591m KL 0015m holen Depressor u. DTS a.D. 08 27,99 N 084 26,42 W
15:35 Depressor und DTS mit Streamer a.D. WT 2579m 08 37,53 N 084 20,33 W

Profil 46 Aufnahme OBHs 12x mit Hydralift 2 und Schlauchboot
17:00 bis 17:37 auslösen aller 12 OBHs 08 36,47 N 084 21,10 W
17:38 1.OBH aufgetaucht Wind:SW 2,c5/8,1009,2 hPa,t27,8C, tw28,5 C, 240° 6s 1,5m
17:40 Schlauchboot mit 3 Personen z.W.
18.00 OBH 1 a.D. 08 37,46 N 084 20,99 W
18:46 OBH 11 a.D. - 1 OBH von WP 03 fehlt noch 08 37,03 N 084 19,74 W
18:48 Schlauchboot a.D., Anfahrt WP 03 Hydrophon z.W. erneuter Auslöseversuch
19:03 Hydrophon z.W. WT 2560m akust. Abstand 500m 08 37,51 N 084 20,56 W
19:08 OBH aufgetaucht, Schlauchboot z.W.
19:17 alle 12 OBHs wohlbehalten a.D., Schlauchboot a.D. 08 37,39 N 084 20,45 W
Anfahrt Profil 47 rw 004 ° D 19 sm v 8,0 kn max
Posidonia Lotschacht ausgefahren, zahlreiche Langleinen im Kurs

Profil 47 Auslage 9x OBHs Hydralift 2

22:28 OBS 1 z.W. WT 1012m 08 55,98 N 084 18,76 W
22:42 OBH 2 z.W. WT 0985m 08 55,84 N 084 18,63 W
22:47 OBS 3 z.W. WT 1007m 08 55,75 N 084 18,56 W
22:59 OBS 4 z.W. WT 1020m 08 55,64 N 084 18,47 W
23:13 OBS 5 z.W. WT 1028m 08 55,52 N 084 18,38 W
23:25 OBH 6 z.W. WT 1037m 08 55,42 N 084 18,31 W
23:33 OBH 7 z.W. WT 1007m 08 55,36 N 084 18,24 W
23:42 OBH 8 z.W. WT 1044m 08 55,18 N 084 18,10 W
23:45 OBT 9 z.W. WT 1040m 08 55,14 N 084 18,07 W

So., 20.07.2003

Profil 48 DTS ohne Airgun und ohne Streamer
00:46 DTS mit Streamer z.W. WT 531m 08 50,90 N 084 14,43 W
01:03 Depressor z.W. WT 626m 08 51,28 N 084 14,81 W
02:00 WT 1009m KL 1044m Streamer am Fisch defekt 08 52,94 N 084 16,15 W
02:25 Beginn Profil 48 DTS WT 1104m KL 1486m D 4,6 sm 08 53,89 N 084 16,89 W
03:00 WT 1033m KL 1604m KüG 321° FüG 3,0 kn nur SSS 08 55,25 N 084 18,00 W
Wind: WSW 3, c 4/8, 1009,0 hPa, t 27,5 C, tw 28,6 C, RF 79% Dünung 200° 06s 1,5 m
04:13 Ende Profil 48 WT 1041m KL 1488m D 4,6 sm 08 58,11 N 084 20,25 W
Anfahrt Profil 49 über Bb mit grosser Schleife

Profil 49 DTS ohne Airgun und ohne Streamer
07:49 Beginn Profil 49 DTS KüG 042° FüG 3,0 kn 08 54,07 N 084 20,29 W
08:18 Langleine der Fischerei überfahren WT 1051m KL 1932m 08 55,18 N 084 19,25 W
09:00 WT 931m KL 1487m 08 56,71 N 084 17,83 W
10:00 WT 801m KL 1090m 08 58,86 N 084 15,79 W
11:00 WT 582m KL 0663m 09 01,17 N 084 13,65 W
11:23 Ende Profil 49 WT 495m KL 503m **D 11sm** 09 02,03 N 084 12,84 W
Drehen über Stb. mit Schleife auf Profil 50
Profil 50 DTS ohne Airgun und ohne Streamer
11:50 Beginn Profil 50 DTS KüG 222° FüG 3,0 kn WT 499m 09 01,34 N 084 12,67 W
12:00 WT 530m KL 454m 09 00,98 N 084 12,98 W
13:00 WT 717m KL 765m 08 58,83 N 084 15,02 W
13:55 Ende Profil 50 WT 941m KL 1180m **D 6sm** 08 56,82 N 084 16,88 W
14:00 Hieven Gerät an Deck WT 954m KL 1031m 08 56,67 N 084 17,01 W
14:30 DTS mit Kompressor a.D.
Anfahrt Seismikprofil 51 (mit Streamer + GI-Gun über OBHs)
Profil 51 Seismik
16:03 Streamer z.W. WT 0934m 08 52,51 N 084 15,89 W
16:07 GI-Gun z.W. WT 0960m 08 52,64 N 084 16,00 W
16:38 Beginn Profil 51 S WT 1055m KüG 321° v 3,0 kn 08 53,78 N 084 16,99 W
17:00 WT ... 08 54,56 N 084 17,62 W
18:00 WT .... 08 56,62 N 084 19,25 W
19:00 WT ... 08 58,49 N 084 20,76 W
20.00 Ende Profil 51 S WT 917m letzter Schuss **D 9sm** 09 00,65 N 084 22,42 W
20:11 Streamer an Deck
Profil 52 DTS + Seismik
20:25 DTS z.W. WT 889m, GI-Gun z.W.
20:50 Beginn Profil 52 DTS WT 878m KL172m KüG 141° 3,0 kn 09 00,48 N 084 22,16 W
21:00 Position 09 00,11 N 084 21,87 W
21:45 DTS defekt Abbruch Profil WT 955m KL 1020m **D 3 sm** 08 58,50 N 084 20,59 W
22:07 GI-Gun a.D. WT 972m KL 308m
22.35 Depressor und DTS a.D.

Mo., 21.07.2003

Profil 53 DTS

01:09 Streamer DTS z.W. WT 1117m 09 06,11 N 084 34,16 W
01:13 DTS z.W. WT 1117m 09 06,19 N 084 34,18 W
01:21 Depressor z.W. WT 1114m 09 06,39 N 084 34,20 W
02:00 WT 1006m KL 861m 09 07,96 N 084 34,21 W
02:22 Beginn Profil 53DTS WT903m KL1238m KüG360°FüG 3kn 09 08,98 N 084 34,21 W
03:43 Ende 1. Profillinie, KÄ über Bb. WT ... KL 347m **D 5 sm** 09 12,76 N 084 34,20 W
04:00 WT 310m KL 180m 09 13,55 N 084 33,84 W
04:50 Beginn 2. Profillinie KüG 180° v 3 kn WT 347m KL 191m 09 13,09 N 084 34,86 W
05:00 WT 432m KL 351m 09 12,57 N 084 34,87 W
06:00 WT ... KL ..... m 09 09,83 N 084 34,86 W
06:30 Ende 2. Profillinie WT 1012m KL 1178m **D 5 sm** 09 08,44 N 084 34,82 W
07:22 Beginn 3.Profillinie KüG 360° v 3kn WT 956m KL 1348m 09 09.01 N 084 35,50 W
08:00 WT .... m KL .....m 09 10,20 N 084 35,50 W
08:54 Ende 3. Profillinie WT 275m KL 183m **D 5 sm** 09 13,45 N 084 35,49 W
09:24 Beginn 4. Profillinie KüG 180° WT 317m KL 225m 09 13,32 N 084 36,13 W
10:00 WT 564m KL 525m 09 11,46 N 084 36,14 W
11:05 Ende 4. Profillinie WT 1132m KL 1280m **D 5 sm** 09 08,48 N 084 36,13 W

***noch* Mo., 21.07.2003**

11:47 Beginn 5. Profillinie KüG 360° WT 966m KL 1222m 09 09,51 N 084 36,79 W
12:50 Ende 5. Profillinie WT 476m KL 509m KÄ ü Bb. **D 3 sm** 09 12,49 N 084 36,77 W
13:23 Beginn 6. Profillinie KüG 180° WT 549m KL 458m 09 12,16 N 084 37,39 W
14:45 Ende 6. Profillinie WT 1172m KL 1299m **D 4 sm** 09 08,52 N 084 37,31 W
15:00 WT 1258m KL 863m 09 08,20 N 084 37,28 W
15:35 DTS mit Depressor a.D. WT 1371m 09 06,73 N 084 37,07 W
Wind:WNW 3, c 7/8, 1006,4 hPa, t 27,6, tw 29,6 C, RF 82%, Dünung 225° 06 s 1,5 m

Profil 54 S (GI-Gun + Streamer)

16:15 Streamer z.W. WT 1296m 09 07,72 N 084 37,98 W
16:19 GI-Gun z.W. WT 1269m 09 07,83 N 084 38,06 W
16:22 Beginn 7. Profillinie WT 1237 1. Schuss 09 08,05 N 084 38,21 W
17:00 WT 953m KüG 360° v 3,0 kn 09 09,52 N 084 38,65 W
18:00 WT 484m 09 12,32 N 084 38,66 W
18:35 Schlauchboot z.W. zur Kontrolle Streamer
18:36 Ende 7. Profillinie WT 168m drehen über Bb. an **D 6 sm** 09 13,38 N 084 38,66 W
drehen langsam über Stb. auf 180°
19:03 Schlauchboot an Deck/Auftrieb am Streamerende entfernt

20:06 Drehung über Stb. beendet / Anfahrt Profillinie 8 09 14,35 N 084 38,01 W
20:19 Beginn 8. Profillinie KüG 180° FüG 3,0 kn WT 188m 09 13,93 N 084 38,01 W
21:00 WT 0585m 09 12,03 N 084 38,02 W
22:00 WT 1069m 09 09,16 N 084 38,04 W
22:03 Ende Profillinie 8 WT 1155m **D 5 sm** 09 08,99 N 084 38,04 W
22:10 bis 23:10 drehen über Stb.
Wind:West 3, c 6/8, 1005,6 hPa, t 27,7 C, tw 29,0 C, RF 79% Dünung: 225° 6 s 1,5 m

23:20 Beginn 9.Profillinie KüG 360° FüG 3,0 kn WT 1005m 09 09,00 N 084 40,65 W

Di., 22.07.2003

24:00 WT 652m 09 11,03 N 084 40,63 W
Wind:SWzW 4, t/l/r/o, 1006,8 hPa, t 26,5 C, tw 29,0 C, RF 95% Dünung 225° 06s 1,5 m

01:00 WT 230m Gewitterregen 09 13,97 N 084 40,64 W
01:02 Ende Profillinie 9 WT 206m **D 5 sm** 09 14,11 N 084 40,62 W
01:10 bis 01:42 drehen über Stb.

01:47 Beginn 10.Profillinie KüG 180° FüG 3,0 kn WT 226m 09 13,82 N 084 39,33 W
02:00 WT 343m 09 13,16 N 084 39,30 W
02:03 WT 360m Test DTS-Streamer ohne Erfolg 09 12,99 N 084 39,31 W
03:00 WT ..... 09 10,05 N 084 39,30 W
03:27 Ende Profillinie 10 WT .... **D 5 sm** 09 08,81 N 084 39,29 W

04:26 Beginn 11. Profillinie KüG 360° FüG 3,0 kn WT 894m 09 09,33 N 084 41,39 W
05:00 WT 675m 09 10,82 N 084 41,40 W
06:06 Ende Profillinie 11 **D 5 sm** 09 14,00 N 084 41,38 W
Wind:Stille, bedeckt, 1008,4 hPa, t 26,7 C, tw 29,0 C, RF 79% Dünung 225° 6 s 1,5 m

07:06 Beginn 12. Profillinie KüG 180° FüG 3,0 kn WT 200m 09 13,98 N 084 39,80 W
08:00 WT 650m 09 11,27 N 084 39,80 W
08:46 Ende Profillinie 12 WT 1058m **D 5 sm** 09 08,97 N 084 39,79 W
08:52 letzter Schuss WT 1116m GI-Gun a.D. 09 08,63 N 084 39,78 W
09:10 Streamer a.D. WT 1231m 09 07,80 N 084 39,76 W
Anfahrt OBH-Profil KüG 117° 25 sm
noch Di., 22.07.2003

Profil 55/1 DTS
12:00 Anfangspunkt für Profil 55/1 DTS erreicht WT 1283m 09 01,11 N 084 27,03 W
12:11 DTS z.W. Wind: NW 2, c 6/8, 1006,6 hPa, t 27,0, tw 28,7 C Dünung 200° 07 s 1,5 m
12:18 Depressor z.W. WT 995m KüG 142° FüG 2,0 kn 08 58,89 N 084 21,01 W
13:11 Beginn Profil 55/1 DTS KüG 142° FüG 2,6-2,8 kn 08 57,23 N 084 19,67 W
14:00 WT 1035m KL 1333m 08 55,65 N 084 18,29 W
14:58 Ende Profil 55 DTS/1 WT 1111m KL 1198m **D 5 sm** 08 53,60 N 084 16,78 W
Profil 55/2 DTS
16:07 Beginn Profil 55/2 DTS KüG 323° FüG 2,6 – 2,8 kn 08 54,26 N 084 17,47 W
17:00 WT 999m KL 1557m 08 56,17 N 084 18,89 W
17:34 Ende Profil 55/2 WT 921m KL 1342m **D 5 sm** 08 57,57 N 084 19,03 W
18:00 WT 868m KL 615m 08 58,59 N 084 18,45 W
18:36 DTS mit Streamer am Fisch an Deck 09 00,28 N 084 17,72 W

Profil 56 / Aufnahme 4xOBH/4xOBS/1xOBT 9x gesamt Schlauchboot und Hydralift 2
18:00 Wind Süd 1-2, c7/8, 1007,2hPa, t30,5C, tw29,2C, RF 68% Dünung 200° 8s 1,5 m
19:28 Schlauchboot z.W. / Aufnahme der Bodenmessgeräte 08 56,33 N 084 18,89 W
19:28 bis 19:43 alle 9 Geräte ausgelöst per Hydrophon WT981m (4xOBS, 4xOBH; 1xOBT)
19:45 Geräte tauchen auf (9x)
20:00 bis 14:41 alle Geräte eingesammelt und unversehrt a. B. 08 55,08 N 084 18,29 W
20:45 Schlauchboot an Deck / Anfahrt Profil 57 DTS rw 141° 7sm 08 54,08 N 084 17,43 W
Wind:Stille, bedeckt, 1007,0 hPa, t 29,7 C, tw 29,2 C, RF 71 % Dünung 200° 07s 1,5 m
21:10 DTS-Streamer z.W. – defekt, vorgesehenes DTS-Profil wird gestrichen
Anfahrt Arbeitsgebiet
Profil 57 SIMRAD- und Magnetikprofil
22:06 Posidonia außer Betr,., Beginn SIMRAD-Profil KüG 284 VV 08 50,60 N 084 14,80 W
23:36 ä.K. auf rw 309° WT 1879m 08 53,96 N 084 28,33 W
Mi., 23.07.2003
00:11 ä.K. auf rw 282° WT 1617m 08 58,98 N 084 34,89 W
04:46 Magnetometer z.W. WT 2935m **SIMRAD D 177 sm**
04:46 Beginn Magnetikprofil KüG 282° v 11,0 kn **D 121 sm** 09 11,47 N 085 30,38 W
06:00 WT 3470m 09 14,27 N 085 43,45 W

07:00 WT 3502m 09 16,24 N 085 54,52 W
08:00 WT 3430m 09 19,10 N 086 05,16 W
09.00 WT 3345m 09 21,63 N 086 16,41 W
10:00 WT 3260m 09 23,98 N 086 26,98 W
11:00 WT 3171m 09 26,44 N 086 37,93 W
12:00 WT 3085m 09 28,84 N 086 48,70 W
13:00 WT 3143m 09 31,30 N 086 59,64 W
14:00 WT 3154m 09 33,69 N 087 10,32 W
15:00 WT 3208m 09 36,03 N 087 20,88 W
15:58 WT 3250m Ende Magnetikprofil 57 Magnetometer a.D. 09 38,07 N 087 28,90 W

Profil 58 – Auslage OBS (18x) in NE-Richtung mit Hydralift Nr. 2

16:16 OBH 01 z.W. WT 3233m 09 38,23 N 087 30,47 W
16:43 OBH 02 z.W. WT 3234m 09 39,90 N 087 28,77 W
17:16 OBH 03 z.W. WT 3183m 09 41,97 N 087 26,75 W
17:57 OBH 04 z.W. WT 3176m 09 44,20 N 089 24,36 W
18:35 OBH 05 z.W. WT 3169m 09 46,21 N 087 22,37 W
19:11 OBH 06 z.W. WT 3156m 09 48,19 N 087 20,38 W
19:40 OBH 07 z.W. WT 3069m 09 49,77 N 087 18,79 W
20:08 OBH 08 z.W. WT 3090m 09 51,04 N 087 17,50 W
noch Mi., 23.07.2003 / Auslage OBH Profil 57

20:35 OBH 09 z.W. WT 3061m 09 52,50 N 087 16,03 W
21:06 OBH 10 z.W. WT 3116m 09 54,49 N 087 14,01 W
21:35 OBH 11 z.W. WT 3114m 09 56,39 N 087 12,10 W
22:06 OBH 12 z.W. WT 3069m 09 58,11 N 087 10,36 W
22:40 OBH 13 z.W. WT 3070m 10 00,22 N 087 08,25 W
22:57 OBH 14 z.W. WT 3071m 10 00,21 N 087 08,35 W
23:29 OBH 15 z.W. WT 3081m 10 02,32 N 087 06,13 W
24:00 OBH 16 z.W. WT 3098m 10 04,77 N 087 03,65 W
Do., 24.07.2003
24:31 OBH 17 z.W. WT 3174m 10 07,16 N 087 01,23 W
01:03 OBH 18 z.W. WT 3360m/ Anfahrt Profil 59 10 09,69 N 086 58,68 W
02:00 WT 4267m 10 17,38 N 086 50,89 W
Wind EzN 2, c 3/8, 1009,2 hPa, t 28,3 C, tw 28,6 C, RF 74% Düng.020°+180°6s 1,5m
03:00 WT 4493m 10 23,28 N 086 44,97 W

Profil 59 S 3x Airguns 32 Ltr.

03:03 Bb. -Airgun 32 Ltr. z.W. WT 4493m 1. Schuss 10 23,28 N 086 44,97 W
Beginn Seismikprofil 59 KüG 225 ° FdW 3,5 kn Profillänge: 68 sm
03:14 Stb.-Airgun 32 Ltr. z.W. WT 4285m 1. Schuss 10 23,01 N 086 45,20 W
03:25 Mitte-Airgun 32 Ltr. z.W. WT 4479m 1. Schuss 10 22,73 N 086 45,49 W
05:16 Ausfall der Mitte-Airgun – an Deck bis 05:30
06:00 WT 4185m 10 17,27 N 086 51,04 W
Wind WNW 3-4, o/p, 1010,0 hPa, t 27,9 C, tw 28,7 C, RF 85% Dünung 045° 07 s 2,0 m
07:06 WT 3857m 10 14,96 N 086 53,35 W
08:00 WT 3693m 10 13,02 N 086 55,30 W
09:06 WT 3352m 10 10,48 N 086 57 86 W
09:19 Mitte Airgun z.W. WT 3343m Seillänge 26m/23m 10 10,08 N 086 58,27 W
10:00 WT ..... m 10 08,68 N 086 59,69 W
11:00 WT 3137m Seillänge Mitte auf 36m vergrößert 10 06,35 N 087 02,03 W
12:00 WT 3057m 10 04,13 N 087 04,26 W
13:00 WT 3065m 10 01,84 N 087 06,61 W
14:00 WT 3074m 09 59,44 N 087 09,03 W
Wind NEzN 3, c 5/8, 1008,6 hPa, t 28,9 C, tw 28,6 C, RF 75% Dünung 190° 7s 1,5-2m

15:00 WT 3105m 09 57,18 N 087 11,32 W
16:00 WT 3122m 09 54,87 N 087 13,65 W
17:00 WT 3062m 09 52,57 N 087 15,96 W
18:00 WT 3085m 09 50,22 N 087 18,39 W
19:00 WT 3153m 09 47,83 N 087 20,74 W
20:00 WT 3157m 09 45,21 N 087 23,40 W
21:00 WT 3185m 09 42,98 N 087 25,64 W
22:00 WT 3209m 09 40,59 N 087 28,04 W
22:59 WT 3232m Airgun Mitte an Deck- defekt 09 38,36 N 087 30,65 W
23:10 WT 3227m Airgun Bb.- an Deck- defekt 09 38,07 N 087 30,60 W
24:00 WT 3226m 09 36,08 N 087 32,62 W
Wind:NNE 3-4, c 7/8, 1007,4 hPa, t 28,1 C, tw 28,6 C, RF 79%Dünung 190°+010° 7s 2,5m

Fr., 25.07.2003

00:28 WT 3223m Airgaun Mitte z.W. 09 34,93 N 087 33,78 W
00:47 WT 3246m Ende Profil 59 – letzter Schuß **D 68 sm** 09 34,24 N 087 34,46 W
01:08 WT 3250m Stb.+Mitte Kanonen a.D., Anfahrt Pr. 60 Regen

01:19 WT 3237m DTS-Streamer z.W. / Gerätetest
01:35 WT 3247m DTS-Streamer a.D. : i.O.

noch Fr., 25.07.2003

Profil 60 S Gl-Gun + Streamer

01:42 WT 3230m Gl-Gun z.W. 09 33,23 N 087 35,17 W
01:45 Seismikstreamer z.W.
01:51 WT 3236m Beginn Profilmessung KüG 045° FüG 5,0 kn 09 33,46 N 087 35,07 W
02:00 WT 3250m 09 33,78 N 087 34,71 W
03:05 WT 3240m 09 37,66 N 087 31,03 W
03:33 WT 3250m Gl-Gun zur Rep. a.D. 09 38,78 N 087 29,88 W
03:58 WT 3250m Gl-Gun z.W. 09 38,65 N 087 29,86 W
05:00 WT 3191m 09 42,12 N 087 26,52 W
06:10 WT 3170m Ende Profil 60 drehen über Stb. **D 18 sm** 09 45,65 N 087 22,37 W

Profil 61 S Gl-Gun + Streamer

06:43 WT 3152m Beginn Profilmessung KüG 267° FüG 5,0 kn 09 44,16 N 087 23,10 W
07:00 WT 3175m 09 44,01 N 087 24,50 W
07:50 WT 3178m Ende Profil 61 drehen über Stb. **D 05 sm** 09 43,90 N 087 28,45 W

Profil 62 S Gl-Gun + Streamer

08:07 WT 3176m Beginn Profilmessung KüG 181° FüG 5,0 kn 09 43,73 N 087 28,40 W
09:06 WT 3233m 09 39,40 N 087 28,52 W
09:25 WT 3244m Ende Profil 62 drehen über Stb. **D 06 sm** 09 37,68 N 087 28,57 W
09:30 WT 3238m Gl-Gun a.D.
09:42 WT 3236m Streamer a.D.

Profil 63 Aufnahme OBHs 18x

09:44 WT 3226m Hydrophon z.W.
10:03 WT ..... OBH 1 ausgelöst
10:11 WT ..... OBH 2 ausgelöst
10:54 WT ..... OBH 1 an Deck 09 38,15 N 087 30,62 W
11:02 WT ..... OBH 3 ausgelöst
11:32 WT ..... OBH 2 an Deck 09 39,61 N 087 29,15 W
11:57 WT ..... OBH 4 ausgelöst
12:23 WT ..... OBH 3 an Deck 09 41,89 N 087 27,29 W
12:50 WT ..... OBH 5 ausgelöst
13:16 WT ..... OBH 4 a.D. 09 44,37 N 087 24,87 W
13:48 WT ..... OBH 6 ausgelöst

14:23 WT	OBH 5 a.D.	09 46,51 N 087 23,06 W
15:04 WT	OBH 6 a.D.	09 48,53 N 087 21,02 W
15:10 WT	OBH 7 + 8 ausgelöst	
16:08 WT	OBH 7 a.D.	09 50,14 N 087 19,23 W
16:12 WT	OBH 9 ausgelöst	
16:58 WT	OBH 10 ausgelöst	
17:25 WT	OBH 9 a.D.	09 53,15 N 087 16,67 W
17:33 WT	OBH 11 ausgelöst	
18:03 WT	OBH 10 a.D.	09 55,26 N 087 14,67 W
18:10 WT	OBH 12 ausgelöst	
18:45 WT	OBH 11 a.D.	09 57,10 N 087 12,79 W
18:55 WT	OBH 13-14 ausgelöst	
19:25 WT	OBH 12 a.D.	09 58,76 N 087 10,99 W
20:03 WT	OBH 13 a.D.	10 00,52 N 087 08,69 W
20:07 WT	OBH 14 a.D.	
20:12 WT	OBH 15 ausgelöst	
20:43 WT	OBH 16 ausgelöst	
21:05 WT	OBH 15 a.D.	10 02,55 N 087 06,38 W

noch Fr., 25.07.2003 / Profil 63 - Aufnahme OBHs

21:10 WT	OBH 17 ausgelöst	
21:58 WT	OBH 16 a.D.	10 05,22 N 087 04,09 W
22:02 WT	OBH 18 ausgelöst ???	
22:39 WT	OBH 17 a.D.	10 07,67 N 087 01,89 W
22:42 WT	OBH 18 ausgelöst	
23:16 WT	OBH 18 a.D. (alle 18 Geräte wieder a.D.)	10 10,08 N 086 59,15 W

Sa., 26.07.2003

Station 64 Auslösertest Winde W 6

00:38 Auslöser z.W. Winde W 6 WT 4574m	10 19,67 N 086 48,85 W
00:40 Hydrophon z.W.	
01:00 WT ..... ? Lotanlage ausgeschaltetKL 690 m	10 19,82 N 086 48,84 W
02:21 WT 4530m SL 4300m hieven	10 20,27 N 086 48,94 W
03:35 WT 4365m Auslöser a.D.	10 20,44 N 086 49,01 W
Wind:umlfnd 1, c6/8, 1009,8hPa, t25,9C, tw28,7C, RF75%	Düng 020°+190° 6s1,5m

Profil 65 Auslage 4x OBHs Hydralift Nr. 4

04:52 OBH 1 z.W. WT 3383m	10 10,03 N 086 57,02 W
05:52 OBH 2 z.W. WT 3050m	10 03,07 N 086 03,53 W
Wind:Stille, c 5/8, 1010,2 hPa, t 26,7 C, tw 28,7 C, RF 79%	Dünung: 190° 06s 1,5 m
06:50 OBH 3 z.W. WT 3126m	09 56,03 N 086 58,52 W
07:54 OBH 4 z.W. WT 3546m	10 03,99 N 086 50,56 W

Profil 66 Einmessen Posidonia-Antenne

11:21 OBH z.W. WT 1237m	10 14,50 N 086 14,49 W
11:35 OBT z.W. WT 1239m	10 14,36 N 086 14,36 W
11:42 Posidonia-Antenne im Lotschacht ausgefahren	
12:05 Beginn Einmessen Posidonia-Antenne WT 1251m	10 14,51 N 086 14,51 W
Wind:varr. 1, 1009,0 hPa, t 27,3 C, tw 28,3 C, RF 80%	Dünung 020 05 s 1,5 m
13:35 Ende Einmessen Posidonia-Antenne WT 1287m	10 14,44 N 086 14,86 W
13:35 OBH ausgelöst	
14:00 OBH an Deck WT 1245m	10 14,52 N 086 14,63 W
Wind:SW1, c3/8, 1010,0hPa, t 27,6C, tw 28,5 C, RF 77%, Düng	350° + 180° 5s 1,0 m

Profil 67 DTS + GI-Gun

14:52 DTS z.W. WT 1376m 10 12,39 N 086 14,03 W
15:00 WT 1465m KL 056m fieren Kabel mit 0,3m/sec KüG 318° FüG 3,0 kn
15:20 GI-Gun z.W. WT 1536m 10 13,12 N 086 15,11 W
15:24 Beginn Profilmessung Profil 67 DTS + GI-Gun 1. Schuss 10 13,36 N 086 15,23 W
16:00 WT 1513m KüG 318° FüG 3,0 kn 10 14,73 N 086 16,32 W
17:00 WT 1663m KL 2757m 10 16,85 N 086 18,21 W
18:00 WT 1774m KL 2942m 10 18,93 N 086 20,05 W
19:18 WT 1866m KL 3217m Profilende drehen ü. Stb. **D 9 sm** 10 21,63 N 086 22,45 W
20:06 WT 1756m GI-Gun vorgeholt KL 2006m 10 22,57 N 086 21,69 W

Profil 68 DTS + GI-Gun

20:17 WT 1771m KL ..... m erster Schuss Profillänge 10 sm 10 22,24 N 086 21,40 W
21:00 WT 1722m KL 2841m KüG 138° FüG 3,0 kn 10 20,63 N 086 19,99 W
Wind:Stille, o, Regen, 1009,6 hPa, t 27,7 C, tw 28,9 C, RF 86% Düng. 180+020° 6s 1,5m
22:00 WT 1594m KL 2871m 10 18,67 N 086 18,26 W
23:00 WT 1466m KL 2342m 10 16,38 N 086 16,31 W
24:00 WT 1257m KL 1977m Profilende drehen ü. Stb. **D 11 sm** 10 14,29 N 086 14,40 W

So., 27.07.2003

Profil 69 DTS + GI-Gun

00:50 WT 1342m KL 1724m Beginn Profil 69 KüG 318° FüG 3kn 10 14,09 N 086 15,00 W
01:00 WT 1373m KL 1841m 10 14,46 N 086 15,36 W
02:00 WT 1594m KL 2567m 10 16,57 N 086 17,23 W
Wind:varr.1, o, 1011,3 hPa, t 26,3 C, tw 28,8 C, RF 89%, Dünung 180° + 020° 05 s 1,5 m
03:00 WT 1691m KL 2896m 10 19,03 N 086 19,39 W
04:00 WT 1824m KL 3629m 10 21,50 N 086 21,57 W
04:30 WT 1813m KL 3322m Profilende, drehen ü. Stb. **D 11 sm** 10 22,40 N 086 22,46 W

Profil 70 DTS+GI-Gun

05:00 WT 1798m KL 2336m 10 23,30 N 086 23,54 W
06:00 WT 1683m KL 1722m 10 23,52 N 086 22,19 W
Wind:E-l.1-2, o, 1011,1 hPa, t 27,0 C, tw 28,7 C, RF 82% Dünung 180° 06 s 1,5 m
06:16 WT 1742m KL 2159m Beginn Profil 70 KüG 139° FüG 3 kn 10 22,91 N 086 21,87 W
07:00 WT 1792m KL 2737m 10 21,23 N 086 20,76 W
08:00 WT 1627m KL 2852m 10 19,02 N 086 18,83 W
09:00 WT 1529m KL 2620m 10 17,03 N 086 17,11 W
09:38 WT 1435m KL 2490m Profilende, drehen ü. Stb. **D 10 sm** 10 15,55 N 086 15,83 W

Profil 71 DTS+GI-Gun

10:00 WT 1224m KL ..... m 10 15,30 N 086 14,81 W
11:00 WT 1471m KL 1423m 10 14,74 N 086 15,99 W
11:18 WT 1552m KL 2015m Beginn Profil 71 KüG318° FüG 3,0kn 10 15,61 N 086 16,73 W
12:00 WT 1622m KL 3267m 10 17,48 N 086 18,38 W
Wind:NE 3, c 5/8, 1009,0 hPa t 26,9C tw 28,6C RF80% Dünung200° 07 s 1,5 – 2,0 m
13:00 WT 1790m KL 3775m 10 20,18 N 086 20,71 W
13:02 WT 1820m KL 3802m Profilende, drehen ü. Stb. **D 6,2 sm** 10 20,30 N 086 20,85 W

Profil 72 DTS+GI-Gun

14:00 WT 1948m KL 1948m 10 22,05 N 086 23,34 W
15:00 WT 1798m KL 1912m 10 21,61 N 086 21,41 W
15:27 WT 1771m KL 2457m Beginn Profil 72 KüG 138° FüG 3,0kn10 20,78 N 086 20,65 W
16:00 WT 1716m KL 2656m 10 19,68 N 086 19,67 W
17:00 WT 1588m KL 2526m 10 17,61 N 086 17,83 W
17:58 WT 1469m KL 1478m Profilende, drehen ü. Stb. **D 7,2 sm** 10 15,61 N 086 16,08 W

Profil 73 DTS+GI-Gun

19:00 WT 1048m KL 1611m 10 16,73 N 086 14,08 W
20:00 WT 0994m KL 1120m 10 18,79 N 086 13,92 W
20:14 WT 1130m KL 1120m Beginn Profil 73 KüG 225°FüG 3,0kn 10 18,42 N 086 14,48 W

21:00 WT 1784m KL 1401m 10 16,95 N 086 16,01 W
22:00 WT 1736m KL 2510m 10 14,94 N 086 18,07 W
Wind:SE 1-2, o/r, 1008,8 hPa, t 27,5C, tw 29,3C, RF78 %Dünung 360°+200° 08s 1-2 m
22:32 WT 1892m KL 2751m Profilende, drehen ü. Stb. **D 6,3 sm** 10 13,97 N 086 19,05 W

Profil 74 DTS+GI-Gun
23:00 WT2027m KL 2095m 10 13,56 N 086 20,35 W
23:31 überlaufen Langleine
24:00 WT 1816m KL 2475m 10 16,18 N 086 19,81 W
Mo., 28.07.2003
00:05 WT 1804m KL2659m Beginn Profil 74 KüG 045° FüG 3,0kn 10 16,32 N 086 19,66 W
01:00 WT 1555m KL 2625m 10 17,98 N 086 17,95 W
02:00 WT 1200m KL 2040m 10 19,84 N 086 16,03 W
02:23 WT 0979m KL 1550m Profilende, drehen ü. Stb. **D 6 sm** 10 20,55 N 086 15,29 W
02:42 bis 02:54 Kontrollieren Posidonia-Antenne Lotschacht

noch Mo., 28.07.2003

Profil 75 DTS+GI-Gun
03:00 WT 0778m KL 0568m 10 21,23 N 086 13,98 W
04:00 WT 1126m KL1105m Beginn Profil 75 KüG 225° FüG 2,5kn 10 19,04 N 086 14,87 W
05:00 WT 1480m KL 1872m 10 17,09 N 086 16,68 W
06:00 WT 1781m KL 2253m 10 15,20 N 086 18,67 W
Wind:West 1, c 4/8, 1010,0 hPa, t 26,7 C, tw 28,8 C, RF 81% Dünung 350+200° 6s 1,5 m
06:18 WT 1865m KL 2316m Profilende, drehen ü. Stb. **D 6 sm** 10 14,64 N 086 19,21 W
Profil 76 DTS+GI-Gun
07:00 WT 1850m KL 2406m 10 15,24 N 086 20,80 W
07:30 WT 1834m KL 2637m Beginn Profil 76 KüG 046° FüG3,0kn 10 16,16 N 086 20,09 W
08:00 WT 1743m KL 2843m 10 17,11 N 086 19,10 W
09:00 WT 1390m KL 2646m 10 19,04 N 086 17,08 W
09:47 WT 1020m KL 1776m Profilende, drehen ü. Stb. **D 6 sm** 10 20,51 N 086 15,50 W
Profil 77 DTS+GI-Gun
10:00 WT 1001m KL 1310m 10 20,92 N 086 15,06 W
10:46 WT 1098m KL 1258m Beginn Profil 77 KüG 225° FüG 3,0kn10 19,39 N 086 15,12 W
11:00 WT 1234m KL 1462m 10 18,89 N 086 15,69 W
12:00 WT 1632m KL 2386m 10 16,81 N 086 17,81 W
Wind:NE 3-4, c 1/8, 1009,4 hPa, t 28,0 C, tw 28,3 C, RF 72%, Dünung 350+200° 10s 1-2m
12:43 WT 1825m KL 2902m Profilende, drehen ü. Stb. **D 6 sm** 10 15,31 N 086 19,38 W
Profil 78 DTS+GI-Gun
13:00 WT 1925m KL 2306m 10 14,72 N 086 20,03 W
14:00 WT 1873m KL 1914m 10 16,00 N 086 20,53 W
Wind:E 3, c 1/8, 1010,7 hPa, t 27,6 C, tw 28,5 C, RF75% Dünung 350+200° 08 s 1-2 m
14:19 WT 1818m KL 2450m Beginn Profil 78 KüG 045° FüG 3,0kn10 16,58 N 086 19,94 W
15:00 WT 1765m KL 2669m 10 18,22 N 086 18,24 W
16:00 WT 1313m KL 2260m 10 19,68 N 086 16,68 W
16:37 WT 1044m KL 1397m Profilende, drehen ü. Stb. **D 6 sm** 10 20,94 N 086 15,40 W
17:00 WT 0908m KL 0706m 10 21,04 N 086 14,57 W
17:08 Ausfall DTS, holen Gerät a.D. 10 20,57 N 086 14,78 W
17:20 GI-Gun a.D.
17:45 DTS mit Depressor a.D. WT 1141m 10 19,82 N 086 15,45 W

Station 79 Gerätetest
18:28 Schwimmtest für Auslöser-Auftrieb bis 19:06
20:00 Posidonia-Antenne Lotschacht eingefahren

Station 80 Aufnahme OBS
20:45 Hydrophon z.W. bis 20:56 10 15,01 N 086 15,16 W
21:08 OBS aufgetaucht / Anlauf
21:23 OBS an Deck WT 1254m 10 14,52 N 086 14,63 W
22:13 Test für Aurtrieb Auslöser

Profil 81 DTS+GI-Gun
22:18 Test DTS-Streamer: i.O.
22:37 DTS z.W. WT 967m KüG 225° FüG 2,5 kn 10 20,38 N 086 14,97 W
22:43 Depressor z.W.
22:52 Posidonia-Antenne Lotschacht ausgefahren
23:00 WT 1144m KL 0385m 10 19,73 N 086 15,49 W
23:04 GI-Gun z.W.
23:22 WT 1274m KL 1283m Beginn Profil 81 DTS KüG 225°3,0kn 10 19,08 N 086 16,17 W
24:00 WT 1489m KL 1759m 10 18,02 N 086 17,24 W
Di., 29.07.2003
01:00 WT 1776m KL 2545m 10 16,22 N 086 19,12 W
01:12 WT 1842m KL 2942m Profilende drehen ü. Stb. **D 5,0 sm** 10 15,61 N 086 19,78 W
Profil 82 DTS+GI-Gun
02:00 WT 2047m KL 1970m 10 14,93 N 086 21,84 W
02:51 WT 1843m KL 2658m Begin Profil 82 KüG 045° FüG 2,5 kn 10 16,63 N 086 20,43 W
03:00 WT 1812m KL 2791m 10 16,91 N 086 20,15 W
03:12 bis 03:25 weichen Fischereifahrzeug aus KüG 080° dann zurück auf Profillinie
04:48 WT 1155m KL2258m Profilende holen Geräte ein **D 5,2 sm** 10 20,29 N 086 16,56 W
04:48 WT 1155m KL 2258m hieven DTS
04:53 GI-Gun a.D., Posidonia-Antenne eingefahren
05:00 WT 1129m KL 1650m 10 20,72 N 086 16,14 W
05:43 WT 0862m Depressor a.D.
05:56 WT 0861m DTS a.D. am DTS-Streamer Langleine von Fischerei
06:00 WT 0862m Streamer a.D. Langleine frei und im Wasser
06:12 Anlauf Caldera D 120 sm SIMRAD-Profilmessung 10 22,24 N 086 14,49 W
16:00 SIMRAD-Datenaufzeichnung eingestellt 09 39,51 N 084 55,99 W

18:00 Reiseunterbrechung Caldera

Mi., 30.07.2003

14:00 Fortsetzung der Reise / Abfahrt Caldera

16:30 Start Datenaufzeichnungen SIMRAD KüG 225° FüG 13 kn 09 37,40 N 084 58,00 W
17:23 ändern Kurs auf 300° WT 174m 09 24,31 N 085 06,27 W
20:49 ändern Kurs auf 287° WT 341m 09 50,07 N 085 43,24 W
21:38 ändern Kurs auf 311° WT 879m 09 53,00 N 085 52,50 W
Do., 31.07.2003
02:44 ändern Kurs auf 323° WT 2351m 10 39,39 N 086 45,32 W
03:28 ändern Kurs auf 352° WT 2341m 10 47,59 N 086 51,20 W
05:03 Ende SIMRAD-Profil / Vermessungsfahrt 10 54,45 N 086 52,31 W

Profil 83 Kalibrierung Posidonia-Antenne
05:03 Auslage OBH WT 1221m 10 56,50 N 086 51,39 W
05:13 Posidonia-Antenne im Lotschacht ausgefahren
05:13 Beginn Kalibrierung Posidonia-Antenne Acht um OBH über Stb.2,5 - 3,0 kn r 750m
Wind:NE 5-6, c 6/8, 1010,2 hPa, t 27,3 C, tw 28,5 C, RF 74% Dünung 360° 05 s 1,5 m
07:04 Ende der Kalibrierung WT 1213m 10 56,53 N 086 51,47 W
07:13 OBH ausgelöst / 07:30 OBH aufgetaucht und gesichtet

07:44 OBH an Deck WT 1212m 10 56,54 N 086 51,55 W
Anfahrt Profil 84 rwK 210° 8,0 sm

Profil 84 DTS+GI-Gun

08:22 Aussetzen DTS WT 1630m 10 54,76 N 086 53,09 W
Wind:NE 4, o, 1009,2 hPa, t 26,8 C, tw 27,4 C, RF 89% Dünung 060° 06 s 1-2 m
09:06 WT 1249m GI-Gun z.W.
09:15 Beginn DTS-Profil 84 WT 1587m KüG 312° FüG 3,0 kn 10 56,35 N 086 54,90 W
10:00 WT 1614m KL 2600m 10 57,69 N 086 56,42 W
11:00 WT 1532m KL 2898m 10 59,62 N 086 58,51 W
12:00 WT 1599m KL 2747m 11 01,56 N 087 00,65 W
13:00 WT 1671m KL 2872m 11 03,47 N 087 02,79 W
14:00 WT 1780m KL 2872m 11 05,41 N 087 04,92 W
15:00 WT 1753m KL 3286m 11 07,48 N 087 07,23 W

noch Profil 84 DTS+GI-Gun

16:00 WT 1522m KL 3173m 11 09,55 N 087 09,54 W
17:00 WT 1505m KL 2507m 11 11,32 N 087 11,44 W
18:00 WT 1701m KL 2827m 11 13,14 N 087 13,48 W
Wind:EzN 4, o, 1010,4 hPa, t 27,9 C, tw 27,9 C, RF 77% Dünung 070° 06 s 2,0 m
19:06 WT 1736m KL 3162m 11 15,37 N 087 15,97 W
20:46 WT 1450m KL 2690m Ende Profil 84 **D 30 sm** 11 18,65 N 087 19,56 W

Profil 85 DTS+GI-Gun

22:00 WT 1119m KL 1453m 11 20,91 N 087 18,38 W
Wind:Ost 5, c 6/8, 1008,8 hPa, t 27,3 C, tw 27,8 C, RF 80ß% Dünung 060° 6 s 2 m
22:26 WT 1131m KL 1453m Profilbeginn KüG132° FüG 3,0 kn 11 20,46 N 087 17,35 W
23:00 WT 1226m KL 1570m 11 19,41 N 087 16,18 W
24:00 WT 1297m KL 1934m 11 17,41 N 087 13,98 W

Fr., 01.08.2003

01:00 WT 1248m KL 2013m 11 15,40 N 087 11,77 W
02:00 WT 1157m KL 1585m 11 13,52 N 087 09,68 W
03.00 WT 1194m KL 1641m 11 11,54 N 087 07,55 W
04:00 WT 1280m KL 1854m 11 09,68 N 087 05,42 W
Wind:ENE 5-6, c 6/8, 1011,5 hPa, t 26,7 C, tw 27,4 C, RF 75% Dünung 060° 6 s 2,0 m
05:00 WT 1345m KL 1660m 11 07,91 N 087 03,46 W
06:00 WT 1193m KL 1682m 11 06,01 N 087 01,38 W

07:00 WT 1193m KL 1888m 11 03,86 N 086 58,99 W
08:00 WT 1197m KL 1660m 11 02,03 N 086 56,98 W
09:03 WT 1276m KL 1600m Profilende drehen ü. Stb. **D 30 sm** 11 00,09 N 086 54,84 W

Profil 86 DTS+GI-Gun

10:24 WT 1505m KL 2207m Profilbeginn KüG 312° FüG 3,0 kn 10 59,12 N 086 56,86 W
Wind:NE 5-6, c 7/8, 1009,2 hPa, t 26,3 C, tw 27,3 C, RF 80% Dünung 060 06s 1,5-2m
11:00 WT 1440m KL 2446m 11 00,26 N 086 58,16 W
12:00 WT 1528m KL 2518m 11 02,21 N 087 00,34 W
13:00 WT 1613m KL 2739m 11 04,12 N 087 02,47 W
14:00 WT 1630m KL 2781m 11 06,09 N 087 04,61 W
Wind:ENE 4-3, o, 1011,3 hPa, t 26,7 C, tw 27,4 C, RF 80% Dünung 060 ° 06s 2 m
15:00 WT 1616m KL 2899m 11 08,09 N 087 06,80 W
16:00 WT 1424m KL 2782m 11 09,91 N 087 08,90 W
17:00 WT 1414m KL 2407m 11 11,89 N 087 11,03 W
18:00 WT 1581m KL 2429m 11 13,73 N 087 13,74 W
Wind:ENE 4-3, o, 1011,5 hPa, t 27,5 C, tw 27,6 C, RF 75% Dünung 060+180° 10m 2m
19:00 WT 1610m KL 2655m 11 15,23 N 087 15,24 W

20:00 WT 1438m KL 2713m 11 17,57 N 087 17,30 W
20:44 WT 1369m KL 2455m Profilende, drehen ü. Stb. **D 29 sm** 11 18,95 N 087 18,85 W

Profil 87 DTS+GI-Gun + Oberflächenstreamer
22:00 WT 1067m KL 1361m 11 21,22 N 087 17,46 W
22:40 WT 1151m KL 1465m Profilbeginn KüG 132° FüG 3,0 kn 11 20,10 N 087 15,89 W
23:00 WT 1169m KL 1503m 11 19,46 N 087 15,19 W
24:00 WT 1200m KL 1600m 11 17,53 N 087 13,07 W
Wind:ESE 3, o, 1009,8 hPa, t 27,4 C, tw 27,6 C, RF 82%, Dünung 060°+180° 10s 2 m
Sa., 02.08.2003
00:36 WT 1146m KL 1738m Oberflächenstramer z.W. 11 16,35 N 087 11,76 W
01:00 WT 1149m KL 1558m 11 15,60 N 087 10,93 W
02:00 WT 1042m KL 1472m 11 13,65 N 087 08,76 W

noch Sa., 02.08.2003 / Profil 87
03:00 WT 1096m KL 1475m 11 11,69 N 087 06,59 W
04:00 WT 1122m KL 1706m 11 09,82 N 087 04,52 W
05:00 WT 1084m KL 1692m 11 07,86 N 087 02,36 W
06:00 WT 1076m KL 1510m 11 05,98 N 087 00,30 W
Wind:ENE 4-5, c 5/8, 1010,9 hPa, t 27,0 C, tw 27,7 C, RF 83% Dünung 060+180° 8s 2 m
07:00 WT 1113m KL 1631m 11 04,01 N 086 58,12 W
07:12 WT 1123m KL 1557m Oberflächenstreamer a.D. 11 03,57 N 086 57,61 W
08:06 WT 1062m KL 1574m 11 01,89 N 086 55,77 W
08:43 WT 1096m KL 1464m Profilende, drehen ü. Stb. **D 29 sm** 11 00,60 N 086 54,33 W

Profil 88 DTS+GI-Gun
09:00 WT 1123m KL 1280m 10 59,74 N 086 54,13 W
09:57 WT 1425m KL 1990m Profilbeginn KüG 312° FüG 3,0 kn 10 59,60 N 086 56,43 W
10:00 WT 1400m KL 2142m 10 59,77 N 086 56,59 W
11:00 WT 1384m KL 2243m 11 01,67 N 086 58,69 W
12:00 WT 1428m KL 2307m 11 03,62 N 087 00,86 W
Wind:NE 6, c 6/8, 1009,2 hpa, t 26,5 C, tw 27,4 C, RF 81 % Dünung 080° 6s 2,5 m
13:00 WT 1478m KL 2458m 11 05,58 N 087 03,02 W
14:00 WT 1521m KL 2569m 11 07,51 N 087 05,15 W
15:00 WT 1503m KL 2412m 11 09,43 N 087 07,29 W
16:00 WT 1297m KL 2136m 11 11,32 N 087 09,37 W
17:00 WT 1390m KL 2048m 11 13,26 N 087 11,51 W
18:00 WT 1487m KL 2413m 11 15,15 N 087 13,62 W
Wind:NE 4-5, c 4/8, 1010,7 hPa, t 27,4 C, tw 27,6 C, RF 72% Dünug 080+200° 10s 1,5m
19:00 WT 1451m KL 2534m 11 17,13 N 087 15,77 W
20:06 WT 1292m KL 2344m 11 19,21 N 087 18,08 W
20:11 WT 1271m KL 2267m Profilende, drehen ü. Stb. **D 29 sm** 11 19,43 N 087 18,33 W
20:35 WT 1139m KL 1317m Langleine überfahren 11 20,37 N 087 18,85 W
21:00 WT 1049m KL 1234m 11 21,63 N 087 18,15 W

Profil 89 DTS+GI-Gun + Oberflächenstreamer
22:00 WT 1066m KL 1234m 11 20,99 N 087 15,82 W
22:10 WT 1062m KL 1326m Profilbeginn KüG 132° FüG 3,0 kn 11 20,60 N 087 15,40 W
22:23 WT 1088m KL 1358m Oberflächenstreamer z.W. 11 20,19 N 087 14,93 W
23:00 WT 1122m KL 1437m 11 19,03 N 087 13,68 W
24:00 WT 1105m KL 1540m 11 17,13 N 087 11,57 W
Wind:E 3, c 1/8, 1008,0 hPa, t 28,3 C, tw 27,9 C, RF 71%, Dünung 090+200° 10 s 2m
So., 03.08.2003
01:00 WT 0961m KL 1413m 11 15,22 N 087 09,44 W
02:00 WT 0909m KL 1125m 11 13,19 N 087 07,21 W

03:00 WT 1136m KL 1485m 11 11,17 N 087 04,98 W
04:00 WT 1069m KL 1236m 11 09,32 N 087 02,91 W

05:00 WT 1059m KL 1236m 11 07,45 N 087 00,88 W
06:00 WT 1196m KL 1308 11 05,64 N 086 58,83 W
Wind:EzN 4, c 2/8, 1010,9 hPa, t 27,6, tw 27,7 C, RF 78% Dünung090+200°10s 2m
06:09 WT 1054m KL 1506m Oberflächenstreamer a.D. 11 05,18 N 086 58,31 W
07:06 WT 1078m KL 1324m 11 03,35 N 086 56,32 W
08:12 WT 0978m KL 1218m Profilende, drehen ü. Stb. **D 29 sm** 11 01,23 N 086 53,97 W
09:06 WT 1362m KL 1190m 10 59,54 N 086 55,29 W

noch So., 03.08.2003

Profil 90 DTS+GI-Gun
09:21 WT 1283m KL 1590m Profilbeginn KüG 312° FüG 3,0 kn 11 00,13 N 086 55,90 W
10:00 WT 1262m KL 1590m 11 01,44 N 086 57,38 W
11:00 WT 1277m KL 1977m 11 03,39 N 086 59,42 W
12:00 WT 1309m KL 2047m 11 05,18 N 087 01,49 W
Wind:ENE 3, c 5/8, 1010,0 hPa, t 26,7 C, tw 27,6, RF 79 % Düng70°+200° 09s 2,0m
13:00 WT 1391m KL 2204m 11 07,09 N 087 03,63 W
14:00 WT 1395m KL 2384m 11 09,07 N 087 05,81 W
15:00 WT 1248m KL 2206m 11 11,01 N 087 07,95 W
16:00 WT 1234m KL 1931m 11 13,05 N 087 10,20 W
17:00 WT 1362m KL 2051m 11 14,98 N 087 12,35 W
18:00 WT 1385m KL 2224m 11 16,91 N 087 14,48 W
Wind:EzN 4, c 7/8, 1010,7 hPa, t 27,3 C, tw 27,7 C, RF 72% Dünung 225° 08 s 1,5 m
19:06 WT 1290m KL 2159m 11 19,04 N 087 16,85 W
19:28 WT 1197m KL 2147m Profilende, drehen ü. Bb. **D 29 sm** 11 19,83 N 087 17,70 W
20:06 WT 1236m KL 1373m 11 20,13 N 087 19,34 W

Profil 91 DTS+GI-Gun
21:00 WT 1519m KL 1622m 11 18,29 N 087 20,29 W
21:40 WT 1587m KL 2104m Profilbeginn KüG 132° FüG 3,0 kn 11 17,00 N 087 19,00 W
22:00 WT 1625m KL 2190m 11 16,36 N 087 18,23 W
23:00 WT 1767m KL 3076m 11 14,46 N 087 16,06 W
24:00 WT 1821m KL 2948m 11 12,51 N 087 13,89 W

Mo., 04.08.2003
01:00 WT 1634m KL 2797m 11 10,58 N 087 11,74 W
02:00 WT 1715m KL 2552m 11 08,56 N 087 09,51 W
03:00 WT 1921m KL 3024m 11 06,50 N 087 07,18 W
04:00 WT 1908m KL 3402m 11 04,61 N 087 05,11 W
05:00 WT 1772m KL 3279m 11 02,66 N 087 02,95 W
06:00 WT 1703m KL 2828m 11 00,72 N 087 00,79 W
Wind:SE 4, o/p/l, 1010,0 hPa, t 26,8 C, tw 27,8C,RF83% Dünung 180+090° 6s 1,5 m
07:06 WT 1656m KL 2685m 10 58,62 N 086 58,48 W
07:49 WT 1705m KL 2644m Profilende, drehen ü. Stb. **D 29 sm** 10 57,18 N 086 56,87 W

Profil 92 DTS+GI-Gun
09:00 WT 2245m KL 2660m 10 55,50 N 086 59,27 W
09:21 WT 2232m KL 2882m Profilbeginn KüG 312° FüG 3,0 kn 10 56,10 N 086 59,91 W
10:00 WT 2168m KL 3792m 10 57,16 N 087 01,09 W
11:00 WT 2079m KL 4458m 10 59,30 N 087 03,40 W
12:00 WT 2142m KL 4366m 11 01,39 N 087 05,68 W
Wind:E 4, c 6/8, 1008,4 hPa, t 26,7 C, tw 27,7 C, RF 80% Düng.200+080°7s 1-2 m

13:00 WT 2374m KL 4521m 11 03,34 N 087 07,82 W
14:00 WT 2339m KL 4809m 11 05,25 N 087 09,93 W
14:19 WT 2261m KL 4750m Profilende hieven DTS **D 14 sm** 11 05,90 N 087 10,63 W
15:00 WT 2446m KL 2339m 11 07,18 N 087 12,01 W

Profil 93 DTS+GI-Gun + Oberflächen-Streamer
16:00 WT 1896m KL 1904m 11 09,40 N 087 12,68 W
16:53 WT 1758m KL 2328m Profilbeginn KüG 132° FüG 3,0 kn 11 08,62 N 087 10,63 W
18:00 WT 2015m KL 3043m 11 06,48 N 087 08,26 W
Wind:ENE 4, o/p, 1009,0 hPa, t 26,9 C, tw 27,8 C, RF 81%, Düng 080°+200°7s 2,0 m
19:00 WT 1937m KL 3340m 11 04,48 N 087 06,14 W
noch Mo., 04.08.2003 / Profil 93

19:15 WT 2003m KL 3440m Oberflächen-Streamer z.W. 11 04,12 N 087 05,64 W
20:06 WT 1924m KL 3499m 11 02,43 N 087 03,75 W
21:06 WT 1806m KL 3270m 11 00,32 N 087 01,42 W
22:00 WT 1784m KL 3059m 10 58,61 N 086 59,52 W
22:56 WT 1854m KL 3223m Profilende **D 18 sm** 10 56,61 N 086 57,31 W
23:00 WT 1845m KL 3123m 10 56,48 N 086 57,17 W
23:19 WT 1903m KL 2545m Oberflächen-Streamer a.D. 10 55,58 N 086 56,64 W
24:00 Wind EzS 3, c 6/8, 1007,8 hPa, t 27,0 C, tw 28,0 C, RF 82%, Dünung 200° 06s 1-2 m

Di., 05.08.2003

Profil 94 DTS+GI-Gun
00:00 WT 2167m KL 2515m 10 55,25 N 086 58,22 W
00:42 WT 2092m KL 3513m Profilbeginn KüG 312° FüG 3,0 kn 10 56,76 N 086 59,62 W
00:48 WT 2082m KL 3478m GI-Gun an Deck 10 56,87 N 086 59,78 W
01:00 WT 2001m KL 3618m 10 57,28 N 087 00,15 W
01:09 WT 1999m KL 3648m GI-Gun zu Wasser 10 57,56 N 087 00,46 W
02:00 WT 1985m KL 3952m 10 59,95 N 087 02,43 W
03:00 WT 2078m KL 3943m 11 01,35 N 087 04,63 W
04:00 WT 2243m KL 4094m 11 03,33 N 087 06,80 W
05:05 WT 2244m KL 4485m 11 05,43 N 087 09,13 W
05:30 WT 2184m KL 4234m Profilende, hieven DTS **D 14 sm** 11 06,14 N 087 09,90 W
06:00 WT 2214m KL 3124m 11 07,09 N 087 11,04 W
Wind:Ost 2-3, c/p/o, 1009,6 hPa, t 27,1 C, tw 27,8 C, RF 82% Dünung 200° 6s 2,0 m

Profil 95 DTS+GI-Gun
07:00 WT 2156m KL 2563m 11 08,63 N 087 13,50 W
08:00 WT 2056m KL 2669m 11 08,39 N 087 11,37 W
08:11 WT 1930m KL 3050m Profilbeginn KüG 132° FüG 3,0 kn 11 07,99 N 087 10,92 W
09:00 WT 2100m KL 3384m 11 06,36 N 087 09,13 W
10:00 WT 2235m KL 3683m 11 04,49 N 087 07,06 W
11:00 WT 2039m KL 3695m 11 02,49 N 087 04,87 W
12:00 WT 1910m KL 3604m 11 00,43 N 087 02,59 W
Wind:NE 5, c 7/8, 1007,0 hPa, t 27,3 C, tw 28,3 C, RF 79% Düng 190+070° 8s 1,5m
13:00 WT 1864m KL 3198m 10 58,43 N 087 00,37 W
14:00 WT 1961m KL 3430m 10 56,40 N 086 58,14 W
14:11 WT 1973m KL 3324m Profilende, hieven DTS **D 18 sm** 10 56,02 N 086 57,70 W
15:00 WT 2196m KL 2444m 10 53,99 N 086 57,48 W

Profil 96 DTS+GI-Gun
16:00 WT 2430m KL 2900m 10 55,07 N 086 59,85 W
16:26 WT 2402m KL 3929m Profilbeginn KüG 312° FüG 3,0 kn 10 55,90 N 087 00,77 W

17:00 WT 2311m KL 4290m 10 56,90 N 087 01,90 W
18:00 WT 2190m KL 4695m 10 59,02 N 087 04,17 W
Wind:NE 5, c 4/8, p, 1009,2 hPa, t 27,0 C, tw 28,6 C, RF 81% Düng 190+070° 8s 2,5 m
19:16 WT 2417m KL 4550m Profilende **D 08 sm** 11 01,62 N 087 06,99 W
19:51 WT 2471m KL 3154m GI-Gun an Deck hieven DTS 11 02,61 N 087 08,18 W
21:00 WT 2690m KL 465m 11 03,77 N 087 11,12 W
21:30 WT 2800m DTS und Depressor an Deck 11 04,35 N 087 12,31 W
21:30 Ende der Stationsarbeiten / SIMRAD-Profilfahrt auf dem Weg nach Caldera
21:37 WT 2800m Posidonia-Antenne Lotschacht eingefahren 11 04,36 N 087 13,00 W

Profil 97 SIMRAD-Vermessungsfahrt
21:37 WT 2800 m KüG 137° VV 11 04,36 N 087 13,00 W
Mi., 06.08.2003
01:21 WT 3006m passieren WP 1 D 39,0 sm 10 33,00 N 086 43,50 W
05:51 WT 2478m ändern Kurs WP 2 D 56,6 sm 09 51,00 N 086 05,00 W
08:06 WT 1192m ändern Kurs WP 3 D 28,0 sm 09 37,00 N 085 40,50 W
09:27 WT ..... m ändern Kurs WP 4 D 18,0 sm 09 29,00 N 085 24,00 W
09:27 Ende der Vermessungsfahrt / Ende der Datenaufzeichnungen der Reise SO 173.1
Anfahrt Caldera / Restdistanz 52 sm

13:24 Ende der Seereise / Caldera Reede 09 55,00 N 084 45,00 W

Appendix E:
Station List
SO173/3 and SO173/4

SO173/3

Date 2003	St.No. SO173/3	Instrument	Begin	Start ACS Program	End ACS Program	End	Duration hh:mm	Lat. Begin	Long. Begin W	Lat. End	Long. End W	Water depth [m]	Remarks	Rec. Gear	Pic. Gear	Responsible	Area	Target Feature
05.09.2003	1	Current Meter			12:00	13:08	12:00	10:17.17	-86.17.89	10:17.17	-86:17.89	1624	deployed during SO173-2, was not switched on	x	x	Mau	Mound Culebra	Mound
05.09.2003	2	OFOS	19:27			19:42	00:15	11.15.54	-87:09.70	11:12.00	-87:11.00	960	tech. Problems at 250m, back to surface, station skipped		x	Sahling	Mound Baula	Mound
05.09.2003	3-1	SIMRAD/PS	21:30				00:00	11:12.00	-87:11.00	11:12.00	-87:10.00	1400	At Scarp below mound Baula			Suess	Mound Baula	Scarp (Slide?)
05.09.2003	3-2	SIMRAD/PS					00:00	11:12.00	-87:10.00	11:08.60	-87:15.00	1400				Suess		Scarp (Slide?)
05.09.2003	3-3	SIMRAD/PS					00:00	11:08.60	-87:15.00	11:05.50	-87:12.00	1400				Suess		Scarp (Slide?)
05.09.2003	3-4	SIMRAD/PS					00:00	11:05.50	-87:12.00	11:07.00	-87:10.60	1400				Suess		Scarp (Slide?)
05.09.2003	3-5	SIMRAD/PS					00:00	11:07.00	-87:10.60	11:12.00	-87:15.60	1400				Suess		Scarp (Slide?)
05.09.2003	3-6	SIMRAD/PS					00:00	11:12.00	-87:15.60	11:18.00	-87:21.50	1400				Suess		Scarp (Slide?)
05.09.2003	3-7	SIMRAD/PS					00:00	11:18.00	-87:21.50	11:17.90	-87:21.50	1400				Suess		Scarp (Slide?)
05.09.2003	3-8	SIMRAD/PS					00:00	11:17.90	-87:21.50	11:08.60	-87:15.00	1400				Suess		Scarp (Slide?)
05.09.2003	3-9	SIMRAD/PS					00:00	11:08.60	-87:15.00	11:07.80	-87:16.00	1400				Suess		Scarp (Slide?)
05.09.2003	3-10	SIMRAD/PS				02:00	04:30	11 07.80	-87:16.00	11:16.00	-87:24.00	1400				Suess		Scarp (Slide?)
06.09.2003	4	OFOS	02:40	03:16	11:55	12:31	09:51	11:12.55	-87:11.22	11:10.44	-87:08.13	1382	3 Videotapes			Sahling	Mound Quetzal Area	Mounds
06.09.2003	5-0	GC-6m	13:20	13:50		14:15	00:55	11:12.44	-87:10.88	11:12.44	-87:10.88	1340	hard ground, no rec. except some carb. clasts in cc		x	Stein	Mound Quetzal	Mound
06.09.2003	5-1	GC-3m	14:51	15:14	15:14	15:50	00:59	11:12.50	-87:10.86	11:12.50	-87:10.86	1334	Recovery 3m, Penetr. 3,48m			Schmidt	Mound Quetzal	Mound
06.09.2003	6-0	GC-6m	16:20	16:45	16:45	17:10	00:50	11:12.34	-87:10.86	11:12 34	-87:10.86	1315	hard ground, no rec. except some carb. clasts in cc		x	Schmidt	Mound Quetzal	Mound
06.09.2003	6-1	GC-6m	17:25	17:49	17:51	18:15	00:50	11:12.26	-87:10.83	11:12.25	-87:10.83	1330	Recovery 4.5m, Penetr. ~6m			Schmidt	Mound Quetzal	Mound
06.09.2003	7	CTD	18:50	19:30		20:28	01:38	11:12.25	-87:10.95	11:12.25	-87:10.99	1358	with SSBC, 4,7,11,19,21 and others need new rubber bands		x	Rehder	Mound Quetzal	Mound
06.09.2003	8	TV-G	20:50	21:33	22:00	22:40	01:50	11:12.32	-87:10.85	11:12.37	-87:10.78	1317	Carbonate Block, 1 Videotape			Suess	Mound Quetzal	Mound
07.09.2003	9	OFOS	01:26	02:00	04:16	04:43	03:15	11:15.69	-87:09.48	11:15.66	-87:09.49	994	1 Videotape, station delayed due to technical problems			Sahling	Mound Baula	Mound
07.09.2003	10	CTD	12:00	12:20	13:20	13:20	01:20	12:00.00	-88:09.0	12:00.00	-88:09.0	1622	1000m CTD, Part of Redox-Transect			Rehder	Slope off Nicaragua	Redox
07.09.2003	11	GC-6m	13:26	13:58	13:59	14:35	01:09	12:00.00	-88:09.01	11:59.99	-88:09.006	1636	recov. 6m, penetr. 8m			Kutterolf	Slope off Nicaragua	Ash Layers
07.09.2003	11-1	GC-12m	15:15	15:43		16:15	01:00	12:00.00	-88:09.00	12:00.00	-88.09.0	1622	recov. 12m, penetr. 12m			Kutterolf	Slope off Nicaragua	Ash Layers
07.09.2003	12	CTD	19:19	19:40	20:40	20:40	01:21	11:28.00	-88:27.00	11:28.00	-88:27.0	4102	1000m CTD, Part of Redox-Transect			Rehder	Incoming Plate off Nicaragua	Redox
07.09.2003	13	GC-12m				23:45	00:00	11:28.00	-88:27.00	11:28.00	-88:27.0	4100	bent at 2m, recovered some consolidated clay clasts		x	Kutterolf	Incoming Plate off Nicaragua	Ash Layers
08.09.2003	13-1	GC-9m	00:50	02:12	02:12	03:26	02:36	11:26.37	-88:28.00	11:26.37	-88:28.00	4134	Recovery 6m, Penetration ~8m			Kutterolf	Incoming Plate off Nicaragua	Ash Layers
08.09.2003	14	CTD	10:36		11:52	11:52	01:13	11:04:00	-89:18.00	11:04 00	-89:18.00	3450				Rehder	Incoming Plate off Nicaragua	Redox
08.09.2003	15	GC-9m	16:30	17:39		18:40	02:10	10:43.16	-88:54.09	10:43.14	-88.54.15	3288	recov. 6m, penetr. 10m			Kutterolf	Incoming Plate off Nicaragua	Ash Layers
08.09.2003	16	CTD	19:03		20:10	20:10	01:07	10:45 00	-88:53.00	10:45.00	-88:53.00	3200				Rehder	Incoming Plate off Nicaragua	Redox
09.09.2003	17	GC-9m	01:35	02:31		03:25	01:50	11:15.79	-88:12.60	11:15.79	-88:12.60	3216	recov. 2.3m, penetr. 9m			Kutterolf	Incoming Plate off Nicaragua	Ash Layers
09.09.2003	18	GC-9m	12:30	12:53	12:53	13:15	00:45	11:36.00	-87:36.00	11:36.00	-87:36.00	1606	recov. 8.5m, penetr. 9m			Kutterolf	Slope off Nicaragua	Ash Layers
09.09.2003	19	OFOS	17:02	17:31	20:03	20:45	03:43	11:12.10	-87:09.40	11:12.45	-87:09.348	1255	1 Videotape, 190 fotos			Sahling	Mound Iguana	Mound
09.09.2003	20	TV-MUC	21:29			22:00	00:31	11:12.20	-87:9.437	11:12.20	-87:09.44	1236	technical failure at 150m		x	Suess	Mound Iguana	Mound
09.09.2003	21	OFOS	23:26	00:01	03:07	03:49	04:23	11:16.13	-87:15.42	11:16.81	-87:15.49	1569	1 Videotape, 4 Profiles			Sahling	Mound Carablanca	Mound
10.09.2003	22	CTD	05:15		07:50	07:50	02:35	11:12.200	-87:09.30	11:12.200	-87:09.30	1230				Rehder	Mound Iguana	Mound
10.09.2003	23	CTD	09:10		11:05	11:05	01:55	11:07.70	-87:11.505	11:07 70	-87:11.505	2270				Rehder	off Nicaragua	Slide
10.09.2003	24	OFOS	12:32	13:13	14:38	15:17	02:45	10:59.90	-87:00.60	11:00.55	-87:00.46	1749	1 Videotape, 1 Profile			Sahling	Mound Morpho	Mound
10.09.2003	25	GC-6m	16:15	16:30	16:32	16:46	00:34	11:08.30	-87:02.80	11:08.30	-87:02.80	1229	Recov. 2.8, Penetr. 5			Schmidt	off Nicaragua	Canyon
10.09.2003	26	TV-MUC	18:20	19:07	20:00	20:45	02:25	11:16.42	-87:15.31	11:16.38	-87:15.12	1435	mit Tiefseepumpe, 4 Cores			Suess	Mound Carablanca	Mound
10.09.2003	27	TV-G	21:42	22:14	22:35	23:35	01:53	11:16.44	-87:15.25	11:16.46	-87:15.20	1432	Carbonate Block, 1 Videotape			Liebetrau	Mound Carablanca	Mound
11.09.2003	28	TV-MUC	00:34	01:14	01:56	02:58	02:22	11:16.48	-87:15.26	11:16.42	-87:15.29	1425	+Tiefsee Pumpe			Suess	Mound Carablanca	Mound
11.09.2003	29	TV-MUC	02:42	03:31	04:36	05:35	02:53	11:16.46	-87:15.30	11:16.44	-87:15.30	1425	+Tiefsee Pumpe			Suess	Mound Carablanca	Mound
11.09.2003	30	BWS	06:05	07:16	07:50	08:50	02:45	11:16.43	-87:15.24	11:16.43	-87:15.24	1426	stopped at 1453m, didn't release		x	Rehder	Mound Carablanca	Mound
11.09.2003	31	CTD	08:56		09:43	09:43	00:47	11:16.43	-87:15.24	11:16.43	-87:15.24	1428				Rehder	Mound Carablanca	Mound
11.09.2003	32	BWS	10:55	11:45	12:23	13:23	02:28	11:16.43	-87:15.24	11:16.43	-87:15.24	1430				Rehder	Mound Carablanca	Mound
11.09.2003	33	GC-6m	13:41	14:08	14:08	14:30	00:49	11:16.33	-87:15.11	11:16.33	-87:15.11	1479	recov. 0.8m, penetr. 1.0m, Eastern slope of Carabalanca			Schmidt	Mound Carablanca	Mound Transect
11.09.2003	34	GC-6m	15:00	15:21	15:22	15:50	00:50	11:16.42	-87:15.32	11:16 42	-87:15.32	1430	recov. 4.5m, penetr. 6.0m, Eastern mid of Carabalanca			Schmidt	Mound Carablanca	Mound Transect
11.09.2003	35	GC-6m	16:25	16:47	16:48	17:35	01:10	11:16.51	-87:15.37	11:16.51	-87:15.37	1452	recov. 4.5m, penetr. 6.0m, northwest slope of Carabalanc			Schmidt	Mound Carablanca	Mound Transect
11.09.2003	36	GC-3m	17:40	18:00	18:00	18:30	00:50	11:18.41	-87:15.23	11:16.41	-87:15.23	1438	recov. 3m, penetr. 3m			Schmidt	Mound Carablanca	Mound Transect

Date 2003	Station No.	Instrument	Time [UTC]	Start Bot. Procedure	End Bot. Procedure	Start Ascent	Duration [hh:mm]	Latitude N°	Longitude W°	Latitude N°	Longitude W°	Water depth [m]	Recovery Remarks	Rec. Stat.	Fail. Stat.	Supervisor	Area	Target Feature
11.09.2003	37	TV-G	21:17	21:54	22:21	23:10	01:53	11:00.17	-87:00.56	11:00.24	-87:00.47	1679	big piece of carbonate			Liebetrau	Mound Morpho	Mound
11.09.2003	38	TV-MUC	23:48	00:28	00:39	01:52	02:04	11:00.15	-87:00.54	11:00.16	-87:00.55	1670				Suess	Mound Morpho	Mound
12.09.2003	39	TV-MUC	02:10	02:45	04:02	05:22	03:11	11:00.11	-87:00.68	11:00.11	-87:00.60	1669				Suess	Mound Morpho	Mound
12.09.2003	40	GC-8m	14:00	14:31	14:31	15:10	01:10	10:00.47	-86:11.46	10:00.47	86:11.46	2283	recov. 6m+Bomb			Gerbe-Schönberg	Mound 10	Mound
12.09.2003	41	Mooring	17:10				00:00	10:17.16	-86:17.87			1604				Mau	Mound Culebra	Mound
12.09.2003	42	Mooring	18:41				00:00	10:18.86	-86:18.82			1638				Mau	Mound Culebra	Mound
12.09.2003	43	CTD	19:22	20:01	21:04	21:04	01:42	10:17.61	-86:17.83	10:17.61	-86:17.83	1590				Rehder	Mound Culebra	Mound
12.09.2003	44	CTD	22:30	23:10	00:00	00:00	01:30	10:18.31	-86:18.85	10:18.31	-86:18.85	1644				Rehder	Mound Culebra	Mound
13.09.2003	45	OFOS	00:45	01:01	02:20	02:40	01:54	10:18.95	-86:11.44	10:18.82	-86:10.47	635	1 Video, no evidence for seeps			Sahling	Mound Culebra Area	Fault
13.09.2003	46	OFOS	03:50	04:27	11:38	12:18	08:28	10:15.65	-86:17.22	10:15.92	-86:16.41	1592	2 Videos, calmfields at fault, very small area			Sahling	Mound Culebra Area	Fault
13.09.2003	47	CTD	12:46	14:10	15:00	15:00	02:14	10:17.35	-86:18.55	10:17.35	-86:18.55	1660				Rehder	Mound Culebra	Mound
13.09.2003	48	CTD	16:37	17:10	18:00	18:00	02:23	10:18.45	-86:18.1	10:18.45	-86:18.1	1602				Rehder	Mound Culebra	Mound
13.09.2003	49	GC-9m	17:45	18:18		18:45	01:00	10:15.941	-86:16.605	10:15.941	-86:16.605	1530	penetration 10m, recov. 9m			Schmidt	Mound Culebra Area	Fault
13.09.2003	50	OFOS	19:38	20:23	21:17	22:13	02:35	10:16.004	-86:16.168	10:17.373	-86:16.349	1529				Sahling	Mound Culebra	Mound
13.09.2003	51	GC-6m	22:48	23:09		23:40	00:54	10:17.66	-86:18.32	10:17.66	-86:18.32	1617	recov. 6m, Penetr. 6m, basalt clasts			Schmidt	Mound Culebra	Mound
14.09.2003	52	TV-MUC	00:30	01:09	01:21	02:20	01:50	10:18.09	-86:18.35	10:18.00	-86:18.32	1531	+ Deep Sea Pump			Suess	Mound Culebra	Mound
14.09.2003	52-1	TV-MUC	03:05	03:42	04:02	04:51	01:45	10:18.18	-86:18.42	10:17.91	-86:18.32	1522	+ Deep Sea Pump			Suess	Mound Culebra	Mound
14.09.2003	53	CTD	05:30	06:10	07:07		-05:30	10:17.51	-86:18.14	10:17.51	-86:18.14	1616	18 bottles didnt release			Rehder	Mound Culebra	Mound
14.09.2003	54	CTD	08:54		10:42		-08:54	10:18.20	-86:16.84	10:18.20	-86:18.84	1682	bottle 18 didnt release			Rehder	Mound Culebra	Mound
14.09.2003	55	Mooring			11:58	12:50	12:50			10:17.22	-86:18.40	1659	recovered from Station 41, recorded ok	x		Mau	Mound Culebra	Mound
14.09.2003	56	Mooring			13:06	13:51	13:51			10:18.47	-86:18.54	1632	recovered from Station 42, recorded ok	x		Mau	Mound Culebra	Mound
15.09.2003	57	OFOS	02:08	02:22	04:21	04:36	02:27	9:12.15	-84:39.97	9:11.54	-84:39.34	614	surveyed headwall of BGR-slide			Sahling	BGR-Slide	Slide
15.09.2003	58	CTD	11:00	11:26	11:58	12:08	01:08	9:11.65	-84:40.00	9:11.65	-84:40.00	625				Rehder	BGR-Slide	Slide
15.09.2003	59	GC-6m	12:15	12:28	12:28	12:45	00:30	9:11.76	-84:40.00	9:11.76	-84:40.00	559	rec. 3.5, penetr., 4m			Schmidt	BGR-Slide	Slide
15.09.2003	59-1	GC-6m	13:00	13:10	13:10	13:25	00:25	9:11.834	-84:39.867	9:11.834	-84:39.867	554	rec. 6m, penetr. 6m			Schmidt	BGR-Slide	Slide
15.09.2003	60	CTD	14:10	15:17			-14:10	9:11.70	-84:37.26	9:11.70	-84:37.26	660				Rehder	GEOMAR-Slide	Slide
15.09.2003	61	GC-6m	15:21	15:46	15:46	16:01	00:33	9:11.47	-84:37.24	9:11.47	-84:37.24	662	6m recov, 7m penetr, 1m in bomb			Schmidt	GEOMAR-Slide	Slide
15.09.2003	61-1	GC-6m	16:25	16:43	16:43	17:08	00:47	9:11.798	-84:37.243	9:11.798	-84:37.243	654	recov 5.6m			Schmidt	GEOMAR-Slide	Slide
15.09.2003	62	OFOS	20:32	20:45	22:21	22:36	02:00	8:48.72	-84:11.972	8:48.13	-84:13.44	303	609 fotos			Sahling	Quepos Slide	Slide
15.09.2003	63	TV-MUC	[redacted]	23:31	23:48	00:08	-23:08	8:51.11	-84:13.08	8:51.14	-84:13.03	405	6 cores			Suess	Quepos Slide	Slide
16.09.2003	64	TV-MUC	00:35	00:52	01:01		-00:35	8:51.08	-84:13.08	8:51.12	-84:13.04	407	6 cores			Suess	Quepos Slide	Slide
16.09.2003	65	BWS	[redacted]	02:27	02:45	03:12	01:10	8:51.10	-84:13.04	8:51.10	-84:13.04	403				Rehder	Quepos Slide	Slide
16.09.2003	66	TV-MUC	03:35	03:51	04:05	04:30	00:54	8:51.101	-84:13.09	8:51.16	-84:13.00	404	6 cores			Suess	Quepos Slide	Slide
16.09.2003	67	BWS	05:13	05:46	06:17	05:46	01:35	8:48.20	-84:13.80	8:48.20	-84:13.80	770				Rehder	Quepos Slide	Slide
16.09.2003	68	Mooring	12:03	12:03			-12:03	9:06.96	-84:50.74			1877	deployment of mooring			Mau	Jaco Scarp	Scarp
16.09.2003	69	Mooring	12:38	12:03			-12:38	9:05.64	-84:49.80			2036	deployment of mooring			Mau	Jaco Scarp	Scarp
End of SO173-3																		

Date 2003	Station	Gear	Time [UTC]	Time [UTC]	Time [UTC]	Time [UTC]	Latitude [°N]	Longitude [°W]	Depth [m]	Comment					Area	Remarks
Start of SO173-4																
18.09.2003	70	OFOS	13:55	14:08	17:03	17:12	8:51.19	-84:13.12	8:51.16	-84:13.35	405	bacteria mats		Sahling	Quepos Slide	Slide
18.09.2003	71	TV-MUC	16:01	16:15	18:26	18:42	8:51.23	-84:13.13	8:51.196	-84:13.19	398	6 cores		Suess	Quepos Slide	Slide
18.09.2003	72	CTD	18:56	19:19	19:54	20:03	8:51.01	-84:13.16	8:51.20	-84:13.18	402			Mau	Quepos Slide	Slide
18.09.2003	73	TV-MUC	20:00	20:28	20:39	20:48	8:51.084	-84:13.122	8:51.175	-84:13.126	404	6 cores		Suess	Quepos Slide	Slide
18.09.2003	74	GC	21:31	21:41	22:00	00:26	8:51.19	-84:13.15	8:51.19	-84:13.15	405	penetr. 6m, recov. 5.5m		Schmidt	Quepos Slide	Slide
18.09.2003	75	BWS	22:10	22:40	23:06	23:24	8:51.14	-84:13.19	8:51.17	-84:13.19	398			Mienke	Quepos Slide	Slide
19.09.2003	76	CTD	04:45	05:30	06:56	06:56	09:14	-84:50.6	9:0.89	-84:50.8	1953			Mau	Jaco Scarp	Scarp
19.09.2003	77	OFOS	13:51	14:29	18:41	19:54	9:40.06	-85:52.51	8:39.16	-85:53.22	1947	2 Videos, Survey of Fault		Sahling	Mound Jaguar	Mound
19.09.2003	78	TV-MUC	22:21	23:17	23:39	00:28	9:00.54	10:00.54	8:59.11.32	10:00.42	2264	4-barrel MUC, recovered 4-cores		Suess	Mound 10	Mound
20.09.2003	79	TV-MUC	01:19	02:17	02:21	03:44	09:00.48	10:00.55	8:59.11.47	10:00.55	2276	coil voltage, intermitly sphere imploding	x	Suess	Mound 10	Mound
20.09.2003	80	OFOS	06:19	06:04	11:33	12:24	09:00	10:00.59	8:59.11.83	10:0.953	2421	Mapping of Mound 10		Sahling	Mound 10	Mound
20.04.2003	81	GC	13:10	13:50	14:30	17:00	01:19	10:00.51	8:59.11.39	10:00.51	2271	Recov. 2m, penetr.3m		Schmidt	Mound 10	Mound
20.09.2003	82	LORA	16:32	16:33			-16:32	10:17.106	8:59.17.86		1610	deployment of LOng RAnger		Linke	Mound Culebra	Mound
20.09.2003	83	CTD	17:45	18:28	18:45	19:26	01:41	10:18.07	8:59.17.76	10:18.02	1550			Mau	Mound Culebra	Mound
20.09.2003	84	CTD	20:50	21:26	21:40	22:26	01:35	10:17.90	8:59.18.29	10:17.90	1514	no transponder		Mau	Mound Culebra	Mound
21.09.2003	85	BC-L	00:56	00:56	02:37	03:26	03:24	10:18.37	8:59.18.54	10:17.91	1603	premature loss of weight	x	Linke	Mound Culebra	Mound
21.09.2003	86	CTD	04:01	04:45	05:07	05:07	01:06	10:17.99	8:59.18.30	10:17.99	1512	no transponder		Mau	Mound Culebra	Mound
21.09.2003	87	GC-8m	13:52	14:20	14:45	17:00	00:58	10:17.83	8:59.18.45	10:17.83	1524	recov. 2m, penetr. 3m		Schmidt	Mound Culebra	Mound
21.09.2003	88	BC-L	16:00	17:03	17:26	18:20	02:15	10:18.112	8:59.18.404	10:18.014	1616	Loss of one weight	x	Linke	Mound Culebra	Mound
21.09.2003	84-1	BC-L	19:21	20:14	20:15	20:56	01:34	10:18.14	8:59.18.43	10:18.14	1634	Loss of one weight	x	Linke	Mound Culebra	Mound
21.09.2003	89	LORA			14:55	15:30	15:30	10:17.108	8:59.17.99	10:17.108	1610	recovered from station 62	x	Linke	Mound Culebra	Mound
21.09.2003	90	TV-G	23:40	00:21	03:07	03:47	04:00	10:00.40	8:59.11.42	10:00.31	2274	1 Video, long of mud		Liebetrau	Mound 10	Mound
22.09.2003	91	BWS	04:58	06:16	06:49	08:03	03:06	10:00.50	8:59.11.41	10:00.50	2287			Mienke	Mound 10	Mound
22.09.2003	92	CTD	08:25	09:10	09:36	10:33	00:08	10:00.45	8:59.11.42	10:00.45	2290			Mau	Mound 10	Mound
22.09.2003	93	CTD	12:20	12:54	13:17	13:17	00:57	10:18.19	8:59.18.38	10:18.17	1632			Mau	Mound Culebra	Mound
22.09.2003	94	TV-MUC	14:13	14:36	15:09	15:19	01:06	10:18.126	8:59.18.441	10:17.886	1644	little recovery		Suess	Mound Culebra	Mound
22.09.2003	95	TV-MUC	16:58	17:35	18:26	18:17	02:19	10:18.024	8:59.18.361	10:17.901	1565			Suess	Mound Culebra	Mound
22.09.2003	96	TV-MUC	19:54	20:33	21:05	21:55	02:01	10:17.886	8:59.18.492	10:17.967	1554			Suess	Mound Culebra	Mound
22.09.2003	97	GC-8m	23:14	23:33	23:33	00:05	00:56	10:15.93	8:59.16.61	10:15.93	1531	penetr. 8m, recov. 8.5m		Schmidt	Mound Culebra Area	Fault
23.09.2003	98	GC-8m	00:36	00:56	00:56	01:20	00:45	10:17.79	8:59.18.59	10:17.79	1567	penetr. 7m, recov. 5m		Schmidt	Mound Culebra	Mound
23.09.2003	99	CTD	11:30	12:32	13:26	13:46	02:16	09:05.39	8:59.49.62	09:05.39	1900			Mau	Jaco Scarp	Scarp
23.09.2003	100	Mooring	14:05	14:05	14:05	14:55	00:51	09:6.69	8:59.50.47	09:6.69	1977		x	Mau	Jaco Scarp	Scarp
23.09.2003	101	Mooring	15:15	15:15	15:15	16:05	00:50	09:6.54	8:59.49.72	09:6.54	1977		x	Mau	Jaco Scarp	Scarp
23.09.2003	102	BC-L	19:38	19:50	20:05	20:15	00:40	8:51.2509	8:59.13.178	8:51.238	391			Linke	Quepos Slide	Slide
23.09.2003	103	BWS	20:31	20:54	21:14	21:14	01:10	8:51.18	8:59.13.04	8:51.18	401			Mienke	Quepos Slide	Slide
24.09.2003	104	Mooring	00:02	00:02	00:02	00:02	00:01	8:55.616	8:59.18.405	8:56.07	1021			Mau	Mound 12	Mound
24.09.2003	105	LORA	00:55	00:55	00:55	00:55	00:00	8:55.616	8:59.18.405	8:55.616	1023			Linke	Mound 12	Mound
24.09.2003	106	CTD	01:30	01:58	02:59	02:59	01:22	8:56.85	8:59.18.60	8:55.90	953			Schollen	Mound 12	Mound
24.09.2003	107	OFOS	03:44	04:08	11:50	12:18	06:31	8:56.04	8:59.18.27	8:56.24	896			Sahling	Mound 11	Mound
24.09.2003	108	FLUFO	22:06	22:24	22:26	22:45	00:40	8:51.25	8:59.13.207	8:51.255	402			Linke	Quepos Slide	Slide
24.09.2003	109	BC-L	22:45	22:45	22:45	23:05	00:20	8:51.2509	8:59.13.178	8:51.238	391	recovered from station 102	x	Linke	Quepos Slide	Slide
24.09.2003	110	GC-8m	23:57	00:10	00:10	00:28	00:56	8:55.78	8:59.18.78	8:55.78	1003	no recovery	x	Schmidt	Mound 12	Mound
25.09.2003	110-1	GC-8m	00:36	00:46	00:46	01:10	00:34	8:56.74	8:59.18.81	8:56.74	1008	recov. 1.4m, penetr. 2m		Schmidt	Mound 12	Mound
25.09.2003	111	CTD	01:28	01:54	02:11	02:35	01:07	8:56.03	8:59.18.82	8:56.15	1003			Schollen	Mound 12	Mound
25.09.2003	112	BWS	03:45	04:36	05:01	05:42	01:58	8:56.74	8:59.18.81	8:56.74	1011			Mienke	Mound 12	Mound
25.09.2003	113	OFOS	06:21	06:41	07:55	07:55	01:34	8:57.77	8:59.20.28	8:57.32	1026			Sahling	Canon NW of Mound 12	Cann
25.09.2003	114	OFOS	08:52	09:10	11:19	11:43	02:51	8:58.65	8:59.17.85	8:58.117	855			Sahling	Hounds Pulga and Luciemaja	Mound
25.09.2003	115	GC-8m	12:29	12:36	13:00	13:00	00:37	8:55.68	8:59.18.62	8:55.68	1008	recov. 6m, penetr. 7m		Schmidt	Mound 12	Mound

SO173/4 Station list

			Time (UTC)					Begin / on position		End / off position						
Date 2003	Station	Instrument	Start	Start bot.	End bot.	End	Duration	Latitude N	Longitude W	Latitude N	Longitude W	Water depth (m)	Recovery Remarks	Rec Stat.	Fail. Stat.	Supervisor	Area	Target Feature
25.09.2003	116	BC-L	15:04	15:04	15:10	15:38	00:34	8:55.686	-84:18.801	8:55.692	-84:18.797	1004				Linke	Mound 12	Mound
25.09.2003	117	GC-6m	16:06	16:25	16:25	16:40	00:34	8:56.30	-84:18.88	8:56.30	-84:18.88	986	penetr. 7m, recov. 6.35m			Schmidt	Mound 12	Mound
25.09.2003	118	TV-MUC	17:36	18:05	18:10	18:45	01:08	8:55.667	-84:18.846	8:55.69	-84:18.84	1018				Suess	Mound 12	Mound
25.09.2003	119	CTD	19:00	19:27	20:24	20:51	01:51	8:55.64	-84:18.47	8:55.64	-84:18.47	1028				Scholten	Mound 12	Mound
25.09.2003	120	TV-MUC	21:12	21:39	22:01	22:01	00:49	8:55.89	-84:18.97	8:55.73	-84:18.84	1011				Suess	Mound 12	Mound
25.09.2003	121	FLUFO	23:45	23:45	00:05	00:05	00:20	8:51.25	-84:13.207	8:51.255	-84:13.195	402	Recovery from Station 108	x		Linke	Quepos Slide	Slide
26.09.2003	122	GC-6m	03:10	03:15	03:15	03:30	00:20	9:11.65	-84:39.10	9:11.65	-84:39.10	567	recov. 6m, penetr. 7m			Schmidt	BGR-Slide	Slide
26.09.2003	123	CTD	06:55	07:15	07:15	07:38	00:43	9:20.05	-85:17.17	9:20.05	-85:17.17	592				Mau	Rio Bongo Scarp	Scarp
26.09.2003	124	CTD	11:44	12:20	12:46	13:18	01:34	8:57.47	-84:38.99	8:57.47	-84:38.99	1618				Mau	Parrita Scarp	Scarp
26.09.2003	125	CTD	15:11	15:27	16:10	16:34	01:23	8:55.46	-84:18.64	8:55.46	-84:18.64	1041				Mau	Mound 12	Mound
26.09.2003	126	BC-L	16:40	16:42	16:42	17:13	00:33	8:55.66	-84:18.81	8:55.66	-84:18.81	1004	recovery from station 116	x		Linke	Mound 12	Mound
26.09.2003	127	TV-MUC	18:15	18:45	19:40	20:20	02:05	8:55.31	-84:18.22	8:55.32	-84:18.25	1012	4 cores with bact. Mats, degassing			Suess	Mound 11	Mound
26.09.2003	128	TV-G	20:52	21:12	21:28	21:28	00:36	8:55.343	-84:18.175	8:55.32	-84:18.24	1013	grabbed next to bacterial mat			Liebetrau	Mound 11	Mound
26.09.2003	129	FLUFO	23:20	23:50	00:39	01:07	-22:13	8:55.676	-84:18.834	8:55.648	-84:18.816	1021	no SSBL available			Linke	Mound 12	Mound
27.09.2003	130	BC-L	01:40	02:16	03:11	03:39	01:59	8:55.44	-84:18.006	8:55.3506	-84:18.226	1010	Bacterial Mat			Linke	Mound 11	Mound
27.09.2003	131	CTD	04:03	04:32	05:00	05:21	01:18	8:55.85	-84:18.97	8:55.81	-84:19.04	1018				Mau	Mound 12	Mound
27.09.2003	132	Mooring	14:34	14:34	14:34	15:17	00:43	8:55.78	-84:19.17	8:55.71	-84:18.66	1028	recovery from station 104	x		Mau	Mound 12	Mound
27.09.2003	133	LORA	15:22	15:22	15:22	15:58	00:33	8:55.606	-84:18.562	8:55.606	-84:18.562	1023	recovery from station 105	x		Linke	Mound 12	Mound
27.09.2003	134	FLUFO	16:07	16:07	16:07	16:40	00:33	8:55.515	-84:18.761	8:55.515	-84:18.767	1021	recovery from station 129	x		Linke	Mound 12	Mound
27.09.2003	135	GC-6m	20:27	20:39	20:39	20:58	00:31	8:55.70	-84:18.81	8:55.70	-84:18.81	1015	no recovery		x	Schmidt	Mound 12	Mound
27.09.2003	135-1	GC-6m	21:08	21:22	21:22	21:45	00:37	8:55.69	-84:18.81	8:55.69	-84:18.81	1015	penetration 6.5m, recovery 6m, last section with gas hydrates			Schmidt	Mound 12	Mound
27.09.2003	136	BC-L	22:03	22:03	22:45	22:45	00:42	8:54.97	-84:18.17	8:54.97	-84:18.17	1010	recovery from station 130		x	Linke	Mound 11	Mound
End of SO 173/4																		

CTD (Conductivity temperature depth)
TV-MUC (TV-Multicorer)
GC (Gravity Corer)
PC (Piston Corer)
TV-G (TV-Grab sampler)
OFOS (Ocean floor observation system)
VESP-L (Vent Lander)
BC (Benthic Chamber lander)
BWS (Bottom Water Sampler)
PS (Parasound)
ISP (In Situ Pump)
LORA (Long Ranger)
FLUFO (Fluid Flux Sampler)

Appendix F: Core Photography

ATTENTION

Appendix F is not included with this report. It can be downloaded and printed from the SFB574 website at http://www.sfb574.geomar.de /downloads/reports/so173/27_appendix_f.pdf

Appendix G:
Core Descriptions

ATTENTION

Appendix G is not included with this report. It can be downloaded and printed from the SFB574 website at http://www.sfb574.geomar.de /downloads/reports/so173/28_appendix_g.pdf

Appendix H: Physical Properties

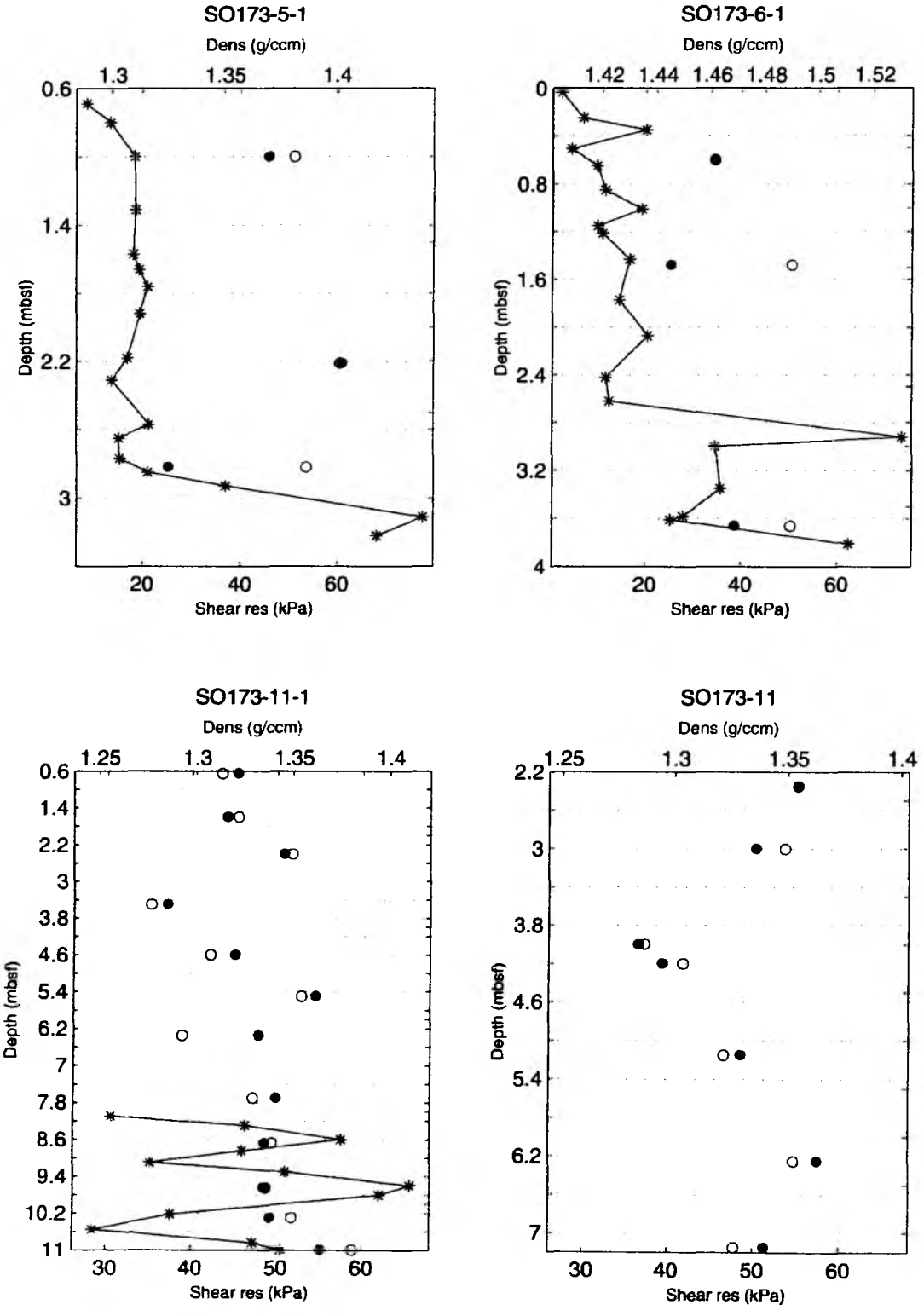

* Undrained shear resistance
● Volumetric wet bulk density
○ Recalculated, grain density based, wet bulk density

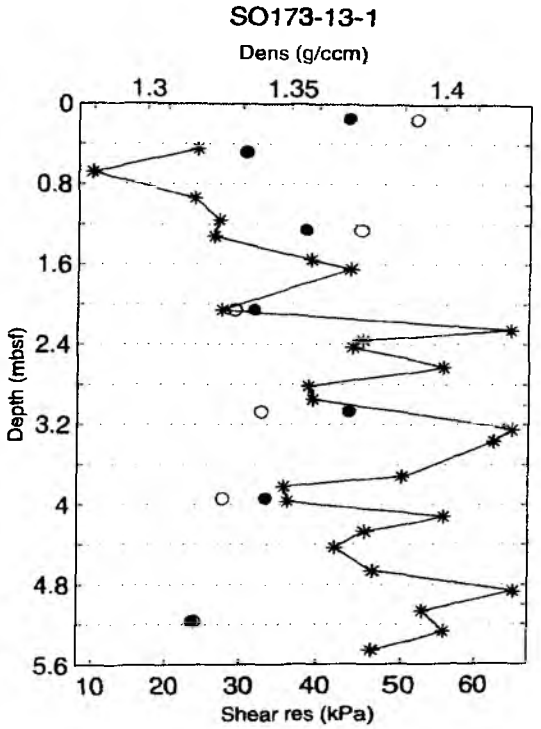

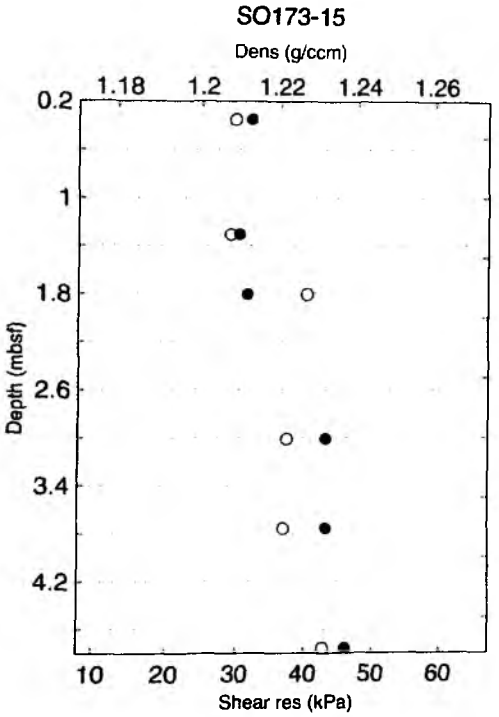

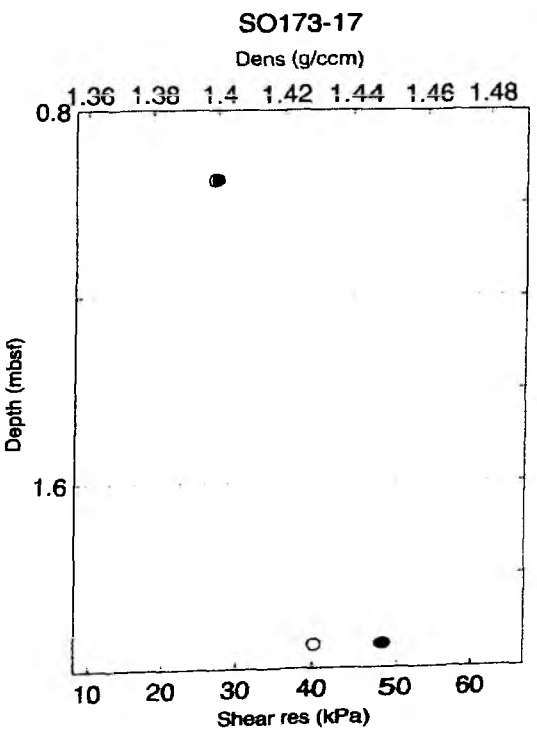

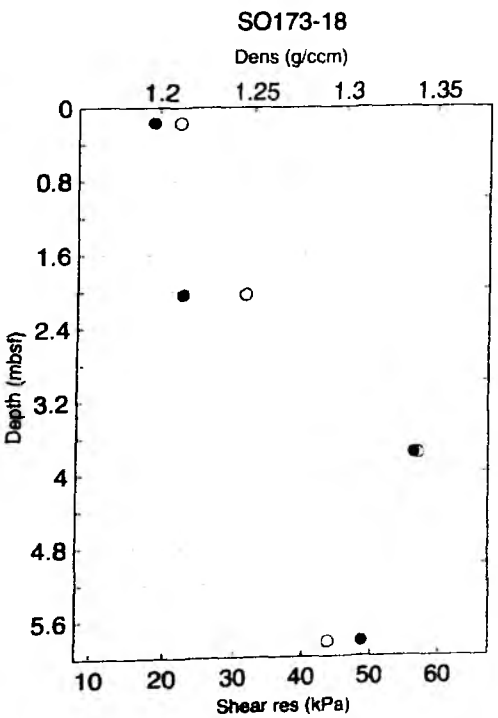

* Undrained shear resistance
● Volumetric wet bulk density
○ Recalculated, grain density based, wet bulk density

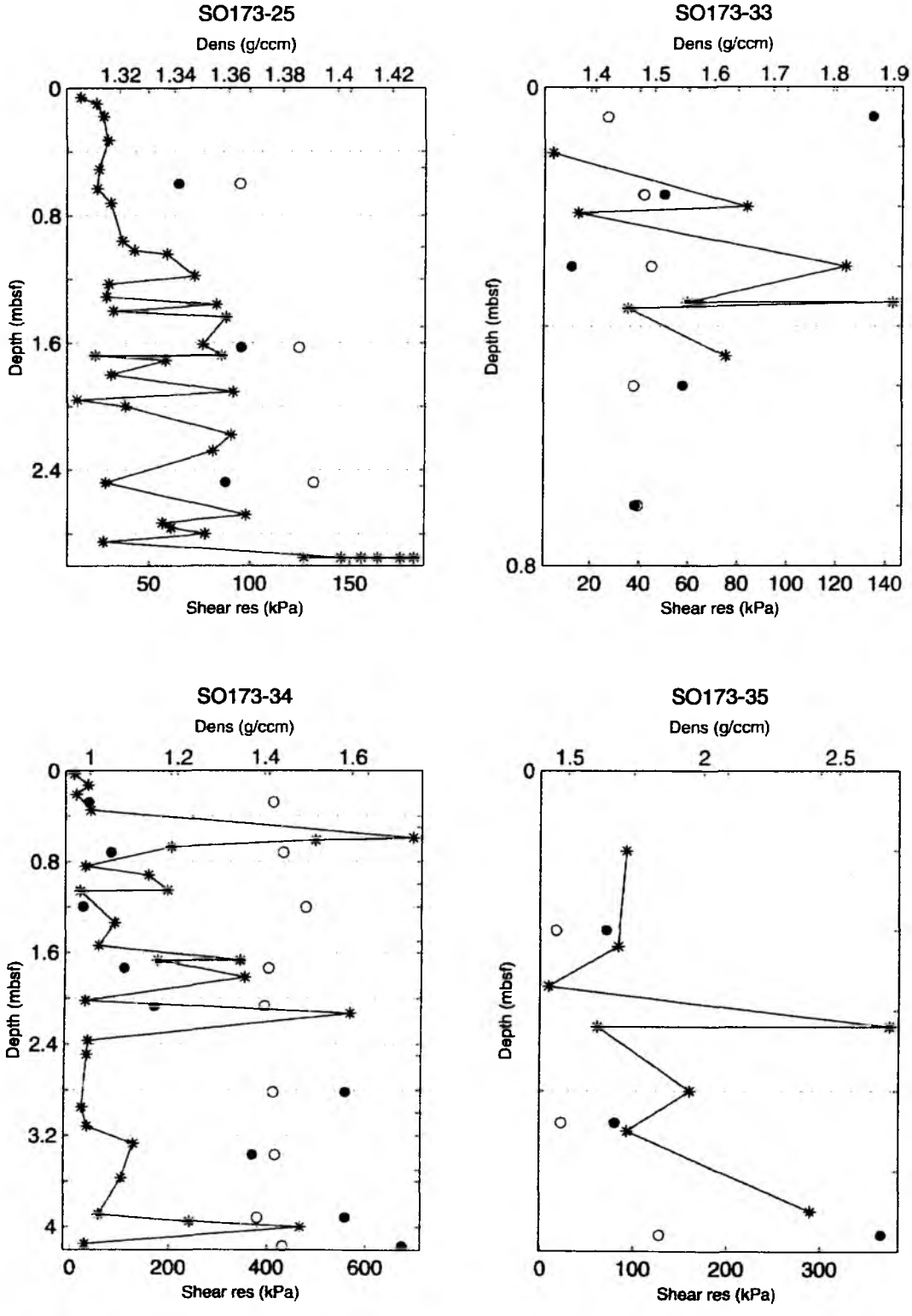

* Undrained shear resistance
• Volumetric wet bulk density
○ Recalculated, grain density based, wet bulk density

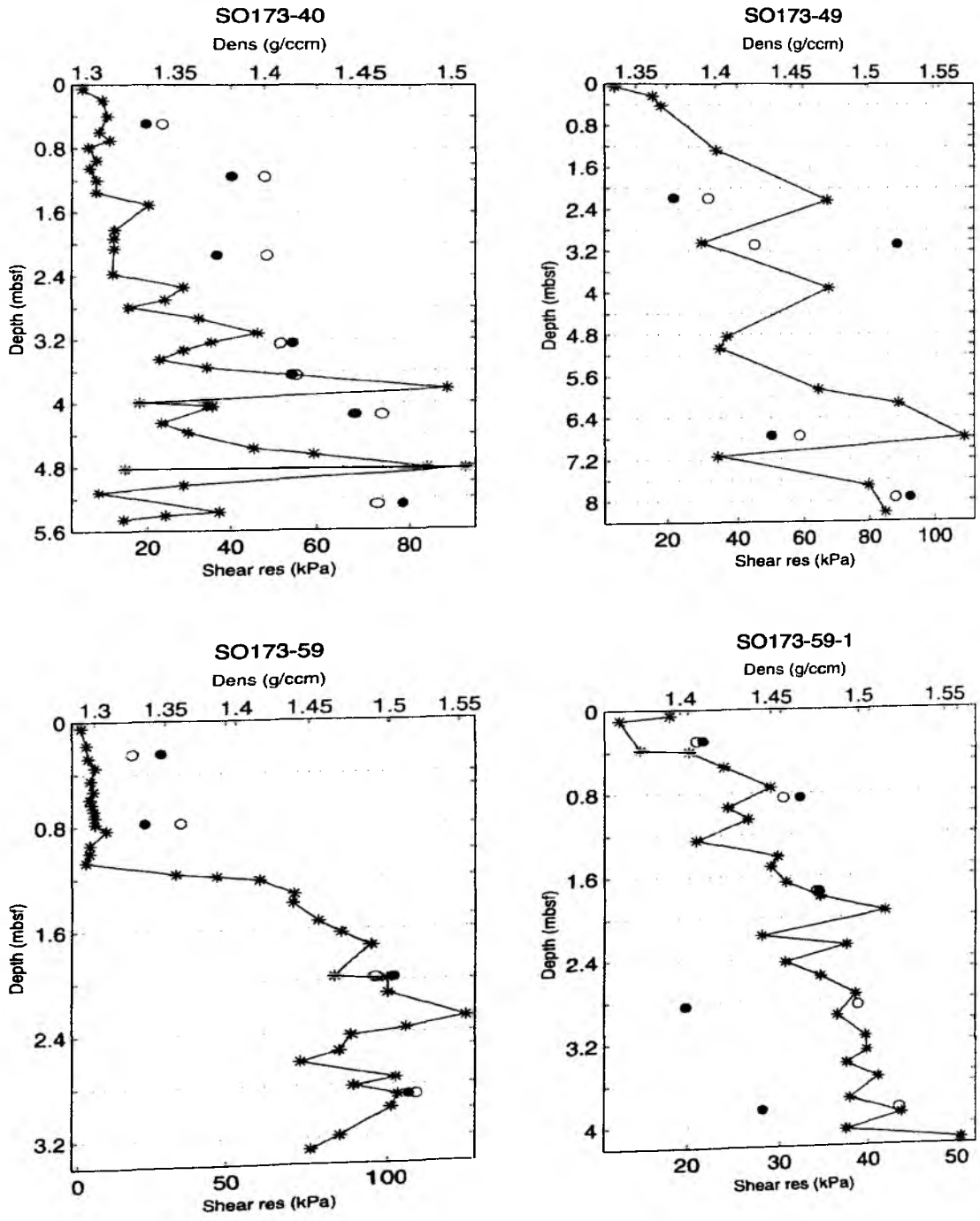

* Undrained shear resistance
● Volumetric wet bulk density
○ Recalculated, grain density based, wet bulk density

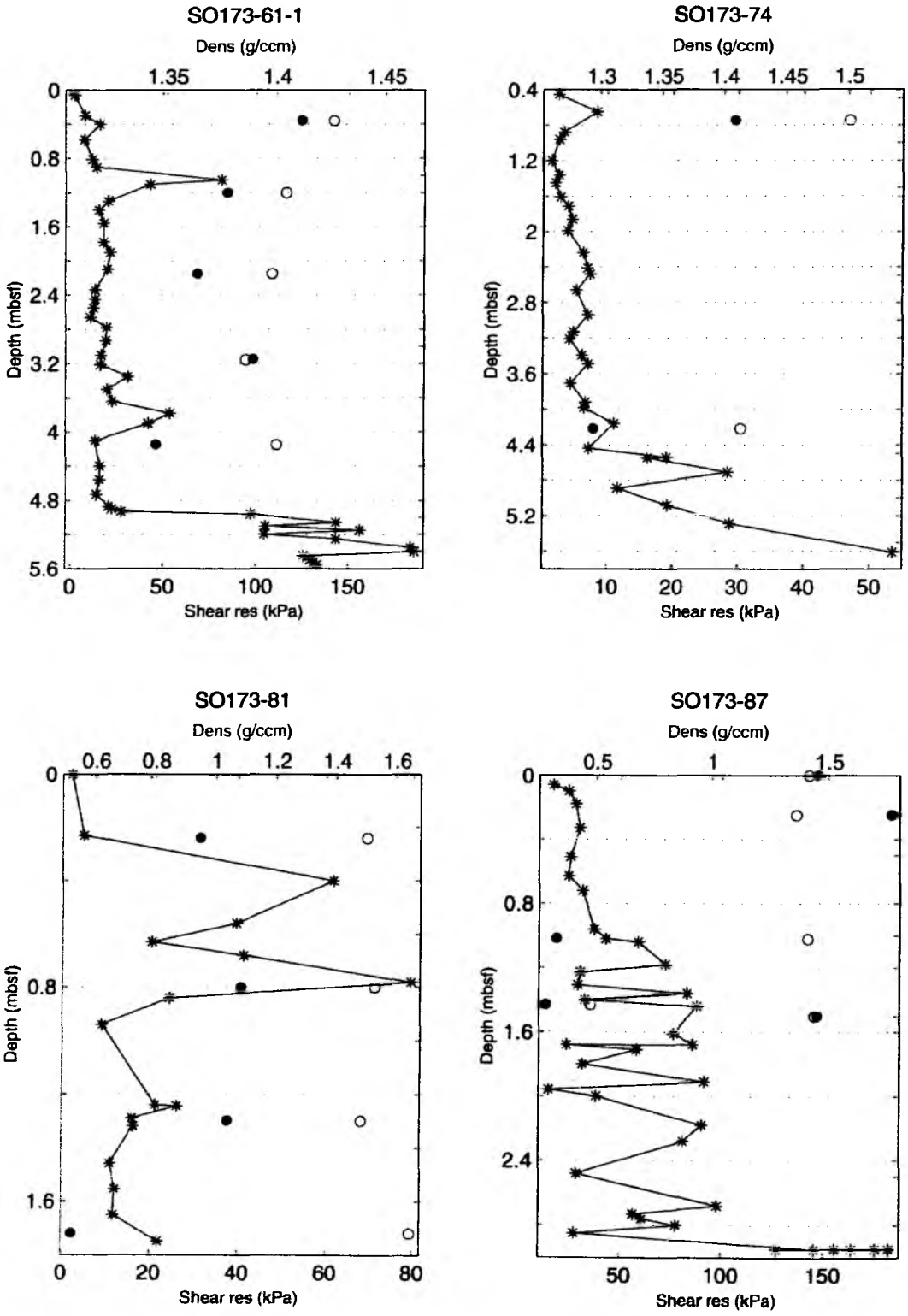

* Undrained shear resistance
• Volumetric wet bulk density
○ Recalculated, grain density based, wet bulk density

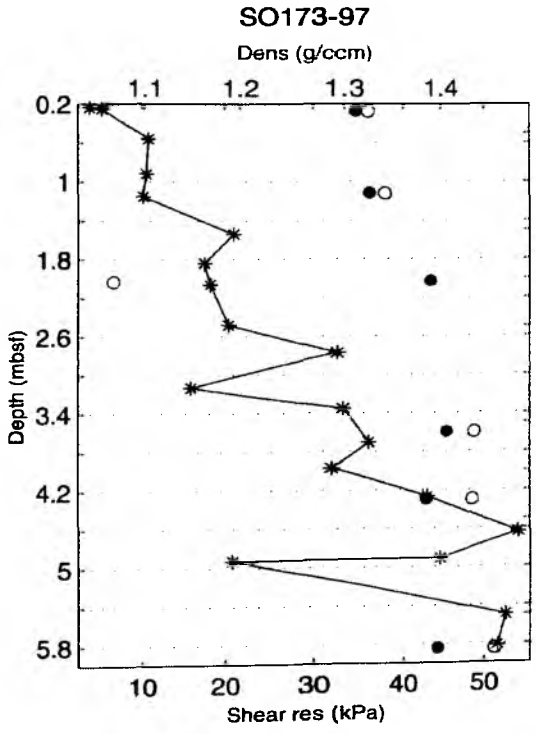

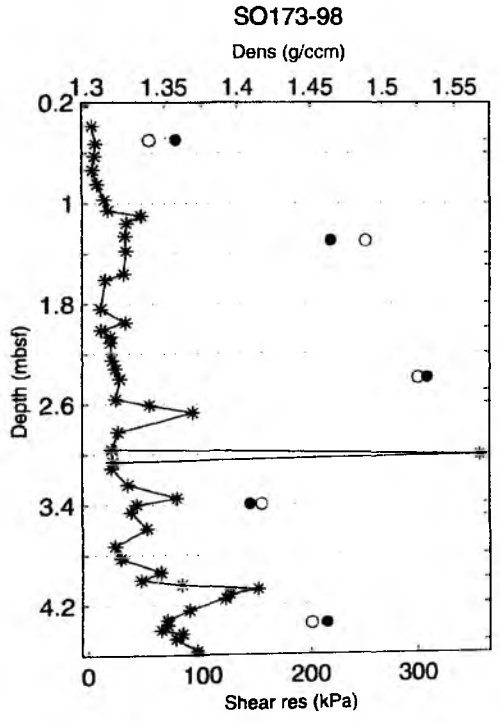

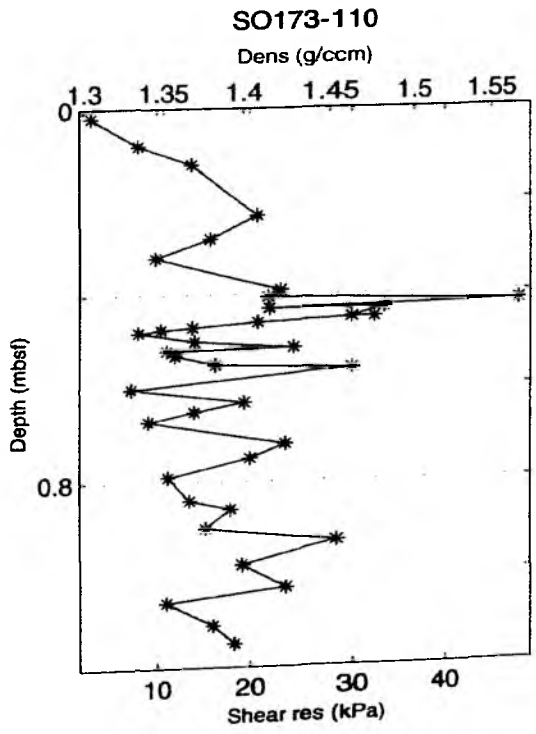

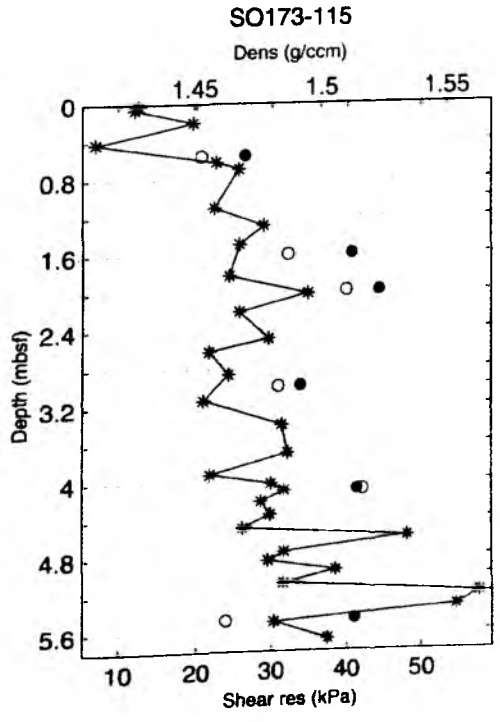

* Undrained shear resistance
● Volumetric wet bulk density
○ Recalculated, grain density based, wet bulk density

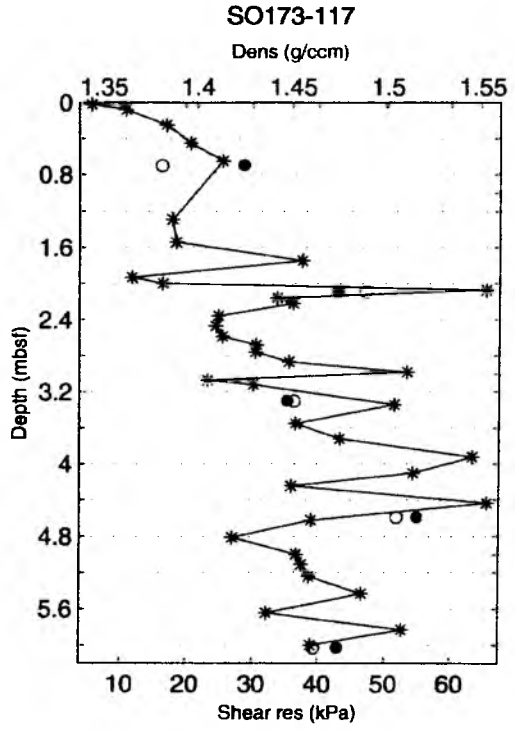

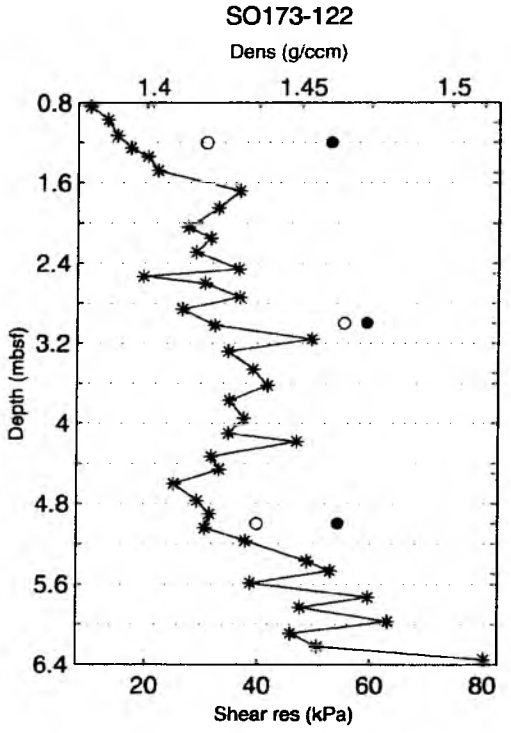

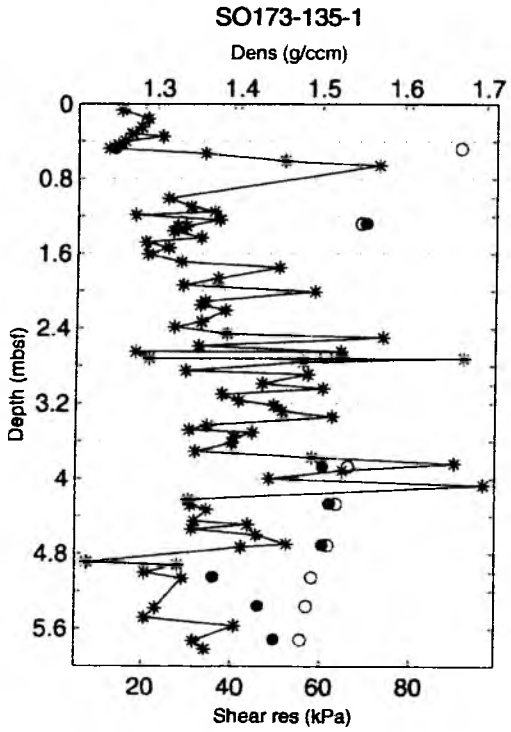

* Undrained shear resistance
● Volumetric wet bulk density
○ Recalculated, grain density based, wet bulk density

Appendix I:
Press Clippings

10 07 2003

REVISTA

La Prensa / 5B

Barco científico zarpa de Panamá con buenas noticias

SOFIA K. DE KOSMAS

skosmas@prensa.com

Foto/Cortesía de GEOMAR

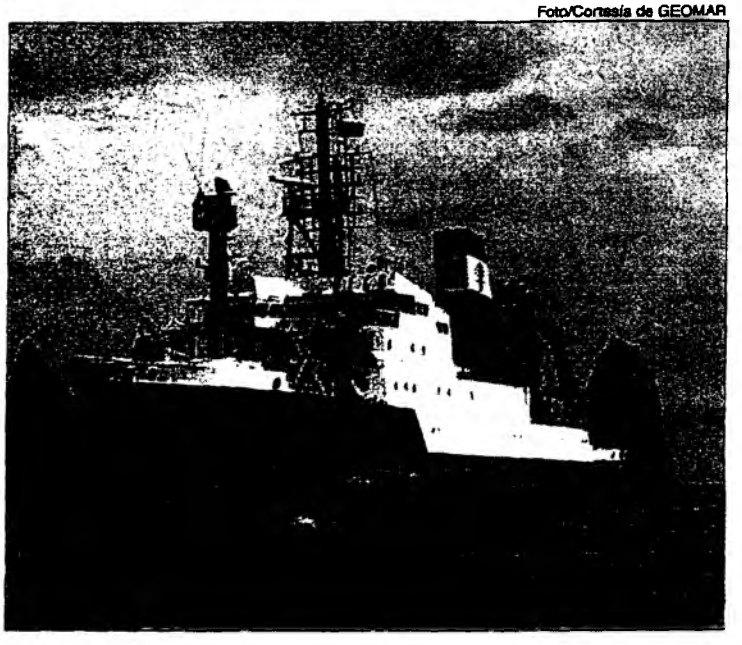

Al abordar la nave F.S. Sonne, el tripulante se siente como si estuviera en un barco de navegación común. Pero un recorrido por las instalaciones revela su estatus como un centro multid .plinario de investigación científica en alta mar.

I nave, que pertenece a la compa. . alemana GEOMAR, mide 97.6 metros de largo zarpó ayer de la base de Rodman, luego de haber anclado por unas 24 horas en Panamá esperando completar el equipo de 18 científicos que participarán en esta travesía.

Su próximo destino son las costas del Pacífico en Costa Rica y Nicaragua, en donde estudiarán los movimientos sísmicos de los platos teutónicos bajo el mar y los volcanes de esas áreas.

El director de la expedición, el sismólogo Ernst Flueh, explicó a La Prensa, cómo esta nave, originalmente un barco pesquero, fue transformada por el gobierno alemán hace 13 años exc ivamente para la investigación de la geología, paleontología, petrogí volcanología, que se desarrolla en l océanos.

El mantenimiento de esta nave, que ha recorrido las costas del Pacífico de Chile, Perú, EU e Indonesia, cuesta 35 mil dólares diarios, y está en funcionamiento 340 días al año.

El científico comentó que estas investigaciones se enfocan en los movimientos teutónicos que con el tiempo tienen un impacto directo en la población humana, ya sea como terremotos o como erupciones volcánicas. Alrededor del 70 % de la población mundial vive a lo largo de las costas, que sufren el primer impacto de estos movimientos.

Pero la ubicación de Panamá nos da una ventaja: seguridad. El científico explicó que esto se debe al desarrollo del Istmo como una "transición" (o puente fijo) entre la altamente activa zona sísmica de Centroamérica y la calma que sigue a lo largo de los Andes desde Chile hasta Colombia).

"De hecho, sólo vamos crear un estudio de alta resolución del fondo del mar panameño rumbo a Costa Rica", comenta Flueh. Esta es una de las pocas veces que la tripulación hace esto, ya que por lo general no cuentan con el permiso para investigar las aguas panameñas.

La sismóloga costarricense Ileana Boschini también es parte de este equipo investigativo.

Según ella, la red de estudios sismológicos y volcánicos entre Panamá y Costa Rica es eficiente y requiere de una estrecha cooperación entre el

el Instituto de Geociencias de la Universidad de Panamá y el Centro Sismológico de Centroamerica. Cuando hay temblores en la zona fronteriza, ambos países intercambian información valiosa para la seguridad de la población.

Ambos científicos detallaron minuciosamente la importancia de estos estudios, mientras mostraban las instalaciones del barco, cuyos instrumentos pueden medir las temperaturas del océano con precisión exacta, utilizando cables de hasta 8 kilómetros de largo, los cuales cubren un 95% de las profundidades del mar.

"El objetivo de cualquier estudio es salvar vidas y en la medida en que conozcamos las fuentes sísmicas, podemos ir conociendo las áreas donde pueden ocurrir terremotos", dijo Boschini, agregando que estos estudios los utilizan los ingenieros civiles para determinar qué materiales de construcción usar en áreas con mayores riegos sísmicos o volcánicos.

¿Está el Istmo en peligro? De acuerdo a Flueh, en un escala geológica, el Istmo de Panamá cambiará, pero tomarán miles de años antes que eso ocurra. De hecho, explicó que las rocas que forman la base del Istmo tienen unos 80 millones de años desde su formación, pero el puente terrestre solo se formó hace unos 4 millones de años, lo que significa que el área es bastante segura.

Laboratorio de alta mar

pasa por Panamá

Elizabeth González A.
egonzalez@epasa.com

Las cálidas aguas panameñas recientemente fueron visitadas por la "Nave de Investigación Científica F.S. Sonne", de la República de Alemania, embarcación que se encuentra en la misión de ir a Costa Rica y Nicaragua para hacer trabajos geofísicos y geológicos en esos países.

En sus travesías por los océanos Pacífico e Índico, 25 científicos acompañados por 30 tripulantes, desarrollan un programa de investigación desde hace casi 10 años para entender los procesos de las placas oceánica y continental hasta las cadenas de volcanes. La idea es entender, medir y cuantificar el flujo de carbón y agua, además de otros elementos fundamentales desde el punto de vista científico y no comercial.

Según Ernst Flueh, geofísico que trabaja en la investigación, el año pasado en Costa Rica colocaron un sismómetro en el fondo del mar para estudiar terremotos pequeños; el mismo que será colocado este año en otra región de ese país.

Con esos estudios los especialistas podrán entender mejor los procesos que suceden en las grandes profundidades de la tierra y que generan terremotos desastrosos.

"Normalmente hay sismómetros de tierra en todos los países, pero con ellos no se pueden estudiar los que ocurren en el mar. En este sentido hay pocos institutos a nivel mundial que tienen este sistema que trabaja hasta unos seis mil metros de profundidad".

Es importante mencionar que la visita por cuatro días de esta nave a Panamá fue específicamente de paso y no para desarrollar investigación alguna en nuestro territorio.

No obstante, durante el paso hasta Costa Rica, los geofísicos aplicarán en aguas panameñas una medición alta de precisión de la topografía submarina, debido a que hay canales y montes submarinos que no son conocidos.

De acuerdo con Flueh, Panamá no es motivo de estudio debido a que en este país la situación tectónica y geológica es muy diferente a la de Costa Rica, que sí tiene cadenas de volcanes; además advierte que en Panamá, por ser una micro placa, hay únicamente movimientos de rotación y traslación que generalmente se producen en el mar y que causan pocos daños a la población.

La Nave de Investigación Científica F.S. Sonne opera desde los años '70. Su función es de trabajar como un laboratorio en alta mar, en la mayoría de los casos al servicio de los científicos del mar de la ciudad de Kiel, en el norte de Alemania.

El prestigio de la oceanografía alemana, basada entre otros, en la Universidad Christian Albrecht en Kiel (Centro de Investigación de Geociencias Marinas y el Instituto de Oceanografía), se debe considerablemente a la existencia de barcos cómo la nave "Sonne".